

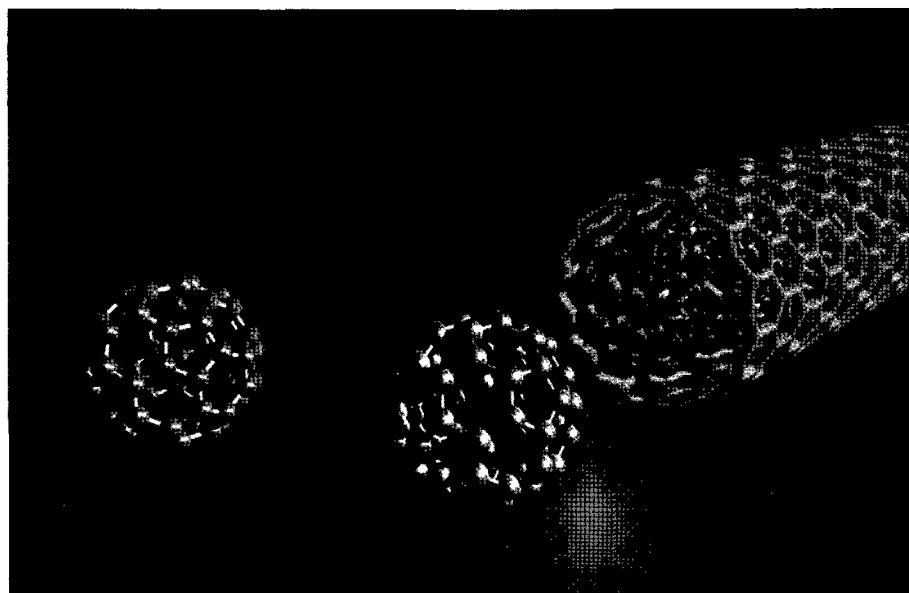
Abstracts

The 33rd Fullerene-Nanotubes General Symposium

第33回フラーレン・ナノチューブ

総合シンポジウム

講演要旨集



July 11–13, 2007, Fukuoka city, Fukuoka

平成19年7月11日～13日

九州大学病院キャンパス百年講堂

The Fullerenes and Nanotubes Research Society

フラーレン・ナノチューブ学会

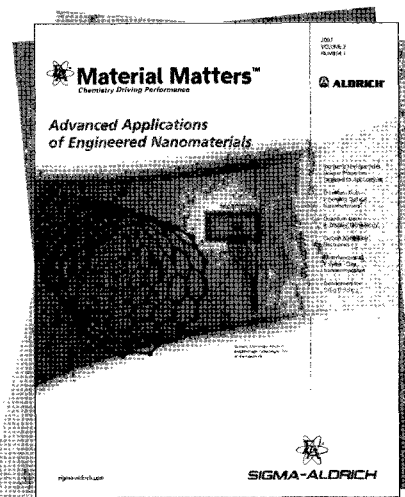
Nanomaterials



製品名 / 製品番号	構造式	容量	価格 (円)
N-methylfulleropyrrolidine (MP-C ₆₀)		100mg	50,000
668184			
(1,2-methanofullerene C ₆₀)-61-carboxylic acid		10mg	26,500
64251		25mg	50,000
658847		50mg	95,700
tert-Butyl (1,2-methanofullerene C ₆₀)-61-carboxylate		10mg	32,500
64245		50mg	128,800
Diethyl (1,2-methanofullerene C ₆₀)-61,61-dicarboxylate		10mg	53,600
64247		50mg	211,900
Diethyl (1,2-methanofullerene C ₇₀)-71,71-dicarboxylate		10mg	74,200
64248		50mg	293,700

フラーレン、カーボンナノチューブ等の
ナノマテリアルを特集した、
Material Matters™ Vol.2 No.1 (英語版)
が発行になりました。
sigma-aldrich.com/matsciからPDFを
ダウンロードいただけます。

日本語版発行準備中!
(8月頃発行予定)



Material Matters™
Chemistry Driving Performance

日本版既刊好評配布中!

第一線の研究者による、テクニカルレビュー、
アプリケーションノートを紹介した
ニュースレターです!

日本語版既刊:
Vol.1 No.1 高分子材料
Vol.1 No.2 分子自己組織化

材料関連の詳細情報は、sigma-aldrich.com/matsci (USサイト) および
sigma-aldrich.com/japan (日本サイト) をご覧ください!

新規登録および
既存カタログのご請求は、
日本サイトから!



SIGMA-ALDRICH
シグマ アルドリッチ ジャパン株式会社

〒140-0002 東京都品川区東品川2-2-24 天王洲セントラルタワー4F
TEL:03-5796-7330 FAX:03-5796-7335
e-mail:sialjpts@sial.com

Abstracts
The 33rd Fullerene-Nanotubes General Symposium

第 33 回 フラーレン・ナノチューブ
総合シンポジウム

講演要旨集

The Fullerenes and Nanotubes Research Society

The Chemical Society of Japan

Japan Society of Applied Physics

The Electrochemical Society of Japan

The Society of Polymer Science, Japan

主催：フラーレン・ナノチューブ学会

共催：日本化学会

協賛：応用物理学会・電気化学会・高分子学会

Date: July 11th(Wed)–13th(Fri), 2007

Place: Centennial Hall Kyushu University School of Medicine
3-3-1 Maidashi Higashi-ku, Fukuoka, Fukuoka, 812-8582
TEL: 092-642-6257

Presentation: Special Lecture (25 min presentation, 5 min discussion)
General Lecture (10 min presentation, 5 min discussion)
Poster Preview (1 min presentation, no discussion)

日時：平成 19 年 7 月 11 日（水）～13 日（金）

場所：九州大学医学部百年講堂

〒812-8582 福岡県福岡市東区馬出 3-1-1

TEL：092-642-6257

発表時間：特別講演 (発表 25 分・質疑応答 5 分)
一般講演 (発表 10 分・質疑応答 5 分)
ポスタープレビュー (発表 1 分・質疑応答 なし)

展示団体御芳名(五十音順、敬称略)

(株)エリオニクス
大塚電子(株)
コスモ・バイオ(株)
サイバネットシステム(株)
(株)島津製作所
(株)セントラル科学貿易
ナカライテスク(株)
フロンティアカーボン(株)
(株)堀場製作所
(株)名城ナノカーボン
福岡県工業技術センター

広告掲載団体御芳名(五十音順、敬称略)

(株)ATR
(株)エリオニクス
エムエス機器(株)
大塚電子(株)
(株)サイエンスラボラトリーズ
サイバネットシステム(株)
サーモフィッシャーサイエンティフィック(株)
(株)産業タイムズ社
(株)三和
シグマアルドリッチジャパン(株)
(株)島津製作所
(株)新興精機
住友商事(株)
(株)セントラル科学貿易
(株)東京プログレスシステム
東レ(株)
東洋炭素(株)
ナカライテスク(株)
日本電子(株)
日本分析工業(株)
(株)日立ハイテクノロジーズ
フロンティアカーボン(株)
(株)堀場製作所
(株)名城ナノカーボン
和光純薬工業(株)

Contents

Time Table	1
Chairperson	3
Program	
Japanese	4
English	15
Abstracts	
Special lecture	27
General lecture	33
Poster preview	79
Author Index	227

目次

早見表	1
座長一覧	3
プログラム	
和文	4
英文	15
講演予稿	
特別講演	27
一般講演	33
ポスター発表	79
発表索引	227

プログラム早見表

各項目敬称略

7月11日(水)		7月12日(木)		7月13日(金)	
	受付 8:00~		受付 8:00~		受付 8:00~
9:00	特別講演 (飯島澄男)	9:00	特別講演 (田代健太郎)	9:00	特別講演 (森口勇)
9:30	一般講演 4件 (ナノチューブの物性)	9:30	一般講演 4件 (金属内包フラーレン) (フラーレン生成・高次フ ラーレン)	9:30	一般講演 4件 (ナノホーン・内包ナノ チューブ) (ナノチューブの応用)
10:30	休憩	10:30	休憩	10:30	休憩
10:45	一般講演 5件 (ナノチューブの物性)	10:45	一般講演 5件 飯島賞受賞対象者講演	10:45	一般講演 5件 (ナノチューブの応用)
12:00	昼食	12:00	昼食	12:00	昼食
13:00	特別講演 (Lunhui Guan)	13:00	総会	13:00	特別講演 (二瓶史行)
13:30	一般講演 4件 (ナノチューブ:生成と精 製)	13:15	特別講演 (表研次)	13:30	一般講演 2件 (炭素ナノ粒子・その他)
14:30	休憩	13:45	一般講演 3件 大澤賞受賞対象者講演	14:00	ポスタープレビュー
14:45	一般講演 5件 (ナノチューブ:生成と精 製)	14:30	休憩	15:00	ポスターセッション
16:00	ポスタープレビュー	14:45	一般講演 4件 (フラーレン固体・フラー レンの化学)	16:30	
17:00	ポスターセッション	15:45	ポスタープレビュー		
18:30		16:45	ポスターセッション		
		18:30	懇親会		

Time Table

Wed. July 11		Thu. July 12		Fri. July 13	
	Registration (from 8 am)		Registration (from 8 am)		Registration (from 8 am)
9:00	Special Lecture (S. Iijima)	9:00	Special Lecture (K. Tashiro)	9:00	Special Lecture (I. Moriguchi)
9:30	General Lecutures [4] (Properties of Nanotubes)	9:30	General Lecutures [4] (Metallofullerenes) (Fullerene Formation)	9:30	General Lecutures [4] (Nanohorns and Endohedral Nanotubes)
10:30	Break	10:30	Break	10:30	Break
10:45	General Lecutures [5] (Properties of Nanotubes)	10:45	Lectures by Candidates for the Iijima Award [5]	10:45	General Lecutures [5] (Applications of Nanotubes)
12:00	Lunch	12:00	Lunch	12:00	Lunch
13:00	Special Lecture (L. Guan)	13:00	Meeting	13:00	Special Lecture (F. Nihey)
13:30	General Lecutures [4] (Formation and Purification of Nanotubes)	13:15	Special Lecture (K. Omote)	13:30	General Lecutures [2] (Science of Nanocarbons)
14:30	Break	13:45	Lectures by Candidates for the Osawa Award [3]	14:00	Poster Preview
14:45	General Lecutures [5] (Formation and Purification of Nanotubes)	14:30	Break	15:00	Poster Session
16:00	Poster Preview	14:45	General Lecutures [4] (Fullerene Solids, Chemistry of Fullerenes)	16:30	Poster Session
17:00	Poster Session	15:45	Poster Preview		
18:30		16:45	Poster Session		
		18:30	Banquet		

座長一覧

7月11日(水)

(敬称略)

	時 間	座 長
特 別 講 演 (飯島)	9:00 ~ 9:30	中嶋 直敏
一 般 講 演	9:30 ~ 10:30	片浦 弘道
一 般 講 演	10:45 ~ 12:00	村越 敬
特 別 講 演 (Guan)	13:00 ~ 13:30	坂東 俊治
一 般 講 演	13:30 ~ 14:30	岡崎 俊也
一 般 講 演	14:45 ~ 16:00	牧 英之
ポスタープレビュー	16:00 ~ 17:00	竹延 大志
		小塩 明

7月12日(木)

	時 間	座 長
特 別 講 演 (田代)	9:00 ~ 9:30	藤ヶ谷 剛彦
一 般 講 演	9:30 ~ 10:30	米村 弘明
一 般 講 演	10:45 ~ 12:00	若林 知成
特 別 講 演 (表)	13:15 ~ 13:45	森田 良美
一 般 講 演	13:45 ~ 14:30	吾郷 浩樹
一 般 講 演	14:45 ~ 15:45	北浦 良
ポスタープレビュー	15:45 ~ 16:45	菅井 俊樹
		野田 優

7月13日(金)

	時 間	座 長
特 別 講 演 (森口)	9:00 ~ 9:30	中嶋 直敏
一 般 講 演	9:30 ~ 10:30	大野 雄高
一 般 講 演	10:45 ~ 11:45	前田 優
特 別 講 演 (二瓶)	13:00 ~ 13:30	水谷 孝
一 般 講 演	13:30 ~ 14:00	柳 和宏
ポスタープレビュー	14:00 ~ 15:00	梅山 有和
		新留 康郎

7月11日(水)

特別講演 発表25分・質疑応答5分
一般講演 発表10分・質疑応答5分
ポスターレビュー 発表1分・質疑応答なし

特別講演(9:00-9:30)

- 1S-1 産総研/ナノカーボン研究センターにおけるカーボンナノチューブの研究:基礎と応用 27
飯島澄男

一般講演(9:30-10:30)

ナノチューブの物性

- 1-1 単層カーボンナノチューブにおける環境効果 33
○宮内雄平、齋藤理一郎、佐藤健太郎、大野雄高、岩崎真也、水谷孝、Jie Jiang、丸山茂夫
- 1-2 サファイア上に配向したSWNTのカイラリティの結晶面依存性 34
○石神直樹、吾郷浩樹、今本健太、辻正治、Konstantin Iakoubovskii、南信次
- 1-3 酸素分子およびオゾン分子によるカーボンナノチューブの酸化 35
○河合孝純、宮本良之
- 1-4 金属表面に吸着した単層カーボンナノチューブラマンスペクトルの構造依存性 36
武田憲彦、○村越敬

☆☆☆☆☆☆ 休憩 (10:30-10:45) ☆☆☆☆☆☆

一般講演(10:45-12:00)

ナノチューブの物性

- 1-5 カーボンナノチューブに対する電界ドーピングの第一原理計算 37
○内田和之、岡田晋
- 1-6 ボロンドープした多層ナノチューブ集合体における可変長ホッピング伝導 38
○坂東俊治、沼尾茂悟、飯島澄男
- 1-7 ホウ素ドーピングカーボンナノチューブの電子構造 39
○是常隆、齋藤晋
- 1-8 単層カーボンナノチューブの光学遷移におけるカイラル角依存性と励起子効果 40
○佐藤健太郎、齋藤理一郎、Jie Jiang、Gene Dresselhaus、Mildred S. Dresselhaus
- 1-9 一軸引っ張り歪印加による孤立単層カーボンナノチューブのバンドギャップ連続制御 41
○牧英之、佐藤徹哉、石橋幸治

☆☆☆☆☆☆ 昼食 (12:00-13:00) ☆☆☆☆☆☆

特別講演(13:00-13:30)

- 1S-2 HRTEM Imaging of the Doped Single-walled Carbon Nanotubes and Fullerene Nanopeapods 28
Lunhui GUAN

一般講演(13:30-14:30)

ナノチューブ:生成と精製

- 1-10 ナノチューブ成長モデルー成長過程におけるカイラル依存性ー 42
○阿知波洋次
- 1-11 カーボンナノチューブの成長に関する炭素透過法の研究 43
○日方威、林和彦、水越朋之、桜井芳昭、石神逸男、青木学聡、瀬木利夫、松尾二郎
- 1-12 ディーゼル煤からの単層カーボンナノチューブの生成 44
○内田貴司、橋勝、小島謙一
- 1-13 残留触媒が無いSWNTフォレストに不純物はないのか?ーグラフィティック炭素不純物の存在 45
○保田諭、平岡樹、二葉N ドン、湯村守雄、飯島澄男、島賢治

☆☆☆☆☆☆ 休憩 (14:30-14:45) ☆☆☆☆☆☆

一般講演(14:45-16:00)

ナノチューブ:生成と精製

- 1-14 コンビナトリアル手法を用いたカーボンナノチューブ触媒成長の基礎と応用 46
○野田優、杉目恒志、長谷川馨、寛和憲、丸山茂夫、山口由岐夫
- 1-15 Co-フェリチン触媒を用いたCVDによる単層カーボンナノチューブ成長のその場ラマン観察 47
○内田貴司、田沢雅也、山崎明、小林慶裕

7月11日(水)

1-16	気相触媒化学蒸着によるカーボンナノチューブのための触媒ナノ粒子のサイズ制御 ○大原賢治、根尾陽一郎、三村秀典、井上翼、石田明広	48
1-17	インパクト法で分級した触媒微粒子による2層・単層カーボンナノチューブの低温成長 ○近藤大雄、佐藤信太郎、山口佳孝、岩井大介、栗野祐二	49
1-18	単層カーボンナノチューブのCVD成長プロセスにおけるSiO ₂ 上の触媒観察 ○村上俊也、長谷部祐樹、木曾田賢治、西尾弘司、一色俊之、播磨弘	50

ポスタープレビュー(16:00-17:10)

ポスターセッション(17:00-18:00)

フラーレンの化学

1P-1	フェノチアジン-C ₆₀ 連結化合物の光誘起分子内電子移動反応からのピラジカルにおける新規磁場効果と時間分解EPRスペクトル ○米村弘明、森部真也、脇田佑哉、山田淳、藤原好恒、谷本能文	79
1P-2	β-カロテン退色法による水溶性[60]フラーレンならびに[60]フラーレンエポキシドの抗酸化能の速度論的評価 ○小久保研、後藤忠示、都賀谷京子、青島央江、大島巧	80
1P-3	フラーレンを用いたカーボン/エポキシ複合材料の界面制御 田島 右副、○山崎大輔、松浦孝伯、沼田陽平、川村博昭、大背戸浩樹	81
1P-4	結晶性C ₆₀ とC ₇₀ の材料電気伝導率の温度依存性 ○河野剛、高倉剛、高瀬 剛、中村英嗣、孫勇	82
1P-5	イリジウムポルフィリン環状二量体ー著しく高い親和性ー ○柳沢誠、田代健太郎、相田卓三	83
1P-6	クロラミンTのフラーレンへの付加ー環化における選択性の制御 ○窪岡亮治、南方聖司、小松満男	84
1P-7	酸素雰囲気におけるフラーレンと水のメカノケミカル反応による水酸化フラーレンの効率的合成 ○石山雄一、渡辺洋人、仙名保	85
1P-8	フラーレンC ₆₀ および開口C ₆₀ 誘導体の二価アニオン種に内包された水素分子のNMR観測 ○村田理尚、越智雄大、田邊史行、村田靖次郎、小松紘一	86
1P-9	高い溶解性を有するフラーレン誘導体とそのプロセス開発 ○橋口昌彦、出島栄治、矢野智美、田中克知	87
1P-10	ニトロフラーレン中間体を用いたアミノフラーレン誘導体の合成 ○関戸大、大野正富	88

金属内包フラーレン

1P-11	Luクラスター内包フラーレンの光電子分光 ○宮崎隆文、加藤真之、古川浩之介、隅井良平、梅本久、沖本治哉、菅井俊樹、篠原久典、日野照純	89
1P-12	Gg@C ₈₂ のBingel反応付加体のESRスペクトル ○金住誠、竹松裕司、若原孝次、土屋敬広、古川貢、赤阪健、加藤立久	90
1P-13	アルカリ金属内包フラーレンのキャラクタリゼーション:凝集クラスター構造 ○岡田 洋史、表 研次、笠間 泰彦、横尾 邦義、小野 昭一、宮崎 孝道、安東 真理子、前川 英己、秋山 公男、小室 貴士、飛田博実	91
1P-14	Pr@C ₈₂ の可逆的構造転移と構造解析 ○北浦良、北村豊、沖本治哉、西堀英治、青柳忍、坂田誠、篠原久典	92

フラーレン固体

1P-15	マグネシウム添加フラーレン化合物の金属相 ○平郡論、木全希、小林本忠	93
1P-16	ナトリウム添加フラーレンNa _x C ₆₀ の超伝導 ○木全希、平郡論、小林本忠	94
1P-17	C ₆₀ (111)面上における銅フタロシアニンの分子線エピタキシー成長 鈴木秀俊、山下侑佑、○小島信晃、山口真史	95

ナノチューブ:生成と精製

1P-18	アルコール封入CVD法によるサブミリメートル長SWNTの合成 ○鈴木義信、島津智寛、大島久純、丸山茂夫	96
1P-19	触媒構造変化によるカーボンナノチューブのミリメートル成長の停止 ○諸隈慎吾、長谷川馨、野田優、丸山茂夫、山口由岐夫	97
1P-20	直径制御したRh/PdおよびCo粒子からの触媒担持化学的気相成長法による単層カーボンナノチューブの成長 ○小林慶太、北浦良、熊井葉子、後藤康友、稲垣伸二、篠原久典	98
1P-21	白金触媒を用いた直径の細い単層カーボンナノチューブの生成 ○浦田圭輔、鈴木信三、長澤浩、阿知波洋次	99

1P-22	Fe/Co/Mo触媒およびMgO担持体を用いたCVD法によるDWNTの効率的成長 ○内藤亮治、村上俊也、長谷部祐樹、木曾田賢治、西尾弘司、一色俊之、播磨弘	100
1P-23	水素直流アーク放電で合成されたSWNTsの精製 ○B. Chen、鈴木智子、趙新洛、井上栄、橋本剛、安藤義則	101
1P-24	液相中における配向カーボンナノチューブの1段合成 ○山際清史、三上真史、竹内恒晴、山口吉弘、岩尾有里子、齋藤守弘、桑野潤	102
1P-25	温度勾配を利用したカーボンナノチューブの直径分布の制御 ○中山崇、鶴岡泰広、鈴木信三、阿知波洋次	103
1P-26	ACCVD法による垂直配向SWNT合成における反応条件と触媒条件のマッチング ○杉目恒志、野田優、丸山茂夫、山口由岐夫	104
1P-27	ブラシ状カーボンナノチューブの成長における残留アセチレンガスの影響 ○山口整郎、潘路暉、秋田成司、中山喜萬	105
1P-28	低圧エタノールCVDによるカーボンナノチューブ成長の触媒金属に関するその場光電子分光による研究 ○前田文彦、鈴木哲、小林慶裕	106
1P-29	カーボンナノチューブ及び触媒微粒子のTEM平面観察とSWNT成長における触媒活性の検討 ○長谷部祐樹、村上俊也、木曾田賢治、播磨弘、西尾弘司、一色俊之	107
1P-30	膜厚を連続的に変化させた触媒からのカーボンナノチューブ成長の不連続性 ○寛和憲、野田優、丸山茂夫、山口由岐夫	108

ナノホーン

1P-31	Close-Open-Close Evolution of Holes in Single-Wall Carbon Nanohorns Caused by Heat Treatment ○范晶、湯田坂雅子、宮脇仁、弓削亮太、河合孝純、飯島澄男	109
1P-32	シスプラチン徐放のためのシスプラチン内包ナノホーンの化学修飾 ○安嶋久美子、湯田坂雅子、村上達也、張民芳、飯島澄男	110
1P-33	葉酸標識カーボンナノホーンの癌細胞への選択的取り込み ○宮脇仁、村上達也、湯田坂雅子、安嶋久美子、張民芳、澤田浩秀、土田邦博、飯島澄男	111
1P-34	アーク放電法によって作製されるボロドープナノホーン粒子 ○原田学、稲垣貴之、坂東俊治、飯島澄男	112
1P-35	過酸化水素処理で損傷したカーボンナノホーンの先端構造の電子顕微鏡観察 ○山口貴司、坂東俊治、湯田坂雅子、飯島澄男	113
1P-36	カーボン・ナノホーンの超遠心分離 ○田村豪主、坂東俊治、湯田坂雅子、飯島澄男	114

ナノチューブの物性

1P-37	ホウ素添加MWNTにおける伝導率の増加 ○石井聡、渡邊徹、小河原昭吾、奥津貴史、富岡史明、上田真也、津田俊輔、山口尚秀、高野義彦	115
1P-38	その場観察電子顕微鏡法による架橋した多層ナノチューブの電子輸送 鈴木泰伸、安坂幸師、○齋藤弥八	116
1P-39	紫外ラマン分光による単層カーボンナノチューブの評価 ○片浦弘道、宮田耕充、真庭豊、柳和宏	117
1P-40	単層カーボンナノチューブと高配向性グラファイトのラマンスペクトルの温度依存性 ○北田典央、加藤健一、小島謙一、橘勝	118
1P-41	Effects of doping to the G'Raman spectra of single and double-wall carbon nanotubes ○Eduardo B. Barros, Jin Sung Park, Georgii G. Samsonidze, Riichiro Saito, Mildred Dresselhaus	119
1P-42	DNA/MWNTの結合系創製とDNA薄膜の電気特性 ○井出光隆、齋藤允俊、河野浩明、村田尚義、春山純志	120
1P-43	蜂の巣配置された多層ナノチューブアレイにおけるマイスナー効果 ○村田尚義、春山純志、上田延輝、松平将治、八木優子、中村仁、野沢響子、清水台生、ErikEinarsson、千足昇平、丸山茂夫、菅井俊樹、岸直希、篠原久典	121

ナノチューブの応用

1P-44	シクロデキストリン-カーボンナノチューブ複合体を用いたゲスト応答性カーボンナノチューブヒドロゲル ○生越友樹、山岸忠明、中本義章、原田明	122
1P-45	ゲスト分子-シクロデキストリン包接錯体によるカーボンナノチューブの可溶性 ○生越友樹、山岸忠明、中本義章、原田明	123
1P-46	カーボンナノチューブ/PVAコンポジット材料を用いた偏光子の作製 ○庄司暁、鈴木秀昌、河田聡	124
1P-47	カーボンナノチューブ合成基板電極上でのグルコースオキシダーゼの直接電子移動反応 富永昌人、○野村真也、西村敏史、谷口功	125
1P-48	カーボンナノチューブ膜の作成と物性 ○宇尾基弘、赤坂司、阿部薫明、亘理文夫、笹森賢一郎、木村久道、佐藤義倫、田路和幸	126

7月11日(水)

1P-49 表面修飾を施した高結晶性単層カーボンナノチューブの電気二重層キャパシタンス 127
○荻野真一、佐藤義倫、名村優、大泉亘、紙透浩幸、本宮憲一、伊藤隆、バラチャンドラン ジャヤデワン、田路和幸

その他

1P-50 Fabrication of Carbon Nanotubes Through Metal-free Chemical Vapor Deposition 128
○Jarrn-Hong Lin, Hui-Ling Ma, Ching-Shiun Chen, Chen-Yin Hsu, Hsiu-Wei Chen

7月12日(木)

特別講演 発表25分・質疑応答5分
一般講演 発表10分・質疑応答5分
ポスタープレビュー 発表1分・質疑応答なし

特別講演(9:00-9:30)

2S-1 ナノカーボン/金属ポルフィリン複合化の精密制御 田代 健太郎 29

一般講演(9:30-10:30)

金属内包フラーレン

2-1 $(M_2C_2@C_{82})(C_6H_5CH_3)$ と $(M_2C_2@C_{82})(C_6H_5CH_3)_2$ の結晶構造 51
○西堀英治、石原将行、寺内伊久哉、青柳忍、坂田誠、高田昌樹、井上崇、伊藤靖弘、梅本久、森部裕江、篠原久典

2-2 エルビウムカーバイド内包フラーレンの $1.5\mu m$ 近赤外蛍光 52
○伊藤靖浩、岡崎俊也、大窪清吾、赤地祐彦、沖本治哉、大野雄高、水谷孝、中村哲也、北浦良、菅井俊樹、篠原久典

フラーレン生成・高次フラーレン

2-3 タイタン衛星は炭素クラスター合成工場ではないか？—衝突合成実験より— 53
○三重野哲、長谷川直

2-4 極性溶媒中におけるSWNT-フラーレン超分子複合体の光誘起電荷分離 54
○伊藤攻、荒木保幸、アツラ サンダナヤカ、ルグー チイタ、フランシス ドゾーサ

☆☆☆☆☆☆ 休憩 (10:30-10:45) ☆☆☆☆☆☆

一般講演(10:45-12:00)

飯島賞受賞対象者講演

2-5 Optical Enrichment of SWNTs 55
○Xiaobin Peng, Naoki Komatsu, Takahide Kimura, Atsuhiko Osuka

2-6 内包色素分子にとって透明なカーボンナノチューブの開発 56
○柳和宏、宮田耕充、片浦弘道

2-7 カーボンナノチューブ中の飽和炭化水素鎖の電子顕微鏡観察 57
○越野雅至、田中隆嗣、ソリン・ニクラス、末永和知、磯部寛之、中村栄一

2-8 ZnPc-ナノホーン-蛋白質ナノハイブリッドの構築とその光線力学治療への応用 58
○張 民芳、湯田坂雅子、安嶋久美子、宮脇仁、飯島澄男

2-9 半導体微粒子からのカーボンナノチューブ成長 59
○高木大輔、日比野浩樹、鈴木哲、小林慶裕、本間芳和

☆☆☆☆☆☆ 昼食 (12:00-13:00) ☆☆☆☆☆☆

総会(13:00-13:15)

特別講演(13:15-13:45)

2S-2 $Li@C_{60}$ の合成 表研次、笠間泰彦 30

一般講演(13:45-14:30)

大澤賞受賞対象者講演

2-10 新規開発したパルスイオンバルブによるイオン移動能測定 60
○菅井俊樹、篠原久典

2-11 HRTEMによる C_{60} フラーレン単分子の観察と電子ビームによる C_{60} フラーレンの変形過程 61
○劉曄、末永和知、Ales Mrzel、片浦弘道、飯島澄男

2-12 化学修飾によるフラーレンケージに内包された金属原子の配向制御 62
○山田道夫、染谷知香、若原孝次、土屋敬広、赤阪健、前田優、与座健治、溝呂木直美、永瀬茂

☆☆☆☆☆☆ 休憩 (14:30-14:45) ☆☆☆☆☆☆

一般講演(14:45-15:45)

フラーレン固体・フラーレンの化学

2-13 十二重および十三重付加型[60]フラーレンの合成、構造および光学特性 63
○藤田健志、松尾豊、中村栄一

2-14	トリアリアルメタン色素系カチオンで安定化したC ₆₀ フラーライド単結晶の示す低次元カラム配列 ○森山広思、杉浦崇仁	64
2-15	多様なアルカンチオールで修飾されたAu電極を用いたC ₆₀ 薄膜FETデバイス ○太田洋平、川崎菜穂子、長野高之、藤原明比古、久保園芳博	65
2-16	フラーレン繊維の作成と重合 ○スディップマリック、藤田典史、新海征治	66

ポスタープレビュー(15:45-16:45)**ポスターセッション(16:45-18:15)****フラーレン生成・高次フラーレン**

2P-1	金属および半導体カーボンナノチューブ上の吸着原子に働く電流誘起力 ○イヴァン ギラード、山本貴博、渡辺一之	129
2P-2	フラーレンの形成過程 ○上野裕亮、斎藤晋	130

フラーレンの化学

2P-3	C ₆₀ -フェノチアジン系の混合ナノクラスターを修飾した電極の形態・電気化学・光電気化学特性に及ぼす磁場印加プロセスの効果 ○脇田佑哉、米村弘明、黒田憲寛、山田淳、藤原好恒、谷本能文	131
2P-4	[70]フラーレン三重付加体の合成と電気化学特性 ○一木孝彦、松尾豊、中村栄一	132
2P-5	フラーレン類によるPMMAの熱分解抑制機構 ○寺田 智仁、松浦孝伯、佐々木健夫、田島右副	133
2P-6	インドリノ[60]フラーレンの合成及び電気化学的性質 ○川嶋淳一、原拓生、松浦孝伯、沼田陽平、田島右副	134

金属内包フラーレン

2P-7	Scカーバイド内包フラーレンの固体NMR ○沖本治哉、Wilhelm Hemme、伊藤靖浩、Helmut Eckert、篠原久典	135
2P-8	M@C ₇₄ の構造と振電相互作用 ○佐藤徹、葛本泰崇、徳永健、今堀博、田中一義	136
2P-9	spiro[2-Adamantane-2,3'-3H-Diazirine]との反応によるLi@C ₆₀ の化学修飾 ○石川真介、小室貴士、岡田洋史、表研次、笠間泰彦、横尾邦義、小野昭一、飛田博実	137
2P-10	Sc@C ₈₂ の構造と電子的特性 ○蜂屋誠、飯塚裕子、若原孝次、土屋敬広、前田優、赤阪健、溝呂木直美、永瀬茂	138
2P-11	Missing Metallofullerene: La@C _{2n} ○二川秀史、菊池隆、山田智也、若原孝次、仲程司、G. M. Aminur RAHAMAN、土屋敬広、前田優、赤阪健、与座健治、Ernst HORN、山本和典、溝呂木直美、Zdenek Slanina、永瀬茂	139

フラーレン固体

2P-12	振動リード法によるフラーレン薄膜の内部摩擦測定 ○脇田慎也、松本修一、吉井尊範、桐本賢太、孫勇	140
2P-13	パーフルオロアルキル基を有するC ₆₀ 誘導体塗布膜のTFT特性 ○近松真之、板倉篤志、吉田郵司、阿澄玲子、八瀬清志	141
2P-14	ホール輸送材料の量子化学的設計:水素化フラーレン ○徳永健、大森滋和、川畑弘、松重和美	142
2P-15	圧縮粉末及び液中成長したフラーレンの自由電子レーザー照射によるポリマー化 ○岩田展幸、安藤慎悟、飯尾靖也、野苺家亮、山本寛	143
2P-16	MgドープC ₆₀ 薄膜の電気伝導特性 ○小島信晃、寺山隆志、鈴木 秀俊、名取雅人、山口真史	144
2P-17	内包H ₂ @C ₆₀ の物理的物性 ○谷垣勝己、良知健、熊代良太郎、村田靖次郎、小松紘一、垣内徹、澤博、小濱芳充、泉沢悟、川路均、阿竹徹	145

炭素ナノ粒子

2P-18	生体分子の炭化によるカーボンナノ粒子の作製 富永昌人、○宮原勝也、野村真也、谷口功	146
2P-19	グラフェンへの高速イオン衝突による電子励起効果 ○宮本良之、アルカディ カラシニコフ、デエイヴィッド トマネク	147
2P-20	ポリインのレーザー誘起発光 ○若林知成、永山寛幸、大極孝太、清岡洋介、橋本健朗	148

2P-21	C ₆₀ -エチレンジアミンナノ粒子の作製と光電気化学的応用 松岡健一、瀬尾英孝、○秋山毅、山田淳	149
2P-22	高密度炭素アーク放電法による多面体グラファイト粒子の形成 ○片桐洋次、小塩明、馬淵淳平、小海文夫	150
2P-23	ナノグラファイトのエネルギー論: 端形状と電子状態 ○岡田晋	151

内包ナノチューブ

2P-24	ナノチューブ内におけるC ₆₀ のエネルギー論 ○岡田晋	152
2P-25	銅ナノワイヤーで完全に充填されたカーボンナノチューブの高効率形成 ○水野直樹、小塩明、鬼頭大信、小海文夫	153
2P-26	フラーレン及びヘテロフラーレンを用いたピーポッド合成とその電氣的輸送特性 ○李永峰、金子俊郎、西垣昭平、畠山力三、表研次、笠間泰彦	154
2P-27	単層カーボンナノチューブに吸着したメタンのNMR 廣津智之、○松田和之、鷹子貴之、門脇広明、真庭豊、片浦弘道	155
2P-28	マイクロ波プラズマ化学気相成長法によるAAO基板上への金属内包カーボンナノチューブの成長 ○松岡洋平、内藤綱彦、林靖彦、藤田武志、種村真幸、曾我哲夫	156

ナノチューブ: 生成と精製

2P-29	その場吸光測定による垂直配向単層カーボンナノチューブの生成メカニズムの解明 ○小倉一晃、門脇政幸、大川潤、Erik Einarsson、丸山茂夫	157
2P-30	長尺カーボンナノチューブ合成とカーボンナノチューブコーティング ○柿畑和行、廣野友作、堀江寿紀、井上翼、石田明広、三村秀典	158
2P-31	単層カーボンナノチューブの分散挙動に及ぼす超音波効果 ○田島勇、Catalin Romeo Luclescu、鈴木芳枝、内田勝美、石井忠浩、矢島博文	159
2P-32	金フェリチンを触媒に用いたサファイア基板上での配向単層カーボンナノチューブ成長 ○山寄明、高木大輔、大塚康之、鈴木哲、本間芳和、吉村英恭、小林慶裕	160
2P-33	アルコール化学気相堆積法による分岐カーボンナノチューブの生成 (3) - Co/Moモル比によるCNT成長の違い ○前川将之、須田善行、菅原広剛、酒井洋輔	161
2P-34	Fe-Sn触媒による多層カーボンナノコイルの作製 ○金田亮、潘路軍、秋田成司、平原佳織、中山喜萬	162

ナノホーン

2P-35	SWNH-Streptavidin: an Effective Anticancer Drug Delivery System ○Xu Jianxun, Masako Yudasaka, Minfang Zhang, Sumio Iijima	163
2P-36	近赤外光駆動型カーボンナノホーンの開発と感染症治療への応用 ○都英次郎、長田英也、平野研、槇田洋二、仲山賢一、廣津孝弘	164

ナノチューブの物性

2P-37	ナノピーポッドから製作した2層カーボンナノチューブの共鳴ラマンによる評価 ○鄭 淳吉、岡崎俊也、岸直希、Zujin Shi、飯島澄男	165
2P-38	単層カーボンナノチューブと <i>p</i> -フェニレン-1,1'-ビニリデン欠陥構造を主鎖に有するポリ(<i>p</i> -フェニレン-1, 2-ビニレン)との複合体 ○門田直樹、梅山有和、手塚記庸、俣野善博、今堀博	166
2P-39	水吸蔵単層カーボンナノチューブのガス吸着 ○客野遥、小笠原俊介、日比寿栄、宮田耕充、松田和之、門脇広明、鈴木信三、阿知波洋次、片浦弘道、斎藤毅、大嶋哲、湯村守雄、飯島澄男、真庭豊	167
2P-40	二層カーボンナノチューブの高温高圧処理 ○金森佑輔、川崎晋司、岩井勇樹、岩田篤志、村松寛之、林卓哉、金隆岩、遠藤守信	168
2P-41	RNA/単層カーボンナノチューブ複合体の光特性 ○若松信雄、野口悠一、藤ヶ谷剛彦、中嶋直敏	169
2P-42	SWNT-DNA複合物質の合成および電気力顕微鏡による観察 ○浅田有紀、桑原彰太、菅井俊樹、北浦良、篠原久典	170
2P-43	電気力顕微鏡によるカーボンナノチューブの欠陥検出 ○沖川侑揮、榎坂武夫、大野雄高、岸本茂、水谷孝	171

ナノチューブの応用

2P-44	液相プロセスを用いた単層カーボンナノチューブトランジスタによる論理回路の作製 ○富田晴雄、小倉明夫、片浦弘道、野内亮、白石誠司	172
-------	--	-----

7月12日(木)

2P-45	皮下組織におけるカーボンナノ物質の生体適合性 ○平田恵理、横山敦郎、佐藤義倫、野田坂佳伸、宇尾基弘、赤坂司、田路和幸、亘理文夫	173
2P-46	サファイア上の配向SWNTの電子輸送特性 ○鈴木朋子、吾郷浩樹、石神直樹、辻正治、生田竜也、高橋厚史	174
2P-47	二層カーボンナノチューブの物理化学的性質に与える化学酸化の影響 ○前田範子、内田勝美、石井忠浩、矢島博文	175
その他		
2P-48	グラフェンナリボンにおけるフォノン散乱ダイナミクス ○高橋徹、山本貴博、渡辺一之	176
2P-49	両親媒性単層カーボンナノチューブ分散剤としてのイオン性ゲル化剤の合成と機能 ○吉田勝、甲村長利、三澤善大、玉置信之、松本一、カザウイ サイ、南信次	177
2P-50	炭化ランタン内包グラファイトカプセルの固化体の調製 ○脇一平、佐藤義倫、名村優、本宮憲一、バラチャンドラン ジャヤデワン、大久保昭、木村久道、田路和幸	178

7月13日(金)

特別講演 発表25分・質疑応答5分
一般講演 発表10分・質疑応答5分
ポスタープレビュー 発表1分・質疑応答なし

特別講演(9:00-9:30)

3S-1 カーボン・金属酸化物ナノ複合材料の創製 森口勇 31

一般講演(9:30-10:30)

ナノホーン・内包ナノチューブ

- 3-1 ポリインピーボッドのラマン分光 67
○若林知成、西出大亮、片浦弘道、阿知波洋次、篠原久典
- 3-2 ピーボットへの単一電子注入 68
○春山純志、水林 潤、武末出美、岡崎俊哉、篠原久典、原田康則、栗野祐二
- 3-3 カーボンナノホーンを使ったサブナノメートルサイズの白金粒子の作製 69
○弓削亮太、湯田坂雅子、張民芳、吉武務、飯島澄男

ナノチューブの応用

- 3-4 C₆₀を内包した単層カーボンナノチューブによる抵抗スイッチング効果 70
○菅洋志、柳和宏、堀川昌代、片浦弘道、清水哲夫、内藤泰久

☆☆☆☆☆☆ 休憩 (10:30-10:45) ☆☆☆☆☆☆

一般講演(10:45-12:00)

ナノチューブの応用

- 3-5 カーボンナノチューブ上のアルミニウムクラスターの原子分解FEM像 71
松川知弘、山下徹也、安坂幸師、中原仁、○齋藤弥八
- 3-6 ポルフィリン修飾単層カーボンナノチューブを用いた光電気化学素子 72
○梅山有和、藤田充、手塚記庸、門田直樹、俣野善博、今堀博
- 3-7 ナノ分散したカーボンナノチューブ・ネットワークによる電氣的・光学的ガス検出 73
○南信次、カルティゲヤン・アンナマライ、ヤクボブスキー・コンスタンチン
- 3-8 スーパーグロス単層カーボンナノチューブ電気化学キャパシタ 74
○イザディナジャファバディ アリ、畠賢治、平岡樹、山田健郎、二葉N. ドン、保田諭、君塚統、棚池修、羽鳥浩章、湯村守雄、飯島澄男
- 3-9 インクジェット法によるナノチューブ薄膜トランジスタの作製 75
○竹延大志、美浦徳子、浅野武志、深尾朋寛、白石誠司、岩佐義宏

☆☆☆☆☆☆ 昼食 (11:45-13:00) ☆☆☆☆☆☆

特別講演(13:00-13:30)

3S-2 マルチチャネルCNTトランジスタの特性 二瓶史行 32

一般講演(13:30-14:00)

炭素ナノ粒子・その他

- 3-10 水分散性グラフィティックナノチューブの作製 76
○金武松、張関心、福島孝典、相田卓三
- 3-11 円錐形キャビティー列を有する垂直配向カーボンナノファイバーの構造:グラファイトコーンの一次元配列 77
○小塩明、丹後佑太、山崎貴之、鈴木健太郎、小海文夫

ポスタープレビュー(14:00-15:00)

ポスターセッション(15:00-16:30)

ナノチューブの応用

- 3P-1 高配向、高含有した単層カーボンナノチューブーエポキシコンポジットフィルムの力学的特性 179
○西野秀和、平岡樹、山田健郎、二葉ドン、畠賢治
- 3P-2 DNAを用いたカーボンナノチューブのガラス基板上への固定とパターン形成 180
○庄司暁、城野純一、河田聡
- 3P-3 単層カーボンナノチューブ分散液の温度依存性による光学特性 181
○種村亜紀奈、Catalin Romeo Luculescu、内田勝美、石井忠浩、矢島博文
- 3P-4 CNTs/キトサン複合フィルムへのイオンビーム照射による細胞接着性制御 182
○鎮目瑠美、高橋克宗、内田勝美、鈴木嘉昭、矢島博文

3P-5	垂直配向単層カーボンナノチューブ膜面上への金属蒸着と金属面への接合 ○渡辺誠、小倉一晃、石川桂、大川潤、エリック エイナルソン、丸山茂夫	183
3P-6	チューブ直径に依存するDNA-SWNTハイブリッドの分散状態 ○戸板翔、姜東哲、小島謙一、橘勝	184
3P-7	タンパク質による単層カーボンナノチューブの高安定分散 ○田中丈士、金赫華、今中忠行、藤原伸介、片浦弘道	185
3P-8	meso-meso縮環ポルフィリンによる単層カーボンナノチューブの可溶化 ○渡辺健一、藤ヶ谷剛彦、中嶋直敏	186
3P-9	半導体と金属カーボンナノチューブを分離する電界クロマトグラフィーの開発 ○佐野正人、和田佳祐	187
3P-10	金属性単層カーボンナノチューブの分離と透明導電性薄膜の作製 ○前田優、橋本正博、長谷川正、神田信、土屋敬広、若原孝次、赤阪健、Said Kazaoui、南信次、丸山茂夫、永瀬茂	188
3P-11	ドライプロセスで作製したSWNT薄膜の評価 ○斎藤毅、大嶋哲、大森滋和、湯村守雄、飯島澄男	189
3P-12	中性粒子ビームによるカーボンナノチューブダメージフリー表面改質 ○和田章良、佐藤義倫、石田真彦、二瓶史行、田路和幸、寒川誠二	190
3P-13	Polybenzimidazole-CNT複合体の新機能開発 ○岡本稔、藤ヶ谷剛彦、中嶋直敏	191
3P-14	お茶によるカーボンナノチューブの可溶化 ○中村元気、成松香織、中嶋直敏	192

ナノチューブの物性

3P-15	酸化/エステル化処理カーボンナノチューブのポルフィリン修飾 ○新井徹、信國真吾、高橋康介、下手義和	193
3P-16	電界効果トランジスタにおけるカーボンナノチューブのフォトルミネッセンス及び光誘起電流の同時測定 ○小林篤史、大野雄高、岸本茂、水谷孝	194
3P-17	孤立単層カーボンナノチューブのバンドル再構成 ○宮田耕充、柳和宏、真庭豊、片浦弘道	195
3P-18	単層カーボンナノチューブにおけるラマン強度の長さ依存性 ○朴珍成、齋藤理一郎、佐藤健太郎、Jie Jiang、Gene Dresselhaus、Mildred S. Dresselhaus	196
3P-19	2層カーボンナノチューブの持つ層間相互作用のSTMによる観察 ○福井信志、加藤裕子、吉田宏道、菅井俊樹、平家誠嗣、藤森正成、諏訪雄二、橋詰富博、篠原久典	197
3P-20	In Situ Manipulation and Engineering of Carbon Nanotubes Inside a Transmission Electron Microscope ○金伝洪、末永和知、飯島澄男	198
3P-21	垂直配向SWNT膜内の狭いバンドル構造 ○エリックエイナルソン、山本剛久、張正宜、幾原雄一、丸山茂夫	199
3P-22	SWNTs-FET特性に対する化学修飾の影響 ○熊代良太郎、阿部有希、赤坂健、前田優、小林長夫、谷垣勝己	200
3P-23	単層カーボンナノチューブの低エネルギー照射損傷の閾エネルギー ○鈴木哲、小林慶裕	201
3P-24	レドックス反応に伴う半導体性SWNTsの分光特性 ○平山康平、藤ヶ谷剛彦、新留康郎、中嶋直敏	202
3P-25	高純度単層カーボンナノチューブの光物性 ○宮田耕充、柳和宏、真庭豊、片浦弘道	203
3P-26	カーボンナノチューブのフォトルミネッセンスに対する環境の効果 ○大野雄高、岩崎慎也、村上陽一、岸本茂、丸山茂夫、水谷孝	204
3P-27	単層カーボンナノチューブ蛍光発光のエタノールガス圧依存性 ○千足昇平、渡部智史、花島干城、本間芳和	205

フラーレン生成・高次フラーレン

3P-28	気相カーボン挿入反応によるC ₆₀ からフラーレンC ₇₀ の合成 ○尾形照彦、三重野哲、畳谷仁男	206
3P-29	Sc ₂ C ₈₄ (II)の構造に関する研究 ○中嶋康二、飯塚裕子、若原孝次、土屋敬広、前田優、赤阪健、溝呂木直美、永瀬茂	207

金属内包フラーレン

3P-30	La@C ₈₂ とシクロペンタジエン誘導体の可逆反応 ○佐藤悟、前田優、稲田浩司、長谷川正、山田道夫、土屋敬広、赤阪健、加藤立久、溝呂木直美、永瀬茂	208
3P-31	窒素原子内包フラーレン合成に関与する窒素プラズマの発光特性 ○西垣昭平、金子俊郎、畠山力三	209

ナノチューブ:生成と精製

- 3P-32 超音波処理によるCMC分散SWNTの構造変化 210
○大森滋和、斎藤毅、大島哲、湯村守雄、飯島澄男
- 3P-33 mmスケールの垂直配向SWNT成長条件と高速成長機構 211
○長谷川馨、野田優、杉目恒志、笥和憲、張正宜、丸山茂夫、山口由岐夫
- 3P-34 触媒パターンを用いたサファイア表面上での配向SWNTの成長メカニズムの検討 212
○吾郷浩樹、石神直樹、大堂良太、辻正治、生田竜也、高橋厚史
- 3P-35 3C-SiC (111)表面からのCNT生成初期段階の第一原理分子起動力学法による研究 213
○森分博紀、平山司、楠美智子

内包ナノチューブ・ナノ炭素粒子

- 3P-36 カーボンナノチューブ・MgB₂ナノチューブ複合系の設計 214
○斎藤晋
- 3P-37 フラレン内包による単層カーボンナノチューブの光学的バンドギャップ変調 215
○岡崎俊也、大窪清吾、中西毅、斎藤毅、大谷実、岡田晋、坂東俊治、飯島澄男
- 3P-38 磁気および光応答性ナノダイヤモンド 216
○小松直樹、森田将史、瀧本竜哉、木村隆英、犬伏俊郎

その他

- 3P-39 SiCナノチューブとSiC系複合ナノチューブの作製と微細組織観察 217
○田口富嗣、井川直樹、山本博之、社本真一
- 3P-40 円錐形キャビティ一列を有する垂直配向カーボンナノファイバーの成長における温度の影響 218
○丹後佑太、小塩明、鈴木健太郎、山崎貴之、小海文夫
- 3P-41 放射状単層カーボンナノチューブを補強材としたゴムの調製と特性 219
○佐藤義倫、長谷川研二、伊藤信幸、本宮憲一、バラチャンドラン ジャヤデワン、田路和幸
- 3P-42 カラム分離したDNA/カーボンナノチューブの安定性 220
○野口悠一、藤ヶ谷剛彦、新留康郎、中嶋直敏
- 3P-43 印刷型フィールドエミッタに向けたカーボンナノツイストペーストの調製 221
○細川雄治、横田真志、滝川浩史、伊藤茂生、山浦辰雄、三浦光治、吉川和男、伊奈孝
- 3P-44 カーボンナノウォールの微細構造解析 222
○小林健一、谷村誠、中井宏、吉村昭彦、吉村博史、小島謙一、橋勝
- 3P-45 TEM-STM複合型顕微鏡法によるカーボン原子状ワイヤーの原子直視観察 223
○安坂幸師、奥村 健介、中原仁、齋藤弥八
- 3P-46 ポリイミド・カーボンナノチューブ複合体 224
○藤ヶ谷剛彦、岡本稔、友清亮輔、中嶋直敏
- 3P-47 グラフェン薄膜へのスピン注入 225
○大石恵、白石誠司、野内亮、野崎隆行、新庄輝也、鈴木義茂

July 11th, Wed.

Special Lecture: 25 min (Presentation) + 5 min (Discussion)

General Lecture: 10 min (Presentation) + 5 min (Discussion)

Poster Preview: 1 min (Presentation), No Discussion

Special Lecture (9:00-9:30)

- 1S-1 Carbon nanotubes research at AIST/Research Center for Advanced Carbon Materials: From basic to industrial applications 27
Sumio Iijima

General Lecture (9:30-10:30)

Properties of Nanotubes

- 1-1 Environmental Effect of Single-Walled Carbon Nanotubes 33
○Yuhei Miyauchi, Riichiro Saito, Kentaro Sato, Yutaka Ohno, Shinya Iwasaki, Takashi Mizutani, Jie Jiang, Shigeo Maruyama
- 1-2 Crystal Face Dependence of Chiralities of Aligned SWNTs on Sapphire 34
○Naoki Ishigami, Hiroki Ago, Kenta Imamoto, Masaharu Tsuji, Konstantin Iakoubovskii, Nobutsugu Minami
- 1-3 Oxidative Reaction of Carbon Nanotubes with O₂ and O₃ 35
○Takazumi Kawai, Yoshiyuki Miyamoto
- 1-4 Structural Dependence of Raman Spectrum of Single-walled Carbon Nanotube Adsorbed on Metal Electrode 36
Norihiko Takeda, ○Kei Murakoshi

☆☆☆☆☆☆ Coffee Break (10:30-10:45) ☆☆☆☆☆☆

General Lecture (10:45-12:00)

Properties of Nanotubes

- 1-5 Field-Effect Doping in Carbon Nanotubes 37
○Kazuyuki Uchida, Susumu Okada
- 1-6 Variable Range Hopping Conduction in Boron doped MWNT Assembly 38
○Shunji Bandow, Shigenori Numao, Sumio Iijima
- 1-7 Electronic Structure of Boron-doped Carbon Nanotube 39
○Takashi Koretsune, Susumu Saito
- 1-8 Chirality dependence and excitonic effect of optical transition of single wall carbon nanotubes 40
○Kentaro Sato, Riichiro Saito, Jie Jiang, Gene Dresselhaus, Mildred S. Dresselhaus
- 1-9 Band-Gap Tuning of an Individual Single-Walled Carbon Nanotube with Uniaxial Strain 41
○Hideyuki Maki, Testuya Sato, Koji Ishibashi

☆☆☆☆☆☆ Lunch Time (12:00-13:00) ☆☆☆☆☆☆

Special Lecture (13:00-13:30)

- 1S-2 HRTEM Imaging of the Doped Single-walled Carbon Nanotubes and Fullerene Nanopeapods 28
Lunhui GUAN

General Lecture (13:30-14:30)

Formation and Purification of Nanotubes

- 1-10 A growth model for single walled carbon nanotubes-Why near armchair structure is so special- 42
○Yohji Achiba
- 1-11 Study of Carbon Transmitting Method for Growth of Carbon Nanotubes 43
○Takeshi Hikata, Kazuhiko Hayashi, Tomoyuki Mizukoshi, Yoshiaki Sakurai, Itsuo Ishigami, Takaaki Aoki, Toshio Seki, Jiro Matsuo
- 1-12 Synthesis of single-wall carbon nanotubes from diesel soot 44
○Takashi Uchida, Tachibana Masaru, Kojima Kenichi
- 1-13 Are Catalyst Free SWNT Forests Free From Impurities ? Existence of Graphitic Carbonaceous Impurities 45
○Satoshi Yasuda, Tatsuki Hiraoka, Don N. Futaba, Motoo Yumura, Sumio Iijima, Kenji Hata

☆☆☆☆☆☆ Coffee Break (14:30-14:45) ☆☆☆☆☆☆

July 11th, Wed.

General Lecture (14:45-16:00)

Formation and Purification of Nanotubes

1-14	Combinatorial Control of Catalyst for Basics and Applications of Carbon Nanotube Growth ○Suguru Noda, Hisashi Sugime, Kei Hasegawa, Kazunori Kakehi, Shigeo Maruyama, Yukio Yamaguchi	46
1-15	<i>In-situ</i> Raman observation of single-wall carbon nanotube growth by CVD using Co-filled apoferritin catalyst ○Takashi Uchida, Masaya Tazawa, Akira Yamazaki, Yoshihiro Kobayashi	47
1-16	Size control of catalyst nanoparticles for carbon nanotube growth by gas-phase catalytic chemical vapor deposition ○Kenji Ohara, Yoichiro Neo, Hidenori Mimura, Yoku Inoue, Akihiro Ishida	48
1-17	Low-temperature growth of double and single-walled carbon nanotubes on a substrate using catalyst nanoparticles size-classified with an impactor ○Daiyu Kondo, Shintaro Sato, Yoshitaka Yamaguchi, Taisuke Iwai, Yuji Awano	49
1-18	Observation of catalyst in a CVD growth process of single-walled carbon nanotubes on SiO ₂ ○Toshiya Murakami, Yuki Hasebe, Kenji Kisoda, Koji Nishio, Toshiyuki Isshiki, Hiroshi Harima	50

Poster Preview (16:00-17:00)

Poster Session (17:00-18:30)

Chemistry of Fullerenes

1P-1	Novel Magnetic Field Effects and Time-Resolved EPR Spectra of Biradicals from Photoinduced Intramolecular Electron Transfer Reactions in Phenothiazine-C ₆₀ Linked Compounds ○Hiroaki Yonemura, Shinya Moribe, Yuya Wakita, Sunao Yamada, Yoshihisa Fujiwara, Yoshifumi Tanimoto	79
1P-2	Kinetic Study of Antioxidant Activity of Water-soluble [60]Fullerene and [60]Fullerene Epoxide by beta-Carotene Bleaching Assay ○Ken Kokubo, Tadashi Goto, Kyoko Togaya, Hisae Aoshima, Takumi Oshima	80
1P-3	Kinetic Control of Interfacial Energy in Carbon/Epoxy Composites by using Fullerenes Yusuke Tajima, ○Daisuke Yamazaki, Takanori Matsuura, Youhei Numata, Hiroaki Kawamura, Hiroki Osedo	81
1P-4	Temperature Dependence of Conductivity of Crystalline C ₆₀ and C ₇₀ Pellets Gou Kawano, ○Tsuyosi Takakura, Tsuyosi Takase, Hidetsugu Nakamura, Yong Sun	82
1P-5	Cyclic Dimers of Iridium Porphyrins - Extraordinary High Affinities toward Fullerenes ○Makoto YANAGISAWA, Kentaro TASHIRO, Takuzo AIDA	83
1P-6	Control of Selectivity in Addition-Cyclization of Chloramine-T to C ₆₀ ○Ryoji Tsuruoka, Satoshi Minakata, Mitsuo Komatsu	84
1P-7	Efficient synthesis of fullereneols by mechanochemical reaction of C ₆₀ with H ₂ O under O ₂ atmosphere ○Yuichi Ishiyama, Hiroto Watanabe, Senna Mamoru	85
1P-8	NMR Studies of Molecular Hydrogen Encapsulated in Dianions of Fullerene C ₆₀ and Open-Cage C ₆₀ Derivatives ○Michihisa Murata, Yuta Ochi, Fumiyuki Tanabe, Yasujiro Murata, Koichi Komatsu	86
1P-9	Highly soluble fullerene derivative and its production process development ○Masahiko Hashiguchi, Eiji Dejima, Tomomi Yano, Katsutomo Tanaka	87
1P-10	Synthesis of Various Amino-Functionalized [60]Fullerene Derivative via Nitrofullerene ○MASARU SEKIDO, MASATOMI OHNO	88

Metallofullerenes

1P-11	Ultraviolet Photoelectron Spectroscopy of Lu-encapsulated Metallofullerenes ○Takafumi Miyazaki, Masayuki Kato, Konosuke Furukawa, Ryohei Sumii, Hisashi Umemoto, Toshiya Okimoto, Toshiki Sugai, Hisanori Shinohara, Shojun Hino	89
1P-12	ESR Spectra of Bingel Mono-adducts of Gd@C ₈₂ ○Makoto Kanazumi, Yuji Takematsu, Takatsugu Wakahara, Takahiro Tsuchiya, Ko Furukawa, Takeshi Akasaka,	90
1P-13	Characterization of Alkali Endohedral Fullerene: The Aggregated Cluster Structure ○Hiroshi Okada, Kenji Omote, Yasuhiko Kasama, Kuniyoshi Yokoo, Shoichi Ono, Takamichi Miyazaki, Mariko Ando, Hideki Maekawa, Hideki Maekawa, Takashi Komuro, Hiromi Tobita	91
1P-14	A Reversible Crystal Structural Transformation and Structural Characterization of Pr@C ₈₂ Metallofullerene. ○Kitaura Ryo, Kitamura Yutaka, Okimoto Haruya, Nishibori Eiji, Aoyagi Shinobu, Sakata Makoto, Shinohara Hisanori	92

Fullerene Solids

1P-15	Metallic Phase in Magnesium Fullerides ○Heguri Satoshi, Kimata Nozomu, Kobayashi Mototada	93
1P-16	Superconductivity in sodium fullerenes Na_xC_{60} ○Nozomu Kimata, Satoshi Heguri, Mototada Kobayashi	94
1P-17	Molecular beam epitaxy of copper phthalocyanine on C_{60} (111) surface Hidetoshi Suzuki, Yusuke Yamashita, ○Nobuaki Kojima, Masafumi Yamaguchi	95

Formation and Purification of Nanotubes

1P-18	Sub-millimeter long single-walled carbon nanotubes synthesis by alcohol enclosed catalytic chemical vapor deposition. ○Yoshinobu Suzuki, Tomohiro Shimazu, Hisayoshi Oshima, Shigeo Maruyama	96
1P-19	Growth termination of carbon nanotubes at millimeter thickness due to structural change in catalyst. ○Shingo Morokuma, Kei Hasegawa, Suguru Noda, Shigeo Maruyama, Yukio Yamaguchi	97
1P-20	Single-Wall Carbon Nanotubes Grown from Size Controlled Rh/Pd and Co Nanoparticles by Catalyst-supported Chemical Vapor Deposition ○Keita Kobayashi, Ryo Kitaura, Yoko Kumai, Yasutomo Goto, Shinji Inagaki, Hisanori Shinohara	98
1P-21	Synthesis of small diameter SWNTs by ACCVD method using platinum as catalyst ○Keisuke Urata, Shinzo Suzuki, Hiroshi Nagasawa, Yohji Achiba	99
1P-22	Efficient growth of double-walled carbon nanotube by CVD using a mixed catalyst Fe/Co/Mo with MgO supporter ○Ryoji Naito, Toshiya Murakami, Yuki Hasebe, Kenji Kisoda, Koji Nishio, Toshiyuki Isshiki, Hiroshi Harima	100
1P-23	Purification of SWNTs fabricated by hydrogen DC arc discharge ○Beibei Chen, Tomoko Suzuki, Xinluo Zhao, Sakae Inoue, Takeshi Hashimoto, Yoshinori Ando	101
1P-24	One-step Synthesis of Aligned Carbon Nanotubes in Liquid Phase ○Kiyofumi Yamagiwa, Masafumi Mikami, Tsuneharu Takeuchi, Yoshihiro Yamaguchi, Yuriko Iwao, Morihiro	102
1P-25	Controlling diameter distribution of SWNTs by refining temperature gradient in laser ablation method ○Takashi Nakayama, Yasuhiro Tsuruoka, Sinzou Suzuki, Yohji Achiba	103
1P-26	Matching between Reaction and Catalyst Conditions in Growing VA-SWNTs by ACCVD ○Hisashi Sugime, Suguru Noda, Shigeo Maruyama, Yukio Yamaguchi	104
1P-27	Influence of residual acetylene gas on growth of brush-shaped carbon nanotubes ○Masao Yamaguchi, Lujun Pan, Seiji Akita, Yoshikazu Nakayama	105
1P-28	<i>In situ</i> photoelectron spectroscopy study of metal catalysts for carbon nanotube growth by low-pressure ethanol CVD ○Fumihiko Maeda, Satoru Suzuki, Yoshihiro Kobayashi	106
1P-29	Plan-viewed TEM observation of carbon nanotubes and catalyst particles and evaluation of catalyst activity for SWNT growth ○Yuki Hasebe, Toshiya Murakami, Kenji Kisoda, Hiroshi Harima, Koji Nishio, Toshiyuki Isshiki	107
1P-30	Discontinuous Change in Carbon Nanotubes Caused by Continuous Change in Catalyst Nominal Thickness ○Kazunori Kakehi, Suguru Noda, Shigeo Maruyama, Yukio Yamaguchi	108

Nanohorns

1P-31	Close-Open-Close Evolution of Holes in Single-Wall Carbon Nanohorns Caused by Heat Treatment ○Jing Fan, Masako Yudasaka, Jin Miyawaki, Ryota Yuge, Takazumi Kawai, Sumio Iijima	109
1P-32	Modification of cisplatin-incorporated single-wall carbon nanohorns to release cisplatin slowly ○Kumiko Ajima, Masako Yudasaka, Tatsuya Murakami, Minfang Zhang, Sumio Iijima	110
1P-33	Folate-Receptor Mediated Uptake of Single-Walled Carbon Nanohorns by Cultured Cancer Cells ○Jin Miyawaki, Tatsuya Murakami, Masako Yudasaka, Kumiko Ajima, Minfang Zhang, Hirohide Sawada, Kunihiro Tsuchida, Sumio Iijima	111
1P-34	Boron doped Nanohorn Aggregates Produced by means of Arc Discharge ○Manabu Harada, Takayuki Inagaki, Shunji Bandow, Sumio Iijima	112
1P-35	Electron microscopy study of nanohorn tip structure damaging with hydrogen peroxide treatment ○Takashi Yamaguchi, Shunji Bandow, Masako Yudasaka, Sumio Iijima	113
1P-36	Ultracentrifugal Separation of Single-wall Carbon Nanohorns ○Goshu Tamura, Shunji Bandow, Masako Yudasaka, Sumio Iijima	114

July 11th, Wed.

Properties of Nanotubes

- 1P-37** Enhancement of conductivities in boron-doped MWNTs 115
○Satoshi Ishii, Tohru Watanabe, Showgo Ogawara, Takashi Okutsu, Fumiaki Tomioka, Shinya Ueda, Shunsuke Tsuda, Takahide Yamaguchi, Yoshihiko Takano
- 1P-38** Electronic transport study of a suspended MWNT by in situ TEM 116
Yasunobu Suzuki, Koji Asaka, ○Yahachi Saito
- 1P-39** Evaluation of single wall carbon nanotubes by UV-Raman spectroscopy 117
○Hiromichi Kataura, Yasumitsu Miyata, Yutaka Maniwa, Kazuhiro Yanagi
- 1P-40** Temperature dependence of the Raman spectra of single-wall carbon nanotube and highly oriented pyrolytic graphite 118
○Norihito Kitada, Kenichi Kato, Kenichi Kojima, Masaru Tachibana
- 1P-41** Effects of doping to the G-Raman spectra of single and double-wall carbon nanotubes 119
○Eduardo B. Barros, Jin Sung Park, Georgii G. Samsonidze, Riichiro Saito, Mildred Dresselhaus
- 1P-42** Fabrication of DNA/MWNTs junctions and electrical measurements of DNA thin films 120
○Mitsutaka Ide, Masatoshi Saito, Hiroaki Kohno, Naoyoshi Murata, Junji Haruyama
- 1P-43** Meissner effect in honeycomb arrays of multi-walled carbon nanotubes 121
○Naoyoshi Murata, Junji Haruyama, Ueda Nobuteru, Masaharu Matsudaira, Yuko Yagi, Jin Nakamura, Kyouko Nozawa, Taisei Shimizu, Erik Einarsson, Syouhei Chiashi, Shigeo Maruyama, Toshiki Sugai, Naoki kishi, Hisanori Shinohara

Application of Nanotubes

- 1P-44** Chemically-Responsive Sol-Gel Transition of Supramolecular Single-Walled Carbon Nanotubes (SWNTs) Hydrogel Made by SWNTs-Cyclodextrins Hybrids 122
○Tomoki Ogoshi, Tada-aki Yamagishi, Yoshiaki Nakamoto, Akira Harada
- 1P-45** Water Soluble Single-Walled Carbon Nanotubes Using Inclusion Complex of Cyclodextrin with Guest Molecules 123
○Tomoki Ogoshi, Tada-aki Yamagishi, Yoshiaki Nakamoto, Akira Harada
- 1P-46** Fabrication of optical polarizer made of CNT/PVA composite material 124
○Satoru Shoji, Hidemasa Suzuki, Satoshi Kawata
- 1P-47** Direct electron transfer reaction of glucose oxidase with carbon nanotubes synthesized on a electrode 125
Masato TOMINAGA, ○Shinya NOMURA, Toshifumi NISHIMURA, Isao TANIGUCHI
- 1P-48** Preparation and Properties of Carbon Nanotube Films 126
○Motohiro Uo, Tsukasa Akasaka, Shigeaki Abe, Fumio Watari, Ken-ichiro Sasamori, Hisamichi Kimura, Yoshinori Sato, Kazuyuki Tohji
- 1P-49** Electric Double Layer Capacitance of the Surface Modified Fine-Crystallined Single-Walled Carbon Nanotubes 127
○Shin-ichi Ogino, Yoshinori Sato, Masaru Namura, Wataru Oizumi, Hiroyuki Kamisuki, Kenichi Motomiya, Takashi Itoh, Balachandran Jeyadevan, Kazuyuki Tohji

Miscellaneous

- 1P-50** Fabrication of Carbon Nanotubes Through Metal-free Chemical Vapor Deposition 128
○Jarrn-Horng Lin, Hui-Ling Ma, Ching-Shiun Chen, Chen-Yin Hsu, Hsiu-Wei Chen

July 12th, Thur.

Special Lecture: 25 min (Presentation) + 5 min (Discussion)

General Lecture: 10 min (Presentation) + 5 min (Discussion)

Poster Preview: 1 min (Presentation), No Discussion

Special Lecture (9:00-9:30)

- 2S-1 Precision Control of Hybridization of Nanocarbon and Metalloporphyrins 29
Kentaro Tashiro

General Lecture (9:30-10:30)

Metallofullerenes

- 2-1 Crystal Structures of $(M_2C_2@C_{82})(C_6H_5CH_3)$ and $(M_2C_2@C_{82})(C_6H_5CH_3)_2$ 51
○Eiji Nishibori, Masayuki Ishihara, Ikuya Terauchi, Shinobu Aoyagi, Makoto Sakata, Masaki Takata, Takashi Inoue, Yasuhiro Ito, Hisashi Umemoto, Hiroe Moribe, Hisanori Shinohara
- 2-2 Enhanced 1.5 μ m Fluorescence from Erbium-Carbide Metallofullerenes 52
○Yasuhiro Ito, Toshiya Okazaki, Shingo Ohkubo, Masahiro Akachi, Haruya Okimoto, Yutaka Ohno, Takashi Mizutani, Tetsuya Nakamura, Ryo Kitaura, Toshiki Sugai, Hisanori Shinohara

Fullerene Formation

- 2-3 Titan satellite has been a carbon-cluster factory? -From collisional explosion experiment- 53
○Tetsu Mieno, Sunao Hasegawa
- 2-4 Photo-Induced Charge-Separation of Supramolecular SWNT-Fullerene Hybrids in Polar Solvent 54
○Osamu Ito, Yasuyuki Araki, Atula Sandanayaka, Rughu Chitta, Francis D'Souza

☆☆☆☆☆☆ Coffee Break (10:30-10:45) ☆☆☆☆☆☆

General Lecture (10:45-12:00)

Lecture by Candidates for the Iijima Award

- 2-5 Optical Enrichment of SWNTs 55
○Xiaobin Peng, Naoki Komatsu, Takahide Kimura, Atsuhiko Osuka
- 2-6 Transparent Carbon Nanotubes for Encapsulated Dyes 56
○Yanagi Kazuhiro, Miyata Yasumitsu, Kataura Hiromichi
- 2-7 Imaging of single alkyl chains in carbon nanotubes by transmission electron microscopy 57
○Masanori Koshino, Takatsugu Tanaka, Niclas Solin, Kazutomo Suenaga, Hiroyuki Isobe, Eiichi Nakamura
- 2-8 Fabrication of ZnPc-Nanohorn-Protein Nanohybrid for Photodynamic Therapy 58
○Minfang Zhang, Masako Yudasaka, Kumiko Ajima, Jin Miyawaki, Sumio Iijima
- 2-9 Carbon Nanotube Growth from Semiconductor Nanoparticles 59
○Takagi Daisuke, Hibino Hiroki, Suzuki Satoru, Kobayashi Yoshihiro, Homma Yoshikazu

☆☆☆☆☆☆ Lunch Time (12:00-13:00) ☆☆☆☆☆☆

General Meeting (13:00-13:15)

Special Lecture (13:15-13:45)

- 2S-2 Synthesis of Alkali Endohedral Fullerenes ($Li@C_{60}$) 30
○Kenji Omote, Yasuhiko Kasama

General Lecture (13:45-14:30)

Lecture by Candidates for the Osawa Award

- 2-10 Ion Mobility Measurement with a Newly Developed Pulsed Ion Valve 60
○Toshiki Sugai, Hisanori Shinohara
- 2-11 HRTEM observation of an Individual C_{60} Fullerene Molecule and its Deformation Process 61
○Zheng liu, Kazu Suenaga, Ales Mrzel, Hiromichi Kataura, Sumio Iijima
- 2-12 Positional Control of Encapsulated Metal Atoms Inside a Fullerene Cage by Exohedral Chemical Functionalization 62
○Michio Yamada, Chika Someya, Takatsugu Wakahara, Takahiro Tsuchiya, Takeshi Akasaka, Yutaka Maeda, Kenji Yoza, Naomi Mizorogi, Shigeru Nagase

July 12th, Thur.

☆☆☆☆☆ Coffee Break (14:30-14:45) ☆☆☆☆☆

General Lecture (14:45-15:45)

Chemistry of Fullerenes and Fullerene Solids

- 2-P-13 Syntheses, Structures and Optical Properties of Dodeca- and Trideca(organo)[60]fullerene 63
○Takeshi Fujita, Yutaka Matsuo, Eiichi Nakamura
- 2-P-14 Low-dimensional Columnar Alignment of C₆₀ Fulleride Single Crystals Stabilized by Triarylmethane Dye Cations 64
○Moriyama Hiroshi, Sugiura Takahito
- 2-P-15 C₆₀ thin film field-effect transistor devices with gold electrodes modified by various types of alkanethiols 65
○Yohei Ohta, Naoko Kawasaki, Takayuki Nagano, Akihiko Fujiwara, Yoshihiro Kubozono
- 2-P-16 preparation and characterization of C₆₀ and C₇₀ fibrillar super structures and its polymerization by gamma-ray irradiation 66
○Sudip Malik, Norifumi Fujita, Seiji Shinkai

Poster Preview (15:45-16:45)

Poster Session (16:45-18:15)

Fullerene Formation

- 2P-1 Current-induced forces on adatoms on metallic and semiconducting carbon nanotubes 129
○Yvan Girard, Takahiro Yamamoto, Kazuyuki Watanabe
- 2P-2 Formation Process of Fullerenes 130
○Yusuke Ueno, Susumu Saito

Chemistry of Fullerenes

- 2P-3 Effects of Magnetic Processing on Morphological, Electrochemical, and Photoelectrochemical Properties of Electrodes Modified with Mixed Nanoclusters of C₆₀-Phenothiazine System 131
○Yuya Wakita, Hiroaki Yonemura, Norihiro Kuroda, Sunao Yamada, Yoshihisa Fujiwara, Yoshifumi Tanimoto
- 2P-4 Synthesis and Electrochemical Property of [70]fullerene derivatives 132
○Takahiko Ichiki, Yutaka Matsuo, Eiichi Nakamura
- 2P-5 Degradation Kinetics of Poly(methyl methacrylate) with fullerenes 133
○Tomohito Terada, Takanori Matsuura, Takeo Sasaki, Yusuke Tajima
- 2P-6 Synthesis and Electrochemical Properties of Indolino-[60]Fullerene 134
○Junichi Kawashima, Takumi Hara, Takanori Matsuura, Youhei Numata, Yusuke Tajima

Metallofullerenes

- 2P-7 Solid State ⁴⁵Sc- and ¹³C-NMR of Sc₂C₂@C₈₂ Carbide Metallofullerene 135
○Haruya Okimoto, Wilhelm Hemme, Yasuhiro Ito, Helmut Eckert, Hisanori Shinohara
- 2P-8 Structure and Vibronic Interaction of M@C₇₄ 136
○Tohru Sato, Yasutaka Kuzumoto, Ken Tokunga, Hiroshi Imahori, Kazuyoshi Tanaka
- 2P-9 Chemical Functionalization of Li@C₆₀ by Its Reaction with spiro[3-Adamantane-2,3'-3H-Diazirine] 137
○Shinsuke Ishikawa, Takashi Komuro, Hiroshi Okada, Kenji Omote, Yasuhiko Kasama, Kuniyoshi Yokoo, Shoichi Ono, Hiromi Tobita
- 2P-10 Structure and Electronic Property of Sc@C₈₂ 138
○Makoto Hachiya, Yuko Iiduka, Takatsugu Wakahara, Takahiro Tsuchiya, Yutaka Maeda, Takeshi Akasaka, Naomi Mizorogi, Shigeru Nagase
- 2P-11 Missing Metallofullerene: La@C_{2n} 139
○Hidefumi NIKAWA, Takashi KIKUCHI, Tomoya YAMADA, Takatsugu WAKAHARA, Tsukasa NAKAHODO, G. M. Aminur RAHAMAN, Takahiro TSUCHIYA, Yutaka MAEDA, Takeshi AKASAKA, Kenji YOZA, Ernst HORN, Kazunori YAMAMOTO, Naomi MIZOROGI, Zdenek Slanina, Shigeru NAGASE

Fullerene Solids

- 2P-12 Internal Friction Measurement of Fullerene Films by Vibrating Reed Method 140
○Shinya Wakita, Shuichi Matsumoto, Takamori Yoshii, Kenta Kirimoto, Yong Sun
- 2P-13 Solution-Processed Organic Thin-Film Transistors Based on Perfluoroalkyl Substituted C₆₀ Derivatives 141
○Masayuki Chikamatsu, Atsushi Itakura, Yuji Yoshida, Reiko Azumi, Kiyoshi Yase

July 12th, Thur.

2P-14	A DFT study on Fullerene Hydrides C ₆₀ H ₂ : Hole Transport Materials	142
	○Ken Tokunaga, Shigekazu Ohmori, Hiroshi Kawabata, Kazumi Matsushige	
2P-15	Polymerization of pressed powder and solution-grown fullerene with free electron laser irradiation	143
	○Iwata Nobuyuki, Andou Shingo, Iio Yasunari, Nokariya Ryou, Yamamoto Hiroshi	
2P-16	Electrical Properties of Mg-doped C ₆₀ Thin Films	144
	○Nobuaki Kojima, Takashi Terayama, Hidetoshi Suzuki, Masato Natori, Masafumi Yamaguchi	
2P-17	Physical Properties of H ₂ Endohedral C ₆₀	145
	○Katsumi Tanigaki, Takeshi Rachi, Ryotaro Kumashiro, Yasujiro Murata, Koichi Komatsu, Toru Kakiuchi, Hiroshi Sawa, Yoshimitsu Kohama, Satoru Izumisawa, Hitoshi Kawaji, Toru Atake	

Carbon Nanoparticles

2P-18	Preparation of carbon nanoparticles by biomolecules carbonization	146
	Masato TOMINAGA, ○Katsuya MIYAHARA, Shinya NOMURA, Isao TANIGUCHI	
2P-19	Influence of Electronic Excitation upon High-Speed Ion Irradiation on Graphene Sheet	147
	○Yoshiyuki Miyamoto, Arkady Krasheninnikov, David Tomanek	
2P-20	Laser Induced Emission of Polyynes	148
	○Tomonari Wakabayashi, Hiroyuki Nagayama, Kota Daigoku, Yosuke Kiyooka, Kenro Hashimoto	
2P-21	Fabrication of C ₆₀ Fullerene - Ethylenediamine Nanoparticles and Their Photoelectrochemical Application	149
	Ken-ichi Matsuoka, Hidetaka Seo, ○Tsuyoshi Akiyama, Sunao Yamada	
2P-22	Formation of Polyhedral Graphite Particles by High-density Carbon Arc Discharge	150
	○Yoji katagiri, Akira Koshio, Junpei Mabuchi, Fumio Kokai	
2P-23	Energetics of Nanographite: Edge Geometries and Electronic Structure	151
	○Susumu Okada	

Endohedral Nanotubes

2P-24	Energetics of C ₆₀ Encapsulated in Carbon Nanotubes	152
	○Susumu Okada	
2P-25	Effective Formation of Carbon Nanotubes Filled Perfectly with Copper Nanowire	153
	○Naoki Mizuno, Akira Koshio, Hironobu Kito, Fumio Kokai	
2P-26	Synthesis, characterization and electrical transport properties of fullerenes and heterofullerene peapods	154
	○Yongfeng Li, Toshiro Kaneko, Syohei Nishigaki, Rikizo Hatakeyama, Kenji Omote, Yasuhiko Kasama	
2P-27	¹ H NMR Study of CH ₄ confined inside Single-Wall Carbon Nanotubes	155
	Tomoyuki Hirotsu, ○Kazuyuki Matsuda, Takayuki Ganko, Hiroaki Kadowaki, Yutaka Maniwa, Hiromichi Kataura	
2P-28	Synthesis of metal-filled carbon nanotubes on anodic aluminum oxide substrate by microwave plasma-enhanced chemical vapor deposition	156
	○Yohei Matsuoka, Tsunahiko Naitou, Yasuhiko Hayashi, Takeshi Fujita, Masaki Tanamura, Tetsuo Soga	

Formation and Purification of Nanotubes

2P-29	Growth mechanism of vertically aligned SWNTs by in-situ absorption measurements	157
	○Kazuaki Ogura, Masayuki Kadowaki, Jun Okawa, Erik Einarsson, Shigeo Maruyama	
2P-30	Growth of ultra long carbon nanotube and carbon nanotube coating	158
	○Kazuyuki Kakihata, Yusaku Hirono, Toshinori Horie, Yoku Inoue, Akihiro Ishida, Hidenori Mimura	
2P-31	Ultrasonication Effects on Debundling and Cutting of Single-Walled Carbon Nanotubes dispersed in Aqueous Solution	159
	○Isamu Tajima, Catalin Romeo Luclescu, Yoshie Suzuki, Katsumi Uchida, Tadahiro Ishii, Hirofumi Yajima	
2P-32	Gold-filled apoferritin catalyst for aligned single-walled carbon nanotube growth on sapphire substrates	160
	○Akira Yamazaki, Daisuke Takagi, Yasuyuki Otsuka, Satoru Suzuki, Yoshikazu Homma, Hideyuki Yoshimura, Yoshihiro Kobayashi	
2P-33	Growth of branched carbon nanotubes by alcohol chemical vapor deposition (3) -Difference in CNTs growth by Co/Mo molar ratio-	161
	○Masayuki Maekawa, Yoshiyuki Suda, Hirotake Sugawara, Yosuke Sakai	
2P-34	Synthesis of multiwalled carbon nanocoils using catalyst of Fe-Sn	162
	○Ryo Kanada, Lujun Pan, Seiji Akita, Kaori Hirahara, Yoshikazu Nakayama	

Nanohorns

2P-35	SWNH-Streptavidin: an Effective Anticancer Drug Delivery System	163
	○Xu Jianxun, Masako Yudasaka, Minfang Zhang, Sumio Iijima	

July 12th, Thur.

- 2P-36 Near-Infrared Laser-Triggered Carbon Nanohorns for Selective Elimination of Various Microorganisms 164
○Eijiro Miyako, Hideya Nagata, Ken Hirano, Yoji Makita, Ken-ichi Nakayama, Takahiro Hirotsu

Properties of Nanotubes

- 2P-37 Resonance Raman Study of Nanopeapod-Derived Double-Walled Carbon Nanotubes 165
○Soon-Kil Joung, Toshiya Okazaki, Naoki Kishi, Zujin Shi, Sumio Iijima
- 2P-38 Composites of Single-Walled Carbon Nanotubes and Poly(*p*-Phenylene-1,2-Vinylene) with Structural Defect of *p*-Phenylene-1,1-Vinylidene Units in the Main Chain 166
○Naoki Kadota, Tomokazu Umeyama, Noriyasu Tezuka, Yoshihiro Matano, Hiroshi Imahori
- 2P-39 Gas adsorption in water-SWCNTs 167
○Haruka Kyakuno, Syunsuke Ogasawara, Toshihide Hibi, Yasumitsu Miyata, Kazuyuki Matsuda, Hiroaki Kadowaki, Shinzo Suzuki, Yohji Achiba, Hiromichi Kataura, Takeshi Saito, Satoshi Ohsima, Morio Yumura, Sumio Iijima, Yutaka Maniwa
- 2P-40 High-pressure and high-temperature treatments of double-walled carbon nanotubes 168
○Kanamori Yusuke, Kawasaki Shinji, Iwai Yuki, Iwata Atsushi, Muramatsu Hiroyuki, Hayashi Takuya, Kim Yoong-Ahm, Endo Morinobu
- 2P-41 Near-IR Absorption and Photoluminescence Spectral Properties of Carbon Nanotubes Dissolved in RNA Aqueous Solutions 169
○Nobuo Wakamatsu, Yuichi Noguchi, Tsuyohiko Fujigaya, Naotoshi Nakashima
- 2P-42 Observation and Characterization of SWNT-DNA Hybrids by Electric Force Microscopy 170
○Yuki Asada, Shota Kuwahara, Toshiki Sugai, Ryo Kitaura, Hisanori Shinohara
- 2P-43 Defect Detection in Carbon Nanotubes by Electrostatic Force Microscopy 171
○Yuki Okigawa, Takeo Umesaka, Yutaka Ohno, Shigeru Kishimoto, Takashi Mizutani

Application of Nanotubes

- 2P-44 Fabrication of logic circuits using solution-processed single-walled carbon nanotube transistors 172
○Haruo Tomita, Akio Ogura, Hiromichi Kataura, Ryou Nouchi, Masashi Shiraishi
- 2P-45 Biocompatibility of Carbon Nanosubstances in the Subcutaneous Tissue 173
○Eri Hirata, Atsuro Yokoyama, Yoshinori Sato, Yoshinobu Nodasaka, Motohiro Uo, Tsukasa Akasaka, Kazuyuki Tohji, Fumio Watari
- 2P-46 Electron Transport Study of Horizontally-Aligned SWNTs on Sapphire 174
○Tomoko Suzuki, Hiroki Ago, Naoki Ishigami, Masaharu Tsuji, Tatsuya Ikuta, Koji Takahashi
- 2P-47 Effects of Chemical Oxidation on the Physicochemical Properties of Double-Walled Carbon Nanotubes 175
○Noriko Maeda, Katsumi Uchida, Tadahiro Ishii, Hirofumi Yajima

Miscellaneous

- 2P-48 Phonon wavepacket dynamics simulation on graphene nanoribbon junctions 176
○Toru Takahashi, Takahiro Yamamoto, Kazuyuki Watanabe
- 2P-49 Novel Ionic Gelator as an Amphiphilic Dispersant for Single-Walled Carbon Nanotube 177
○Masaru Yoshida, Nagatoshi Koumura, Yoshihiro Misawa, Nobuyuki Tamaoki, Hajime Matsumoto, Said Kazaoui, Nobutsugu Minami
- 2P-50 Solidification of Lanthanum Carbide-Encapsulating Carbon Nanocapsules 178
○Ipppei Waki, Yoshinori Sato, Masaru Namura, Kenichi Motomiya, Balachandran Jeyadevan, Akira Okubo, Hisamichi Kimura, Kazuyuki Tohji

July 13th, Fri.

Special Lecture: 25 min (Presentation) + 5 min (Discussion)
General Lecture: 10 min (Presentation) + 5 min (Discussion)
Poster Preview: 1 min (Presentation), No Discussion

Special Lecture (9:00-9:30)

- 3S-1 Development of Carbon/Metal Oxide Nanocomposite Electrode Materials 31
○Isamu Moriguchi, Hirotooshi Yamada

General Lecture (9:30-10:30)

Nanohorns and Endohedral Nanotubes

- 3-1 Raman Spectroscopic Study of Polyynes Peopods 67
○Tomonari Wakabayashi, Daisuke Nishide, Hiromichi Kataura, Yohji Achiba, Hisanori Shinohara
3-2 Single electron injection into C₆₀-encapsulated carbon nano-peapod quantum dots 68
○J. Haruyama, J. Mizubayashi, I. Takesue, T. Okazaki, H. Shinohara, Y. Harada, Y. Awano
3-3 Preparation of subnanometer-sized Pt particles using single-wall carbon nanohorns 69
○Ryota Yuge, Masako Yudasaka, Minfang Zhang, Tsutomu Yoshitake, Sumio Iijima

Application of Nanotubes

- 3-4 Non-volatile Memory using SWCNT Encapsulating Fullerene 70
○Hiroshi Suga, Kazuhiro Yanagi, Masayo Horikawa, Hiromichi Kataura, Tetsuo Shimizu, Yasuhisa Naitoh

☆☆☆☆☆☆ Coffee Break (10:30-10:45) ☆☆☆☆☆☆

General Lecture (10:45-12:00)

Application of Nanotubes

- 3-5 Atomically-resolved field emission image of aluminum clusters deposited on carbon nanotubes 71
Tomohiro Matsukawa, Tetsuya Yamashita, Koji Asaka, Hitoshi Nakahara, ○Yahachi Saito
3-6 Porphyrin-Modified Single-Walled Carbon Nanotubes for Photoelectrochemical Devices 72
○Tomokazu Umeyama, Mitsuru Fujita, Noriyasu Tezuka, Naoki Kadota, Yoshihiro Matano, Hiroshi Imahori
3-7 Electrical and Optical Gas Sensing Using Nanoscopically Dispersed Carbon Nanotube Networks 73
○Nobutsugu Minami, Annamalai Karthigeyan, Konstantin Iakoubovskii
3-8 Super-Growth Single-Walled Carbon Nanotube Electrochemical Capacitors 74
○Ali Izadi-Najafabadi, Kenji Hata, Tatsuki Hiraoka, Takeo Yamada, Don N. Futaba, Satoshi Yasuda, Osamu Kimizuka, Osamu Tanaike, Hiroaki Hatori, Motoo Yumura, Sumio Iijima
3-9 Ink-jet Printing of Carbon Nanotube Film Transistors 75
○Taishi Takenobu, Noriko Miura, Takeshi Asano, Tomohiro Fukao, Masashi Shiraishi, Yoshihiro Iwasa

☆☆☆☆☆☆ Lunch Time (11:45-13:00) ☆☆☆☆☆☆

Special Lecture (13:00-13:30)

- 3S-2 Characteristics of Multi-Channel Carbon Nanotube Transistors 32
Fumiyuki Nihey

General Lecture (13:30-14:00)

Carbon Nanoparticles and Miscellaneous

- 3-10 Formation of Water-Dispersible Nanotubular Graphitic Assembly 76
○Wusong JIN, Guanxin ZHANG, Takanori FUKUSHIMA, Takuzo AIDA
3-11 Structure of Vertically Aligned Carbon Nanofibers Containing Conical Cavity Array: One-dimensional Array of Graphitic Cones 77
○Akira Koshio, Yuta Tango, Takayuki Yamasaki, Kentaro Suzuki, Fumio Kokai

Poster Preview (14:00-15:00)

Poster Session (15:00-16:30)

July 13th, Fri.

Application of Nanotubes

3P-1	Reinforcement of Epoxy Composite Sheets by Highly Oriented, Highly-Loaded Single-Walled Carbon Nanotubes ○Hidekazu Nishino, Tatsuki Hiraoka, Takeo Yamada, Don N. Futaba, Kenji Hata	179
3P-2	DNA-assisted fixation and patterning of carbon nanotubes on glass substrate ○Satoru Shoji, Jun-ichi Jono, Satoshi Kawata	180
3P-3	Temperature Effects on the Optical Properties of SWNTs Dispersed in Aqueous Solutions ○Akina Tanemura, Catalin Romeo Luculescu, Katsumi Uchida, Tadahiro Ishii, Hirofumi Yajima	181
3P-4	Ion beam modification of CNTs/chitosan composite film For cell attachment control ○Rumi Shizume, Katsumune Takahashi, Katsumi Uchida, Yoshiaki Suzuki, Hirofumi Yajima	182
3P-5	Metal vapor deposition onto vertically aligned single-walled carbon nanotubes and bonding to metal surfaces ○Makoto Watanabe, Kazuaki Ogura, Kei Ishikawa, Jun Ookawa, Erik Einarsson, Shigeo Maruyama	183
3P-6	Dependence of the isolation of SWNTs by DNA wrapping on their diameter ○Sho Toita, Dongchul Kang, Kenichi Kojima, Masaru Tachibana	184
3P-7	Stable Dispersion of Single-Wall Carbon Nanotubes by a Protein ○Takeshi Tanaka, Hehua Jin, Tadayuki Imanaka, Shinsuke Fujiwara, Hiromichi Kataura	185
3P-8	Solubilization of Carbon Nanotubes by Using meso-meso Linked Zn(II) porphyrin ○Kenchi Watanabe, Tsuyohiko Fujigaya, Naotoshi Nakashima	186
3P-9	Field Effect Chromatography that Separates Metallic and Semiconducting Carbon Nanotubes ○Masahito Sano, Keisuke Wada	187
3P-10	Separation of Metallic Single-walled Carbon Nanotubes and Preparation of Transparent and Conductive Thin Films from the Nanotubes ○Yutaka Maeda, Masahiro Hashimoto, Tadashi Hasegawa, Makoto Kanda, Takahiro Tsuchiya, Takatsugu Wakahara, Takeshi Akasaka, Said Kazaoui, Nobutsugu Minami, Shigeo Maruyama, Shigeru Nagase	188
3P-11	Characterization of SWNT Thin Films Deposited by Dry-Process ○Takeshi Saito, Satoshi Ohshima, Shigekazu Ohmori, Motoo Yumura, Sumio Iijima	189
3P-12	Damage-free Surface Modification of Carbon Nanotubes using Advanced Neutral Beam ○Akira Wada, Yoshinori Sato, Masahiko Ishida, Fumiyuki Nihey, Kazuyuki Tohji, Seiji Samukawa	190
3P-13	The New Feature Development of Carbon Nanotubes-Polybenzimidazole Composite ○Minoru Okamoto, Tsuyohiko Fujigaya, Naotoshi Nakashima	191
3P-14	Teas Solution Individually Solubilizes Single-walled Carbon Nanotubes ○Genki Nakamura, Kaori Narimatsu, Naotoshi Nakashima	192

Properties of Nanotubes

3P-15	Side-wall attachment of porphyrins to the shortened and esterified carbon nanotubes ○Toru Arai, Shingo Nobukuni, Kohsuke Takahashi, Yoshikazu Shimote	193
3P-16	Simultaneous Spectroscopy of Photoluminescence and Photocurrent of Individual Carbon Nanotubes in Field-Effect Transistor ○Atsushi Kobayashi, Yutaka Ohno, Shigeru Kishimoto, Takashi Mizutani	194
3P-17	Bundle Reconstruction of Isolated Single Wall Carbon Nanotubes ○Yasumitsu Miyata, Kazuhiro Yanagi, Yutaka Maniwa, Kataura Hiromichi	195
3P-18	Length dependence of Raman intensity of the single wall carbon nanotube ○Jin Sung Park, Saito Riichiro, Kentaro Sato, Jie Jiang, Gene Dresselhaus, Mildred S. Dresselhaus	196
3P-19	Imaging Inter-layer Interaction of Double-Wall Carbon Nanotubes by UHV-STM ○Nobuyuki Fukui, Yuko Kato, Hiromichi Yoshida, Toshiki Sugai, Seiji Heike, Masaaki Fujimori, Yuji Suwa, Tomihiro Hashizume, Hisanori Shinohara	197
3P-20	In Situ Manipulation and Engineering of Carbon Nanotubes Inside a Transmission Electron Microscope ○Chuanhong JIN, Kazutomo SUENAGA, Sumio IJIMA	198
3P-21	Predominance of small bundles within vertically aligned SWNT arrays ○Erik Einarsson, Takahisa Yamamoto, Zhengyi Zhang, Yuichi Ikuhara, Shigeo Maruyama	199
3P-22	Effect of Chemical Modification for SWNTs-FET Properties ○Ryotaro Kumashiro, Yuki Abe, Takeshi Akasaka, Yutaka Maeda, Nagao Kobayashi, Katsumi Tanigaki	200
3P-23	Threshold Energy of Low-Energy Irradiation Damage in Single-Walled Carbon Nantoubes ○Satoru Suzuki, Yoshihiro Kobayashi	201
3P-24	Regulated near-IR optical properties of individually dissolved semiconducting SWNTs via redox reaction ○Kouhei Hirayama, Tsuyohiko Fujigaya, Yasuro Niidome, Naotoshi Nakashima	202
3P-25	Optical Properties of High-Purity Single Wall Carbon Nanotubes Sorted by Electronic Structure ○Yasumitsu Miyata, Kazuhiro Yanagi, Yutaka Maniwa, Hiromichi Kataura	203

3P-26	Environmental effects on photoluminescence of carbon nanotubes ○Yutaka Ohno, Shinya Iwasaki, Yoichi Murakami, Shigeru Kishimoto, Shigeo Maruyama, Takashi Mizutani	204
3P-27	Ethanol Gas Pressure Dependence of Photoluminescence from SWNTs ○Shohei Chiashi, Satoshi Watanabe, Tateki Hanashima, Yoshikazu Homma	205
Fullerene Formation		
3P-28	Synthesis of Fullerene C ₇₀ from C ₆₀ by Gaseous Carbon Insertions into CC Bonds ○Teruhiko Ogata, Tetsu Mieno, Yoshio Tatamitani	206
3P-29	Structural study of Sc ₂ C ₈₄ (II) ○Koji Nakajima, Yuko Iiduka, Takatsugu Wakahara, Takahiro Tsuchiya, Yutaka Maeda, Takeshi Akasaka, Naomi Mizorogi, Shigeru Nagase	207
Metallofullerenes		
3P-30	Reversible Reaction of La@C ₈₂ with Cyclopentadiene Derivatives ○Satoru Sato, Yutaka Maeda, Koji Inada, Tadashi Hasegawa, Michio Yamada, Takahiro Tsuchiya, Takeshi Akasaka, Tatsuhisa Kato, Naomi Mizorogi, Shigeru Nagase	208
3P-31	Optical Emission of Nitrogen Plasmas Yielding the Synthesis of Nitrogen Atom Encapsulated Fullerenes ○Shohei Nishigaki, Toshiro Kaneko, Rikizo Hatakeyama	209
Formation and Purification of Nanotubes		
3P-32	Ultrasonication Induced Structural Change of SWNTs Dispersed in the CMC Aqueous Solution ○Shigekazu Ohmori, Takeshi Saito, Satoshi Ohshima, Motoo Yumura, Sumio Iijima	210
3P-33	Growth Window and Possible Mechanism of Millimeter-Thick Single-Walled Carbon Nanotube Forests ○Kei Hasegawa, Suguru Noda, Hisashi Sugime, Kazunori Kakehi, Zhengyi Zhang, Shigeo Maruyama, Yukio Yamaguchi	211
3P-34	Growth Mechanism of Horizontally-Aligned SWNTs on Sapphire Surface Studied with Patterned Catalyst ○Hiroki Ago, Naoki Ishigami, Ryota Ohdo, Masaharu Tsuji, Tatsuya Ikuta, Koji Takahashi	212
3P-35	First-principle Molecular dynamics study on initial stage of CNT formation from 3C-SiC (111) surface ○Hiroki Moriwake, Tsukasa Hirayama, Michiko Kusunoki	213
Endohedral Nanotubes, Carbon Nanoparticles		
3P-36	Design of Carbon-MgB ₂ Hetero-Double-Walled Nanotube ○Susumu Saito	214
3P-37	Optical Bandgap Modulation of Single-Walled Carbon Nanotubes by Encapsulated Fullerenes ○Toshiya Okazaki, Shingo Okubo, Takeshi Nakanishi, Takeshi Saito, Minoru Otani, Susumu Okada, Shunji Bandow, Sumio Iijima	215
3P-38	Magnetically and Fluorescently Visualized Nanodiamond ○Naoki Komatsu, Masahito Morita, Tatsuya Takimoto, Takahide Kimura, Toshiro Inubushi	216
Miscellaneous		
3P-39	Preparation and microstructural observation of SiC nanotubes and SiC composite nanotubes; C-SiC, SiC-SiO ₂ and C-SiC-SiO ₂ coaxial nanotubes ○Tomitsugu Taguchi, Naoki Igawa, Hiroyuki Yamamoto, Shinichi Shamoto	217
3P-40	Growth Temperature Influence on Vertically Aligned Carbon Nanofibers Containing Conical Cavity Array ○Yuta Tango, Akira Koshio, Kentaro Suzuki, Takayuki Yamasaki, Fumio Kokai	218
3P-41	Preparation and properties of rubber filled with radial single-walled carbon nanotubes ○Yoshinori Sato, Kenji Hasegawa, Nobuyuki Ito, Kenichi Motomiya, Balachandran Jeyadevan, Kazuyuki	219
3P-42	Stability of DNA-dissolved Carbon Nanotubes Separated by Size-Exclusion Chromatography ○Yuichi Noguchi, Tuyohiko Fujigaya, Yasuro Niidome, Naotoshi Nakashima	220
3P-43	Preparation of Carbon Nanotwist Paste for Printing-Type Field Emitter ○Y. Hosokawa, M. Yokota, H. Takikawa, S. Itoh, T. Yamaura, K. Miura, K. Yoshikawa, T. Ina	221
3P-44	Nanostructure Analysis of Carbon Nanowalls ○Ken-ichi Kobayashi, Makoto Tanimura, Hiroshi Nakai, Akihiko Yoshimura, Hirofumi Yoshimura, Kenichi Kojima, Masaru Tachibana	222
3P-45	Atomistic structural dynamics of carbon atomic wires by TEM-STM combined microscopy ○Koji Asaka, Kensuke Okumura, Hitoshi Nakahara, Yahachi Saito	223
3P-46	Polyimide/Carbon nanotube composites ○Tsuyohiko Fujigaya, Minoru Okamoto, Ryosuke Tomokiyo, Naotoshi Nakashima	224

July 13th, Fri.

3P-47 Spin Injection into a Graphite Thin Film

○Megumi Ohishi, Masashi Shiraishi, Ryo Nouchi, Takayuki Nozaki, Teruya Shinjo, Yoshishige Suzuki

225

特別講演
Special Lecture

1S - 1 ~ 1S - 2

2S - 1 ~ 2S - 2

3S - 1 ~ 3S - 2

Carbon nanotubes research at AIST/Research Center for Advanced Carbon Materials: From basic to industrial applications

S. Iijima

*Research Center for Advanced Carbon Materials (AIST), Meijo University and NEC
1-501 Shiogamaguchi, Tenpaku, Nagoya 468-8502, Japan*

The first modern nanocarbon materials, particularly, carbon nanotubes, have reported 16 years ago. The materials attracted many researchers in the field of basic sciences and industrial applications and have initiated new fields of nanoscience and nanotechnology. Nanocarbon has started with fullerene in 1985 and its main interest has shifted toward carbon nanotubes, and in the last couple of years the new graphene science, which deals with a single sheet of flat graphite, has come out and rapidly grown. Obviously, nanocarbon materials have created rich fields of scientific excitements as well as possible industrial applications.

In this talk I would like to introduce some of research activities which have been conducted at the Research Center for Advanced Carbon Materials at AIST in Tsukuba. The Center consists of three laboratories of nanotube synthesis and applications led by K. Hata, nanotube (TEM) characterization led by K. Suenaga and nano-diamond coating led by M. Hasegawa, together with some independent research experts such as T. Okazaki and T. Saito. In recent years their activities have become visible internationally, which we have aimed at. The center's activities have been supported mostly by public agencies at substantial financial level. Because of this social background I, as the director of the center, feel some responsibilities to inform to the public on our activities and therefore I asked the organizers a time allocation for my presentation in this symposium.

For the reason mentioned above, I would like to present recent research highlights of our research center and ask your comments and opinions.

Corresponding Author : Sumio Iijima

E-mail : ijimas@ccmfs.meijo-u.ac.jp, **Tel&Fax** : +81-52-834-4001

HRTEM Imaging of Doped Single-walled Carbon Nanotubes and Fullerene Nanopeapods

Lunhui Guan^{1,2*}, Kazu Suenaga¹, Zujin Shi², Zhennan Gu² and Sumio Iijima¹

¹ *Research Center for Advanced Carbon Materials, National Institute of Advanced Industrial Science and Technology (AIST) Tsukuba, 305-8565, JAPAN*

² *College of Chemistry and Molecular Engineering, Peking University, Beijing, 100871, China*

Encapsulation of foreign materials into the hollow cavity of single-walled carbon nanotubes (SWNTs) is of scientific importance in two different viewpoints; (i) Doping SWNTs is known to significantly modify the properties of host SWNT, and (ii) the properties of guest materials can be also altered by being encapsulated. Thus, it is quite important to reveal the doping sites and structural transformation of dopant in confined nanospace.

In this talk, we report direct evidence for the doping site of alkali (*n*-type doping) and halogen (*p*-type doping) atoms in SWNTs and fullerene peapods (C₆₀@SWNTs) by means of high-resolution transmission electron microscopy (HR-TEM). The structures of iodine inside SWNT are polymorphic and quite sensitive to the diameter of the host SWNT. [1] It is proven that potassium and iodine atoms can be doped at the intermolecular sites within C₆₀ peapods.[2,3] The doped intratubular iodine atom(s) have some catalytic effect to trigger the coalescence of the C₆₀ molecules inside SWNTs, eventually inducing the transformation of C₆₀ into a tubular structure. It is also reported how the smallest SWNTs with diameter of 0.4-0.5 nm are derived from the catalytic reaction confined in SWNTs. [4, 5]

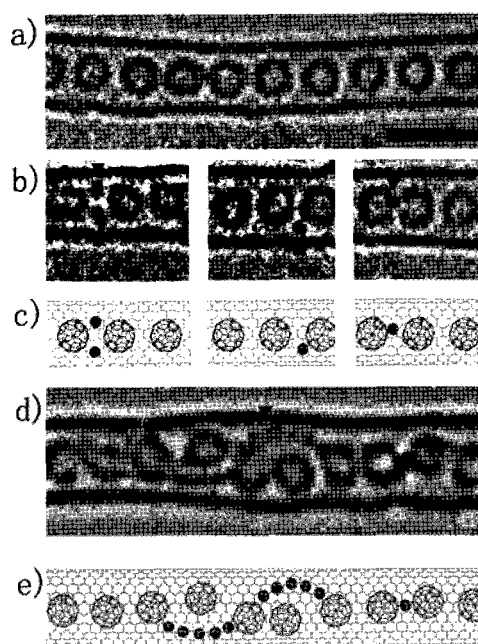


Fig.1 HRTEM images and simulated models of iodine doped C₆₀ peapods

Reference

- [1] Guan LH, Suenaga K, Shi ZJ, Gu ZN, Iijima S, *Nano letters*, ASAP
- [2] Guan LH, Suenaga K, Shi ZJ, Gu ZN, Iijima S, *Physical Review Letters*, 94, 045502 (2005)
- [3] Guan LH, Suenaga K, Shi ZJ, Gu ZN, Iijima S, Submitted.
- [4] Guan LH, Shi ZJ, Li MX, Gu ZN *Carbon*, 43, 2780-2785(2005)
- [5] Guan et al. (unpublished)

Corresponding Author: Lunhui Guan

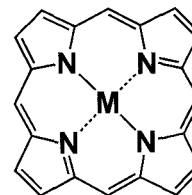
TEL: +81-29-861-5694, FAX: +81-29-861-4806, E-mail: guan-lunhui@aist.go.jp

Precision Control of Hybridization of Nanocarbon and Metalloporphyrins

Kentaro Tashiro

School of Engineering, The University of Tokyo, Tokyo 113-8656, Japan

Supramolecular interactions between fullerenes and metalloporphyrins have been found to occur in the solid state and constrained media. While the hybridization of fullerenes with such largely π -conjugated moieties is an interesting subject in molecular and materials sciences of carbon nanoclusters, there were two considerable limitations. Namely, the fullerene–metalloporphyrin interactions are generally hardly detectable in solution. On the other hand, although segregation of fullerenes and metalloporphyrins in their hybrids is necessary for the highly efficient photoelectric conversion, the two components tend to form alternating arrangements in their hybrids as the result of the donor-acceptor type interactions. Here we report our strategies to overcome these limitations and precisely control the hybridization of fullerenes with metalloporphyrins [1].



In order to obtain stable fullerene–metalloporphyrin hybrids in solution, we have designed cyclic dimers of metalloporphyrins having a π -electronic cavity for the complexation with fullerenes. The inclusion complexes composed of such metalloporphyrin hosts and fullerene guests do not dissociate even under chromatographic conditions. The binding capability of the hosts are widely tunable using the central metal ions of the porphyrin moieties, where the association constants of a cyclic dimer of methyliridium(III) porphyrin and fullerenes are one of the largest values among those for any host-guest complexation events. One of the applications of the metalloporphyrin dimers is the selective extraction of rare fullerenes and enantiomers of chiral fullerenes, which has been successfully achieved after optimizing the structures of the porphyrin framework and linker parts, together with the proper choice of the central metal ions [2].

Very recently, we have found that introduction of amphiphilicity into the molecular structure allows segregation of fullerenes and metalloporphyrins, despite of their interactions, in the fullerene–metalloporphyrin hybrid materials. A fused porphyrin Cu complex bearing alkyl and triethylene glycol chains at the periphery forms a liquid crystalline (LC) phase from -20 to 70 °C. Since an analogous hydrophobic porphyrin having alkyl chains displays LC phase with a much narrower temperature range, amphiphilic structure of the molecule should mostly restrict the orientation of the fused porphyrin moiety and stabilize the LC phase. In general, liquid crystallinity of metalloporphyrin derivatives is lost upon addition of fullerenes due to the intercalation of fullerenes between stacked metalloporphyrin moieties. In contrast, the LC phase of the fused porphyrin survives and is rather stabilized after hybridization with an alkylated fullerene. Absorption spectroscopy of the film samples of the fused porphyrin and its hybrid with the fullerene derivative demonstrated that the stacking of fused porphyrin moieties are retained in the hybrid [3].

[1] K. Tashiro and T. Aida, *Chem. Soc. Rev.*, **36**, 189 (2007).

[2] Y. Shoji, K. Tashiro, and T. Aida, *J. Am. Chem. Soc.*, **126**, 6570 (2004); *ibid.*, **128**, 10690 (2006).

[3] T. Sakurai *et al.*, in preparation.

Corresponding Author: Kentaro Tashiro

TEL: +81-3-5841-8803, FAX: +81-3-5841-7310, E-mail: tashiro@macro.t.u-tokyo.ac.jp

Synthesis of Alkali Endohedral Fullerenes (Li@C₆₀)

○Kenji Omote, Yasuhiko Kasama,
Tomohiro Konno, Hiroki Takahashi, Fuyuko Yamashita, Hiroshi Okada, Haruna Oizumi,
Kazuhiko Kawachi, Yuzo Mizobuchi, Kuniyoshi Yokoo and Shoichi Ono

Ideal Star Inc., Sendai 989-3204, Japan

Endohedral fullerenes have been energetically investigated in chemical and physical fields, because they have characteristics which empty fullerenes can't realize [1-3]. They belong to piezoelectric semiconductors and are expected to be new nano-materials of electronics for the next generation [4]. One of the characteristics comes from the nanoscale electronic polarization by a charge transfer from enclosed atoms to carbon cages. Since the technology strategy map 2006 of Ministry of Economy, Trade and Industry places this characteristic as a central agenda item, it is expected to apply to the optical memory materials with a nano-meter size, means petabyte memory [5].

Alkali endohedral fullerenes have attracted wide interests for a viewpoint of charge transfer. Campbell et al. produced Li@C₆₀ by using low energy ion implantation [6]. In EU, NICE project (Nanoscale Integrated Circuits using Endohedral Fullerenes) which produces Li@C₆₀ has taken effect for four years [7]. However, the satisfactory characterization of Li@C₆₀ has not been succeeded because of the difficulty of mass production and their purification [1,8], so that they have not been made practicable yet [4].

We have tried a new synthesis method of alkali endohedral fullerenes by getting a hint from the plasma process developed at Tohoku University [9]. In this presentation, we introduce our recent results of the mass production of Li@C₆₀ by using a Li plasma process.

- [1] H. Shinohara, *Rep. Phys. Prog. Phys.*, **63**, 843 (2000)
- [2] *Endofullerenes: A New Family of Carbon Clusters*; T. Akasaka and S. Nagase (Eds.), Kluwer Academic Publishers, 2002.
- [3] *Quarterly Fullerene: The Forefront of Science & Technology*; Dia Research Martech Inc., **1-47**, (1993-2004)
- [4] K. Omote and K. Yokoo, *NEDO Research Report: The Investigation Regarding the Predominance in Regard to Industrial Utilization of Endohedral-Fullerenes FY2006 result report*, **06002242-0-1**, 1-278 (2007)
- [5] Ministry of Economy, Trade and Industry, *Technology Strategy Map 2006*, 226 (2006)
- [6] R. Tellmann, N. Krawez, S. H. Lin, I. V. Hertel and E. E. B. Campbell, *Nature*, **382**, 408 (1996)
- [7] NMRC, University of Cambridge, University of Cothenborg and IBM Zurich, Covering Period : (2000-2004), *Final Project Report: Nanoscale Integrated Circuits using Endohedral Fullerenes*, 1-102 (2004)
- [8] T. Akasaka, *Special Lecture of the 27th Fullerene-Nanotubes General symposium*, **3S-8** (2004)
- [9] T. Hirata, R. Hatakeyama, T. Mieno and N. Sato, *J. Vac. Sci. Technol. A*, **14**, 615 (1996)

Corresponding Author: Kenji Omote

TEL: +81-22-303-7336, FAX: +81-22-303-7339, E-mail: kenji.omote@idealstar-net.com

Development of Carbon/Metal Oxide Nanocomposite Electrode Materials

○ Isamu Moriguchi, Hirotochi Yamada

*Department of Applied Chemistry, Faculty of Engineering, Nagasaki University,
Nagasaki 852-8521, Japan*

There is growing interest in electrical/electrochemical energy storage devices with both high-power and high-energy densities because of possible applications as auxiliary power sources for electric and/or hybrid-electric vehicles. The performance of conventional power sources is however not enough for the auxiliary power sources. Many studies have been made from the following approaches to develop high performance power sources;

- Improving electric double layer capacitive property by increasing surface area and controlling the porous structure of carbons
- Developing pseudocapacitor materials by modifying carbon surface with redox active materials
- Increasing power density of secondary batteries by nanostructural control of electrode materials

For all the cases, it is important to develop a nanostructured electrode that enables high-rate and high-capacitive electrochemical reactions, that is, to design and fabricate a high surface area electrode structure effective to electrochemical processes, such as ion-transport at a quasi-three-dimensional electrode interface, ion-diffusion in active material solid, electron transfer accompanied with a faradic reactions, and so on.

Here I will focus on nanoporous materials such as porous carbons and carbon/metal oxide porous composites as one of candidates of electrode materials for high power sources. Topics will be as follows;

Topic 1: Development of mesoporous and macroporous carbons as EDLC materials [1-4]

Topic 2: Development of nanoporous composites of Li-intercalation host/carbon as high rate Li-intercalation materials

(2-1) Nanoporous Li-intercalation host materials (TiO₂, LiFePO₄, Graphite) [5-9]

(2-2) Bicontinuous porous nanocomposites of Li-intercalation hosts and carbons such as SWNTs [10]

(2-3) Post-modification of the surface of porous carbons with metal oxide nanolayers [11]

- [1] H. Yamada, H. Nakamura, Y. Watanabe, I. Moriguchi, T. Kudo, *J. Phys. Chem. C*, **111**, 227 (2007).
- [2] M. Kodama, J. Yamashita, Y. Soneda, H. Hatori, K. Kamegawa, I. Moriguchi, *Chem. Lett.*, **35**, 680 (2006).
- [3] I. Moriguchi, F. Nakahara, H. Yamada, T. Kudo, *Stud. Surf. Sci. Catal.*, **156**, 589 (2005).
- [4] I. Moriguchi, F. Nakahara, H. Yamada, T. Kudo, *Electrochemical and Solid State Letters*, **7**, A221 (2004).
- [5] I. Moriguchi, R. Hidaka, H. Yamada, T. Kudo, *Solid State Ionics*, **176**, pp.2361-2366 (2005).
- [6] I. Moriguchi, Y. Shono, H. Tachikawa, H. Yamada, T. Kudo, Y. Teraoka, T. Nishimi, *Chem. Lett.*, **34**(4), 610 (2005).
- [7] H. Yamada, T. Yamato, I. Moriguchi, T. Kudo, *Solid State Ionics*, **175**, 195 (2004).
- [8] H. Yamada, T. Yamato, I. Moriguchi, T. Kudo *Chemistry Letters*, **33**(12), 1548 (2004)
- [9] I. Moriguchi, Y. Katsuki, H. Yamada, T. Kudo, T. Nishimi *Chemistry Letters*, **33**(9), 1102 (2004)
- [10] I. Moriguchi, R. Hidaka, H. Yamada, T. Kudo, H. Murakami, N. Nakashima., *Adv. Mater.*, **18**, 69 (2006).
- [11] H. Yamada, K. Tagawa, M. Komatsu, I. Moriguchi, T. Kudo, *J. Phys. Chem. C*, in press (2007).

Corresponding Author: Isamu Moriguchi

E-mail: mrgch@nagasaki-u.ac.jp

Characteristics of Multi-Channel Carbon Nanotube Transistors

Fumiyuki Nihey

*Nano Electronics Research Laboratories, NEC Corporation,
34 Miyukigaoka, Tsukuba 305-8501, Japan*

Carbon nanotubes (CNTs) are attracting much attention because of their peculiar mechanical and electrical properties. Especially, their chemical stability, mechanical flexibility, and excellent carrier mobility are suitable for the next-generation electronics. In this talk, we present three aspects of multi-channel CNT field-effect transistors (CNTFETs); high-frequency characteristics, low-temperature fabrication on plastic substrates, and yield estimation from the switching point of view.

We have developed a high density multiple-channel CNTFET structure whose output impedance is much lower than conventional single channel CNTFETs, and the de-embedding procedure that removes parasitic impedance components in measured S-parameters of small-signal devices. We have obtained a cut-off frequency over 10 GHz and maximum oscillation frequency higher than 3 GHz. These values are among the highest ever published. We also made an equivalent circuit RF model for the CNTFETs, which appeared to be consistent with the experimental results. Detailed analysis revealed that decreasing parasitic capacitances of electrodes and resistances of CNT extensions greatly improve the high-frequency performance of CNTFETs.

We have also fabricated CNT network transistors on plastic substrates. “CNT ink”, in which single-wall carbon nanotubes were dispersed in organic solvent, was spin-coated onto the plastic substrates with predefined electrodes (source, drain, and gate). The maximum process temperature can be below 100°C, which is suitable for reliable fabrication on plastic substrates. Field mobility reached 100 cm²/Vs with on/off current ratio ranging from 10 to 10³. By using these devices, we succeeded in driving organic light-emitting diodes (OLEDs).

Controlling CNT density is found to be important for achieving excellent switching property. CNTs can be metallic or semiconducting, depending on their chirality. One third of CNTs are believed to be metallic, which may degrade the switching behavior due to the creation of metallic paths between source and drain. This can be overcome by controlling CNT density. We simulated device characteristics of CNT network transistors focusing on the impact of CNT length on switching behavior. Although CNT consists of 1/3 of metallic content, we found that device yield of more than 99.9% could be obtained by reducing CNT length less than 1/5 of source-drain distance.

[1] Kaoru Narita, Hiroo Hongo, Masahiko Ishida, and Fumiyuki Nihey, *Phys. Stat. Sol. (a)* **204**, 1808 (2007).

Corresponding Author: Fumiyuki Nihey

TEL: +81-29-850-1584, FAX: +81-29-856-6139, E-mail: nihey@cd.jp.nec.com

一般講演
General Lecture

1-1 ~ 1-18

2-1 ~ 2-16

3-1 ~ 3-11

Environmental Effect of Single-Walled Carbon Nanotubes

○Yuhei Miyauchi¹, Riichiro Saito², Kentaro Sato², Yutaka Ohno³, Shinya Iwasaki³,
Takashi Mizutani³, Jie Jiang⁴, Shigeo Maruyama¹

¹*Department of Mechanical Engineering, The University of Tokyo, Tokyo 113-8656, Japan*

²*Department of Physics, Tohoku University and CREST, Sendai 980-8578, Japan*

³*Department of Quantum Engineering, Nagoya University, Nagoya 464-8603, Japan*

⁴*Center for High Performance Simulation and Department of Physics, North Carolina State University, Raleigh, North Carolina 27695-7518, USA*

Optical transition energies of single-walled carbon nanotubes (SWNTs) are affected up to 80meV by the change of environment materials around SWNTs [1], which is known as an environmental effect. Here, we have calculated the environmental effect for optical transition energies of an exciton [2] for many different (n,m) SWNTs [3]. In the calculation, we solve the Bethe-Salpeter equation within the extended tight-binding model [2] in which we adopted a polarization function for the valence π electrons and a static dielectric constant κ for the effects of the core electrons and the surrounding materials. The static dielectric constant κ used in the exciton calculation can be expressed as a harmonic average (serial connection of two capacitors) of two dielectric constants of the surrounding material κ_{env} and SWNT κ_{tube} [3], that is $1/\kappa = C_{\text{env}}/\kappa_{\text{env}} + C_{\text{tube}}/\kappa_{\text{tube}}$, where C_{env} and C_{tube} are coefficients for the outside and inside of a SWNT, respectively. In Fig.1(a), we show a schematic view for the serial connection of electric flux and how the κ is related to κ_{env} and κ_{tube} . In Fig.1(b), the shift of the experimentally observed E_{11} energy is plotted as a function of κ_{env} for different (n,m) SWNTs (left) [1] and the corresponding calculated results (right) [3]. The calculated results reproduce well the environmental effects for the experimental transition energies for various surrounding materials and for various diameters.

[1] Y. Ohno, S. Iwasaki, Y. Murakami, S. Kishimoto, S. Maruyama, T. Mizutani, arXiv:0704.1018v1 [cond-mat.mtrl-sci] (2007).

[2] J. Jiang, R. Saito, G.G. Samsonidze, A. Jorio, S.G. Chou, G. Dresselhaus, M.S. Dresselhaus, Phys. Rev. B **75**, 035407 (2007).

[3] Y. Miyauchi, R. Saito, K. Sato, Y. Ohno, S. Iwasaki, T. Mizutani, J. Jiang, S. Maruyama, Chem. Phys. Lett., in press (arXiv:0704.1380v1 [cond-mat.mtrl-sci]).

Corresponding Author: Shigeo Maruyama

TEL&FAX: +81-3-5841-6983

E-mail: maruyama@photon.t.u-tokyo.ac.jp

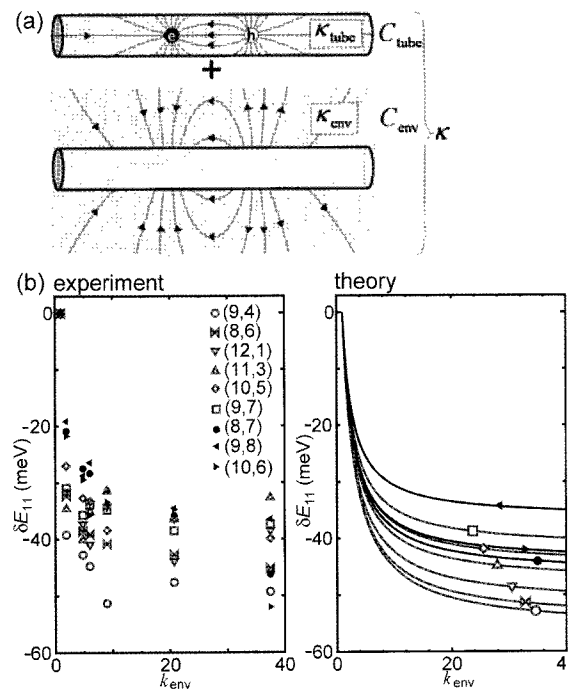


Fig.1 (a) Schematic of the connection of the dielectric constants. (b) Transition energy dependence plotted as a function of κ_{env} : (left) experiment (right) theory.

Crystal Face Dependence of Chiralities of Aligned SWNTs on Sapphire

Naoki Ishigami¹, Hiroki Ago^{*,1,2}, Kenta Imamoto¹, Masaharu Tsuji^{1,2},
Konstantin Iakoubovskii³, and Nobutsugu Minami³

¹ Graduate School of Engineering Sciences, Kyushu University, Fukuoka 816-8580, Japan

² Institute for Materials Chemistry and Engineering, Kyushu University

³ Nanotechnology Research Institute, AIST, Tsukuba 305-8565, Japan

The directional control of single-walled carbon nanotubes (SWNTs) on a substrate is one of the most important issues for fabrication of SWNT-based devices. In our previous work, we succeeded to grow horizontally-aligned SWNTs on A- and R-faces of sapphire substrates [1]. The influence of the crystal face on the structure of aligned SWNTs is interesting from the view point of epitaxial growth. Here, we report on the characterization of the aligned SWNTs by Raman and photoluminescence (PL) spectroscopies.

SWNTs were grown on A-, R-, C-face sapphire and SiO₂ substrates by chemical vapor deposition (CVD) after immersing the substrates in Co-based catalyst solution (Fig. 1). The diameter distribution estimated from the Raman spectra were found to depend on the crystal face of sapphire (Fig. 2). The surfaces which aligned SWNTs gave relatively narrow diameter distribution, which may suggest the interaction between the surface and metal nanoparticles. Interestingly, we could observe the PL from the aligned SWNTs on sapphire, even though the SWNTs were not covered with surfactant. The polarized PL measurement confirmed the alignment of nanotubes. This is the first demonstration of the PL emission from uncovered SWNTs deposited on a substrate, as far as we know, because tube-substrate interactions are supposed to quench the luminescence. The chirality distribution shown in Fig. 3 agreed with the diameter distribution obtained by the Raman measurements.

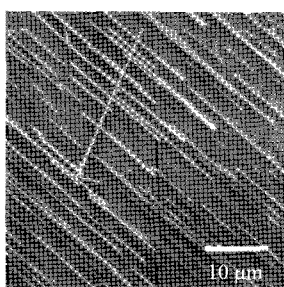


Fig. 1 A typical SEM image of aligned SWNTs on R-face sapphire.

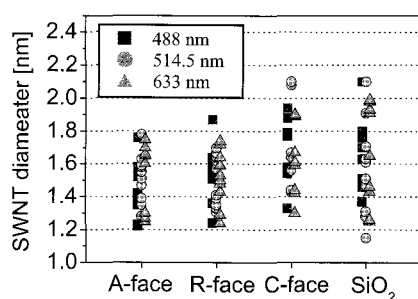


Fig. 2 Diameter distributions of SWNTs grown on A-, R-, C-face sapphire and SiO₂ determined from Raman spectra ($d_{\text{NT}}=248/\omega_{\text{RBM}}$).

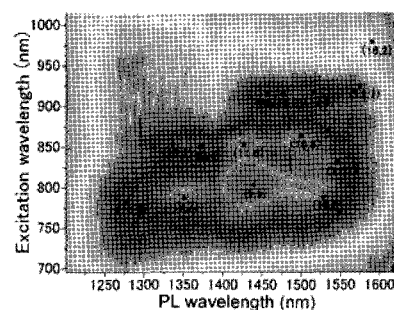


Fig. 3 PL map of aligned SWNTs on R-face sapphire. The PL detection range is $< 1.7 \mu\text{m}$, corresponding to about 1.4 nm of SWNT.

Acknowledgements: This work is supported by Grant-in-aid for Scientific Research from MEXT (# 18681020), Industrial Technology Research Program from NEDO, CREST-JST, and Joint Project of Chemical Synthesis Core Research Institution.

References: [1] H. Ago et al., *Chem. Phys. Lett.*, **408**, 433 (2005).

Corresponding Author: Hiroki Ago (TEL&FAX: +81-92-583-7817, E-mail: ago@cm.kyushu-u.ac.jp)

Oxidative Reaction of Carbon Nanotubes with O₂ and O₃

○Takazumi Kawai and Yoshiyuki Miyamoto

*Nano Electronics Research Laboratories, NEC Corporation
34, Miyukigaoka, Tsukuba, Ibaraki 305-8501, JAPAN*

The process of refinement is one of the most important issues for various device applications of carbon nanotubes, since amorphous carbons and defective nanotubes would often inhibit the original functions of intact nanotubes. The chirality selection of nanotubes is also important role of the refinement process. Oxidation is one of the promising candidates for the refinement process[1]. Although the understanding of atomic-scale mechanisms for oxidative reaction should be important to increase efficiency of the refinement, the detailed mechanism is unclear due to the complexity of the process.

Recently, we have done the first-principles calculations for the process of breaking C-C bond after cyclo-addition of O₂ [2]. We found that the reaction barriers for the breaking C-C bond are depending largely on the local curvature radius along the C-C bond about to break. The reaction barriers are also depending on the electronic states of initial cyclo-addition and transition state (saddle point) configurations at the Fermi level. Thus, the hole-doping effect changes the reaction barriers dramatically, and even change the order of barrier heights. We also discuss the refinement of nanotubes with O₃ molecules, which is known for more reactive oxidative adduct.

References:

- [1] Y. Miyata, Y. Maniwa, and H. Kataura, *J. Phys. Chem. B* 110, 25, (2006), Y. Miyata, T. Kawai, Y. Miyamoto, K. Yanagi, Y. Maniwa, H. Kataura, accepted for publication in *J. Phys. Chem. C*.
[2] T. Kawai and Y. Miyamoto, submitted.

Corresponding Author: Takazumi Kawai

E-mail: takazumi-kawai@mua.biglobe.ne.jp

Tel&Fax: +81-29-850-1554, +81-29-856-6136

Structural Dependence of Raman Spectrum of Single-walled Carbon Nanotube Adsorbed on Metal Electrode

Norihiko Takeda¹ and Kei Murakoshi^{1,2}

¹Japan Science and Technology Agency, Sapporo, Hokkaido 060-0810, Japan

²Division of Chemistry, Graduate School of Science, Hokkaido University, Sapporo, Hokkaido 060-0810, Japan

Single-walled carbon nanotubes (SWNTs) are attractive materials for new generation of devices such as nano-scale electronic circuits, field emission displays, and fuel cells to name a few. Although researches on physical properties of SWNTs had progressed significantly in the past, much of information about structure dependent properties are based on theoretical calculations. The difficulties in experimentally evaluating structure-property relationships of SWNTs are partly due to the lack of abilities to select specific tube structures in the current synthesis methods. The band position in the absolute energy scale, i.e. the redox potential of SWNT is an important factor in determining its chemical reactivity. Variations of Fermi energies of isolated SWNTs were found in Raman spectroelectrochemical studies [1,2]. The Fermi levels became more positive in the electrochemical scale with decreasing diameters. Diameter-dependent charge transfer reactivities of SDS-dispersed SWNTs to electron acceptors in solution were interpreted as a result of the Fermi level shifts. In the present study, resonant Raman scattering spectra of single-walled carbon nanotubes (SWNTs) were investigated under electrochemical potential control in aqueous electrolytes. Raman spectra of the radial breathing mode (RBM) with a 785 nm laser excitation were monitored while slowly scanning the electrode potential. Six resolved RBM peaks all showed decreasing intensities when the electrode was positively biased due to depletion of valence band electrons associated with resonant excitation. General trends of more positive potentials for electrochemical oxidation of narrower diameter tubes with higher RBM frequencies were observed (Figure). This is consistent with the larger bandgaps of narrower diameter tubes which would have the valence bands at more positive potential. However, the large Fermi level shifts reported for isolated SWNTs were not observed in the bundle system (3). The bundled tubes could have constant Fermi energy much like a bulk solid materials and/or the surrounding SDS micelles could shield the solvent molecules which could affect the stabilities of oxidized tubes.

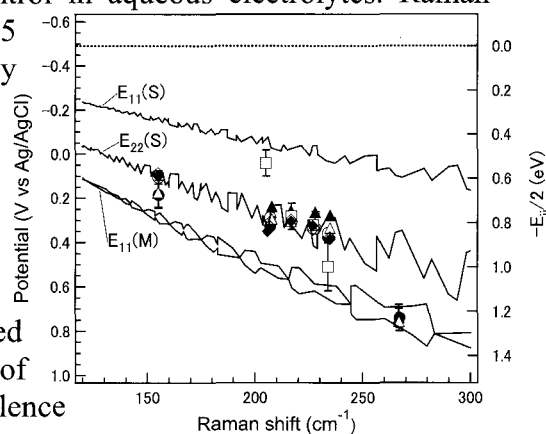


Figure. Plots of half-intensity potentials of RBM peaks against their peak positions. Different symbols refer to different data sets. Potential values refer to the left axis. Solid lines are plots of locations of valence state edges from midgap energy in panel a (Fermi level) for semiconducting (v1(s), v2(s)) and metallic (v1(m)) tubes $-E_i/2$ referencing to the right axis.

References: (1) N. Takeda and K. Murakoshi, *Anal. Bioanal. Chem.*, **388**, 103 (2007); (2) K. Murakoshi and K.-i. Okazaki, *Electrochem. Acta*, **50**, 3069 (2005); (3) K.-i. Okazaki, Y. Nakato and K. Murakoshi, *Phys. Rev. B*, **68**, 035434 (2003).

Corresponding Author: Kei Murakoshi

Tel: +81- 11-706-2704, **Fax:** +81- 11-706-4810, **E-mail:** kei@sci.hokudai.ac.jp

Field-Effect Doping in Carbon Nanotubes

○Kazuyuki Uchida and Susumu Okada

*Center for Computational Sciences, University of Tsukuba, 1-1-1 Tennodai, Tsukuba
305-8577, Japan*

*CREST, Japan Science and Technology (JST) Agency, 4-1-8 Honcho, Kawaguchi,
Saitama 332-0012, Japan*

Abstract: Carbon nanotubes (CNTs) are considered to be a premier material for the constituent of nanometer-scale electronic devices in the next generation. Indeed, it has been demonstrated that the individual semiconducting CNT work as field-effect transistors (FETs) [1,2]. Although experiments on CNT-FET are rapidly advancing, little is known as to fundamentals of the CNTs in FET structures. In particular, electronic property of charged CNTs under electronic field is not addressed yet. In this work, to uncover the issue, we perform first-principles density-functional calculations on the electronic structures of the charged CNTs under electronic field.

Here we take a (7,0) CNT placed over an electrode, which is considered to be a structural model of the CNT-FET with a back (top) gate electrode. By applying the gate voltage, carriers are injected into the CNT and the accumulated charges are distributed in a part of the CNT facing to the electrode. Using this distribution of the accumulated charge, we can estimate electrostatic component of the capacitance between the CNT and the electrode. We also point out that the capacitance strongly depends on the bias voltage, reflecting the electronic structure of the CNT. The result indicates that the characteristics of CNT-FETs sensitively depend on the diameter and chirality of the constituent CNTs.

References

- [1]S. J. Tans et al, Nature **393**, 49 (1998).
- [2]R. Martel et al., Appl. Phys. Lett. **73**, 2447 (1998).

Corresponding Author: Kazuyuki Uchida

E-mail: kuchida@comas.frsc.tsukuba.ac.jp

Tel: 029-853-5600-8233

Variable Range Hopping Conduction in Boron doped MWNT Assembly

○ Shunji Bandow, Shigenori Numao^a, Sumio Iijima

*Department of Materials Science and Engineering, Meijo University,
1-501 Shiogamaguchi, Tenpaku, Nagoya 468-8502, Japan*

^a *The Graduate University for Advanced Studies, Institute for Molecular Science,
38 Nishigo-Naka, Myodaiji, Okazaki 444-8585*

Enlargement on the innermost tube diameters for the multiwall carbon nanotubes (MWNTs) can be achieved by the vaporization of the boron containing carbon rod in RF-plasma [1]. ESR study for these RF-driven B-MWNTs indicated the growth of new signals at $g = 2.001$ and 2.002 with increasing the boron concentration [1]. In the present study, we measured the electrical resistivity for the pellet formed MWNT assembly as a function of the boron concentration.

Figure 1 is the SEM images taken for the pellet-formed MWNT assemblies. Surface structures are similar between these samples, suggesting that the resistance does not closely depend on the porosity. Electrical resistivities were measured in the temperature range between 6 and 290 K by the 4-probes method. Figure 2 is the temperature dependences of the electrical resistivity ρ together with the boron concentration dependence of ρ_{RT} (ρ at room temperature) as an inset figure. These temperature dependences clearly indicate that the electrical conduction is governed by the 3 dimensional Mott's variable range hopping (3D-VRH) mechanism and the resistivity indicates monotonic decrease as a function of the boron concentration. Analyses of the characteristic temperature T_0 for 3D-VRH clearly indicated the enhancement on the electronic DOS that consists quantitatively with the results from ESR. This enhancement is due to a fact of doping the boron to the tube wall.

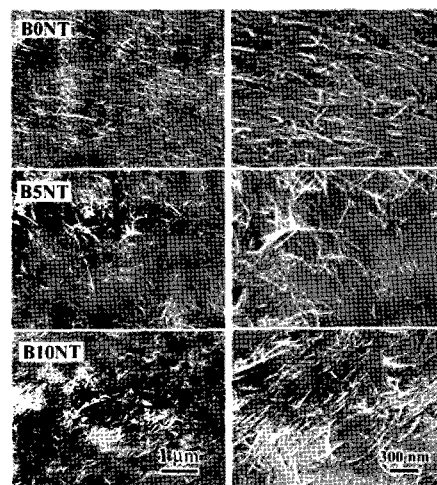


Fig. 1. Surfaces of the pellet-formed B-MWNT assemblies. B0NT corresponds un-doped MWNTs and B5NT means MWNTs from 5 % of B-containing C rod.

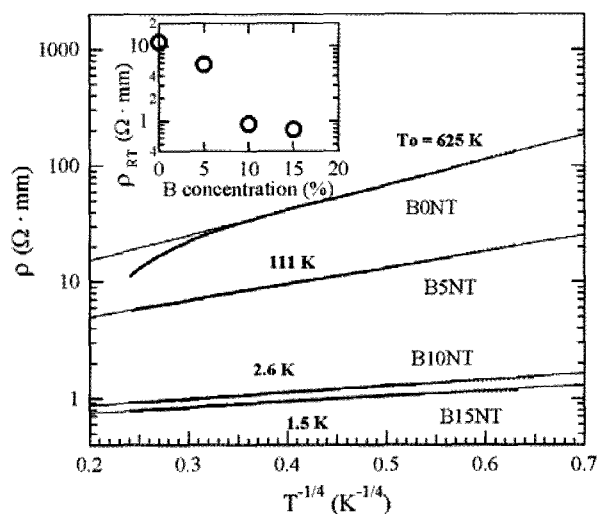


Fig. 2. Temperature and boron concentration dependences of the electrical resistivity. Mechanism for the electrical conduction is represented by the Mott's 3D-VRH.

[1] S. Numao, S. Bandow, S. Iijima, *J. Phys. Chem. C* **111**, 4543 (2007).

Corresponding Author: Shunji Bandow, **E-mail:** bandow@ccmfms.meijo-u.ac.jp, **Tel&Fax:** +81-52-834-4001

Electronic Structure of Boron-doped Carbon Nanotube

○Takashi Koretsune and Susumu Saito

*Department of Physics, Tokyo Institute of Technology
2-12-1 Ookayama, Meguro-ku, Tokyo 152-8551*

Since the discovery of the superconductivity in boron-doped diamond [1], the carrier doping, especially boron doping in carbon materials attracts much attentions. For the carbon nanotubes, however, the effect of boron doping as well as the possibility of the superconductivity [2] have not been well understood yet. Thus, we study the boron-doped single-walled zig-zag carbon nanotube using density functional theory to explore the basic properties of boron doped nanotubes.

We first discuss the result of the structure optimization and the total energy. Since boron atom has larger atomic radius than carbon atom, a boron atom in the optimized structure locates slightly outside of the original carbon nanotube. It is found that narrower tube needs lower energy cost to exchange a carbon atom to a boron atom. We also discuss the doping rate dependences of band structure and the density of states.

For the (10,0) nanotube, which has a moderate band gap, the result indicates that boron doping can be understood as a hole doping in the rigid band picture. Doping rate within our calculation (0.8at%) is too large to achieve the high density of states using the van Hove singularity at the edge of the one-dimensional band. We speculate that the low boron concentration is sufficient to realize the superconductivity in boron-doped nanotube, which is in sharp contrast to the boron-doped diamond.

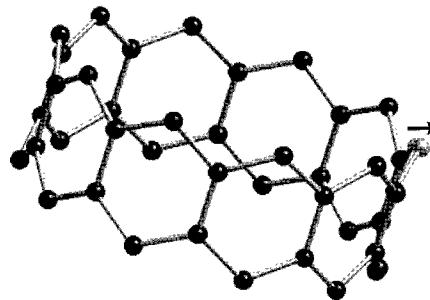


Fig 1. Optimized structure of boron-doped (10,0) carbon nanotube.

References:

- [1] E.A. Ekimov et al., *Nature* **428** 542 (2004).
[2] I. Takesue et al., *Phys. Rev. Lett.* **96** 057001 (2006).

Corresponding Author: Takashi Koretsune

E-mail: koretune@stat.phys.titech.ac.jp

Tel: 03-5734-2387

Chirality dependence and excitonic effect of optical transition of single wall carbon nanotubes

○Kentaro Sato¹, Riichiro Saito¹, Jie Jiang², Gene Dresselhaus³, Mildred S. Dresselhaus⁴

¹*Department of Physics, Tohoku Univ. and CREST JST, Sendai, 980-8578, Japan*

²*Department of Physics, NC State Univ., Raleigh, NC 27695-7518, USA*

³*Francis Bitter Magnet Laboratory, Massachusetts Institute of Technology,
Cambridge, MA 02139-4307, USA*

⁴*Department of Physics, Massachusetts Institute of Technology,
Cambridge, MA 02139-4307, USA*

Since the exciton binding energy of single wall carbon nanotubes (SWNTs) is large (0.3-0.5 eV), the exciton exists in the room temperature. Thus we should consider the excitonic effect for optical transitions. The exciton energy is a sum of the single particle energy and many body energy ($\Sigma - E_{bd}$), where Σ is the self energy, and E_{bd} is the binding energy [1]. In the case of E_{11}^S and E_{22}^S optical transitions, the chirality dependence of the exciton binding energy is almost cancelled by that of the self energy. Thus the origin of the family pattern for E_{11}^S and E_{22}^S optical transitions come from the chirality dependence of the single particle energy [1].

Recently, some experiments show that the diameter dependence of E_{33}^S and E_{44}^S is different from that of E_{11}^S and E_{22}^S [2, 3]. The chirality dependence of the excitonic effect becomes important [2]. We calculate exciton energy, self energy and binding energy of optical transitions ($E_{11}^S, E_{22}^S, E_{11}^M, E_{33}^S, E_{44}^S, E_{11}^M, E_{55}^S, E_{66}^S, E_{33}^M$) of SWNTs by solving the Bethe-Salpeter equation within an extended tight binding method. We show that the chirality dependence of the excitonic effect becomes important when we consider the origin of the family pattern of E_{33}^S and E_{44}^S optical transitions. Since the self energy becomes larger than the exciton binding energy for E_{33}^S and E_{44}^S , the chirality dependence of the binding energy is not canceled by that of the self energy. Thus the chirality dependence of the excitonic effect becomes important for the origin of the family pattern of E_{33}^S and E_{44}^S optical transitions [4].

References:

- [1] J. Jiang *et al.*, Phys. Rev. B 75, 035407 (2007).
- [2] P. T. Araujo *et al.*, Phys. Rev. Lett. 98, 067401 (2007).
- [3] T. Michel *et al.*, Phys. Rev. B 75, 155432 (2007).
- [4] K. Sato *et al.*, Vibrational Spectroscopy, in press (2007).

Corresponding Author: Kentaro Sato

E-mail: Kentaro@flex.phys.tohoku.ac.jp, Tel: +81-22-795-6445

Band-Gap Tuning of an Individual Single-Walled Carbon Nanotube with Uniaxial Strain

Hideyuki Maki¹, Tetsuya Sato¹, and Koji Ishibashi²

¹*Department of Applied Physics and Physico-Informatics, Faculty of Science and Technology, Keio University, Hiyoshi, Yokohama 223-8522, Japan*

²*Advanced Device Laboratory, The Institute of Physical and Chemical Research (RIKEN), Wako, Saitama 351-0198, Japan*

The emission energy obtained from photoluminescence (PL) and electrically induced optical emission is determined by the band gap that depends on the chirality of SWNT. However, it was theoretically reported that the band gap is varied by the strain of SWNT and the change of the band gap depends on their chirality and deformation mode.¹ In our study, we have fabricated the new devices for applying strain to the individual suspended SWNTs. Using this device, the emission energy shift due to the band gap change caused by the elastic strain is observed from the PL measurement for the individual SWNT.

Figure 1(a) shows schematic pictures of a device for applying stretch to the suspended SWNTs. Suspended SWNTs were formed over the crack of the substrate. One side of the crack is opened; therefore, extension can be directly applied to the suspended SWNTs by applying piezo voltage (V_{piezo}) to the piezoelectric device. This device has very small size (maximal length of ~ 7 mm); hence it is easy to insert this device into various experimental instruments. In this study, the form of individual SWNT under stretching was directly observed by SEM under applying piezo voltage. In addition, PL spectra from individual SWNTs under stretching were also measured using microscope objective at room temperature in air.

Figure 2a shows the V_{piezo} dependence of the PL spectra for the SWNT which have emission energy around 1.125 eV. As applied V_{piezo} is increased, the emission peak is shifted toward lower energy. Moreover, the peak goes back to the normal position, when the applied V_{piezo} is reduced to 0 V following application of $V_{\text{piezo}} = 39$ V. Figure 2b shows the V_{piezo} dependence of the emission energy. The emission energy is linearly shifted toward lower energy in the range from $V_{\text{piezo}} = 15.0$ to 32.4 V (region II). This shift can be understood by the band gap narrowing due to uniaxial strain.

[1] L. Yang, J. Han, *Phys. Rev. Lett.*, **85**, 154, (2000).

Corresponding Author: Hideyuki Maki

E-mail: maki@appi.keio.ac.jp, Tel: +81-45-566-1643, FAX: +81-566-1587

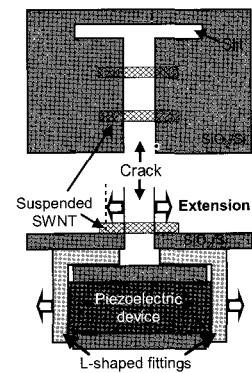


Fig. 1. Schematic top view and cross-section of the fabricated device for applying strain to the suspended SWNTs.

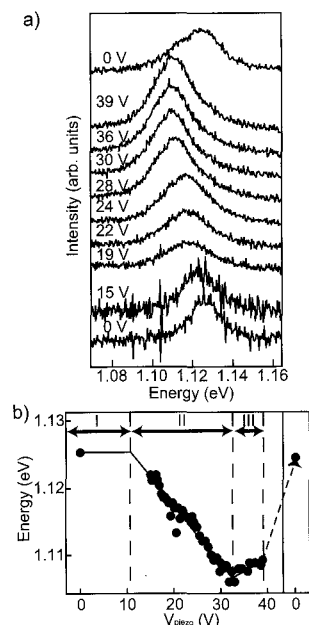


Fig. 2. a) V_{piezo} dependence of the PL spectra for sample A. The applied V_{piezo} is reduced to 0 V after application of $V_{\text{piezo}} = 39$ V. b) V_{piezo} dependence of the emission energy.

A growth model for single walled carbon nanotubes

-Why near armchair structure is so special-

Y. Achiba

Department of Chemistry, Tokyo Metropolitan University, Tokyo 192-0397, Japan

One of the most intriguing aspect of the growth process in the field of single walled carbon nanotubes (SWNTs) is represented by the question whether there is the preferential growth of the SWNT with a specific chiral angle or not. Actually, the results deduced by the recent photoluminescence experiments have strongly suggest the presence of a sort of the propensity in the selection of chiral angle; favorite formation of near armchair structures. On the other hand, the resonant Raman scattering experiments rather suggest strong preference in the optical processes, depending on type of the family, chiral angle, tube diameter, etc.

With use of the laser ablation method, so far we have reported the preferential growth of (7, 6) and (6,5) SWNTs under the refined condition of laser ablation. Furthermore, the further refining the experimental condition suggested that even the preferential formation of (5,4) nanotubes would be possible [1]. All these experimental results has clearly shown that the formation of the SWNT family characterized by the $(n-m) = 1$ index is very much pronounced. In order to understand these experimental evidence, here in the present work, we would like to propose a new growth model by which the preferential growth of the SWNTs with the $(n-m) = 1$ family is safely interpreted in terms of a very simple mechanism.

The growth model presented here is based on several assumptions such that; 1) at the early stage of the tube growth, a fullerene cap is formed, 2) the preferential growth of SWNT with a specific chiral angle is controlled by the difference in the growth rate of the tubes (not the growth rate of the fullerene cap), 3) major carbon source used for the tube growth is C_2 species produced on the metal catalyst. 4) a paired dangling bond (p-DB) might be kinetically much more stable in comparison with a single dangling bond (s-DB).

Under such assumption, we can easily deduce an essential property of the $(n-m) = 1$ family which might differentiate the one from many other (n,m) family. The unique property of each (n,m) family should appear in the DBs, sitting on the periphery of the cap structure, which acts as a radical site. For example, the $(n-m) = 0$ family, so called “armchair” structure, is well represented by the presence of all p-DBs, while the $(n-m) = n$ family, “zigzag” structure, all s-DBs. As a result, these two families might have different experience during the growth under the assumption mentioned above; for the armchair, every cycle of the C_2 addition reproduces the kinetically stable same edge structure with all p-DBs, and for the zigzag, after finishing the C_2 addition every one round, the edge structure necessarily requires the addition of C_1 or C_3 species, this is out of the situation of assumption 3). All other chiral family possesses combination of these p- and s-DBs. Among them, only the $(n-m) = 1$ family possesses the structure with the combination of only one s-DB connected with p-DBs. For this particular case, the C_2 addition is possibly taken place smoothly every minute without any congestion in the growth direction.

[1] Y. Tsuruoka, K. Urata, S. Suzuki and Y. Achiba, unpublished data.

Corresponding Author: Yohji Achiba

TEL: 042-667-2534, E-mail: achiba-yohji@tmu.ac.jp

Study of Carbon Transmitting Method for Growth of Carbon Nanotubes

○Takeshi Hikata¹, Kazuhiko Hayashi¹, Tomoyuki Mizukoshi²,
Yoshiaki Sakurai², Itsuo Ishigami², Takaaki Aoki³, Toshio Seki³, and Jiro Matsuo³

¹Sumitomo Electric Industries, Ltd., Osaka 554-0024, Japan

²Technology Research Institute of Osaka Prefecture, Osaka 594-1157, Japan

³Faculty of Engineering Quantum Science and Engineering Center, Kyoto University,
Kyoto 606-8501, Japan

Carbon nanotubes (CNTs) have been expected as ideal electric wires with the excellent properties of low resistivity, high strength and light weight. However, it is difficult to fabricate the long length wires with the excellent properties because it is difficult to maintain the growth of CNT by covering of unnecessary harmful carbon formed on nano-sized metal particle catalysts in thermal CVD process. We propose the Carbon Transmitting Method for continuous growth of CNT with the concept of the separation between carbon source gas supply and CNT growth as shown in Fig.1. [1]

The catalyst has Fe filament shape through the Ag foil as the separator between the carbon source gas and CNT growth site. The composite structure of Fe nano filaments and Ag matrix was fabricated by deformation process of metal wire drawing techniques. The composite wires with diameter of 10 mm was cut and polished until the thickness of about 50 μm to the foil shape. The both end of Fe filaments in the Ag foil were exposed with length of a few μm on Ag surface. The Fe filaments were tape shape with thickness of about 30nm to sub μm and width of about 200nm to a few μm .

The carbon source gas, CO was provided on one end of Fe filaments (side A) and Ar gas was provided on the other end of Fe filaments (side B) at 850 $^{\circ}\text{C}$ for 1 hour. As the result of the heat treatment, the tape shaped carbon nano filaments were generated on side B in Ar gas. The carbon nano filaments were observed by TEM as shown in Fig.2. These results indicate that the source carbon has been provided on the end of Fe filaments and move to the other end, and then carbon nano filaments generated according to the tape shape of the end of Fe filaments. The tape shaped CNT is expected to become the bundled CNT conductors with high conductivity because of low contact resistance between the flat surface of the taped CNT filaments.

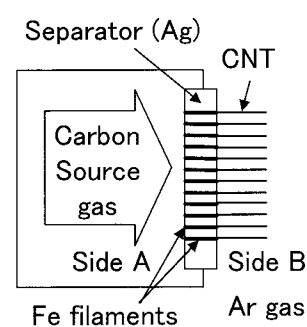


Fig.1 Concept of Carbon Transmitting Method

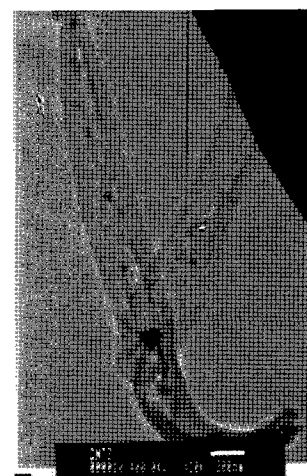


Fig.2 TEM photograph of tape-shaped carbon nano filaments

Corresponding Author: Takeshi Hikata /E-mail: hikata-takeshi@sei.co.jp

TEL: +81-6-6466-5790, FAX: +81-6-6466-6583

[1] T.Hikata et al., The 32nd Fullerene-Nanotubes General Symposium, 3P-2(2007).

Synthesis of single-wall carbon nanotubes from diesel soot

○Takashi Uchida*, Masaru Tachibana, Kenichi Kojima

Graduate School of Integrated Science, Yokohama City University, 22-2, Seto, Kanazawa-ku, Yokohama 236-0027, Japan

**Present address: NTT Basic Research Laboratories, NTT Corporation, Japan*

Single-wall carbon nanotubes (SWNTs) have been synthesized by electric arc-discharge, laser vaporization and chemical vapor deposition methods. Each method has its own merits and demerits in terms of quality, yield, growth control and cost. In electric arc-discharge and laser vaporization methods, graphite is generally used as a carbon source. However, few studies have shown the synthesis of SWNTs from other carbon sources, among them synthesis from fullerenes by a laser vaporization method [1]. Recently, a unique technique for effectively collecting diesel soot has been developed [2]. The diesel soot is the exhaust soot from diesel engines operating with light or heavy oil that causes air pollution and leads to global warming and adverse health effects. To prevent this pollution, diesel soot should be rendered harmless or collected before emission into the environment. It is desirable that the collected diesel soot is recycled for useful applications. In this letter, we demonstrate the synthesis of SWNTs from diesel soot by laser vaporization. As-grown materials were characterized by Raman spectroscopy and transmission electron microscopy (TEM).

Figure 1 shows the Raman spectra of a typical as-grown material synthesized from diesel soot by laser vaporization method taken at excitation energies of 1.96 and 2.33 eV. The Raman spectra exhibit two strong bands at low (100 - 300 cm^{-1}) and high (1500 - 1600 cm^{-1}) frequencies, which correspond to the radial breathing modes and tangential modes (the G band) of SWNTs respectively. These Raman features show that SWNTs were successfully synthesized by laser vaporization, even from a diesel soot carbon source. The presence of SWNTs in as-grown materials is also confirmed by TEM images.

These results indicate that diesel soot can be recycled as a carbon source for the synthesis of SWNTs. The collection of diesel soot for the synthesis of SWNTs is an example of recycling to benefit the environment. SWNTs produced in this way should provide economic benefits and also contribute to a cleaner environment.

This work has been published on JJAP 45 (2006) 8027.

[1] T. Nishimoto, PCT Int. Appl. WO 2005049983 (2005).

[2] Y. Zhang and S. Iijima, APL 75 (1999) 3087.

Corresponding Author: Takashi Uchida

TEL/FAX: +81-46-240-4319/+81-46-240-4718

E-mail: uchida@will.brl.ntt.co.jp

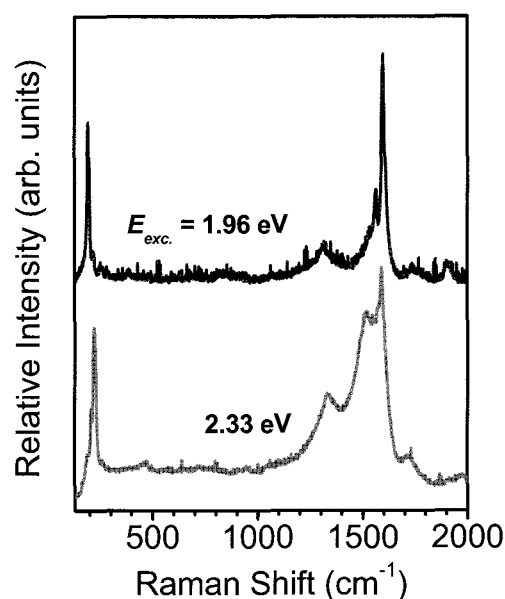


Fig. 1. Raman spectra of a typical as-grown material synthesized from diesel soot.

Are Catalyst Free SWNT Forests Free From Impurities? – Existence of Graphitic Carbonaceous Impurities

○Satoshi Yasuda, Tatsuki Hiraoka, Don N. Futaba,
Motoo Yumura, Sumio Iijima, and Kenji Hata

¹*Reserach Center for Advanced Carbon Materials, National Institute of Advanced Industrial Science and Technology (AIST), Tsukuba, 305-8576, Japan*

The “Super-growth” CVD technique has enabled synthesis of millimeter-long, vertically aligned and catalyst free SWNTs forest by adding a small and controlled level of water into the growth environment [1,2]. Super-growth is a promising approach for the mass production of SWNTs, and might open the door for the scientific and industrial application of SWNTs, such as electrical devices, nano-reactors, and especially, super capacitors for compact energy-storage devices [3]. Although the carbon purity of SWNTs synthesized by super-growth technique reaches more than 99.98%[1], this result does not exclude the possibility of carbonaceous impurities in forms different from nanotubes existing in the synthesized material. From a practical point, it is important to estimate the carbonaceous impurities in the forests and study their influence on physical and chemical properties. With this in view, we investigated the amount and characteristics of carbon impurity in SWNTs synthesized by super-growth CVD. TEM measurement shows that the nanotubes at 5 mins growth time are clean SWNTs free from carbonaceous and metal catalysts (Figure 1(a)). However, we found a large amount of carbonaceous impurities on SWNTs synthesized at 90 mins growth time. We interpret this carbonaceous impurities are due to expose of the SWNT forests to the carbon source gas for a long time (Figure 1(b)). The adhesion rate and characteristics of the carbon impurity will be discussed in the conference.

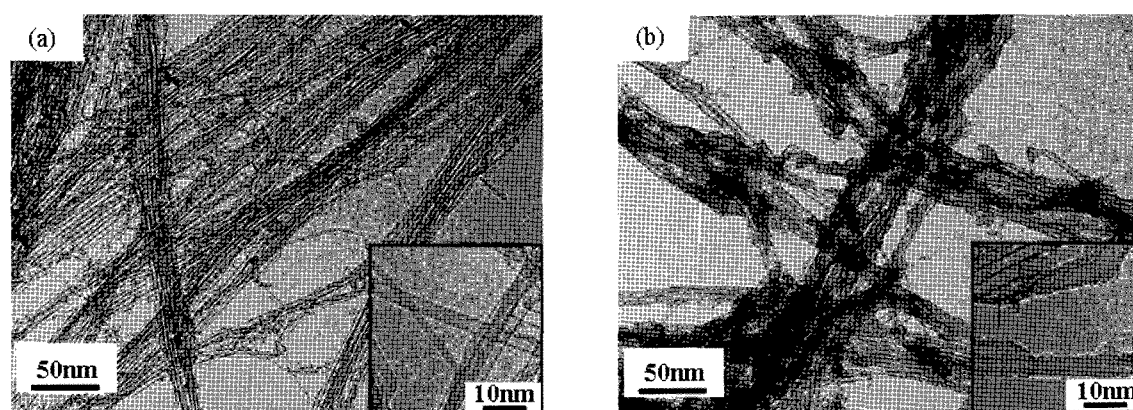


Figure 1 TEM images of (a) SWNTs at 5 mins and (b) 90 mins growth times, respectively.

[1] K. Hata, D. N. Futaba, K. Mizuno, T. Namai, M. Yumura, and S. Iijima, *Science* 2004, **306**, 1362.

[2] D. N. Futaba, K. Hata, T. Yamada, K. Mizuno, M. Yumura, and S. Iijima *Phys. Rev. Lett.* 2005, **95**, 056104

[3] D. N. Futaba, K. Hata, T. Yamada, T. Hiraoka, Y. Hayamizu, Y. Kakudate, O. Tanaike, H. Hatori, M. Yumura, and S. Iijima *Nature Material* 2006, **5**, 987

Corresponding Author: Kenji Hata

TEL: +81-29-861-4656, FAX: +81-29-861-4851, E-mail: kenji-hata@aist.go.jp

Combinatorial Control of Catalyst for Basics and Applications of Carbon Nanotube Growth

○Suguru Noda¹, Hisashi Sugime¹, Kei Hasegawa¹, Kazunori Kakehi¹,
Shigeo Maruyama² and Yukio Yamaguchi¹

¹*Dept. of Chemical System Engineering, The University of Tokyo, Tokyo 113-8656, Japan*

²*Dept. of Mechanical Engineering, The University of Tokyo, Tokyo 113-8656, Japan*

Control of catalyst nanoparticles is a key for further progress in both SWNT production and understanding of its growth mechanism. We have developed "combinatorial masked deposition (CMD)" method [1], in which a series of catalyst nanoparticles are formed on a substrate from a catalyst gradient thickness profile preformed by sputtering through a physical filter. We have applied this CMD to alcohol catalytic CVD (ACCVD) [2] and realized SWNT films by Co/SiO₂ [3] and Ni/SiO₂ [4], and VA-SWNTs by Co-Mo/SiO₂ [5].

This time we studied ACCVD in detail. Co/SiO₂ grew SWNTs and MWNTs efficiently at Co thickness of 0.1-0.2 nm and 1-2 nm at 973 K, respectively, and hardly grew nanotubes in between. Co-Mo/SiO₂ yielded VA-SWNTs under several conditions, including Co/Mo atomic ratio of (i) 1/2 reported for CO disproportion [6] and (ii) 1.6/1 for ACCVD [7] (Fig. 1). We also found the third region with pure Co (iii) highly efficient under 4 kPa C₂H₅OH, yielding VA-SWNTs with a bimodal diameter distribution. Catalyst layers of different thickness yield different particles, which are catalytically active for different conditions.

We also applied CMD to "supergrowth [8]" and reproduced it [9]. Figure 2 shows a millimeter-thick forest grown in 10 min by 0.2-3-nm-thick Fe on Al₂O₃/SiO₂. Thin Fe (~ 0.5 nm) yielded SWNTs under a limited condition, and thicker Fe yielded thicker nanotubes under wider conditions. CMD enabled efficient optimization because CVD condition can be adjusted to lead the threshold Fe thickness for VA-CNTs smaller. Aluminum oxide, which is a well-known catalyst in hydrocarbon reforming, had an essential role in enhancing the nanotube growth by dissociating carbon species and supplying them to Fe nanoparticles.

SWNT growth at a low areal density is important as well. The as-grown network of thick bundles resulted from sparse, long SWNTs (Fig. 3a) by ACCVD showed a transparent conducting property much better than that of thin bundles from short, dense SWNTs (Fig. 3b).

In summary, there remains abundant potential in catalytic growth of nanotubes and CMD is effective in both understanding and developing supported catalysts.

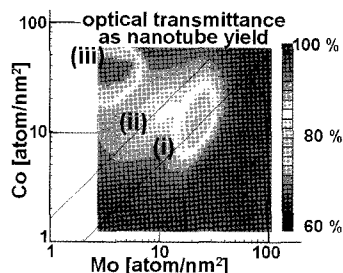


Fig. 1. Co-Mo activity map.

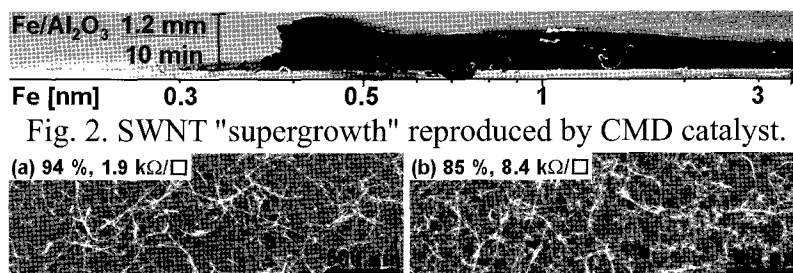


Fig. 2. SWNT "supergrowth" reproduced by CMD catalyst.

- [1] S. Noda, et al., *Appl. Surf. Sci.*, **225**, 372 (2004). [2] S. Maruyama, et al., *Chem. Phys. Lett.*, **360**, 229 (2002). [3] S. Noda, et al., *Appl. Phys. Lett.*, **86**, 173106 (2005). [4] K. Kakehi, et al., *Chem. Phys. Lett.*, **428**, 381 (2006). [5] S. Noda, et al., *Carbon*, **44**, 1414 (2006). [6] J.E. Herrera, et al., *J. Catal.*, **204**, 129 (2001). [7] Y. Murakami, et al., *Chem. Phys. Lett.*, **385**, 298 (2004). [8] K. Hata, et al., *Science*, **306**, 1362 (2004). [9] S. Noda, et al., *Jpn. J. Appl. Phys.*, **46**, L399 (2007).

Corresponding Author: Suguru Noda, Tel/Fax: +81-3-5841-7330/7332, E-mail: noda@chemsys.t.u-tokyo.ac.jp

***In-situ* Raman observation of single-wall carbon nanotube growth by CVD using Co-filled apoferritin catalyst**

○Takashi Uchida^{1,2}, Masaya Tazawa^{1,3}, Akira Yamazaki^{1,4}, and Yoshihiro Kobayashi^{1,2}

¹*NTT Basic Research Laboratories, NTT Corporation, Atsugi 243-0198, Japan*

²*CREST/JST, Japan Science and Technology Corporation*

³*Department of Physics, Tokyo University of Science, Shinjuku, Tokyo 162-8601, Japan*

⁴*Department of Physics, Meiji University, Kawasaki 214-8571, Japan*

Clarifying the growth mechanism of single-wall carbon nanotubes (SWNTs) is indispensable for the control of SWNT growth. *In-situ* observation by scanning electron microscopy and Raman spectroscopy is very useful for investigating the growth mechanism of SWNTs [1,2]. In these previous studies, the chiralities of growing SWNTs were not specified. We have succeeded in observing the diameter-dependent growth behavior through the observation of chirality-sensitive RBM signals in *in-situ* Raman spectra using Co thin film catalyst [3]. However, the correlation between the growth behavior and the CVD conditions has not been clarified because the size of the catalyst particle formed from thin film also depends on the CVD conditions. Metal nanoparticle catalysts, such as Co-filled apoferritins (Co-ferritin) [4], are useful for investigating the initial growth stage of SWNTs because their diameter remains fixed regardless of the CVD conditions. In this report, we report on *in-situ* Raman observation during CVD growth of SWNTs using Co-ferritin as a catalyst.

In-situ Raman spectra were obtained with a micro-Raman system (633-nm excitation wavelength; 2- μ m laser spot) combined with an ethanol-CVD system.

Figure 1 shows a series of typical RBMs in the *in-situ* Raman spectra observed during CVD growth. The growth temperature was 720 °C and the ethanol gas pressure was 0.8 Torr. Each spectrum was integrated for 30 s. It is clearly observed that the RBM intensities around 130 - 215 cm^{-1} increase with increasing growth time. In particular, the increase in the RBM intensities at around 130 cm^{-1} and 215 cm^{-1} is delayed compared to those at 160 - 190 cm^{-1} . Furthermore, the RBM at 250 cm^{-1} appeared at the growth time of about 1600 s. These results indicate that the incubation time of SWNT growth depends on the chirality. *In-situ* Raman observation of CVD growth using Co-ferritin catalyst enables us to analyze the details of the kinetics of SWNT growth under various CVD conditions.

This work was partly supported by JSPS Grant-in-Aid for Scientific Research (B).

[1] Y. Homma et al., APL 88 (2006) 023115.

[2] S. Chiashi et al., CPL 386 (2004) 89.

[3] M. Tazawa et al., 32th F&NT General Symposium 2007, 2P-3.

[4] G. -H. Jeong et al., JACS 127 (2005) 8328.

Corresponding Author: Takashi Uchida

TEL/FAX: +81-46-240-4319/+81-46-240-4718

E-mail: uchida@will.brl.ntt.co.jp

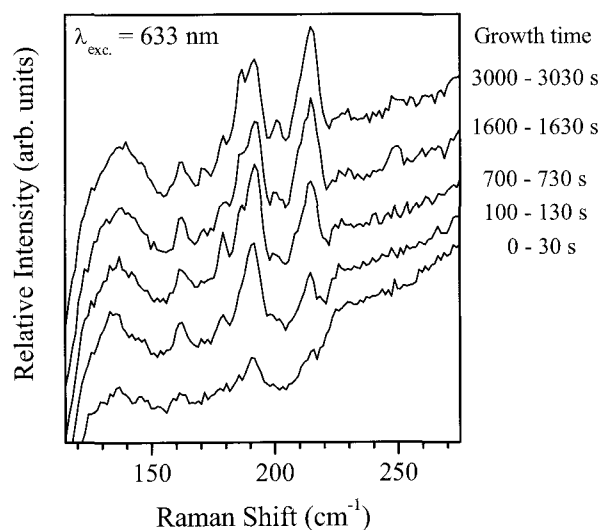


Fig. 1. Typical RBMs in the *in-situ* Raman spectra observed during CVD growth.

Size control of catalyst nanoparticles for carbon nanotube growth by gas-phase catalytic chemical vapor deposition

○K. Ohara¹, Y. Neo², H. Mimura², Y. Inoue³ and A. Ishida³

¹Grad. Schl. of Electron. Sci. and Technol., Shizuoka University,
Hamamatsu 432-8011, Japan

²Research Institute of Electronics, Shizuoka University, Hamamatsu 432-8011, Japan

³Dept. of Electrical and Electronic Eng., Shizuoka University, Hamamatsu 432-8561, Japan

Diameter control of carbon nanotubes (CNTs), including single wall carbon nanotubes (SWCNTs) and multi wall carbon nanotubes (MWCNTs), is very important, because the characteristics of CNT change with the diameter. Since CNT structures are strongly related to catalyst nanoparticles, control of the size and density is very important issue. To control the size of catalyst nanoparticles, we performed gas-phase catalytic chemical vapor deposition (CVD) in which carbonyl iron used for the catalyst precursor. Until now, this method has been reported by many researchers for the purpose of high mass production [1,2]. In these reports, CNTs were grown by the floating growth. In this study, we are focusing on the detailed control of the nanoparticles size on the substrate by employing the gas-phase catalyst.

To form nanoparticles, organic Fe complex gas was used as a precursor. Size and density of nanoparticles can be controlled by varying the molar flow rate, decomposition temperature and flow time. The substrates were quartz and Si. The nanoparticles were formed at a substrate temperature of 600 °C. Following the formation of nanoparticles, CNTs were successively grown by thermal CVD at 800 °C. Acetylene was used as a carbon source. Figure 1(a) and (b) show AFM images of Fe nanoparticles under pressures of 1 and 2 Torr, and at flow rate of 4.4 and 2.9 $\mu\text{mol}/\text{min}$, respectively. The average particle size increases with the pressure and carbonyl iron flow rate. Figure 2 shows the SEM image of CNTs. The CNTs were vertically aligned to the substrate. The size control of catalyst nanoparticles and resulting CNT growth will be presented.

[1] P. Nikolaev, M. J. Bronikowski, R. K. Bradley, F. Rohmd, D. T. Colbert, K.A. Smith, R. E. Smalley: Chemical Phys. Lett. 313 (1999) 91-97

[2] H.M. Cheng, F. Li, X. Sun, S.D.M. Brown, M.A. Pimenta, A. Marucci, G. Dresslhaus, M.S. Dresselhaus: Chemical Phys. Lett. 289(1998) 602-610

Corresponding Author: Kenji Ohara

TEL:+81-53-478-1319 FAX:+81-53-478-1321 e-mail:k_ohara@nvr.rie.shizuoka.ac.jp

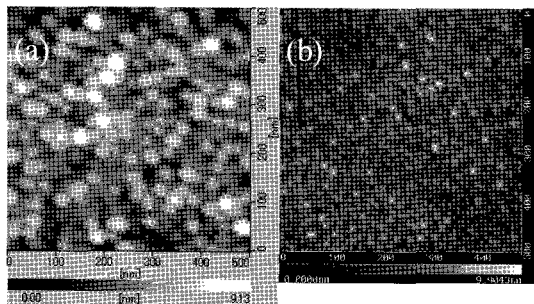


Fig.1 AFM images of Fe nanoparticles
(a):2Torr, 4.4 $\mu\text{mol}/\text{min}$ and (b):1Torr, 2.9 $\mu\text{mol}/\text{min}$

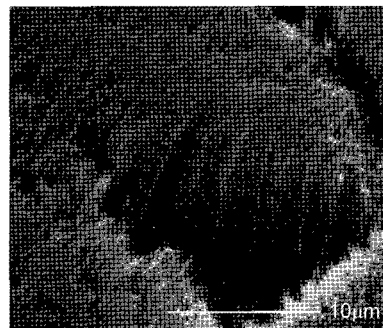


Fig.2 SEM image of CNTs

Low-temperature growth of double and single-walled carbon nanotubes on a substrate using catalyst nanoparticles size-classified with an impactor

⁰Daiyu Kondo^{1,2,3}, Shintaro Sato^{1,2,3}, Yoshitaka Yamaguchi², Taisuke Iwai^{1,2,3}, Yuji Awano^{1,2,3}

¹Fujitsu Limited, ²Nanotechnology Research Center, Fujitsu Laboratories Ltd., ³CREST/JST

Due to their peculiar electrical properties, double and single-walled carbon nanotubes (DWNTs and SWNTs) have been attracting a great deal of interest as a candidate for future electronic devices. Applying them to electronic devices such as high frequency transistors, it is important to control the chirality of DWNTs and SWNTs which determines their electrical properties. The diameter-controlled growth of DWNTs and SWNTs is the first step to such control. However, it is difficult to control their diameters using conventional metal films as a catalyst, because catalyst particles formed by annealing metal films have a wide diameter distribution in general. To overcome this problem, size-classified catalyst nanoparticles with a newly-designed impactor [1] were used. This classification method leads to a higher yield of metal catalyst nanoparticles with diameters smaller than 2 nm on a desired substrate in comparison with a method using a differential mobility analyzer [2].

Growth of DWNTs and SWNTs was performed using size-classified iron nanoparticles as a catalyst by hot-filament chemical vapor deposition (CVD). The iron nanoparticles of diameters of 1.1, 1.8 and 2.1 nm (standard deviation: ~54%, 31% and 34%) were obtained by a dry process including size-classification with an impactor. The particles were then deposited on a silicon oxide substrate. As the carbon source, a mixture of acetylene and argon gases was introduced into a CVD chamber, in which the substrate was placed. Hydrogen was also added during the growth and the substrate temperature was 590°C. After the CVD process, carbon nanotubes (CNTs) grown uniformly all over the substrate were observed using scanning electron microscopy. From the Raman spectroscopy and transmission electron microscopy, it was found that high-quality DWNTs and SWNTs were grown from iron nanoparticles with a diameter of 2.1 nm, and high-quality SWNTs grown from those with a diameter below 1.8 nm. The radial breathing modes in the Raman spectra (figure 1) show that SWNTs from nanoparticles below 1.8 nm have a narrower diameter distribution centering around 1.3 nm than those metal catalyst films (not shown). Furthermore, DWNTs from 2.1-nm nanoparticles are found to have smaller diameter than those from metal catalyst films [3].

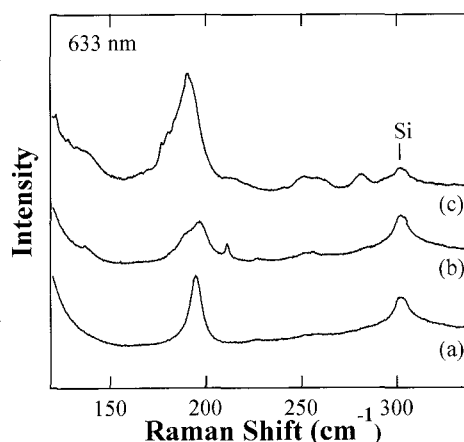


Figure 1 Raman spectra of SWNTs and DWNTs grown from nanoparticles with diameters of (a) 1.1 nm, (b) 1.8 nm and (c) 2.1nm.

References: [1]Y. Awano *et al.*, *phys. stat. sol. (a)* **203** (2006) 3611. [2]S. Sato *et al.*, *Chem. Phys. Lett.* **382** (2003) 361. [3]D. Kondo *et al.*, 2nd Korea-Japan symposium on Carbon Nanotube, 1P-06 (2005).

Corresponding Author: Daiyu Kondo

E-mail: kondo.daiyu@jp.fujitsu.com, Tel&Fax: 046-250-8234&046-248-8844

Observation of catalyst in a CVD growth process of single-walled carbon nanotubes on SiO₂

[○]Toshiya Murakami¹, Yuki Hasebe¹, Kenji Kisoda², Koji Nishio¹,
Toshiyuki Isshiki¹ and Hiroshi Harima¹

¹Department of Electronics, Kyoto Institute of Technology, Kyoto 606-8585, Japan

²Physics Department, Wakayama University, Wakayama 640-8510, Japan

Clarifying the growth mechanism of single-walled carbon nanotube (SWNT) is a key step for its future chirality-controlled growth. Rich information may be obtained by observing the correspondence between the SWNT characteristics and the growth parameters such as the carbon source, the catalyst species and the supporting material. By transmission electron microscopy (TEM), we carefully observed morphology of catalyst particles and SWNT simultaneously in the as-grown state, and considered how the catalyst formed a compound or aggregated in the growth process, and affected the growth of SWNT.

SWNTs were grown by chemical vapor deposition (CVD) at 800°C using ethanol as the carbon source and Co or Fe as the catalyst. To support the catalyst, amorphous SiO₂ powder or a SiO₂ plate thinned to less than 50 nm for TEM observation was employed. First, catalyst-related products after the growth process were analyzed by X-ray diffraction (XRD). As shown in Fig.1 for Co (upper) and Fe (lower), β-Co and Fe₂SiO₄ were mainly formed, respectively. Raman scattering and TEM observation showed that SWNT grew efficiently from Co catalyst, but not from Fe. It means that formation of iron silicate during the growth process deprived iron of the catalytic activity.

Figure 2 shows the change of TEM image of a SiO₂ substrate; loaded with Co catalyst before growth (a) and after growth (b). When the growth started, reaction of ethanol vapor with the catalyst promoted aggregation of Co to nm-sized particles. We found furthermore that large particles with size > ~6 nm showed no catalytic activity, while smaller particles with diameter < ~3 nm grew SWNT with almost the same tube diameter.

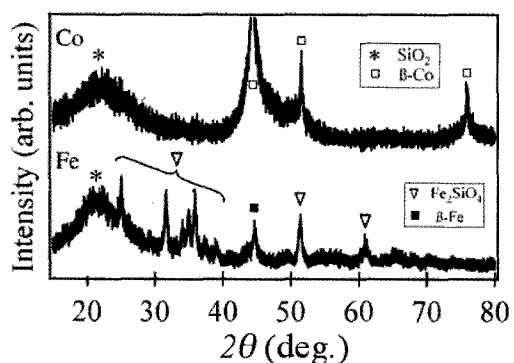


Fig. 1 XRD pattern of the samples after the growth process

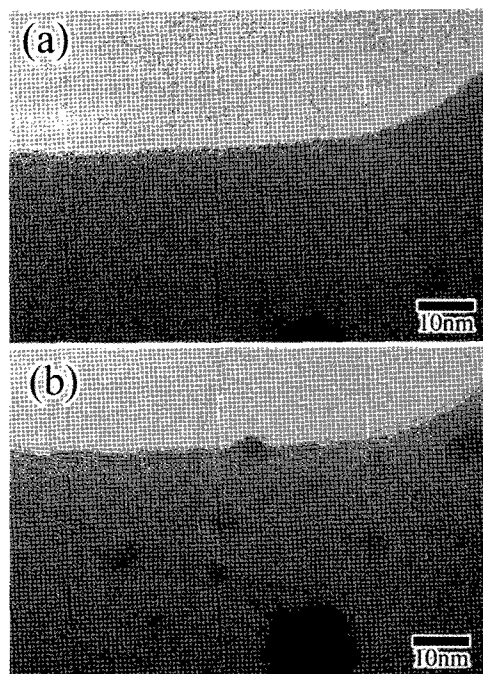


Fig. 2 TEM images of SiO₂ substrate before (a) and after growth (b).

Corresponding Author: T. Murakami, TEL: +81-75-724-7417, E-mail: d5830004@edu.kit.ac.jp

Crystal Structures of $(M_2C_2@C_{82})(C_6H_5CH_3)$ and $(M_2C_2@C_{82})(C_6H_5CH_3)_2$

○Eiji Nishibori¹, Masayuki Ishihara¹, Ikuya Terauchi¹, Shinobu Aoyagi¹, Makoto Sakata¹, Masaki Takata^{2,5}, Takashi Inoue³, Yasuhiro Ito³, Hisashi Umemoto³, Hiroe Moribe³, and Hisanori Shinohara^{3,4,5}

¹*Department of Applied Physics, Nagoya University, Nagoya 464-8603, Japan*

²*RIKEN SPring-8 Center, 1-1-1 Kouto, Sayo-cho, Sayo-gun, Hyogo 679-5148, Japan*

³*Department of Chemistry, Nagoya University, Nagoya 464-8602, Japan*

⁴*Institute for Advanced Research, Nagoya University, Nagoya 464-8602, Japan*

⁵*CREST, Japan Science and Technology Corporation, Japan*

Metal-carbide endohedral-metallofullerenes have attracted interests due to their unique structures and characteristic properties. The metallofullerene molecules are crystallized with several kinds of solvent molecule such as toluene and carbon disulfide. Previously, we have determined the crystal structures of $(M_2C_2@C_{82})(C_6H_5CH_3)$ ($M=Sc[1], Y[2]$) by synchrotron radiation (SR) powder diffraction. The ratio between fullerene and toluene molecules in the crystal so far determined was 1:1. Recently, we managed to crystallize the powder specimen of $(M_2C_2@C_{82})(C_6H_5CH_3)_2$, which has different ratio of fullerene and solvent toluene molecules, that is 1:2. In this presentation, we report a structural analysis of the $(M_2C_2@C_{82})(C_6H_5CH_3)_2$ ($M=Sc, Er, Lu$) determined from the powder specimen.

The SR X-ray powder patterns of $(M_2C_2@C_{82})(C_6H_5CH_3)_2$ ($M=Sc, Er, Lu$) were collected by Large Debye-Scheerer Camera installed at SPring-8 BL02B2. The powder patterns of $(M_2C_2@C_{82})(C_6H_5CH_3)$ ($M=Sc, Er, Lu$) were also collected for the references. The obtained data were analyzed by the MEM/Rietveld analysis.

It is found that the $M_2C_2@C_{82}$ molecules form two-dimensional layer in the $(M_2C_2@C_{82})(C_6H_5CH_3)_2$ crystal. The toluene molecules also show layer structure between the fullerene layers. It is also found that the molecular arrangement of metal-carbide metallofullerene in $(M_2C_2@C_{82})(C_6H_5CH_3)_2$ is different from that in $(M_2C_2@C_{82})(C_6H_5CH_3)$.

[1] Nishibori, E., Ishihara, M., Takata, M., Sakata, M., Ito, Y., Inoue, T., Shinohara, H., *Chem. Phys. Lett.* **433** (2006) 120-124.

[2] Nishibori, E., Narioka, S., Takata, M., Sakata, M., Inoue, T., Shinohara, H., *ChemPhysChem*, **7**(2006) 345-348.

Corresponding Author: Eiji Nishibori

TEL: +81-52-789-3702, FAX: +81-52-789-3724, E-mail: eiji@mcr.nuap.nagoya-u.ac.jp

Enhanced 1.5 μm Fluorescence from Erbium-Carbide Metallofullerenes

Yasuhiro Ito¹, Toshiya Okazaki², Shingo Ohkubo², Masahiro Akachi¹, Haruya Okimoto¹, Yutaka Ohno³, Takashi Mizutani³, Tetsuya Nakamura⁴, Ryo Kitaura^{1,5}, Toshiki Sugai^{1,5} and Hisanori Shinohara^{1,5,6}

¹Department of Chemistry and Institute for Advanced Research, Nagoya University, Nagoya 464-8602, Japan

²Research Center for Advanced Carbon Materials, National Institute of Advanced Industrial Science and Technology (AIST), Tsukuba 305-8565, Japan

³Department of Quantum Engineering, Nagoya University, Furo-cho, Chikusa-ku, Nagoya 464-8603, Japan

⁴Japan Synchrotron Radiation Research Institute, SPring-8, Sayo, Hyogo 679-5143, Japan

⁵CREST, Japan Science and Technology Agency, c/o Department of Chemistry, Nagoya University, Nagoya 464-8602, Japan

⁶Institute for Advanced Research, Nagoya University, Nagoya 464-8602, Japan

Recently, we found that $(\text{Er}_2\text{C}_2)@\text{C}_{82}(\text{III})$, an di-Er-metal-carbide fullerene, exhibits an enhanced near infrared (IR) fluorescence which is the strongest IR fluorescence among the several isomers of $\text{Er}_2@\text{C}_{82}$ and $(\text{Er}_2\text{C}_2)@\text{C}_{82}[1]$. The present optical study indicates that the encapsulated C_2 molecule does not contribute to the f - f transition of the encapsulated Er^{3+} . The insertion of the C_2 molecule into the C_{82} cage, however, induces an enlargement of the HOMO-LUMO gap of the C_{82} cage. By comparing the HOMO-LUMO energy gap of C_{82} cage and the excited ($^4\text{I}_{15/2} - ^4\text{I}_{13/2}$) electronic state gap of Er^{3+} , the mechanism of intra-fullerene energy transfer may be divided into three types, which are shown in Figure 1.

The energy transfer from the LUMO of the C_{82} cage to $^4\text{I}_{13/2}$ level in encapsulated Er^{3+} is the most efficient process (Type 1). The energy transfer from the C_{82} cage to Er^{3+} and the relaxation to the HOMO of C_{82} may occur simultaneously (Type 2), which induces the reduction of the efficiency of energy transfer from the C_{82} cage to Er^{3+} . Vibrationally excited HOMO states of the C_{82} cage may rapidly decay nonradiatively to the LUMO state without the energy transfer to Er^{3+} (Type 3).

In any of these fluorescence mechanisms, the HOMO-LUMO gap of the C_{82} cage plays a crucial in inducing the IR fluorescence of Er-dimetallofullerenes. If the HOMO-LUMO gap can be varied by reduction/oxidation or chemical derivatization, the corresponding IR fluorescence can be obtained even from mono-Er-metallofullerenes such as $\text{Er}@\text{C}_{82}$, in which no such IR fluorescence has been obtained so far.

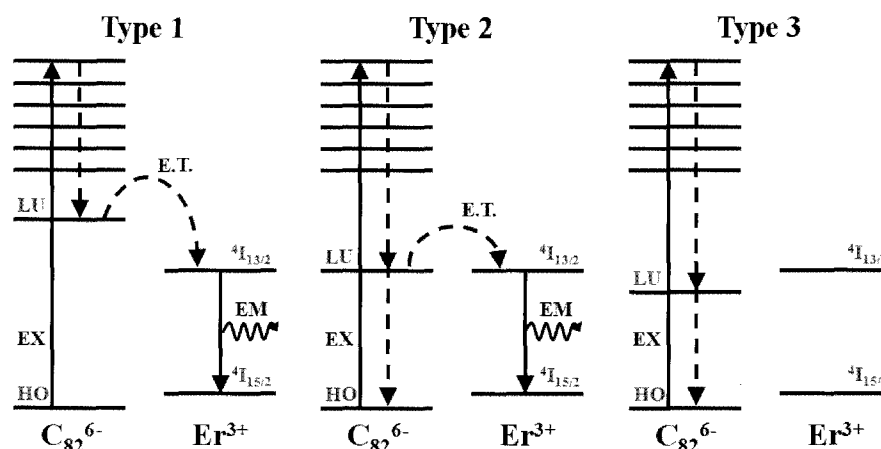


Figure 1. Schematic Energy Diagrams for the observed IR fluorescence of Er-dimetallofullerenes. Type 1, 2, 3 may be applied to $(\text{Er}_2\text{C}_2)@\text{C}_{82}(\text{III})$, $\text{Er}_2@\text{C}_{82}(\text{I, III})$ and $(\text{Er}_2\text{C}_2)@\text{C}_{82}(\text{I})$, $\text{Er}_2@\text{C}_{82}(\text{II})$ and $(\text{Er}_2\text{C}_2)@\text{C}_{82}(\text{II})$ cases, respectively.

References

[1] Y. Ito *et al.*, 31st Fullerene-Nanotube General Symposium, 2P-15 (2006).

Corresponding Author: Hisanori Shinohara **E-mail:** Noris@cc.nagoya-u.ac.jp **Tel/Fax:** +81-52-789-2482/1169

Titan Satellite Would Be a Carbon-Cluster Factory in Space – From Explosive-Reaction Experiment –

○Tetsu Mieno¹, Sunao Hasegawa²

¹*Dept. Physics, Shizuoka University. Ooya, Suruga-ku Shizuoka-shi 422-8529, Japan*

²*Inst. Space & Astronautical Science, JAXA, Sagami-hara-shi, Kanagawa, 229-8510, Japan*

Huge amount of carbon atoms have been produced in fixed stars and they are diffusing into cosmic space. From the successful exploration of Cassini mission to Titan satellite by NASA, we could recognize huge methane-seas on the surface of Titan. [1] From these pioneer explorations, we expect that Titan is a carbon-cluster factory in space. As the surface temperature of Titan is low, coming methane molecules are stored as liquid or solid in nitrogen atmosphere. As there were large number of collisions by space asteroids and debris, explosive reactions by these collisions have been naturally carried out on Titan, which would make many kinds of carbon clusters and hydro-carbon molecules. Main parts of these products are stored on the Titan's surface, and a part was flown off into space (inter-stellar region) and diffused to another stars. Therefore, we expect that many kinds of carbon clusters are stored in Titan's methane seas.

In order to simulate this collisional explosion-reaction, a 2-stage light-gas gun and a rail gun set in ISAS/JAXA are used. In the gas-gun experiment, a stainless-steel ball (3 mm ϕ) is accelerated in a metal tube to 3.7 km/s and it hits a surface of a metal substrate, which makes large explosion and the surface materials are blown off. When the ball hits on liquid propanol in 1 atm of He gas, it blows off the liquid. After this explosion, produced carbon soot is carefully collected and analyzed by a laser-desorption TOF mass-analyzer. Figure 1 shows a obtained mass spectrum of this soot. We can clearly confirm that higher-fullerenes are produced by this reaction. When we use a rail-gun, and a poly-carbonate projectile is accelerated by electro-magnetic force to about 6 km/s, which hits a surface of a stainless steel target. A large explosion takes place and a big crater is formed. From this reaction we could find production of fullerenes, [2] carbon capsules and balloon-like carbons.

From the simulation experiment, we can expect that many kinds of carbon clusters were produced and stored on the surface of Titan satellite.

[1] See a homepage of "NASA Cassini mission". [2] T. Mieno, A. Yamori, *Jpn. J. Appl. Phys.* **45** (2006) 2768.

Corresponding Author: Tetsu Mieno

E-mail: piero@sannet.ne.jp,

Tel & Fax: +81-54-238-4750



Fig. 2. The ISAS gas-gun.

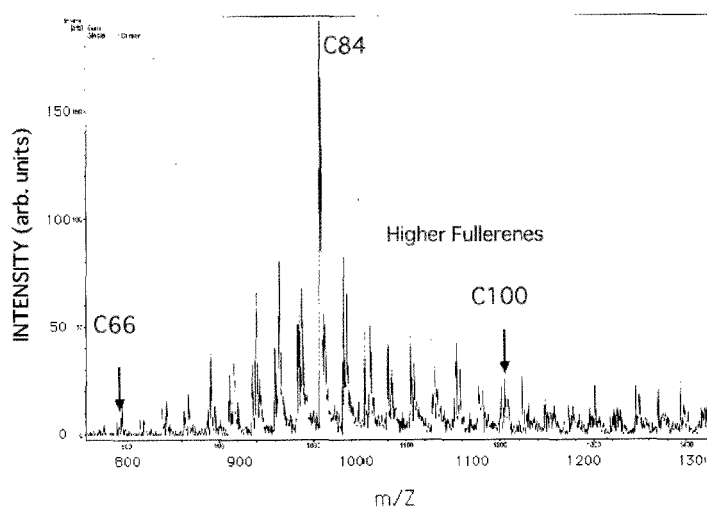


Fig. 1. A mass spectrum of the soot by a LD-TOF-MS.

Photo-Induced Charge-Separation of Supramolecular SWNT-Fullerene Hybrids in Polar Solvent

○ Osamu Ito^{1,3}, Yasuyuki Araki¹, Atula Sandanayaka^{1,4}, Raghu Chitta², Francis D'Souza²

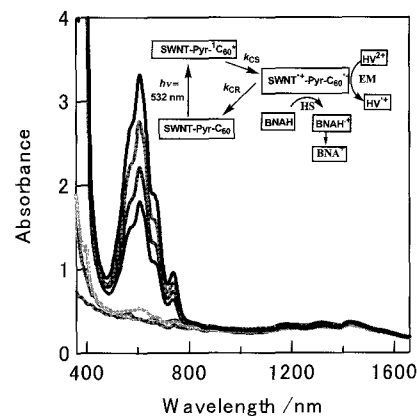
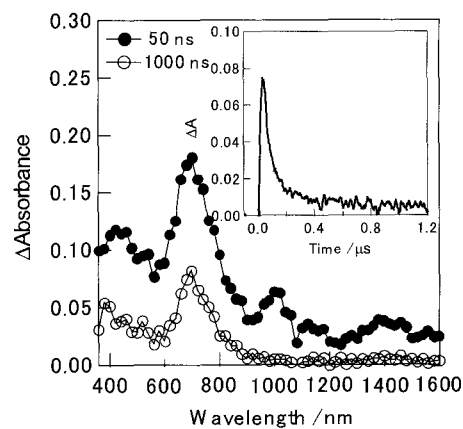
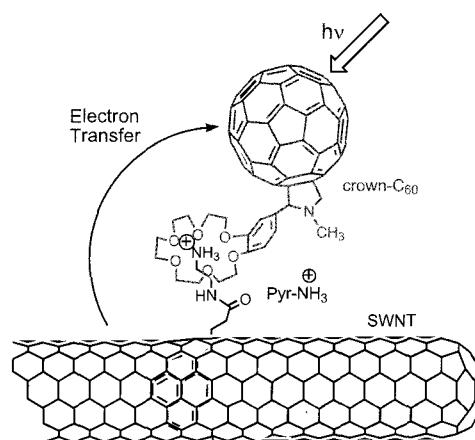
¹IMRAM, Tohoku University, Sendai 980-8577, Japan

²Department of Chemistry, Wichita State University, Kansas 67260-0051, USA

³CarbonPhotoScience, Sendai, Japan

⁴School of Material Science, JAIST, Ishikawa 923-1292, Japan

In order to spread the utilization of SWNTs, we have studied the light-induced processes. Here, SWNTs were noncovalently functionalized using alkyl ammonium functionalized pyrene (PyrNH₃⁺) to form SWNT/PyrNH₃⁺, to which crown-C₆₀ was added to yield SWNT/Pyr-NH₃⁺/crown-C₆₀ (See right Scheme). The nanohybrids were characterized by HR-TEM, UV-visible-near IR and electrochemical methods. Free energy calculations suggested charge-separation from SWNTs to the singlet excited C₆₀ (¹C₆₀^{*}) in the SWNT/Pyr-NH₃⁺/crown-C₆₀ in polar solvents. The fluorescence studies revealed efficient quenching of ¹C₆₀^{*} in the nanohybrids. Nanosecond transient absorption studies confirmed charge-separation mechanism, in which C₆₀ anion radical was spectrally characterized at 1000 nm (see right figure). The rates of charge separation, k_{CS} and charge recombination, k_{CR} were found to be $3.5 \times 10^9 \text{ s}^{-1}$ and $1.0 \times 10^7 \text{ s}^{-1}$, respectively, in DMF. The calculated lifetime of the radical ion-pair was found to be over 100 ns suggesting charge stabilization in this novel supramolecular nanohybrids. The generated radical ion-pair of the nanohybrids was further utilized to pump up an excess electron on C₆₀ to hexyl-viologen dication (HV²⁺) in the presence of appropriate a hole shifting reagent in solution. Accumulation of the radical cation of HV²⁺ at 610 nm as an evidence of electron pooling was observed (see right figure), which confirms the photoinduced charge-separation, suggesting utilizations of SWNT/Pyr-NH₃⁺/crown-C₆₀ in light energy harvesting applications.



[1] Chitta, R.; Sandanayaka, A. S. D.; Schumacher, A. L.; D'Souza, L.; Araki, Y.; Ito, O.; D'Souza, F. *J. Phys. Chem. C* **2007**, *111*, 6947-6955.

Corresponding Author: Osamu Ito

TEL (& FAX): +81-22-376-5970, E-mail: ito@tagen.tohoku.ac.jp

Optical Enrichment of SWNTs

○Xiaobin Peng^{1,2}, Naoki Komatsu¹, Takahide Kimura¹, and Atsuhiko Osuka³

¹Department of Chemistry, Shiga University of Medical Science, Seta, Otsu 520-2192, Japan,

²International Innovation Center, Kyoto University, Nishikyo-ku, Kyoto 615-8520, Japan,

³Department of Chemistry, Graduate School of Science, Kyoto University, Sakyo-ku, Kyoto 606-8502, Japan

At the last two conferences, we reported the optically active SWNTs obtained through the preferential extraction of the left- or right-handed structure of SWNTs with chiral diporphyrin nano-tweezers (Fig. 1), and the enhanced ability of the tweezers for extracting and discriminating SWNTs by changing the spacer unit from benzene (**1**) to pyridine (**2**) [1]. Herein, chiral diporphyrins linked with carbazole (**3**) and dibenzothiophene (**4**) are newly designed, synthesized and examined for optical enrichment of SWNTs.

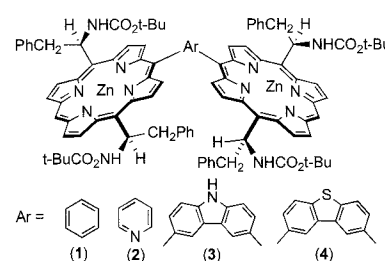


Fig. 1 Diporphyrin nano-tweezers with different spacers ((*R*)-**1** – **4**).

After the porphyrin nano-tweezers was removed completely from the porphyrin-SWNTs complexes, pairs of symmetrical CD spectra were obtained from the D₂O/SDBS solutions of the SWNTs extracted with (*R*)- and (*S*)-**3** (Fig. 2b), and (*R*)- and (*S*)-**4** as in the case of those with **1** and **2** (Fig. 2a). The CD intensity of (7,5) SWNTs is largest in the spectra of SWNTs extracted with **3** (Fig. 2b) and **4**, while **2** showed higher discriminating ability to (6,5) SWNTs than that to other chiralities of SWNTs (Fig. 2a). These results indicate that optical enrichment of the specific chiral SWNTs can be realized by choosing appropriate chiral nano-tweezers.

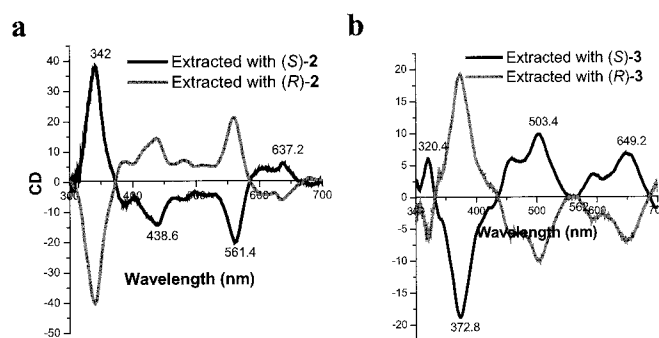


Fig. 2. CD spectra of SWNTs extracted with (*R*)- and (*S*)-nano-tweezers **2** (a) and **3** (b).

References: [1] X. Peng, *et al*, The 31st and 32nd Fullerene-Nanotubes General Symposium; X. Peng, N. Komatsu, *et al*, *Nature Nanotechnology*, advance online publication.

Corresponding Author: Xiaobin Peng,

TEL: +81-77-548-2102, FAX: +81-77-548-2354, E-mail: xiaobin@belle.shiga-med.ac.jp

Transparent Carbon Nanotubes for Encapsulated Dyes

-Toward the complete separation of metallic and semiconducting SWCNTs-

○K. Yanagi, Y. Miyata, H. Kataura

Nanotechnology Research Institute, National Institute of Advanced Industrial Science and Technology (AIST)

Abstract: Complete separation of metallic and semiconducting single-wall carbon nanotubes (SWCNTs) from their mixture is one of the most important subjects for applications of SWCNTs. Recently, Arnold et al.¹ suggested a sorting method of SWCNTs from the mixture through density-gradient centrifugation. In this study, with additional improvements to their method, a technique to obtain a large amount of SWCNTs of a single electronic type [metallic (or semiconducting) purity is ~99%] was developed (Fig. 1). The technique enables us to investigate their intrinsic properties under the cover of the mixture situation. For example, although dye molecules do exhibit remarkable photophysical properties inside SWCNTs,² efficient photoexcitation of the encapsulated dyes was difficult in the mixture. To overcome this problem, dyes encapsulated SWCNTs of a single electronic type were prepared using our sorting method. β -Carotene, which is a model for one dimensional π -conjugated molecules, encapsulated into metallic or semiconducting SWCNTs (Car@Metal_{cnt} and Car@Semi_{cnt}) were selectively obtained. The absorption band of encapsulated β -Carotene is located in a region where metallic tubes have a low extinction coefficient. This situation enables resonant excitation of β -Carotene at an off-resonance condition for its surrounding tubes in Car@Metal_{cnt}. Figure 2 shows the Raman spectra of Car@Metal_{cnt} and Car@Semi_{cnt}. Compared with negligibly small Raman signals caused by SWCNTs, signals originating from encapsulated β -Carotene were significantly large in Car@Metal_{cnt}, indicating the transparency of the surrounding tubes for encapsulated dye molecules.

References: [1] Arnold et al., *Nature Nano.*, **1** (2006) 60, [2] Yanagi et al., *JACS*, **129** (2007) 4992.

Corresponding Author: K. Yanagi, E-mail: k-yanagi@aist.go.jp, Tel&Fax: 029-861-3132, 029-861-2786

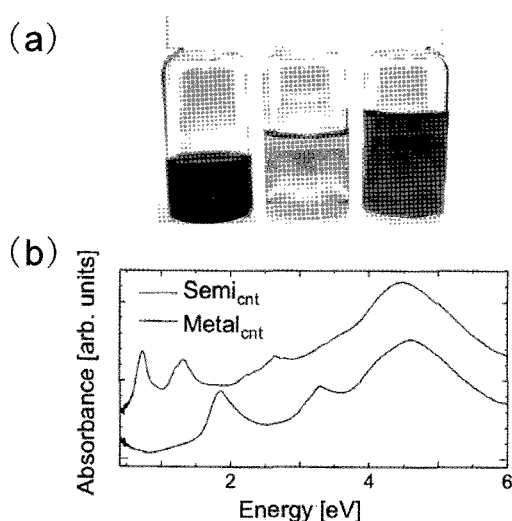


Fig. 1 (a) The colors of pristine (left), metallic (Metal_{cnt}, center), and semiconducting (Semi_{cnt}, right) SWCNT solutions. (b) Absorption spectra of thin films of Metal_{cnt} and Semi_{cnt}.

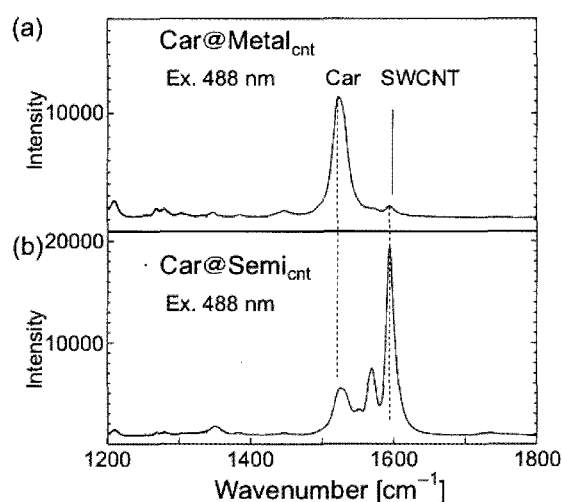


Fig. 2. Raman spectra of (a) Car@Metal_{cnt} and (b) Car@Semi_{cnt} at 488 nm excitation.

Imaging of single alkyl chains in carbon nanotubes by transmission electron microscopy

○Masanori Koshino,^{1,2} Takatsugu Tanaka,³ Niclas Solin,³ Kazutomo Suenaga,²
Hiroyuki Isoe,⁴ Eiichi Nakamura,^{1,3}

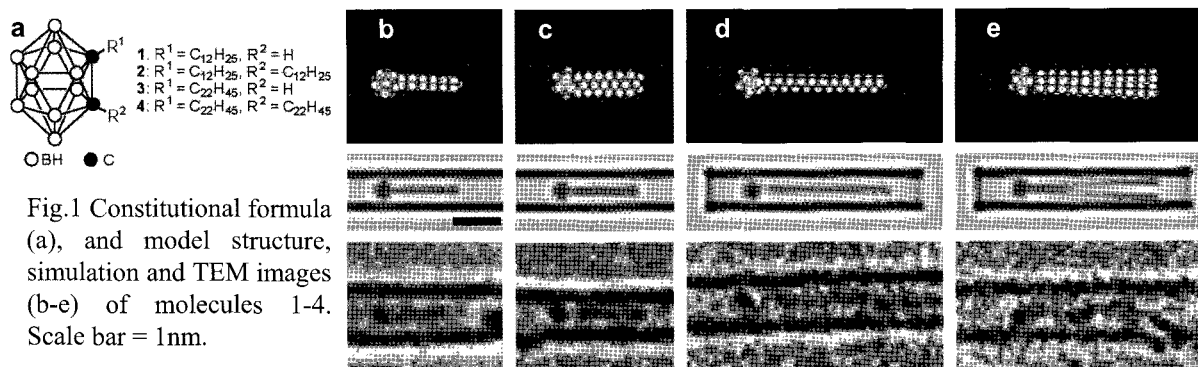
¹ERATO, Nakamura Functional Carbon Cluster Project, JST, ²Research Centre for Advanced Carbon Materials, National Institute of Advanced Industrial Science and Technology (AIST), Higashi, Tsukuba, Ibaraki 305-8565, Japan. ³Department of Chemistry, The University of Tokyo, Hongo, Bunkyo-ku, Tokyo 113-0033, Japan. ⁴Department of Chemistry, Tohoku University, Aoba-ku, Sendai 980-8578 Japan

For organic compounds, the assumed high sensitivity of light elements such as hydrocarbons to damage by electron impact has discouraged previous exploration by transmission electron microscopy (TEM)^[1]. We recently reported, with near-atomic resolution (2.4 Å resolution), the observation of a single small organic molecule either at rest or translating within a single-wall carbon nanotube (CNT) by TEM^[2].

We chose, for this proof-of-principle study, molecules 1-4 with hydrocarbon chains covalently attached to an ortho-carborane end group (Fig.1a; C₂B₁₀H₁₂, ca. 0.8 nm diameter), which serves as a tag for identification by its characteristic element and shape. As the molecular container, we chose a mixture of CNTs with diameters of 0.9 to 1.2 nm, from which we could combinatorially investigate size matching between the host and guest.

Under the condition of room temperature TEM (120 kV) with 0.5 s electron irradiation (~40,000 e⁻/nm²) imaging intervals, the alkyl chain molecules 1-4 in narrow CNTs were immobilized and its head/tail structure was clearly visualized (Fig.1b-e) over several seconds to a minute. The measured length of alkyl chains (C₁₂ and C₂₂) and image contrast between the head and tail structures agree very well with the simulation. Electron energy loss spectroscopy (EELS) analysis supported the presence of carborane.

These results highlight the unanticipated utility of TEM for single-molecule chemical analysis relevant to fundamental reactivity as well as to engineering applications, such as tribology and gas absorption/storage in activated carbon. The mechanism of the electron impact on the organic molecules in CNTs is not fully understood, but the applied method, i.e. isolation of molecules in inert CNT that has high thermal and electron conductivity, must contribute to the stability of guest molecules under the TEM observation.



References: [1] R. F. Egerton, *et al.*, *Micron* **2004**, 35, 399. [2] M. Koshino, *et al.*, *Science* **2007**, 316, 853.

Corresponding Author: M. Koshino, E-mail: m-koshino@aist.go.jp

Tel&Fax: +81(0)29-861-4424, +81(0)29-861-4415

Fabrication of ZnPc-Nanohorn-Protein Nanohybrid for Photodynamic Therapy

OM. Zhang¹, M. Yudasaka^{1,2}, K. Ajima¹, J. Miyawaki¹, S. Iijima^{1,2,3}

¹*SORST-JST, c/o NEC, 34 Miyukigaoka, Tsukuba, Ibaraki 305-8501, Japan*

²*NEC, 34 Miyukigaoka, Tsukuba, Ibaraki 305-8501, Japan*

³*Meijo Univ. 1-501 Shiogamaguchi, Tenpaku-ku, Nagoya 468-8502, Japan*

Photodynamic therapy (PDT) is an innovative treatment for several types of cancers and noncancer diseases. This therapy utilizes photosensitizing agents that absorb light and generate cytotoxic species. Zinc phthalocyanine (ZnPc) is a promising PDT agent due to its strong optical absorption in the phototherapeutic window (600-800 nm) and high efficiency in generating cytotoxic species. However, ZnPc is hydrophobic and prone to self-aggregate in aqueous solutions, which limit its delivery and photosensitizing efficiency. Thus, it must be administered in vivo by means of delivery system. Comparing with other drug carriers such as liposomes, single-wall carbon nanohorns (SWNHs) are π -electron conjugated material, and can have holes on the walls by the oxidation, which allow ZnPc to adsorb on the SWNH-walls, and even enter inside SWNHs, thereby the self-aggregation is avoided. In addition, the solubility of SWNHs in aqueous solution can be enhanced by modification with BSA protein as we proved in the previous study [1]. Therefore, BSA modified SWNHs is favorable to carry ZnPc for PDT.

For loading ZnPc, we first treated SWNHs by light assisted oxidation using H_2O_2 to open holes and generate carboxylic groups at the holes edges. Then the SWNHs were immersed in a ZnPc-saturated solution followed by filtration. After loading of ZnPc, the SWNHs were chemically modified with BSA via diimide-activated amidation. The obtained ZnPc-SWNH-BSA was well dispersed in phosphate buffered saline (PBS) and its homogeneous dispersion state was kept for several weeks. When the rat cancer cells were incubated with the culture medium solution containing ZnPc-SWNH-BSA for about 24 h, the confocal microscopy and flow cytometry results indicated that the ZnPc-SWNH-BSA could get inside of almost rat cancer cells. Because of such effective uptake of ZnPc-SWNH-BSA by the cells, the light irradiation (about 60 mW/cm², wavelength of 600-700 nm) for 5 minutes made the cell to die (Fig.1). This proves that the bio-inorganic nanohybrid of ZnPc-SWNH-BSA is potentially useful in the photodynamic therapy.

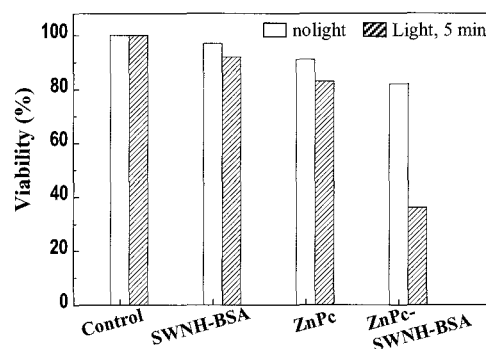


Fig. 1 Viability of rat cancer cells incubated with ZnPc-SWNH-BSA under light (600-700 nm) irradiation for 5 minutes.

References

[1] Zhang, M.; Yudasaka, M.; Ajima, K.; Iijima, S. 32 th F-NT symposium, 2-14.

Corresponding authors: M. Zhang, minfang@frl.cl.nec.co.jp, M. Yudasaka, yudasaka@frl.cl.nec.co.jp
Tel: 0081-29-856-1940, Fax: 0081-298-50-1366

Carbon Nanotube Growth from Semiconductor Nanoparticles

○Daisuke Takagi^{1,3}, Hiroki Hibino², Satoru Suzuki^{2,3},
Yoshihiro Kobayashi^{2,3}, Yoshikazu Homma^{1,3}

¹*Department of Physics, Tokyo University of Science, Shinjuku, Tokyo 162-8601, Japan*

²*NTT Basic Research Laboratories, NTT Corporation, Atsugi, Kanagawa 243-0198, Japan*

³*CREST, JST, Kawaguchi, Saitama 332-0012, Japan*

In this report, we show that semiconductor (SiC, Ge, and Si) nanoparticles can produce carbon nanotubes (CNTs) as catalyst.

The size of semiconductor particles is the key to CNT synthesis (1-5 nm). To obtain small crystalline semiconductor particles, we used the epitaxial relationship between particles and substrates. We monitored the formation process of crystalline particles by reflection high-energy electron diffraction (RHEED) in an ultrahigh vacuum (UHV) and terminated the formation process at the initial growth stage. SiC nanoparticles were formed on Si(111) substrate, and Ge and Si nanoparticles were formed on SiC(0001) substrates. CNTs were synthesized by alcohol chemical vapor deposition. The grown CNTs and catalyst particles were characterized by SEM, TEM, AFM, and Raman spectroscopy.

Figure 1a is a RHEED pattern from SiC nanoparticles on Si substrate. The transmission diffraction spots, one of which is denoted by an arrow, indicate that SiC(111) crystalline particles were epitaxially formed on the Si(111)7×7 substrate. The AFM image of the surface in Fig. 1b shows that the SiC nanoparticle size is less than 5 nm. Double- and single-walled carbon nanotube (DWCNT and SWCNT) growth was confirmed from TEM images (Fig. 1c). In the Raman scattering spectra (Fig. 1d), signals due to the radial breathing mode (RBM) indicate that metallic and semiconducting SWCNTs can be synthesized from semiconductor SiC nanoparticles. CNTs were also synthesized from Ge and Si crystalline nanoparticles.

For the CNT synthesis, metal particles, such as iron, platinum, and gold, have been used¹. As an interpretation of the metal-catalyzed CNT growth mechanism, the vapor-liquid-solid model has been proposed. On the other hand, SiC is a high-melting-point semiconductor material, and we confirmed from RHEED that SiC nanoparticles remained solid in the UHV even at 1000 °C, which is much higher than the CNT growth temperature (850 °C). This indicates that CNTs grow from the solid catalyst surface. The present results mean that CNTs can be synthesized from nanosize structures, regardless of species (metal or semiconductor) and phase (liquid or solid). The essential role of the catalyst particles would be the provision of a template for CNT cap nucleation.

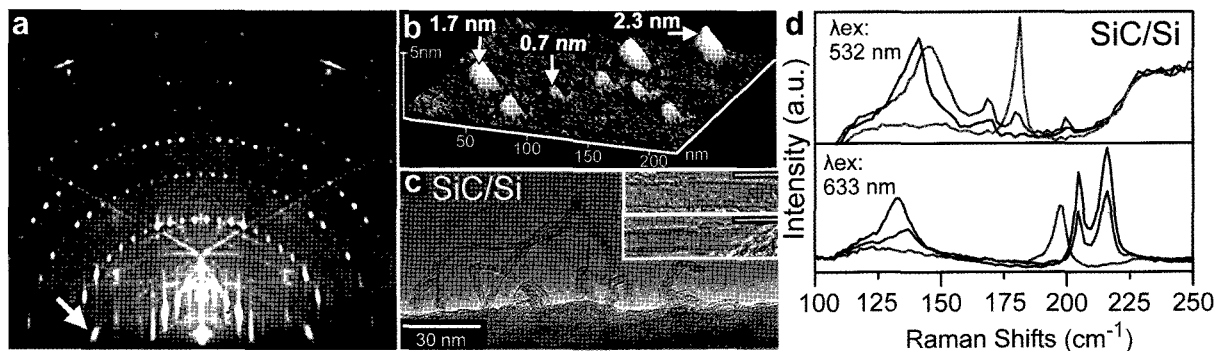


Fig.1. (a) RHEED pattern of epitaxially-grown SiC nanoparticles on Si(111)7×7. (b) AFM image of SiC nanoparticles. (c) TEM image of grown CNTs (inset scale bars: 5 nm). (d) Raman spectra from grown CNTs.

[1] D. Takagi, *et al.*, *Nano Lett.*, **2006**, *6*, 2642-2645.

Corresponding Author: Daisuke Takagi

TEL: +81-3-5228-8244, FAX +81-3-5261-1023, E-mail: daisuke@will.brl.ntt.co.jp

Ion Mobility Measurement with a Newly Developed Pulsed Ion Valve

○T. Sugai¹, H. Shinohara^{1,2,3}

¹*Department of Chemistry (RCMS), Nagoya University*

²*Institute for Advanced Research, Nagoya University*

³*CREST, Japan Science and Technology Agency*

Ion mobility measurements on fullerenes have clarified novel carbide structures and formation processes[1,2]. These achievements are accomplished by the high sensitivity and the high measurement throughput of the method. However, the mobility or structural resolution and upper mass limitation prevent us to apply this method to fullerene isomer identification and nanotube growth observation. To overcome these limitations, we have developed a pulsed ion valve (PIV), which is the key interface to couple a high-pressure drift cell (DC) to a high-vacuum time of flight mass spectrometer (TOF). Here we present the mobility measurement with this system and the expected resolution to identify fullerene isomers.

The measurement system consists of a laser desorption ion source, PIV, and TOF. The mobility measurements were performed with the air origin ions produced by the laser. The ionization point was 60 mm apart from PIV where 1 kV was applied. The ions were introduced from the air side into TOF through PIV only when the PIV opening timing was set after 1 ms of the ion production showing that the drift velocity is around 60 m/s(Fig. 1).

The PIV worked at more than 10 atm, where we expect to separate C₈₂ isomers in 200 ms together with a drift cell length of 1 m and a drift voltage of 100 kV(Fig. 2). With this PIV, we are planning to explore new structures of fullerenes and to observe the nanotube growth processes utilizing this HPLC level resolution.

References:

[1] T. Sugai *et al.*, *J. Am. Chem. Soc.* **123**, 6427 (2001).

[2] von Helden *et al.*, *J. Chem. Phys.* **95**, 3835 (1991).

e-mail: sugai@nano.chem.nagoya-u.ac.jp tel:

+81-52-789-2477 fax: +81-52-789-1169

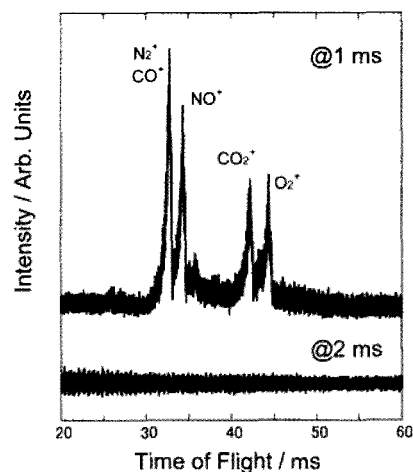


Fig. 1 PIV timing dependence

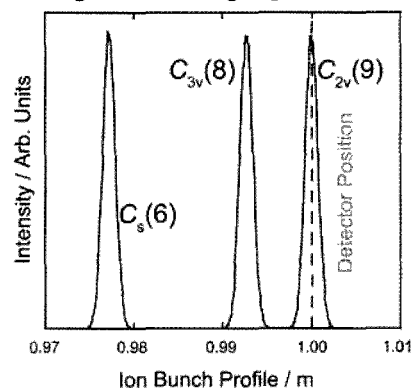


Fig. 2 Expected Resolution for C₈₂

HRTEM observation of an Individual C₆₀ Fullerene Molecule and its Deformation Process

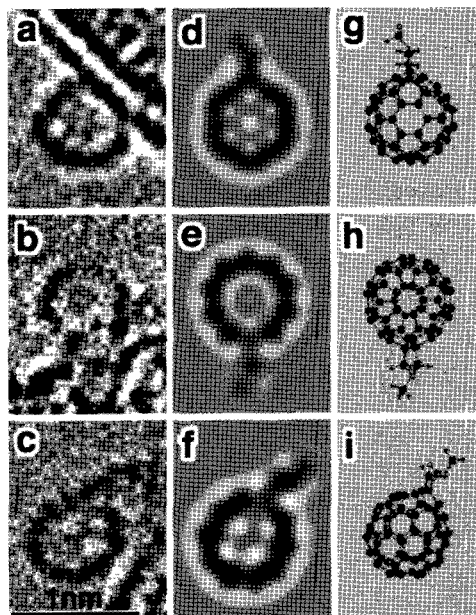
○Zheng Liu¹, Kazu Suenaga¹, Aleš Mrzel², Hiromichi Kataura² and Sumio Iijima¹

¹Research Center for Advanced Carbon Materials, National Institute of Advanced Industrial Science and Technology (AIST), Tsukuba, 305-8565, Japan

²Nanotechnology Research Institute, National Institute of Advanced Industrial Science and Technology (AIST), Tsukuba, 305-8562, Japan

The fullerene molecules (C₆₀) with a functional group of C₃NH₇ (C₆₀-C₃NH₇), which are prepared by following the Prato reaction¹, confined inside single-wall carbon nanotubes (SWNTs) have already been visualized.² However, higher spatial resolution is definitively required to visualize the intramolecular structure of fullerenes. Since the resolution of TEM is determined by the spherical aberration coefficient (C_s) of objective lens and the wave length (λ) of incident electron beam, the C_s must be minimized to achieve the best performance because the reduction of the λ (equal to elevate the accelerating voltage) causes beam damage to the carbon materials. A high-resolution transmission electron microscope (HRTEM, JEM-2010F) equipped with a C_s corrector (CEOS)³ was operated at a moderate accelerating voltage (120kV). Although the point resolution of 0.14 nm was obtained, HRTEM simulations were necessary in order to investigate the images of fullerenes taken under different projections. SWNT is used as a specimen support in this experiment. We observed

the fullerene molecules which were located on the surface of the SWNTs perpendicular to the incident electron beam (not the ones inside the SWNTs), so that the carbon network of the SWNT does not interfere in the direct imaging of the fullerene intramolecular structures by HRTEM. For this purpose the C₆₀ fullerenes were chemically functionalized with pyrrolidine¹ so that the functional groups attached to each fullerene molecule should act as anchors² and the functionalized C₆₀ fullerenes are relatively stabilized on the surface of SWNT during the TEM observations. In this work, the intramolecular structure, such as pentagons and hexagons, of the individual C₆₀ fullerene was visualized (shown in the figure). The deformation of C₆₀ fullerene due to the electron irradiation was also investigated. Three C₅₈ molecules with C₁ symmetry are depicted as reasonably well fitted models.



a-c) HRTEM images of C₆₀-C₃NH₇ attached to the surface of SWNTs. The intra-molecular structures are clearly visible for each fullerene. d-f) Image simulations of C₆₀ fullerene derivatives for various orientations and the corresponding atomic models (g-i).

References

- (1) Prato, M. et al., *Tetrahedron* **1996**, 52, 5221.
- (2) Liu, Z. et al., *Phys. Rev. Lett.* **2006**, 96, 088304.
- (3) Haider, M. et al., *Nature* **1998**, 392, 768.

Corresponding Author: Zheng Liu

E-mail: liu-z@aist.go.jp

Tel: 029-861-2514

Fax: 029-861-4806

Positional Control of Encapsulated Metal Atoms Inside a Fullerene Cage by Exohedral Chemical Functionalization

○ Michio Yamada,¹ Chika Someya,¹ Takatsugu Wakahara,¹ Takahiro Tsuchiya,¹ Takeshi Akasaka,¹ Yutaka Maeda,² Kenji Yoza,³ Naomi Mizorogi,⁴ and Shigeru Nagase⁴

¹Center for Tsukuba Advanced Research Alliance, University of Tsukuba, Tsukuba, Ibaraki 305-8577, Japan ²Department of Chemistry, Tokyo Gakugei University, Koganei, Tokyo 184-8501, Japan ³Bruker AXS K. K., Yokohama, Kanagawa 221-0022, Japan ⁴Institute for Molecular Science, Okazaki, Aichi 444-8585, Japan

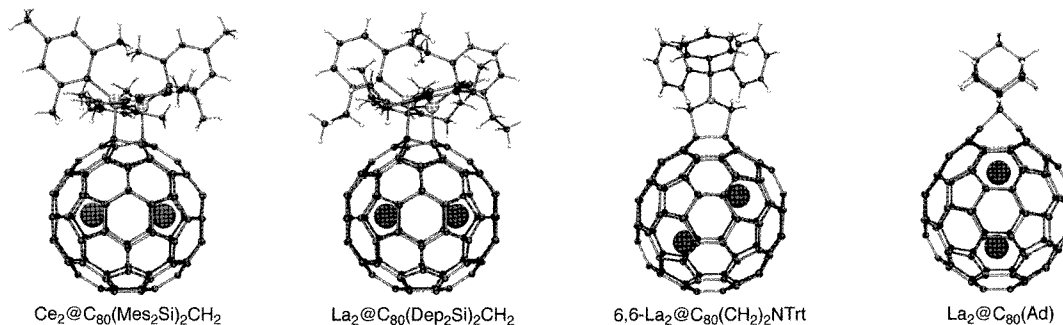
Among many kinds of metallofullerenes,¹ $M_2@C_{80}$ has attracted special attention for the dynamics of the encapsulated metal atoms because of their three-dimensional random motion.² Positional control of the metal atoms within a cage is expected to be very valuable in designing functional molecular devices with new electronic or magnetic properties.

We successfully prepared an exohedrally silylated $Ce_2@C_{80}$, $Ce_2@C_{80}(Mes_2Si)_2CH_2$, in which the random motion of two Ce atoms is fixed at specific positions. We also synthesized an exohedrally silylated $La_2@C_{80}$, $La_2@C_{80}(Dep_2Si)_2CH_2$, in which the two La atoms hop two-dimensionally along the equator of the cage.⁴ These results reveal that exohedral functionalization of the fullerene surface can regulate the motion of the metal atoms drastically.

It is very interesting to know what controls the dynamic behavior of the metal atoms. We synthesized and characterized two regioisomers of endohedral pyrrolidinometallofullerene, $La_2@C_{80}(CH_2)_2NTrt$.⁵ We revealed that two La atoms in 6,6-closed adduct are localized at the slantwise position. Meanwhile, theoretical calculation for the 5,6-closed adduct suggests that two La atoms can rotate rather freely. These results indicate that the motion of the metal atoms is controllable by addition position of the addends.

Furthermore, we found that the selective addition of the adamantylidene carbene occurs at the 6,6-junction of the $M_2@C_{80}$ ($M = La \& Ce$) to afford the formation of 6,6-open adduct, $M_2@C_{80}(Ad)$.⁶ The location of the metal atoms is regulated below the Ad group.

From the viewpoint of designing functional molecular devices, it is important to regulate the metal position to the desirable one inside the cage. We expect this study enhances the possibilities for the application of metallofullerenes.



[1] Akasaka, T.; Nagase, S. *Endofullerenes: A New Family of Carbon Clusters*; Kluwer: Dordrecht, The Netherlands, 2002. [2] Akasaka, T. et al. *Angew. Chem., Int. Ed. Engl.* **1997**, *36*, 1643. [3] Yamada, M. et al. *J. Am. Chem. Soc.* **2005**, *127*, 14570. [4] Wakahara, T. et al. *Chem. Commun.* **2007**, in press. [5] Yamada, M. et al. *J. Am. Chem. Soc.* **2006**, *128*, 1402. [6] Yamada, M. et al. submitted.

Corresponding Author: Takeshi Akasaka, **Tel&Fax:** +81-29-853-6409, **E-mail:** akasaka@tara.tsukuba.ac.jp

Syntheses, Structures and Optical Properties of Dodeca- and Trideca(organo)[60]fullerenes

○Takeshi Fujita¹, Yutaka Matsuo², Eiichi Nakamura^{1,2}

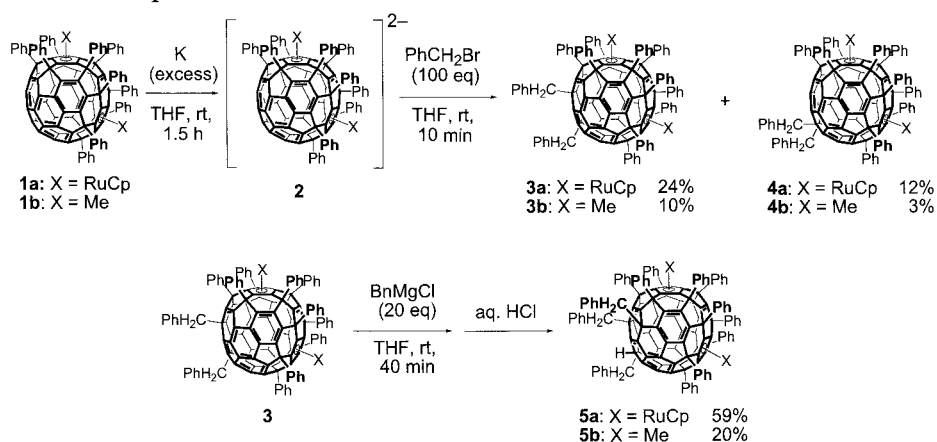
¹*Department of Chemistry, The University of Tokyo, Hongo, Bunkyo-ku, Tokyo 113-0033, Japan*

²*Nakamura Functional Carbon Cluster Project, ERATO, Japan Science and Technology Agency (JST), Hongo, Bunkyo-ku, Tokyo 113-0033, Japan*

The detraction of the π -electron conjugated system for [60]fullerene by functionalization is a powerful method to construct new hoop- and bowl-shaped π systems[1]. Such compounds showed unique luminescence by changing electronic structures of [60]fullerene[2]. Herein we report on syntheses, structural determination, and optical properties of dodeca- and trideca(organo)[60]fullerenes bearing new curved π systems.

Treatment of decaadducts $C_{60}Ph_{10}X_2$ (**1a**: X = C_5H_5Ru ; **1b**: X = Me) with potassium metal afforded dianions **2**, which were trapped with an excess amount of benzyl bromide to give two kinds of dodecaadducts **3** and **4**. The sequential nucleophilic addition reaction of benzylmagnesium chloride to **3** afforded tridecaadduct $C_{60}Ph_{10}X_2(CH_2Ph)_3H$ (**5**). Unambiguous structural determination of dodeca- and tridecaadducts were achieved by X-ray crystallographic analysis with ruthenium complex **3a**, **4a**, and **5a**. Dodecaadduct **3a** and **4a** has C_1 and C_{2v} symmetry. Tridecaadduct **5a** has an indene part surrounded by three benzyl groups. Dodecaadducts **3b** and **4b** and tridecaadduct **5b** exhibited characteristic luminescence for each π systems. The colors of emission for **3b**, **4b**, and **5b** are yellow, green, and blue, respectively. Note that **5b** shows the highest luminescent quantum yield among all fullerene compounds.

These fullerene multiadducts having new curved π -electron conjugated systems are expected to be new optical materials.



[1] (a) E. Nakamura, K. Tahara, Y. Matsuo, M. Sawamura, *J. Am. Chem. Soc.*, **125**, 2834 (2003). (b) Y. Matsuo, K. Tahara, M. Sawamura, E. Nakamura, *J. Am. Chem. Soc.*, **126**, 8725 (2004).

[2] Y. Matsuo, K. Tahara, K. Morita, K. Matsuo, E. Nakamura, *Angew. Chem. Int. Ed.*, **46**, 2844 (2007).

Corresponding Author: Yutaka Matsuo and Eiichi Nakamura

TEL/FAX: +81-3-5841-1476; E-mail: matsuo@chem.s.u-tokyo.ac.jp; nakamura@chem.s.u-tokyo.ac.jp

Low-dimensional Columnar Alignment of C₆₀ Fulleride Single Crystals Stabilized by Triarylmethane Dye Cations

○Hiroshi Moriyama*, Takahito Sugiura †

Department of Chemistry, Toho University, Miyama 2-2-1, Funabashi, 274-8510 Japan

The novel low-dimensional nanostructural alignment of a C₆₀ anion radical moiety was revealed by single crystal structure analysis of C₆₀ fulleride salts stabilized by triarylmethane dye cations formed by electrocrystallization.

Discrete fulleride anions¹⁾ have drawn much attention, as the electron-accepting ability of C₆₀ is its most characteristic chemical property, results in intriguing physical properties, such as superconducting of alkali-metal doped C₆₀ and unique ferromagnetic behavior of TDAE-C₆₀. However, there has been rather a limited number of well-characterized C₆₀ anion radical salts predominantly because of their sensitivity to air. We have succeeded in obtaining single crystals of C₆₀ anion radical salts stabilized by cationic triarylmethane dyes²⁾ (Fig. 1), some of which were found to give rise to an intriguing nanostructural columnar alignment of C₆₀ fullerides.

Fig 2. shows the single-crystal structure of [Crystal Violet]⁺C₆₀⁻·C₆H₅Cl. The C₆₀ fulleride aligns with the columnar structure along the *a* axis (crystal growth direction), as well as a zigzag structure along the *b* axis, with contacts of almost van der Waals magnitude (*ca.* 10 Å, distance of the C₆₀ – C₆₀ centers), stabilized by mutual interactions of C₆₀⁻ and dye, such as π–π, face-to-face, and CH–π. SQUID measurement showed that some salts demonstrate antiferromagnetic interaction between the C₆₀ fullerides, as well as magnetic phase transition.

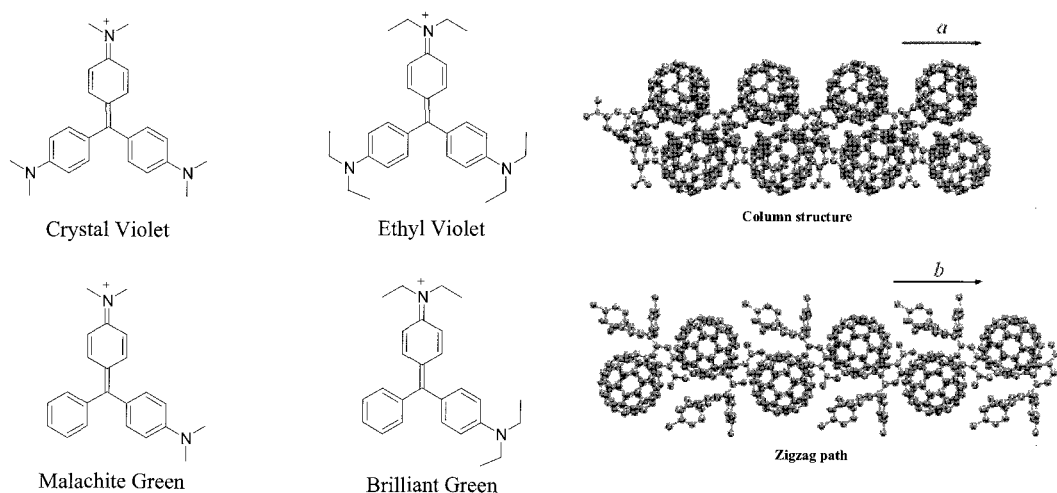


Fig. 1. Triarylmethane Dyes

Fig. 2 Crystal Structure of [Crystal Violet]⁺C₆₀⁻·C₆H₅Cl along the *a* and *b* axis.

- 1) C. A. Reed and R. D. Bolskar, *Chem. Rev.*, **100**, 1075-1120 (2000).
- 2) T. Sugiura, E. Osawa, and H. Moriyama, Abstracts of 30th Fullerene-Nanotubes General Symposium 2-13 (2006); H. Moriyama and T. Sugiura, *New Diamond*, **22**, 30-31(2006).

Corresponding Author: Hiroshi Moriyama e-mail; moriyama@chem.sci.toho-u.ac.jp
Tel: 047-472-1211, Fax: 047-476-9449 † Present Address: The University of Tokyo

C₆₀ thin film field-effect transistor devices with gold electrodes modified by various types of alkanethiols

○ Yohei Ohta,^a Naoko Kawasaki,^a Takayuki Nagano,^a Akihiko Fujiwara^b and Yoshihiro Kubozono^a

- a) Research Laboratory for Surface Science (RLSS), Okayama University, Okayama 700-8530, Japan
 b) Japan Advanced Institute for Science and Technology, Ishikawa 923-1292, Japan

C₆₀ thin film field-effect transistor devices are fabricated with gold (Au) source/drain electrodes modified with various types of 1-alkanethiols (C_nH_{2n+1}SH, n = 4 – 18) in order to study carrier injection barriers at the interface between electrodes and C₆₀ thin films. We have analyzed the drain current density J_D vs drain-source voltage V_{DS} curve, which shows concave-up nonlinear behavior at low V_{DS} region (Fig.1), on the basis of a thermionic emission model for double Schottky barriers. From the analyses 1-alkanethiols are found to form large tunneling barrier at the interface. In the device modified with 1-hexadecanethiol (C₁₆H₃₃SH), effective Schottky barrier ϕ_B^{eff} which consists of tunneling barrier and pristine Schottky barrier for the contact of Au – C₆₀ is 0.591(2) eV in application of gate voltage $V_G = 100$ V, and 85% of ϕ_B^{eff} is produced by the tunneling barrier. The tunneling efficiency, β , between electrodes and C₆₀ thin films is 1.12(6) Å⁻¹, whose value is close to that, 0.87 Å⁻¹, junction of n-Si-(hexadecane)-Hg.¹⁾

Above 320 K, the concave-up nonlinear behavior in $I_D - V_{DS}$ changed to normal curve (linear and saturation) (Fig. 2) because of a large fluctuation of 1-hexadecanethiol; its melting point is ~310 K. This implies a destruction of tunneling barrier at the interface. Furthermore, thickness dependences of photoemission spectra on the pristine Au electrodes and the modified electrodes are also studied in order to clarify electronic structures at the interfaces. In the conference, the tunneling barriers and β s will also be reported for the devices modified with other 1-alkanethiols and the alkyl-chain length dependence of ϕ_B^{eff} will be clearly shown. Part of this work was recently published in JPC.²⁾

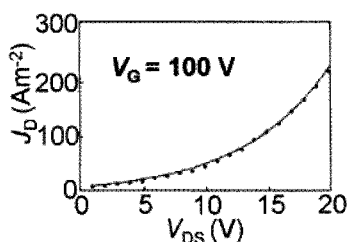


Fig. 1: J_D - V_{DS} plots for the C₆₀ FET device with Au source/drain electrodes modified by 1-hexadecanethiol.

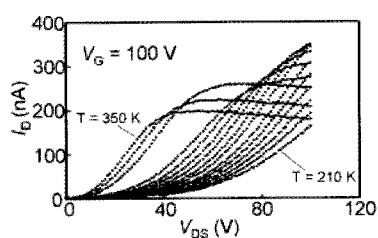


Fig. 2: I_D - V_{DS} plots for the C₆₀ FET device measured from 210K to 350K.

- 1) E. Faber, *ChemPhysChem*. 6, 2153 (2005).
 2) T.Nagano et al., *J. Phys. Chem. C* 111, 7211 (2007).

Corresponding Author : Yohei Ohta

E-mail: y-ota@cc.okayama-u.ac.jp, Tel : +81-86-251-7850, Fax : +81-86-251-7853

Preparation and characterization of C₆₀ and C₇₀ fibrillar superstructures and its polymerization by γ -ray irradiation

Sudip Malik, Norifumi Fujita and Seiji Shinkai

Department of Chemistry and Biochemistry, Graduate School of Engineering, Kyushu University, 744 Moto-oka, Nishi-ku, 819 0395 Fukuoka, Japan

Fullerenes (C₆₀ or C₇₀) are dissolved in solid and sublimable solvents such as naphthalene, ferrocene and camphor, respectively. After removing these solvents by sublimation process, the formation of fibrillar superstructures of fullerene has been observed by scanning electron microscopy (SEM) as shown in Figure 1. X-ray powder diffraction study and ATR/IR analysis reveal that fullerene superstructures preserve fcc lattice as like in pristine in case of C₆₀. NMR together with elemental analysis proposes the presence of significantly less amount of solvent in the superstructures. We have attempted to polymerize these superstructures by γ -ray irradiation to achieve polyC₆₀ or polyC₇₀ that is the material composed only fullerenes connected by covalent bonds without any additional linkage.[1] We have characterized these materials by TEM/HRTEM as well as PL studies. The approach that provides not only an easy, simple and efficient technique for the production of fibrous fullerene or polyfullerene but also to control over the morphological aspects will be the promising pathways to prepare fullerene based material for the development of realistic applications.

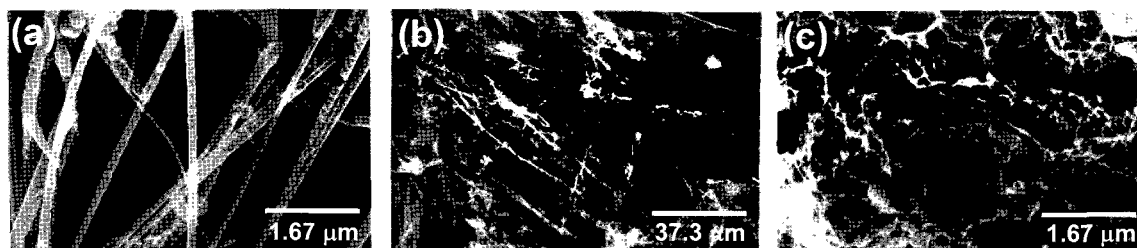


Figure 1: The typical SEM images of C₆₀ superstructure after sublimation of solid solvents : (a) naphthalene, (b) ferrocene and (c) camphor respectively

[1] F. Giacalone and N. Martin, *Chem. Rev.*, **106**, 5136 (2006).

Corresponding Author: Seiji Shinkai

TEL: +81-92-802-2818, FAX: +81-92-802-2820, E-mail: seijitcm@mbox.nc.kyushu-u.ac.jp

Raman Spectroscopic Study of Polyynes Peopods

○Tomonari Wakabayashi¹, Daisuke Nishide², Hiromichi Kataura³,
Yohji Achiba⁴, and Hisanori Shinohara^{2,5}

*Department of Chemistry, School of Science and Engineering, Kinki University,
Higashi-Osaka 577-8502, Japan¹*

Department of Chemistry, Nagoya University, Nagoya 464-8602, Japan²

*Nanotechnology Research Institute, National Institute of Advanced Industrial Science and
Technology (AIST), Tsukuba 305-8562, Japan³*

*Graduate School of Science, Tokyo Metropolitan University, Hachioji 192-0397, Japan⁴
Institute for Advanced Research, Nagoya University, and CREST, Japan Science and
Technology Agency (JST), Nagoya 464-8602, Japan⁵*

The SWNT that contains $C_{2n}H_2$ polyynes inside has been prepared and its advantages as a spectroscopic tool for stabilizing the highly reactive molecules have been demonstrated. This work is a follow-up research of the previous publications on the demonstration for trapping $C_{10}H_2$ polyynes inside SWNTs [1] and its thorough research on $C_{2n}H_2$ ($n=4-6$) [2].

In the present Raman spectra of polyynes $C_{2n}H_2$ ($n=4-8$) inside SWNTs reveals Raman activities of CH-stretching, CCC-bending overtones in addition to the reported strong activities of the CC-stretching fundamentals and overtones. Along with the recent studies on normal Raman [3] and resonance Raman spectra of pristine polyynes in solution [4], the mechanism of the overtone of stretching of polyynes and nanotube and other weak Raman modes is discussed in more detail.

[1] D. Nishide *et al.* *Chem. Phys. Lett.* **428**, 356 (2006).

[2] D. Nishide *et al.* *J. Phys. Chem. C* **111**, 5178 (2007).

[3] H. Tabata *et al.* *Carbon* **44**, 3168 (2006).

[4] T. Wakabayashi *et al.* *Chem. Phys. Lett.* **433**, 296 (2007).

Corresponding Author: Tomonari Wakabayashi

E-mail: wakaba@chem.kindai.ac.jp

Tel: +81-6-6730-5880 (ex.4101), **Fax:** +81-6-6723-2721

Single electron injection into C₆₀-encapsulated carbon nano-peapod quantum dots

J.Haruyama^{1,5}, J.Mizubayashi¹, I.Takesue^{1,5}, T.Okazaki², H.Shinohara^{3,5}, Y.Harada^{4,5},
Y.Awano^{4,5}

¹*Aoyama Gakuin University, 5-10-1 Fuchinobe, Sagamihara, Kanagawa 229-8558 Japan*

²*National Institute of Advanced Industrial Science and Technology, Tsukuba, 305-8565, Japan*

³*Nagoya University, Furo-cho, Chigusa, Nagoya 464-8602 Japan*

⁴*Fujitsu Laboratory, 10-1 Wakamiya, Morinosato, Atsugi, Kanagawa 243-0197 Japan,*

⁵*JST-CREST, 4-1-8 Hon-machi, Kawaguchi, Saitama 332-0012 Japan*

Carbon nano-peapods have recently attracted considerable attention [1, 2], because their unique nano-structures are expected to yield exotic electronic states [3], quantum charge (spin) transports, and one-dimensional (1D) quantum phenomena. There are, however, still a few reliable reports that experimentally reported such electronic states and quantum phenomena [4][5].

Here, we report anomalous charging effect of single electrons (Coulomb diamonds) observed in carbon nano-peapods quantum dots that encapsulate a series of C₆₀ molecules [6]. We find that behaviors of diamonds are anomalously sensitive to back-gate voltages (V_{bg}), exhibiting two evidently different V_{bg} regions and a large polarity on V_{bg} . In particular, we find only a sequence of one large diamond followed by three smaller ones existing around ground state. Magnetic field dependence indicates presence of shell filling by spin singlet to doubly degenerate electronic levels for these. The encapsulated C₆₀ molecules indirectly affect this shell filling at low V_{bg} possibly via nearly free electrons. In contrast, they act as individual quantum dots coupled in series in high V_{bg} region. It directly contributes to highly overlapped very large diamonds.

Moreover, we report power law behaviors on conductance versus energy relationships observed in the same peapods and discuss about correlation of the anomalous power values with orbital-related Tomonaga-Luttinger liquid.

References

1. B.W.Smith, et al., *Nature* **393**, 323 (1998)
2. M. Yudasaka, S. Iijima, et al., *Chem. Phys. Lett.*, **380**, 42 (2003).
3. S.Okada, S.Saito, and A.Oshiyama, *Phys.Rev.Lett.* **86**, 3835 (2001)
4. J.Lee, T.Okazaki, H.Shinohara, Y.Kuk, et al., *Nature* **415**, 1006 (2002)
5. K.Hirahara, T.Okazaki, H.Shinohara, et al., *Phys.Rev.Lett.* **85**, 5384 (2000)
6. J.Mizubayashi, J.Haruyama, T.Okazaki, et al., *Phys.Rev.B* **75**, 205431 (2007)

Corresponding author: Junji Haruyama J-haru@ee.aoyaoyama.ac.jp

Preparation of subnanometer-sized Pt particles using single-wall carbon nanohorns

○Ryota Yuge¹, Masako Yudasaka^{1,2}, Minfang Zhang², Tsutomu Yoshitake¹, and Sumio Iijima^{1,2,3}

¹*NEC, 34 Miyukigaoka, Tsukuba 305-8501, Japan*

²*SORST-JST, 34 Miyukigaoka, Tsukuba 305-8501, Japan*

³*Meijo University, 1-501 Shiogamaguchi, Tenpaku-ku, Nagoya, 468-8502, Japan*

Single-wall carbon nanohorns (SWNHs), a type of single-wall carbon nanotubes, adsorb various materials, thus being potentially useful in many fields. Surface areas inside and outside of SWNH aggregates measured by N₂-adsorption were about 600 and 400 m²/g, respectively [1]. Mechanism of storage and release of materials into/from SWNHs was well studied [2, 3]. We previously reported that Pt particles with sizes of about 2 nm can be loaded on the outside surface of the pristine SWNHs or inside of SWNHs if holes were opened. The Pt deposition method employed there was the colloidal one carried out at 70°C. On the other hand, the smaller-sized Pt particles about 1.7 nm were available on the pristine SWNHs by depositing Pt-ammine complexes at room temperature [4]. Since the small-sized Pt particles are more useful in various catalytic-applications [5], we developed a new method to decrease the Pt-particle sizes.

Recently, it was shown that abundant oxygen-containing functional groups were formed on SWNHs by light-assisted oxidation (LAOx) [6]. In LAOx, SWNHs were dispersed in hydrogen peroxide solution at 80°C for 6 hours, wherein the light from a Xe lamp was irradiated. We made Pt-SWNHs using LAOx-SWNHs and Pt-ammine complexes, and observed the obtained Pt loaded LAOx-SWNH with transmission electron microscope, X-ray diffraction, and others. As a result, it was found that the Pt particles were well supported on SWNHs, and the Pt-particle sizes were in the range of sub-nanometers. We consider that the abundant oxygen-containing functional groups of LAOx-SWNH had certain effects in decreasing the Pt particle sizes. The details are shown in the presentation.

Acknowledgement:

We thank T. Azami for preparing SWNH samples.

Reference:

- [1] K. Murata, et al. *J. Phys. Chem.* **B105**, 10210 (2001).
- [2] K. Ajima et al. *Adv. Mater.* **16**, 397 (2004).
- [3] R. Yuge et al. *J. Phys. Chem.* **B109**, 17861(2005).
- [4] K. Murata et al. *Carbon*, **44**, 799 (2006).
- [5] T. Yoshitake, et al. *Physica B* **323**, 124 (2002).
- [6] M. Zhang et al. *The 32th Fullerene-Nanotubes General Symposium*, 38 (2006).

Corresponding Author: M. Yudasaka and R. Yuge.

TEL: +81-29-850-1566, FAX: +81-29-856-6137 E-mail: yudasaka@ftrl.cl.nec.co.jp, ryuge@ftrl.cl.nec.co.jp

Non-volatile Memory using SWCNT Encapsulating Fullerene

○Hiroshi Suga^{1,2}, Kazuhiro Yanagi¹, Masayo Horikawa¹, Hiromichi Kataura¹,
Tetsuo Shimizu¹ and Yasuhisa Naitoh^{1,3}

¹*Nanotechnology Research Institute, Advanced Industrial Science and Technology, Ibaraki
305-8562, Japan*

²*College of Science and technology, Nihon University, Chiba 274-8501, Japan*

³*PRESTO, Japan Science and Technology Corporation, Tokyo 102-0075, Japan*

A reproducible resistance switch effect is observed in the I-V characteristics of a simple metal nanogap junction when high-bias voltages are applied. This phenomenon is only occurs for gap widths slightly under about 10 nm [1]. The switching effect is caused by the following process; applied bias voltage induces the changes of the gap width between the metal electrodes, and the change of the gap width affects the resistance of the gap. As a result, such gap junctions can exhibit a non-volatile resistance hysteresis, leading to the resistance switching. Due to the simplicity of the construction process of the metal nanogaps, this device has great potential for non-volatile memory and other information storage devices. To achieve such switching in a few nanometer line electrodes, however, is required for the applications to these devices. The diameter of single wall carbon nanotubes (SWCNT) is approximately 1~2 nm, thus SWCNT is one of the possible candidates for the nanometer line electrodes of the nanogap switching. In this study, we constructed nanogaps using carbon nanotubes to achieve the switching in the 1 nm line scale range. For the switching, fullerene peapods were prepared, because the position changes of encapsulated fullerenes will lead to the change of resistance similar to that of metal gaps. The nanogap parts were fabricated by electromigration and breakdown methods [2]. Figure 1 shows resistances of the peapod nanogap junction in on-off cycles. The nanogap does exhibit switching behavior, indicating the observation of resistance switching between ~1 nm scale electrodes.

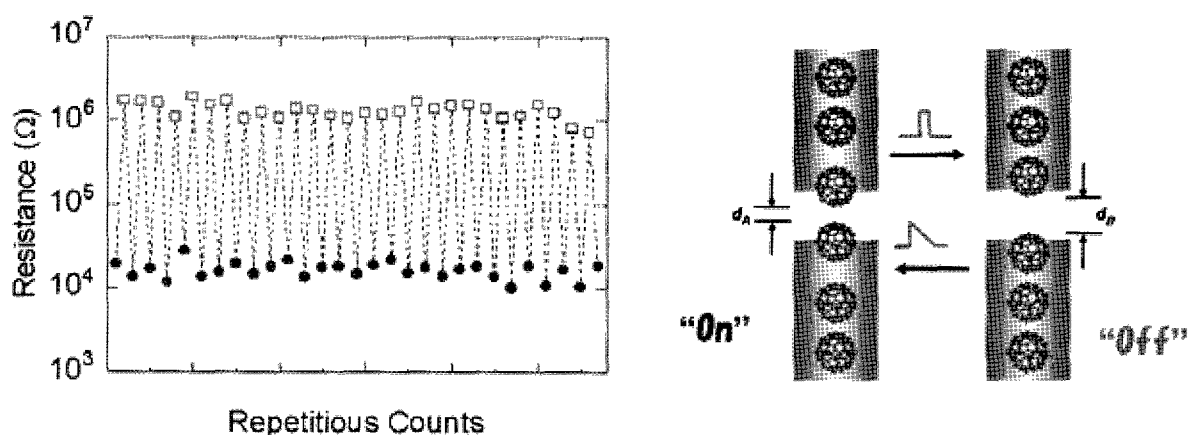


Figure 1. Resistances of a peapod nanogap junction at 0.2V in On-Off cycles.

[1] Y. Naitoh, M. Horikawa, H. Abe, and Tetsuo Shimizu, *Nanotechnology*, **17**, 5669 (2006).

[2] R. V. Seidel, A. P. Graham, B. Rajasekharan, E. Unger, M. Liebau, G. S. Duesberg, F. Kreupl, and W. Hoenlein, *J. Appl. Phys.*, **96**, 6694 (2004).

Corresponding Author: Yasuhisa Naitoh

TEL: +81-29-861-7892, FAX: +81-29-861-2786, E-mail: ys-naitou@aist.go.jp

Atomically-resolved field emission image of aluminum clusters deposited on carbon nanotubes

T. Matsukawa, T. Yamashita, K. Asaka, H. Nakahara and ○Y. Saito

Department of Quantum Eng., Nagoya University, Furo-cho, Nagoya 464-8603

Field emission of electrons from multiwall carbon nanotubes (MWNTs) with a closed cap occurs preferentially from pentagons at the cap when the nanotube surface is clean [1]. Enhancement of electron emission occurs when residual gas molecules are adsorbed on the nanotube surface [2]. In this work, effect of aluminum (Al) deposition on MWNT field emitters was studied by field emission microscopy (FEM), and FEM images of Al clusters in atomic-resolution and the suppression of current fluctuation were observed.

MWNTs produced by arc discharge were attached to a tungsten hairpin by graphite-bond, and Al was deposited onto apex regions of MWNTs in the FEM chamber. The amount of Al deposited on MWNT caps was in a range from ~ 1 nm to ~ 10 nm in terms of mean film thickness. The base pressure of the FEM chamber was 7×10^{-8} Pa.

Figure 1 shows FEM images of an MWNT emitter before and after Al deposition. Before the Al deposition, pentagon patterns characteristic of clean caps of MWNTs (two MWNTs are visible in this image) are observed as revealed in Fig. 1 (a). By the deposition of Al, as shown in Fig. 1 (b), a spotty pattern with a high symmetry (4-fold symmetry in this case) appeared instead of the clean pentagon patterns. The contrast of the spotty pattern reminiscent of the structure of an atom cluster with a shape of cubo-octahedron, which is the crystal form characteristic of face-centered cubic metals. A model of the structure consisting of 79 Al atoms is illustrated in Fig. 2. The polyhedral image, rotating and migrating, disappeared at several seconds after its appearance, and finally the original clean cap was recovered.

Although the fluctuation of emission current was large just after the Al deposition, flickering of spots in the FEM and current fluctuation considerably decreased after the first current-voltage measurement. This may be due to the gettering action of Al clusters deposited on MWNT emitters.

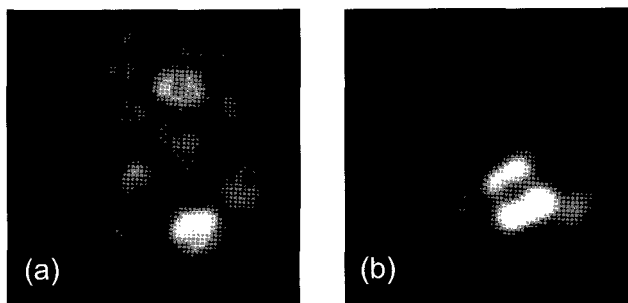


Fig. 1. FEM images of (a) clean MWNT caps and (b) an Al cluster.

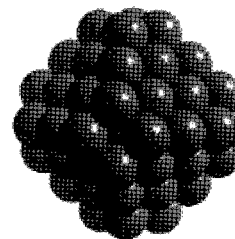


Fig. 2. Cubo-octahedron of an Al_{79} cluster

[1] Y. Saito, K. Hata and T. Murata: *Jpn. J. Appl. Phys.* **39**, L271 (2000).

[2] K. Hata, A. Takakura and Y. Saito: *Surface Sci.* **490**, 296-300 (2001).

Corresponding Author: Yahachi Saito

TEL: +81-52-789-4459, FAX: +81-52-789-3703, E-mail: ysaito@nagoya-u.jp

Porphyrin-Modified Single-Walled Carbon Nanotubes for Photoelectrochemical Devices

Tomokazu Umeyama¹, Mitsuru Fujita¹, Noriyasu Tezuka¹, Naoki Kadota¹,
Yoshihiro Matano¹ and Hiroshi Imahori¹

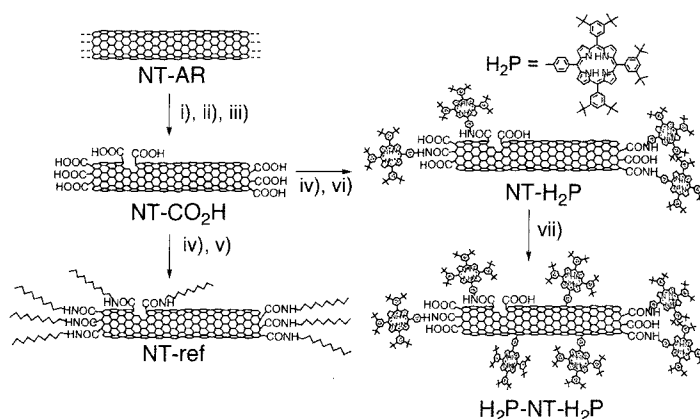
¹Graduate School of Engineering, Kyoto University, Kyoto 615-8501, Japan

In recent years, carbon nanomaterials including fullerenes and single-walled carbon nanotubes (SWNTs) have extensively been applied to photovoltaic and photoelectrochemical devices. While fullerenes are moderately soluble in organic solvents, SWNTs form bundle structures, resulting in poor dispersibility in organic solvents due to their strong π - π interaction between the individual SWNTs. In this study, photoactive molecules (i.e., porphyrin) have been tethered to SWNTs to increase the dispersibility in organic solvents and then the composites have been deposited electrophoretically onto semiconductor electrodes to construct photoelectrochemical devices.

Sequential covalent modification of SWNTs with bulky porphyrin units was carried out to disentangle large bundles of SWNTs as shown in Scheme 1.¹ The electrochemically deposited films of NT-H₂P and H₂P-NT-H₂P on nanostructured SnO₂ electrodes exhibited incident photon-to-photocurrent efficiencies (IPCEs) as high as 4.0 % and 4.9 %, respectively, under an applied potential of 0.08 V vs SCE, while the maximum IPCEs of NT-CO₂H and NT-ref were 2.3 % and 2.6 %.

The more efficient photocurrent generation in the porphyrin-SWNT composite devices can be rationalized by the exfoliation abilities of the bulky porphyrins that yield more exfoliated SWNTs in the deposited films, which was confirmed by AFM and TEM measurements. In spite of efficient quenching of the porphyrin excited singlet state by the SWNTs in the porphyrin-linked SWNTs, the photocurrent action spectra revealed that the excitation of the porphyrin moieties makes no contribution to the photocurrent generation. Direct electron injection from the excited states of the SWNTs to the conduction band of the SnO₂ electrode is responsible for the photocurrent generation. This is the first example of photoelectrochemical devices in which porphyrins are covalently linked to SWNTs.

Scheme 1



Reagents and conditions: i) 200 °C, air, 24 h, ii) conc. HCl, sonication, 15 min, iii) 2.6 M HNO₃, reflux, 24 h, iv) SOCl₂, reflux, 24 h, v) *n*-C₁₀H₂₁NH₂, 130 °C, 3 days, vi) H₂P-NH₂, DMF, 130 °C, 3 days, vii) H₂P-NH₂, isoamyl nitrile, ODCB, microwave, 100 °C, 30 min.

[1] T. Umeyama, M. Fujita, N. Tezuka, N. Kadota, Y. Matano, K. Yoshida, S. Isoda and H. Imahori, *J. Phys. Chem. C*, in press.

Corresponding Author: Tomokazu Umeyama

TEL: +81-75-383-2568, FAX: +81-75-383-2571, E-mail: umeyama@scl.kyoto-u.ac.jp

Electrical and Optical Gas Sensing Using Nanoscopically Dispersed Carbon Nanotube Networks

○Nobutsugu Minami, Annamalai Karthigeyan, Konstantin Iakoubovskii

Nanotechnology Research Institute, National Institute of Advanced Industrial Science and Technology (AIST), Central 5, 1-1-1 Higashi, Tsukuba, Ibaraki 305-8565, Japan

Single-wall carbon nanotubes (SWNTs) show great promise as a gas sensing material because of their extremely small size and large surface area (per unit volume). Accordingly, to maximize their gas sensing ability, it is essential to prepare a finely dispersed SWNT network down to a nanometer-scale. Following this line and extending our previous work of cellulose-derivative aided dispersion and thin film fabrication of SWNT [1], we have developed an ultra-sensitive gas sensor.

SWNTs finely dispersed in an aqueous solution of a cellulose derivative were spin coated on a quartz substrate, followed by matrix removal by burning in vacuum, realizing well exposed and mostly individualized SWNT networks. A sensor was completed by vacuum depositing a pair of interdigitated gold electrodes (100 μ m gap) on top of the SWNT network.

The sensor demonstrated a sizable increase in current upon exposure to 25ppb NO₂ (Fig. 1) or even lower; this is one of the most sensitive NO₂ detection ever reported for pristine (non-functionalized) SWNTs. UV-induced photodesorption was used to recover the baseline. As is generally accepted, the current increase results from hole doping by NO₂, reflecting the p-type nature of oxygen-doped SWNTs. When exposed to 5ppm NH₃, on the other hand, a considerable reduction in current was observed, attributable to carrier compensation by electron donation from NH₃ to p-doped SWNTs.

These charge transfer processes were further studied by investigating the effect of gas exposure on absorption and photoluminescence (PL). We found that upon exposure to NO₂, PL from an SWNT network derived from the S₁₁ optical transition considerably decreased, while it increased upon exposure to NH₃ (Fig. 2). Indeed, this is the first demonstration of optical gas sensing with SWNT, and the trend of the PL change is fully consistent with the charge transfer mechanism mentioned above.

[1] N. Minami *et al.*, Appl. Phys. Lett. **88**, 093123 (2006).

Corresponding Author: Nobutsugu Minami

TEL: +81-29-861-9385, FAX: +81-29-861-6309, E-mail: n.minami@aist.go.jp

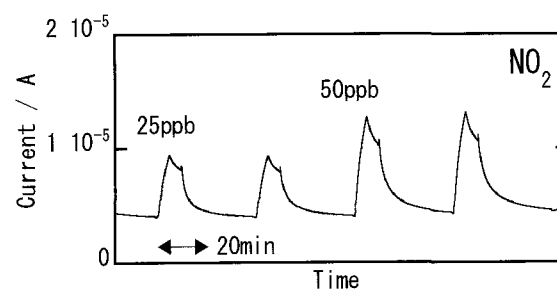


Fig.1 Electrical response to 25ppb and 50ppb NO₂.

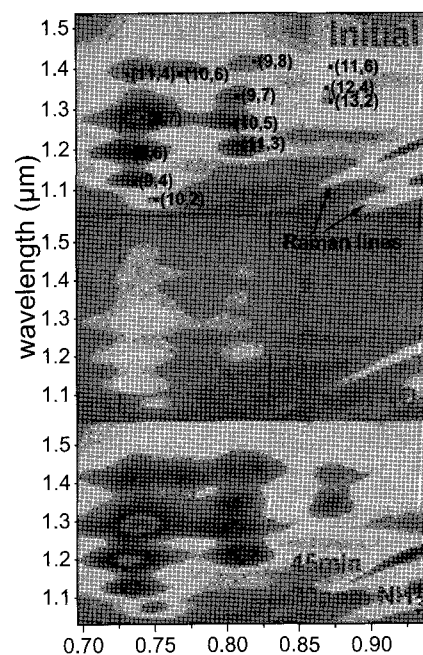


Fig.2 PL change induced by gas exposure (100ppmNO₂ & 30ppmNH₃).

Super-Growth Single-Walled Carbon Nanotube Electrochemical Capacitors

○Ali Izadi-Najafabadi^{1,2,3}, Kenji Hata^{1,2}, Tatsuki Hiraoka^{1,2}, Takeo Yamada^{1,2}, Don N. Futaba^{1,2}, Satoshi Yasuda^{1,2}, Osamu Kimizuka², Osamu Tanaike², Hiroaki Hatori², Motoo Yumura^{1,2} and Sumio Iijima^{1,2,3,4}

¹*Research Center for Advanced Carbon Materials, Tsukuba 305-8565, Japan*

²*National Institute of Advanced Industrial Science and Technology (AIST), Tsukuba 305-8565, Japan*

³*21st Century COE, Nano-factory, Department of Material Science and Engineering, Meijo University, Nagoya 468-8502, Japan*

⁴*NEC Corporation, Tsukuba, 305-8501, Japan*

With the advent of global warming and its ever present impact, zero-emission renewable energy sources and conversion devices have garnered much attention within the scientific community and beyond. One promising source of compact energy storage devices is the electrochemical capacitor, also called supercapacitor. Able to simultaneously deliver high energy density and high power density, supercapacitors operate on the principle of double layer charging; therefore, a potential electrode material is based on its accessible specific surface area, electronic conductivity, chemical stability and operating voltage range.

It is thought that SWNTs, due to their crystallinity (i.e. high electrical conductivity) and high surface area possess the potential for becoming next-generation electrode material. Super-growth SWNT (SGT) forests have shown the highest reported specific surface area for CNT material [1]. Here we report the performance of electrochemical capacitors based on super-growth forests, and showcase their potential to exceed performance of other types of supercapacitors.

[1] D. N. Futaba, K. Hata, T. Yamada, T. Hiraoka, Y. Hayamizu, Y. Kakudate, O. Yanaike, H. Hatori, M. Yumura and S. Iijima, *Nat. Mater.*, **5** (12), 987 (2006)

Corresponding Author: Kenji Hata

TEL: +81-298-861-6763, FAX: +81-298-61-4654, E-mail: kenji-hata@aist.go.jp

Ink-jet Printing of Carbon Nanotube Film Transistors

○Taishi Takenobu^{1,2}, Noriko Miura³, Takeshi Asano³, Tomohiro Fukao⁴,
Masashi Shiraishi⁴ and Yoshihiro Iwasa^{1,2}

¹*Institute for Materials Research (IMR), Tohoku University, Sendai 980-8577, Japan*

²*CREST, Japan Science and Technology Corporation, c/o IMR,
Tohoku University, Sendai 980-8577, Japan*

³*BROTHER INDUSTRIES, Ltd, Nagoya 467-0841, Japan*

⁴*Graduate School of Engineering Science, Osaka University, Toyonaka 560-8531, Japan*

Fundamental studies of charge transport through individual single-walled carbon nanotubes (SWNTs) reveal remarkable room-temperature properties, including mobilities more than ten times larger than that of silicon, current-carrying capacities as high as 10^9 Acm⁻² and ideal subthreshold characteristics in single-tube transistors. The implications of these behavior could be significant for many applications in electronics, optoelectronics, sensing and other areas. Devices that use single SWNTs as functional elements might not, however, form a realistic basis for these technologies, due to part to their low current outputs and small active areas. More importantly, integration of single SWNT devices into scalable integrated circuits requires a solution to the very difficult problem of synthesizing and accurately positioning large numbers of individual, electrical homogeneous tubes.

Currently, researchers are developing thin-film transistors (TFTs) using various organic semiconductors in order to construct electronics on polymeric materials for such “macroelectronic” applications as lightweight flexible display, inexpensive radio frequency identification, etc., whereby the performance merit is not driven by Moore’s law scaling as in conventional microelectronics but is instead determined by the low-cost per unit area and the compatibility with large-area, non-crystallines substrates. We recently proposed an alternative semiconducting material for such applications that consists of a two-dimensional random network of solution-processed SWNTs and have reported high-performance SWNT TFTs on inflexible Si substrates [1] and on flexible plastic substrates [2]. One of the main technological attractions for solution-processed SWNT TFTs is that an TFT can be deposited and patterned at low/room temperature by a combination of low-cost solution-processing and direct-write printing, which makes them ideally suitable for realization of low-cost, large-area electronic functions on flexible substrates. Here we applied inkjet printing to the fabrication process of SWNT TFTs. Transistors have been successfully fabricated *via* inkjet printing with high reproducibility. The detail of fabrication process and device performance will be presented at the meeting.

This study was supported by Industrial Technology Research Grant Program in 2006 from New Energy and Industrial Technology Development Organization (NEDO) of Japan.

[1] M. Shiraishi, T. Takenobu, T. Iwai, Y. Iwasa, H. Kataura and M. Ata, *Chem. Phys. Lett.*, **394**, 110 (2004).

[2] T. Takenobu, T. Takahashi, T. Kanbara, K. Tsukagoshi, Y. Aoyagi and Y. Iwasa, *Appl. Phys. Lett.*, **88**, 33511 (2006).

Corresponding Author: Taishi Takenobu

TEL: +81-22-215-2032, FAX: +81-22-215-2031, E-mail: takenobu@imr.tohoku.ac.jp

Formation of Water-Dispersible Nanotubular Graphitic Assembly

○ Wusong Jin¹, Guanxin Zhang¹, Takanori Fukushima^{1,2} and Takuzo Aida^{1,2}

¹ERATO-SORST Nanospace Project, Japan Science and Technology Agency (JST), National Museum of Emerging Science and Innovation, Tokyo 135-0064, Japan

²Department of Chemistry and Biotechnology, School of Engineering, and Center for NanoBio Integration, The University of Tokyo, Tokyo 113-8656, Japan

Recently, we have reported that Gemini-shaped hexa-*peri*-hexabenzocoronene (HBC) amphiphiles self-assemble to form π -electronic, discrete nanotubular objects [1]. Due to the well-defined one-dimensionality, the nanotubes are attractive in view of electronic and optoelectronic materials. By taking advantage of this study an isothiuronium ion-appended HBC amphiphile **1** is newly synthesized (Fig. 1). Incorporation of the ionic functionality as a pendant allows the resultant nanotube to disperse in water owing to effective hydration as well as electrostatic repulsion (Fig. 2). Furthermore, we also succeeded in post supramolecular functionalization of the nanotube surface with oxoanion guests [2].

HBC **1** is the first examples of ionically charged Gemini-shaped HBC amphiphile. After many attempts, we found that **1** can self-assemble specifically in CH_2Cl_2 to form nanotubular objects. Although compound **1** was insoluble in water even under boiling conditions, tubularly assembled **1** was finely dispersed in water at room temperature. For example, a CH_2Cl_2 suspension of the nanotubes (1 mL, 1 mg/mL) was centrifuged at 25 °C, and the resulting solid substance was subjected to immersion in MeCN (2 mL) followed by centrifugation. After repeating this washing treatment, deionized water (2 mL) was added to the residue, whereupon a yellow-colored, transparent solution resulted. TEM and SEM microscopy of an air-dried aqueous dispersion clearly displayed that the individual nanotubes are well separated from each other. Making use of a specific interaction of the isothiuronium pendants with oxoanionic species, we demonstrated post surface functionalization of the uniformly dispersed nanotubes in water. While excitation of the nanotubes in water/MeCN (1:1 v/v) at 427 nm resulted in a fluorescence emission at 526 nm with a shoulder at 562 nm, upon titration with sodium anthraquinone-2-carboxylate (SAQ), the fluorescence stepwise decreased in intensity. The Stern–Volmer constant (K_{sv}) for the fluorescence quenching was determined to be $3.3 \times 10^6 \text{ M}^{-1}$ from the initial fluorescence intensity change at 526 nm. The fluorescence quenching is obviously due to a long-range photoinduced electron transfer from the HBC units in the graphitic tubular wall to surface-bound SAQ molecules.

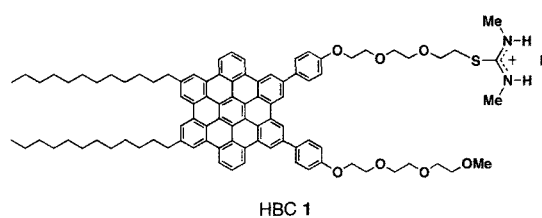


Fig. 1. Molecular structure of isothiuronium ion-appended hexa-*peri*-hexabenzocoronene (HBC) **1**.

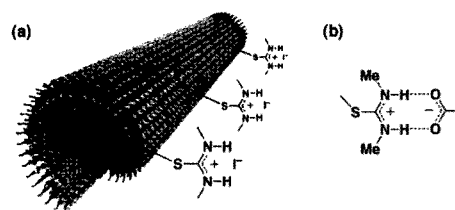


Fig. 2. (a) Schematic structure of a graphitic nanotube from **1**. (b) Possible binding structure of the isothiuronium ion pendant with a guest containing an oxoanion group, through a hydrogen-bonding interaction.

[1] J. P. Hill, W. Jin, A. Kosaka, T. Fukushima, H. Ichihara, T. Shimomura, K. Ito, T. Hashizume, N. Ishii and T. Aida, *Science* **304**, 1481 (2004).

[2] G. Zhang, W. Jin, T. Fukushima, A. Kosaka, N. Ishii and T. Aida, *J. Am. Chem. Soc.*, **129**, 719 (2007).

Corresponding Author: Wusong Jin

TEL: +81-3-3570-9182, FAX: +81-3-3570-9182, E-mail: jin@nanospace.miraikan.jst.go.jp

Structure of Vertically Aligned Carbon Nanofibers Containing Conical Cavity Array: One-dimensional Array of Graphitic Cones

○Akira Koshio, Yuta Tango, Takayuki Yamasaki, Kentaro Suzuki, and Fumio Kokai

*Division of Chemistry for Materials, Graduate School of Engineering, Mie University,
1577 Kurimamachiya-cho, Tsu, Mie 514-8507, Japan*

Catalytic chemical vapor deposition (CVD) has been extensively investigated as a promising method for growing carbon nanofibers (CNFs). It is well known that various types of CNFs can be formed by controlling the growth conditions, such as metal catalysts and reactant gases. We have previously reported that CNFs having an array of conical cavities that are 300–800 nm long were formed by alcohol CVD using indium tin oxide (ITO) and Fe as the metal catalysts (Fig. 1(a))[1]. We named these CNFs “conical-cavity CNFs (CC-CNFs)” because they have a unique structure containing conical cavities in a one-dimensional array at uniform intervals. In this study we inspected the structure of CC-CNFs using electron microscopies. We found that the conical cavities in CC-CNFs consisted of a one-dimensional array of graphitic cones confined by disclination defects in the hexagonal graphitic network.

Figure 1(b) shows a typical TEM image of one of the conical cavities in CC-CNF. The

TEM observation revealed that the CC-CNF had two graphitic structures, which were parallel to the fiber axis (Fig. 1(c)) and the wall of the conical cavity (Fig. 1(d)). The graphitic structures correspond to multi-wall carbon nanotubes and graphitic cones [2], respectively. We

observed a few limited angles by deducing them from the projected dimensions of the tilted conical cavity. This means that the conical cavity is confined to seven possible cone structures by the total disclination (TD) of the graphitic network decided by the number of pentagons (P) in the tip (Fig. 2).

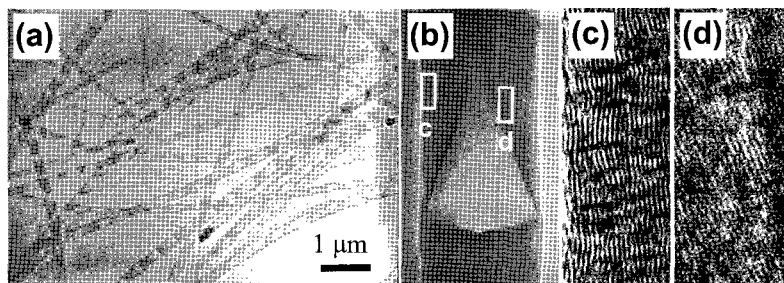


Fig. 1 TEM images of (a) CC-CNFs, (b) one conical cavity, (c) outer graphitic structure shown in (b), and (d) inner graphitic structure shown in (b).

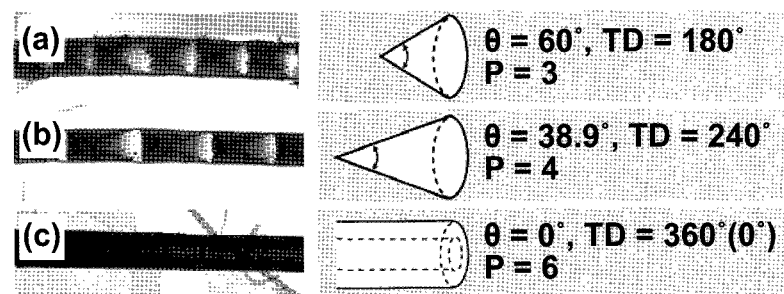


Fig. 2 Examples of conical cavities corresponding to graphitic cones. The tip angles of the conical cavities indicate $\theta = 60^\circ$ and $\theta = 38.9^\circ$ in (a) and (b), respectively. Image (c) shows the hollow MWNTs corresponding to the tip angle $\theta = 0^\circ$.

References: [1] A. Koshio *et al.*, *The 31st Fullerene-Nanotube General Symposium*, 1-18.

[2] A. Krishnan *et al.*, *Nature*, **388**, 451(1997).

Corresponding author: Akira Koshio

E-mail: koshio@chem.mie-u.ac.jp **Tel & Fax:** +81-59-231-5370

ポスター発表
Poster Preview

1P-1 ~ 1P-49

2P-1 ~ 2P-50

3P-1 ~ 3P-47

1P-1

Novel Magnetic Field Effects and Time-Resolved EPR Spectra of Biradicals from Photoinduced Intramolecular Electron Transfer Reactions in Phenothiazine-C₆₀ Linked Compounds

○Hiroaki Yonemura¹, Shinya Moribe¹, Yuya Wakita¹, Sunao Yamada^{1,2},
Yoshihisa Fujiwara³, and Yoshifumi Tanimoto³

¹Department of Applied Chemistry, Kyushu University, Fukuoka 819-0395, Japan

²Center for Future Creation, Kyushu University, Fukuoka 819-0395, Japan

³Department of Mathematical and Life Sciences, Hiroshima University, Higashi-Hiroshima 739-8526, Japan

We examined photoinduced electron-transfer reactions and magnetic field effects (MFEs) on the photogenerated biradicals in phenothiazine(Ph)-C₆₀ linked compounds, **Ph(n)C₆₀** (**n=6,8,10,12**), where photoinduced intramolecular electron-transfer reactions occur from Ph to the excited triplet state of C₆₀ in benzonitrile [1]. We also investigated a system of porphyrin-C₆₀ linked compounds (**ZnP(n)C₆₀** (**n=4,8**)) [2] and have found the novel MFEs in both the **Ph(n)C₆₀** and **ZnP(n)C₆₀** systems.

In the study, we have examined the effects of temperature, solvent, and a salt on the dynamics of the biradical of **Ph(n)C₆₀(n=4-12,BP)** (Fig. 1) in benzonitrile [3] and THF at various magnetic fields (0-14 T) and temperatures (283-343K) to verify the mechanism of the novel MFEs.

Transient absorption spectra indicated that triplet biradicals were generated by intramolecular electron-transfer reactions from the Ph to triplet excited state of C₆₀.

The reverse MFE, that the lifetime of the biradical increases first and then decreases with increasing magnetic field, was clearly observed at low magnetic fields (0.1~0.2 T) in **Ph(n)C₆₀** (**n=4-12,BP**). The MFEs were drastically changed by temperature, solvent, a salt, and a spacer.

The present MFEs can be explained by the contribution of not only spin-lattice relaxation mechanism but also spin-spin relaxation mechanism related to exchange interaction of the biradical. The time-resolved EPR spectra in **Ph(n)C₆₀(n=4-12)** are assigned to spin-correlated radical pairs. The time-resolved EPR spectra also support the mechanism suggested in MFEs.

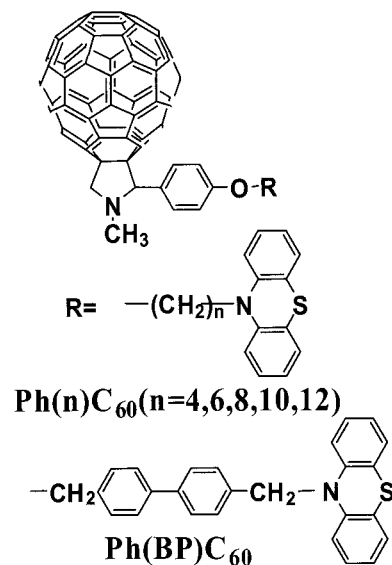


Fig. 1. Molecular structures of Ph-C₆₀ linked compounds

[1] S. Moribe, H. Yonemura, and S. Yamada, *C. R. Chimie*, **9**, 247 (2006).

[2] H. Yonemura, S. Harada, S. Moribe, S. Yamada, H. Nakamura, Y. Fujiwara, and Y. Tanimoto, *Mol. Phys.*, **104**, 1559 (2006).

[3] S. Moribe, H. Yonemura, and S. Yamada, *Chem. Phys.*, **334**, 242 (2007).

Corresponding Author: Hiroaki Yonemura

TEL: +81-92-802-2814, FAX: +81-92-802-2815, E-mail: yonetcm@mbox.nc.kyushu-u.ac.jp

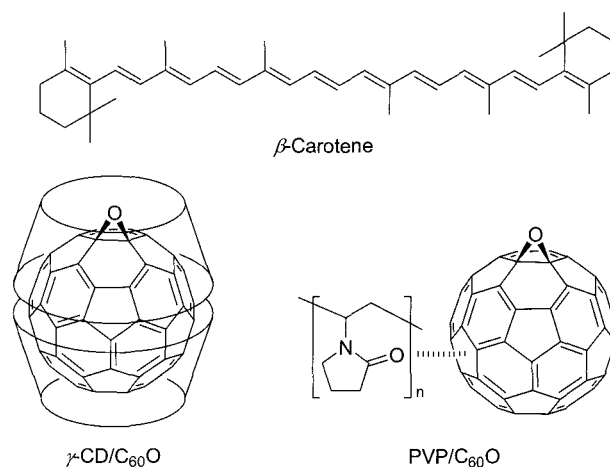
Kinetic Study on Antioxidant Activity of Water-soluble [60]Fullerene and [60]Fullerene Epoxide by β -Carotene Bleaching Assay

○Ken Kokubo¹, Tadashi Goto¹, Kyoko Togaya¹, Hisae Aoshima² and Takumi Oshima¹

¹*Division of Applied Chemistry, Graduate School of Engineering, Osaka University
Suita, Osaka 565-0871, Japan*

²*Vitamin C60 BioResearch Corporation, 1-8-7, Kyobashi, Chuo-ku, Tokyo 104-0031, Japan*

Water-soluble fullerenes have been found to behave as potent reactive oxygen species (ROS)-scavengers in cell cultures and can protect human skin keratinocytes from UV irradiation and oxidative damage by *tert*-butyl hydroperoxide [1,2]. Despite numerous studies on the radical scavenging activity of water-soluble fullerenes, little is known about the comparative assay of fullerenes versus carotenoids, which are known to behave as a radical scavenging type antioxidant. Recently, we evaluated the antioxidant activity of unfunctionalized water-soluble fullerenes, such as γ -cyclodextrin (CD)-bicapped [60]fullerene and polyvinylpyrrolidone (PVP)-entrapped [60]fullerene, by β -carotene bleaching assay and found a significant inhibitory effect of these water-soluble fullerenes on the oxidative discoloration of β -carotene induced by coupled autoxidation of linoleic acid [3]. In the present study, we investigated the antioxidant activity of water-soluble [60]fullerene epoxides as well as other fullerenes in a wide range of concentrations. We found that the γ -CD-bicapped [60]fullerene monoepoxide showed slightly higher antioxidant activity (%AOA) than that of γ -CD-bicapped [60]fullerene with the relative rate constant k_{rel} of 1.30 at 50°C.



[1] L. Xiao, H. Takada, K. Maeda, M. Haramoto and N. Miwa, *Biomed. Pharmacother.* **2005**, *59*, 351–358.

[2] L. Xiao, H. Takada, X. H. Gan and N. Miwa, *Bioorg. Med. Chem. Lett.* **2006**, *16*, 1590–1595.

[3] H. Takada, K. Kokubo, K. Matsubayashi and T. Oshima, *Biosci. Biotechnol. Biochem.* **2006**, *70*, 3088–3093.

Corresponding Author: Ken Kokubo

TEL: +81-6-6879-4592, FAX: +81-6-6879-4593, E-mail: kokubo@chem.eng.osaka-u.ac.jp

1P-3

Kinetic Control of Interfacial Energy in Carbon/Epoxy Composites by using Fullerenes

Yusuke Tajima^{1,2}, ○Daisuke Yamazaki^{1,2}, Takanori Matsuura¹, Youhei Numata¹
Hiroaki Kawamura^{1,3}, Hiroki Osedo^{1,3}

¹Nano-Integration Materials Research Unit, RIKEN, Wako 351-0198

²Department of Chemical Engineering, Saitama University, Saitama 338-8570

³Toray Industries Inc., New Frontiers Research Laboratories, Kamakura 248-8555.

Composite materials consist of carbon and matrix resins (ca. epoxy resins) are widely used in transport and architecture industries. The interfacial condition of carbon/matrix has received much attention recently, as it is generally accepted that this region can influence the properties of composites strongly. Control of carbon surface energy is one of the ways to improve the interfacial adhesion between carbon and matrix resins. In this study, we tried to control the surface free energy of carbon by fullerenes coating. We also investigated the reinforcement effect of fullerenes for flexural modulus of epoxy resins.

The surface free energies (γ_s^d , γ_s^p , γ_s^h , γ_s) of carbon wafers applied with or without fullerenes were assessed by contact angles of standard test liquids (water, glycerin, ethyleneglycole, etc.) using the expanded Fowkes method [1]. Adhesion work between carbon wafers and epoxy resins (W) was determined by the liquid surface tension of epoxy resins and the contact angles of epoxy resins on carbon wafers using the Young-Dupré equation. As shown in Table 1, γ_s and W varied depending upon the structures of fullerenes. The relation between weight ratio of fullerenes and flexural modulus for epoxy resins seems not to obey theoretical curve derived from rule of mixture.

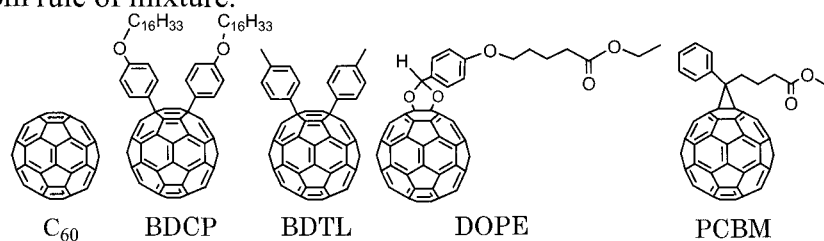


Table 1 γ_s and W of carbon wafers applied with or without fullerenes [mN/m]

Fullerenes	γ_s^d	γ_s^p	γ_s^h	γ_s	W
Non	43.5	0.2	0.1	43.8	90.1
C ₆₀	41.8	0.3	0.1	42.2	90.6
PCBM	41.5	4.3	0.0	45.8	92.0
DOPE	34.5	15.5	0.7	50.7	92.4
BDTL	41.9	0.6	0.5	43.0	90.1
BDCP	38.1	0.1	0.6	38.8	75.2

[1] T. Hata, Y. Kitazaki, *J. Adhesion*, **1972**, 8, 131

Corresponding author: Yusuke Tajima

Tel: +81-48-467-9309, Fax: +81-48-462-4702, E-mail: tajima@riken.jp

1P-4

Temperature Dependence of Conductivity of Crystalline C₆₀ and C₇₀ Pellets

○Gou Kawano¹, Tsuyoshi Takakura¹, Tsuyoshi Takase², Hidetsugu Nakamura¹ and Yong Sun¹

¹Department of Applied Science for Integrated System Engineering, Graduate school of Engineering, Kyushu Institute of Technology, 1-1 Sensui, Tobata, Kitakyushu, Fukuoka 804-8550, Japan

²Faculty of Modern Communication, Baiko Gakuin University, 1-1-1 Koyochō Shimonoseki, Yamaguchi 750-8511, Japan

Using the samples produced in pellet form, the conductivity of crystalline C₆₀ and C₇₀ fullerenes was measured. The conductivity of C₆₀ sample is shown in Fig.1 as a function of temperature. The conductivity depends on temperature process of the sample, and is almost constant at temperatures below 300K.

At temperatures above 300K, the conductivity rapidly decreases with increasing temperature. Moreover, a hysteresis on the conductivity is observed in the temperature region from 410K to 480K during upping and downing the temperature. Thermal activation energies of about 0.6 and 0.7eV on the conductivity are obtained in the temperature regions of 300-410K and above 480K, respectively. X-ray diffraction showed that the crystalline C₆₀ sample has fcc lattice structure at room temperature.

Based on the above results, we

believe that there are three crystal phases, sc phase below 300K, fcc1 phase between 300-410K, and fcc2 phase above 480K. Here, lattice constant of fcc2 phase should be larger than that of fcc1 phase. The temperature dependence of the conductivity below 300K is related to a disordered orientation of C₆₀ molecule in sc lattice, and the hysteresis between 410K and 480K may be due to the phase transition between fcc1 and fcc2.

Reference: 篠原久典、齋藤弥八: フラーレンの化学と物理 (名古屋大学出版会、1997).

TEL/FAX: 81-93-884-3564. E-mail: g348913g@tobata.isc.kyutech.ac.jp

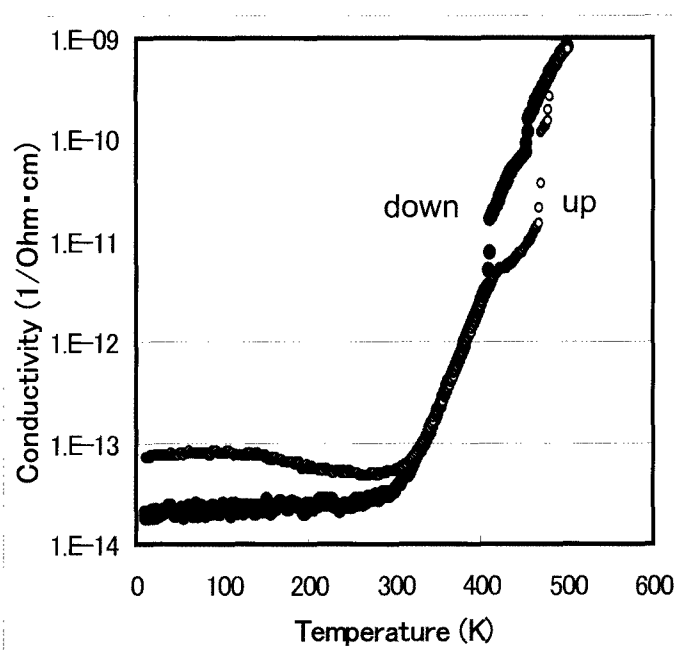


Fig.1 Conductivity of crystalline C₆₀ sample as a function of temperature

Iridium(III) Porphyrin Cyclic Dimer as a Bond-Forming Host for Fullerenes

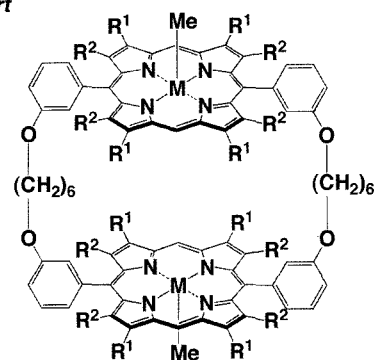
○Makoto Yanagisawa, Kentaro Tashiro, Takuzo Aida

*Department of Chemistry and Biotechnology, School of Engineering, The University of Tokyo
7-3-1 Hongo, Bunkyo-ku, Tokyo 113-8656*

Design of host molecules having bond-forming capability with fullerenes is interesting in that the structures as well as chemical/physical properties of the carbon cages can be modified through host/guest chemistry. Here we report that a cyclic dimer of methyliridium porphyrin (**1**; **Chart**) displays an extraordinary affinity toward fullerenes, as the result of a bond-forming host-guest interaction [1]. Because of the binding of two iridium centers to the opposite sides of included C_{60} , the fullerene deforms from a spherical shape to an oval shape upon inclusion.

From spectroscopic titrations, the association constant K_{assoc} between **1** and C_{60} in benzene was estimated at 10^{10} M^{-1} , which is one of the largest values among those for any host-guest complexation events reported. In order to investigate the origin of such an extraordinary affinity of **1** toward C_{60} , we conducted an X-ray crystallographic study on the inclusion complex **1** $\supset C_{60}$. Two iridium centers in **1** bind to the opposite ends of the C_{60} frame, where each of the iridium atoms coordinates in an η^2 fashion to a 6:6 ring-juncture C–C bond of C_{60} . The coordinated C–C bonds are definitely longer than a C–C bond at a 6:6 ring but shorter than that at a 5:6 fusion in uncomplexed C_{60} . Bound C_{60} exhibits a marked elongation along the Ir---Ir axis, thereby adopting an oval shape. In sharp contrast to **1** $\supset C_{60}$, an analogous inclusion complex of C_{60} with a zinc porphyrin cyclic dimer (**2** $\supset C_{60}$; **Chart 1**) displays neither such bond-forming signatures nor detectable distortions of included C_{60} [2–5].

Chart



1: M = Ir, R¹ = Hex, R² = Me
2: M = Zn, R¹ = R² = Et

[1] M. Yanagisawa *et al.*, *submitted*.

[2] K. Tashiro *et al.*, *J. Am. Chem. Soc.*, **121**, 9477 (1999).

[3] J.-Y. Zheng *et al.*, *Angew. Chem. Int. Ed.*, **40**, 1857 (2001).

[4] H. Sato *et al.*, *J. Am. Chem. Soc.*, **127**, 13086 (2005).

[5] K. Tashiro and T. Aida, *Chem. Soc. Rev.*, **36**, 189 (2007).

Corresponding Authors: Takuzo Aida and Kentaro Tashiro

E-mail: yanagisawa@macro.t.u-tokyo.ac.jp

Tel +3-5841-8803; **Fax** +3-5841-7310

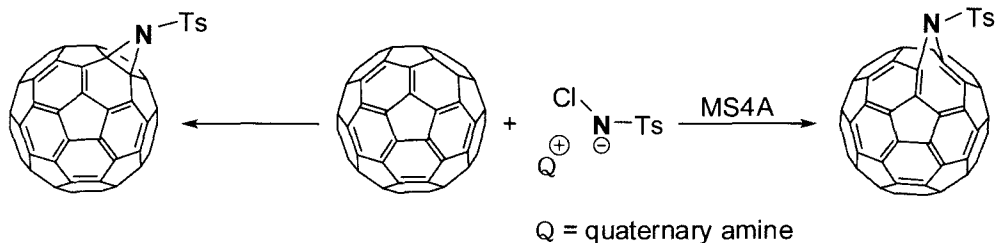
Control of Selectivity in Addition–Cyclization of Chloramine-T to C₆₀

○Ryoji Tsuruoka¹, Satoshi Minakata¹, and Mitsuo Komatsu²

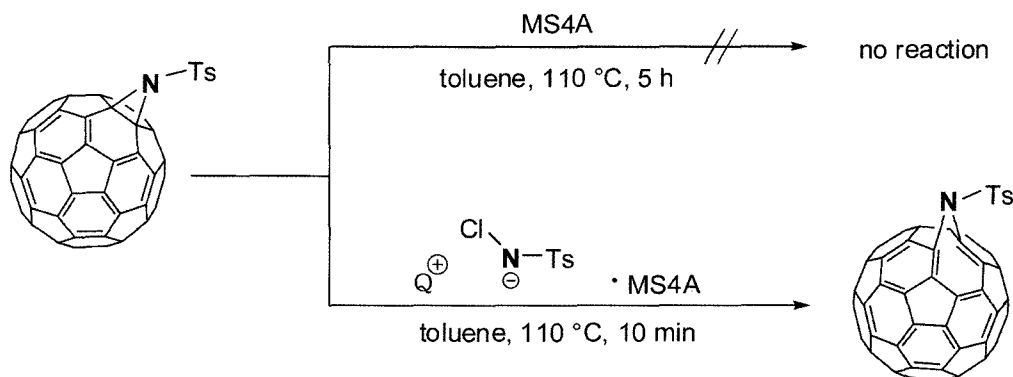
¹Department of Applied Chemistry, Graduate School of Engineering, Osaka University,
Suita, Osaka 565-0871, Japan

²Anan National College of Technology, Anan, Tokushima 774-0017, Japan

The development of a facile and basic method for functionalization of C₆₀ is still an important challenge because of recent demand of carbon nanomaterials. The known procedures so far for the functionalization have just employed conventional transformation of electron-deficient olefins. Among these methods, introduction of N₁ unit to C₆₀ leading to azafulleroids and aziridinofullerenes is limited to use of azides with need for careful treatment.¹ We have already reported in this symposium that C₆₀ was directly converted to an aziridinofullerene with Chloramine-T in the presence of phase-transfer catalyst. Here we found that azafulleroid, which is an isomer of aziridinofullerene, was produced by addition of MS4A to the above reaction system. The investigation of the reaction conditions could successfully control the selective formation of aziridinofullerene and azafulleroid.



In addition, to confirm the reaction pathway, isolated aziridinofullerene was treated with MS4A under the thermal conditions, but the reaction did not proceed at all. On the other hand, when the aziridinofullerene and chloramine-T were heated in toluene in the presence of MS4A, the azafulleroid was produced. These results indicate that the aziridinofullerene was rearranged to azafulleroid by the combination of MS4A and chloramine-T.



[1] M. Prato, Q. C. Li, F. Wudl, and V. Lucchini, *J. Am. Chem. Soc.* **115**, 1148 (1993).

Corresponding Author: Satoshi Minakata

TEL: +81-6-6879-7403, FAX: +81-6-6879-7402, E-mail: minakata@chem.eng.osaka-u.ac.jp

Efficient synthesis of fullerlenols by mechanochemical reaction of C₆₀ with H₂O under O₂ atmosphere

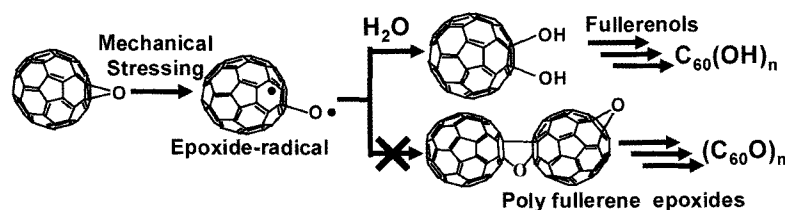
○Yuichi Ishiyama, Hiroto Watanabe, Mamoru Senna

*Faculty of Science and Technology, Keio University
3-14-1 Hiyoshi Kohoku-ku, Yokohama, 223-8522, Japan*

Fullerenols have attracted much interest in industrial chemistry and biochemistry. They are known to be free-radical scavengers or water-soluble antioxidant in biological systems. Hydroxylation of fullerene has been performed in not only liquid phase with toxic organic solvents [1], but also under solvent-free conditions using high-speed vibration mill (HSVM) techniques [2]. While HSVM methods do not need any solvents, then take a lot of trouble with eliminating metallic salts remaining in reaction products. Therefore, we developed a more efficient synthesis method of fullerlenols, without any catalyst.

We recently demonstrated a solid-state oxidation of fullerene under mechanical stressing by ambient gaseous oxygen [3]. Major products were polymerized fullerene epoxides (C₆₀O)_n. We supposed the polymerization of epoxides to have initiated by oxygen radical generated during destruction of unstable epoxy rings on a fullerene cage [4]. We further assumed that the trapping of those radicals by water results in introduction of hydroxyl groups on fullerene, and inhibition of further polymerizations at the same time (Scheme 1).

We here examine generation of fullerlenols during mechanochemical reaction of fullerene with H₂O under O₂ atmosphere, without adding any catalyst and toxic reagents. We milled crystallite C₆₀ with water under O₂ atmosphere, using vibration mill with a single milling ball (Fritsch, Pulversitte 0). Obtained products showed water solubility. From the IR spectra, we observed the peak assigned to hydroxyl groups, and it is totally different from those of polymerized fullerene epoxides.



Scheme 1 Hydroxylation of fullerene

Finally, we developed a very simple and clean synthetic method of fullerlenols, by only using O₂ and H₂O. Therefore, this method will be wide spread to many industrial applications in fullerene chemistry.

References:

- [1] Long Y. Chiang, J.B. Bhonsle, Leeyih Wang, S.F. Shu, T.M. Chang, and Jih Ru Hwu, *Tetrahedron Lett.*, **1996**, 52, 4963-4972
- [2] Pu Zhang, Hualong Pan, Dongfang Liu, Zhi-Xin Guo, Fushi Zhang, and Daoben Zhu, *Synth. Commun.*, **2003**, 33, 2469-2474
- [3] Watanabe H, *et al.*, Abstracts of The 30th Fullerene-Nanotubes general symposium, p.152, 2006
- [4] Watanabe H, *et al.*, Abstracts of The 32nd Fullerene-Nanotubes general symposium, p.120, 2007

Corresponding Author: Mamoru Senna **Tel:** +81-045-566-1569; **fax:** +81-045-564-0950; **E-mail** senna@applc.keio.ac.jp

NMR Studies of Molecular Hydrogen Encapsulated in Dianions of Fullerene C₆₀ and Open-Cage C₆₀ Derivatives

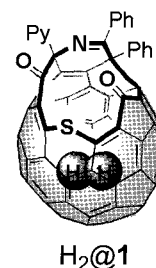
○Michihisa Murata¹, Yuta Ochi¹, Fumiyuki Tanabe¹, Yasujiro Murata^{1,2}, and Koichi Komatsu^{1,3}

¹ Institute for Chemical Research, Kyoto University, Uji, Kyoto 611-0011, Japan

² PRESTO, Japan Science and Technology Agency

³ Department of Environmental and Biotechnological Frontier Engineering, Fukui University of Technology, Gakuen, Fukui 910-8505, Japan

We have already reported that a hydrogen molecule encapsulated in fullerene C₆₀ cage can be used as a sensitive NMR probe for chemical functionalization at the exterior of the fullerene cage [1]. The NMR signals of H₂ inside C₆₀ or its derivatives were observed in high-field region ($\delta < -1.4$ ppm) because of strong shielding effect of the fullerene cage. In this study, we carried out two-electron reduction of C₆₀ and open-cage C₆₀ derivatives encapsulating H₂ and examined the ¹H NMR chemical shifts of inside H₂.



Dianion of open-cage fullerene derivative **1** having a 13-membered-ring orifice encapsulating hydrogen (H₂@**1**) was successfully generated within one hour by treating with CH₃SNa in acetonitrile-*d*₃ under vacuum. ¹H NMR spectrum of the resulting brown solution showed a signal for the encapsulated hydrogen at δ 8.13 ppm, which was downfield shifted by ca. 15 ppm as compared to that of neutral H₂@**1** (δ 7.25 ppm in 1,2-dichlorobenzene-*d*₄). More drastic downfield shift was observed when the pristine C₆₀ encapsulating H₂ (H₂@C₆₀) acquired two electrons. An NMR spectrum of dianion of H₂@C₆₀, which was generated in the same way as that of H₂@**1**, exhibited a signal for encapsulated H₂ at such a downfield as δ 26.36 ppm in acetonitrile-*d*₃ as shown in Figure 1. These large downfield shifts of H₂ signals upon two-electron reduction indicated significant decrease of overall aromaticity of the fullerene π -conjugated systems and were interpreted based on the GIAO and NICS calculations. We will also discuss NMR chemical shifts for H₂ encapsulated in dianion of open-cage C₆₀ derivatives with different orifice sizes.

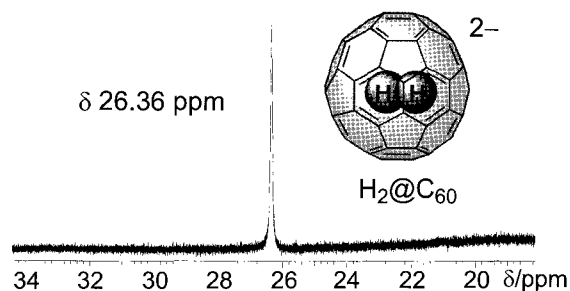


Figure 1. ¹H NMR spectrum of dianion of H₂@C₆₀ in acetonitrile-*d*₃.

[1] M. Murata, Y. Murata and K. Komatsu, *J. Am. Chem. Soc.* **128**, 8024 (2006).

Corresponding Authors:

Yasujiro Murata, Tel: +81-774-38-3173, Fax: +81-774-38-3178, E-mail: yasujiro@scl.kyoto-u.ac.jp

Koichi Komatsu, Tel: +81-776-29-7864, Fax: +81-776-29-7891, E-mail: komatsu@fukui-ut.ac.jp

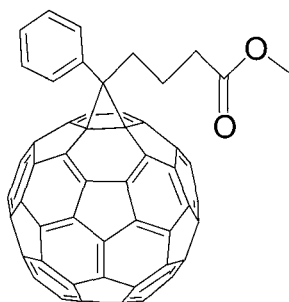
1P-9

Highly soluble fullerene derivatives and their production process development

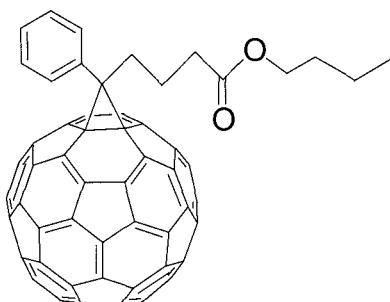
○Masahiko HASHIGUCHI, Eiji DEJIMA, Tomomi YANO, Katsutomo TANAKA

*Frontier Carbon Corporation
Engineering and Development Center
MCC-Group, Kurosaki, Yahatanishi-ku Kitakyushu-shi 806-0004 Fukuoka, Japan*

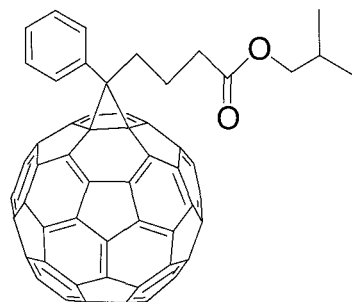
Recently the fullerene application development as the real industrial materials, has been progressed in many variety of the product are as such as the energy devices or the cosmetics. Though C_{60} , the most popular fullerene molecular, can be dissolved, the customers require the more solubility. By adding some functions using the chemical modification, the very high solubility can be attained for many kinds of the solvents. For example, PCBM families (refer to the following figures), it is found that the solubility has been dramatically changed by the different types of ester structure added to C_{60} . These types of molecular are now studied as the electron acceptor of the organic thin film photo voltaic cell all over the world[1,2].



PCBM



PCBNB



PCBIB

Frontier Carbon Corporation (FCC) has been developing the fullerene derivatives and the production process with Mitsubishi Chemical Science and Technology Research Center, and can supply the various fullerene derivatives which solubility is suitable for many industrial applications with the reasonable prices and the reliable qualities. In this poster some of the fullerene derivatives are introduced with some property data, as well as the FCC fullerene derivative development activity.

[1] G. Yu et al., *Science*, **270**, 1789 (1995).

[2] L. Zheng et al., *J. Phys. Chem. B*, **108**, 11921 (2004).

Corresponding Author: Masahiko HASHIGUCHI

TEL: +81-93-643-4400, FAX: +81-93-643-4401, E-mail: 6206530@f-carbon.com

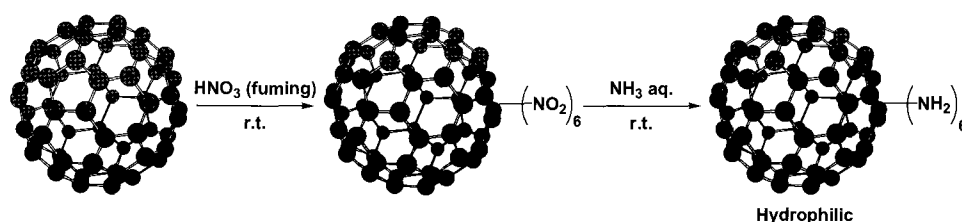
1P-10

Synthesis of Various Amino-Functionalized [60]Fullerene Derivative *via* Nitrofullerene Intermediate

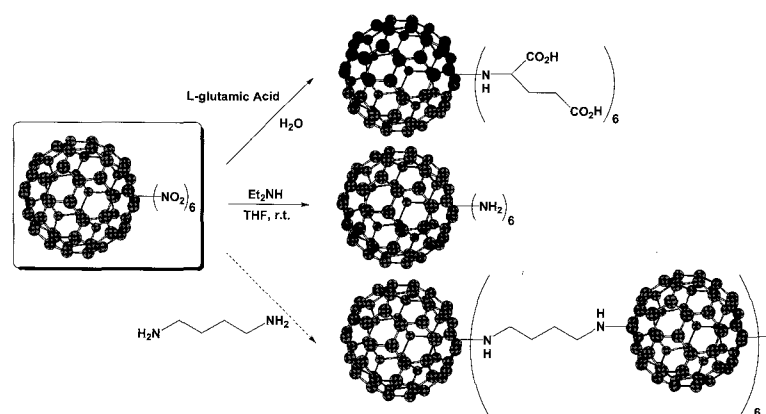
○Masaru Sekido, Masatomi Ohno

*Department of Advanced Science and Technology, Toyota Technological Institute
2-12-1 Hisakata, Tempaku, Nagoya 468-8511, Japan*

We have developed the effective methods to prepare the nitrofullerene intermediate¹⁾ and its application to synthesize hydrophilic fullerene derivatives, such as hydroxyfullerene derivatives. Aiming at the further application of the nitrofullerene intermediate, various amino functional groups were introduced to give aminofullerene derivatives. Typically nitrofullerene intermediate was prepared by the reaction of C₆₀ with HNO₃ (fuming) at room temperature without using any solvents to give the nitrofullerene intermediate as an orange crystal. Then NH₃ was added to the THF solution of this nitrofullerene intermediate to give the amino-fullerene derivative, which was soluble in water.



By using the similar methods various amino groups were introduced to give hydrophilic and lipophilic fullerene derivatives. For example, amino acid, such as L-glutamic acid, was introduced to give the corresponding hydrophilic fullerene derivatives, which may have interesting biological activity. Synthesis of the fullerene-knot network by using 1,4-diaminobutane was also attempted to obtain a fullerene-based material.



References: V. Anantharaj, J. Bhonsle, T. Canteenwala, and L. Y. Chiang, *J. Chem. Soc., Perkin Trans. 1*, 1999, 31-36.

Corresponding Author: Masaru Sekido, sekido@toyota-ti.ac.jp, tel:052-802-1841, fax:052-809-1721

Ultraviolet Photoelectron Spectroscopy of Lu-encapsulated Metallofullerenes

○Takafumi Miyazaki¹, Masayuki Kato², Konosuke Furukawa², Ryohei Sumii^{3,4}, Hisashi Umemoto⁵, Toshiya Okimoto⁵, Toshiaki Sugai⁵, Hisanori Shinohara⁵, Shojun Hino¹,

¹ Graduate School of Science & Technology, Ehime University

² Graduate School of Science & Technology, Chiba University

³ Institute for Molecular Science

⁴ Research Center for Materials Science, Nagoya University

⁵ Graduate School of Science, Nagoya University

The valence band electronic structure of C₈₂ endohedral fullerenes containing Lu atom(s) was studied by ultraviolet photoelectron spectroscopy.

Figure 1 shows the ultraviolet photoelectron spectra (UPS) of Lu-encapsulated C₈₂ obtained by hv=40eV irradiation. Their spectral onsets are 1.1 eV (C₈₂), 0.23 eV (Lu@C₈₂(I)), 0.60 eV (Lu₂@C₈₂(II)), 0.87 eV (Lu₂@C₈₂(III)), 0.61 eV (Lu₂C₂@C₈₂(II)) and 0.80 eV (Lu₂C₂@(III)). A large difference is observed in the structures between 0 – 4 eV. However, similarity is observed in the UPS of Lu₂@C₈₂(II) and Lu₂C₂@C₈₂(II), and in those of Lu₂@C₈₂(III) and Lu₂C₂@C₈₂(III). Lu₂@C₈₂(II) and Lu₂C₂@C₈₂(II) have the same C_{2v} cage structure and Lu₂@C₈₂(III) and Lu₂C₂@(III) have the same C_{3v}. It seems that the cage structure dominates the electronic structure derived from π-electrons.

Their spectral structures between 5~9eV are almost analogous, which suggests that the electronic structure of skeletal σ-bonds are almost the same. It should be noted that there are two structures at around 9.5 eV and 11.0 eV, which are not observed in the UPS of other fullerenes. These two structures are attributed to Lu 4f electrons.

Corresponding Author : S. Hino, E-mail : hino @ eng. ehime-u.ac.jp, phone : 089-927-9924

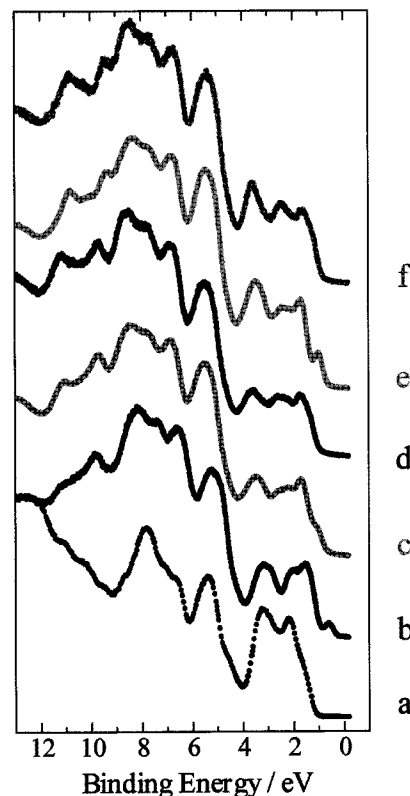


Figure 1 UPS of Lu-encapsulated C₈₂: (a) C₈₂, (b) Lu@C₈₂(I), (c) Lu₂@C₈₂(II), (d) Lu₂@C₈₂(III), (e) Lu₂C₂@C₈₂(II), and (f) Lu₂C₂@(III).

ESR Spectra of Bingel Mono-adducts of Gd@C₈₂

○Makoto Kanazumi^{J)}, Yuji Takematsu^{T)}, Takatsugu Wakahara^{T)}, Takahiro Tsuchiya^{T)},
Ko Furukawa^{J)}, Takeshi Akasaka^{T)}, Tatsuhisa Kato^{J)*}

^{J)}Department of Chemistry, Josai University, Sakado 350-0295, Japan, ^{T)} Center for
Tsukuba Advanced Research Alliance, University of Tsukuba, Ibaraki 305-8577, Japan,

^{J)} Institute for Molecular Science, Okazaki 444-8585, Japan,

Two kinds of Bingel mono-adducts of Gd@C₈₂ exhibited a sharp contrast on ESR spectra. The reaction of La@C₈₂ with diethyl bromomalonate in the presence of base (the Bingel reaction) has generated five monoadducts^{1), 2)}. The Tsukuba group of the authors recently synthesized two mono-adducts of Gd@C₈₂ which were well purified, mono-A and mono-E. ESR spectra of the adducts were obtained by using a high-field (W-band) ESR spectrometer at low temperature in solution, which show a remarkable

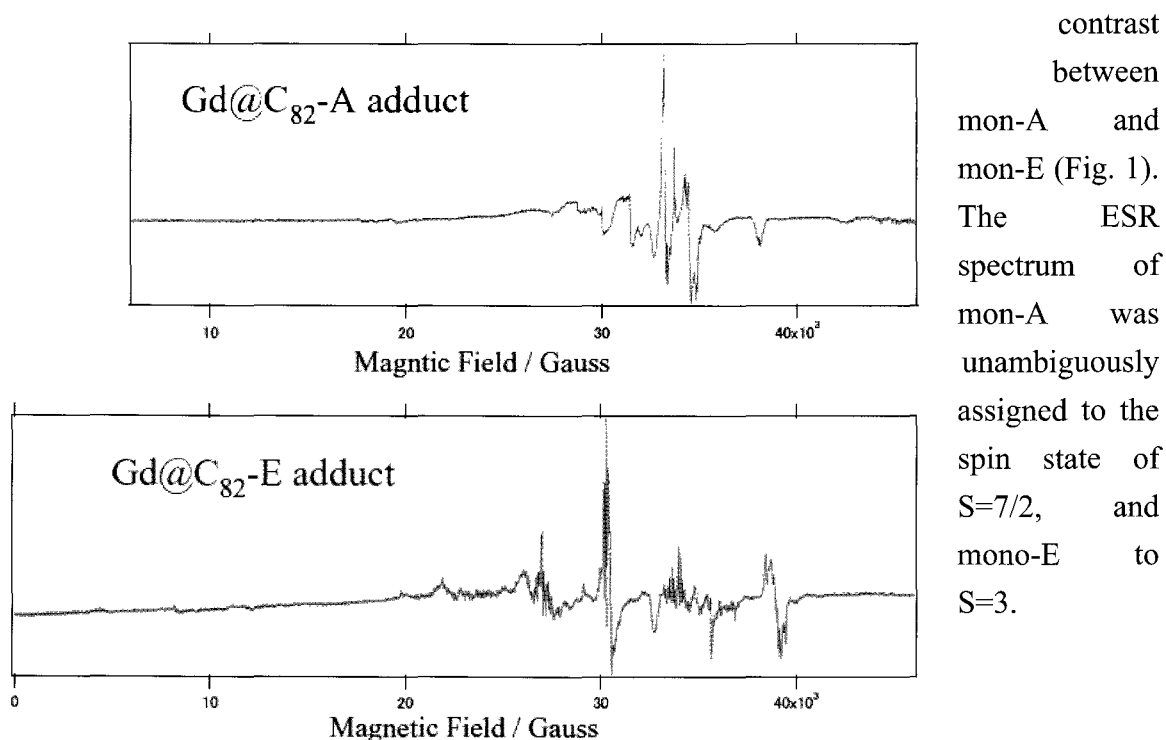


Fig. 1

References: 1) L. Feng et al., *J. Am. Chem. Soc.*, **127**, 17136-17137 (2005). 2) L. Feng et al., *Chem. Eur. J.*, **12**, 5578-5586 (2006).

Corresponding Author: Tatsuhisa Kato

Tel: 049-271-7295 **Fax:** 049-271-7985 **E-mail:** rik@josai.ac.jp

Characterization of Alkali Endohedral Fullerene: The Aggregated Cluster Structure

○Hiroshi Okada^{1,5}, Kenji Omote¹, Yasuhiko Kasama¹, Kuniyoshi Yokoo¹, Shoichi Ono¹,
Takamichi Miyazaki², Mariko Ando^{2,3}, Hideki Maekawa³, Kimio Akiyama⁴,
Takashi Komuro⁵, and Hiromi Tobita⁵

¹*Ideal Star Inc.,*

ICR Bldg, 6-6-3 Minamiyoshinari, Aoba-ku, Sendai 989-3204, Japan

²*Technical Division, Graduate School of Engineering, Tohoku University,
Sendai 980-8579, Japan*

³*Department of Metallurgy, Graduate School of Engineering, Tohoku University,
Sendai 980-8579, Japan*

⁴*Institute of Multidisciplinary Research for Advanced Materials, Tohoku University,
Sendai 980-8577, Japan*

⁵*Department of Chemistry, Graduate School of Science, Tohoku University,
Sendai 980-8578, Japan*

In 1996, Campbell et al. reported for the first time the synthesis of an alkali endohedral fullerene $\text{Li}@C_{60}$ using ion implantation technique [1] and described its extraction and purification [2]. They have investigated the properties of alkali endohedral fullerenes extensively (thermal stability, electric conductivity, IR, Raman, ESR, etc.) [3]. However, the structural characterization has not been achieved yet.

We have developed the mass production technique for $\text{Li}@C_{60}$ using the reaction of empty C_{60} with Li plasma and have examined its extraction with organic solvents and characterization of the extracted product.

The LDI-TOF MS spectrum of the extracted sample shows a strong molecular ion peak at $m/z = 727$ (Figure 1). The ICP analysis of Li revealed that the sample contains 0.05-0.07 wt% of Li. This result indicates that the $\text{Li}@C_{60}$ molecules in the extracted sample aggregate with empty C_{60} molecules to form a cluster structure formulated as $(\text{Li}@C_{60})(C_{60})_x$ ($x = 12 \sim 20$). The particle size of the extracted sample, 3-7 nm in diameter, determined by TEM (Transmission Electron Microscope) and DLS (Dynamic Light Scattering) in solution is consistent with the above-mentioned cluster structure.

In this poster, we report the extraction process for $\text{Li}@C_{60}$ and analytical data for the extracted material. Its ^7Li NMR and ESR spectra will also be discussed.

[1] Campbell et al., *Nature*, **382**, 407 (1990).

[2] Campbell et al., *Appl. Phys.*, **A66**, 293 (1998).

[3] (a) Campbell et al., *Eur. Phys. J. D*, **9**, 345 (1999).

(b) Campbell et al., *J. Phys. Chem. B*, **107**, 11290

(2003). (c) Campbell et al., *Solid State Communications*, **133**, 499 (2005).

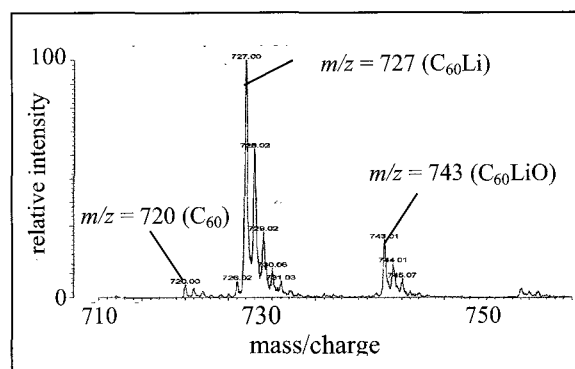


Figure 1. A mass spectrum of the extracted product

Corresponding Author: Hiroshi Okada

TEL: +81-22-303-7336, FAX: +81-22-303-7339, E-mail: hiroshi.okada@idealstar-net.com

A Reversible Crystal Structural Transformation and Structural Characterization of Pr@C₈₂ Metallofullerene.

Ryo Kitaura, Yutaka Kitamura, Eiji Nishibori, Shinobu Aoyagi, Makoto Sakata, Haruya Okimoto, Hisanori Shinohara*.

Endohedral metallofullerenes have attracted much attention during the past decade and added a new dimension to materials-directed physics and chemistry; properties and applications of these materials range from magnetism, photoluminescence, transport and mechanical properties, molecular switches, field effect transistors and drug deliveries.^{1, 2} M@C₈₂ (M = rare earth metal ions) is one of the most abundant metallofullerenes, where water-soluble Gd@C₈₂ is a promising candidate for MRI contrast agents of next generation. Elucidation of molecular and packing structure of these metallofullerenes is essential to understand their properties and promote further applications.

Synchrotron X-ray powder diffraction (SXRD) followed by MEM/Rietveld analysis is one of the most powerful techniques to determine the structure of novel metallofullerenes. We have promoted systematic structural characterization of M@C₈₂ metallofullerenes using the SXRD-MEM/Rietveld method, and successfully determined the structure of Eu, Gd, Ce, Dy and Er encapsulating M@C₈₂ metallofullerenes. In this presentation, we will focus on Pr@C₈₂ whose molecular and crystal structure is still unknown.

Pr@C₈₂ was synthesized by using arc-discharge and purified by high-performance liquid chromatography. By controlling temperature and growing speed of the sample preparation, we have prepared two crystals, one is monoclinic and the other is triclinic crystal system. Both of crystal structures were successfully determined by the MEM/Rietveld method. In the triclinic crystal, Pr@C₈₂ molecules form 2-dimensional array separated by layers of toluene molecules, whereas 3-dimensional packing of Pr@C₈₂ was formed in the monoclinic crystal. We also found that a reversible crystal structural transformation from the monoclinic to triclinic structure occurs by exposing Pr@C₈₂ crystals to toluene vapors.

1. Kitaura, R. & Shinohara, H. Carbon-nanotube-based hybrid materials: Nanopeapods. *Chemistry-an Asian Journal* 1, 646-655 (2006).
2. Shinohara, H. Endohedral metallofullerenes. *Reports on Progress in Physics* 63, 843-892 (2000).

Corresponding Author: Hisanori Shinohara
TEL: +81-52-789-2482, FAX: +81-52-789-1169, E-mail: noris@cc.nagoya-u.a.jp

Metallic Phase in Magnesium Fullerides

○Satoshi Heguri, Nozomu Kimata, Mototada Kobayashi

*Department of Material Science, Graduate School of Material Science
University of Hyogo, Ako, Hyogo 678-1297, Japan*

The divalent magnesium ion Mg^{2+} has a small ionic radius. A large number of Mg^{2+} will be accommodated into fullerene lattice and it may be possible to control a doping level widely. We have reported structural and physical properties of magnesium fullerides Mg_xC_{70} [1,2]. The x-ray powder diffraction profile of magnesium saturated phase Mg_5C_{70} is shown in Fig.1. It can be assigned to a simple orthorhombic structure with $a=1.684$, $b=1.462$ and $c=1.384$ nm. The molar ratio x was determined by weight uptake measurement. Figure 2 shows the temperature dependence of the spin susceptibility of the Mg_5C_{70} derived from the intensity of the ESR signal. The spin susceptibility was estimated to be 4.1×10^{-5} emu/mol at 300K. This value is one order smaller than those of typical metallic fullerides. Mg_5C_{70} was suggested to be insulating.

We adopted thin film technique in order to reveal possible metallic phases. Evaporation technique may improve the diffusivity of magnesium into fullerene lattice. Pristine C_{70} film of 100nm thickness was deposited on a glass substrate at 423K under high vacuum of the order of 10^{-4} Pa. Mg metal was deposited onto the film in the evaporation chamber afterward. Electrical resistivity measurement was performed by four-probe method during the deposition. The substrate was maintained at 473K throughout the Mg deposition process. The composition x of Mg_xC_{70} film was estimated from the thickness ratio of Mg to C_{70} . The thickness was measured by using a quartz oscillator thickness monitor. Mg concentration dependence of the electrical resistivity for Mg_xC_{70} films, together with Mg_xC_{60} , will be discussed at the meeting.

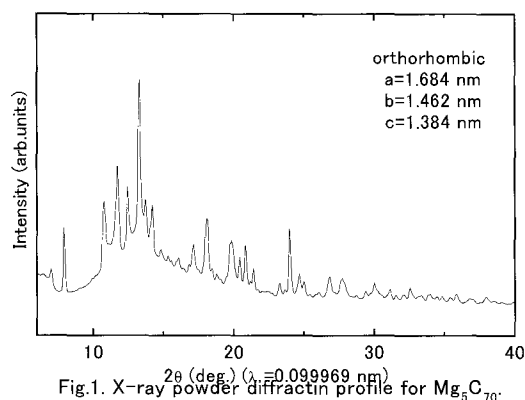


Fig.1. X-ray powder diffraction profile for Mg_5C_{70} .

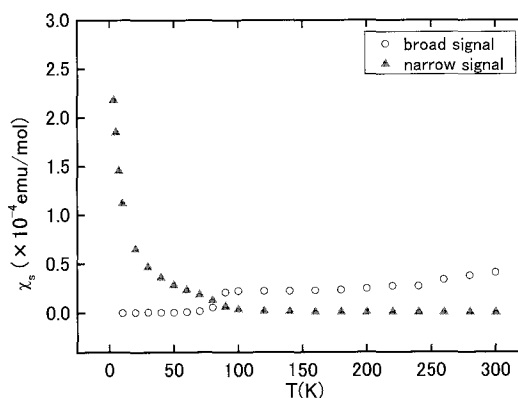


Fig.2. Temperature dependence of the spin susceptibility for Mg_5C_{70} derived from ESR intensity.

- References:** [1] S. Heguri et al., The 23rd Commemorative Fullerene&Nanotubes Symposium, 2p-84(2003).
[2] S. Heguri et al., The 25th Commemorative Fullerene&Nanotubes Symposium, 1P-34(2004).

Corresponding Author: Satoshi Heguri

E-mail: rk07d004@stkt.u-hyogo.ac.jp

Tel&Fax: +81-791-58-0156/+81-791-58-0132

1P-16

Superconductivity in sodium fullerenes Na_xC_{60}

○Nozomu Kimata, Satoshi Heguri, and Mototada Kobayashi

*Department of Material Science, Graduate School of Material Science,
University of Hyogo, Ako, Hyogo 678-1297, Japan*

The structure and physical properties of sodium fullerenes Na_xC_{60} are very interesting because they are different from those of other alkali-doped C_{60} . Since the Na^+ ion has a small ionic radius, Na_xC_{60} with large x value can be expected. Yildirim *et al.* reported the synthesis of $\text{Na}_{9.7}\text{C}_{60}$ with an face-centered cubic(fcc) structure and suggested the Na-saturated phase to be $\text{Na}_{11}\text{C}_{60}$ [1]. Superconductivity in Na_xC_{60} has not yet been found. We report here the results of structure and magnetic susceptibility and superconductivity for Na_xC_{60} .

Sodium doped fullerenes were prepared from sublimed C_{60} powder with 99.95% purity (MTR Ltd.) and Na metal. The mixture of degassed C_{60} and Na metal was encapsulated into a stainless steel tube and sealed into a Pyrex glass tube after evacuating. Thermal treatments in a furnace were carried out at 723K for 192 hours. The molar composition x of products were determined by weight uptake measurement.

The X-ray powder diffraction profiles for Na_xC_{60} ($6 \leq x$) at room temperature using $\text{MoK}\alpha$ radiation are shown in Fig.1. All profiles can be assigned to be a hexagonal lattice. Lattice parameters of $\text{Na}_{10.8}\text{C}_{60}$ are $a=1.023$ and $c=1.662$ nm, respectively. Figure 2 shows the temperature dependence of the magnetic susceptibility for $\text{Na}_{8.2}\text{C}_{60}$ by using SQUID magnetometer. Clear superconducting transition was observed below $T_c=14\text{K}$. The magnitude of the flux exclusion for the zero-field-cooled curve corresponds to 0.5% volume fraction. Details will be discussed at the meeting.

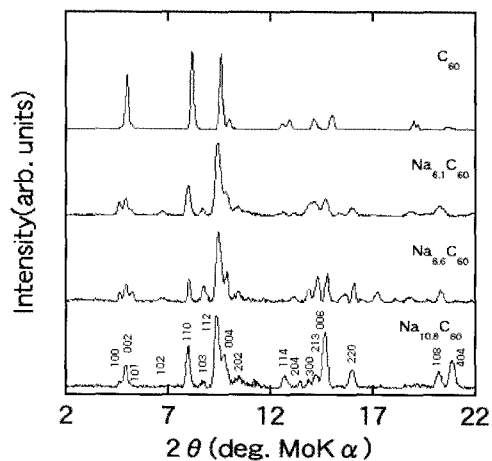


Fig.1 X-ray diffraction profiles for Na_xC_{60} with $x=0,6,9$ and 11 by using $\text{MoK}\alpha$ radiation

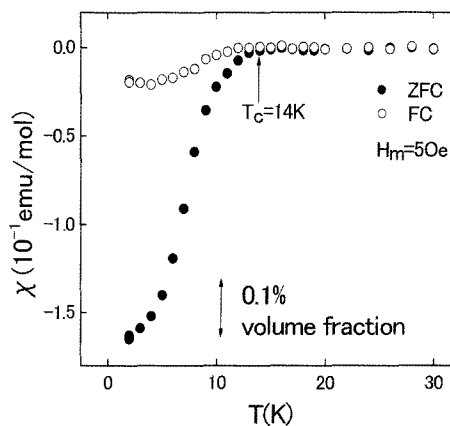


Fig.2 Temperature dependence of magnetic susceptibility for $\text{Na}_{8.2}\text{C}_{60}$ by using SQUID.

[1] T.Yildirim, O.Zhou, J.E.Fischer, N.Bykovetz, R.A.Strongin, M.A.Cichy, A.B.Smith III, C.L.Lin and R.Jelinek, *Nature*, **360**, 568(1992).

Corresponding Author: Nozomu Kimata

TEL: +81-791-58-0156, FAX:+81-791-58-0132, E-mail: ri07v005@stkt.u-hyogo.ac.jp

Molecular beam epitaxy of copper phthalocyanine on C₆₀ (111) surface

H. Suzuki, Y. Yamashita, ○N. Kojima and M. Yamaguchi

Toyota Technological Institute, 2-12-1 Hisakata, Tempaku, Nagoya 468-8511 Japan

C₆₀ and copper phthalocyanine (CuPc) are expected as a prospective combination to fabricate an organic solar cell with high conversion efficiency, because they have high carrier mobility in organic semiconductors. So far, 5.7 % of conversion efficiency has been achieved by the combination [1]. However, separation and transport processes of carriers between C₆₀ and CuPc have been not clear yet. To analyze the processes precisely, it is necessary to prepare highly ordered CuPc/C₆₀ structure. Molecular beam epitaxy method is a useful technique to fabricate such ordered structures. In this study, we selected a C₆₀ (111) surface as a template for epitaxial growth of CuPc.

C₆₀ (111) surfaces were prepared by MBE method on cleaved mica substrates in an ultra high vacuum chamber. The C₆₀ (111) surfaces were evidenced by reflection high-energy electron diffraction. Continuously, CuPc was evaporated on the C₆₀ (111) surfaces at 60~160°C. After evaporation, the samples were removed from the chamber. Lattice constant and orientation of CuPc crystals were evaluated by x-ray diffraction (XRD) and surface morphology was observed by scanning electron microscopy (SEM).

Typical surface morphology of a CuPc crystal on C₆₀ (111) is shown in Fig.1. For comparison, that on a mica substrate is also shown. In case of mica, CuPc agglutinated each other and the bare mica substrate was observed (white region in the figure). In case of C₆₀, CuPc forms fiber shape crystals and covered whole region of the surface. In addition, CuPc crystals were aligned along 3 directions equivalent to <112> on C₆₀ (111), although few fibers were dispersed randomly on the top of the surface. These results indicated that epitaxial CuPc crystals could be grown on C₆₀ (111) by MBE.

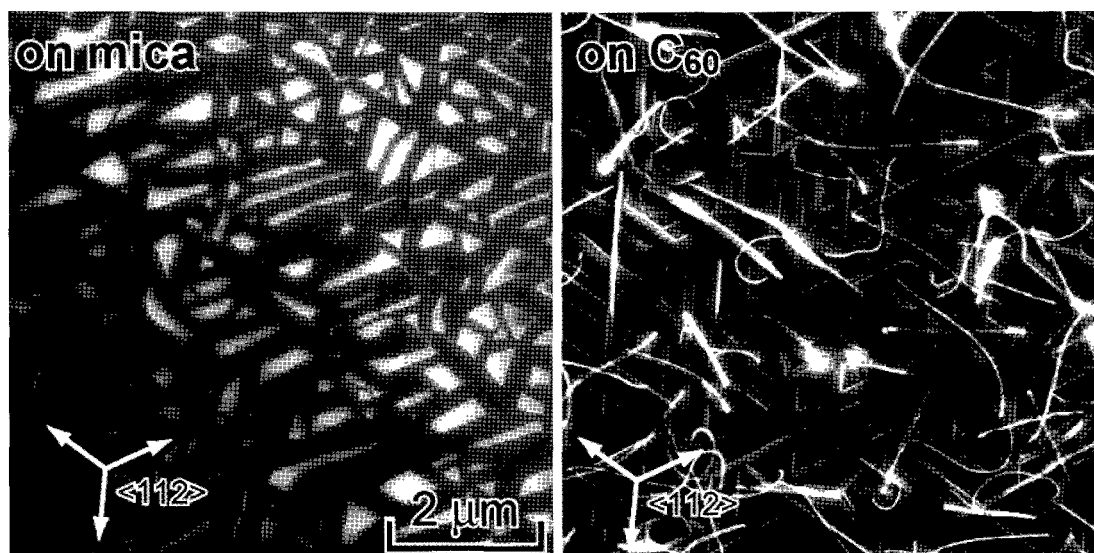


Fig.1: SEM images of CuPc crystals grown on mica (left) and C₆₀ (111) (right).

References: [1] J. Xue, et. al., Appl. Phys. Lett., 85 (2004) 5757

Corresponding Author: H. Suzuki, E-mail: ssk@toyota-ti.ac.jp, Tel&Fax: +81-52-809-1830

Sub-millimeter long single-walled carbon nanotubes synthesis by alcohol enclosed catalytic chemical vapor deposition

○Yoshinobu Suzuki¹, Tomohiro Shimazu¹, Hisayoshi Oshima¹, and Shigeo Maruyama²

¹Research Laboratories, DENSO Corporation

500-1 Minamiyama, Komenoki, Nisshin-shi, Aichi 470-0111, Japan

²Department of Mechanical Engineering, The University of Tokyo

7-3-1 Hongo, Bunkyo-ku, Tokyo 113-8656, Japan

To obtain longer vertically aligned single-walled carbon nanotube films using alcohol catalytic vapor deposition (ACCVD)[1], we have developed a novel method. Using a conventional ACCVD system, ethanol vapor was filled up and enclosed in a reactor tube with Co/Mo catalysts formed on a quartz substrate during growth period.

Comparing gas flow type ACCVD, gas enclosed type ACCVD increased the film thickness up to 0.11mm for 30min growth. Gas elements during CVD were investigated by means of Fourier transform infrared spectroscopy (FT-IR) and quadrupole mass spectrometer (QMAS). Ethanol was thermally decomposed into ethylene, acetylene, acetaldehyde, and water, and at CVD temperature. A possible mechanism for the increase of film thickness is suppression of carbon coating on catalysts by produced water and enhancement of SWNTs growth by new generated carbon sources such as ethylene.

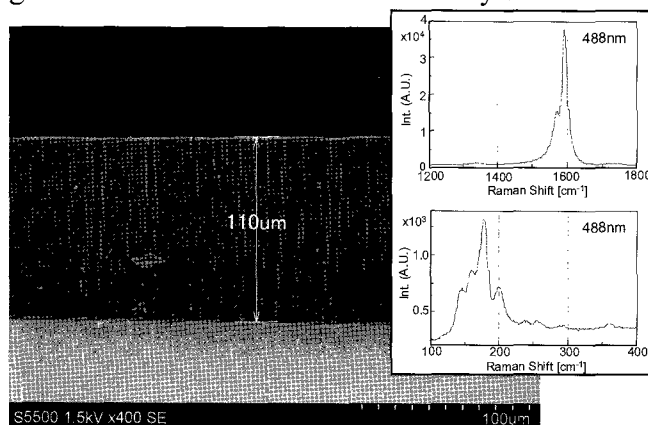


Fig.1 A typical cross-section SEM image and Raman spectrum excited by 488nm laser
Growth conditions: enclosed initial pressure 2.7kPa at 840°C for 30min

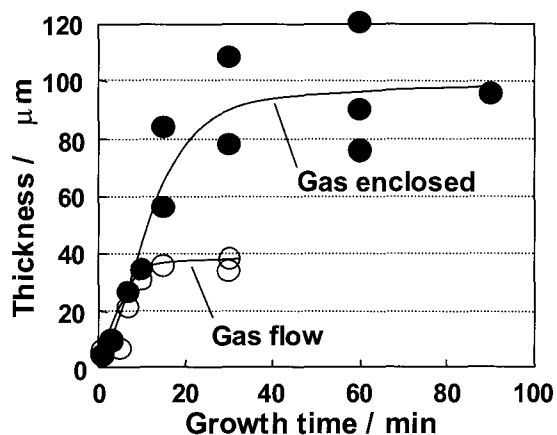


Fig.2 SWNTs film thickness as a function of growth time. Gas enclosed conditions: initial pressure 2.7kPa at 840°C. Gas flow conditions: Pressure 1.3kPa at 840°C

[1] Y. Murakami, S. Chiashi, Y. Miyauchi, M. Hu, M. Ogura, T. Okubo, and S. Maruyama, *Chem. Phys. Lett.*, **385**, 298 (2004)

Corresponding Author: Hisayoshi Oshima

E-mail: hoosima@rlab.denso.co.jp Tel.: +81-561-75-1860 Fax.: +81-561-75-1193

Growth Termination of Carbon Nanotubes at Millimeter Thickness Due to Structural Change in Catalyst

○Shingo Morokuma¹, Kei Hasegawa¹, Suguru Noda¹, Shigeo Maruyama², Yukio Yamaguchi¹

¹*Dept. of Chemical System Engineering, The University of Tokyo, Tokyo 113-8656, Japan*

²*Dept. of Mechanical Engineering, The University of Tokyo, Tokyo 113-8656, Japan*

The water-assisted growth method, so-called "supergrowth [1]", realized millimeter-thick vertically-aligned single-walled carbon nanotubes (VA-SWNTs). Later, it is reported that "supergrowth" rate decreases with reaction time and finally the growth terminates [2]. Our group recently reproduced "supergrowth" [3] and observed similar "supergrowth" termination within a few tens minutes. In this work, we analyzed substrate surface before and after CVD to clarify the mechanisms of catalyst deactivation.

0.5-2-nm-thick Fe catalyst was prepared on Al₂O₃/SiO₂ substrate by sputtering method. After 10 minutes reduction of this catalyst under 27 kPa H₂/ 0.010 kPa H₂O/ Ar balance at atmospheric pressure, 8.0 kPa C₂H₄ was introduced and CVD was carried out at 1093 K for 3-30 min. After removing CNT by oxidation in air at 1000 K, substrate surfaces were investigated by SEM and XPS. SEM images of substrate surfaces showed that the mean diameter of catalyst particles increased while number density of catalyst particles decreased with an increasing CVD time (Fig. 1). Fe/Al intensity ratio by XPS decreased with reaction time, and this change occurred quickly for thinner Fe (Fig. 2). The decrease in Fe/Al ratio is caused by the increase in Fe particle size rather than by the decrease in the amount of Fe. The coarsening of Fe particles during CVD is possibly the fundamental cause of the growth termination under our experimental conditions. More details will be reported.

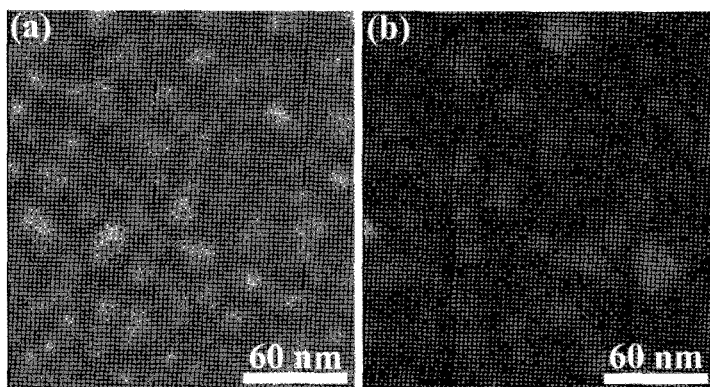


Fig. 1 SEM images of 2 nm Fe/ Al₂O₃/SiO₂ sample surfaces after CVD for (a) 3 min and (b) 30 min. VA-CNTs were removed by oxidizing under air at 1000 K.

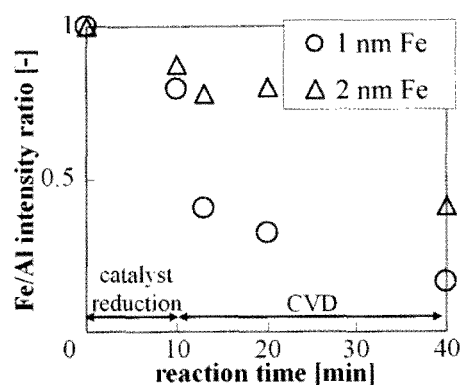


Fig. 2 Change of XPS intensity with reduction/CVD time at 1093 K. Intensity ratio was normalized by the initial value.

References

- [1] K. Hata, et al., *Science*, **306**, 1362 (2004).
 [2] D. N. Futaba, et al., *Phys. Rev. Lett.*, **95**, 056104 (2005).
 [3] S Noda, et al., *Jpn. J. Appl. Phys.*, **46**, L399 (2007).

Corresponding Author: Suguru Noda

TEL: +81-3-5841-7330, FAX: +81-3-5841-7332, E-mail: noda@chemsys.t.u-tokyo.ac.jp

Single-Wall Carbon Nanotubes Grown from Size Controlled Rh/Pd and Co Nanoparticles by Catalyst-supported Chemical Vapor Deposition

○Keita Kobayashi¹, Ryo Kitaura¹, Yoko Kumai³, Yasutomo Goto³, Shinji Inagaki³ and Hisanori Shinohara^{1,2}

¹Department of Chemistry, Nagoya University, Nagoya 464-8062, Japan

²Institute for Advanced Research, Nagoya University, and CREST/JST

³Toyota Central R&D Labs., Inc., Nagakute, Aichi, 480-1192, Japan

In chemical vapor deposition (CVD) growth of carbon nanotubes (CNTs), preparation of size-controlled metal catalyst nanoparticles is essential to realize diameter-controlled growth of CNTs; the diameter of CNTs depends on the size of catalyst nanoparticles employed. Mesoporous materials such as

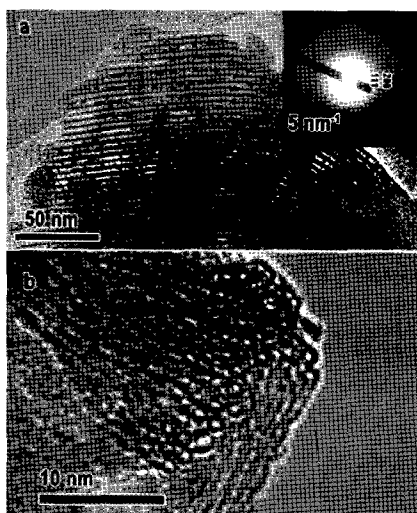


Figure 1. (a)TEM image and the corresponding electron diffraction pattern (inset) of FSM-16 impregnating size-ordered Rh/Pd particles (b) Typical TEM image of the SWNTs obtaining after CCVD

FSM-16 [1, 2] have ideal one-dimensional (1D) channels with a narrow size distribution, which provides suitable nano-sized ordered space to prepare regulated nano-sized metal particles [3]. In a previous study, we reported synthesis of single-wall carbon nanotubes (SWNTs) by catalyst-supported CVD (CCVD) using size-ordered Rh/Pd nanoparticles which are supported in 1D channels of FSM-16[4, 5]. The diameter of obtained SWNTs is smaller than the size of Rh/Pd nanoparticles (Fig. 1), indicating that the diameter distribution of SWNTs depends not only on the size of catalyst particles but also on specimen of catalysts. Here, we report the growth of SWNTs by CCVD using size-controlled Co and Rh/Pd particles supported on the mesoporous materials.

A mixture solution of $\text{RhCl}_3/\text{H}_2\text{PdCl}_2$ or $\text{CoCl}_2 \cdot 6\text{H}_2\text{O}$ was used as a source of catalyst metals, which were mixed with a powder of FSM-16. The $\text{RhCl}_3/\text{H}_2\text{PdCl}_2$ or $\text{CoCl}_2 \cdot 6\text{H}_2\text{O}$, which were incorporated in 1D channel of FSM-16, were reduced by a high temperature H_2 reaction. Prior to alcohol CCVD, the Rh/Pd particles were treated at 1173 K in air to enhance the catalyst activity [6]. The alcohol CCVD was carried out at 1173 K under an Ar gas flow. Obtained SWNTs were characterized by TEM observations and Raman spectroscopy.

We will discuss the correlation between the diameter distribution of SWNTs and size of catalyst metal nanoparticles.

- [1] T. Yanagisawa et al., *Bull. Chem. Soc. Jpn.*, **63**, 988 (1990).
- [2] S. Inagaki et al., *Chem. Commun.*, 680 (1993).
- [3] A. Fukuoka et al., *Microporous Mesoporous Mat.*, **48**, 171 (2001).
- [4] K. Kobayashi et al., *Proc. 32nd Fullerene nanotubes symposium*, 397 (2006).
- [5] K. Kobayashi et al., in preparation.
- [6] D. Takagi et al., *Nano Lett.*, **6**, 2642 (2006).

Corresponding Author : Hisanori Shinohara

TEL: +81-52-789-2482, FAX:+81-52-789-1169, E-mail: noris@cc.nagoya-u.ac.jp

Synthesis of small diameter SWNTs by ACCVD method using platinum as catalyst

○Keisuke Urata¹, Sinzo Suzuki², Hiroshi Nagasawa³, and Yohji Achiba¹

¹*Department of Chemistry, Tokyo Metropolitan University, Tokyo 192-0397, Japan*

²*Department of Physics, Kyoto Sangyo University, Kyoto 603-8555, Japan*

³*Life Science System Division, EBARA Corporation,
Kanagawa 251-8502, Japan,*

It is well known that ambient temperature, carbon source materials, and the kind of catalyst are important parameters for controlling the production of SWNTs. Actually, so far we have reported that platinum catalyst gives rise to very narrow diameter distribution of SWNTs [1]. The diameter distribution was also found to be very much dependent on the pore size of the porous glass used as a supported material [1,2]. In this presentation, the effect of alcohol pressure (density of carbon supply) on the diameter distribution of SWNTs was carefully investigated by means of so called alcohol-CCVD (ACCVD) method.

The SWNTs samples were synthesized by ACCVD method using ethanol as carbon source, and platinum was used as a catalyst deposited on PG. The ambient temperature and an inner pressure of ethanol were systematically changed with the aim of synthesizing the smaller and the narrower diameter distributions of SWNTs. The obtained SWNTs were analyzed by TEM, Raman spectroscopy, and fluorescence spectroscopy. Typical example of Raman spectra are shown in Figs.1 (a) and (b). Under the higher pressure condition, the average diameter of SWNT sample tends to shift to the larger one, but the lower pressure condition results in the production of the SWNTs with the smaller diameter, peaking at 311cm^{-1} (6,5) and 370cm^{-1} (5,4). Furthermore, it was also found that the relative ratio of these two peaks changes by changing the ambient temperature.

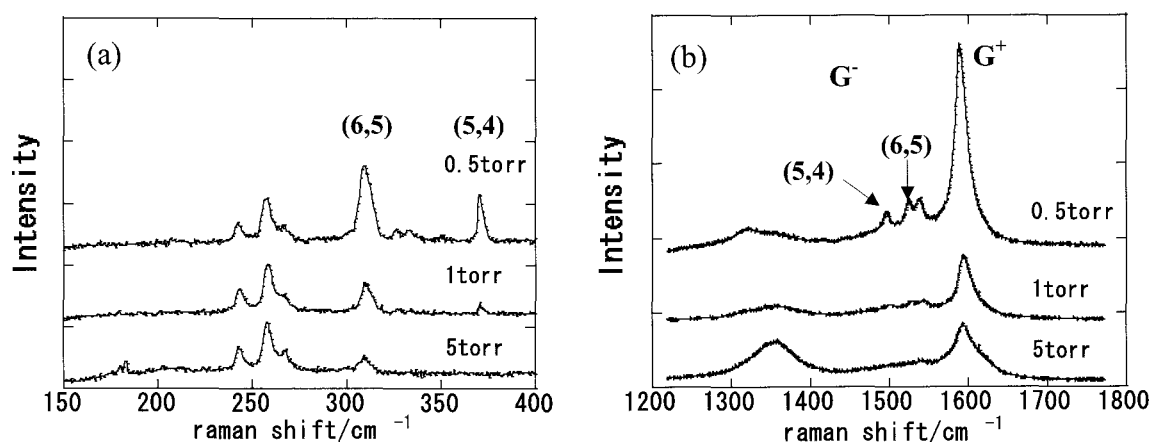


Figure.1.: Raman spectra of SWNTs synthesized at 850°C

with different pressure of ethanol. (488nm)

References:[1] K. Urata et al., The 31th Fullerene-Nanotubes General Symposium, 1P-30 (2006).

[2] Y.Aoki et al., Chem. Lett., **562**, 34(2005)

Corresponding Author: Yohji Achiba

E-mail: achiba-yohji@c.metro-u.ac.jp, **TEL:**042-677-2534

Efficient growth of double-walled carbon nanotube by CVD using a mixed catalyst Fe/Co/Mo with MgO supporter

○Ryoji Naito¹, Toshiya Murakami¹, Yuki Hasebe¹, Kenji Kisoda², Koji Nishio¹, Toshiyuki Isshiki¹ and Hiroshi Harima¹

¹Department of Electronics, Kyoto Institute of Technology, Kyoto 606-8585, Japan

²Physics Department, Wakayama University, Wakayama 640-8510, Japan

Double-walled carbon nanotubes (DWNT) have great potential for future nm-sized devices due to their robustness and quasi one-dimensionality. It is, however, very difficult to grow DWNT selectively in an efficient manner. We have already reported the growth of high purity DWNT by chemical vapor deposition (CVD) using MgO as a supporting material and Fe/Co/Mo as a catalyst.[1] Here we studied in more detail to find the key parameters for growing DWNT and discussed the growth mechanism.

The DWNT sample was grown by CVD at 850 °C using n-hexane as a carbon source. They were purified by post-oxidation in air at 700°C to remove single-walled carbon nanotubes (SWNT) and other carbon impurities. Here we tested various catalyst compositions between Fe, Co and Mo, and also compared catalyst supporting materials between MgO, SiO₂ and Al₂O₃.

As a result, we found that DWNTs grew only on MgO, and mixed catalysts of Co/Mo, Fe/Mo and Fe/Co/Mo worked more efficiently than any single elemental catalyst. In the case of ternary mixture, Fe/Co/Mo, the Mo concentration greatly affected the DWNT content in the as-grown samples. As shown by TEM images in Fig.1, DWNT grew more efficiently for composition of Fe/Co/Mo=1/1/5.5 wt% (b) than for 1/1/1.8 wt% (a). All these results suggest important role of Mo, and we may optimize the Mo content for efficient growth of DWNT.

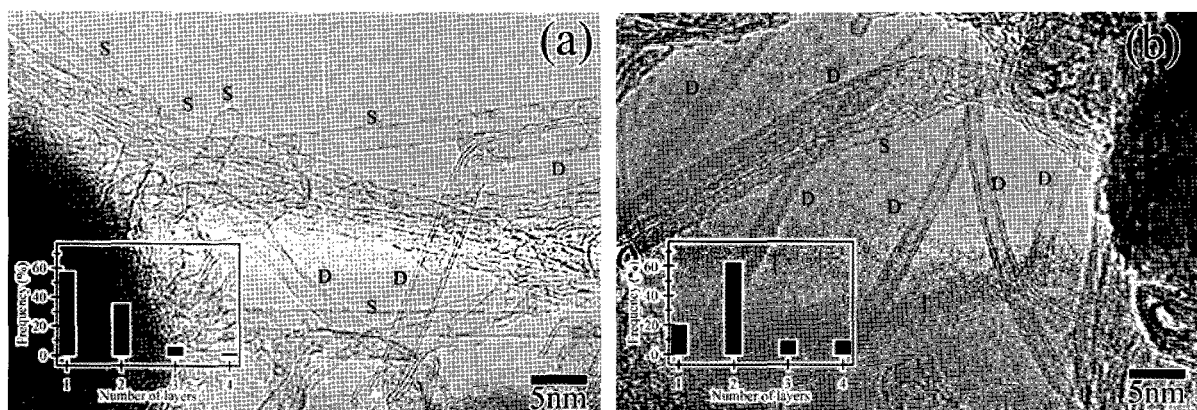


Figure 1. TEM images of as-grown samples for (a) Fe/Co/Mo=1/1/1.8wt% and (b) Fe/Co/Mo=1/1/5.5wt%. Insets are histograms of wall numbers of observed nanotubes; 1 for SWNT, 2 for DWNT, and so on. Symbols “S” and “D” indicate SWNT and DWNT, respectively.

[1] K. Matsumoto, T. Murakami, T. Isshiki, K. Kisoda and H. Harima, *Diamond and Related Materials*, **16** (2007) 1188.

Corresponding Author: Ryoji Naito

TEL: +81-75-724-7417, E-mail: m7621018@edu.kit.ac.jp

Purification of SWNTs fabricated by hydrogen DC arc discharge

○ B. Chen^a, T. Suzuki^a, X. Zhao^a, S. Inoue^a, T. Hashimoto^b, and Y. Ando^a

^a21st COE Program "Nano Factory", Department of Material Science & Engineering,
Meijo University, Tenpaku-ku, Nagoya 468-8502, Japan

^bMeijo Nano Carbon Co., Ltd., Naka-ku, Nagoya 460-0002 Japan

Single-walled carbon nanotubes (SWNTs) with high crystallization have been synthesized by a hydrogen DC arc discharge with evaporation of carbon anode containing 1at% Fe catalyst in H₂-Ar mixture gas[1]. It is also very clear that some impurities such as metal particles and amorphous carbon coexist in the SWNTs soot. In order to obtain high quality of SWNTs, various purification methods have been attempted. As we know, refluxing by H₂O₂ is an efficient method for SWNTs purification. However, it is necessary to use a lot of toxic H₂O₂ and take a long time. In this study, a high-pressure microreactor has been utilized instead of refluxing instrument. Therefore, even with a little H₂O₂ by shorter time, the purification of SWNTs can be efficiently realized. The purified SWNTs have been confirmed by scanning electron microscopy (SEM, as shown in Fig. 1) and transmission electron microscopy (TEM, as shown in Fig. 2).

By the result of thermogravimetric analysis (TGA), it is known that Fe particles are almost near to zero. After the purification, the nitrogen cryo-adsorption isotherms have been measured. The specific surface area (SSA) of purified SWNTs calculated using the Brunauer-Emmett-Teller is about two times as large as that of as-grown SWNTs.

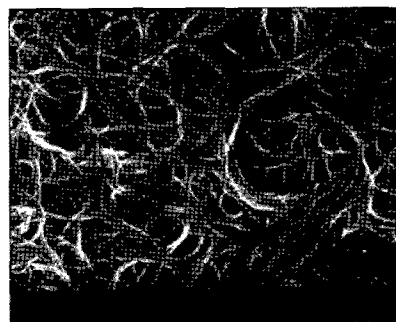


Fig. 1 SEM image of purified SWNTs



Fig. 2 TEM image of purified SWNTs

Reference: [1] X. Zhao, et al., *Chem. Phys. Lett.*, **373**, 266-271 (2003)

Corresponding Author: Beibei Chen

Tel: +81-52-838-2409, Fax: +81-52-832-1170

E-mail: m0641507@ccmailg.meijo-u.ac.jp

One-step Synthesis of Aligned Carbon Nanotubes in Liquid Phase

○Kiyofumi Yamagiwa, Masafumi Mikami, Tsuneharu Takeuchi, Yoshihiro Yamaguchi,
Yuriko Iwao, Morihito Saito, Jun Kuwano

*Department of Industrial Chemistry, Faculty of Engineering, Tokyo University of Science,
12-1 Ichigayafunagawara-cho, Shinjuku-ku, Tokyo 162-0826, Japan*

Ando *et al.* have recently reported the liquid-phase synthesis of highly aligned carbon nanotubes (CNTs) by resistance heating of a small Si substrate in liquid organic compounds [1,2]. However, the Fe metal catalyst was deposited on the substrate by a vacuum process, namely sputtering. The whole process thus consisted of two-step processes.

In this study, we have developed a novel one-step process for liquid-phase synthesis of highly aligned CNTs[3,4]. We used the substrate of stainless steel (SUS304) and homogeneously dissolved cobaltocene $\text{Co}(\text{C}_5\text{H}_5)_2$ in alcohols as a catalyst source. Commercially available stainless steel (SUS304) substrates were used without any surface treatments. The substrate ($5 \times 25 \times 0.1 \text{ mm}^3$) was heated at 800°C for 15 min in an alcohol (200 ml) by applying a direct current. Straight-chain primary alcohol with $n_c=1-6$ (n_c : the number of carbon atoms), 1,2-ethanediol, cyclohexanol and *tert*-butanol were used as a carbon source to examine the effects of the molecular structures on the morphologies and alignment of CNTs.

Fig. 1 shows a SEM image of highly aligned CNTs prepared from methanol containing cobaltocene. Vertically aligned multi-walled CNTs were grown on the stainless steel substrates in all the alcohols except 1,2-ethanediol and *tert*-butanol. Methanol brought the best purity and alignment of CNTs of all the alcohols. A large amount of amorphous carbon and irregularly deposited CNTs were prepared from 1,2-ethanediol. Only a small amount of amorphous carbon was prepared from *tert*-butanol.

Distinctive features of this method are simple, low cost and a one-step process involving none of vacuum processes and catalyst preparation processes.

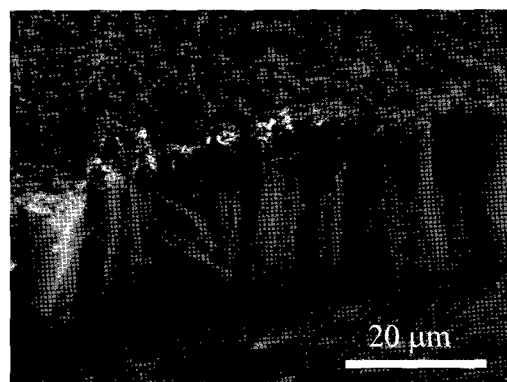


Fig. 1. SEM image of highly aligned CNTs prepared from methanol containing cobaltocene.

[1] Y. F. Zhang, M. N. Gamo, C. Y. Xiao and T. Ando, *Physica B*, **323**, 293 (2002).

[2] Y. F. Zhang, M. N. Gamo, C. Y. Xiao and T. Ando, *Jpn. J. Appl. Phys*, **41**, L411 (2002).

[3] K. Yamagiwa *et al.*, *Key Eng. Mater.*, in press.

[4] M. Mikami *et al.*, *Key Eng. Mater.*, in press.

Corresponding Author: Jun Kuwano

TEL/FAX: +81-3-5228-8314, E-mail: kuwano@ci.kagu.tus.ac.jp

Controlling diameter distribution of SWNTs by refining temperature gradient in laser ablation method

○T. Nakayama¹, Y. Tsuruoka¹, S. Suzuki^{1,2}, Y. Achiba¹

¹ *Department of Chemistry, Tokyo Metropolitan University, Tokyo 192-0397, Japan*

² *Department of Physics, Kyoto Sangyo University, Kyoto 603-8555, Japan*

In the case of the laser ablation-furnace method, properly choosing the furnace temperature, the kinds of ambient gas as well as catalyst has been found to be important factors by which a specific SWNT with a very narrow diameter distribution and/or a limited number of chiral structures is selectively produced [1]. In order to find the better condition for the production of the SWNT with a specific chiral index ((6,5) tube, for example), in the present work, we intended to understand the effect of temperature history of the plume (a vapor cloud of network forming carbons) after laser irradiation, particularly placing special attention to the temporal change of the effective temperature resulting from the time and spatial evolution of the plume which immediately starts to move after ablation and continues for several hundreds millisecond, or in some cases, even for the minute time range.

Since there is a distinct temperature gradient inside a furnace (maximum 100°C between center and inlet or outlet), it is obvious that by changing the position of the laser ablation target (graphite rod), we are able to make the condition so that the plume would have different temperature experience during traveling inside the furnace. For example, when the target is arranged close to exit of the furnace, the resulting plume travels in the ambience of the temperature from low to high within 1-2 ms, and then it stays for a while in the ambience at high temperature with in 10-20 ms, and finally slowly moves to the lower temperature by taking several seconds.

Figure 1 shows Raman spectra of the raw soot collected at the outlet area of the furnace by changing the position of the target inside the furnace from -40mm to +140mm (here, we define zero position as the center of the furnace and + means the distance from the center to the outlet direction, -, the inlet direction). Figure 2 shows plots of intensity of two peaks at 260cm⁻¹ (8,5) (solid line) and 310cm⁻¹ (6,5) (broken line) in Fig. 1 as a function of the position of the target. The detailed results and discussion will be shown in the symposium.

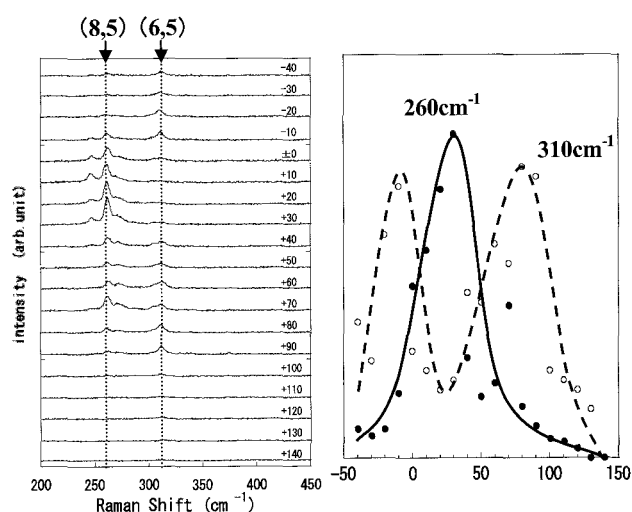


Fig. 1 Raman spectra of the soot by excitation of 488nm laser line

Fig. 2 Change of intensity of two peaks at 260cm⁻¹ and 310cm⁻¹ in Fig. 1 as a function of the target position

[1] Y. Tsuruoka et al., The 31st Fullerene-Nanotubes General Symposium, 2P-28 (2006)

Corresponding Author: Yohji Achiba

TEL: 042-667-2534, E-mail: achiba-yohji@tmu.ac.jp

Matching between Reaction and Catalyst Conditions in Growing VA-SWNTs by ACCVD

○Hisashi Sugime¹, Suguru Noda¹, Shigeo Maruyama² and Yukio Yamaguchi¹

¹Dept. of Chemical System Engineering, The University of Tokyo, Tokyo, 113-8656, Japan

²Dept. of Mechanical Engineering, The University of Tokyo, Tokyo, 113-8656, Japan

In the direct growth of SWNTs on substrates by CVD methods, preparation of the catalyst nanoparticles is a crucial issue. Co-Mo binary catalysts effectively grow SWNTs either from CO [1] or from alcohol [2]. However, different values are reported as the optimum Co/Mo atomic ratio; 1/3 for the former [1] and 1.6/1 for the latter [2]. The structure of catalyst nanoparticles should be determined not only by the composition but also by the amount of catalyst metals, and optimum conditions should depend on the CVD conditions.

In this study, SWNT growth by alcohol catalytic CVD with Co-Mo catalyst was systematically investigated, by mapping the SWNT yield against the orthogonal gradient thickness profiles of Co and Mo [3]. Vertically-aligned SWNT forests grew in 10 minutes at several regions including Co/Mo ratios of 1/3 and 1.6/1 mentioned above. The temperature for catalyst reduction before CVD did not affect the regions for forests so much compared to the temperature for CVD. Maximum heights of forests were about 30 μm either at 1123 K or 1023 K under different catalyst conditions. Figure 1 shows TEM images of the as-grown SWNTs obtained under the optimum condition and histograms of their diameter distribution. SWNTs had a monomodal diameter distribution when they were grown by Co-Mo catalyst at 1123 K, on the other hand it had bimodal distribution when they were grown by Co catalyst at 1023 K. The bimodal distribution was possibly caused by the bimodal size distribution of catalyst particles evolved by Ostwald ripening process during CVD.

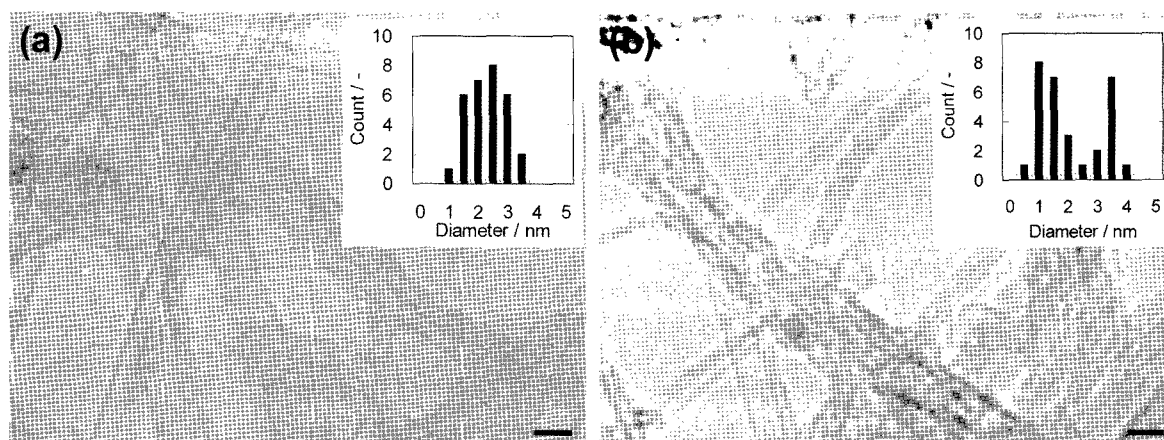


Fig. 1 TEM images and histograms of diameter distribution of as-grown SWNTs

(a) Co:0.22nm Mo:0.14nm Temperature:1123 K (b) Co:0.78nm Mo:0nm Temperature:1023 K
Scale bar: 5 nm

[1] J. E. Herrera, L. Balzano, A. Borgna, W. E. Alvarez and D. E. Resasco, *J. Catal.* 204, 129 (2001).

[2] M. Hu, Y. Murakami, M. Ogura, S. Maruyama and T. Okubo, *J. Catal.* 225, 230 (2004).

[3] S. Noda, H. Sugime, T. Osawa, Y. Tsuji, S. Chiashi, Y. Murakami and S. Maruyama, *Carbon* 44, 1414 (2006).

Corresponding Author: Suguru Noda

TEL: +81-3-5841-7330, FAX: +81-3-5841-7332, E-mail: noda@chemsys.t.u-tokyo.ac.jp

Influence of residual acetylene gas on growth of brush-shaped carbon nanotubes

○Masao Yamaguchi¹, Lujun Pan¹, Seiji Akita¹ and Yoshikazu Nakayama²

¹*Department of Physics and Electronics, Osaka Prefecture University, 1-1 Gakuen-cho, Naka-ku, Sakai, Osaka 599-8531, Japan.*

²*Department of Mechanical Engineering, Graduate School of Engineering, Osaka University, Japan*

Abstract: Brush-shaped carbon nanotubes (CNTs) are expected to have wide applications due to their structural anisotropy. It is important to control the gas components in the whole process of CVD, especially in the heating process. In this report, we have investigated the effect of a small amount of residual C_2H_2 in the gas system on the formation of the catalyst particles, which results in the different states of CNTs growth.

Iron films with a thickness of 4 nm deposited on the SiO_2/Si substrates were used as catalyst. The samples were heated from room temperature to $700^\circ C$ at a rate of $20^\circ C/min$ in a He atmosphere, where a small of C_2H_2 resident in the gas supplying system was monitored by a quadrupole mass spectrometer (QMS). After holding the temperature at $700^\circ C$ for 2 min, C_2H_2 with a flow rate of 15 sccm were introduced in the chamber for 10 min for the growth of CNTs.

Figure 1 shows the AFM image of Fe particles on substrate after heating to $700^\circ C$ in He atmosphere, during which the amount of acetylene is extremely small (below the detectable level of QMS). It is found that there are two kinds of particles formed in this process. One kind is the relatively large particles with an average diameter of 40 nm and the other kind is the particles with an average diameter of tens of nanometer. With the increase of the amount of residual C_2H_2 (Maximum 8.7cc), as shown in Fig. 2, the number of larger particles is largely increased. After CVD, the length and density of CNTs grown by the catalyst of Fig. 1 (about $110\mu m$ and $25mg/cm^3$) are larger than those by the catalyst of Fig. 2 (about $100\mu m$ and $20mg/cm^3$). It is considered that the formation of large sized particles is by the adoption the carbon from the residual C_2H_2 during the heating process, which may cause the reduction of the catalyst activities for the growth of CNTs. The CNTs are considered to be grown only from the smaller sized Fe particles without poisoned by the residual C_2H_2 gas. The increase of the amount of residual C_2H_2 would result in the decreasing of the number of smaller sized Fe particles and hence decreasing the density of the grown CNTs, which is evidence by the experimental results. These results suggest that the states of grown CNTs can be controlled by the heating conditions with an addition of a small amount of reaction gas.

Acknowledgement: This work was partially supported by the Osaka Prefecture Collaboration of Regional Entities for the Advancement of Technological Excellence, JST.

Corresponding Author L. Pan

E-mail pan@pe.osakafu-u.ac.jp **Tel&Fax** +81-72-254-9265

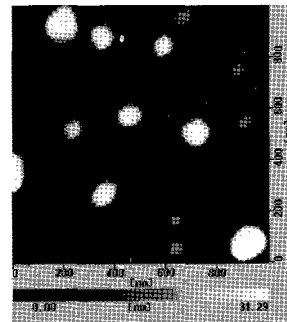


Fig.1 AFM image of the substrate heated in He with a very small amount of acetylene.

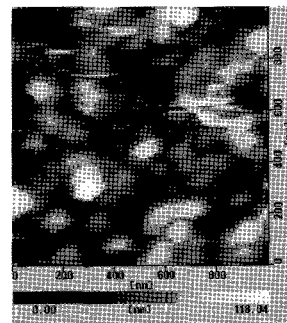


Fig.2 AFM image of the substrate heated in He with a larger amount of acetylene.

***In situ* photoelectron spectroscopy study of metal catalysts for carbon nanotube growth by low-pressure ethanol CVD**

○Fumihiko Maeda, Satoru Suzuki, and Yoshihiro Kobayashi

NTT Basic Research Laboratories, NTT Corporation, and CREST, JST, 3-1 Morinosato-Wakamiya, Atsugi-shi, Kanagawa 243-0198, Japan

Though metal catalysts play an important role in the growth of carbon nanotubes (CNTs), we do not have a clear understanding of the chemical and physical states of catalysts during CVD. Therefore, we have been investigating these states using *in situ* x-ray photoelectron spectroscopy (XPS) [1]. A real-time analysis is desirable but is technically difficult. Therefore, in this work, we looked at the reaction product of the catalyst nanoparticles obtained after CVD by analyzing the surface *in situ* in a stable state in an ultra-high vacuum.

Si substrates with a thin SiO₂ layer were used. We prepared two samples. For one, Co was deposited in a growth chamber, followed by the CNT growth without exposure to air (metallic sample). The other sample was exposed to air to oxidize a Co thin film after the deposition (oxidized sample). The samples were heated at 600°C in an ethanol ambient with a pressure of ~0.05 Torr. Then, the as-grown surfaces were analyzed by *in situ* XPS without exposure to air.

The Co 2*p* spectra of the metallic sample (right) and oxidized sample (left) are shown in Fig. 1. From these spectra, we found that, in the metallic sample, the Co remained in the metallic state after the CNT growth process. For the oxidized sample, Co oxide was reduced during the annealing process, resulting in a spectrum identical to that of the metallic sample. In C 1*s*, after the CNT growth in both samples, no peak was found at the binding energy corresponding to Co carbide, but asymmetric single peaks were observed, which are attributed to graphite or amorphous carbon. These results indicate that the oxide state and the state involving carbon are not stable but that the metallic state is stable for Co under this CNT growth condition. Meanwhile, the intensity of C 1*s* of the metallic sample was much larger than that of the oxidized sample, although the density of CNTs is too small to explain this C 1*s* intensity. Here, Co nanoparticles and CNTs covered with thick films were observed in a SEM image. Thus, the high intensity is ascribed to this thick film, i.e., the thick graphitic film adheres to the CNTs and Co nanoparticles. Since the CNT growth yield for the metallic sample was larger than that for the oxidized sample, these results suggest that a high growth yield was obtained as the result of the high efficiency of the decomposition of ethanol by the metallic Co.

[1] F. Maeda et al., Jpn. J. Appl. Phys. **46** (2007) L148.
Corresponding Author;
Fumihiko Maeda
E-mail;
fmaeda@will.brl.ntt.co.jp
Tel; +81-46-240-3423
Fax; +81-46-240-4711

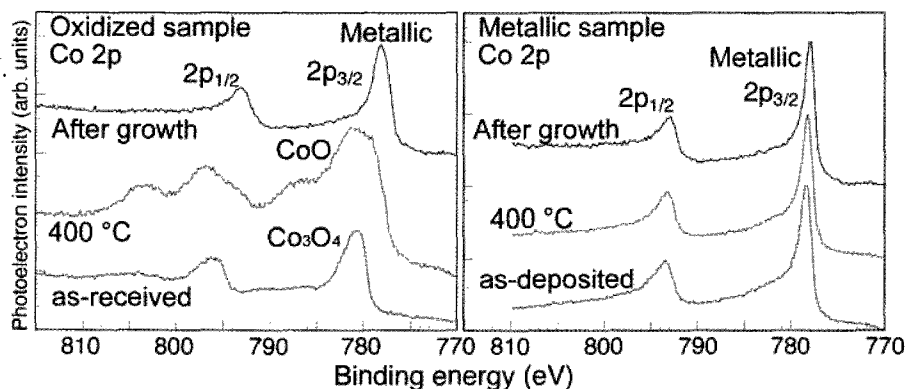


Fig. 1. Co 2*p* spectra of oxidized sample (left) and metallic sample (right).

Plan-viewed TEM observation of carbon nanotubes and catalyst particles and evaluation of catalyst activity for SWNT growth

Yuki Hasebe¹, Toshiya Murakami¹, Kenji Kisoda², Hiroshi Harima¹,
Koji Nishio¹ and Toshiyuki Isshiki¹

¹Department of Electronics, Kyoto Institute of Technology, Kyoto 606-8585, Japan

²Physics Department, Wakayama University, Wakayama 640-8510, Japan

Chemical vapor deposition (CVD) is a conventional technique for growth of carbon nanotubes on various substrates. Optimizing catalyst species and their diameter for each substrate are much important to grow carbon nanotubes efficiently with controlling their chirality. We have investigated the relation between nanotubes and catalyst particles on substrates after CVD process by transmission electron microscopy (TEM) [1].

Before loading catalyst source, a substrate was processed enough thin to observe by TEM. The substrate was dipped in ethanol solution dispersed catalyst, and then was dried in air. CVD was carried out at 800°C using ethanol as a carbon source. As-grown sample was immediately observed by TEM without any process. This sample preparation technique makes possible to observe SWNTs and catalyst particles on substrate simultaneously.

Figure 1 shows a TEM image of as-grown sample with Co catalyst on thin SiO₂ substrate. Single-walled carbon nanotubes (SWNTs) and catalyst particles (dark spots) were clearly observed on the substrate. No multi-walled carbon nanotubes were observed. The diameter distribution of SWNTs and catalyst particles is shown in Fig. 2. The mean diameter of Co particles (~3.5 nm) was significantly larger than that of SWNTs (~1.5 nm). This difference indicates that activity of catalyst drastically decreased as increasing the diameter of Co particles. In the present growth, the ratio of Co particles effective for SWNTs growth to amount of Co particles was only around 10% in particle number. It is expected that the ratio of the active particles will increase by controlling CVD parameters as the mean diameter of Co particles will be suppressed around 2nm equal to diameter of growing SWNTs.

[1] T. Murakami *et al.*, J. Applied Physics, **100**(9) 094303-1–094303-4

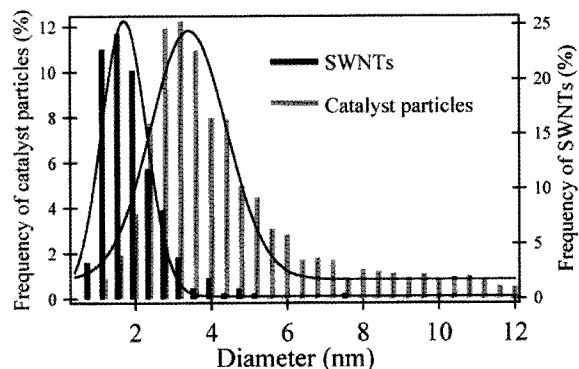
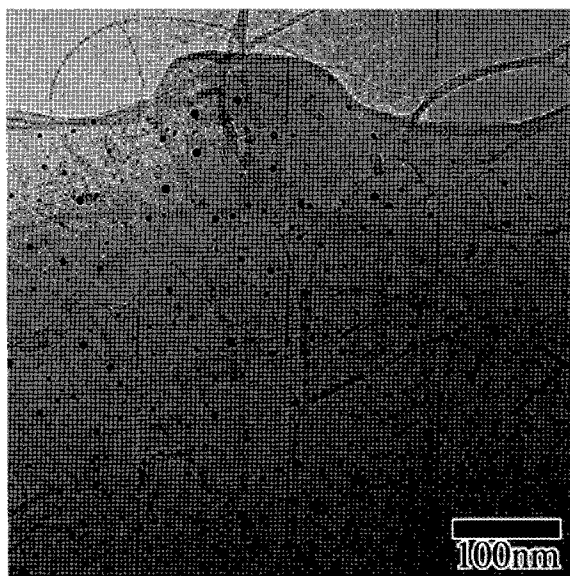


Figure 2. Diameter distribution of SWNTs and catalyst particles

Figure 1. TEM image of the as-grown sample after CVD.

Corresponding Author: Y. Hasebe, TEL:+81-75-724-7448, E-mail: m6621030@edu.kit.ac.jp

Discontinuous Change in Carbon Nanotubes Caused by Continuous Change in Catalyst Nominal Thickness

°Kazunori Kakehi¹, Suguru Noda¹, Shigeo Maruyama² and Yukio Yamaguchi¹

¹*Dept. of Chemical System Engineering, The University of Tokyo, Tokyo 113-8656, Japan*

²*Dept. of Mechanical Engineering, The University of Tokyo, Tokyo 113-8656, Japan*

Controlled growth of single-walled carbon nanotubes (SWNTs) on substrates is crucial for many of their device applications. SWNT growth is largely dependent on both catalyst conditions (element of catalyst, diameter, etc.) and reaction conditions (source of carbon, temperature, pressure, etc.). Effects of these conditions interact with each other complicatedly.

Previously, we prepared a thickness profile of Co on a SiO₂/Si substrate [1] and that of Ni on quartz glass substrate [2] by our ‘combinatorial masked deposition (CMD)’ method [3], carried out alcohol catalytic CVD (ACCVD) [4], and grew SWNTs by metal nanoparticle catalysts spontaneously forming from nominal monolayers of metal. The thickness profiles formed by this method enable preparation of a series of nanoparticles with various sizes and areal densities on one substrate. Thus we can investigate influence of reaction and catalyst conditions systematically.

In this work, we studied the relationship between the structure of catalyst and that of growing nanotubes by preparing a gradient thickness profile (about 0.06-3.5 nm) of Co by using CMD method and by growing carbon nanotubes (CNTs) by ACCVD at 873-1123K. At 973K, two active regions appeared with an inactive region in between. SWNTs mainly grew at a thin Co region (~ 0.1 nm, Fig. (a)), small amount of short CNTs grew at a medium region (~ 0.4 nm, Fig. (b)), and multi-walled carbon nanotubes grew at a thick region (~ 1.5 nm, Fig. (c)). In the medium region, the dissolution of carbon into catalysts and the precipitation of carbon as CNTs from them may be unbalanced and the growth may not be sustainable.

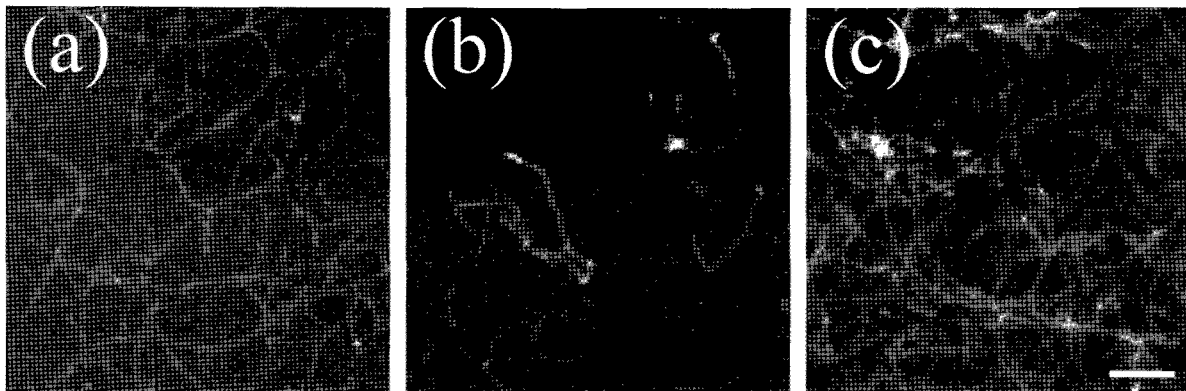


Fig. Plan-view FE-SEM images of CNTs at the nominal Co thickness of (a) 0.13, (b) 0.29 and (c) 0.92 nm. All images are in the same scale and the scale bar is 100 nm.

[1] S. Noda, et al., *Appl. Phys. Lett.* **86**, 173106 (2005). [2] K. Kakehi, et al., *Chem. Phys. Lett.* **428**, 381 (2006).

[3] S. Noda, et al., *Appl. Surf. Sci.* **225**, 372 (2004). [4] S. Maruyama, et al., *Chem. Phys. Lett.* **360**, 229 (2002).

Corresponding Author: Suguru Noda

TEL: +81-3-5841-7330 FAX: +81-3-5841-7332, E-mail: noda@chemsys.t.u-tokyo.ac.jp

Close-Open-Close Evolution of Holes in Single-Wall Carbon Nanohorns Caused by Heat Treatment

○ Jing Fan¹, Masako Yudasaka^{1,2}, Jin Miyawaki¹, Ryota Yuge²,
Takazumi Kawai², Sumio Iijima^{1,2,3}

1) SORST/JST, NEC Corporation, 34 Miyukigaoka, Tsukuba 305-8501, Japan

2) NEC Corporation, 34 Miyukigaoka, Tsukuba 305-8501, Japan

3) Meijo University, 1-501 Shiogamaguchi, Tenpaku-ku, Nagoya 468-8502, Japan

Experimental results and theoretical calculations indicated that the holes at the tips of single-wall carbon nanohorns (SWNHs) can be closed by heating treatment of 1200 °C in Ar atmosphere [1]. We have examined the effect of heating temperatures (HT 600~ 1200 °C) on closing of the hole of SWNHs opened at different oxidizing temperatures (Tox 350~ 550 °C). It was found that the number of closed holes increased with the HT temperature. When Tox was higher than 500 °C, the hole closing mainly occurred at HT 1200 °C. In this study, we further investigated the hole closing rate of SWNHs by changing the heating periods.

To open the holes, SWNHs were oxidized in flowing air by slow combustion method [2] (NHox) with various target temperatures (Tox 300~ 500 °C). For closing the holes, NHox was heat-treated at 1200 °C in Ar for 0~ 3 h. The hole closing was examined by measuring xylene-adsorption quantity using thermogravimetric equipment. As a result, we found that the holes show the tendency of closing with HT duration period. However, we also noticed that the closed holes were once again opened during HT, which will be explained in the presentation.

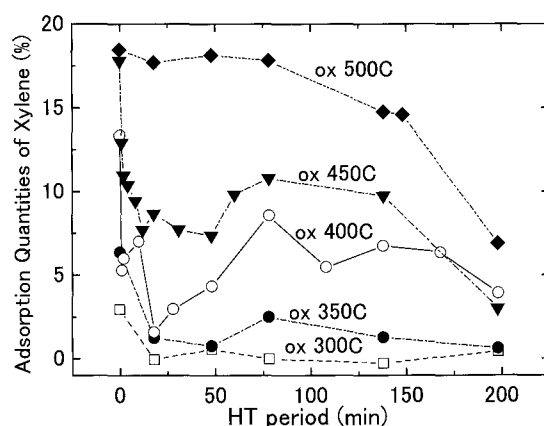


Fig. 1 Adsorption quantities of xylene by NHox (Tox 300~ 500 °C) depending on HT duration periods. The heat treatment temperature was 1200 °C, and the atmosphere was Ar (760 Torr).

References:

[1] J. Miyawaki et al., *J. Phys. Chem. C* **111** (2007) 1553-5.

[2] J. Fan et al., *J. Phys. Chem. B* **110** (2006) 1587-91.

Corresponding Author: Yudasaka Masako

E-mail: yudasaka@frl.cl.nec.co.jp Tel:+0081-29-850-1190; Fax: +0081-29-850-1366.

Modification of cisplatin-incorporated single-wall carbon nanohorns to release cisplatin slowly

○Kumiko Ajima¹, Masako Yudasaka^{1,2}, Tatsuya Murakami³, Minfang Zhang¹ and Sumio Iijima^{1,2,4}

¹JST/SORST, c/o NEC, 34 Miyukigaoka, Tsukuba, Ibaraki 305-8501, Japan

²NEC, 34 Miyukigaoka, Tsukuba, Ibaraki 305-8501, Japan

³Fujita Health University, 1-98 Dengakugakubo, Kutsukake-cho, Toyoake, Aichi 470-1192, Japan

⁴Meijo Univ., 1-501 Shiogamaguchi, Tenpaku, Nagoya 468-8502, Japan

We have been studying applications of single-wall carbon nanohorns (NH) to drug delivery systems (DDS). Previous experiments showed that cisplatin (CDDP), an anticancer drug, could be incorporated into NH by the precipitation method using H₂O, and that the CDDP released from CDDP-incorporated NH (CDDP@NH) showed strong anticancer-effects against human-lung cancer cell *in vitro*. *In vivo* anticancer effect of CDDP@NH was also confirmed using tumor-bearing nude-mice.

To apply CDDP@NH to DDS, release rate of CDDP from CDDP@NH needs to be slow; however, CDDP was quickly released from the as-prepared CDDP@NH in phosphate-buffered saline (PBS). We show in this report that the surface modification of NH of CDDP@NH is effective to make the CDDP release slow. Several modification methods were examined using various materials such as bovine serum albumin, polyethylene glycol (PEG), PEG-doxorubicin, lactic acid, and benzoic acid. The modifications by these materials also enhance dispersibility of CDDP@NH in H₂O. The materials were solved in a small amount of H₂O and mixed with CDDP@NH powders. The small amount of H₂O was indispensable because the CDDP in CDDP@NH easily went out in H₂O. After the mixture, x-ray diffractions were measured to check whether the CDDP crystals exist outside NH. The CDDP clusters remained in CDDP@NH were checked with high-resolution transmission electron-microscopy. Then the release rates of CDDP from CDDP@NH in PBS were measured by dialysis method. The quantities of released CDDP were measured by atomic absorption spectroscopy.

We will discuss about the release rates of CDDP from CDDP@NH depending on the NH-surface modification materials.

Corresponding author: Kumiko Ajima, Masako Yudasaka

E-mail: kumikoajima@frl.cl.nec.co.jp, yudasaka@frl.cl.nec.co.jp

Tel: +81-(0)29-856-1940, Fax: +81-(0)29-850-1366.

Folate-Receptor Mediated Uptake of Single-Walled Carbon Nanohorns by Cultured Cancer Cells

○Jin Miyawaki¹, Tatsuya Murakami², Masako Yudasaka^{1,3}, Kumiko Ajima¹, Minfang Zhang¹, Hirohide Sawada², Kunihiro Tsuchida², and Sumio Iijima^{1,3,4}

¹*JST/SORST, c/o NEC, 34 Miyukigaoka, Tsukuba, Ibaraki 305-8501, Japan*

²*Fujita Health University, 1-98 Dengakugakubo, Kutsukake, Toyoake, Aichi 470-1192, Japan*

³*NEC, 34 Miyukigaoka, Tsukuba, Ibaraki 305-8501, Japan*

⁴*Meijo University, 1-501 Shiogamaguchi, Tempaku, Nagoya 468-8502, Japan*

Drug carrying ability [1,2] and low toxicity [3] of single-walled carbon nanohorns (SWNHs) [4] present their potential usage as a drug delivery carrier. To maximize therapeutic efficiency and reduce adverse side effects, however, targeted delivery of drugs to diseased sites is crucial issue. It is known that many human cancer cells significantly overexpress receptors for vitamin folic acid (FA) on their surface membranes [5], thus conjugation with FA is considerably promising for the selective delivery of SWNHs to the cancer cells. Herein, we demonstrate preferential uptake of the FA-labeled SWNHs into cultured cancer cells.

To increase dispersibility in physiologic solutions, SWNHs were first modified with fluorescently labeled protein BSA (BSA-NH) [6], and then, FA was covalently attached to BSA-NH via carbodiimide-activated amidation (FA-BSA-NH). The KB human cancer cells, derived from an epidermal carcinoma of oral cavity, were cultured in folate-free medium. Following 24-h incubation of the KB cells with FA-BSA-NH or BSA-NH, the cellular uptakes were investigated by confocal laser scanning microscopy and flow cytometry. Both analyses showed that the uptake of FA-BSA-NH by the KB cells was preferential as compared with that of BSA-NH. On the other hand, no difference in uptake quantity was observed between FA-BSA-NH and BSA-NH for normal human cells having much less amount of the FA receptors. These results indicate that the chemical modification of SWNHs with FA enabled selective delivery of SWNHs to the cancer cells having the folate receptors.

References:

[1] T. Murakami et al., *Mol. Pharm.*, **1**, 399 (2004).

[2] K. Ajima et al., *Mol Pharm.*, **2**, 475 (2005).

[3] J. Miyawaki et al., *Abstract of the 32nd Fullerene-Nanotubes General Symposium*, 71 (2007).

[4] S. Iijima, et al., *Chem. Phys. Lett.*, **309**, 165 (1999).

[5] J. A. Reddy and P. S. Low, *Crit. Rev. Ther. Drug Carr. Syst.*, **15**, 587 (1998).

[6] M. Zhang, et al., *Abstract of the 32nd Fullerene-Nanotubes General Symposium*, 38 (2007).

Corresponding Author: Jin Miyawaki and Masako Yudasaka

TEL: +81-29-856-1940, FAX: +81-29-850-1366, E-mail: jin_m@frl.cl.nec.co.jp (Miyawaki), yudasaka@frl.cl.nec.co.jp (Yudasaka)

Boron doped Nanohorn Aggregates Produced by means of Arc Discharge

○ Manabu Harada, Takayuki Inagaki, Shunji Bandow, Sumio Iijima

*Department of Materials Science and Engineering, Meijo University,
1-501 Shiogamaguchi, Tenpaku, Nagoya 468-8502, Japan*

Nanohorn (NH) aggregates can be produced by the vaporization of the carbon rod using the arc discharge with a power density of $\sim 5 \text{ kW/cm}^2$ [1]. NH aggregates thus prepared have rather small diameter than those produced by the laser vaporization [2]. In the previous study, we examined to produce the boron nano-particles deposited on the NH aggregates by the arc-vaporization of boron containing rod [3]. As results, when the NHs were prepared from 30 % of boron containing rod, we succeeded to observe frequently the boron particles depositing on the NHs. However, the NHs from the lower concentration of boron containing rod, we could not observe obvious change in the morphological structures of NHs as compared with those from the pure carbon rod. In the present study, we examined the temperature dependence on the electrical conduction for the NHs prepared from the low concentrations of boron containing rod.

Electrical resistance was measured for the pellet formed NH aggregates with 4-probes method. Results of the temperature dependence on the electrical resistance are shown in Fig. 1. From this figure, we can find that the electrical conduction is governed by the 3 dimensional Mott's variable range hopping (3D-VRH) mechanism, and the characteristic temperature T_0 for each sample is systematically changed in accordance with the change of boron concentration in the carbon rod. Furthermore, it was found that the heat-processes for opening the nano-windows do not significantly modify the value of T_0 . According to the transmission and scanning electron microscopy observations, we concluded that the localization lengths for 3D-VRH un-change between the samples. Because NH aggregates have almost the same in size (see Fig. 2). Therefore, the change in T_0 should be resultant from the change in the electronic DOS of NHs, suggesting the boron doping to the nanohorn wall.

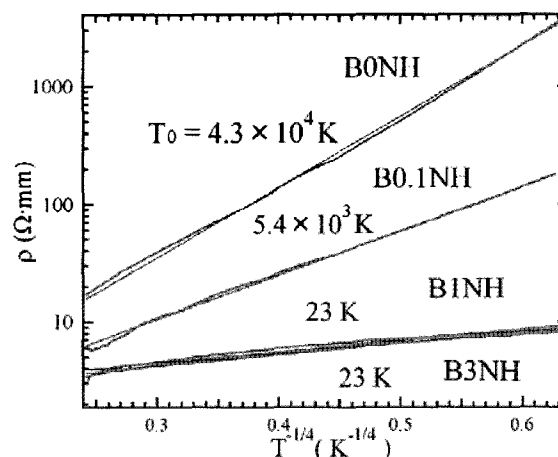


Fig. 1. Temperature and boron concentration dependences on the electrical resistivity.

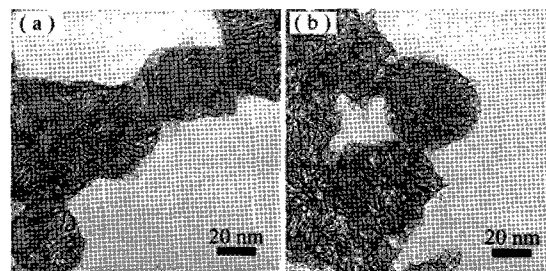


Fig. 2. TEM images of (a) B0NH and (b) B3NH

[1] T. Inagaki *et al.*, The 32nd F&NT General Symp., (2007) **3P-24**. [2] T. Yamaguchi *et al.*, *Chem. Phys. Lett.* **389**, 181 (2004). [3] T. Inagaki *et al.*, The 32nd F&NT General Symp., (2007) **3P-23**.

Corresponding Author: Manabu Harada, **E-mail:** m0634039@ccmailg.meijo-u.ac.jp, **Tel&Fax:** +81-52-834-4001

Electron microscopy study of nanohorn tip structure damaging with hydrogen peroxide treatment

○T. Yamaguchi¹, S. Bandow¹, M. Yudasaka² and S. Iijima^{1,2}

¹*Department of Materials Science and Engineering, Nano-Factory, Meijo Univ.,
1-501 Shiogamaguchi, Nagoya 468-8502, Japan*

²*SORST-JST, NEC Corporation,
34 Miyukigaoka, Tsukuba 305-8501, Japan*

Amorphous carbon can be removed from nano-carbon materials by the mild combustion in oxygen flux at around 400°C. However, this combustion method only works well for the nano-carbon materials locating at the interfacial region with gas flux. In addition, during the combustion, the surfaces of the nano-carbon materials such as nanotubes and nanohorns receive serious damage, and sometimes their structures were completely destroyed.

In the present study, we used aqueous solution of hydrogen peroxide (30 %) for removing the amorphous carbon from the nanohorns and for opening the nano-windows on the nanohorn wall. First experimental evidence for opening the nano-windows by using hydrogen peroxide was carried out in 2002 by Bekyarova *et al* [1]. They found the effective opening of the nano-windows on the nanohorn wall. Although this liquid phase method for purifying the nano-carbon materials and also opening the nano-windows has a merit of homogenous chemical reaction all around the sample, the details on the local structural changes around the nanohorn tips have not been studied systematically. Hence we study here the effect of liquid phase oxidation on the local structures around the nanohorn tips by using a 90°C mild treatment in hydrogen

peroxide. Time trace for the change in the tip structures can be seen in Fig. 1. From this figure, one can find that the tip structures are started to destroy for the period of more than 30 min (Fig. 1c). Details will be explained in the poster.

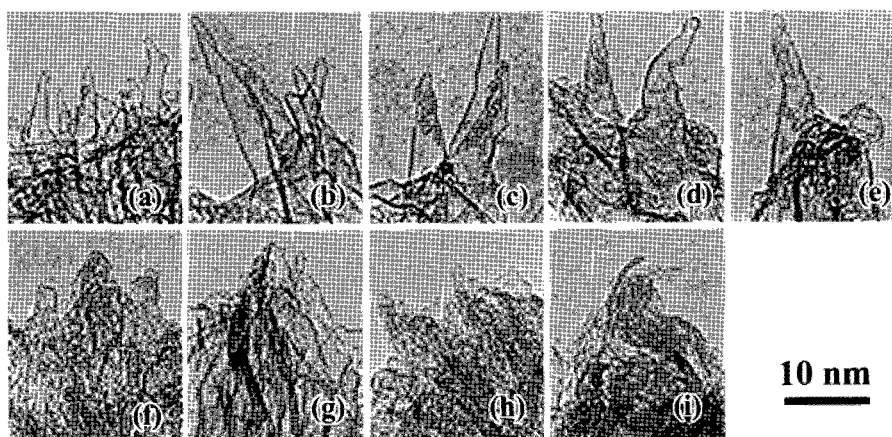


Fig. 1. TEM images of tip structures for the carbon nanohorns treated by hydrogen peroxide at various periods. (a) is taken for as-grown NHs, (b) for 10 min treatment, (c) 30 min, (d) 60 min, (e) 120 min, (f) 180 min, (g) 240 min, (h) 24 hours and (i) 72 hours.

Reference : [1] E. Bekyarova et al., *Adv. Mater.* **14**, 1117 (2002).

Corresponding Author : Takashi Yamaguchi

E-mail : nanocyma@ccmfs.meijo-u.ac.jp, **Tel&Fax** : +81-52-834-4001

Ultracentrifugal Separation of Single-wall Carbon Nanohorns

○Goshu TAMURA¹⁾ Shunji BANDOW¹⁾ Masako YUDASAKA²³⁾ Sumio IJIMA¹²³⁾

1) Graduate School of Science and Technology "Nano Factory" Meijo University
Shiogamaguchi 1-501 Tempaku-ku Nagoya-city Aichi 468-8502 Japan

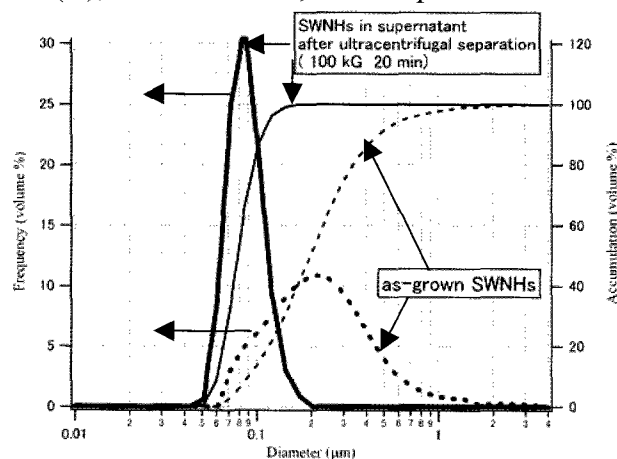
2) JST-SORST c/o NEC Miyukigaoka 34 Tsukuba-city Ibaraki 305-8501 Japan

3) NEC Corporation Miyukigaoka 34 Tsukuba-city Ibaraki 305-8501 Japan

Abstract: Primary particles of as-grown single-wall carbon nanohorns (SWNHs) have a variety of sizes. In case of SWNHs made by laser ablation, their particle sizes are between 70nm and 300 nm. Their mean volume diameters are around 200 nm. If technological application is considered, especially for bio-medical field such as drug delivery system (DDS), the narrower size distribution is required.

Normally as grown SWNH particles contain micrometer-sized and graphite-based impurities, named GG (giant graphite) balls, and many of these particles form agglomeration with a size of over micrometer-order in dry or even wet condition before sonication. If many SWNH and GG ball particles are aggregated, we cannot separate out SWNHs and GG balls, and moreover primary SWNH particles as well. Once SWNH particles, however, can be well dispersed in ethanol, they can be separated from GG balls, so that we can classify SWNHs in terms of size using the difference in chemical or physical character of each primary particle. On the 29th Symposium in 2005, we had poster presentation that we achieved high dispersion of SWNHs in ethanol by ultrasonication using bath type sonicator. And on the 30th one in 2006, we also had poster presentation that SWNHs in ethanol suspension can be easily purified, and separated from GG balls by natural gravitation (1G). SWNHs were still in supernatant, otherwise only GG balls could be sediment under 1G.

This time, we treated ultracentrifugal separation on the ethanol dispersion to classify SWNHs using difference of sedimentation velocity. As gravitation is increased, we could sediment even large size SWNHs. A size distribution of SWNHs in supernatant became narrower, and shifted toward the smaller side. SWNHs size distributions could be controlled by rotating speed (G), treatment time, and the position of extraction.



SWNHs sizes distributions before (solid lines) and after (dot lines) ultracentrifugal separation measured by DLS (dynamic light scattering) particle size analyzer

For example, we got small SWNHs: their mean volume diameters became 80 nm under 100 kG for 20 minutes. We achieved classification of SWNHs using ultracentrifugal separation.

Corresponding Author: Goshu TAMURA

E-mail: m0441505@ccmailg.meijo-u.ac.jp

Tel&Fax: (+81)- 52-834-4001

Enhancement of conductivities in boron-doped MWNTs

○Satoshi Ishii, Tohru Watanabe, Showgo Ogawara, Takashi Okutsu, Fumiaki Tomioka, Shinya Ueda, Shunsuke Tsuda, Takahide Yamaguchi and Yoshihiko Takano

Nano System Functionality Center, National Institute for Materials and Science, 121, Sengen, Tsukuba, Ibaraki 305-0047, Japan

Boron-doped multi-walled carbon nanotubes (MWNTs) were grown by chemical vapor deposition (CVD) using methanol (CH_3OH) solution of boric acid (H_3BO_3). Boric acid was used to dope the boron atoms into the MWNTs. The MWNTs were grown on the surface of Si substrates coated with Fe_2O_3 nano particles as catalyst.

In this study, methanol containing 1.0 atm% of boron atoms was used as source material. The diameters of obtained MWNTs were about 40 nm and lengths of those were more than 10 μm . In order to evaluate the electronic transport properties of boron-doped MWNTs, temperature dependence of conductivities were measured from room temperature to 0.6 K. For accurate evaluation, an individual MWNT was measured by four-point method. The nanosized electrodes were fabricated by means of electron beam lithography technique (Fig. 1).

We can see that our MWNTs showed one or two orders of magnitude higher conductivities than reference sample. Furthermore, our MWNTs still showed high conductivities even at very low temperatures while conductivity of reference sample decreased and became insulator (Fig. 2). This result seems to indicate that boron atoms were successfully doped into MWNTs and enhanced conductivities.

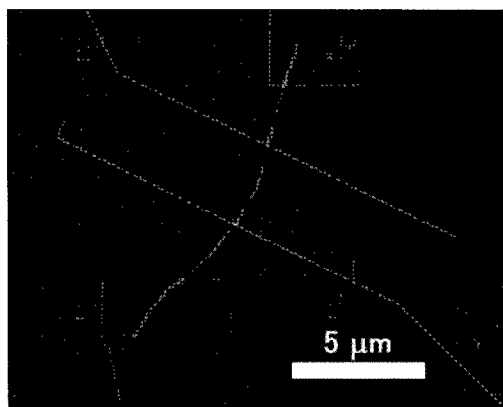


Fig. 1 SEM image of individual MWNT with four point contact.

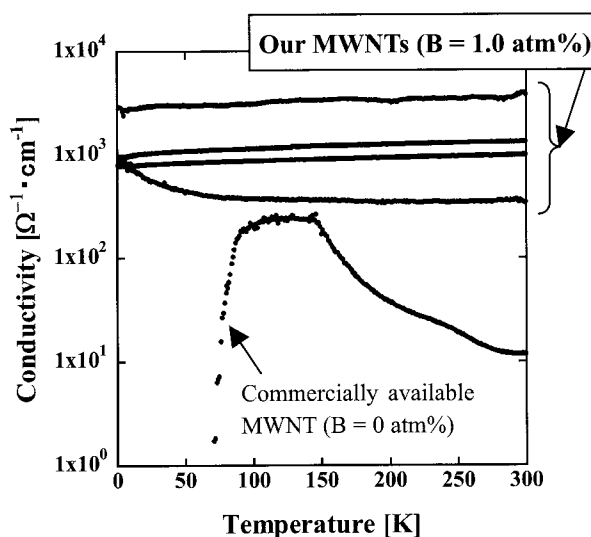


Fig. 2 Temperature dependence conductivities of MWNTs.

Corresponding Author: Satoshi Ishii

E-mail: ISHII.Satoshi@nims.go.jp

Tel: +81-29-859-2644, **Fax:** +81-29-859-2601

Electronic transport study of a suspended MWNT by in situ TEM

Yasunobu Suzuki, Koji Asaka and ○Yahachi Saito

Department of Quantum Engineering, Nagoya University, Nagoya 464-8607, Japan

Carbon nanotubes, with their strong interatomic bonds, are robust against electromigration and have high current carrying capacities exceeding $10 \mu\text{A}/\text{nm}^2$. Thus, metallic nanotubes, particularly multiwall nanotubes (MWNTs), are promising as reliable, metallic wires and interconnects in the future molecular-scale electronic devices. For such applications of MWNTs, understanding their electron transport under the high field, high current is required. We carried out high bias transport experiment using a free suspended MWNT in a transmission electron microscope (TEM), and derived the intrinsic conductivity of a MWNT and the contribution of contact resistances.

A small bundle or a single MWNT produced by arc discharge technique was attached to the tip of a platinum-coated tungsten (W) needle. The W needle with a MWNT and a copper plate covered with low-melting poing metal (In or In-Ga alloy) were mounted in a special sample holder for TEM. A free tip of MWNT was attached to the metal reservoir, and voltage variation under constant current at various bridge lengths and conductance versus bias voltage were measured. Figure 1 shows TEM images of a suspended MWNT (31 nm in diam.) carrying $40 \mu\text{A}$ at various bridge lengths (x). The In-Ga droplet was in a liquid phase, and so the nanotube slid freely on the surface of the droplet. We analysed the two terminal resistance of the nanotube bridge by using classical expression of the total resistance R_{tot} as

$$R_{\text{tot}} = R_W + \rho_{LM} \frac{1}{l-x} + \rho_{NT} \frac{x}{\pi r^2}$$

where R_W is the contact resistance at the nanotube/Pt-covered W, ρ_{LM} and ρ_{NT} are respectively the contact resistance per unit length of the nanotube/liquid metal interface and the resistivity of the MWNT. l and r are the total length and the radius of the MWNT, respectively. $R_W \approx 27.5 \text{k}\Omega$, $\rho_{LM} \approx 3.67 \times 10^{-2} \Omega \cdot \text{cm}$ and $\rho_{NT} \approx 3.79 \times 10^{-4} \Omega \cdot \text{cm}$ were derived from R_{tot} values measured for various x using Newton's method. Figure 2 shows a conductance (G) versus bias-voltage (V) characteristics of the suspended MWNT for $x = 1072$ nm. The zero-bias conductance is nearly $0.2 G_0$ (where $G_0 = 2e^2/h$), and G increases with the increase of V in accordance with the increase of DOS of electrons contributing conduction. At the high current and elevated temperature ($\sim 200^\circ\text{C}$) the transport in MWNTs was seemingly diffusive, and the resistivity of MWNTs was $2 - 4 \times 10^{-4} \Omega \cdot \text{cm}$, being consistent with the values measured previously by the four-terminal method.

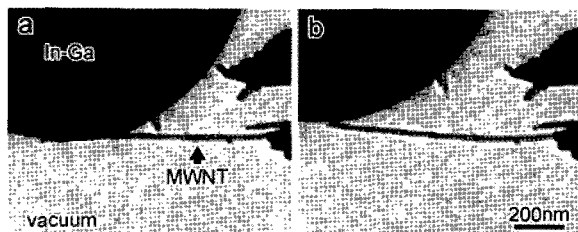


Fig. 1 TEM images of a suspended MWNT.

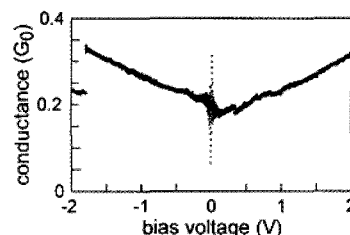


Fig. 2 G - V characteristics

Corresponding Author: Yahachi Saito

TEL: +81-52-789-4459, FAX: +81-52-789-3703, E-mail: ysaito@nagoya-u.jp

Evaluation of single wall carbon nanotubes by UV-Raman spectroscopy

○Hiromichi Kataura¹, Yasumitsu Miyata^{1,2}, Yutaka Maniwa², Kazuhiro Yanagi¹

¹Nanotechnology Research Institute (NRI), AIST, Tsukuba, Ibaraki 305-8562, Japan

²Department of Physics, Tokyo Metropolitan University, Tokyo 192-0397, Japan

Abstract:

Raman spectroscopy is easy and powerful tool to evaluate the single wall carbon nanotube (SWCNT). Raman measurement can be done without any pretreatment of the sample while photoluminescence measurement requires dispersion process. Since radial breathing mode (RBM) frequency is proportional to the inverse diameter of SWCNT, diameter distribution of SWCNT sample can be estimated. Further, from G-band and D-band intensities, purity of the sample can be roughly estimated. Since the Raman process is dominated by the resonance effect, however, Raman spectrum has limited information of specific SWCNTs on resonance. Several different laser wavelengths have to be used to cover all chirality. This selectivity is very useful for the scientific research of SWCNT but is disadvantage for the sample evaluation. One possible solution of this problem is to use ultraviolet (UV) light. One can find less selective resonance feature for UV excitation. UV-Raman spectroscopy is thought to be a good tool for easy evaluation of SWCNT sample.

Problems of the UV-Raman measurement are mostly on the equipments, such as less transmittance of lenses, less resolution of spectrometer, and less sensitivity of detectors. Here we would like to demonstrate the UV-Raman results of typical SWCNT samples. Figure 1 indicates preliminary Raman spectra in RBM and G-band for HiPco and CoMoCAT SWCNTs. The measurements were done in Tokyo sales office, HORIBA Company using LabRAM HR-800 with 2400 g/mm grating and HeCd laser. Used laser wavelength was 324 nm.

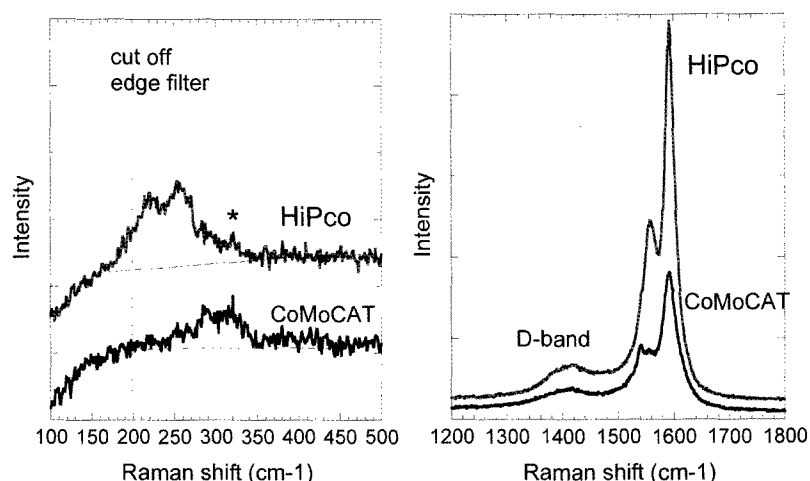


Figure 1 UV-Raman spectra of HiPco and CoMoCAT SWCNTs measured by LabRAM HR-800 UV at Tokyo sales office, HORIBA Company. Excitation wavelength is 324 nm. Asterisk indicates artificial peak.

Although S/N is not sufficient to go deep analysis, RBM spectra have less structure than visible Raman spectra. G-band structure also shows more averaged feature reflecting less selective resonance condition. D-band and G'-band also have further information about diameter distribution of the sample. Detailed analysis will be discussed.

Corresponding Author: Hiromichi Kataura

E-mail: h-kataura@aist.go.jp

Tel&Fax: 029-861-2551, 029-861-2786

Temperature dependence of the Raman spectra of single-wall carbon nanotube and highly oriented pyrolytic graphite

○Norihito Kitada, Kenichi Kato, Kenichi Kojima and Masaru Tachibana

*Graduate School of Liberal Arts and Science, Yokohama City University, 22-2 Seto,
Kanazawa-ku, Yokohama, 236-0027, Japan*

The structural properties of single-wall carbon nanotubes (SWNTs) are unique due to their extremely small diameters and the curved C-C bonds. The curvature of the SWNTs is responsible for some of the surprising properties. The thermal stability and temperature-dependent properties of SWNTs are very important for the fabrication of SWNT-based devices.

Resonant Raman spectroscopy is one of the most powerful tools for characterizing the structural and electronic properties of SWNTs. So far the study on the temperature dependence of Raman spectra of SWNTs has been carried out by many groups [1-3]. However, the understanding of the temperature-dependent behaviors is still insufficient. This is due to the quality, or breakdown, of SWNTs in the higher temperature, the difficulty of the experimental technique in the lower temperature, and so on. These make it difficult to interpret the temperature-dependent Raman feature. In this paper, we report the temperature-dependent Raman spectra of high quality SWNTs in the higher temperature.

G and 2D Raman bands in SWNTs are clearly observed at around 1590 and 2600 cm^{-1} . The temperature dependence of these bands was examined in the higher temperature above 300 K. The G and 2D can be also observed for highly oriented pyrolytic graphite (HOPG) with planar C-C bonds. The behaviors of G and 2D bands in SWNTs are compared with those in HOPG. In addition, D band observed at around 1300 cm^{-1} that is related to defects was also examined. Actually synthesized SWNTs will include some types of defects. The defects often greatly influence the properties of SWNTs. More recently, the thermal relaxation process of defects in SWNTs was examined by Raman spectroscopy [4]. We also discuss the behavior of D band in the higher temperature.

[1]P. Tan et al., Phys. Rev. B **58**, 5435 (1998).

[2]P. Corio et al., Chem. Phys. Lett. **360**, 557(2002).

[3] Z. Zhou et al., J. Phys. Chem. B **110**, 1206(2006).

[4]T. Uchida et al., J. Appl. Phys. **101**, 084313 (2007).

Corresponding Author: Masaru Tachibana

E-mail: tachiban@yokohama-cu.ac.jp

Tel: +81-45-787-2307, Fax: +81-45-787-2172

Effects of doping to the G' Raman spectra of single and double-wall carbon nanotubes

○Eduardo B. Barros^{1,2,4}, Jin Sung Park¹, Georgii G. Samsonidze^{3,4}, Riichiro Saito¹, Mildred Dresselhaus⁴

¹ *Department of Physics, Tohoku University and CREST, Sendai, 980-8578, Japan*

² *Departamento de Física, Universidade Federal do Ceara, Fortaleza, Ceara, 60455-760 Brazil*

³ *Materials Sciences Division, Lawrence Berkeley National Laboratory, Berkeley, California 94720, USA*

⁴ *Department of Electrical Engineering and Computer Science, Massachusetts Institute of Technology, Cambridge, MA, 02139-4307, U.S.A.*

In this work, we performed a study of the effect of donor and acceptor doping to the G' Raman spectra of carbon nanotubes. The G' band is a second-order Raman feature which is usually observed in graphitic systems.[1] The strong intensity of this second-order peak is usually attributed to a double resonance process involving two phonons.[2] For this reason, both the frequency and the intensity of the G' band are strongly dependent on the electronic structure of the nanotube. To better understand the effect of doping to the G' band, the electronic structure of the carbon nanotubes is calculated using the extended tight-binding formalism (ETB), where both the σ and π orbitals are taken into consideration. The structure of each (n,m) nanotube is optimized by minimizing the total electron energy and the effect of doping is included by changing the occupation of the electronic bands (controlling the Fermi energy). The G' band frequency and intensity is calculated within the framework of the double resonance process as a function of the Fermi energy variation. The calculated results are then compared to Raman spectroscopy experiments performed on single (SWNT) and double wall carbon nanotube (DWNT) bucky papers treated with H₂SO₄. The H₂SO₄ is known to act as an acceptor for the electrons of graphitic materials. The effects of H₂SO₄ doping on the electronic and vibrational properties of SWNTs and DWNTs were analyzed with 7 different laser excitation energies, allowing different nanotubes, in resonance with the different laser energies, to be probed.

[1] M. S. Dresselhaus and G. Dresselhaus, in *Light Scattering in Solids III*, edited by M. Cardona Springer, Berlin (1982).

[2] C. Thomsen and S. Reich, *Phys. Rev. Lett.* **85**, 5214 (2000).

Corresponding Author: Barros Eduardo

TEL: +81-90-2996-2906, E-mail: ebarros@flex.phys.tohoku.ac.jp

Fabrication of DNA/MWNTs junctions and electrical measurements of DNA thin films

M.Ide, M.Saito, H.Kohno, N.Murata, and J. Haruyama

Aoyama Gakuin University, 5-10-1 Fuchinobe, Sagamihara, Kanagawa 229-8558 Japan

Study of electrical conductivity in DNA has recently attracted considerable attention. DNA has been interpreted as semiconductor with a wide band gap, which shows insulative behavior [1]. In contrast, recent some works have reported transport of electrons and Cooper pairs through DNA [2]. It may be due to different chemical treatment of interface of DNA and metal electrodes. Moreover, magnetization of DNA has been also reported [3]. On the other hand, it is known that DNA tends to connect with Au, Ag, and carbon nanotubes (CNTs). Indeed, single electron tunneling in Au nano-wire coated on DNA [4] and CNTs - FET[5] have been realized.

Here, we report connection of DNA to the top ends of multi-walled CNTs (MWNTs), which were synthesized in nano-porous alumina template and results of electrical measurements. We used λ -DNA with length of 42~8000 (nm). After dissolving this DNA into Tris EDTA solution, we dropped this solution on the top ends of arrays of MWNTs and dried out solution. Figure 1(a) shows a schematic cross sectional view of the sample and Fig.1(b) and (c) exhibit SEM top views of the sample before evaporating electrodes. The top ends of MWNTs are covered by accumulation of DNAs in (b) and (c). Because these DNAs could not be etched out even by wet etching using some kinds of solutions, this result stresses that the connection between DNAs and MWNTs are very strong. This is consistent with previous reports of DNA/CNT junction. The results of electrical measurements of DNAs will be also discussed.

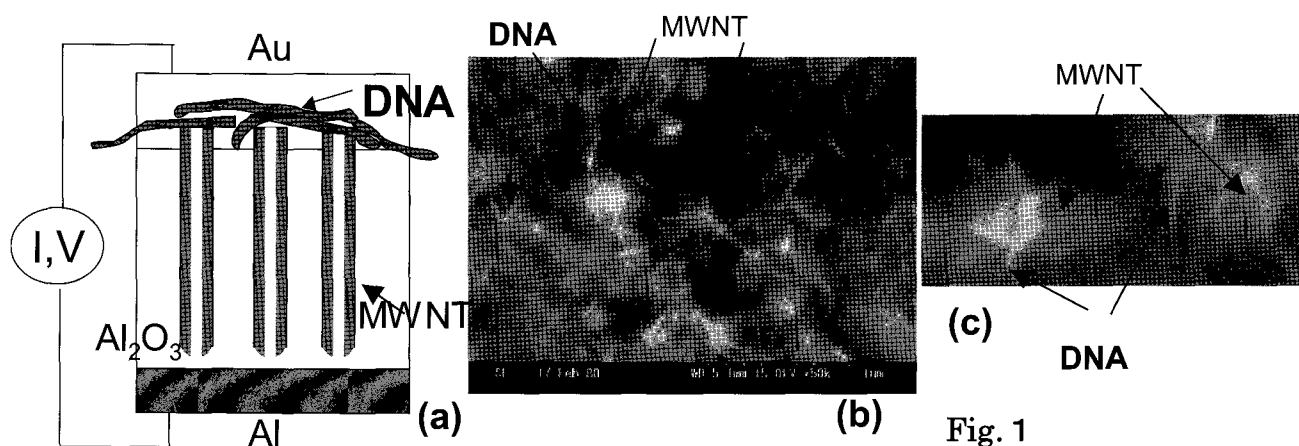


Fig. 1

References

- [1] P.J.de Pablo, et al., Phys. Rev. Lett. 85, 4992 (2000)
- [2] A. Yu. Kasumov, H. Bouchiat et al., Science **291**, 280 (2001).
- [3] S.Nakamae, H.Bouchiat et al., Phys.Rev.Lett. 94, 248102 (2005)
- [4] E.Braun et al., Science **391**, 775 (1998)
- [5] E.Braun et al., Science 302, 1380 (2003)

Corresponding author: Junji Haruyama J-haru@ee.aoyayama.ac.jp

Meissner effect in honeycomb arrays of multi-walled carbon nanotubes

N.Murata^{1,4}, J.Haruyama^{1,4,*}, N.Ueda¹, M.Matsudaira¹, Y.Yagi⁴, J.Nakamura¹,
K.Nozawa¹, T.Shimizu¹, E.Einarsson², S.Chiashi², S.Maruyama², T.Sugai^{3,4}, N.Kishi³,
H..Shinohara^{3,4}

¹*Aoyama Gakuin University, 5-10-1 Fuchinobe, Sagami-hara, Kanagawa 229-8558 Japan*

²*Tokyo University, 7-3-1 Hongo, Bunkyo-ku, Tokyo 113-0033 Japan*

³*Nagoya University, Furo-cho, Chigusa, Nagoya 464-8602 Japan*

⁴*JST-CREST, 4-1-8 Hon-machi, Kawaguchi, Saitama 332-0012 Japan*

New carbon-based superconductors, such as C₆Ca with a transition temperature (T_c) of 11.5 K (1) and highly boron-doped diamond with T_c = 4 K (2), have been recently found and attracted considerable attention, because a small mass of carbon may lead to high-T_c superconductivity like MgB₂. Superconductivity in carbon nanotubes (CNTs) has also attracted increasing attention (3–5). Three groups have experimentally reported superconductivity in different kinds of CNTs as follows; 1. with a T_c as low as 0.4 K for resistance drops (T_{cR}) in ropes of single-walled CNTs (SWNTs) (3), 2. with a T_{cR} as high as 12 K for an abrupt resistance drop in arrays of our multi-walled CNTs (MWNTs) entirely end-bonded by gold electrode (4), and 3. with a T_c of 15 K for magnetization drops (T_{cH}) in SWNTs with diameters as small as 0.4 nm (5). However, no groups could report the observation of both the Meissner effect and the resistance drop down to 0 Ω in their respective systems. Moreover, it is crucial to reveal how shielding currents for Meissner effect or superconducting vortexes occur and behave in one-dimensional space of CNTs.

Here, we report Meissner effect for type-II superconductors with a maximum T_c of 19 K, which is the highest value among those in new-carbon related superconductors, found in the honeycomb arrays of MWNTs. Drastic reduction of ferromagnetic catalyst and efficient growth of MWNTs by deoxidization of catalyst make the finding possible. The weak magnetic anisotropy, superconductive coherence length (~ 7 nm), and disappearance of the Meissner effect after dissolving array structure indicate that the graphite structure of an MWNT and those intertube coupling in the honeycomb array are dominant factors for the mechanism.

References

1. T.E.Weller, M.Ellerby, et al., *Nature Physics* 1, 39 (2005)
2. E.A.Ekimov et al., *Nature* 428, 542 (2004)
3. M. Kociak, et al., *Phys. Rev. Lett.* 86, 2416 (2001)
4. I.Takesue, J.Haruyama et al., *Phys. Rev. Lett.* 96, 057001 (2006)
5. Z. K. Tang, et al., *Science* 292, 2462 (2001)

Corresponding author; J.Haruyama (J-haru@ee.aoyama.ac.jp)

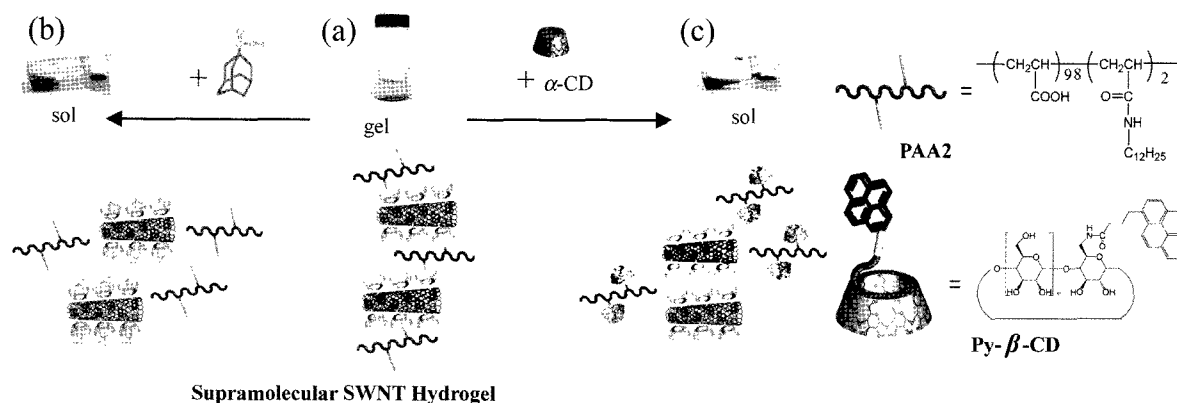
Chemically-Responsive Sol-Gel Transition of Supramolecular Single-Walled Carbon Nanotubes (SWNTs) Hydrogel Made by Hybrids of SWNTs and Cyclodextrins (CDs)

○Tomoki Ogoshi¹, Tada-aki Yamagishi¹, Yoshiaki Nakamoto¹ and Akira Harada²

¹Graduate School of Natural Science and Technology, Kanazawa University,
Kakuma-machi, Kanazawa 920-1192, Japan

²Graduate School of Science, Osaka University, Toyonaka, Osaka 560-0043, Japan

Single-walled carbon nanotubes (SWNTs) have received a great deal of interests because of their unique structural, electrical, and mechanical properties. However, their applications have been extremely limited due to their low solubility in solvents. Therefore, solubilization of SWNTs has been one of hot topics for the past few years. Herein, we report novel chemically-responsive supramolecular SWNT hydrogel by using soluble SWNTs functionalized cyclodextrin (CD) moieties on SWNT surface. Since CD shows high solubility in water, water-soluble SWNTs carrying CDs are obtained by using π - π interaction between pyrene modified β -CDs and SWNTs (Py- β -CD/SWNT hybrids) [1].



Scheme 1. Supramolecular SWNT Hydrogel Prepared from Py- β -CD/SWNT Hybrids and Guest Modified Polymer (PAA2).

By utilizing host-guest interactions between poly(acrylic acid) carrying dodecyl groups (PAA2) and β -CDs of Py- β -CD/SWNT hybrids, nanocomposites of polymer and SWNTs were prepared. By mixing Py- β -CD/SWNT hybrids and PAA2 in aqueous media (Scheme 1a), a homogeneous SWNT hydrogel formed, indicating that host-guest complexes between β -CD moieties immobilized on the SWNT surface and dodecyl groups in PAA2 act as cross-links to form network structures which showed gel-like behavior. Furthermore, SWNT hydrogels composed of Py- β -CD/SWNT hybrids and PAA2 changed to sol by adding competitive guests or host compounds. When sodium adamantane carboxylate (AdCNa, 100 eq. to dodecyl moieties of PAA2) was added to the hydrogel as a competitive guest, gel to sol transition was observed (Scheme 1b). Upon addition of α -CD (100 eq. to dodecyl groups of PAA2) as a competitive host, the gel also changed to sol (Scheme 1c).

[1] T. Ogoshi et al. *J. Am. Chem. Soc.*, 129, 4878 (2007).

Corresponding Author: Akira Harada Tel&Fax 06-6850-5445 E-mail harada@sci.chem.osaka-u.ac.jp

Water Soluble Single-Walled Carbon Nanotubes Using Inclusion Complex of Cyclodextrin with Guest Molecules

○Tomoki Ogoshi¹, Tada-aki Yamagishi¹, Yoshiaki Nakamoto¹ and Akira Harada²

¹Graduate School of Natural Science and Technology, Kanazawa University,
Kakuma-machi, Kanazawa 920-1192, Japan

²Graduate School of Science, Osaka University, Toyonaka, Osaka 560-0043, Japan

Single-walled carbon nanotubes (SWNTs) have been an area of intense research since their discovery in 1993 because of their unique structural, electrical, and mechanical properties and potential applications. However, their applications have been extremely limited due to their low solubility. Therefore, solubilization of SWNTs has been one of hot topics over the past decade. For solubilization of SWNTs in solvents, chemical modification of SWNTs and physical adsorption of organic molecules on SWNT surfaces are useful strategies. Soluble SWNTs in aqueous media are obtained using physical adsorption of surfactants and polymers. Herein, we firstly report soluble SWNTs by using host-guest inclusion complex between cyclodextrin (CD) and guest compound. Surprisingly, SWNTs are soluble in aqueous media with host-guest complex, while SWNTs are insoluble with only CD or guest compound. To the best of our knowledge, it is first example of solubilization of SWNTs with host-guest inclusion complexes. It is little known that two different kinds of compounds cooperatively act as solubilizer of SWNTs.

To suspension of SWNTs (1.0 mg) in aqueous solution (5.0 mL), β -CD (20 mg) and sodium adamantane carboxylate (AdCNa, 2.14 mg, 1 equivalent to β -CD) were added and then the resulting solution was sonicated for 3 h at room temperature. During the sonication, the aqueous solution changed from colorless to black, indicating solubilization of SWNTs in aqueous solution. After the sonication, insoluble SWNTs were removed by centrifugation. The supernatant was homogeneous black solution and stable for more than a month (Figure 1a). On the other hand, SWNTs were insoluble with β -CD or AdCNa (Figure 1b). These observations indicate that SWNTs are soluble using the mixture of β -CD and AdCNa. Formation of the complex between β -CD and AdCNa is necessary to solubilize SWNTs.

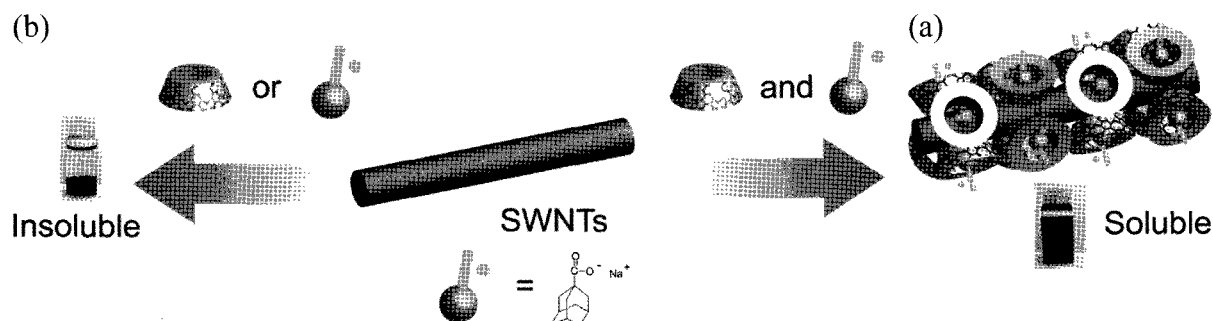


Figure 1. Aqueous SWNTs solution with (a) β -CD (3.52 mM) and AdCNa (3.52 mM), (b) β -CD or AdCNa after sonication.

Fabrication of optical polarizer made of CNT/PVA composite material

○Satoru Shoji^{1,3}, Hidemasa Suzuki¹, and Satoshi Kawata^{1,2,3}

¹*Department of Applied Physics, Osaka University, Yamadaoka 2-1, Suita, Osaka
565-0871, Japan*

²*Nanophotonics Laboratory, RIKEN, Wako, Saitama, 351-0198, Japan*

³*CREST, Japan Corporation of Science and Technology, Japan*

We prepared a uniaxially stretched carbon nanotube/PVA film to study the property of aligned carbon nanotubes as optical polarizer. Carbon nanotubes (HiPco single-wall carbon nanotubes: Carbon Nanotechnologies inc.) were uniformly dispersed in water solution of TritonX-100 under ultrasonication. The solution was then mixed with PVA powder and exposed under additional ultrasonication for several hours. The carbon nanotubes/PVA mixture was cast on a glass plate and dried out to form a solid film. The film was peeled from the glass plate and mechanically stretched along uniaxial direction so that carbon nanotubes were aligned in the PVA film in the stretching direction. We investigated degree of polarization (DOP) of the developed film by measuring transmission spectra with linear polarized light parallel/perpendicular to the stretching direction. The film showed DOP of 88% with transmission of 12% at the wavelength of 800 nm. Thanks to the broad absorption spectrum of carbon nanotubes originated from π plasmon, the film shows flat transmission spectrum and keeps the high DOP almost constantly through spectral region from near infrared (800 nm) to ultraviolet (down to 350 nm). We further improved the DOP by using carbon nanotubes shortened into the length of ~ 200 nm.

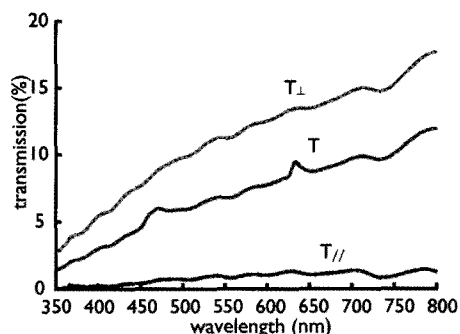


Figure 1. Transmission spectra of the SWCNT/PVA optical polarizer measured with linear polarized light parallel/perpendicular to the orientation of CNTs.

Corresponding Author: Satoru Shoji
TEL: +81-6-6879-7847, FAX: +81-6-6879-7330
E-mail: shoji@ap.eng.osaka-u.ac.jp

Direct electron transfer reaction of glucose oxidase with carbon nanotubes synthesized on a electrode.

Masato Tominaga, ○Shinya Nomura, Toshifumi Nishimura and Isao Taniguchi

Graduate School of Science and Technology, Kumamoto University,
Kumamoto 860-8555, Japan

Direct electron transfer reaction of enzymes at an electrode has been extensively studied from the viewpoints of both understanding the fundamental features of enzymes, and applications to enzyme-biofuel cell, biodevice and biosensors. It is expected that carbon nanotubes (CNTs) work as an excellent electrode material for direct electron transfer reaction of enzyme because of their unique electronic properties. In this study, direct electron transfer reaction of glucose oxidase (GOD) adsorbed on carbon nanotubes-synthesized electrode was demonstrated.

GOD (from *Aspergillus niger*, EC 1.1.3.4) was obtained from Tokyo Chemical Ind. Co., and was used as received. Platinum substrate was polished by a SiC paper followed by ferritin immobilization onto it (ferritin/Pt). To prepare iron nano-particles as catalysts for CNTs synthesis, the ferritin/Pt was heated at 400 °C for 60 min to eliminate the protein shell of ferritin. The prepared iron nano-particle size on Pt was evaluated to be approximately 5±1 nm in diameter by transmission electron microscope (TEM) measurement. The CNTs were synthesized by alcohol catalyst chemical vapor deposition (ACCVD) method. Diameter of the prepared CNTs on Pt plate was evaluated to be 5-10 nm by TEM, which were multi-walled CNTs. The electrochemical measurements were investigated by cyclic voltammetry. An Ag / AgCl (saturated KCl) and Pt plate were used as reference and auxiliary electrode, respectively.

GOD was immobilized CNTs/Pt electrode (GOD/CNTs/Pt) by the immersion of the electrode into a phosphate buffer solution of 550 units ml⁻¹ GOD for 12 hours, followed by rising with the buffer solution. Cyclic voltammogram of glucose oxidation of GOD/CNTs/Pt is shown in Fig. 1. Catalytic oxidation current was observed from around -0.4 V in a phosphate buffer (pH 7) in the presence of 3 mmol dm⁻³ glucose. Such catalytic current was not observed in the absence of glucose. When the CNTs/Pt and Pt electrode were used, no catalytic oxidation current was observed. The GOD/CNTs/Pt electrode indicated substrate specificity: the catalytic current was not obtained when mannose and galactose instead of glucoses were used as substrate. The obtained facts let us to know that the direct electron transfer occurred between GOD and CNTs.

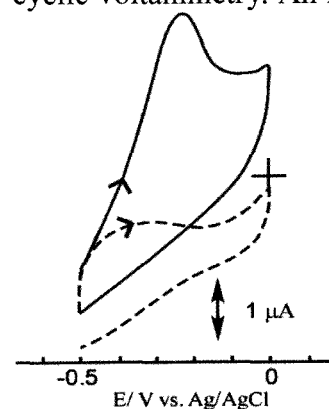


Fig. 1 Cyclic voltammograms of glucose oxidation at GOD immobilized on CNT/Pt electrode in a phosphate buffer in the presence (solid line) and absence (broken line) of 3 mmol dm⁻³ glucose. Scan rate: 5 mV s⁻¹. Electrode area: 0.246 cm².

Corresponding Author: Masato Tominaga

E-mail: masato@gpo.kumamoto-u.ac.jp

Tel&Fax: 096-342-3656

Preparation and Properties of Carbon Nanotube Films

○Motohiro Uo¹, Tsukasa Akasaka¹, Shigeaki Abe¹, Fumio Watari¹, Ken-ichiro Sasamori², Hisamichi Kimura², Yoshinori Sato³ and Kazuyuki Tohji³

¹*Department of Biomedical Materials & Engineering, Graduate School of Dental Medicine, Hokkaido University, Sapporo 060-8586, Japan*

²*Institute for Materials Research, Tohoku University, Sendai 980-8577, Japan*

³*Graduate School of Environmental Studies, Tohoku University, Sendai 980-8579, Japan*

Carbon nanotubes (CNTs) have a very high aspect ratio with high mechanical, electrical and chemical properties. Also, the good cell adhesion on the CNTs have been reported[1]. In this study, we prepared the multi-walled carbon nanotube (MWCNTs) films and their tensile strength were estimated.

The raw material of MWCNTs (20 to 50nm in diameter ; CNT Co.Ltd., Seoul, Korea) were purified and dispersed in distilled water or surfactant solution (1wt% of Triton X-100) to be 50mg in 100ml and sonicated for 20 minutes. The collagen (Cellgen, Koken, Tokyo, Japan) solution was added into MWCNTs solution while the sonication. The MWCNT/collagen mixture was filtered using polycarbonate membrane filter (pore diameter = 0.8μm). The stacked MWCNT/collagen film on the membrane filter was rinsed with distilled water and dried at 50°C. The obtained film was cut into 3mm in width and applied for the tensile test. The micro structure of the film was observed by SEM.

The obtained MWCNTs/collagen composite films were flexible and did not decomposed in water. Fig.1 shows the SEM images of MWCNTs/collagen composite with 5, 10 and 15% of collagen content. The fibrous structure of MWCNTs are clearly observed and adherent substances on the MWCNTs, which were assumed as the collagen, were observed. The film prepared without collagen was brittle. Therefore, collagen would act as binder of MWCNTs. The tensile strength of the film containing 15wt% of collagen was 14MPa. The strength was increased with the collagen content. Also, the tensile strength of composite films prepared using the surfactant was higher than that without surfactant.

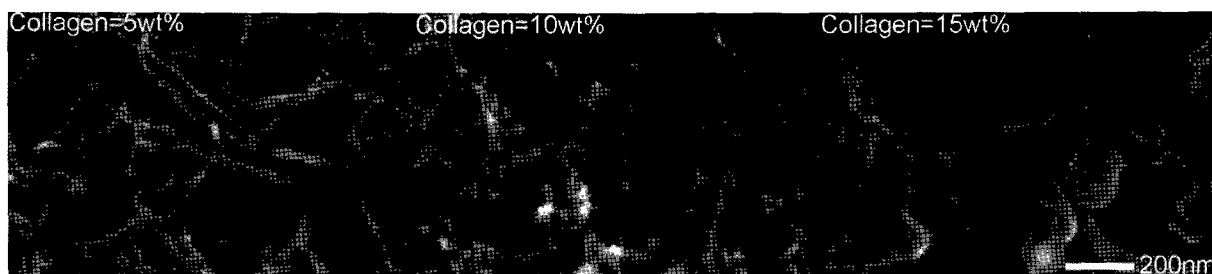


Fig.1 SEM images of MWCNTs/collagen composite films.

[1] N.Aoki, A.Yokoyama, Y.Nodasaka, T.Akasaka, M.Uo, Y.Sato, K.Tothji and F.Watari, Chemistry Letters, 2006, 35, 508-509.

Corresponding Author: Motohiro Uo

E-mail: uo@den.hokudai.ac.jp, **Tel&Fax:** 011-706-4251

Electric Double Layer Capacitance of the Surface Modified Fine-Crystallined Single-Walled Carbon Nanotubes

○Shin-ichi Ogino¹, Yoshinori Sato¹, Masaru Namura¹, Wataru Oizumi², Hiroyuki Kamisuki²,
Kenichi Motomiya¹, Takashi Itoh³, Balachandran Jeyadevan¹ and Kazuyuki Tohji¹

¹Graduate School of Environmental Studies, Tohoku University, Sendai 980-8579, Japan

²NEC TOKIN Corporation, Sagamihara 229-1198, Japan

³Center for Interdisciplinary Research, Tohoku University, Sendai 980-8578, Japan

Electric double layer capacitors (EDLCs) are kind of energy storage devices that exhibit high power density, rapid charge-discharge, and long cycle life. In this presentation, we report the electrochemical behavior of EDLCs built from fine-crystallined single-walled carbon nanotubes (SWCNTs). Fine-crystallined SWCNTs possess extremely low electric resistance through the influence of long mean free path by ballistic transport. Therefore, they can utilize electrons effectively.

We prepared fine-crystallined SWCNTs by the following steps. Firstly, we synthesized as-grown SWCNTs by an arc-discharge method using Fe/Ni mixture particles as a metal catalyst simultaneously. Secondly, The as-grown SWCNTs were air oxidized and treated with hydrochloric acid to remove amorphous carbon and catalytic metal particles respectively (purified-SWCNTs). Finally, the purified-SWCNTs were annealed under high vacuum ambient atmosphere at 1473 K for 30 minutes (fine-crystallined-SWCNTs). In an effort to modify nanotube surface, the fine-crystallined-SWCNTs were treated with nitric acid at 373 K for a specific period of time to add carboxyl and hydroxyl groups on the surface (surface-modified-SWCNTs). As a consequence, these hydrophilic chemical functions improve the affinity between electrode and electrolyte. EDLC cells were assembled using surface-modified-SWCNTs as both electrode and 30 wt% of sulfuric acid as electrolyte.

Figure 1 is the dependence of electric double layer capacitance of current density for the surface-modified SWCNTs. To achieve higher capacitance, it exhibits the most suitable surface-treating time of nitric acid is four hours. This means that the structure of nanotube is disrupted by excess surface-treating time and the excess surface-modified SWCNTs cannot keep the excellent conductivity. The relation of the capacitance and surface modification will be reported in detail and discussed.

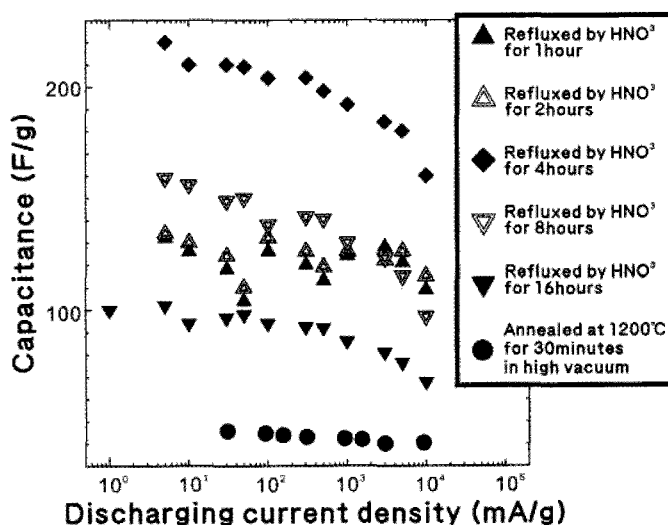


Fig. 1. Dependence of electric double layer capacitance of current density for the surface-modified SWCNTs.

Corresponding Author: Shin-ichi Ogino
E-mail: ogino@bucky1.kankyo.tohoku.ac.jp
Tel&Fax: +81-22-795-7392

Fabrication of Carbon Nanotubes Through Metal-free Chemical Vapor Deposition

○Jarrn-Horng Lin^{1,*}, Hui-Ling Ma^{1,3}, Ching-Shiun Chen², Chen-Yin Hsu³, and Hsiu-Wei Chen^{3,*}

¹Dept. of Materials Science, National University of Tainan, 33, Sec. 2, Shu-Lin St., Tainan, Taiwan, 700, Republic of China.

²Center of General Education, Chang Gung University, 259 Wen-Hwa 1st Rd., Kwei-shan, Tao-Yuan, Taiwan, 333, Republic of China.

³Dept. of Chemistry and Center for Nanoscience and Nanotechnology, National Sun Yat-sen University, Kaohsiung, Taiwan 804, Republic of China.

The fabrication of carbon nanotubes (CNTs) at desired positions and the large-scale production of metal-free CNTs are two key factors that will determine whether CNTs will soon reach their huge potential for application in a wide variety of areas. Arc discharge¹, laser ablation², and catalytic chemical vapor deposition (CCVD)³⁻⁵ techniques have been developed to produce CNTs, with CCVD having the greatest potential for using in large-scale production of CNTs. Although much effort have been exerted into improving the CCVD process, e.g., for controlling the size and morphology of CNTs, some fundamental problems still remain a challenge. One of the major weakness of CCVD is the encapsulation of the metallic catalyst within the nanotube during its growth. The presence of encapsulated metals may have a detrimental effect on the applicability of CNTs, especially in electronic devices. The other major problem of the CCVD approach toward the synthesis of CNTs is migration of the nanoscale catalytic particles during the preparation of the catalysts; this phenomenon makes it difficult to control the positions of the CNT growth sites. Non-catalytic CVD approaches would have the potential to solve these two problems. In this regard, we have developed a simple metal-free CVD method that has the potential to allow the controlled fabrication of CNTs at desired growth sites on graphite surfaces. Multi-Walled CNTs (MWCNTs) can be produced at 800 °C in the flow of C₂H₄/He on graphite surfaces that have been treated with nitric acids, oxygen or laser ablation.

[1] C. R. Wang, T. Kai, T. Tomiyama, T. Yoshida, Y. Kobayashi, E. Nishibori, M. Takata, M. Sakata and H. Shinohara, *Angew. Chem. Int. Ed.*, **40**, 397 (2001).

[1] S. Iijima, *Nature* 354, 56(1991).

[2] T. Guo, P. Nikolaev, A. Thess, D. T. Colbert, R. E. Smalley, *Chem. Phys. Lett.* 243, 49 (1995).

[3] W. Z. Li, L. X. Qian, B. H. Chang, W. Y. Zou, R. A. Zhao and G. Wang, *Science*, 274, 1701 (1996).

[4] D. S. Bethune and C. H. Kiang, *Nature*, 363, 605 (1993).

[5] S. Iijima and T. Ichihashi, *Nature*, 363, 603-605 (1993).

Corresponding Author: Jarrn-Horng Lin

TEL: +886-6-2133111 ext. 240, FAX: +886-6-2133409, E-mail: janusjhlin@mail.nutn.edu.tw

Current-induced Forces On Adatoms on Metallic and Semiconducting Carbon Nanotubes.

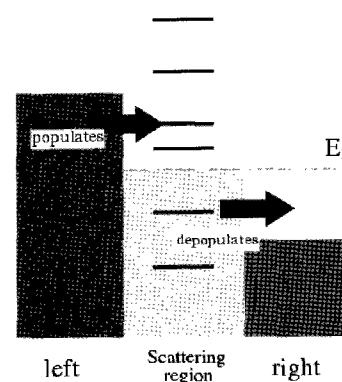
Yvan Girard^{1,2}, Takahiro Yamamoto^{1,2}, Kazuyuki Watanabe^{1,2}

1. Department of Physics, Tokyo University of Science.

2. CREST, Japan Science and Technology Agency.

The forces induced by a steady electric current on several atoms adsorbed on a metallic (5,5) and semi-conducting (8,0) carbon nanotubes were calculated using the non-equilibrium Green's function technique combined with density functional theory. The calculations were performed with five different atoms, viz. B, C, N, O and F, adsorbed onto the nanotubes. Single-zeta basis sets with a LDA functional and considered a fairly large scattering region containing 100 carbon atoms, leads being semi-infinite nanotubes as well. Geometries were optimized at zero bias voltage with adatoms in bridge positions. Atoms were found to be either repelled from the tube or attracted to it and the current-induced forces also pulled the atoms either in the direction of the electron flow or in the opposite direction.

We are able to explain these results in terms of charge transfer, modification of the electron density, and chemical bonding properties of the scattering states, assuming that when the bias is applied, the scattering electrons from the lead with the higher chemical potential (source) populates the states above the original Fermi level and the state below the Fermi level is depopulated by the electron flow toward the lead with the lower chemical potential (drain).



References

1. Girard, Y.; Yamamoto, T.; Watanabe, K. *J. Phys. Chem.* accepted.

Formation Process of Fullerenes

○ Yusuke Ueno and Susumu Saito

*Department of Physics, Tokyo Institute of Technology,
2-12-1 Oh-okayama, Meguro-ku, Tokyo 152-8551*

Contrary to many successful studies on the properties of C_{60} since a macroscopic production of C_{60} fullerene [1], the microscopic formation process of C_{60} and other fullerenes has not been clarified yet. Therefore, the mystery, why icosahedral C_{60} clusters are by far most abundant in carbon soot, still remains unsolved. We address these issues using the molecular-dynamics combined with the transferable tight-binding model (TBMD) parametrized by Omata *et al.* [2]. The reason why we use the new tight-binding model is that, unlike the previous tight-binding model [3], it can accurately describe the long-range force between carbon atoms, which should play an important role in the formation process of fullerenes from C atoms.

We first study the structures of small carbon clusters. It is found that C_{10} is the smallest stable ring at 2000 K. This explains the high abundance of C_{10} in the experimental C_n^- mass spectra [4]. From the density-functional study, we find that binding energy per atom of the C_{10} ring is larger by 0.4 eV/atom than that of the C_{10} chain. This energy preference of a ring to a chain in C_{10} is most prominent among all C_n clusters studied ($5 \leq n \leq 18$).

Next, we examine the formation process of fullerenes, taking C_{10} rings as fundamental parts [4], by performing the TBMD simulation of the reactions between carbon clusters at 1000, 1500, 2000 and 2500 K. Reaction between sp -hybridized C_{10} rings gives rise to the planar sp^2 -network C_{20} cluster (Fig.1 (a)) at more than 1000 K. Surprisingly, reaction between C_{20} and C_{10} clusters is found to give the closed-cage C_{30} (Fig.1 (b)) at 2500 K. These results are different from those by using the previous tight-binding model [3] but are consistent with the experimental result of the ion chromatography by von Helden *et al.* [5]. In addition, it is confirmed that C_{40} , C_{50} and C_{60} clusters have the closed-cage structure at more than 1500 K, which is close to the experimental temperature of fullerene formation.

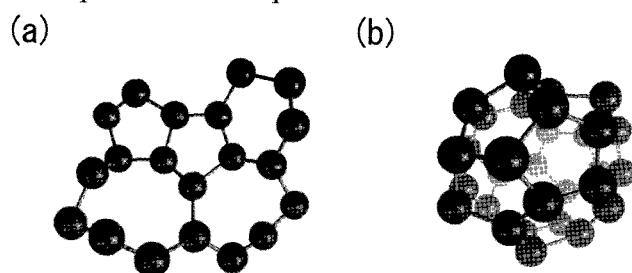


Fig. 1: (a) planar sp^2 -network C_{20} and (b) “fullerene” C_{30}

[1] W. Krateshmer, L. D. Lamb, K. Fostiropoulos and D. R. Huffman, *Nature* **347** (1990) 354.

[2] Y. Omata, Y. Yamagami, K. Tadano, T. Miyake and S. Saito, *Physica E* **29** (2005) 454.

[3] C. H. Xu, C. Z. Wang, C. T. Chan and K. M. Ho, *J. Phys. Condens. Matter* **4** (1992) 6047.

[4] T. Wakabayashi and Y. Achiba, *Chem. Phys. Lett.* **190** (1992) 465.

[5] G. von Helden, M. T. Hsu, N. Gotts and M. T. Bowers, *J. Phys. Chem.*, **97** (1993) 8182.

Corresponding Author: Yusuke Ueno

TEL: 03-5734-2387, FAX:03-5734-2739, E-mail: ueno@stat.phys.titech.ac.jp

Effects of Magnetic Processing on Morphological, Electrochemical, and Photoelectrochemical Properties of Electrodes Modified with Mixed Nanoclusters of C₆₀-Phenothiazine System

○Yuya Wakita¹, Hiroaki Yonemura¹, Norihiro Kuroda¹, Sunao Yamada^{1,2},
Yoshihisa Fujiwara³, and Yoshifumi Tanimoto³

¹Department of Applied Chemistry, Kyushu University, Fukuoka 819-0395, Japan

²Center for Future Creation, Kyushu University, Fukuoka 819-0395, Japan

³Department of Mathematical and Life Sciences, Hiroshima University, Higashi-Hiroshima 739-8526, Japan

We examined photoinduced electron-transfer reactions and magnetic field effects (MFEs) on the dynamics of a radical pair that was generated from the intermolecular electron-transfer reaction between of C₆₀ derivative with positive charge (C₆₀N⁺) and methyl phenothiazine (MePH) (Fig. 1) [1]. We also reported MFEs on the photoelectrochemical reactions of photosensitive electrodes modified with nanoclusters containing of C₆₀N⁺ and MePH, intended for utilization of C₆₀ as photofunctional nanodevices [2].

Applying strong magnetic fields to materials induces huge MFEs. It is expected to create highly functional nano-materials containing new properties, since new interfaces or nanostructures are constructed by strong magnetic fields [3]. In this study, we examined MFEs on morphological, electrochemical, and photoelectrochemical properties of electrodes modified with C₆₀N⁺ and MePH in the presence and the absence of magnetic processing due to strong magnetic field [4].

The AFM measurements indicated that the size of C₆₀N⁺-MePH nanoclusters in the presence of magnetic processing was smaller than that in the absence of magnetic processing. First reduction peaks due to C₆₀N⁺ nanocluster in the presence of magnetic processing were negative-shifted as comparison with that in the absence of magnetic processing. Potential dependencies of the photocurrents of the electrodes modified with C₆₀N⁺-MePH nanoclusters in the presence of magnetic processing were also different from that in the absence of magnetic processing.

The magnetic field effects in AFM, and electrochemical and photoelectrochemical measurements are most likely ascribed to the difference of the reduction potentials between the absence and the presence of magnetic processing due to the morphological change of C₆₀N⁺ nanoclusters.

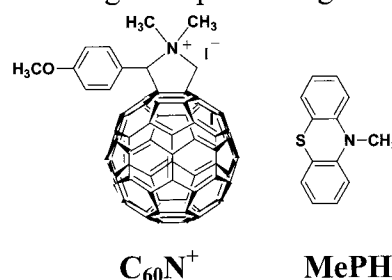


Fig. 1 Molecular structures of C₆₀N⁺ and MePH

[1] H. Yonemura, N. Kuroda, S. Moribe, and S. Yamada, *C. R. Chimie*, **9**, 254 (2006).

[2] H. Yonemura, N. Kuroda, and S. Yamada, *Sci. Technol. Advanced Materials*, **7**, 643 (2006).

[3] M. Yamaguchi and Y. Tanimoto (eds.): *Magnetism-Science Magnetic Field Effects on Materials : Fundamentals and Applications*, Kodansha-Springer, (2006).

[4] H. Yonemura, Y. Wakita, N. Kuroda, S. Yamada, Y. Fujiwara and Y. Tanimoto, submitted for publication in *Jpn. J. Appl. Phys.*, (2007).

Corresponding Author: Yuya Wakita

TEL: +81-92-802-2814, FAX: +81-92-802-2815, E-mail: y-wakitatcm@mbox.nc.kyushu-u.ac.jp

Synthesis and Electrochemical Property of [70]fullerene derivatives

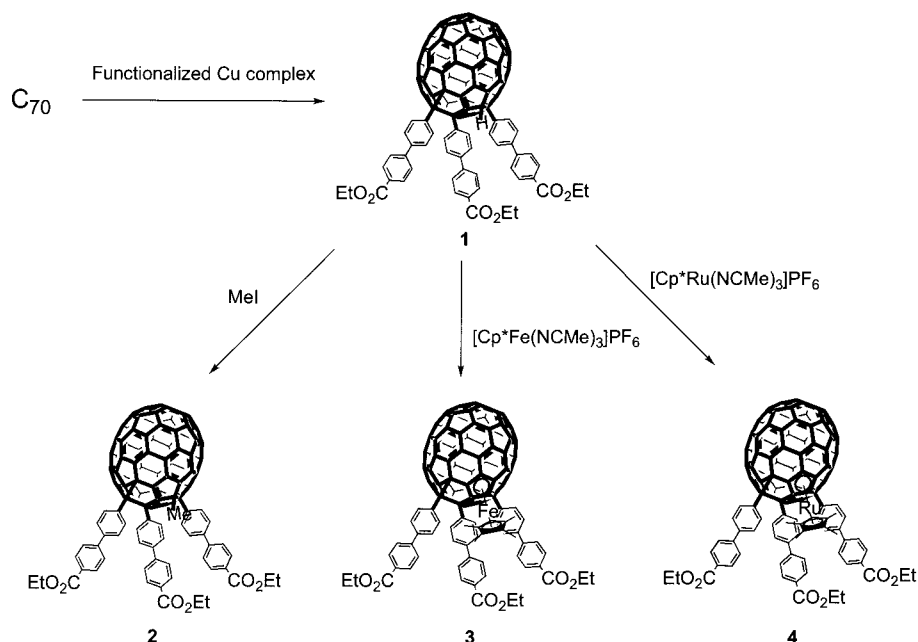
○Takahiko Ichiki¹, Yutaka Matsuo², Eiichi Nakamura^{1,2}

¹Department of Chemistry, The University of Tokyo, Hongo, Bunkyo-ku, Tokyo 113-0033, Japan

²Nakamura Functional Carbon Cluster Project, ERATO, Japan Science and Technology Agency (JST), Hongo, Bunkyo-ku, Tokyo 113-0033, Japan

There are quantitative differences such as structure, aromatic character, symmetry and chemical properties between [60]fullerene and the higher fullerenes available. The development of the chemistry of the higher fullerenes such as [70]fullerene is great significance because they show a high performance of optical and electrochemical properties for the creation of novel molecular devices. The synthesis of tri-adducts [70]fullerene derivatives has been reported in our laboratory[1]. This multi-addition reaction is a powerful method for the functionalization of [70]fullerene to develop abilities or add novel functions to [70]fullerene.

Here, we report the tri-adducts [70]fullerene derivatives which possess biphenyl ester groups. To a suspension of Cu complex in THF was added a solution of $\text{EtOCOC}_6\text{H}_4\text{C}_6\text{H}_4\text{MgBr}$ which was prepared by iodine-magnesium exchange procedure[2]. To the resulting yellow suspension was added a solution of [70]fullerene to obtain $\text{C}_{70}(\text{C}_6\text{H}_4\text{C}_6\text{H}_4\text{CO}_2\text{Et})_3\text{H}$ (**1**). The sequential methylation or complexation of **1** afforded **2**, **3** and **4**. Electrochemical and photophysical properties of these compounds will be presented.



[1] M. Sawamura, M. Toganoh, H. Iikura, Y. Matsuo, A. Hirai, and E. Nakamura, *J. Mater. Chem.* (Fullerene issue), **12**, 2109-2115 (2002).

[2] Y.-W. Zhong, Y. Matsuo, and E. Nakamura, *Org. Lett.*, **8**, 1463-1466 (2006).

Corresponding Author: Yutaka Matsuo and Eiichi Nakamura

TEL/FAX: +81-3-5841-1476; E-mail: matsuo@chem.s.u-tokyo.ac.jp; nakamura@chem.s.u-tokyo.ac.jp

2P-5

Degradation Kinetics of Poly(methyl methacrylate) with Fullerenes

○Tomohito Terada^{1,2}, Takanori Matsuura¹, Takeo Sasaki², Yusuke Tajima¹

¹Nano-Integration Materials Research Unit, RIKEN, Wako, 315-0198

²Department of Chemistry, Graduate School of Science, Tokyo University of Science, Shinjuku-ku, 152-8601

Thermal degradation of radically polymerized polymethylmethacrylate (PMMA) in nitrogen atmosphere is explained by three reaction stages [1]. Differential scanning calorimetry (DSC) curve of the PMMA shows three endothermic peaks corresponding to each stage. With an increase in the content of C₆₀ addition, the first peak disappears and other peaks shift to high temperature.

In this study, we investigate the thermal stability of PMMA with or without fullerenes. The influence of C₆₀, C₆₀O, and [6,6]-phenylC₆₁-butyric acid methyl ester (PCBM), which have different electron affinity (Table1), on the thermal degradation of PMMA are kinetically studied. The apparent activation energies, E_a , associated with the second and third degradation stage of PMMA are calculated by the methods of Flynn-Wall-Ozawa [2] and Kissinger [3].

Calculated kinetic parameters are shown in Table 2. The E_a values of the PMMA containing any kind of fullerenes are comparable to each other and higher than that of pristine PMMA. These results indicate that fullerenes heighten the degradation point of PMMA and are good stabilizer for PMMA. The kinetic compensation parameters for thermal degradation, S_p^* , are calculated according to $S_p^* = E_a / \log A$ [4]. The S_p^* of PMMA with or without fullerenes shows almost constant value. It suggests that shift of the peak top temperature of second and third degradation stage of PMMA does not accompany with the alteration of degradation mechanism of PMMA.

Table1. Reduction potential of fullerenes (vs. Ag/Ag⁺)

	E_{red}^1 / V
C ₆₀	-0.85
C ₆₀ O	-0.81
PCBM	-0.94

Table 2. Kinetic parameters of thermal degradation at the second degradationstage of PMMA calculated by the Kissinger method.

	$E_a / \text{kJ mol}^{-1}$	$A / \text{min}^{-1 \text{ a)}$	S_p^*
PMMA	171.7	4.13×10^{12}	13.6
PMMA/C ₆₀	196.5	7.49×10^{14}	13.2
PMMA/C ₆₀ O	190.5	1.64×10^{14}	13.4
PMMA/PCBM	199.3	1.54×10^{15}	13.1

a) Preexponential factor.

[1] T. Kashiwagi, et al., *Macromol.* **1986**, *19*, 2160. [2] T. Ozawa, *Bull. Chem. Soc. Jpn.* **1965**, *38*, 1881.

[3] H. Kissinger, *Anal. Chem.* **1957**, *29*, 1702. [4] M. Maciejewski, *J. Thermal Anal.* **1988**, *33*, 1269

Corresponding Author: Yusuke Tajima

TEL: +81-48-467-9309, FAX: +81-48-462-4702, E-mail: tajima@riken.jp

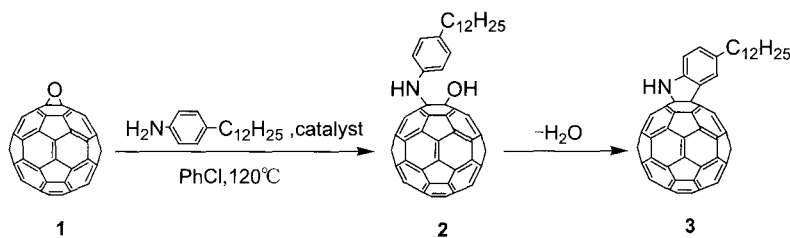
Synthesis and Electrochemical Properties of Indolino-[60]Fullerene

○Junichi Kawashima^{1,2}, Takumi Hara^{1,2}, Takanori Matsuura¹,
Youhei Numata¹, Yusuke Tajima^{1,2}

¹Nano-Integration Materials Research Unit, RIKEN, Wako, 351-0198

²Department of Chemical Engineering, Saitama University, Saitama, 338-8570

Recently, we have shown that fullerene oxide can be transformed into 1,3-dioxolane derivatives or 1,4-bisadducts efficiently[1][2]. In the present study, we report the synthesis of indolino-[60]fullerene derivative by the nucleophilic substitution of epoxy group on C₆₀O (**1**). Reaction of **1** with excess aromatic amine in the presence of acid catalyst affords fullerene derivative (**3**) bearing five-membered heterocyclic structure.



The structure for **3** was confirmed by using FT-IR, MS, ¹H- and ¹³C-NMR measurements. The reactions in the presence of several catalysts under the similar conditions were carried out, and the results are listed in Table 1. The reaction produced **3** in *ca.* 50 % yield under BiCl₃, which catalyzes opening of epoxide ring with aromatic amines[3]. The production of **3** was also enhanced by the presence of Montmorillonite K10 and Sepiolite, whereas neither *p*-toluenesulfonic acid (TsOH) nor Amberlyst 15 was produced **3** as main product. During the reaction, we observed the formation of 1,2-aminoalcohol (**2**) as an intermediate. These results imply that the reaction proceeds in only aprotic condition *via* a nucleophilic substitution of **1** with aromatic amine followed by a cyclization of **2**.

Table 1. Reaction of **1** with aromatic amine in the presence of catalyst

catalysts	time	yield(%)	temperature(°C)
BiCl ₃	2h	50.3	120
Montmorillonite K10	6h	56.7	120
Sepiolite	6h	63.8	120
TsOH	5d	trace	100
Amberlyst 15	5d	0	120

Table 2. Reduction potentials vs Ag/AgCl

compounds	E^1_{red}	E^2_{red}	E^3_{red}
C ₆₀	-0.85	-1.23	-1.68
C ₆₀ O	-0.81	-1.34	-1.69
PCBM	-0.94	-1.30	-1.81
3	-0.92	-1.29	-1.80

Electrochemical data for the first three reductions of **3** are given with those of C₆₀, C₆₀O and PCBM in Table 2. The first reduction potential of **3** is significantly low and comparable to that of PCBM.

[1] Y. Shigemitsu, M. Kaneko, Y. Tajima, K. Takeuchi, *Chem. Lett.*, **2004**, 33(12), 1604-1605.

[2] Y. Tajima, T. Hara, T. Honma, K. Takeuchi, *Org. Lett.*, **2006**, 8(15), 3203-3205.

[3] T. Ollevier, G. Lavie-Compin, *Tetrahedron Lett.*, **2002**, 43, 7891-7893.

Corresponding Author: Yusuke Tajima

TEL: +81-48-467-9309, FAX: +81-48-462-4702, E-mail: tajima@riken.jp

Solid-State ^{45}Sc - and ^{13}C -NMR of $\text{Sc}_2\text{C}_2@C_{82}$ Carbide Metallofullerenes

○Haruya Okimoto¹, Wilhelm Hemme², Yasuhiro Ito¹, Helmut Eckert² and Hisanori Shinohara^{1,3}

¹Department of Chemistry and Institute for Advanced Research,
Nagoya University, Nagoya 464-8602, Japan

²Institut für Physikalische Chemie and NRW Graduate School of Chemistry, Universität
Münster, Corrensstrasse 30, D-48149, Münster, Germany

³CREST, Japan Science and Technology Corporation, c/o Department of Chemistry,
Nagoya University, Nagoya 464-8602, Japan

Metal carbide fullerenes are an intriguing class of fullerene materials encapsulating metal-carbide cluster inside carbon cages [1]. For example, $\text{Sc}_2\text{C}_2@C_{82}(\text{III})$ encages two Sc metal and C_2 cluster in a carbon cage of C_{3v} symmetry [2,3]. Two Sc ions have been observed to rotate in the carbon cage as revealed by solution NMR [4]. Although many NMR measurements have been reported for metallofullerenes, almost all measurements have been done on liquid-state NMR. Here, we report solid-state NMR of Sc-metallofullerenes and discuss an intra-fullerene motional dynamics of Sc metal atoms in the fullerene solid.

$\text{Sc}_2\text{C}_2@C_{82}(\text{III})$ solid was prepared by drying a purified (99.9 %) metallofullerene in vacuo at room temperature. ^{45}Sc NMR and ^{13}C NMR spectra were recorded at 121.5 and 125.7 MHz, respectively, on a Bruker DSX 500 spectrometer, incorporating a 2.5mm magic angle spinning NMR probe. Spectra were taken on samples spinning at a rate of 0-25 kHz, using 90° pulses of $1.44 \mu\text{s}$ for scandium and $3.00 \mu\text{s}$ for carbon, which was followed by a relaxation delay of 0.5 s. The temperature dependence was observed between 300 and 373 K. The chemical shifts for scandium and carbon atoms were calibrated by using aqueous solution of scandium nitrate and adamantane, respectively.

Figure 1 shows solid state ^{45}Sc -NMR spectra of $\text{Sc}_2\text{C}_2@C_{82}(\text{III})$ at a temperature range from 300 to 373 K. The signals shown in Fig.1 were the only signals obtained in the chemical shift range -500 to 1000 ppm. This also indicates there is no overlap of two resonances with almost similar chemical shifts. The activation energy estimated from the corresponding Arrhenius plot is 6.59 kJ/mol which is lower than 8.49 kJ/mol by a solution ^{45}Sc -NMR reported by Miyake et al. Figure 2 shows solid state ^{13}C -NMR spectrum of $\text{Sc}_2\text{C}_2@C_{82}(\text{III})$ at room temperature. It is suggested that $\text{Sc}_2\text{C}_2@C_{82}(\text{III})$ fullerenes are in a certain (restricted) motion in the solid state judging from the observed sharp ^{13}C -NMR lines.

References: [1]C.-R. Wang *et al.*, *Angew. Chemie. Int. Ed.*, **40**, 397(2001). [2]Iiduka *et al.*, *Chem. Commu.*, 2057 (2006). [3]E.Nishibori *et al.*, *Chem. Phys. Lett.* **433**, 120(2006). [4]Y. Miyake *et al.*, *J. Phys. Chem.*, **100**,9579 (1996).

Corresponding Author Hisanori Shinohara E-mail noris@nano.chem.nagoya-u.ac.jp
Tel +81-52-789-3660

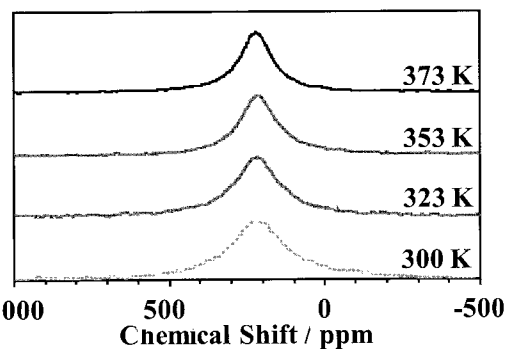


Figure 1. Solid State ^{45}Sc -NMR spectra of $\text{Sc}_2\text{C}_2@C_{82}(\text{III})$

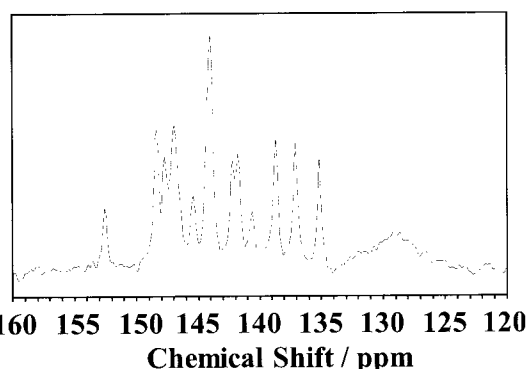


Figure 2. Solid State ^{13}C -NMR spectra of $\text{Sc}_2\text{C}_2@C_{82}(\text{III})$

Structure and Vibronic Interaction of M@C₇₄

○ Tohru Sato^{1,2}, Yasutaka Kuzumoto², Ken Tokunaga², Hiroshi Imahori²,
and Kazuyoshi Tanaka^{2,3}

¹ *Fukui Institute for Fundamental Chemistry, Kyoto University,
Takano-Nishihiraki-cho 34-4, Sakyo-ku, Kyoto 606-8103, Japan*

² *Department of Molecular Engineering, School of Engineering, Kyoto
University, Kyoto 615-8510, Japan*

³ *Core Research for Evolutional Science and Technology, Japan Science and
Technology Agency (JST-CREST)*

From the temperature dependence of ¹³C NMR spectra of Ca@C₇₄, it was found that the symmetry of the cage is D_{3h} and that the Ca atom hops between several sites inside the cage[1]. It was suggested that the Ca deviates from the center of the cage, and the stable structure of Ca@C₇₄ is C_{2v} at low temperature. With increasing temperature, the metal moves within the σ_h plane. Density functional calculations also predicted that the most stable structure of Ca@C₇₄ is C_{2v} [2].

Motion of the encapsulated metal in M@C₇₄ (M=Be, Mg, Ca, Sr, Ba) is studied in terms of vibronic coupling using group theory approach. The selection rule for the symmetry of metal motion is presented. This agrees well with experimental findings for Ca@C₇₄. The metal motion can be regard as a pseudo-Jahn–Teller effect. The electronic structures and adiabatic potential surfaces of M@C₇₄ are calculated using the tight-binding approximation.

[1] T. Kodama, Y. Fujii, Y. Miyake, S. Suzuki, H. Nishikawa, I. Ikemoto, K. Kikuchi, and Y. Achiba, *Chem. Phys. Lett.* **399**, 94(2004).

[2] S. Nagase, K. Kobayashi, and T. Akasaka, *J. Mol. Struct. (Theochem)* **461-462**, 97 (1999).

Corresponding Author: Tohru Sato

E-mail: tsato@scl.kyoto-u.ac.jp

Tel: +81 75 383 2803

Fax: +81 75 383 2255

Chemical Functionalization of Li@C₆₀ by Its Reaction with spiro[2-Adamantane-2,3'-3H-Diazirine]

○Shinsuke Ishikawa¹, Takashi Komuro¹, Hiroshi Okada^{1,2}, Kenji Omote², Yasuhiko Kasama²,
Kuniyoshi Yokoo², Shoichi Ono², and Hiromi Tobita¹

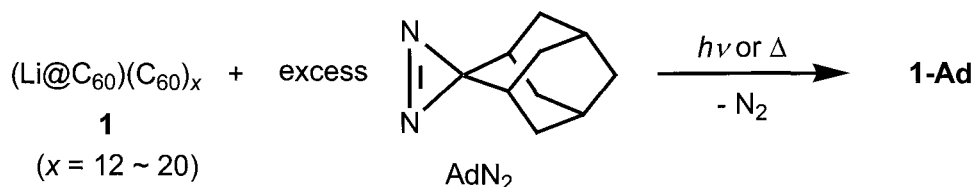
¹*Department of Chemistry, Graduate School of Science, Tohoku University,
Sendai 980-8578, Japan*

²*Ideal Star Inc., ICR Bldg, 6-6-3 Minamiyoshinari, Aoba-ku, Sendai 989-3204, Japan*

Ideal Star Inc. has recently achieved the synthesis of the Li@C₆₀-containing material and its extraction with 1-chloronaphthalene to afford the Li@C₆₀-enriched product. However, several spectroscopic and elemental analyses indicate that the extracted product contains a large amount of empty [C₆₀]fullerene molecules. We suggest that Li@C₆₀ molecule is associated with C₆₀ molecules to form a cluster structure formulated as (Li@C₆₀)(C₆₀)_x (**1**, *x* = 12 ~ 20). Because of low solubility of **1** in common solvents as well as unexpectedly strong intermolecular force between Li@C₆₀ and C₆₀, we have not succeeded in isolation of Li@C₆₀ from **1** by extraction or chromatography.

Thus, we have focused on the chemical functionalization of **1** with a bulky adamantylidene group to improve the solubility as well as ravel out the cluster structure. For example, Akasaka et al. reported the chemical functionalization of La@C₈₂ by spiro[2-adamantane-2,3'-3H-diazirine] (AdN₂) to give La@C₈₂(Ad)¹.

Herein, we report the reaction of (Li@C₆₀)(C₆₀)_x (**1**) with excess AdN₂ and characterization of the reaction product (**1-Ad**). Treatment of **1** with excess AdN₂ in 1-chloronaphthalene gave **1-Ad** as a brown powder. **1-Ad** was characterized by LDI-TOF MS spectroscopy, where the several peaks assignable to Li@C₆₀(Ad)_{*n*} (*n* = 1 ~ 6) were observed. **1-Ad** has higher solubility in *o*-dichlorobenzene and CS₂ compared to **1**.



[1] Y. Maeda et al., *J. Am. Chem. Soc.*, **126**, 6858 (2004).

Corresponding Author: Hiromi Tobita

TEL: +81-22-795-6539, FAX: +81-22-795-6543, E-mail: tobita@mail.tains.tohoku.ac.jp

Structure and Electronic Property of Sc@C₈₂

○Makoto Hachiya¹, Yuko Iiduka¹, Takatsugu Wakahara¹, Takahiro Tsuchiya¹,
Yutaka Maeda², Takeshi Akasaka¹, Naomi Mizorogi³, Shigeru Nagase³

¹*Center for Tsukuba Advanced Research Alliance, University of Tsukuba,* ²*Department of Chemistry, Tokyo Gakugei University,* ³*Department of Theoretical and Computational Molecular Science, Institute for Molecular Science*

Since the first success in the extraction of endohedral metallofullerenes in 1991, M@C₈₂ (M = Sc, Y, La and other lanthanide elements) has been most widely investigated as a prototype of mono-metallofullerenes [1]. For example, the structure and electronic property of La@C₈₂ have been revealed by theoretical calculations and various experimental methods such as ¹³C NMR and X-ray powder diffraction studies and X-ray single-crystal structure analysis. Meanwhile, the structure of Sc@C₈₂ has been reported by X-ray powder diffraction study [2], however, its electronic property and chemical reactivity have not so far been clarified.

Because of the paramagnetic nature, it is difficult to determine the structure of Sc@C₈₂ by ¹³C NMR measurement. We have developed a new method to determine the structures of a series of paramagnetic mono-metallofullerenes by ¹³C NMR measurements in their anionic form [3]. Herein we report the structural determination of Sc@C₈₂ by using this method. Electronic property and chemical reactivity of Sc@C₈₂ were also investigated.

References

- [1] *Endofullerenes: A New Family of Carbon Clusters*; Akasaka, T., Nagase, S., Eds.; Kluwer: Dordrecht, 2002.
- [2] Nishibori, E. et al. *Chem. Phys. Lett.* **1998**, *298*, 79.
- [3] Akasaka, T. et al. *J. Am. Chem. Soc.* **2000**, *122*, 9316.

Corresponding Author: Takeshi Akasaka
TEL&FAX: +81-29-853-6409, E-mail: akasaka@tara.tsukuba.ac.jp

Missing Metallofullerenes: La@C_{2n}

○Hidefumi Nikawa¹, Takashi Kikuchi¹, Tomoya Yamada¹, Takatsugu Wakahara¹, Tsukasa Nakahodo¹, G. M. Aminur Rahman¹, Takahiro Tsuchiya¹, Yutaka Maeda², Takeshi Akasaka¹, Kenji Yoza³, Ernst Horn⁴, Kazunori Yamamoto⁵, Naomi Mizorogi⁶, Zdenek Slanina⁶, and Shigeru Nagase⁶

¹Center for Tsukuba Advanced Research Alliance, University of Tsukuba, Tsukuba, Ibaraki 305-8577, Japan,

²Department of Chemistry, Tokyo Gakugei University, Koganei, Tokyo 184-8501, Japan,

³Bruker AXS K.K., Yokohama, Kanagawa 221-0022, Japan,

⁴Department of Chemistry, Rikkyo University, Tokyo 171-8501, Japan,

⁵Power Reactor & Nuclear Fuel Development Corporation, Tokai, Ibaraki 319-1100, Japan,

⁶Theoretical Molecular Science, Institute for Molecular Science, Okazaki, Aichi 444-8585, Japan

Endohedral metallofullerenes have attracted special interest since they could lead to new spherical molecules with unique structure and properties that are unexpected for empty fullerenes. In 1991, Smalley and co-workers reported that La@C₆₀, La@C₇₄, and La@C₈₂ were produced especially abundantly in the soot, but only La@C₈₂ was extracted with toluene[1]. Since then, the chemistry of soluble endohedral metallofullerenes has been started by centering on that of La@C₈₂, and up to now many soluble endohedral metallofullerenes have been separated and characterized. However, insoluble endohedral metallofullerenes such as La@C₆₀, La@C₇₂, and La@C₇₄, have not yet been isolated although they are regularly observed in the raw soot by mass spectrometry.

We herein report the isolation of La@C₇₂, La@C₇₄, and La@C₇₆ as an endohedral metallofullerene derivative, La@C₇₂(C₆H₃Cl₂)[2], La@C₇₄(C₆H₃Cl₂)[3], and La@C₇₆(C₆H₃Cl₂), respectively. The structural determination has been performed by spectroscopic and finally X-ray crystallographic analysis, and these properties are discussed on the basis of the theoretical study.

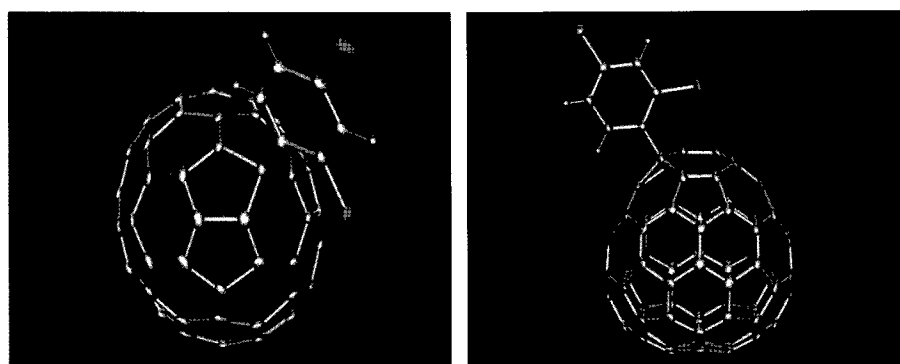


Figure 1. Structure of (a) La@C₇₂(C₆H₃Cl₂) and (b) La@C₇₄(C₆H₃Cl₂)

References:

- [1] Chai, Y.; et al. *J. Phys. Chem.* **1991**, *95*, 7564.
 [2] Wakahara, T.; Nikawa, H.; et al. *J. Am. Chem. Soc.* **2006**, *128*, 14228.
 [3] Nikawa, H.; Kikuchi, T.; et al. *J. Am. Chem. Soc.* **2005**, *127*, 9684.

Corresponding Author: Takeshi AKASAKA

E-mail: akasaka@tara.tsukuba.ac.jp

Tel&Fax: +81-29-853-6409

Internal Friction Measurement of Fullerene Films by Vibrating Reed Method

○Shinya Wakita¹, Shuichi Matsumoto¹, Takanori Yoshii¹,
Kenta Kirimoto² and Yong Sun¹

¹*Faculty of Engineering, Kyushu Institute of Technology, 1-1 Sensui, Tobata, Kitakyushu, Fukuoka 804-8550, Japan*

²*Department of Electrical and Electronic Engineering, Kitakyushu National College of Technology, 5-20-1 Suii, Kokuraminami, Kitakyushu, Fukuoka 802-0985, Japan*

Temperature dependence of the C₆₀ and C₇₀ fullerene films was measured by vibrating reed method in the temperature range from 110K to 500K. The fullerene film was deposited on Cu-alloy substrate of dimensions of 40mm×5mm×0.1mm at 473K by vacuum sublimation in a residual gas pressure below 2.0×10⁻⁶ Torr. Thickness of the fullerene films obtained was confirmed to be about 1000 nm. X-ray diffraction measurements show that no any diffraction

peak was observed. Internal friction of both the Cu-alloy substrate and the fullerene/Cu-alloy sample were measured, and then the temperature dependence of internal friction of the fullerene films was calculated. The temperature dependences of internal friction of the C₆₀ and C₇₀ films are shown in Fig.1. We see in the figure that the internal friction of C₇₀ film is larger than that of C₆₀ film. This may be related to a lower symmetrization of C₇₀ molecule. A strong internal friction peak is

observed around 280K in both fullerene films. We believe that the internal friction around 280K is due to a rotation of C₆₀ or C₇₀ molecule in their amorphous phase. In the figure a weaker peak is observed around 400K in the C₇₀ film only. This internal friction may be related to a rotation of C₇₀ molecule along its shorter axis.

References: Z.S.Li, Q.F.Fang, S.Veprek, S.Z.Li, Mater.Sci.Eng.A 370(2004) 186-190

Corresponding Author : Shinya Wakita

E-mail: g348950s@tobata.isc.kyutech.ac.jp TEL/FAX: 81-93-884-3564

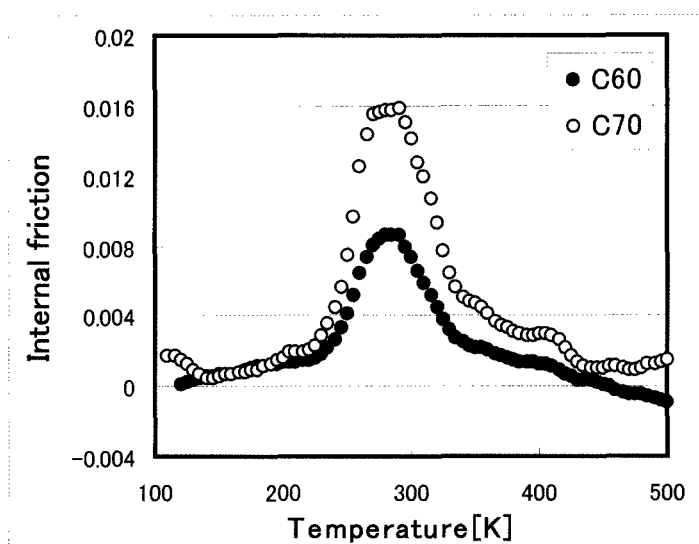


Fig.1 Temperature dependence of internal friction of C₆₀ and C₇₀ film.

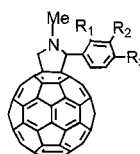
Solution-Processed Organic Thin-Film Transistors Based on Perfluoroalkyl Substituted C₆₀ Derivatives

○M. Chikamatsu, A. Itakura, Y. Yoshida, R. Azumi, K. Yase

Photonics Research Institute, National Institute of Advanced Industrial Science and Technology (AIST), Central 5, 1-1-1 Higashi, Tsukuba, Ibaraki 305-8565, Japan

We have reported that solution-processed organic thin-film transistors (TFTs) based on long-chain alkyl-substituted C₆₀ derivatives exhibit high field-effect electron mobility [1-2]. Recently, we have reported an organic TFT based on a perfluoroalkyl substituted C₆₀ derivative, C₆₀-fused *N*-methylpyrrolidine-*para*-perfluorooctyl phenyl (C60PC8F17), shows high mobility and air-stability [3]. In this study, for evaluating the effect of perfluoroalkyl-chain orientation, we fabricate and characterize TFTs based on various perfluorooctyl substituted C₆₀ derivatives. Films of C₆₀ derivatives were fabricated on highly doped silicon wafers covered with SiO₂ by spin coating from chloroform solution under ambient condition. Source and drain gold electrodes were deposited on the film. The TFT characteristics were measured in a vacuum and air at room temperature.

Table 1 shows electron mobilities of the TFTs in a vacuum and after exposure to air for 5 hours. C60MC8F17- and C60PC8F17-TFT exhibited high electron mobility in a vacuum, whereas the mobility of C60MC8F17-TFT largely decreased in air. C60OC8F17-TFT exhibited low mobility in a vacuum and no active performance in air. These results indicated that perfluoroalkyl-chain orientation of C₆₀ derivatives strongly affects the TFT performance.



C60OC8F17 (R₂=R₃=H, R₁=C₈F₁₇)

C60MC8F17 (R₁=R₃=H, R₂=C₈F₁₇)

C60PC8F17 (R₁=R₂=H, R₃=C₈F₁₇)

Table 1. Electron mobilities of the TFTs

	Mobility (cm ² /Vs)	
	Vacuum	Air (after 5h)
C60OC8F17	0.001	-
C60MC8F17	0.02	4×10 ⁻⁴
C60PC8F17	0.07	0.008

This study was partly supported by Industrial Technology Research Grant Program in 2006 from New Energy and Industrial Technology Development Organization (NEDO) of Japan.

[1] M. Chikamatsu et al., Appl. Phys. Lett. **87**, 203504 (2005).

[2] M. Chikamatsu et al., J. Photoch. Photobio. A **182**, 245 (2006).

[3] M. Chikamatsu et al., The 31th Fullerene-Nanotubes General Symposium, 1P-16 (2006).

Corresponding Author: Masayuki Chikamatsu

TEL: +81-29-861-6252, FAX: +81-29-861-6303, E-mail: m-chikamatsu@aist.go.jp

A DFT study on Fullerene Hydrides C₆₀H₂: Hole Transport Materials

○ Ken Tokunaga¹, Shigekazu Ohmori^{1,a}, Hiroshi Kawabata^{1,2}, and Kazumi Matsushige^{1,2}

¹ Venture Business Laboratory, Kyoto University, Kyoto 606-8501

² Department of Electronic Science and Engineering, Kyoto University, Kyoto 615-8510

Fullerene derivatives are paid attention as one of the tendency to improve carbon materials. We have been working on a quantum-chemical design of conductive materials and career transport materials (for example, polythiophene and polysilane), and reported that the career mobility can be predicted according to the ratio of intermolecular orbital overlap and reorganization energy λ to the injection of the career.

In the present study [1], we focus on the hydrogenation of C₆₀ and its effect on the hole transport property. Density functional theory calculations (B3LYP/6-311G(*d*)) are applied to C₆₀ and 11 isomers of C₆₀H₂ (Figure 1) with small heat of formation ΔH_f° [2], focusing our attention mainly on the reorganization energy λ to the hole injection. It is well known that small reorganization energy λ causes the effective hole transport.

Reorganization energy λ of C₆₀ to the hole injection is 94 meV, and those of C₆₀H₂ are shown in Figure 1. A of two synthesized isomers (0a and 2a [3]) is 65 meV, which is smaller than that of C₆₀. It should be noted that 2b and 3a isomers have further smaller λ (50 and 62 meV, respectively) than 0a and 2a, though they have not been synthesized. These results indicate that some isomers of C₆₀H₂ have potential utility as hole transport materials.

In order to propose the design manual of hole transport materials based on the fullerene derivatives, analysis of the reorganization using vibronic coupling density η [4,5] or nuclear Fukui function ϕ [6] is carried out. Details of the calculation and analysis will be presented in the symposium.

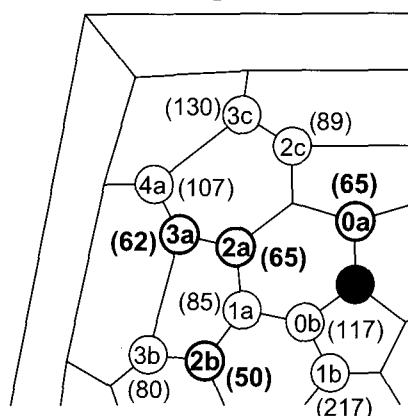


Figure 1. A part of Schlegel diagram of C₆₀ and numbering of carbon atoms. The initial hydrogen is placed at carbon atom colored black and the second hydrogen at one of 0a-4a carbons to produce 11 isomers of C₆₀H₂. Inserted values in the parenthesis are the reorganization energies λ (meV) of each isomer to the hole injection.

[1] K. Tokunaga, S. Ohmori, H. Kawabata, and K. Matsushige, *Synth. Met.*, to be submitted.

[2] N. Matsuzawa, D. A. Dixon, and T. Fukunaga, *J. Phys. Chem.* **96**, 7594 (1992).

[3] C. C. Henderson and P. A. Cahill, *Science* **259**, 1885 (1993); A. G. Avrnt, A. D. Darwish, D. K. Heimbach, H. W. Kroto, M. F. Meidine, J. P. Parsons, C. Remars, R. Roers, O. Ohashi, R. Taylor, and D. R. M. Walton, *J. Chem. Soc. Perkin Trans. 2*, 15 (1994).

[4] K. Tokunaga, T. Sato, and K. Tanaka, *J. Chem. Phys.* **124**, 154303 (2006).

[5] K. Tokunaga, T. Sato, and K. Tanaka, *J. Mol. Struct.*, in press.

[6] M. H. Cohen, M. V. Ganduglia-Pirovano, and J. Kudrnovský, *J. Chem. Phys.* **101**, 8988 (1994).

Corresponding Author: Ken Tokunaga

Tel: +81-75-753-7578, Fax: +81-75-753-7579, E-mail: tokunaga@t27w1425.mbox.media.kyoto-u.ac.jp

^a Present address: National Institute of Advanced Industrial Science and Technology (AIST), Ibaraki 305-8568

Polymerization of pressed powder and solution-grown fullerene with free electron laser irradiation

○Nobuyuki Iwata, Shingo Ando, Yasunari Iio,
Ryou Nokariya and Hiroshi Yamamoto

*College of Science & Technology, Nihon University
7-24-1 Narashinodai, Funagashi-shi Chiba, Japan 274-8501*

We have been studying the polymerization of C_{60} with free electron laser (FEL) irradiation. The FEL has the features of wavelength variability and extremely sharp pulse width, \sim several hundreds femtosecond. The purpose of this work is to synthesize an amorphous and polymerized fullerene bulk. In our previous works the optimization is carried out concerning about the irradiation wavelength, that is 450 \sim 500 nm.[1-2] However the polymerization area is limited to approximately $5\mu\text{m}$ in a diameter, the reason of which is probably the limited directions for polymerization. The directionality is expected to be reduced inserting some molecules with double bonds between C_{60} molecules and then an amorphous C_{60} polymer is also anticipated. In this presentation FEL was irradiated to C_{60} precipitates on the bottom in the saturated toluene. In addition the effect of FEL irradiation against the specimens grown by liquid-liquid interfacial precipitation (LLIP) method as well as the pressed powder will be investigated.

The C_{60} powder (99.5%) was pressed to be bulk specimen and 3rd harmonics 500 nm FEL was irradiated (fundamental energy density was $6.8 \text{ mJ/pulse} \cdot \text{cm}^2$) in vacuum after annealing at 120°C . Another approach is as follows. The C_{60} powder 0.2 g was dissolved in toluene 30 ml subsequently sonicated for 5 min and then was maintained for 3 days. FEL was irradiated for one hour to the remained C_{60} powder at the bottom of a glass bottle filled with the saturated toluene. Irradiated powder was pressed and the surface of it was evaluated by optical microscope and Raman analysis.

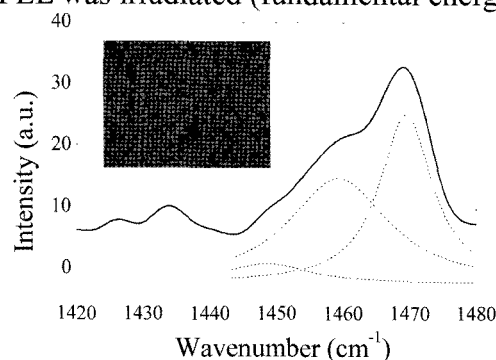


Fig.1 : Raman spectra and optical microscope image of a pressed bulk specimen



Fig.2 : Optical microscope image of the solution-grown C_{60}

In figure 1 optical microscope image and Raman spectra inside the circle, center of the image. Small shiny grain, $\sim 5\mu\text{m}\phi$, was observed and that showed the photo-polymerization demonstrated by the peak around 1460 cm^{-1} in Raman spectrum. Figure 2 shows the optical image of the specimen irradiated in the saturated toluene, the spectrum of which was similar to that of Fig.1. It is clearly seen that a lot of polymerized grains, indicated by the dotted circles, were obtained. It is expected that the solution help polymerize C_{60} molecules.

- [1] The 31st Fullerene and Nanotubes General Symposium 2P-19
- [2] The 32nd Fullerene and Nanotubes General Symposium 1P-39
- [3] Molecular Electronics and Bioelectronics 4 1P-05

Electrical Properties of Mg-doped C₆₀ Thin Films

○Nobuaki Kojima, Takashi Terayama, Hidetoshi Suzuki,
Masato Natori and Masafumi Yamaguchi

Toyota Technological Institute, 2-12-1 Hisakata, Tempaku, Nagoya 468-8511, Japan

C₆₀ solids have been known as high resistive semiconductor materials. For the practical use of this unique semiconducting carbon molecular solid, it is necessary to control conductivity by impurity doping. C₆₀ intercalation has been studied extensively with regard to the superconducting compounds. Alkali and alkali earth metals, such as Li, Na, K, Rb and Ba have been used mostly as guest metals in the previous study. The valence electron level of almost alkali and alkali earth metals lies at higher energy than LUMO-derived band of C₆₀, and the valence electrons of guest metals transfer to the C₆₀ LUMO-derived band. Thus, these compounds show the metallic behavior. For the semiconductor device application, the search for new guest materials is necessary. Mg is one of the promising materials for guest metal showing semiconductor property. R. P. Gupta *et al.* reported the energy band calculation of Mg₂C₆₀ solids, and indicated that Mg₂C₆₀ was semiconductor, since Mg 3s-derived occupied band was formed between C₆₀ HOMO-LUMO levels [1]. In this paper, we will report Mg doping into C₆₀ films by co-evaporation of C₆₀ and Mg, and their electrical properties.

C₆₀ and Mg-doped C₆₀ films were grown by using molecular beam deposition chamber. The base pressure of the chamber was 3×10^{-7} Pa. The pure (99.98%) C₆₀ powder and Mg (99.9%) was evaporated from a Knudsen cell. The beam flux of the each source was monitored by a nude ion gauge at the substrate position. The ratio of Mg/C₆₀ source was changed in the range of 0.04 to 0.7. The growth rate of C₆₀ was 2~3 nm/min, and the total film thickness was around 500 nm. The film composition of Mg:C₆₀ was confirmed by X-ray Photoelectron Spectroscopy (XPS). For the conductivity measurements, Mg-doped C₆₀ films were evaporated on the glass substrates coated with Al stripe electrodes at 0.5 mm spacing and 10 mm long. The conductivity was estimated from I-V characteristics between the adjacent bottom electrodes with variable temperature under the vacuum condition.

Temperature dependence of conductivity of Mg-doped C₆₀ films with different Mg concentrations are shown in Fig. 1. The conductivity at room temperature increases with increasing Mg concentration, and its temperature dependence consists of two or more thermally-activated processes with different activation energy.

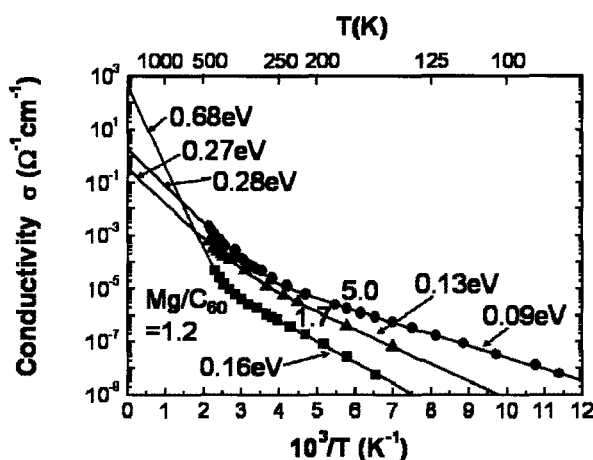


Fig. 1: Temperature dependence of conductivity of Mg-doped C₆₀ films.

[1] R. P. Gupta, M. Gupta, *Physica C*, **219**, (1994) 21-25.

Corresponding Author: Nobuaki Kojima

TEL: +81-52-809-1877, FAX: +81-52-809-1879, E-mail: nkojima@toyota-ti.ac.jp

Physical Properties of H₂ Endohedral C₆₀

Katsumi Tanigaki¹, Takeshi Rachi¹, Ryotaro Kumashiro¹, Yasujiro Murata², Koichi Komatsu²,
Toru Kakiuchi³, Hiroshi Sawa³, Yoshimitsu Kohama⁴, Satoru Izumisawa⁴, Hitoshi Kawaji⁴
and Tooru Atake⁴

¹*Department of Physics, Graduate of Science, Tohoku University*

²*Institute of Chemical Research, Kyoto University*

³*Material Structure Science, KEK*

⁴*Materials and Structures Laboratory, Tokyo Institute of Technology*

¹*6-3 Aoba, Aramaki, Aoba, Sendai 980-8578, Japan*

²*Uji, Kyoto 611-0011, Japan*

³*1-1, Oho, Tsukuba 305-0801, Japan*

⁴*259 Nagatsuta-cho, Midori-ku, Yokohama 226-8503, Japan*

Endohedral Fullerenes have been attracting much attentions in the past decade in both chemistry and physics. Although very intriguing physical properties are expected in endohedral C₆₀ family fullerenes, almost all the studies in physical properties have been focused on atom endohedral C₈₂ fullerenes. This is because the latter can macroscopically be produced. Recently hydrogen molecule endohedral C₆₀ has been synthesized in macroscopic quantity using an elegant molecular surgery method in chemical synthesis. Therefore, we have attempted to study physical properties of this new endohedral fullerene, including the detailed studies on superconductivity upon carrier doping.

The specific heat capacity measurements show two remarkable transition peaks: one is at a high temperature regime for C₆₀ disorder-order transition and the other is at a low temperature regime which is related to the rotation of the endohedral hydrogen molecule. When alkaline metals of K and Rb are doped to this system, superconductivity appears.

In this presentation, we compare the both physical properties and the structure between C₆₀ and H₂@C₆₀ on a basis of specific heat capacity measurements and structural information obtained from high resolution X ray diffraction measurements at SPring-8 and KEK.

The present work is partially supported by the 21st century COE program "Particle Matter Hierarchy" MEXT Japan, and Center for Interdisciplinary Research Project in Tohoku University. This work was performed by a Grant-in-Aid from the Ministry of Education, Science, Sports and Culture of Japan, No. 15201019, 1771088, 18204030, 18651075 and 19014001.

Corresponding Author: Katsumi Tanigaki

TEL: +81-022-795-6469, FAX: +81-022-795-6470, E-mail: Tanigaki@sspns.phys.tohoku.ac.jp

Preparation of carbon nanoparticles by biomolecules carbonization

Masato Tominaga, ○Katsuya Miyahara, Shinya Nomura, and Isao Taniguchi

Graduate School of Science and Technology, Kumamoto University,
Kumamoto 860-8555, Japan

Ferritin, an iron storage protein, is a potential candidate for protein engineering of nanomaterial synthesis. In this study, the fabrication of two-dimensional carbon nanoparticles based on ferritin molecule was prepared via heat treatment in a hydrogen gas atmosphere.

A polished silicon substrate surface was treated by H_2O_2 / NH_4OH / water (1:1:5 (v/v)). Then, the silicon substrate was modified with 3-aminopropyltrimethoxysilane (3-APMS). Ferritin was immobilized onto 3-APMS-modified silicon surface (3-APMS/Si) by immersion of substrate into a phosphate buffer solution of $0.2 \mu\text{mol dm}^{-3}$ ferritin. Tapping-mode atomic force microscope (AFM) measurements were carried out under an atmosphere.

Preparation of carbon nanoparticles on silicon substrate were performed by heat-treatment for ferritin on 3-APMS/Si at $400 \text{ }^\circ\text{C}$ for 60 min under H_2 gas. Fig. 1(a, b) show typical tapping-mode AFM images before and after heat-treatment. Before the treatment, ferritin molecules immobilized onto the silicon surface were observed as shown in Fig. 1(a). The size of each ferritin molecule was evaluated to be approximately $9(\pm 2) \text{ nm}$ in diameter. After the treatment, carbon nanoparticles derived from the carbonization of ferritin were observed as shown in Fig. 1(b), which was evaluated to be approximately 5 nm in diameter. We will discuss the detailed characterization of carbon nanoparticles.

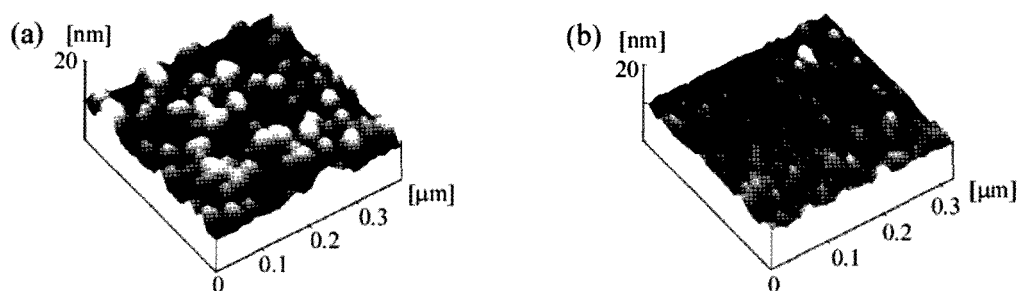


Fig. 1 Tapping-mode AFM images before (a) and after (b) heat-treatment for ferritin immobilized onto 3-APMS-modified silicon substrate at $400 \text{ }^\circ\text{C}$ for 60 min under H_2 gas atmosphere.

Corresponding Author: Masato Tominaga

E-mail: masato@gpo.kumamoto-u.ac.jp

Tel&Fax: 096-342-3656

Influence of Electronic Excitation on High-Speed Ion Irradiation to Graphene Sheet

○Yoshiyuki Miyamoto¹, Arkady Krasheninnikov², and David Tománek³

¹*Nano Electronics Research Labs, NEC, Tsukuba 305-8501, Japan*

²*Accelerator Labs, University of Helsinki, Helsinki 02015, Finland*

³*Physics and Astronomy Dept, Michigan State Univ., Michigan 48824-2320, USA*

Ion-irradiation is a useful tool for inducing structural changes on graphite, nanotube, and many carbon related materials. Despite the utility of ion-irradiation, the atomic scale mechanism of the structural change remains unknown. There was no proper computational method to simulate the atomic scale phenomena of ion-impact on condensed matters especially for high-speed ion irradiations, since the conventional Born-Oppenheimer approximation (BOA) is highly questionable in that cases.

To address validation (or invalidation) of conventional BOA in molecular dynamics (MD) simulations, we examine the cases of H projectile targeting graphene sheet and compared the results between tight-binding (TB) MD method based on the density-functional-theory (DFT) and the MD method based on the time-dependent DFT (TDDFT) [1]. Although nice agreements between these two MD simulations is obtained when kinetic energy of projectile is less than 100 eV, significant stopping power of the projectile is observed only by TDDFT-MD in high-speed region with corresponding kinetic energy beyond 1 KeV.

Even though the kinetic energy transportation from projectile to recoil atom is negligible in both MD simulations under such a high-energy region, the lost of kinetic energy of projectile is significant only in TDDFT-MD simulation. From the energy conservation rule, the stopping power can be interpreted as corrective electronic shakeup by high-speed ion. This shakeup cannot be expressed within BOA. We discuss validation of using the TDDFT-MD method by comparing numerical results obtained by conventional theory of high-speed impacts of ion to condensed matters.

This work was supported by the Next Generation Super Computing Project, Nano Science Program, MEXT Japan.

[1] O Sugino and Y. Miyamoto, Phys. Rev. B. **59**, 2579 (1999); *ibid*, Phys. Rev. B **66**, 089901(E) (2002).

Corresponding Author: Yoshiyuki Miyamoto

TEL: +81-29-850-1586, FAX: +81-29-856-6136, E-mail: y-miyamoto@ce.jo.nec.com

Laser Induced Optical Emission of Polyynes

○Tomonari Wakabayashi¹, Hiroyuki Nagayama¹, Kota Daigoku²,
Yosuke Kiyooka³, and Kenro Hashimoto³

*Department of Chemistry, School of Science and Engineering, Kinki University,
Higashi-Osaka, Osaka 577-8502, Japan¹*

*Department of Chemistry and Biological Science, College of Science and Engineering,
Aoyama Gakuin University, Sagami-hara, Kanagawa 229-8558, Japan²*

*Department of Chemistry, Graduate School of Science, Tokyo Metropolitan University,
Hachioji, Tokyo 192-0397, Japan³*

During the resonance Raman study of vibrational structures of polyyne molecules [1], we found optical emission spectra of the molecules in the visible wavelength regions. From the analysis of the vibrational structures of the emission spectra, the transition was attributed to the forbidden electronic transition. The weak transition was able to be detected after the effort of purification of the sample solution by repetitive HPLC operations. In the emission spectra, vibrational structures were clearly observed for such a relatively large molecule. With the aid of theoretical investigations on the symmetry selection rules, the spectral features were explained by vibronic transitions of characteristic vibrational modes.

In this work, optical emission spectra of polyyne molecules $C_{2n}H_2$ ($n=5-8$) were observed upon UV-laser irradiation for the dipole-allowed transition, ${}^1\Sigma_u^+ \leftarrow X^1\Sigma_g^+$, of size-separated polyyne molecules in *n*-hexane. The emission spectra of $C_{10}H_2$ show distinct peaks at 436 and 480 nm with a separation of $\sim 2100\text{ cm}^{-1}$ for the stretching vibration of the sp-carbon chain. Weak absorption features were also detected nearby UV regions in shorter wavelengths. The spectral features in the emission spectra were assigned to vibronic bands of the forbidden electronic transition, ${}^1\Delta_u \rightarrow X^1\Sigma_g^+$, within the spin-singlet manifold. The emission wavelengths of the series of polyynes increase systematically with increasing size *n*.

[1] T. Wakabayashi *et al.* *Chem. Phys. Lett.* **433**, 296 (2007).

Corresponding Author: Tomonari Wakabayashi

E-mail: wakaba@chem.kindai.ac.jp

Tel: +81-6-6730-5880 (ex.4101), **Fax:** +81-6-6723-2721

Fabrication of C₆₀ Fullerene – Ethylenediamine Nanoparticles and Their Photoelectrochemical Application

Ken-ichi Matsuoka¹, Hidetaka Seo², Tsuyoshi Akiyama^{1,3} and Sunao Yamada^{1,3}

¹*Department of Materials Physics and Chemistry, Graduate School of Engineering, Kyushu University, 744 Moto-oka, Nishi-ku, Fukuoka 819-0395, Japan*

²*Department of Materials Sciences and Engineering, School of Engineering, Kyushu University, 744 Moto-oka, Nishi-ku, Fukuoka 819-0395, Japan*

³*Department of Applied Chemistry, Graduate school of Engineering, Kyushu University, 744 Moto-oka, Nishi-ku, Fukuoka 819-0395, Japan*

Fullerene has been one of promising nanocarbon materials for use in high-performance (photo)electronic devices. Especially, C₆₀ clusters have been attracting much attention, because assemblies of C₆₀ exhibit high mobility of electrons. Thus, application of the C₆₀ clusters to photoelectric conversion devices is quite interesting. On the other hand, early studies reported that the addition reaction between C₆₀ and some aliphatic diamines generated cluster-like precipitates. In this research, we have clarified that the reaction of C₆₀ with a large excess of ethylenediamine (EDA) afforded nanospheres consisting of C₆₀ and EDA and have found that the resultant nanospheres substantially enhanced the photocurrent signal from a polythiophene film.¹⁾

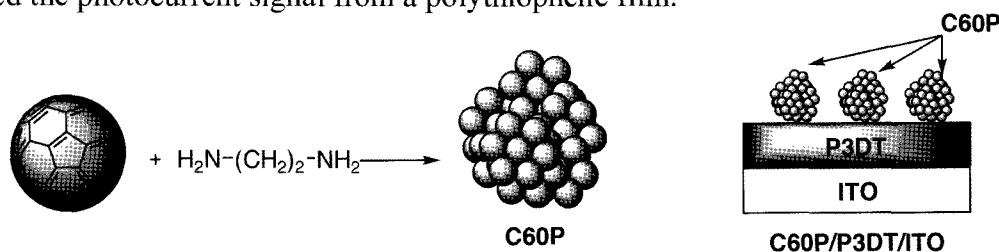


Figure 1. Preparation abstract of C60P and the structures of C60P/P3DT/ITO

Figure 1 shows the abstract of the preparation of fullerene – EDA particle (C60P) and the structure of C60P modified polythiophene film. C60Ps were prepared by mixing of C₆₀ toluene solution and EDA. C60Ps were collected by filtration and dried in vacuo. The result of scanning electron microscope image of C60Ps indicated that the almost C60Ps were roughly spherical with the diameter about 300 nm. C₆₀ layer was superimposed on the poly-3-dodecylthiophene (P3DT) film modified indium-tin-oxide electrode (P3DT/ITO) to give C60P modified composite film C60P/P3DT/ITO. In the presence of sacrificial reagent, C60P/P3DT/ITO was generated the stable photocurrent. The photocurrent from C60P/P3DT/ITO was roughly three-times enhanced as compared with that of reference P3DT/ITO electrode. Experimental details and further discussion will be addressed in the presentation.

Reference

1) K-i. Matsuoka, H. Seo, T. Akiyama and S. Yamada, *Chem. Lett.*, *accepted*.

Corresponding Author: Tsuyoshi Akiyama

E-mail: t-akitem@mbox.nc.kyushu-u.ac.jp

Tel: +81-92-802-2816, FAX: +81-802-2815

Formation of Polyhedral Graphite Particles by High-density Carbon Arc Discharge

○Yoji Katagiri, Akira Koshio, Junpei Mabuchi, and Fumio Kokai

Division of Chemistry for Materials, Graduate School of Engineering, Mie University, 1577 Kurimamachiya-cho, Tsu, Mie 514-8507, Japan

It is known that polyhedral graphite (PG) particles having a structure composed of many polyhedra with 100-500 nm diameters are formed by the laser vaporization of graphite in a high-pressure Ar atmosphere [1]. These PG particles can be used as a lubricant because of their unique structures and properties, such as chemical and mechanical stability during high-pressure compression [2]. We have reported that PG particles can be formed efficiently by using cellulose char as an additional carbon source in the arc discharge (high-density carbon arc discharge) [3]. In this study, we investigated the formation condition of PG particles in more detail and the influence of the carbon density on the PG particle formation in arc plasma.

The PG particles were produced by conventional carbon arc discharge with a cellulose char pellet introduced into the arc plasma in an Ar atmosphere. The cellulose pellet was charred at 350°C for 60 min before arc vaporization. A graphite anode and the cellulose char pellet were simultaneously vaporized in DC arc plasma.

Figure 1 shows a TEM image of some typical PG particles formed by high-density carbon arc discharge. They have facets and highly graphitized concentric structures that are the same as those formed by laser vaporization. The interlayer spacing was approximately 0.34 nm. Figure 2 shows the size distribution of the formed PG particles. The diameters of the particles ranged from 100 to 560 nm and the average diameter was 290 nm. These results are similar to those for laser vaporization. It is usually necessary to have a high-pressure of 0.8 MPa to form PG particles by laser vaporization. However, PG particles can be formed efficiently at a low-pressure of 0.1 MPa by using our arc technique. We assume that the additional carbon source from the cellulose char pellet lead to the high density carbon species equivalent to that of laser vaporization in high-pressure Ar.

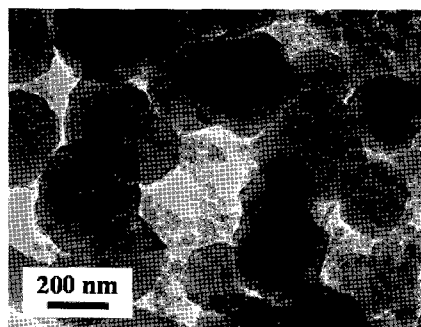


Fig. 1 TEM image of PG particles produced by high-density carbon arc discharge in Ar.

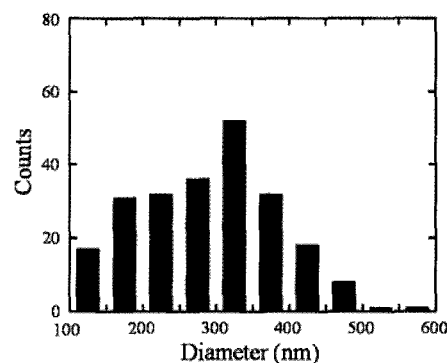


Fig. 2 Size distribution of PG particles produced by high-density carbon arc discharge in Ar.

- References:** [1] F. Kokai *et al.*, *Appl. Phys. A*, **77**, 69 (2003).
 [2] A. Nakayama *et al.*, *Appl. Phys. Lett.* **84**, 5112, (2004).
 [3] A. Koshio *et al.*, *The 31st Fullerene-Nanotubes General Symposium*, 2P-21.

Corresponding Author: Akira Koshio

E-mail: koshio@chem.mie-u.ac.jp, **Tel & Fax:** +81-59-231-5370

Energetics of Nanographite: Edge Geometries and Electronic Structure

○Susumu Okada

*Institute of Physics and Center for Computational Sciences, University of Tsukuba,
Tennodai, Tsukuba 305-8577, Japan
CREST, JST, 4-1-8 Honcho, Kawaguchi, Saitama 332-0012, Japan*

Monolayer graphite sheets with nano-meter scale (nanographite) are fascinating as a new comer for constituent units of the nano-scale electronic devices due to their interesting electronic and geometric properties. For the theoretical studies, graphite ribbons with finite width are usually considered to mimic the nanographite which intrinsically possess edges and nanometer width. There have been a much theoretical works to study the electronic properties of graphite ribbons. Because an interesting class of localized states called edge state has been found in the ribbons with zigzag edges. The edge state is localized at but extended along an edge of the graphite ribbon resulting in the partially filled flat dispersion band in a part of Brillouin zone. Despite a lot of calculations on the electronic properties, the energetics for formation of the nanographites is not addressed yet. Thus, in the present work, we study the energetics of graphite ribbons by using the first-principles total-energy calculations in the framework of the density functional theory. Figures 1(a) and (b) show the edge formation energy of the graphite ribbons with the edges of zigzag and armchair arrangements, respectively. The edge formation energy for the zigzag edge is 0.3 eV/atom. On the other hand, for the armchair edge, the energy is 0.1 eV/atom. Thus the armchair edge is much preferable to the nanographite flakes. However, since the formation energy for the zigzag edge strongly depends on the width of the ribbon, the zigzag edge also emerges around the apex of the flakes and the boundary of the nanographite is formed by the mixture of the armchair and zigzag elements. For the armchair edges, the periodic oscillation of the formation energy is ascribed to the electronic structure of the ribbons.

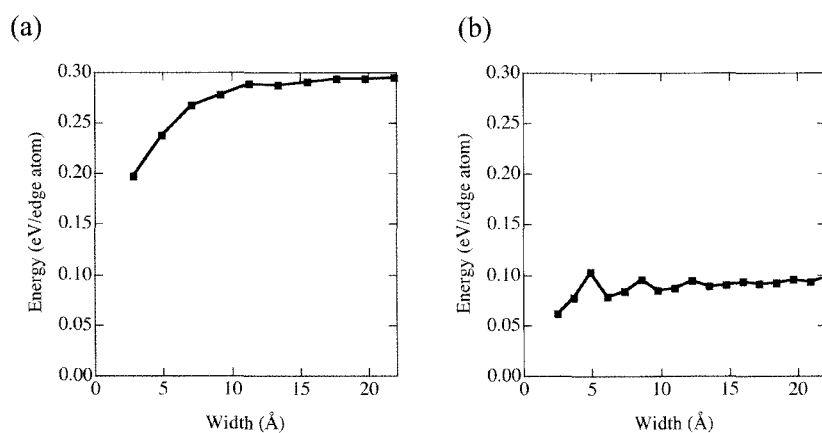


Fig. 1: The edge formation energies of (a) the zigzag and (b) the armchair ribbons as a function of their width.

Corresponding Author: Susumu Okada
E-mail: sokada@comas.frsc.tsukuba.ac.jp
Tel&Fax: 029-853-5921/029-853-5924

Energetics of C₆₀ Encapsulated in Carbon Nanotubes

○Susumu Okada

*Institute of Physics and Center for Computational Sciences, University of Tsukuba,
Tennodai, Tsukuba 305-8577, Japan
CREST, JST, 4-1-8 Honcho, Kawaguchi, Saitama 332-0012, Japan*

Carbon nanotubes are fascinating as host materials to induce various kinds of complexes by containing atoms or molecules inside or outside. In particular, encapsulation of fullerenes into the inner space of nanotubes results in unusual nanometer-scale carbon networks "carbon peapods" of which structures are characterized by an interesting combination of one- and zero-dimensional constituent units. The peapods are thus regarded as new hierarchical solids with mixed dimensionality. Our previous works show that energetics of carbon peapods strongly depend on the space between walls of the fullerenes and the nanotube. However, energetics of encapsulated C₆₀ and the thick nanotubes are still unclear. We here report total-energy calculations performed for peapods consisting of C₆₀ and thick armchair nanotubes of which diameters are thicker than that of the (10,10) to elucidate the stable C₆₀ positions inside the nanotubes and a possibility of the deformation of nanotubes. Figures 1 (a) and (b) show the encapsulation energies (ΔE) of C₆₀ in the cylindrical and deformed (12,12) nanotubes for the various radial positions. The stability is evaluated by calculating the energy difference in the reaction: (12,12) tube + C₆₀ \rightarrow C₆₀@(12,12)- ΔE . The C₆₀ is found to be dislodged from the center of the nanotube to retain the inter-wall distance of 3.3 Å. Furthermore, the encapsulation energy ΔE for the deformed nanotube is deeper than that for the nanotube with cylindrical shape. The encapsulation energies for deformed nanotubes are about 1 eV which is insensitive to the tube thickness [Fig. 1(c)]. The results indicate that the C₆₀ are more tightly bound in the deformed nanotubes than in the cylindrical nanotubes. Further, the competition between the lattice distortion energy and the encapsulation energy may induce the deformation of the thick nanotubes by inserting the fullerenes. Indeed, such deformation has been observed in a TEM experiment recently reported [1].

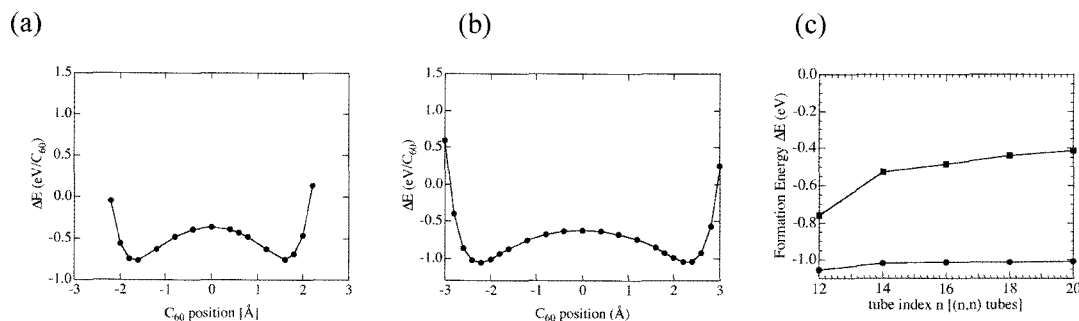


Fig. 1: Encapsulation energies of C₆₀@(12,12) per unit cell for the various radial positions for (a) cylindrical and (b) deformed nanotubes. (c) Encapsulation energies for (n,n) nanotubes with cylindrical and deformed nanotubes. Circles and squares denote the energies for deformed and cylindrical nanotube, respectively.

[1] J. Fan, M. Yudasaka, R. Yuge, D.N. Futaba, K. Hata, S. Iijima, *CARBON*, **45**, 722 (2007).

Corresponding Author: Susumu Okada

E-mail: sokada@comas.frsc.tsukuba.ac.jp

Tel&Fax: 029-853-5921/029-853-5924

Effective Formation of Carbon Nanotubes Filled Perfectly with Copper Nanowire

○Naoki Mizuno, Akira Koshio, Hironobu Kito, and Fumio Kokai

*Division of Chemistry for Materials, Graduate School of Engineering, Mie University,
1577 Kurimamachiya-cho, Tsu, Mie 514-8507, Japan*

Copper nanowires have been extensively studied as a material for next generation electronic nanodevices. However, some problems related to quality, such as stability, crystallinity, and long one-dimensional growth, still remain. The hybridization of copper nanowire and carbon nanotubes has been tried as one of the ideas for improving the quality of copper nanowires. Arc discharge is believed to be one of the better methods for formation of copper nanowire-filled multi-wall carbon nanotubes (Cu-MWNTs). Dai et al. reported that Cu-MWNTs were produced by arc discharge in hydrogen [1], but, that very short copper nanowires were intermittently filled in the MWNTs and that there was not enough yield. Wang et al. reported on the effective production of Cu-MWNTs using coal as a carbon source [2]. Their experiments indicated that more than 40-50% of the as-prepared carbon nanotubes were filled with copper nanowires. We recently found that perfectly filled Cu-MWNTs can be produced at approximately 90% of the filling rate by using the hydrogen arc discharge method.

Cu-MWNTs were produced by the conventional DC arc discharge. A hole (3 mm diameter) was drilled in the center of a graphite anode (5 mm diameter) and filled with copper powder. A 20 mm in diameter graphite rod was used for the cathode. The two electrodes were set vertically in a vacuum chamber. Hydrogen gas was filled up the chamber at a pressure of 0.1 MPa and was flowed at 500 ml/min during arc vaporization. Arc discharge was maintained at 90 A for 1 min.

Cu-MWNTs were included in soot that was deposited in large quantities on the inner wall of the chamber (Fig. 1). Figure 2a shows that the obtained Cu-MWNTs had 10-45 nm diameters and the filling rate of the MWNTs was extremely high. Many TEM observations clarified that approximately 90% of the as-prepared MWNTs were filled perfectly with copper nanowires. The Cu-MWNTs consists of less than 10-nanotube layers and fcc copper crystals inside the MWNT in a long-range order (Fig. 2b). The distance between the lattice fringes of the filled copper crystals was measured at about 0.21 nm, which is identical to the d-spacing of the (111) atomic plane of copper.

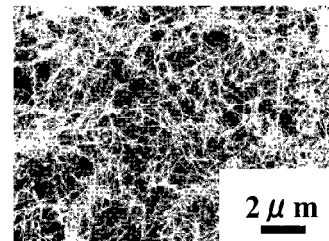


Fig. 1 SEM image of Cu-MWNTs

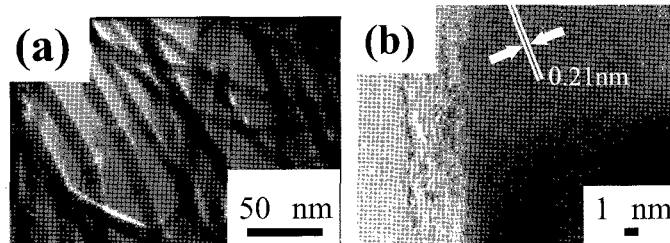


Fig. 2(a) TEM image of Cu-MWNTs (b) High-resolution TEM of Cu-MWNTs

References: [1] Dai et al., *Chem. Phys. Lett.*, **258**, 547(1996).

[2] Wang et al., *Carbon*, **44**, 1845(2006).

Corresponding Author: Akira Koshio

E-mail: koshio@chem.mie-u.ac.jp

Tel & Fax: +81-59-231-5370

Synthesis, characterization and electrical transport properties of fullerenes and heterofullerene peapods

○Y.F. Li¹, T. Kaneko¹, S. Nishigaki¹, R. Hatakeyama¹, K. Omote², and Y. Kasama²

¹*Department of Electronic Engineering, Tohoku University, Sendai 980-8579, Japan*

²*Ideal Star Inc., Minami-Yoshinari 6-6-3, Aoba-ku, Sendai 989-3204, Japan*

Following the discovery of fullerenes and carbon nanotubes, carbon peapods, i.e., single-walled carbon nanotubes (SWNTs) encapsulating fullerenes, have recently attracted great interest as potential building blocks for nanoelectronics. The presence of fullerenes inside SWNTs is expected to significantly modify the band structure of SWNTs and consequently affect their electrical transport properties. It has been reported experimentally that fullerene peapods can exhibit different transport characteristics, such as *p*-type, ambipolar and metallic [1, 2]. More recently, it has been found that transport properties of metallic C₆₀ peapods are dominated by quantum effects at temperatures below 30 K [3]. However, little is known about detailed mechanisms of electronic interaction between SWNTs and fullerenes, and it still remains an open question as to what extent the encapsulated fullerene molecules can affect the transport properties of SWNTs.

In this study, synthesis of three kinds of fullerene (C₆₀, C₇₀, and C₈₄) and one kind of heterofullerene (C₅₉N) peapods is performed, and their transport properties are investigated by fabricating them as the channels of field-effect transistors (FETs). Our measurements indicate that threshold voltages of *p*-type SWNTs are extremely enhanced due to C₆₀ and C₇₀ fullerene encapsulation, demonstrating a strong charge-transfer effect. While ambipolar semiconducting behavior is observed only on the FET devices, in which SWNTs encapsulate higher fullerene C₈₄. More importantly, we find that *n*-type semiconducting SWNTs can be formed by C₅₉N fullerene encapsulation. At low temperatures, it is found that the transport characteristics of all peapod devices are completely dominated with regular Coulomb oscillation peaks, suggesting quantum dots are created in SWNTs after various fullerenes encapsulation.

[1] T. Shimada *et al.* *Physica E* **21**, 1089 (2004).

[2] T. Shimada *et al.* *Appl. Phys. Lett.* **81**, 4067 (2002).

[3] P. Utko *et al.* *Appl. Phys. Lett.* **89**, 233118 (2006).

Corresponding author: Yongfeng Li, E-mail: yfli@plasma.ecei.tohoku.ac.jp

TEL/FAX: 81-022-795-7046/263-9225

^1H NMR Study of CH_4 confined inside Single-Wall Carbon Nanotubes

Tomoyuki Hirotsu¹, Kazuyuki Matsuda¹, Takayuki Ganko¹, Hiroaki Kadowaki¹,
Yutaka Maniwa^{1,3}, and Hiromichi Kataura²

¹ Faculty of Science, Tokyo Metropolitan University, 1-1 Minami-osawa, Hachioji,
Tokyo 192-0397, Japan

² Nanotechnology Research Institute, National Institute of Advanced Industrial Science and
Technology (AIST), Central 4, Higashi 1-1-1, Tsukuba, 305-8562, Japan

³CREST, Japan Science and Technology Corporation

Single-walled carbon nanotubes (SWNTs) assemble themselves into a two-dimensional triangular lattice to form bundles of aligned nanotubes. Thus, the inside of the nanotubes and the interstitial channels in the bundle provide well characterized nanometer-sized cavities in which various kinds of molecules are adsorbed. We have revealed that methane molecules are adsorbed inside SWNTs and the adsorption properties can be described by a two-dimensional (2D) gas model. In this model, methane molecules are confined on the potential minimum surface inside SWNT. Hence, it is interesting to investigate structure and phase behavior of methane adsorbed inside SWNTs. Our X-ray diffraction experiments have confirmed no phase transition in methane inside SWNTs down to 100 K. In order to study the dynamics of methane molecules at low temperatures (T), we have performed ^1H NMR measurements in a

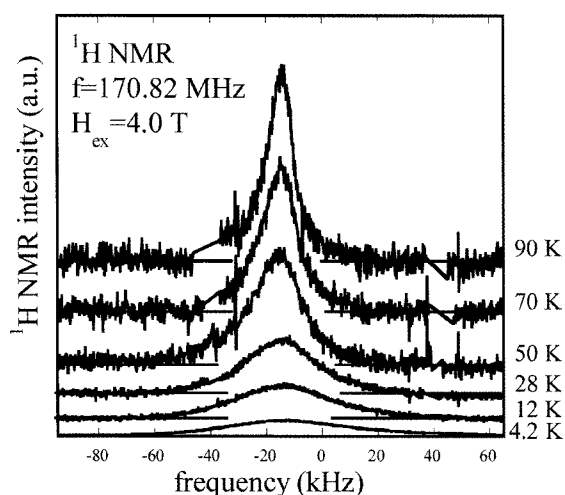


Fig.1 T -dependence of ^1H NMR spectra for CH_4 confined inside SWNTs.

T -range from 4.2 to 100 K. Fig.1 shows the T -dependence of ^1H NMR spectra for methane confined inside SWNTs with an average diameters of 13.5 Å. At high- T , a motionally-narrowed NMR signal is observed, indicating the large amplitude molecular motion of methane on the NMR time scale $\sim 10^{-6}$ s. Below ~ 50 K, the ^1H NMR signal decreases significantly in intensity with decreasing T . This suggests a liquid-to-solid-like phase change of methane inside SWNTs.

Corresponding Author: Kazuyuki Matsuda

TEL: +81-426-77-2498, FAX: +81-426-77-2483, E-mail: matsuda@phys.metro-u.ac.jp

Synthesis of metal-filled carbon nanotubes on anodic aluminum oxide substrate by microwave plasma-enhanced chemical vapor deposition

○Y. Matsuoka¹, T. Naitou¹, Y. Hayashi¹, T. Fujita², M. Tanemura¹, T. Soga¹

¹*Nagoya Institute of Technology, Gokiso, Showa, Nagoya, 466-8555, Japan*

²*Tohoku University, Aoba-ku, Sendai, Miyagi 980-8577, Japan*

A new type of cobalt-based metal-filled carbon nanotubes (MF-CNTs) was fabricated on Co-filled anodic aluminum oxide (AAO) substrate by microwave plasma-enhanced chemical vapor deposition (MPECVD) with the technique of bias enhanced growth method.

In our previous study, we have successfully synthesized the MF-CNTs on pre-deposited catalyst metal (Pd, Co, Ni, etc) on SiO₂/Si substrate. However, obstacles still remain for device realization, such as controlling quality of diameter and density of MF-CNT. Also, we have observed the aggregation of nanoparticles by plasma irradiation during growth of MF-CNTs.

In this study, we have introduced AAO substrate to control density and highly-uniformed diameter of MF-CNT. AAO substrates are ideal templates for the synthesis of highly-ordered MF-CNTs since they are thermally and chemically stable and the pore size can be fully controlled.

We synthesized the MF-CNTs on pre-deposited Co catalyst metal on AAO substrate by MPECVD using a 2.45GHz, 600W microwave power supply. During deposition the H₂ gas was adjusted to achieve various CH₄ concentrations at a total pressure of 20 Torr.

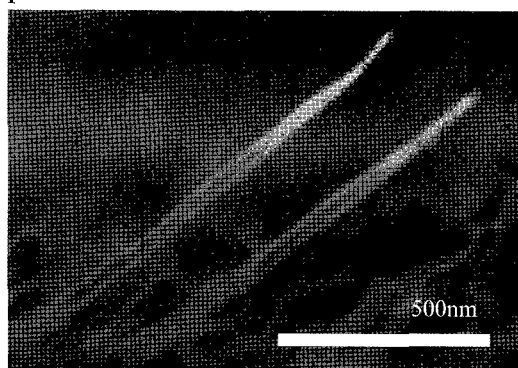


Figure 1 shows the SEM image the MF-CNTs grown on AAO substrate. The resultant MF-CNT arrays exhibit high density and uniformity, with the diameter and length determined, respectively, by the pore diameter and depth of the AAO layer.

Fig. 1. SEM images of MF-CNTs on AAO substrate.

Corresponding Author: Yohei Matsuoka, E-mail: teastalkstar@hotmail.com, Tel&Fax: 052-735-5104

Growth mechanism of vertically aligned SWNTs by in-situ absorption measurements

○Kazuaki Ogura, Masayuki Kadowaki, Jun Okawa, Erik Einarsson, Shigeo Maruyama,

Department of Mechanical Engineering, The University of Tokyo, Tokyo 113-8656, Japan

We have studied the effect of CVD conditions on the thickness of vertically aligned single-walled carbon nanotube (VA-SWNT) films [1]. Real-time observation of the growth process by an in-situ absorbance measurement [2] yielded a growth curve, which was fit to a function with the exponential decay of the growth rate: $L = \gamma_0 \tau (1 - \exp(-t/\tau))$. Here, L is the overall film thickness, and γ_0 , τ are the initial growth rate and catalyst decay time scale, respectively [3]. The final thickness shown in Fig. 1 strongly depends on ethanol pressure and CVD temperature. The initial growth rate and catalyst decay time scale obtained from the growth function are plotted in Fig. 2. The initial growth rate is proportional to pressure up to about 2 kPa, but independent of temperature. This result indicates the mechanism by which SWNT synthesis occurs is essentially a first-order chemical reaction between the ethanol and the catalyst, however there is no clear influence on catalyst decay time. Additionally, characterization by resonance Raman spectroscopy and UV-Vis-NIR absorption spectroscopy suggests the average SWNT diameter becomes smaller when synthesized at pressures above the optimum condition. Overall, this study shows how details of the underlying growth mechanism can be obtained by a systematic investigation of the growth profiles of VA-SWNTs synthesized under various conditions in a well-controlled environment.

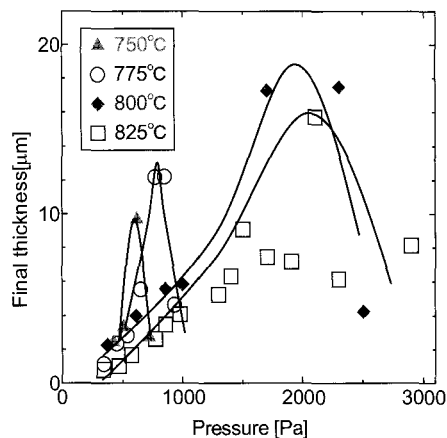


Fig.1 Estimated thickness of VA-SWNT after 10min

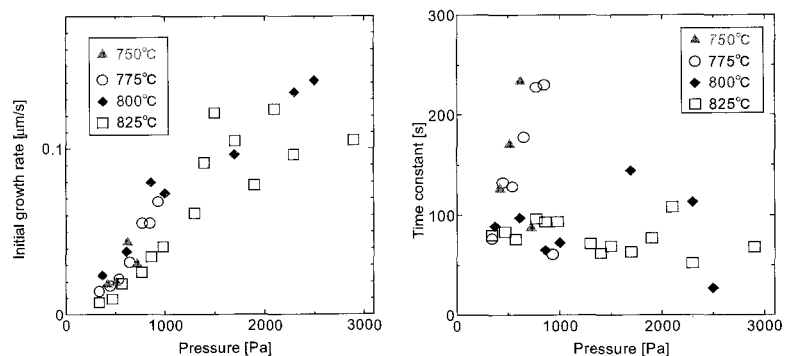


Fig.2 Pressure and temperature dependence of initial growth rate and catalyst decay time scale.

[1] Y. Murakami, S. Chiashi, Y. Miyauchi, M. Hu, M. Ogura, T. Okubo, S. Maruyama, *Chem. Phys. Lett.* **385**, 298 (2004).

[2] S. Maruyama, E. Einarsson, Y. Murakami, T. Edamura, *Chem. Phys. Lett.* **403**, 320 (2005).

[3] E. Einarsson, Y. Murakami, M. Kadowaki, S. Maruyama, *submitted to Carbon* (2007).

Corresponding Author: Shigeo Maruyama

TEL: +81-3-5841-6421, FAX: +81-3-5800-6983, E-mail: maruyama@photon.t.u-tokyo.ac.jp

Growth of ultra long carbon nanotube and carbon nanotube coating

Kazuyuki Kakihata¹, Yusaku Hirono¹, Toshinori Horie¹, Yoku Inoue¹,
Akihiro Ishida¹ and Hidenori Mimura²

¹Dept of Electrical and Electronic Eng., Shizuoka University, Hamamatsu 431-8561 Japan

²Research Institute of Electronics, Shizuoka University, Hamamatsu 431-8561 Japan

Carbon nanotubes (CNTs) are nano-carbon materials with many excellent features, such as strong mechanical strength, high electric conduction characteristics and high heat conduction characteristics. From this point of view, not only the fundamental properties but also industrial applications of CNTs are widely investigated. To achieve the industrial use of CNTs, ultra-long, and high speed growth for high mass production are very important issue.

In this study, we present ultra-long and high-speed growth of multi-walled CNT. Growth method is very simple catalyst-assisted thermal chemical deposition. CNT was grown at 700~800 °C with acetylene as a source gas on a quartz substrate. Scanning electron microscopy (SEM) image of 2mm long CNT is shown in Fig.1. Here, it should be noted that this sample was grown in an hour. Therefore, the 1-hour growth rate corresponds to 2 mm/h. This value is high among the reported results [1,2]. Furthermore, CNTs are highly dense and vertically aligned on the substrate.

On the other hand, this CNT growth method has the feature to obtain the CNTs growth also on the back of the substrate. We obtained the idea of the coating technology with CNT. We performed the CNT coating with quartz wool shown in Fig.2. After the CNT growth, all of the quartz fibers several microns in diameter are completely coated with CNTs. The coating morphology is almost uniform from surface to deep inside of the ball of quartz wool. These results suggest that the CNT coating is capable on the rough, indented and complicated surfaces. We believe that this technology will opens a new CNT application field.

[1] K. Hata *et al.*, Science **306**, 1362 (2004).

[2] L.X. Zheng *et al.*, Nature Mat. **3**, 673 (2004).

Corresponding Author: Yoku Inoue

TEL: +81-53-478-1356, FAX: +81-53-478-1356

E-mail: tyinoue@ipc.shizuoka.ac.jp



Fig.1. SEM image of 2 mm long vertically aligned CNTs on quartz substrate.

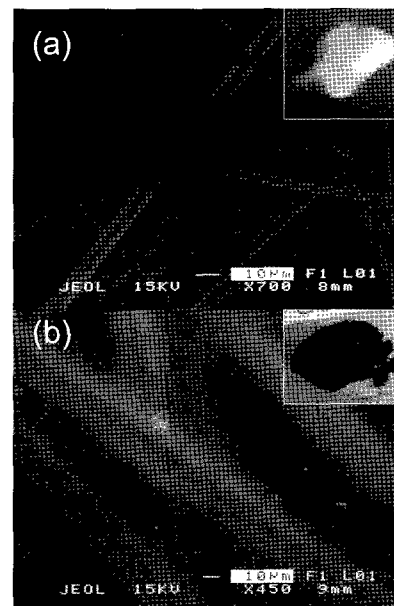


Fig.2. CNT coating of quartz wool. (a)SEM image of bare quartz fibers and (b) CNT coating result. Insets show whole pictures.

Ultrasonication Effects on Debundling and Cutting of Single-Walled Carbon Nanotubes Dispersed in Aqueous Solution

○Isamu Tajima, Catalin Romeo Luclescu, Yoshie Suzuki, Katsumi Uchida,
Tadahiro Ishii, and Hirofumi Yajima

*Department of Applied Chemistry, Faculty of Science, Tokyo University of Science
12-1 Funagawara-machi, Shinjyuku-ku, Tokyo 162-0826, Japan*

The process of debundling of single-walled carbon nanotubes (SWNTs) is based on powerful cavitation effect and subsequent replacement of nanotube-nanotube agglomeration due to powerful van der Waals forces by surfactant micelles or polymer wrapping. The colloidal aqueous dispersions of strongly hydrophobic SWNTs are usually achieved by powerful ultrasonication. At present, two types of ultrasonicators are commercially available: horn (or tip) and cup-horn ultrasonicators. As for horn ultrasonicator, a tip is inserted directly to a vessel, and the ultrasonication power is transferred to samples at a converging local area. A cup-horn ultrasonication gives rather the small input power to the samples because the input power is transferred through a water bath with a relatively homogeneous sound intensity in the sample volume. In this study, we investigated the effect of ultrasonication on the physicochemical properties of SWNTs in aqueous sodium dodecyl sulfate (SDS) solutions by using two commercial ultrasonicators, that is, cup-horn type ultrasonicator (Nanoruptor, TOSHO DENKI Co. Ltd., 350 W, 20 kHz) working in on-off cycles (60 seconds on and 30 seconds off) and horn type ultrasonicator (US-300T, Nippon Seiki Co. Ltd., 20 W, 19.5 kHz). The cup-horn ultrasonication was applied to sealed sample vials inserted in the temperature controlled water bath (4 °C) whereas the horn ultrasonication was directly applied to the vessel in ice bath (0 °C). The samples' pH values were monitored during ultrasonication. The characteristics of ultrasonicated samples were investigated by absorption and Raman spectroscopies and dynamic light scattering (DLS). The pH of the nanotubes dispersed solutions decreased strongly with the ultrasonication time following an exponential law. This is inferred to be ascribed to be the generation of HNO₃ and HNO₂ through a couple of reactions induced by powerful cavitation. In order to avoid pH effects, all measurements were conducted after adjusting samples' pH to ca.7 with a mixed buffer solution of standard potassium phosphate monobasic buffer solution and sodium phosphate dibasic buffer solution at 4:1 ratios. DLS and Raman spectroscopic measurements revealed that the debundling and the cutting of SWNTs occurred with the increase of the sonication time. The cup-horn sonication did not give so large damages to SWNTs in spite of the long time sonication. The characteristic differences between the horn type and cup-horn type ultrasonications will be discussed.

Corresponding Author: Hirofumi Yajima

TEL: +81-3-3260-4272(ext.5760), FAX: +81-3-5261-4631, E-mail: yajima@rs.kagu.tus.ac.jp

Gold-filled apoferritin catalyst for aligned single-walled carbon nanotube growth on sapphire substrates

○ Akira Yamazaki^{1,2}, Daisuke Takagi^{3,4}, Yasuyuki Otsuka², Satoru Suzuki^{1,4}, Yoshikazu Homma^{3,4}, Hideyuki Yoshimura², and Yoshihiro Kobayashi^{1,4}

¹NTT Basic Research Laboratories, NTT Corporation, Japan

²Department of Physics, Meiji University, Japan

³Department of Physics, Tokyo university of Science, Japan

⁴JST/CREST, Japan Science and Technology Corporation

It has been reported that single-walled carbon nanotubes (SWNTs) grow in a specific direction on sapphire substrate. [1, 2] It has recently been found that Au nanoparticles act as catalyst for SWNT growth by CVD. [3] Au is an ideal element for SEM observation of nanoparticles because it has higher secondary electron yield than Fe and Co, which are usually employed as catalysts for CVD growth of SWNTs. Hence, it is expected that SWNTs and Au catalyst particles can be observed simultaneously by SEM, which would give direct evidence to determine the growth mode, such as tip- or root-growth, which is a key issue in clarifying the alignment mechanism. In this report, we show that SWNTs can be aligned on sapphire substrate using Au nanoparticles provided by Au-ferritin and discuss the alignment mechanism based on the observed SEM images.

Figure 1 shows an SEM image of SWNTs grown on an R-face sapphire substrate by CVD using Au-ferritin as the catalyst. Black dots observed in Fig.1 correspond to Au nanoparticles, which were derived from Au-ferritin and tend to condense around protrusions fabricated by photolithography. In addition to Au nanoparticles, grown SWNTs are also clearly visible as relatively dark lines. SWNTs tend to align to a specific direction on the ordered area of the substrate, while the growth in random directions is also observed for some disordered areas, as has already been reported. [4] Au catalyst nanoparticles are regularly detected around the end of the aligned SWNTs, as shown in the inset of Fig.1. Considering that the initial points of SWNT growth locate around the protrusions, this result directly indicates that aligned growth of SWNTs on the sapphire substrates proceeds by the tip-growth mechanism, and strongly suggesting that the catalyst particles should “feel” the atomic arrangements on sapphire substrates and that the catalyst-surface interaction plays an important role in the aligned growth.

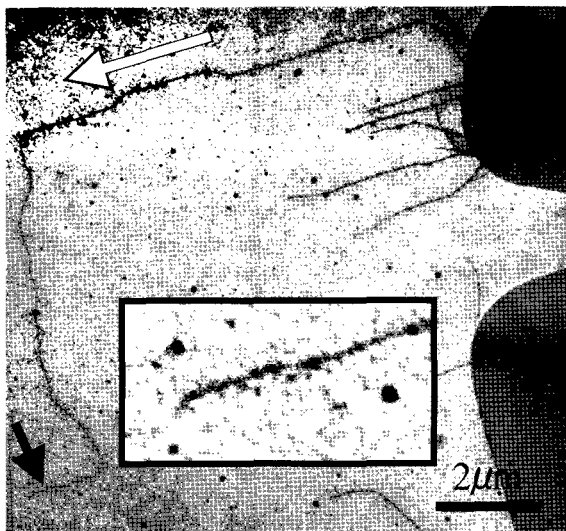


Fig. 1 SEM image of aligned SWNTs growth around protrusions fabricated on R-face sapphire substrate. Inset: magnification of the area indicated by the black arrow. White arrow represents $(1, \bar{1}, 0, \bar{1})$ direction.

Acknowledgement: This work was partly supported by a JSPS Grant-in-Aid for Scientific Research (B).

References: [1] S. Han *et al.*, *JACS* **127** (2005) 5294. [2] H. Ago *et al.*, *CPL* **408** (2005) 433. [3] D. Takagi *et al.*, *Nano Lett.* **6** (2006) 2642. [4] A. Yamazaki *et al.*, the 31st F-NT General Symposium 1P-22 (2006).

Corresponding Author: Akira Yamazaki

E-mail: a.yama@will.brl.ntt.co.jp Tel. & Fax.: +81-46-240-4070/4718

Growth of branched carbon nanotubes by alcohol chemical vapor deposition (3) – Difference in CNTs growth by Co/Mo molar ratio –

○M. Maekawa, Y. Suda, A. Okita, H. Sugawara, Y. Sakai

Division of Electronics for Informatics, Graduate School of Information Science and Technology, Hokkaido University, North 14, West 9, Sapporo 060-0814, Japan

Y-junction carbon nanotubes (Y-CNTs) are interesting for their potential use in three-terminal nanoscale devices such as a transistor [1], because of their branching structures and diameter difference between branch and stem. Thiophene (C_4H_4S) is known as an effective promoter for Y-junction structures. Recently, the growth technique of single-walled Y-CNTs without thiophene was also reported [2]. In that report, forming molybdenum carbide (Mo_2C) is a key factor to synthesize branching structure. However the reports on the growth mechanism of Y-CNTs are only a few, and it is necessary to understand the growth mechanism and develop new growth techniques of Y-junction CNTs.

We have studied variation of CNTs growth from binary catalysts, Co and Mo by alcohol chemical vapor deposition. We found the changes in CNTs number density and G/D ratio of Raman spectra by Co/Mo molar ratio. Especially, we focus on the attachment of growing nanotubes to catalyst particles on substrate, from which we expect to induce Y-junction structures. The CNTs grown were analyzed with scanning electron microscopy (SEM) and Raman spectroscopy.

We prepared Co/Mo catalysts on SiO_2 substrates using a procedure of dip coating [3]. The substrates were placed inside the quartz tubular reactor. The reactor was vacuumed by a rotary pump and heated up to $750^\circ C$ in a vacuum atmosphere. Subsequently, H_2 gas fed into the reactor as reduction for 20 minutes. After H_2 supply was stopped, ethanol vapor was introduced for 60 minutes.

SEM images of the CNTs grown from Co/Mo catalysts with a molar ratio of (a) 1.4, (b) 0.5, (c) 0.2 are shown in Fig. 1. This shows a tendency; the number density of CNTs decreased when Mo composition ratio increased, Moreover, the higher Mo composition ratio, the more catalyst particles attached on CNT surface.

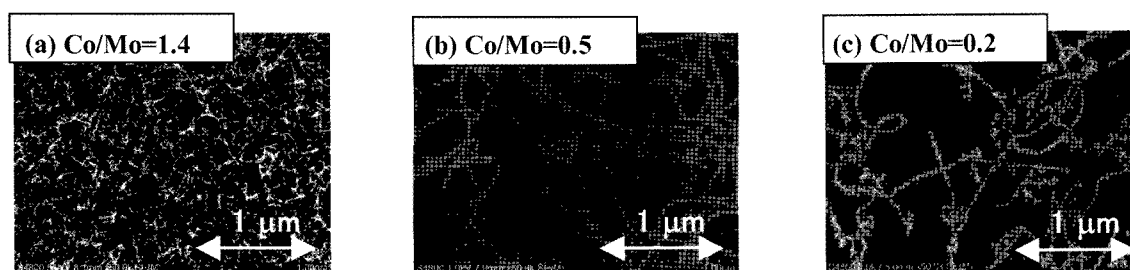


Fig. 1 SEM images of CNTs depending on Mo/Co molar ratio

References: [1] AN Andoitis, et al, Phys. Rev. Lett., **87** (2001) 66802-1-4

[2] YC Choi, et al, Carbon, **43** (2005) 2737-2741

[3] Y Murakami, et al., Chem. Phys. Lett., **377** (2003) 49-54

Corresponding Author M. Maekawa

E-mail maekawa@mars-ei.eng.hokudai.ac.jp

Tel : 81-(0)11-706-6519 **Fax :** 81-(0)11-706-7890

Synthesis of multiwalled carbon nanocoils using catalyst of Fe-Sn

○Ryo Kanada¹, Lujun Pan¹, Seiji Akita¹, Kaori Hirahara² and Yoshikazu Nakayama²

¹*Department of Physics and Electronics, Osaka Prefecture University, 1-1 Gakuen-cho, Sakai, Osaka 599-8531, Japan*

²*Department of Mechanical Engineering, Graduate School of Engineering, Osaka University, Japan*

The catalysts of Fe/ITO [1] or Fe-In-Sn-O [2] has been successfully used for the synthesis of carbon nanocoils so far. However, carbon nanocoils synthesized by these catalysts are lack of crystallinity, which results in their relatively lower mechanical strength and electric conductivity compared with the normal multiwalled carbon nanotubes (CNTs). It is reported that arc plasma gun (APG) can be used for the formation of good quality catalysts, which has been applied for the fabrication of CNTs. It is also desired that high quality carbon nanocoils can be synthesized by using the catalysts produced by APG.

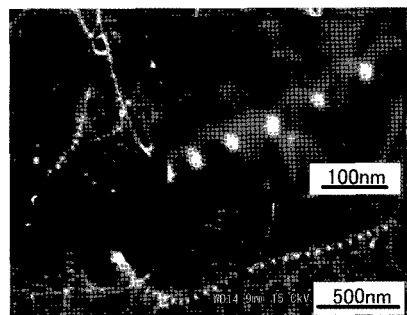


Fig.1 SEM image of the grown MWCNCs.

Two-element-metal Fe-Sn is used as the catalyst, which is produced by two APGs with the evaporating sources of Fe and Sn, respectively. The Fe-Sn catalyst is formed by layer-by-layer deposition or by co-deposition, with the composition controlled by the number of pulse discharge. Then the samples were annealed at 150°C in air for 12 hours in order to oxidize the catalysts to prevent the Sn from vaporization during heating process. Carbon nanocoils were then synthesized by the thermal CVD at 700°C using acetylene as a reaction gas and He as a carrier gas. The growth time was 15 min.

Figure 1 shows the SEM image of the grown multiwalled carbon nanocoils (MWCNCs) using the co-deposited catalysts of Fe and Sn, each of which has a film thickness of 4 nm. The coil diameters of grown MWCNCs are less than 100 nm, which are thinner than those of the conventional carbon nanocoils synthesized by the Fe/ITO catalysts. The line diameters of distributed carbon nanocoils are less than 20 nm, which is the same as the CNTs grown under the same CVD conditions without the catalyst of Sn. Therefore, Sn plays a crucial role for the growth of MWCNCs. It is found that there are a large number of particles, with diameters ranging from 20 to 100 nm, are distributed on the surface of substrate. The MWCNCs are observed to have a possible base growth mechanism, which is different from that of conventional carbon nanocoils. The grown MWCNCs are promising for the applications to NEMS or composites.

Acknowledgement: This work was partially supported by a Grant-in-Aid for Scientific Research from the Japan Society for the Promotion of Science, and by the Osaka Prefecture Collaboration of Regional Entities for the Advancement of Technological Excellence, JST.

Reference: [1] M. Zhang, Y. Nakayama and L. Pan, *Jpn. J. Appl. Phys.* 39 (2000) L1242. [2] T. Nosaka, O. Suekane, and Y. Nakayama: *Abstr. Int. Conf. Science and Application of Nanotubes*, 2003, p. 42.

Corresponding Author: L. Pan,

TEL: +81-72-254-9265, **FAX:** +81-72-254-9265, **E-mail:** pan@pe.osakafu-u.ac.jp

SWNH-Streptavidin: an Effective Anticancer Drug Delivery System

O Xu Jianxun,¹ Yudasaka Masako,¹ Zhang Minfang,¹ Iijima Sumio^{1,2}

¹JST/SORST, c/o NEC, 34 Miyukigaoka, Tsukuba, Ibaraki 305-8501, Japan

²Meijo University, 1-501 Shiogamaguchi, Tenpaku-ku, Nagoya 468-8502, Japan

Single Wall Carbon Nanohorn (SWNH) is a new kind of nano-carbon material, which has horn-like structure with 2~5 nm diameter. Usually about 2,000 SWNHs assemble to form an spherical aggregate with diameter of around 80~100 nm.¹ The SWNH aggregate emerges as an attractive candidate for a drug delivery system (DDS). It is specially promising to carry an anticancer drug, many of which are not water soluble and highly toxic, to make them effectively delivered, and released in a controlled way.

In this study, we incorporated Docetaxel (Doc), an anticancer drug used for stomach cancer, breast cancer, non-small cell lung cancer and so on, into hydrogen peroxide treated SWNHs by modified nano-precipitation method. The weight percent of incorporated Doc is around 20%. Taking advantage of those carboxylic groups on SWNHs, we firstly introduced amine-PEO3-biotin to the conjugate to improve the hydrophilicity. Then, streptavidin, a small protein, was attached on the complex due to the high affinity between streptavidin and biotin. The weight percent of streptavidin is estimated roughly to be 25%. The streptavidin moiety on SWNH makes it easy to attach some other biotinylated peptides/proteins, to introduce more functions to the complex.

Furthermore, we investigated the anticancer effectiveness of Doc@SWNH-Streptavidin using a stomach cancer cell line (ATCC NO.: CRL5973). The cytotoxicity experiment was conducted using WST-1 reagent (Figure 1). The cells were incubated with Doc, SWNH-Streptavidin and Doc@SWNH-Streptavidin (~3 ug/ml) respectively for two days. We found that the viability of the cells with Doc@SWNH-Streptavidin decreased dramatically: only 1/3 of that of the cells with SWNH-Streptavidin. It is noteworthy that Doc@SWNH-Streptavidin has a higher cytotoxicity to the cancer cells than Doc itself.

These indicate that Doc can be delivered by SWNH-Streptavidin into the cells and the released Doc causes cell death. Thus, we think SWNH-Streptavidin could be an effective DDS.

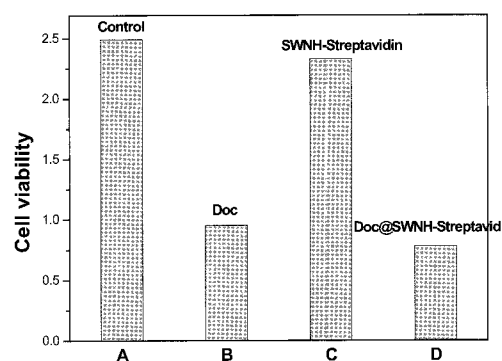


Figure 1. Cytotoxicity experiments using cancer cells incubated with Doc (B), SWNH-Streptavidin (C) and Doc@SWNH-Streptavidin.

References:

1. S. Iijima, M. Yudasaka, R. Yamada, S. Bandow, K. Suenaga, F. Kokai, K. Takahashi *Chem. Phys. Lett.*, **1999**, *309*, 165, and therein cited.

Corresponding Author: Xu Jianxun, Yudasaka Masako; **E-mail:** xu@frl.cl.nec.co.jp, yudasaka@frl.cl.nec.co.jp; **Tel:** 029-856-1940; **Fax:** 029-850-1366

Near-Infrared Laser-Triggered Carbon Nanohorns for Selective Elimination of Various Microorganisms

○Eijiro Miyako, Hideya Nagata, Ken Hirano, Yoji Makita,
Ken-ichi Nakayama, Takahiro Hirotsu

Health Technology Research Center, National Institute of Advanced Industrial Science and Technology (AIST), 2217-14, Hayashi-cho, Takamatsu 761-0395, Japan

Infections of various harmful microorganisms, such as methicillin-resistant *Staphylococcus aureus* (MRSA), severe acute respiratory syndrome (SARS) virus, and human immunodeficiency virus (HIV), have been a worldwide serious problem. Hence, there is a high demand for anti-microbial drugs and materials in a medical field. Here we show that the first application of carbon nanohorn (CNH) as potent laser therapeutic agents for highly selective elimination of various model microorganisms (yeast; *Saccharomyces cerevisiae*, bacteria; *Escherichia coli*, and virus; T7 bacteriophage) (Figure 1).[1]

We successfully prepared molecular recognition element (MRE)-CNH complexes, which when enables to NIR laser irradiation, are able to kill various microorganisms in a highly selective manner. The real-time anti-microbial activities of NIR laser-triggered molecular recognition element (MRE)-CNH complexes were investigated by using a fluorescence microscopy and propidium iodide to stain dead microorganisms (Figure 2).

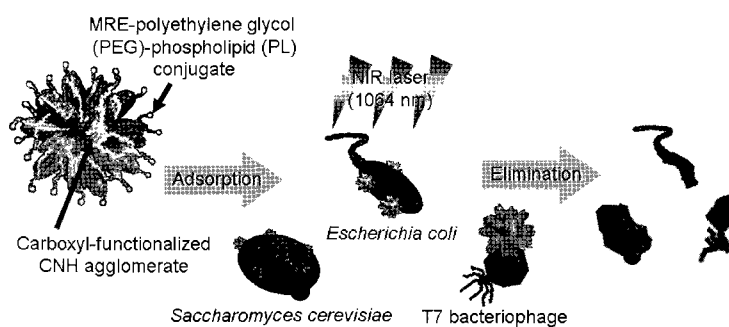


Figure 1. Method for elimination of various microorganisms using MRE-CN complexes and NIR laser irradiation (1064 nm). The MRE selectively targets the microbe, the PEG chains affect the water dispersibility of the CNH-COOH molecules, and the hydrophobic carbon chains of the PL non-covalently bind to the surfaces of the CNH-COOH molecules via hydrophobic interactions.

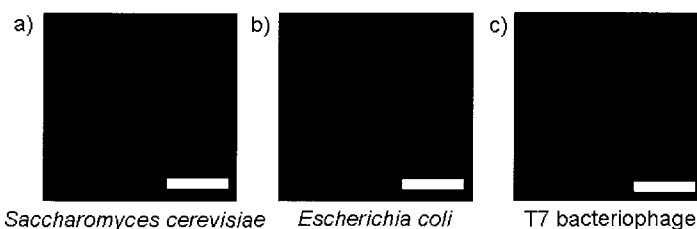


Figure 2. Direct observations of eliminated microorganisms. a) *S. cerevisiae*. b) *E. coli*. c) T7 bacteriophage. Scale bars: 25 μm . Magnification: $\times 20$. Laser power: 1 W. Wavelength: 1064 nm.

[1] E. Miyako, Hideya Nagata, Ken Hirano, Yoji Makita, Ken-ichi Nakayama, Takahiro Hirotsu, *J. Am. Chem. Soc.*, submitted (2007).

Corresponding Author: Eijiro Miyako

TEL: +81-87-869-3574, FAX: +81-87-869-3550, E-mail: e-miyako@aist.go.jp

Resonance Raman Study of Nanopeapod-Derived Double-Walled Carbon Nanotubes

○Soon-kil Joung¹, Toshiya Okazaki¹, Naoki Kishi¹, Zujin Shi² and Sumio Iijima¹

¹*Research Center for Advanced Carbon Materials, AIST, Tsukuba 305-8565, Japan*

²*Department of Chemistry, Peking University, Beijing 100871, P. R. China*

Double-walled carbon nanotubes (DWNTs) have been expected for nanocomposites, field emission sources, nanotube bi-cables and electronic devices because of their superior mechanical properties, thermal conductivity and structural stability [1]. Optical application of DWNTs is also attractive because the inner core tube is protected from environment and its optical properties are preserved.

We have previously reported that photoluminescence (PL) of nanopeapod-derived DWNTs strongly depend on the interlayer spacing between the outer and the inner tubes [2, 3]. For example, while significant PL quenching occurs in DWNTs having smaller interlayer distance, the PL signals of the inner tubes are observable from DWNTs having larger interlayer distance. However, details of the PL behaviors such as chiral indexes of the emissive inner tubes are yet unclear.

We here report the resonance Raman study of the nanopeapod-derived DWNTs having larger interlayer distance for clarifying the structural changes of DWNTs. Using a contour plot of the Raman intensities of the radial breathing modes (RBMs) over the laser excitation wavelengths of 880-1070 nm, we found that smaller diameter tubes such as (6, 5) and (6, 4) tubes are abundant as the inner tubes. Possible PL mechanism and structural changes will be discussed based on the results.

[1] M. Endo, H. Muramatsu, T. Hayashi, Y. A. Kim, M. Terrones, M. S. Dresselhaus., *Nature* **433**, 476 (2005).

[2] T. Okazaki, S. Bandow, G. Tamura, Y. Fujita, K. Iakoubovskii, S. Kazaoui, N. Minami, T. Saito, K. Suenaga, S. Iijima, *Phys. Rev. B*, **74**, 153404 (2006).

[3] T. Okazaki, Z. Shi, T. Saito, H. Wakabayashi, K. Suenaga, S. Iijima, *The 32nd Fullerene-Nanotube General Symposium*, 2P-2 (2007).

Corresponding Author: Toshiya Okazaki

E-mail: toshi.okazaki@aist.go.jp, **Tel:** 029-861-4173, **Fax:** 029-861-4851

Composites of Single-Walled Carbon Nanotubes and Poly(*p*-Phenylene-1,2-Vinylene) with Structural Defect of *p*-Phenylene-1,1-Vinylidene Units in the Main Chain

○Naoki Kadota, Tomokazu Umeyama, Noriyasu Tezuka, Yoshihiro Matano, and Hiroshi Imahori

Graduate School of Engineering, Kyoto University, Kyoto 615-8501, Japan

Many studies have focused on nanocomposites of exfoliated single-walled carbon nanotubes (SWNTs) and conjugated polymers, since they are appealing candidates exhibiting unique photophysical properties in molecular devices. Nevertheless, the photophysical properties including energy transfer (EN) or electron transfer (ET) process between conjugated polymers and SWNTs have not been fully elucidated. Although the emission quenching of the π -conjugated polymers in the composites has been reported, the emission from the SWNTs due to the EN has never been observed. Here we report the first unambiguous demonstration of EN from conjugated polymers to SWNTs in the composites by the near infrared (NIR) emission from the SWNTs. A novel conjugated polymer, poly[*(p*-phenylene-1,2-vinylene)-*co*-(*p*-phenylene-1,1-vinylidene)] (*co*PPV, Figure 1), has been prepared by Heck coupling reaction to examine specific interactions with SWNTs.

The *co*PPV-SWNT nanocomposites were prepared by tip-sonication of a mixture of SWNTs and *co*PPV (1/10, w/w) in THF, centrifugation of the mixture, and filtration of the supernatant. The resultant solid on the filter, *co*PPV-SWNTs, was washed thoroughly and redispersed in THF with the aid of bath sonication. The dark brown solution without discernable particulates remained stable at least for 2 weeks.

UV-vis-NIR absorption spectrum of *co*PPV-SWNT in THF shows characteristic sharp peaks of SWNTs, demonstrating the high dispersing ability of *co*PPV. When fluorescence spectra of *co*PPV and *co*PPV-SWNTs in visible region are compared, the fluorescence intensity in *co*PPV-SWNTs relative to that in *co*PPV is reduced significantly, suggesting the occurrence of interaction between the excited state of *co*PPV and SWNTs. Furthermore, the NIR fluorescence contour plot of *co*PPV-SWNTs (Figure 2) exhibits emission in the excitation wavelength range of 400–500 nm, where SWNTs show no absorption. This emission can be accounted by initial excitation arising from the π - π^* transition of *co*PPV, followed by EN from the excited *co*PPV to the SWNTs in the composites. Although there have been many reports on the NIR fluorescence of exfoliated SWNTs, this is the first example of enhancement of emission intensity by interaction with dispersing agents.

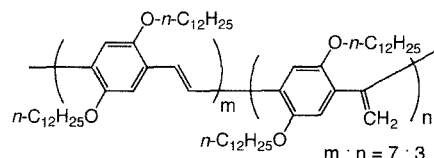


Figure 1. Structure of *co*PPV.

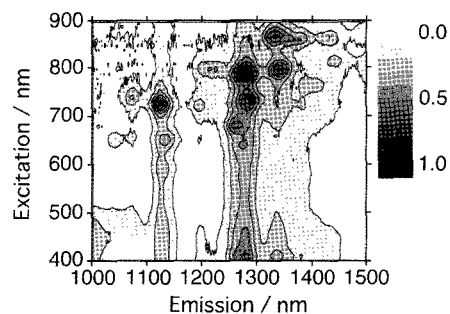


Figure 2. Contour plot of photoluminescence spectrum for *co*PPV-SWNTs in THF.

Corresponding Author: Naoki Kadota

TEL: +81-75-383-2568, FAX: +81-75-383-2571, E-mail: kadotan@t06.mbox.media.kyoto-u.ac.jp

Gas adsorption in water-SWCNTs

○Haruka Kyakuno¹, Syunsuke Ogasawara¹, Toshihide Hibi¹, Yasumitsu Miyata^{1,4},
Kazuyuki Matsuda¹, Hiroaki Kadowaki¹, Shinzo Suzuki³, Yohji Achiba³,
Hiromichi Kataura⁴, Takeshi Saito⁵, Satoshi Ohsima⁵, Morio Yumura⁵,
Sumio Iijima⁵ and Yutaka Maniwa^{1,2}

¹Department of Physics, Faculty of Science, Tokyo Metropolitan University,
Tokyo 192-0397, Japan

²CREST, Japan Science and Technology Corporation (JST), Kawaguchi, 322-0012, Japan

³Department of Chemistry, Faculty of Science, Tokyo Metropolitan University,
Tokyo 192-0397, Japan

⁴Nanotechnology Research Institute, National Institute of Advanced Industrial Science and
Technology (AIST), Ibaraki 305-8562, Japan

⁵Advanced Carbon Materials Research Center, National Institute of Advanced Industrial
Science and Technology (AIST), Ibaraki 305-8565, Japan

It is known that single-wall carbon nanotubes (SWCNTs) can adsorb various kinds of gases. Especially, water molecules inside SWCNTs form ice nanotubes (ice NTs) at low temperature.

Recently, gas adsorption in water-SWCNTs is discussed actively. So, we carried out the study of water-SWCNTs in gas atmospheres, by means of X-ray diffraction (XRD) and electrical resistance. In these experiments, we used SWCNTs samples with an average diameter of 13.5 Å. From the experimental results, we considered that the water filling-ejecting type transition occurred inside SWCNTs in the presence of atmospheric gases. [1] To confirm this consideration, we carried out molecular dynamics (MD) simulations. As shown in Fig.1, the water cluster was completely forced out from the SWCNT by the entering CH₄ molecules. This result clearly shows the presence of the water filling-ejecting transition.

Furthermore, to examine whether the transition's appearance depends on SWCNTs diameters, we also carried out XRD using SWCNTs samples with an average diameter of 20 Å.

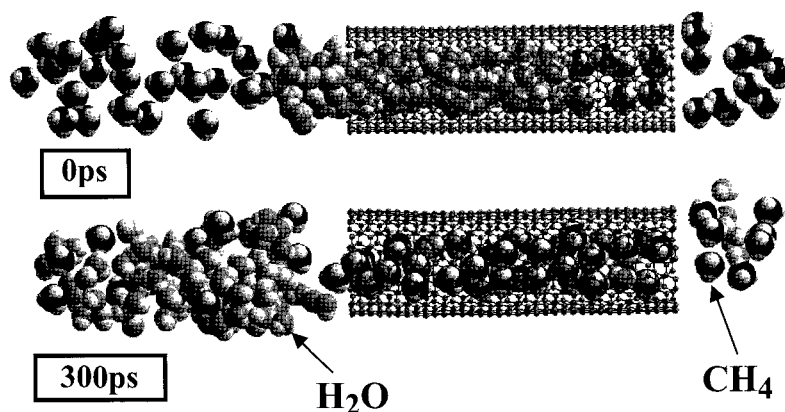


Fig.1

The result of MD simulation

At first, the water molecules are located inside the SWCNT.

After 300ps, CH₄ molecules enter the SWCNT at 200K.

[1] Y. Maniwa *et al.*: Nature Materials 6 (2007) 135-141.

Corresponding Author: Yutaka Maniwa

TEL: +81-42-677-2490, E-mail: maniwa@phys.metro-u.ac.jp

High-pressure and high-temperature treatments of double-walled carbon nanotubes

○Y. Kanamori¹, S. Kawasaki¹, Y. Iwai¹, A. Iwata¹,
H. Muramatsu², T. Hayashi², Y.A. Kim², M. Endo²

¹ Department of Chemistry, Nagoya Institute of Technology, Japan

² Faculty of Engineering, Shinshu University, Japan

Although double-walled carbon nanotubes (DWCNTs) have attracted great attention from both academic and industrial points of view, it had been difficult to produce high purity DWCNT sample. However, recently, Endo et al. [1] developed a selective synthesis method of DWCNTs and it becomes possible to perform structural investigations. In this paper, we report on the structural change of DWCNT samples by HPHT treatments.

DWCNT samples used in the present study were prepared by the CVD method [1]. In situ XRD measurements of DWCNTs under high pressure and at high temperature were performed at AR-NE5C of KEK in Tsukuba. Pressure-Temperature conditions for the HPHT treatments are summarized in Fig. 1.

As shown in Fig. 2, since the DWCNT sample treated at relatively low temperature and low pressure (#1) shows almost the same Raman pattern as that of pristine sample, the #1 sample might keep the original structure. On the other hand, structural change occurred in the other samples (#2 - #5). We will discuss the structural change of the DWCNT sample by HPHT treatment in more detail in the symposium.

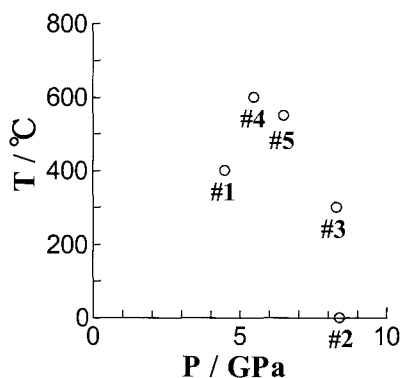


Fig. 1 Pressure-Temperature conditions for the HPHT treatments of DWCNT samples. Experimental run numbers are indicated in the figure.

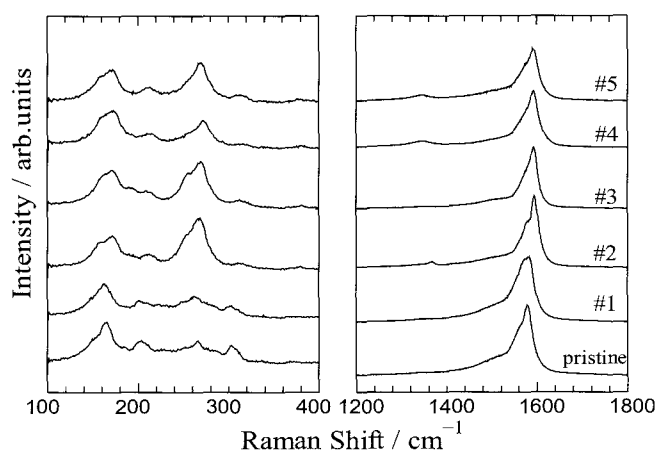


Fig. 2 Raman spectra of the HPHT treated DWCNT samples. The indicated numbers correspond to the numbers in Fig. 1.

[1] M. Endo et al., *Nature*, **433**, 476 (2005)

Corresponding Author: Shinji Kawasaki Fax: +81-(52)-735-5221, E-mail: kawasaki.shinji@nitech.ac.jp

Near-IR Absorption and Photoluminescence Spectral Properties of Carbon Nanotubes Dissolved in RNA Aqueous Solutions

○Nobuo Wakamatsu, Yuichi Noguchi, Tsuyohiko Fujigaya,
and Naotoshi Nakashima

*Department of Applied Chemistry, Graduate School of Engineering, Kyushu University,
Fukuoka, Japan*

Since the finding in 1991[1], carbon nanotubes (CNTs) are nanomaterials of forefront in nanoscience and nanotechnology. Applications of CNTs toward bio and related areas are interesting. CNTs are not dispersed in water, so we have difficulties in using CNTs for applications. We[2] and Zheng[3] described the findings that double-stranded DNA and single-stranded DNA dissolve single-walled carbon nanotubes (SWNTs) in water, respectively. We also described the fabrication of the layer-by-layer assembly of RNA-wrapped single-walled carbon nanotubes on a solid substrate[4]. Here we report the near-IR absorption and photoluminescence (PL) spectral properties of SWNTs dissolved in Poly(U) (or Poly (C)) aqueous solutions. Fig. 1 shows a 2-D mapping of SWNTs dissolved in RNA aqueous solutions. As can be seen in the figure, the PL mapping showed strong pH dependence. The detail mechanism of this behavior will be discussed at the meeting.

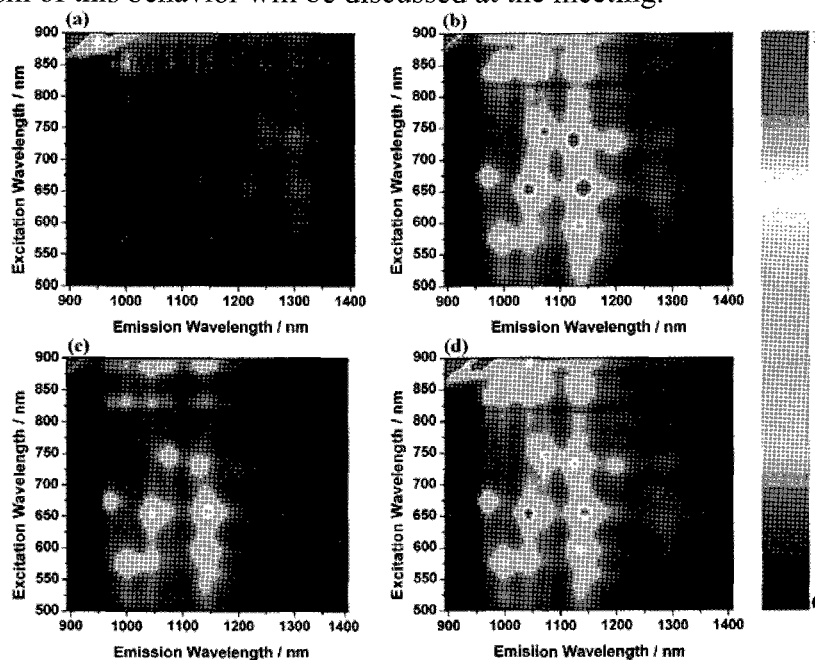


Fig.1. 2-D mapping of Photoluminescence spectra of SWNTs dissolved in RNA aqueous solutions (a)SWNTs/Poly(U) at pH5.8 (b)SWNTs/Poly(U) at pH8.0 (c)SWNTs/Poly(C) at

[1] S. Iijima, *Nature*, **354**, 147 (1991).

[2] N. Nakashima et al., *Chem. Lett.*, **32**, 456 (2003).

[3] M. Zheng et al., *Nat. Mater.*, **2**, 338 (2003).

[4] Nakashima et al., *Chem. Phys. Lett.*, **419**, 574 (2006).

Corresponding Author: Naotoshi Nakashima

TEL:+81-92-802-2840,FAX:+81-92-802-2840,E-mail:nakashima-tcm@mbox.nc.kyushu-u.ac.jp

Observation and Characterization of SWNT-DNA Hybrids by Electric Force Microscopy

○Yuki Asada¹, Shota Kuwahara¹, Toshiki Sugai^{1,2}, Ryo Kitaura¹
and Hisanori Shonohara^{1,2,3}

¹*Department of Chemistry, Nagoya University, Nagoya 464-8602, Japan*

²*Institute for Advanced Research, Nagoya University, Nagoya 464-8602, Japan*

³*CREST, Japan Science and Technology Corporation, c/o Department of Chemistry, Nagoya University, Nagoya 464-8602, Japan*

DNA wrapped single-wall carbon nanotubes (SWNT-DNA hybrid) have been known to exhibit unique characteristics in their structures as well as the high solubility in water [1]. A partial separation of the chirality was achieved by ion exchange chromatography, which is assumed to be due to chirality dependent electric characters of SWNT-DNA hybrids. We have recently reported [2] a preliminary study on the electronic properties of the hybrids by electric force microscopy (EFM) which can visualize and manipulate the hybrid materials. Here, we report a detailed study on the electric properties of SWNT-DNA hybrids by EFM measurement and the effects of DNA wrapping on the electronic structure of SWNTs.

SWNT-DNA hybrid materials were synthesized from SWNTs (HiPco) and single strand DNA (ssDNA) by ultrasonication and centrifugation. The hybrid solution was deposited on a SiO₂ substrate and dried by nitrogen gas. EFM measurements were performed in air at room temperature with a NanoscopeIII (Digital Instruments). EFM images were observed under a non-contact mode while keeping the tip-sample height distance exactly at 30 nm, which was realized by simultaneous measurements of the height information on the hybrids with tapping mode AFM. Furthermore, we are able to image a salient process where DNAs are removed completely from the SWNT-DNA hybrids by thermal oxidation (combustion) on a SiO₂ substrate at 400 °C.

Figure 1 shows EFM images of SWNT-DNA hybrids with a reference topography image (a). Some of the hybrids exhibit no EFM signal (b), which is recovered by the DNA elimination by the combustion(c). These results show that the presence of DNAs wrapped on the SWNTs affects and controls the electronic properties of pristine SWNTs significantly. The EFM/AFM observation also suggests that the wrapping structures and electronic properties of the hybrids are expected to have strong dependence on the length of the hybrids. We are, therefore, currently performing size-exclusion chromatography on the hybrids to further investigate the DNA wrapping effects on the electronic structure of the materials.

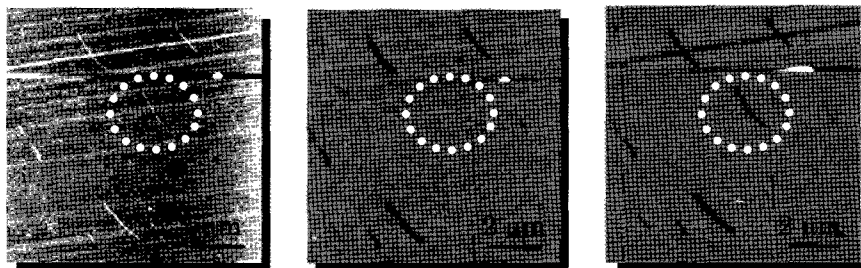


Figure 1. AFM and EFM images of SWNT-DNA hybrids on SiO₂.
(a) AFM topography image, (b) EFM image, (c) EFM image after combustion.

References: [1] Zheng, M. *et al.*, *Nat. Mater.* **2**, 338, (2003).

[2] (a) Y. Asada, *et al.* 86th CJS spring meeting (2006), (b) Y. Asada, *et al.* 87th CJS spring meeting (2007).

Corresponding Author: Hisanori Shinohara

E-mail: noris@cc.nagoya-u.a.jp, **TEL:** +81-52-789-2482, **FAX:** +81-52-789-1169

Defect Detection in Carbon Nanotubes by Electrostatic Force Microscopy

○Yuki Okigawa¹, Takeo Umesaka¹, Yutaka Ohno¹, Shigeru Kishimoto^{1,2}, Takashi Mizutani¹

¹Department of Quantum Engineering, Nagoya University, Nagoya 464-8603, Japan

²Venture Business Laboratory, Nagoya University, Nagoya 464-8603, Japan

Carbon Nanotube (CNT) field-effect transistors (FETs) have been intensively studied because of their high-speed potential with a large transconductance.[1,2] However, there is a concern about the defects in the CNTs which would deteriorate the performance of the CNT-FETs. The potential profile along the CNTs will be affected if the defects exist in the CNTs. In this study we have measured the potential profile along the CNTs by electrostatic force microscopy (EFM) and obtained the non-uniform potential image affected by the defects in the CNTs.

The CNTs used for the fabrication of CNT-FETs with back gate was grown by grid-inserted plasma-enhanced chemical vapor deposition.[3] The device has no passivation film. The potential profile was measured using EFM in vacuum. The EFM is similar to the KFM [4] which has a feedback loop to attain the null electrostatic force. The image obtained by the EFM was better than the KFM even though the absolute value of the potential was not obtained in the case of EFM. Then the EFM is suitable for discussing the effects of the defects on the potential profile along the CNTs. Figure 1(a) shows the atomic force microscopy (AFM) image, and Fig. 1(b) and (c) show EFM images at gate bias voltages of $V_{GS} = 2$ V and -1 V, respectively. Even though the AFM image seems smooth with little feature, the EFM image at $V_{GS} = 2$ V shown in Fig. 1(b) shows non-uniform image with dark area (indicated by arrows) which is probably due to the effects of the defects. The CNT is divided into multiple conducting segments separated by potential barriers at defects. It is notable that the EFM image became smooth when the back gate voltage became negative ($V_{GS} = -1$ V). This is probably due to that the separation of the conducting channel became weak by inducing holes in the channel of p-type CNT-FET.

It has been shown that the EFM is effective in detecting the defects in the CNTs.

[1] S. Rosenblatt, H. Lin, V. Sazonova, S. Tiwari, and P. L. McEuen, *Appl. Phys. Lett.*, **87** 153111 (2005).

[2] A. Javey, J. Guo, D. B. Farmer, Q. Wang, E. Yenilmez, R. G. Gordon, M. Lundstrom, and H. Dai, *Nano Lett.*, **7** 1319 (2004).

[3] Y. Kojima, S. Kishimoto, Y. Ohno, A. Sakai, T. Mizutani, *Jpn. J. Appl. Phys.*, **44** 2600 (2005).

[4] T. Umesaka, H. Ohnaka, Y. Ohno, S. Kishimoto, K. Maezawa, and T. Mizutani, *Jpn. J. Appl. Phys.*, **46** 2496 (2007).

Corresponding Author: Takashi Mizutani

TEL: +81-52-789-5230, FAX: +81-52-789-5232, E-mail: tmizu@nuee.nagoya-u.ac.jp

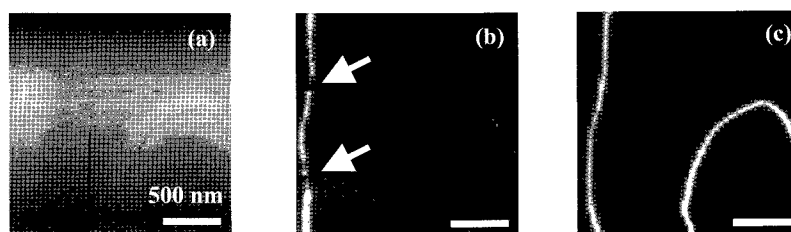


Fig. 1. (a) Topographic AFM image of the device. (b), (c) EFM images at gate bias voltages of $V_{GS} = 2$ V and -1 V, respectively.

Fabrication of logic circuits using solution-processed single-walled carbon nanotube transistors

○ Haruo Tomita¹, Akio Ogura¹, Hiromichi Kataura², Ryo Nouchi¹
and Masashi Shiraishi¹

¹Graduate School of Engineering Science, Osaka University, Toyonaka 560-8531, Japan

²AIST Nanotech. Res. Inst., Tsukuba 305-8562, Japan

Single-walled carbon nanotube field effect transistors (SWNT FETs) will play an important role for the construction of integrated circuits, because semiconducting SWNTs exhibit a high mobility and a large On/Off ratio. Logic circuits using an individual SWNT-FETs have been reported by several groups [1,2], however their fabrication processes contained high temperature treatment [1], or complicated lithography steps [2]. Our group has reported fabrication and various characteristics of thermal-free solution-processed network-SWNT-FETs, in which network SWNTs were used as a channel layer, for flexible device applications [3-6]. Here in this work, we fabricated logic circuits by using the network-SWNT-FETs.

Complementary logic circuits are composed of p-type and n-type FETs. Although a conventional un-doped SWNT-FET shows an ambipolar FET property, it shows a p-type FET property in air because of adsorption of oxygen molecules onto the SWNTs. In order to fabricate logic circuits, we utilized such p-type network-SWNT-FETs, and in addition, we fabricated n-type network-SWNT-FETs by a chemical doping method using polyethyleneimine (PEI) [7]. A schematic diagram of an example of the circuit, inverter, is shown in Fig. 1. An operating voltage was set to be -2 V and the measurement was carried out at an ambient condition. It can be seen that an output voltage was changed as a function of the applied input (gate) voltage (Fig. 2). This result indicates that an inverter characteristic was observed. The detail of the other logic circuits by the network-SWNT-FETs will be discussed in the presentation.

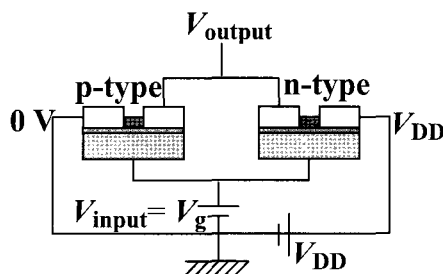


Fig. 1 An inverter circuit

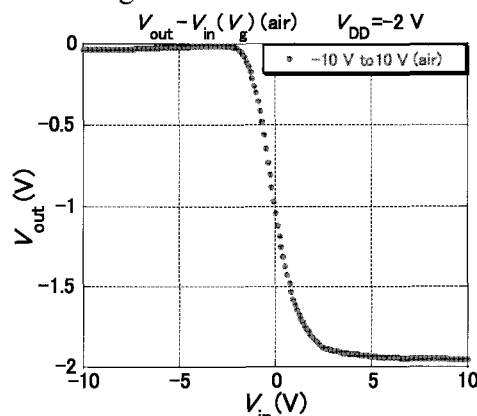


Fig. 2 An inverter characteristic

References: [1] A. Javey et al., *Nano Lett.* **2**, 9 (2002). [2]

Z. Chen et al., *Science* **311**, 24 (2006). [3] M. Shiraishi et

al., *CPL* **394**, 110 (2004) [4] M. Shiraishi et al., *APL* **87**, 93107 (2005). [5] S. Nakamura et al., *APL* **89**,

11312 (2006). [6] T. Fukao et al., *JJAP* **45** 6524 (2006). [7] M. Shim et al., *J. Am. Chem. Soc* **123**, 11512

(2001).

Corresponding Author: Masashi Shiraishi

E-mail: shiraishi@mp.es.osaka-u.ac.jp, Tel: +81-6-6850-6426, Fax: +81-6-6845-4632

Biocompatibility of Carbon Nanosubstances in the Subcutaneous Tissue

○Eri Hirata¹, Atsuro Yokoyama¹, Yoshinori Sato², Yoshinobu Nodasaka¹, Motohiro Uo¹,
Tsukasa Akasaka¹, Kazuyuki Tohji², Fumio Watari¹

¹Graduate School of Dental Medicine, Hokkaido University, Sapporo, 060-8586, Japan

²Graduate School of Environmental Studies, Tohoku University, Sendai, 980-8579, Japan

Recently application of carbon nanoscale substances for biomaterials have attracted. It is necessary to evaluate tissue response in addition to cytotoxicity to develop biomaterials. However, reports on the biocompatibility about them were a few^{1,2)}, especially for long term study. The purpose of this study was to investigate tissue response to carbon nanosubstances implanted in subcutaneous tissue for long term. In the present study, two kinds of carbon nanosubstances were used. Hat-stacked carbon nanofibers (H-CNFs) were produced by thermal CVD using a powdered Ni catalyst in a conventional flow reactor system according to the report of Rodriguez³⁾. The multi-wall carbon nanotubes (MWCNTs) synthesized by CVD method from NanoLab, Inc. The average 590 nm- and 1160 nm-lengths of H-CNFs (600 H-CNFs and 1200 H-CNFs), and the average 220 nm- and 825 nm-lengths of MWCNTs (220 CNTs and 825 CNTs) were implanted in the subcutaneous tissue of rats. Segments of the subcutaneous tissue including specimens were excised and fixed at 1, 4, 16, 52 and 104 weeks after surgery. The fixed specimens were divided into two parts. One part was embedded in paraffin. Hematoxylin and eosin-stained specimens were observed by optical microscopy. The other was observed by transmission electron microscopy. After 1 week, granulation tissue with capillaries and phagocytes was observed around carbon nanosubstances. Some of them were engulfed in macrophages. The degree of inflammation on H-CNFs was slighter than that on MWCNTs. Also, inflammatory responses around smaller sizes of them were slighter than those around larger sizes. Some of 600 H-CNFs were observed in lysosomes, while most of 1200 H-CNFs were diffused in cytoplasm randomly. Most of 220 MWCNTs were in lysosomes, whereas 825 MWCNTs were aggregated in cytoplasm in phagocytes. At 52 weeks after surgery, both sizes of H-CNFs were covered by thin fibrous tissue. On the other, slight granulomatous inflammatory response was observed around MWCNTs. Shortening and decomposition of H-CNFs were suggested, although changes of structures of MWCNTs were not recognized in phagocytes. These results showed that severe inflammatory response such as necrosis and degeneration was not observed around H-CNFs and MWCNTs, and structures of carbon nanosubstances influenced their biocompatibility in the subcutaneous tissue.

References:

- [1] A. Yokoyama, Y. Sato, Y. Nodasaka, S. Yamamoto, T. Kawasaki, M. Shindoh, T. Kohgo, T. Akasaka, M. Uo, F. Watari, K. Tohji. *Nano Lett*, **5**, 157-161, (2005)
- [2] Y. Sato, A. Yokoyama, K. Shibata, Y. Akimoto, S. Ogino, Y. Nodasaka, T. Kohgo, K. Tamura, T. Akasaka, M. Uo, K. Motomiya, B. Jeyadevan, M. Ishiguro, R. Hatakeyama, F. Watari, K. Tohji. *Mol. BioSyst*, **1**, 176-182, (2005)
- [3] N. Rodriguez. *J. Mater. Res*, **8**, 3233-3250, (1993)

Corresponding Author :Atsuro Yokoyama

E-mail:yokoyama@den.hokudai.ac.jp

Tel:+81-11-706-4270, **Fax**:+81-11-706-4903

Electron Transport Study of Horizontally-Aligned SWNTs on Sapphire

○Tomoko Suzuki,¹ Hiroki Ago,^{*,1,2} Naoki Ishigami,¹ Masaharu Tsuji,^{1,2}
Tatsuya Ikuta,³ and Koji Takahashi³

¹Graduate School of Engineering Sciences, Kyushu University, Fukuoka 816-8580, Japan

²Institute for Materials Chemistry and Engineering, Kyushu University

³Graduate School of Engineering, Kyushu University

Recently, we reported the growth of single-walled carbon nanotubes (SWNTs) aligned to the specific crystallographic directions of sapphire (α -Al₂O₃) surfaces [1-3]. This aligned growth is promising for the fabrication of nanoelectronic devices, such as flexible field-effect transistors (FETs), high on-current FETs, and high frequency devices. Here, we have studied the electronic structure of aligned nanotubes by measuring the electron transport properties for further control over the nanotube growth.

The FETs were fabricated with aligned SWNTs grown on an R-plane sapphire substrate, by depositing source/drain Au electrodes using photolithography. Two types of electrode configurations were studied; the channel directions were parallel (device A) and perpendicular (device B) to the SWNT orientation. The devices were characterized with a back-gate structure in air.

We obtained four types of electron transport properties in terms of the V_g dependence; semiconducting channel (S), mixture of metallic and semiconducting channel (M+S), metallic-dominant channel (M), and no current (N). The S and S+M type devices showed p-type behavior as indicated in Fig. 1, and the former showed good FET characteristics with on/off ratio of 10^3 - 10^5 . The M type devices are dominated by high current metallic SWNTs without showing the V_g dependence.

Table 1 compares the electron transport properties measured for devices A and B. The device with a parallel configuration gave the 81 % operation, while the perpendicular configuration gave only 6 % operation, indicating that the alignment is crucial for the device productivity. The effective device mobility (μ_d) of device A was found to be ~ 260 cm²/Vs, suggesting high potential of SWNT-FETs.

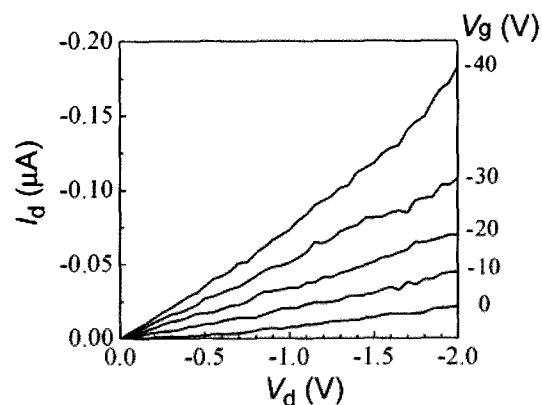


Fig. 1 I_d - V_d characteristic of S type device

Table 1 Distribution of transport characteristics (%)

device	S	S+M	M	N
A	8	71	2	19
B	3	3	0	94

Acknowledgements: This work is supported by Grant-in-aid for Scientific Research from MEXT (#18681020), Industrial Technology Research Program from NEDO, CREST-JST, and Joint Project of Chemical Synthesis Core Research Institutions.

References: [1] H. Ago et al, *Chem. Phys. Lett.*, **408**, 433 (2005); *ibid*, **421**, 399 (2006); *Appl. Phys. Lett.*, **90**, 123112 (2007).

Corresponding Author: Hiroki Ago (Tel&Fax: +81-92-583-7817, E-mail: ago@cm.kyushu-u.ac.jp)

Effects of Chemical Oxidation on the Physicochemical Properties of Double-Walled Carbon Nanotubes

○Noriko Maeda, Katsumi Uchida, Tadahiro Ishii, and Hirofumi Yajima

*Department of Applied Chemistry, Faculty of Science, Tokyo University of Science
12-1 Funagawara-machi, Shinjyuku-ku, Tokyo 162-0826, Japan*

Recently, double-walled carbon nanotubes (DWNTs) have attracted a great deal of attention in their specific optical properties and possible technological applications in various fields of science. In the view of the DWNTs' structural characteristics, they are expected to be more stabler for the chemical modification and thermal treatments, compared to single-walled carbon nanotubes (SWNTs).

In order to develop a novel functionalized material using DWNTs, we have probed the effects of the chemical oxidation on the physicochemical properties of DWNTs, including dispersion behavior in aqueous solutions. DWNTs from Nanolab were used without further purification. The chemical oxidation was made for the DWNTs with 3:1 concentrated H₂SO₄/HNO₃ mixtures (96 % and 60~61 % , respectively) under the sonication in a bath-type ultrasonicator at 40°C for appropriate time; giving rise to the carboxylation for the DWNTs. The oxidated DWNTs were facilitated to be dissolved in water without a dispersant. Then, the resulting characteristics were scrutinized by means of various spectroscopies, such as FT-IR, near-infrared (NIR) absorption/photoluminescence (PL) and Raman spectra, Dynamic Light Scattering (DLS), and Transmission Electron Microscopy (TEM). FT-IR measurements revealed that the number of the derived carboxyl groups, which were anticipated to be located at the open end of the tube from TEM observations, tended to increase with the increasing treatment time. However, the effects of the chemical oxidation on the characteristic Raman bands for the DWNTs, namely G- (1590 cm⁻¹), D- (1350 cm⁻¹), and RBM(Radial breathing mode) region bands, were hard to be recognized. At present, further studies of the physicochemical properties of the oxidated DWNTs with NIR-spectroscopies and DLS are under the progress.

References : [1]T.Takahashi et al. *Jpn.J.Appl.Phys* **43** (2004) 3636

[2]T.Takahashi et al. *Chem.Lett.* **11** (2005) 1516

[3]J.Liu et al. *Science* **280** (1998) 1253

Corresponding Author : Hirofumi Yajima

E-mail : yajima@rs.kagu.tus.ac.jp

Tel : +81-3-3260-4272 (ext.5760) , **Fax :** +81-3-5261-4631

Phonon wavepacket dynamics simulation on graphene nanoribbon junctions

OToru Takahashi¹, Takahiro Yamamoto^{1,2} and Kazuyuki Watanabe^{1,2}

¹Department of Physics, Tokyo University of Science, Tokyo 162-8601, Japan

²CREST, Japan Science and Technology Agency, Saitama 332-0012, Japan

Graphene nanoribbons (GNRs) are one-dimensional carbon materials, which is formed by cutting a single-walled carbon nanotube along the tube axis [1]. There are two basic shapes for graphene edges, namely, armchair (cis-polyacetylene-type) and zigzag (trans-polyacetylene-type) edges. The zigzag GNRs (ZNGRs) are also expected to be potential candidates for spintronics devices [2]. The thermal property of ZNGRs is a key to realize GNR-based nano-devices.

In this talk, we discuss the thermal transport properties of ZNGR junctions as a simple prototype of GNR-based nano-devices. In Fig.1(a), a wide ZNGR with a width W is joined to a thin ZNGR with a width N through the junction region. Thermal current in ZNGRs is dominantly carried by phonons, not by electrons, because they are insulating [3]. In our work, the phonon transmission function is calculated using the phonon wavepacket scattering method [4].

Figure 1(b) shows the transmission function of phonon wavepacket consisting of a longitudinal acoustic (TA) mode for ZNGRs with $1/5$, $2/5$, $3/5$, and $N/W=4/5$. The transmission decreases as the ratio N/W decreases. In other words, the contact thermal resistance increases with decreasing the ratio N/W .

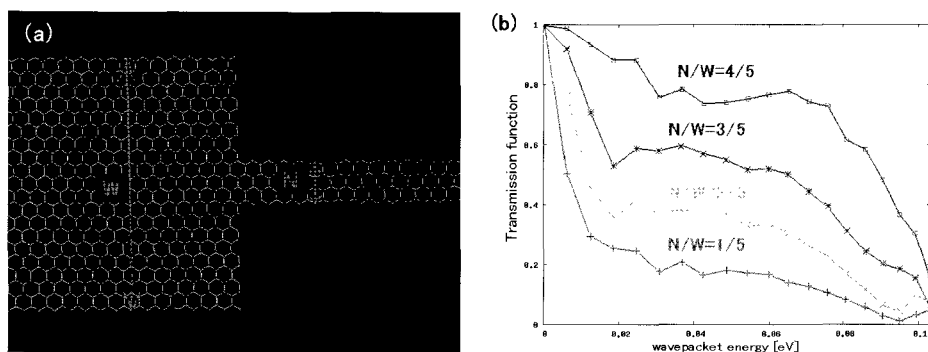


Fig.1: (a) Schematic of a graphene-nanoribbon junction. (b) The transmission function of phonon wavepacket consisting of a TA mode of ZNGRs with $1/5$, $2/5$, $3/5$, and $N/W=4/5$.

[1] M. Fujita, K. Wakabayashi, K. Nakada and K. Kusakabe, J. Phys. Soc. Jpn. **65**, 1920 (1996).

[2] Y.-W. Son, M.L. Cohen and S.G. Louie, Nature **444**, 347 (2006).

[3] Y.-W. Son, M.L. Cohen and S.G. Louie, Phys. Rev. Lett. **97**, 216803 (2006).

[4] N. Kondo, T. Yamamoto and K. Watanabe, Jpn. J. Appl. Phys. **45**, L963 (2006).

Corresponding Author: Toru Takahashi

TEL: +81-3-3260-4665, FAX: +81-3-3260-4665, E-mail: j1207642@ed.kagu.tus.ac.jp

Novel Ionic Gelator as an Amphiphilic Dispersant for Single-Walled Carbon Nanotubes

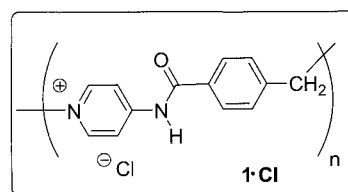
○ Masaru Yoshida,^{1,*} Nagatoshi Koumura,¹ Yoshihiro Misawa,¹ Nobuyuki Tamaoki,¹ Hajime Matsumoto,² Said Kazaoui,³ and Nobutsugu Minami¹

¹Nanotechnology Research Institute, National Institute of Advanced Industrial Science and Technology (AIST), 1-1-1 Higashi, Tsukuba, Ibaraki 305-8565, Japan,

²Research Institute for Ubiquitous Energy Devices, AIST, 1-8-31, Midorigaoka, Ikeda, Osaka 563-8577, Japan,

³Research Center for Advanced Carbon Materials, AIST, 1-1-1 Higashi, Tsukuba, Ibaraki 305-8565, Japan

Dispersant for single-walled carbon nanotubes (SWNT) and SWNT composite gels are potentially important for various applications. We have developed a novel oligomeric electrolyte **1·Cl** as a new structural motif for hydrogelator. Herein we report that **1·Cl** has bifunctional property as a “hydrogelator” and an efficient “dispersant” for SWNT. A mixture of 37.5 mg



of **1·Cl** and 0.5 mg of SWNT (HiPco, CNI) in 5 mL of water was sonicated for 1 hour using a low-power bath sonication (130 W, 35 kHz). A stable dispersion (at least for 6 months) was obtained under those mild conditions. A well-resolved optical absorption spectrum (400-1600 nm) clearly demonstrates that SWNT can be un-bundled and dispersed in an aqueous solution of **1·Cl** (Figure 1a). Dispersion of SWNT using a slightly concentrated solution of **1·Cl** was enough to form a SWNT-containing gel without any other additives (Figure 2). The shape of UV-vis-NIR spectrum of the gel was found to be essentially the same as that of the solution (Figure 1b). We also found that **1·Cl** acted as an amphiphilic dispersant for SWNT in an organic solvent after an exchange of the chloride anions of **1·Cl** by perfluorinated ones.

Acknowledgement. This work was supported by Industrial Technology Research Grant Program in '05 from New Energy and Industrial Technology Development Organization (NEDO) of Japan.

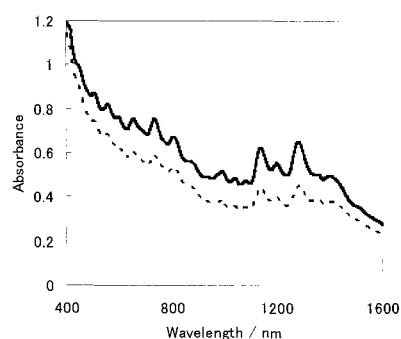


Figure 1. UV-vis-NIR spectra of SWNT in a) the D₂O solution based on **1·Cl** (7.5 g/L) (solid) and b) D₂O gel based on **1·Cl** (20 g/L) (dashed).

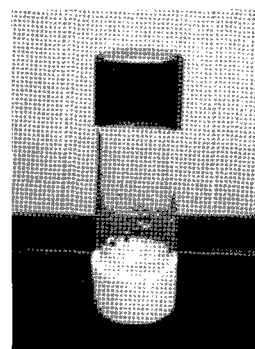


Figure 2. SWNT composite hydrogel prepared by **1·Cl**.

Corresponding Author: Masaru Yoshida

E-mail: masaru.yoshida@aist.go.jp

Tel: +81-29-861-4672, Fax: +81-29-861-4673

Solidification of Lanthanum Carbide-Encapsulating Carbon Nanocapsules

○Ippei Waki¹, Yoshinori Sato¹, Masaru Namura¹, Kenichi Motomiya¹, Balachandran Jeyadevan¹, Akira Okubo², Hisamichi Kimura², and Kazuyuki Tohji¹,

¹*Graduate School of Environmental Studies, Tohoku University, Sendai 980-8579, Japan*

²*Institute of Materials Research, Tohoku University, Sendai 980-8577, Japan*

Mammography screening is one of the test methods to find out the breast cancer. Although the iodinated contrast material is used, the blood capillaries around cancer are not caught well with the present screening techniques. During the radiography, clearer contrasting images can be obtained by characteristic X-rays with an X-ray absorption edge that is shorter than that of the target materials. Lanthanum (La) containing materials are suitable for X-ray target materials as the characteristic X-rays of La are just shorter than the X-ray absorption edge of iodine. X-ray target material requires high melting point, heat conductivity, and electric conductivity. Lanthanum carbide-encapsulating carbon nanocapsules (LaC₂@CNCs), consisting of several graphene sheet capsules, are expected to have higher melting point, heat conductivity and electric conductivity than La or Lanthanum oxide (La₂O₃). Here, we report solidification and evaluation of LaC₂@CNCs.

LaC₂@CNCs were synthesized by a direct current arc-discharge between pure graphite rod and metal-loaded graphite rod. The anode rod was drilled and filled with composite of La₂O₃ and graphite to make rod to contain 1.0 at.% of La. Arc discharge was run with He pressure of 100 Torr and arc-discharge current of 70 A. After arc discharging, the cathode deposit, containing LaC₂@CNCs, was collected and treated with 1M HCl acid to remove La₂O₃. The sample was mixed by satellite mill in dry condition with Lanthanum boride (LaB₆), which is used as a sintering binder. Each composite contained 20, 30, 40, and 50 wt. % of cathode deposit. Spark plasma sintering (SPS) process with the condition of 80 MPa pressure and 1,123 K temperature, was run in an effort to make a sintered solid of 10 mm in diameter. The sintered solid was cut into 1 mm width section, and its electric resistance was measured. The cut surface of sintered solid was observed by scanning electron microscope (SEM). The each result of the sintering solid will be reported in detail and discussed.

Corresponding Author: Ippei Waki

TEL, FAX: +81-22-795-7392, E-mail: waki@bucky1.kankyo.tohoku.ac.jp

3P-1

Reinforcement of Epoxy Composite Sheets by Highly Oriented, Highly-Loaded Single-Walled Carbon Nanotubes

○Hidekazu Nishino, Tatsuki Hiraoka, Takeo Yamada, Don N. Futaba, Kenji Hata*

*Research Center for Advanced Carbon Materials, National Institute of Advanced Industrial
Science and Technology (AIST), 1-1-1 Higashi, Tsukuba, Ibaraki 305-8565, Japan*

Due to their extraordinary high modulus and strength, single-walled carbon nanotube (SWNT) is considered as the most promising reinforcement material to realize high performance composites. (ref.[1]-[2]). For, an individual SWNT, the estimated tensile strength is in the range of 13~53 GPa, and the maximum elastic modulus is close to ~1.5 TPa (ref.[2]), superior than any know existing material. Among polymer composites, high-strength epoxy systems are very important materials for aircraft, automobiles, electronics products, and many other industrial applications. Therefore, many efforts have been carried out to reinforce epoxy composites with SWNTs, which so far has resulted in rather disappointing results.

Here we present a new and rational approach that enables to fabricate well dispersed, highly loaded, and aligned SWNT/epoxy composite sheets made from very pure and long SWNTs. Such SWNT/epoxy composite have shown 2.5 and 3.3 times improvement in tensile strength and elastic modulus when the stress is applied parallel to the alignment direction. The key point to realize such composites was the use of SWNT forests directly grown on flexible metal foils [3]. A forest [4] can be considered as ideally dispersed SWNT material, and SWNTs in these forests are known to be catalyst free, highly aligned, and very long. These features make the SWNT forest a very fascinating starting material to fabricate composites. The challenge is to develop a method to convert the SWNT forests into a composite, with the ability to control the shape of the composite and direction of the alignment of tubes while retaining the fascinating features of forests.

References:

- [1] M. Yu, O. Lourie, M. J. Dyer, T. F. Kelly, R. S. Ruoff, *Science*, 2000, 287, 637.
- [2] M. F. Yu, B. S. Files, S. Arepalli, R. S. Ruoff, *Phys. Rev. Lett.*, 2000, 84, 5552.
- [3] T. Hiraoka, T. Yamada, K. Hata, D. N. Futaba, H. Kurachi, S. Uemura, M. Yumura, S. Iijima, *J. Am. Chem. Soc.* 2006, 128, 13338.
- [4] K. Hata, D. N. Futaba, K. Mizuno, T. Namai, M. Yumura, S. Iijima, *Science* 2004, 306, 1362.

Corresponding Author: Kenji Hata

E-mail: kenji-hata @aist.go.jp

TEL: +81-29-861-4654, **FAX:** +81-29-861-4851

3P-2

DNA-assisted fixation and patterning of carbon nanotubes on glass substrate

○Satoru Shoji^{1,3}, Jun-ichi Jono¹, and Satoshi Kawata^{1,2,3}

¹*Department of Applied Physics, Osaka University, Yamadaoka 2-1, Suita, Osaka 565-0871, Japan*

²*Nanophotonics Laboratory, RIKEN, Wako, Saitama, 351-0198, Japan*

³*CREST, Japan Corporation of Science and Technology, Japan*

For the practical application of mass-produced carbon nanotubes(CNTs) for electrical or optical devices, simple methods to isolate and disperse CNTs, and then organize them into desired patterns are desired. DNA is known as one of good candidate agents to isolate and disperse CNTs in water. In this presentation, we present a method to fix DNA-dispersed CNTs onto a substrate in arbitrary two-dimensional micro-pattern through silane-coupling agent, which is widely used for fixation of biological molecules such as proteins and DNA on glass substrate. A MAS-coated glass plate (Matsunami glass Ind., Ltd.) was used as a substrate, and carbon nanotubes were fixed on the substrate via strong adhesion between MAS and DNA entangled on CNT. First, two-dimensional mask pattern was fabricated with SU-8 photoresist (MicroChem Corp.) on the MAS-coated glass plate by means of photolithography. The solution of DNA-dispersed CNTs was dropped onto the mask pattern and was left for 1 minute. The substrate was then washed with pure water and dried. Figure 1 is a Raman microscope image of the fabricated CNTs stripe pattern. With combination of chirality sorting techniques using DNA reported recently, this method would have a potential for CNT-based nano-electronic device or optical elements.

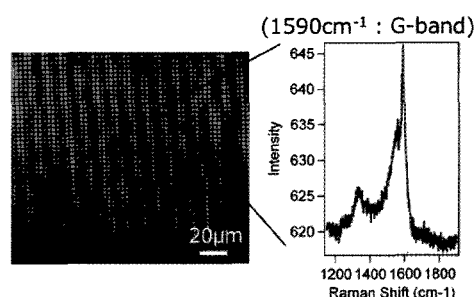


Figure 1 Raman microscope image of the surface of the fabricated CNTs pattern. The image was constructed by mapping the intensity of Raman scattering at 1590cm⁻¹.

Corresponding Author: Satoru Shoji
TEL: +81-6-6879-7847, FAX: +81-6-6879-7330
E-mail: shoji@ap.eng.osaka-u.ac.jp

Temperature Effects on the Optical Properties of SWNTs Dispersed in Aqueous Solutions

○Akina Tanemura, Catalin Romeo Luculescu, Katsumi Uchida,
Tadahiro Ishii, and Hirofumi Yajima

*Department of Applied Chemistry, Faculty of Science, Tokyo University of Science
12-1 Funagawara-machi, Shinjyuku-ku, Tokyo 162-0826, Japan*

Single-walled carbon nanotubes (SWNTs) are one-dimensional tubular carbon structures with various diameters and chiralities. Owing to their outstanding mechanical, electrical and thermal properties, many potential applications have been proposed. However, as a result of strong cohesive van der Waals force between them, SWNTs are easily forming bundles. We have developed the novel dispersion and purification procedures for SWNTs using biopolymers as dispersants [1]. Heller, et al. studied that sonication temperature effects on the dispersion of SWNTs with SDS aqueous solution showed that the relative intensity of chiral structures changed in the intensities of photoluminescence with temperature [2]. It has been known that optical properties of SWNTs are sensitive to the change in the surrounding environments such as temperature and pH [3,4].

In this study, we have investigated with respect to temperature effects on optical characteristic and dispersion behavior of SWNTs. Several dispersed SWNTs aqueous solutions were prepared with biopolymers and surfactants, which have different charges. We used carboxy methyl cellulose (CMC), chitosan, sodium dodecyl sulfate (SDS), and n-tetradecyl trimethyl ammonium bromide as dispersing agents. Then the temperature dependences of the optical properties of the dispersed SWNTs were probed by means of the spectroscopic techniques such as UV-vis-NIR absorption and photoluminescence. The resulting absorption spectra indicated that the peak intensities for S_{11} bands for the dispersed SWNTs were largely changed compared to those of S_{22} bands, regardless of the dispersant species. Using biopolymer as a dispersion agent, absorbance was decreased with increasing temperature. Whereas using SDS, the absorbance was increased with temperature. Likewise, the discrepancy between the biopolymers and surfactants appeared in the pH effects. Those phenomena are suggested to be attributed to the difference in the structural features of the complexation of SWNTs with the dispersants involved in the dispersion behavior of SWNTs.

References:

- [1] T.Takahashi, C.R.Luculescu, K.Uchida, T.Ishii and H.Yajima, *Chem.Lett.* **11**, 1516 (2005)
- [2] D.A.Heller, P.W.Baron, and M.S.Strano, *Carbon* **43**, 651 (2005)
- [3] L-J.Li, R J Nicholas, C-Y. Chen, R C Darton and S C Baker, *Nanotechnology* **16**, S202 (2005)
- [4] P.Finnie, Y.Homma and J.Lefebvre, *Phys. Rev. Lett.* **94**, 247401 (2005)

Corresponding Author: Hirofumi Yajima

E-mail: yajima@rs.kagu.tus.ac.jp

TEL: +81-3-3260-4272(ext.5760) **FAX:** +81-3-5261-4631

Ion beam modification of CNTs/chitosan composite film for cell attachment control

ORumi Shizume¹, Katsumune Takahashi¹, Katsumi Uchida¹,
Yoshiaki Suzuki² and Hirofumi Yajima¹

¹*Department of Applied Chemistry, Tokyo University of Science,
12-1 Funagawara-cho, Ichigaya, Shinjuku-ku, Tokyo 162-0826, Japan*

²*Advanced Development and Supporting Center, RIKEN,
2-1 Hirosawa, Wako, Saitama, 351-0198, Japan*

Recently, the field of tissue engineering has rapidly developed with much efforts being concentrated on the attachment control of cells to the scaffolds such as collagen and PLLA. Additionally, it has been known that the proliferation and differentiation of cells on their scaffolds can be controlled by the surface roughness of materials, and the electric, optical, or mechanical stimulation. We have proposed that cellular behavior would be controlled by utilizing electric, mechanical properties and luminescence characteristics of single carbon nanotubes (SWNTs). In our previous study, it has been found that chitosan was a useful dispersant for SWNTs [1]. The objective of this study is to fabricate a novel stimulus-responsive cell culture material by using SWNTs/chitosan composite film (SCF), combined with ion beam modification. Ion beam irradiation technique is well known as a powerful way to change physicochemical properties of the surfaces without affecting the bulk properties. Suzuki et al. reported that ion beam irradiation to polymer surfaces brings about the improvement of their biocompatibility [2].

The purified HiPco SWNTs from Carbon Nanotechnologies Inc. were used without further purification. SWNTs were mixed with chitosan/2 % acetic acid solution and then treated using an ultrasonic disruptor for 1 hour. The obtained SWNTs dispersions were ultracentrifuged at 163,000g to remove large SWNTs' bundles. SCF was prepared by casting supernatant solution on glass substrates. SCF were irradiated at an energy of 150 kV-Kr⁺ ion with fluences of 1x10¹³, 1x10¹⁴ and 1x10¹⁵ ions/cm² using RIKEN 200 kV ion implanter. Raman spectroscopic analysis showed that the intensity ratio of G band to that of D band with the increase in the fluences, accompanied by the formation of amorphous carbon. This finding was supported by the results of XPS analysis. Amorphous carbon phase is suggested to be constructed as a result of destruction of chitosan and SWNTs structures by ion beam irradiation. Cell attachment test was performed using bovine aortic endothelial cells. Results of 24 hour cultivation indicated that cell attachment was improved on the only sample irradiated with a fluence of 1x10¹⁵ ions/cm² compared with non-irradiated SFC. Consequently, it is inferred that amorphous carbon phase induced by ion beam irradiation is significantly involved in cell attachment, which would be controlled by Kr⁺ ion beam irradiation.

[1] T. Takahashi et al *Chemical Letters*.**11** (2005) 1516

[2] Y. Suzuki *Nuclear Instruments and Methods in Physics Research B* 206 (2003) 501

Corresponding Author: Hirofumi Yajima

TEL: +81-3-3260-4272 (ext.5760), FAX: +81-3-5261-4631, E-mail: yajima@rs.kagu.tus.ac.jp

Metal vapor deposition onto vertically aligned single-walled carbon nanotubes and bonding to metal surfaces

○ Makoto Watanabe, Kazuaki Ogura, Kei Ishikawa, Jun Ookawa,
Erik Einarsson, Shigeo Maruyama

Department of Mechanical Engineering, The University of Tokyo, Tokyo 113-8656, Japan

Vertically aligned single-walled carbon nanotubes (VA-SWNTs) possess unique properties, including superhydrophobicity [1, 2] and high thermal conductivity. With the aim of using these properties to study convective heat transfer and phase change phenomena at a VA-SWNT surface, we have attempted to firmly bond VA-SWNT films to a metal surface by first depositing a thin metal layer onto VA-SWNT surface, and then welding the thin metal layer to a bulk metal surface by high-temperature annealing. Firm bonding between the metal block and the VA-SWNT film was confirmed.

VA-SWNTs were synthesized on quartz [3, 4] by the alcohol CVD method [5]. After synthesis, a 100 nm gold film was deposited onto the VA-SWNTs by vacuum vapor deposition. A cross-sectional SEM image is shown in Fig. 1. From this image, we can see that gold particles have penetrated between the bundles, reaching approximately 1 μm into the VA-SWNT film. A substantial crust of gold has accumulated on the top of the film. After deposition, the sample (Au-coated VA-SWNT film + quartz substrate) was set inside the experimental apparatus (Fig. 2a). A diagram of the inside of the sample chamber is shown in Fig. 2b. With a piece of bonding material between the base heating block and Au-deposited VA-SWNTs, the sample was adhered to the base by annealing between 600 and 850 $^{\circ}\text{C}$ under flowing argon gas. The quartz substrate was then removed using the simple and easy hot-water assisted film transfer technique developed by our group [1, 2], leaving behind the securely attached VA-SWNT film.

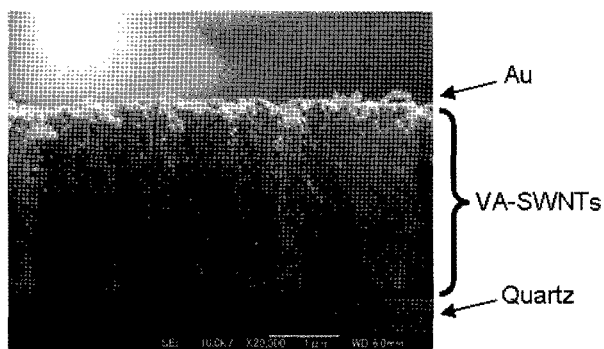


Fig.1: SEM image showing Au deposited onto a VA-SWNT film by vacuum vapor deposition.

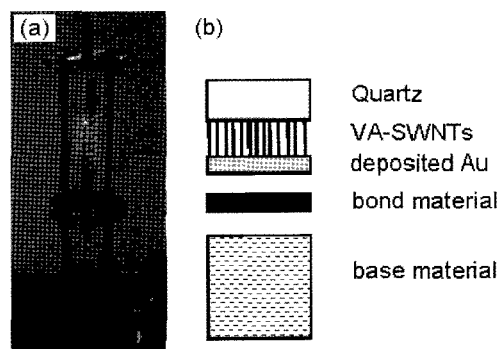


Fig.2: (a) photo of experimental apparatus and (b) diagram of sample chamber interior.

- [1] Y. Murakami and S. Maruyama, *Chem. Phys. Lett.* **422**, 575 (2006).
- [2] M. Watanabe et al., *Proc. 43rd Nat. Heat Transfer Symp. Japan* **1**, 193 (2006).
- [3] Y. Murakami, S. Chiashi, Y. Miyauchi, M. Hu, M. Ogura, T. Okubo, S. Maruyama *Chem. Phys. Lett.* **385**, 298 (2004).
- [4] S. Maruyama, E. Einarsson, Y. Murakami, T. Edamura, *Chem. Phys. Lett.* **403**, 320 (2005).
- [5] S. Maruyama, R. Kojima, Y. Miyauchi, S. Chiashi, M. Kohno, *Chem. Phys. Lett.* **360**, 229 (2002).

Corresponding Author: Shigeo Maruyama

TEL: +81-3-5841-6421, FAX: +81-3-5800-6983, E-mail: maruyama@photon.t.u-tokyo.ac.jp

Dependence of the isolation of SWNTs by DNA wrapping on their diameter

○S.Toita, D.Kang, K.Kojima, M.Tachibana

*International Graduate School of Arts and Science, Yokohama City University,
22-2seto, Kanazawa-ku, Yokohama 236-0027, Japan*

The production of DNA-wrapped single-wall carbon nanotubes (DNA-SWNT hybrids) has triggered to a big advance in the techniques of isolation or separation of SWNTs required for many applications. The characterization of DNA-SWNT hybrids by Raman, photoluminescence (PL), and optical absorption spectroscopies, and atomic force microscopy (AFM) has been carried out by many groups. Some of recent researches are shown in Ref. 1-4. For their applications, the mechanism of the interaction between DNA and SWNT, and the isolation of SWNTs by DNA wrapping need to be understood. In this paper, we report the dependence of the isolation of SWNTs by DNA wrapping on their average diameter.

HiPco and arc-discharge produced SWNTs with average diameter of 0.9 nm and 1.4 nm, respectively, were used as starting materials. 1 mg of SWNTs was mixed in 1 ml aqueous double-stranded DNA solution where the DNA was extracted from salmon's testis. After the mixture was sonicated on ice, the samples were centrifuged to remove insoluble materials, leaving DNA-SWNT hybrid solution. The isolation of SWNTs was examined by photoluminescence and optical absorption measurements, and AFM observation.

HiPco SWNTs by DNA wrapping in solution exhibited strong photoluminescence. Note that the observation of photoluminescence of SWNTs is an indicator of their isolation. It should be noted that no photoluminescence was observed for arc SWNTs with larger diameter by DNA wrapping in solution. This indicates that the isolation of arc SWNTs with larger diameter can not occur by DNA wrapping. These results will provide an important insight for the understanding of the mechanism of the isolation of SWNTs by DNA wrapping. The mechanism will be discussed with the AFM observation.

- [1] H. Kawamoto et al. Chem. Phys. Lett. 431, 118 (2006).
- [2] H. Kawamoto et al. Chem. Phys. Lett. 432, 172 (2006).
- [3] H. Cathcart et al. J. Phys. Chem. C, 111, 66 (2007).
- [4] C. Fantini et al. Chem. Phys. Lett. 439, 138 (2007).

Corresponding Author: Masaru Tachibana

E-mail: tachiban@yokohama-cu.ac.jp

Tel: +81-45-787-2307, Fax: +81-45-787-2172

Stable Dispersion of Single-Wall Carbon Nanotubes by a Protein

○Takeshi Tanaka¹, Hehua Jin¹, Tadayuki Imanaka², Shinsuke Fujiwara³, Hiromichi Kataura¹,

¹*Nanotechnology Research Institute, National Institute of Advanced Industrial Science and Technology (AIST), 1-1-1 Higashi, Tsukuba, Ibaraki 305-8562, Japan,*

²*Department of Synthetic Chemistry and Biological Chemistry, Graduate School of Engineering, Kyoto University, Katsura, Nishikyo-ku, Kyoto 615-8510, Japan,*

³*Department of Bioscience, Nanobiothechnology Research Center, School of Science and Technology, Kwansai Gakuin University, 2-1 Gakuen, Sanda, Hyogo 669-1337, Japan*

Besides applications of carbon nanotube (CNT) to electronic devices, medical applications attract a great deal of attention. When CNT is used as drug or drug carrier, it is very useful that CNTs are modified by proteins which specifically bind the target molecules. As far as we know, only two kinds of protein have been reported to disperse CNTs [1, 2]. Here we report the novel protein which can disperse CNTs. The protein is prefoldin. In the living organisms, the function of prefoldin is to be bound to surface-exposed hydrophobic regions of proteins of which structures are incorrect and to stabilize the proteins to prevent from degradation. So it was expected that prefoldin could bind the hydrophobic surface of CNTs and disperse CNTs well (Fig. 1).

We prepared the prefoldin from hyperthermophilic microorganism by conventional genetic engineering methods. Recombinant proteins were produced in *Escherichia coli* cells and purified. The purified prefoldin and HiPco-CNT were used for CNT dispersion experiment. We found the ability of prefoldin to disperse CNTs at concentrations higher than 0.05% protein. The amount of CNTs dispersed by prefoldin was higher than that of bovine serum albumin but lower than that of lysozyme. Detail comparison between prefoldin and lysozyme was performed at the various pHs and salt concentrations. At pH around pI of prefoldin, the protein could not disperse CNTs as reported on lysozyme. Addition of salt above 10 mM NaCl, in the case of lysozyme, caused the disappearance of dispersibility. On the other hand, prefoldin could disperse CNTs to a similar extent up to 10 mM NaCl, and even at 100 to 1000 mM NaCl retained about 40% dispersibility compared to no addition of the salt. Since the concentration of physiological saline or blood is 150 mM NaCl, prefoldin should be applied to stably disperse and functionalize CNTs in the human body for medical uses.

[1] D. Nepal and K. E. Geckeler, *Small*, **2**, 406 (2006).

[2] K. Matsuura, T. Saito, T. Okazaki, S. Ohshima, M. Yumura and S. Iijima, *Chem. Phys. Lett.*, **429**, 497 (2006).

Corresponding Author: Takeshi Tanaka

TEL: +81-29-861-2903, FAX: +81-29-861-2786,

E-mail: tanaka-t@aist.go.jp

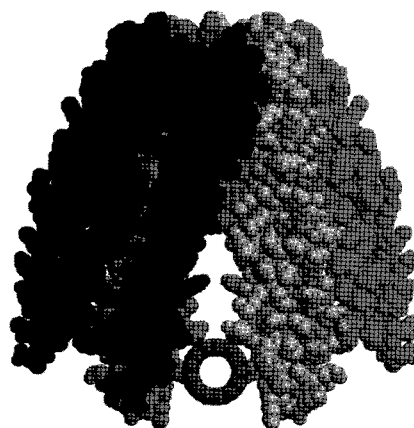


Fig. 1 Binding model of CNT and prefoldin

Solubilization of Carbon Nanotubes by Using a *meso-meso* Linked Zn^{II} Porphyrin

○Kenichi Watanabe, Tsuyohiko Fujigaya, and Naotoshi Nakashima

Department of Applied Chemistry, Graduate School of Engineering, Kyushu University, 744 Motoooka, Nishi-ku, Fukuoka 819-0395, Japan

We already have reported that zinc protoporphyrin IX (ZnPP) dissolve single-walled carbon nanotubes (SWNTs) in organic solutions as long as excess porphyrin is present in solution [1]. However, upon removal of excess ZnPP, it was found that the ZnPP-nanotube complex precipitates within a few days.

Polymerized solubilizer is proved to give more stable dispersion than monomeric one [2]. From the result, polymeric porphyrin is expected to lead the more stable dispersion.

Herein, we designed and synthesized *meso-meso* linked porphyrin (**1**) as described in the literatures [3]. And we carried out solubilization in organic solvents and characterize the *meso-meso* linked porphyrin-SWNTs composites. By means of UV-vis-NIR absorption spectra measurements, it was revealed that compound **1** could disperse SWNTs in DMF solution (**Figure 2**).

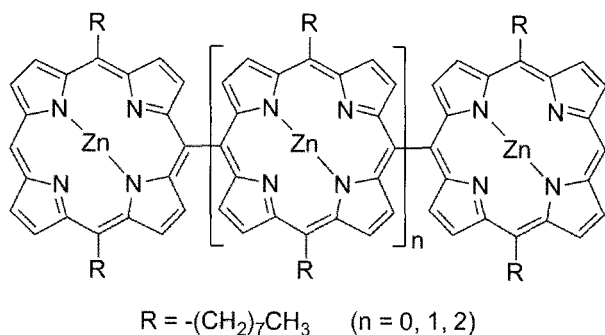


Figure 1. Chemical structure of **1**

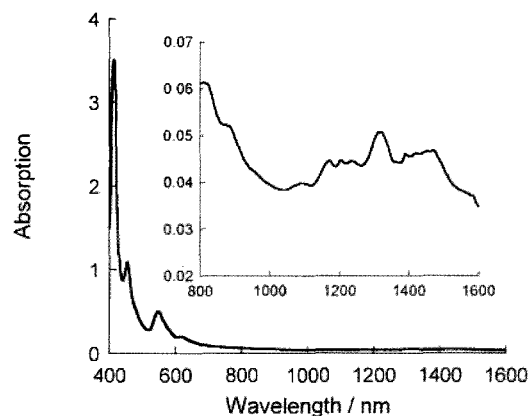


Figure 2. Absorption spectra of SWNTs solubilized with compound **1**.

References

- [1] H. Murakami, T. Nomura, N. Nakashima, *Chem. Phys. Lett.*, **378**, 481 (2003).
 [2] N. Nakashima, S. Okuzono, Y. Tomonari, and H. Murakami, *Trans. Mater. Res. Soc. Jpn.* **29**, 525. (2004).
 [3] (a) A. Osuka, and H. Shimizu, *Angew. Chem. Int. Ed.*, **36**, 135 (1997). (b) A. Tsuda, A. Nakano, H. Furuta, H. Yamochi, A. Osuka, *Angew. Chem. Int. Ed.*, **39**, 558 (2000). (c) A. Tsuda, H. Furuta, A. Osuka, *Angew. Chem. Int. Ed.*, **39**, 2549 (2000).

Corresponding Author: Naotoshi Nakashima

E-mail: nakashima-tcm@mbox.nc.kyushu-u.ac.jp

Tel&Fax: (+81)-92-802-2840

Field Effect Chromatography that Separates Metallic and Semiconducting Carbon Nanotubes

○Masahito Sano and Keisuke Wada

Department of Polymer Science and Engineering, Yamagata University 992-8510, Japan

A separation of metallic and semiconducting carbon nanotubes (CNTs) is of primary importance for fundamental researches as well as applications, particularly, in electrical and optical fields. The separation methods reported so far are based on kinetic differences in chemical reactivity or adsorption, electrophoresis, and centrifugation in solution phase. Here, we report a novel chromatographic technique that can concentrate metallic CNTs by simply letting the mixture flow through a specifically designed column.

Chromatography is a separation technique widely used in chemistry and biology. A mixture to be separated is poured from one end of a column which is filled with a specially designed packing material. The packing material should have a property that the time takes to flow through the column depends on each component of the mixture. Then, solutions coming out of another end at different times contain different amounts of each component. For instance, the packing material may be beads with many nanopores through which only small molecules can enter. Because large molecules cannot enter the pores, the small molecules spent more time in beads. Consequently the large molecules flow through the column faster. Thus, the solution that comes out of the column earlier contains more large molecules.

In this study, we use DC electric field and non-uniform flow to discriminate CNT electronic types. Previously, we have shown that only semiconducting CNTs are electrodeposited on anode surface by DC electric field in anhydrous conditions [1, 2]. In contrast, multi-walled CNTs, which are mostly metallic, are seen to oscillate between the anode and cathode surfaces under certain conditions. These observations indicate that metallic and semiconducting CNTs have different motions across the electrodes under DC electric field. If non-uniform flow is applied between the electrodes perpendicular to the electric field, one component can be carried down faster than another by the flowing liquid.

As a primary study, single-walled CNTs dispersed in an anhydrous organic solvent was placed at the top of the parallel plate electrodes. With a constant supply of the solvent from the top, the dispersion was flown down between the electrodes with DC electric field. The geometry and the flow speed were adjusted so that the liquid near the middle of electrodes flown faster than one near the electrode surfaces. The solution coming out of the bottom of the electrodes was collected by small portions in a consecutive order. Raman spectroscopy showed that a ratio of the metallic to semiconducting peaks is larger for portions that have come out earlier. Thus, we are able to demonstrate that the proposed mechanism can be used to construct a chromatography system for separations of CNTs by electronic types.

[1] Abe, Y., Tomuro, R., Sano, M.; *Adv. Mater.* **17**, 2192-2194 (2005).

[2] Tomuro, R., Matsumoto, T., Sano, M.; *Jpn. J. Appl. Phys.*, **45**, L578-L581 (2006).

Corresponding Author: Masahito Sano

E-mail: mass@yz.yamagata-u.ac.jp

Tel&Fax: +81-238-26-3072

Separation of Metallic Single-walled Carbon Nanotubes and Preparation of Transparent and Conductive Thin Films from the Nanotubes

○ Yutaka Maeda, Masahiro Hashimoto, Tadashi Hasegawa, Makoto Kanda, Takahiro Tsuchiya, Takatsugu Wakahara, Takeshi Akasaka, Said Kazaoui, Nobutsugu Minami, Shigeo Maruyama, and Shigeru Nagase

^aDepartment of Chemistry, Tokyo Gakugei University, Tokyo 184-8501, Japan, ^bPRESTO, Japan Science and Technology Agency, 4-1-8 Honcho Kawaguchi, Saitama 332-0012, Japan, ^cCenter for Tsukuba Advanced Research Alliance, University of Tsukuba, Ibaraki 305-8577, Japan, ^dNational Laboratory of Advanced Industrial Science and Technology, Ibaraki 305-8565, Japan, ^eGraduate School of Engineering, The University of Tokyo, Tokyo 113-8656, Japan, ^fDepartment of Theoretical Molecular Science, Institute for Molecular Science, Aichi 444-8585, Japan

Many potential applications of single-walled carbon nanotubes (SWNTs) have been extensively expected because of their excellent mechanical and electrical properties. However, SWNTs are typically grown as the bundles of metallic and semiconducting SWNTs (m- and s-SWNTs), which is a hindrance to their widespread applications. Since there is no method for selective preparation of SWNTs having specific electrical properties, it is technologically important to separate m-SWNTs and s-SWNTs.¹ The chemical vapor deposition (CVD) method attracts broad attention for one of possible low-cost and large-scale production of SWNTs. We herein report separation of SWNTs produced by several CVD methods and preparation of transparent and conductive thin films made of SWNTs and m-SWNTs, respectively.

A typical procedure for separation of m-SWNTs is as follows: 1mg of SWNTs was added to 10 mL of a tetrahydrofuran (THF) solution containing amine, and then sonicated for 2 hours followed by centrifugation (45 kG).^{2,3} The absorption, photoluminescence, and Raman spectroscopies showed that separation of m-SWNTs from SWNTs was achieved effectively by our method.

Transparent and conductive thin films were prepared by spraying SWNTs dispersion onto substrate with an airbrush. The thin films were characterized by UV-vis spectroscopy and a 4-point probe conductivity measurement. Compare to the films made of SWNTs as received, m-SWNTs films are 10 times more conductive at same transmittance.

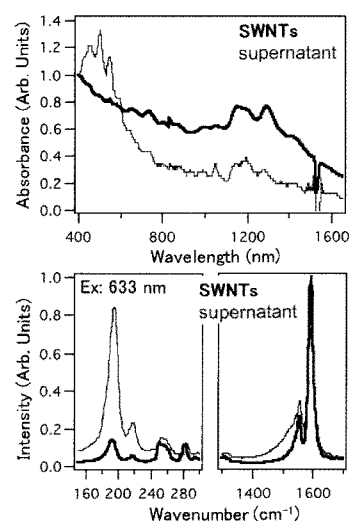


Figure. Vis-NIR and Raman spectra of SWNTs dispersion and supernatant.

References:

- [1] An, K. H. et al., *Nano* **2006**, *1*, 115.
- [2] Maeda, Y. et al., *J. Phys. Chem. B* **2004**, *108*, 18395.
- [3] Maeda, Y. et al., *J. Am. Chem. Soc.* **2005**, *127*, 10287. Maeda, Y. et al., *J. Am. Chem. Soc.* **2006**, *128*, 12239.

Corresponding Author: Yutaka Maeda

E-mail: ymaeda@u-gakugei.ac.jp, Tel&Fax: +81-42-329-7512

Characterization of SWNT Thin Films Deposited by Dry-Process

○Takeshi Saito^{1,2}, Satoshi Ohshima¹, Shigekazu Ohmori¹,
Motoo Yumura¹ and Sumio Iijima^{1,3}

¹ *Research Center for Advanced Carbon Materials, National Institute of Advanced Industrial Science and Technology (AIST), Tsukuba 305-8565, Japan*

² *PRESTO, Japan Science and Technology Agency, Kawaguchi 332-0012, Japan*

³ *Department of Materials Science and Engineering, 21st century COE (Nanofactory), Meijo University, Nagoya 468-8502, Japan*

Single-walled carbon nanotubes (SWNTs) conduct electricity well, which could make them promising for many electronic applications, such as transistor, chemical sensor, solar cell, and so on. However, manufacturing devices using single SWNT is expensive and suffers from reliability problems. Recently, it was found that the thin film constructed by networks of SWNTs could perform a variety of basic electronic functions [1]. The thin film of SWNTs has prepared by wet process using dispersion of SWNTs so far, but that is not generally as easy as it sounds. Once SWNTs are mixed in solvents, they tend to bundle together, requiring surfactants to keep them isolated. It should be expected that surfactants would give an impediment to the electronic conductivity. Therefore development of the dry process for preparing homogeneous thin films of isolated SWNTs is eagerly anticipated.

Here we have tried to develop a dry-process of depositing the thin film of SWNTs synthesized by the enhanced direct injection pyrolytic synthesis (e-DIPS) method. The morphology and optical properties of the SWNT film will be discussed in detailed.

[1] G. Gruner, Scientific American, pp. 76-83, May 2007.

Corresponding Author: Takeshi Saito

TEL: +81-29-861-4863, FAX: +81-29-861-3392, E-mail: takeshi-saito@aist.go.jp

Damage-free Surface Modification of Carbon Nanotubes using Advanced Neutral Beam

○Akira Wada¹, Yoshinori Sato², Masahiko Ishida³,
Fumiyuki Nihey³, Kazuyuki Tohji² and Seiji Samukawa¹

¹*Institute of Fluid Science, Tohoku University, Sendai 980-8577, Japan*

²*Graduate School of Environmental Studies, Tohoku University, Sendai 980-8579, Japan*

³*Fundamental and Environmental Research Laboratories,
NEC Corporation, Tsukuba, 305-8501, Japan*

In an effort to realize carbon nanotube (CNT) FET, it is necessary to modify electric characteristic of grown CNTs by using plasma process. However, the conventional plasma process damages CNTs because charged particles and ultraviolet photons are irradiated to the CNTs. As a result, the CNT FET could not be practically fabricated using conventional plasma processes. Here, we have proposed damage free surface modification by using our developed neutral beam to resolve the problems and to practically fabricate the CNT FET without any damages. Neutral beam can almost eliminate irradiation of charged particles and ultraviolet photons to CNTs. In this study, we irradiated Ar plasma and Ar neutral beam to single-walled carbon nanotubes (SWCNTs). Raman spectra confirmed that the intensity ratio of D-band/G-band in SWCNTs irradiated by neutral beam was still kept at the same as that with no beam irradiation. Conversely, the intensity ratio of D-band/G-band was drastically increased by conventional plasma irradiation. Transmission electron microscopy could also confirm that SWCNTs did not have any damages after the neutral beam irradiation, whereas SWCNTs was destroyed by conventional plasma irradiation. Neutral beam process is very promising candidate for future CNT FET fabrication processes.

Corresponding Author: Seiji Samukawa

TEL: +81-22-217-5240, FAX: +81-22-217-5240, E-mail: samukawa@ifs.tohoku.ac.jp

The New Feature Development of Carbon Nanotubes-Polybenzimidazole Composite

○Minoru Okamoto, Tsuyohiko Fujigaya and Naotoshi Nakashima

*Department of Applied Chemistry, Graduate School of Engineering
Kyushu University, Fukuoka, Japan*

Carbon nanotubes (CNTs) have expected in most areas of science and engineering due to their mechanical properties, electrical properties and so on[1]. But, the application of CNTs is limited because they form bundles each other and possess poor solubility in any solvents. Many researches of dispersing CNTs in solvent and preparing CNTs-polymer composites has been reported[2]. In this time, we focus on Polybenzimidazole (PBI) as polymer materials. PBI is used as super engineering plastic because of the heat stability. In addition, PBI is expected to apply for solid polymer electrolyte membrane of fuel cells.

First, we examined if PBI can solubilize CNTs in solvent. CNTs were added to the solution which PBI was dissolved in dimethyl sulfoxide (DMAc). This solution was sonicated to dissolve CNTs, followed by centrifugation. Fig.1 (A) shows the absorption spectra of the suspension after centrifugation. For comparison, the same operation without PBI was carried out and absorption spectra is shown in Fig.1 (B).

In the case of the solution including PBI (Fig.1 (A)), the characteristic spectral features due to dissolved CNTs were clearly observed in the near-IR region. On the other hand, the characteristic absorption due to CNTs was not observed in the absence of PBI (Fig.1 (B)). This means PBI can act as solubilizer for CNTs. It is attributed that the π - π interaction between PBI and CNTs plays an important role for debandling of CNTs.

Next, the CNTs-PBI composite films and PBI films were prepared by spreading each solution on a glass plate and the solvent was evaporated, (Fig.2). The tensile strength and Young's modulus of each film was measured, and found that those of CNTs-PBI composite film is about 1.6 times higher than PBI film without CNTs.

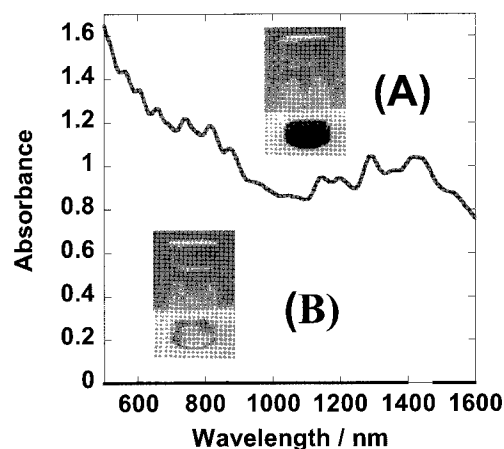


Fig.1 Vis-NIR spectra of CNTs solution (A) with PBI (B) without PBI.

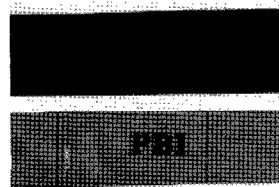


Fig.2 CNTs-PBI composite film and PBI film.

[1] D.Tasis, N. Tagmatarchis, A. Bianco, M. Prato, *Chem. Rev.*, 106, 1105 (2006).

[2] J. N. Coleman, U. Khan, Y. K. Gun'ko, *Adv. Mater.*, 18, 689 (2006).

Corresponding Author: Naotoshi Nakashima

TEL/FAX: +81-92-802-2840, E-mail: E-mail: nakashima-tcm@mbox.nc.kyushu-u.ac.jp

Teas Solution Individually Solubilizes Single-walled Carbon Nanotubes

○Genki Nakamura, Kaori Narimatsu, Naotoshi Nakashima

*Department of Applied Chemistry, Graduate School of Engineering, Kyushu University,
744 Motoooka, Nishi-ku, Fukuoka 819-0395, Japan*

Carbon nanotubes (CNTs) are insoluble in solvents due to their strong intertube van der Waals interactions. Therefore, strategic approaches toward the solubilization of CNTs are highly important in wide fields including chemistry, physics, biochemistry, biology, and pharmaceutical and medical science. Our interest focused on the fundamental and applications of soluble carbon nanotubes in aqueous and organic systems.² We³ and others⁴ have already described that compounds (including polymers) bearing a condensed polycyclic aromatic moiety such as pyrene, anthracene, porphyrin, or polyimide group dissolve CNTs in water or in organic compounds. Double-⁵ and single⁶ stranded-DNAs that are biological compounds carrying polycyclic aromatic moieties are also good CNTs solubilizers in water.

We present here new CNTs solubilizers, that is, teas, which contains numerous components with antioxidant activity including polyphenols, minerals, and vitamins. Catechins⁷ are typical polyphenols that are contained in tea, so we tested catechins to dissolve CNTs. We used single-walled carbon nanotubes (SWNTs) as CNTs since individually dissolved SWNTs show characteristic structural spectral features in the near-IR region.

[1] S. Iijima, *Nature* **1991**, 354, 56.

[2] N. Nakashima, N. *International J. Nanoscience* **2005**, 4, 119.

[3] N. Nakashima, Y. Tomonari, H. Murakami, *Chem. Lett.* **2002**, 31, 638.

[4] H. Paloniemi, T. Ääriralo, T. Laiho, H. Like, N. Kocharova, K. Haapakka, F. Terzi, R. Seeber, J. Lukkari, *J. Phys. Chem. B* **2005**, 109, 8634.

[5] N. Nakashima, S. Okuzono, H. Murakami, T. Nakai, K. Yoshikawa, *Chem. Lett.* **2003**, 32, 456.

[6] M. Zheng, A. Jagota, E. D. Swmke, B. A. Diner, R. S. Mclean, S. R. Lustig, R. E. Richardson, N. G. Tassi, *Nat. Mater.* **2003**, 2, 338.

[7] N. Ihara, Y. Tachibana, J. E. Chung, M. Kunrisawa, H. Uyama, S. Kobayashi, *Chem. Lett.* **2003**, 32, 816.

Corresponding Author: Naotoshi Nakashima

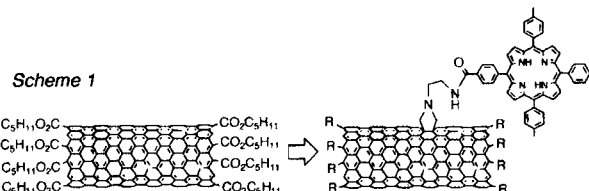
Tel&Fax: 092-802-2840, E-mail: nakashima-tcm@mbox.nc.kyushu-u.ac.jp

Side-wall attachment of porphyrins to the "shortened and esterified" carbon nanotubes

○ Toru Arai, Shingo Nobukuni, Kohsuke Takahashi, Yoshikazu Shimote

*Department of Applied Chemistry, Faculty of Engineering,
Kyushu Institute of Technology, Kitakyushu 804-8550, Japan*

The conjugates of fullerene and porphyrin have been widely studied as potential photoactive devices [1]. However, carbon nanotubes (CNTs)



covalently linked to porphyrins have been limitedly investigated [2,3]. Here we report the synthesis and photochemistry of porphyrin-linked, "shortened and esterified" CNTs.

The SWCNT sample (Aldrich) was sonicated in $\text{HNO}_3 / \text{H}_2\text{SO}_4$. Then $-\text{COOH}$ at the tip of the shortened CNT was converted to pentyl ester (Scheme 1) [4]. Aminoethyl group was grafted via the pyrrolidine ring [3]. Then porphyrin with $-\text{COCl}$ was coupled to yield the porphyrin-linked CNT, which was isolated by silica-gel column chromatography (CHCl_3 -DMF). These modifications of CNTs were characterized by IR and TGA/DSC. The shortening of CNTs could be monitored by MALDI-TOF-MS; the signals at $\sim m/z = 50\ 000$ increased with the progress of the reaction.

UV-vis spectra of the porphyrin-linked CNT (Figure 1a) shows the absorption of porphyrins (419 nm). The emission spectrum of this sample (Figure 1b solid line, $\lambda_{\text{ex}} = 419$ nm) seemed to be a sum of the CNT emission (broad signal at 500~600 nm) and the porphyrin emissions (653 and 720 nm). Interestingly, the porphyrin emission from the porphyrin-linked CNT little differs from the emission of the reference porphyrin (Figure 1b broken line), which indicate a weak interaction between porphyrin and CNT in our porphyrin-linked CNT.

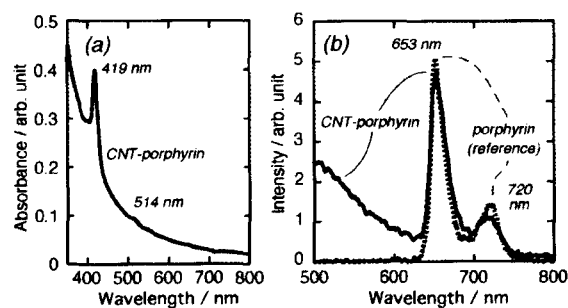


Figure 1 (a) UV-vis and (b) emission spectra ($\lambda_{\text{ex}} = 419$ nm) of porphyrin-linked CNT in DMF.

[1] H. Imahori, *Bull. Chem. Soc. Jpn.*, **80**, 621 (2007).

[2] D. Baskaran *et al.*, *J. Am. Chem. Soc.*, **127**, 6916 (2006).

[3] H. Imahori *et al.*, *Abstracts of the 31st Fullerene-Nanotubes General Symposium*, 3-14.

[4] R. E. Smalley *et al.*, *Science*, **280**, 1253 (1998); H. Garcia *et al.*, *Chem. Phys. Lett.*, **386**, 342 (2004).

Corresponding Author: Toru Arai, Tel and Fax: +81-93-884-3303, E-mail: arai@che.kyutech.ac.jp

Simultaneous Spectroscopy of Photoluminescence and Photocurrent of Individual Carbon Nanotubes in Field-Effect Transistor

○Atsushi Kobayashi¹, Yutaka Ohno^{1,2}, Shigeru Kishimoto¹, and Takashi Mizutani¹

¹*Department of Quantum Engineering, Nagoya University, Nagoya 464-8603, Japan*

²*PRESTO, Japan Science and Technology Agency, Saitama 332-0012, Japan*

Semiconducting single-walled carbon nanotubes (SWNTs) are promising for optical functional materials because they have a near-ideal 1D electronic state and direct bandgap. Photoluminescence (PL) and photocurrent (PC) spectroscopy are useful techniques to study not only 1D exciton physics but also carrier transport phenomenon in SWNTs. [1] In this study, we have simultaneously investigated PL and PC of individual SWNTs in field-effect transistor (FET).

The device has SWNTs bridging over a trench formed on SiO₂/Si substrate, as shown in Figure 1. The both width and depth were $\sim 2 \mu\text{m}$. The metal catalyst pattern, Co/Pt (2/10 nm), were formed on both sides of the trench. The metal catalysts were also used as the source and drain electrodes. SWNTs were synthesized by alcohol chemical vapor deposition technique. A Ti/Sapphire laser was used for an excitation source. The diameter of incident laser spot on the device surface was $\sim 2 \mu\text{m}$, which enable the measurements of a single SWNT.

Biasing the device at off-state, we could obtain PL and PC of a SWNT simultaneously, as shown in Figure 2. These excitation spectra showed good correlation. With increasing the drain bias, PL intensity collapsed and PC increased. We have estimated the optical absorption cross-section of a single free-standing SWNT from the PC.

[1] Y. Ohno, S. Kishimoto and T. Mizutani, *Nanotechnol.* **17**, 549 (2006)

Corresponding Author: Yutaka Ohno

TEL and FAX: +81-52-789-5387, E-mail: yohno@nuee.nagoya-u.ac.jp

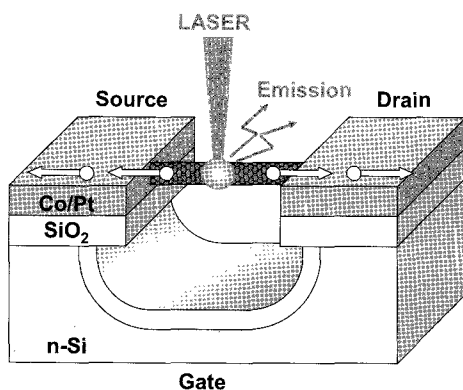


Fig.1 Schematic diagram of PL and PC in nanotube FET.

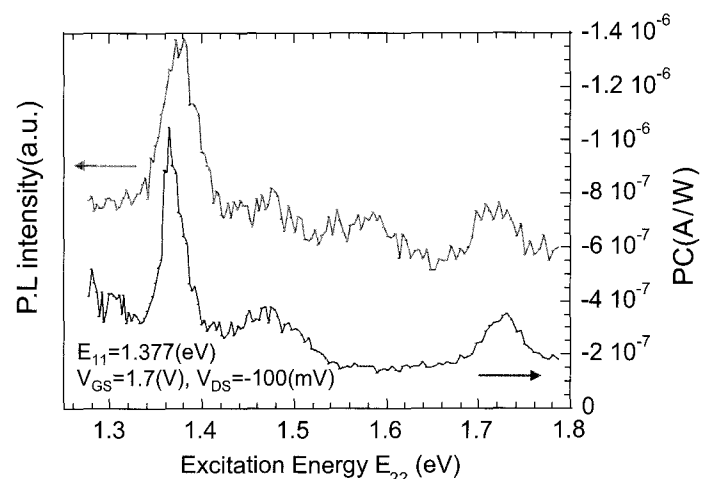


Fig.2 Excitation spectra of the PL and PC of a single SWNT.

Bundle Reconstruction of Isolated Single Wall Carbon Nanotubes

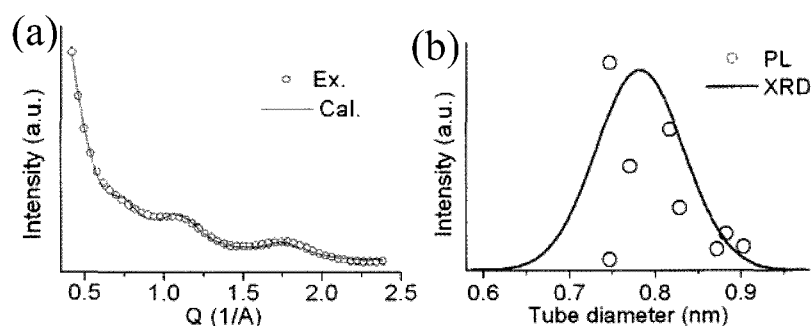
○ Yasumitsu Miyata^{1,2}, Kazuhiro Yanagi², Yutaka Maniwa¹ and Hiromichi Kataura²

¹*Department of Physics, Tokyo Metropolitan University, 1-1 Minami-Osawa, Hachioji, Tokyo 192-0397, Japan*

²*Nanotechnology Research Institute (NRI), National Institute of Advanced Industrial Science and Technology (AIST), 1-1-1 Higashi, Tsukuba 305-8562, Japan*

One of the important issues for understanding of the physical properties of single wall carbon nanotubes (SWCNTs) is the correct characterization of the distribution in both tube diameter and chiral angle. Since the first report on the chirality-assigned optical spectra of individual SWCNTs by Bachilo et al., [1] photoluminescence (PL) and resonance Raman spectroscopy have been widely used for the characterization of the detailed composition of SWCNTs. For example, the PL analysis suggests that the CoMoCAT method mainly produces the specific chiralities, such as (6,5) and (7,5) SWCNTs. [2] However, it is still unclear whether the optical signal really reflects the true chirality distribution of the sample. The problem is mainly due to less information about the chirality dependence of the PL (Raman) cross section and about the possible chirality selection in the dispersion process with surfactant followed by the centrifugation. To solve this problem, it is essential to combine the PL results with non-spectroscopic diameter estimation for the identical sample without any additional dispersion process.

In this work, we investigated the diameter distribution of the CoMoCAT SWCNT by the PL and the x-ray diffraction (XRD). First, well isolated SWCNT dispersion was prepared through the sonication and ultra centrifugation processes. After the PL measurement, a piece of bucky paper was produced from the dispersion. Then, the XRD pattern of the bucky paper was measured (Fig. 1a). Thus the PL and XRD measurements were recorded on the completely identical samples. The XRD analysis shows that the average diameter is 0.78 ± 0.01 nm and its dispersion is 0.12 nm by assuming a Gaussian distribution. As shown in Fig. 1b, the PL intensity of each chirality agrees with the diameter distribution estimated from the XRD result. This result first revealed that the relative PL intensity of the CoMoCAT SWCNTs actually represents their diameter distribution.



References: [1] S.M. Bachilo et al., *Science*, 298, 2361 (2002)

[2] S.M. Bachilo et al. *JACS*, 125, 11185 (2003)

Corresponding Author:

Hiromichi Kataura

E-mail: h-kataura@aist.go.jp

Tel: +81-29-861-2551

Fax: +81-29-861-2786

Fig. 1. (a) The observed XRD pattern of the CoMoCAT SWCNTs (open circle), and the simulated pattern (solid line). (b) The PL intensity of each chirality plotted as a function on diameter (open circle), and the diameter distribution estimated from the XRD result (solid line).

Length Dependence of Raman Intensity of the Single Wall Carbon Nanotube

* Jin Sung Park¹⁾, Riichiro Saito¹⁾, Kentaro Sato¹⁾, Jie Jiang²⁾, Gene Dresselhaus³⁾,
Mildred S. Dresselhaus^{4), 5)}

¹⁾ Department of Physics, Tohoku University and CREST JST, Sendai 980-8578, Japan

²⁾ Department of Physics, North Carolina State University, USA

³⁾ Francis Bitter Magnet Laboratory, ⁴⁾ Department of Electrical Engineering and

⁵⁾ Computer Science, Department of Physics, Massachusetts Institute of Technology,
Cambridge, MA 02139-4307, USA

Since excitonic effects are important in the optical properties of the single wall carbon nanotubes (SWNTs), we should consider an exciton picture to study Raman scattering. We have developed an exciton model by solving the Bethe-Salpeter equation in the SWNTs within tight binding model [1]. Unlike single particle picture, the exciton-photon matrix elements [2], as important factor to calculate the Raman intensity, strongly depend on the diameter but no tube type and no chiral angle dependence. Especially, the exciton-photon matrix element has a larger value for a longer SWNT, because the exciton wave function coefficient depends on tube length related to number of \mathbf{k} points. For the first resonance Raman scattering such like RBM and G-band, the Raman intensity in the range of tube length more than 100 nm does not depend on tube length. However, for very short SWNT, i.e. 20 nm, the Raman intensity considerably becomes weaker relative to tube length more than 100 nm. The reason is that the exciton wave function coefficient to be included in exciton-phonon matrix term quickly decreases with reducing tube length rather than tube length normalization in the Raman intensity formula. We will also compare our calculated results with experiment [3] for double resonance Raman scattering.

Reference:

- 1) J. Jiang, R. Saito, Ge. G. Samsonidze, A. Jorio, S. G. Chou, G. Dresselhaus, and M. S. Dresselhaus, *Phys. Rev. B*, 75, 035407, (2007)
- 2) J. Jiang, R. Saito, K. Sato, J. S. Park, Ge. G. Samsonidze, A. Jorio, G. Dresselhaus, and M. S. Dresselhaus, *Phys. Rev. B*, 75, 035405, (2007)
- 3) S. G. Chou, H. Son, A. Jorio, R. Saito, M. Zheng, G. Dresselhaus, and M. S. Dresselhaus, *Appl. Phys. Lett.*, 90, 131109, (2007)

Imaging Inter-layer Interaction of Double-Wall Carbon Nanotubes by UHV-STM

○N. Fukui¹, Y. Kato¹, H. Yoshida¹, T. Sugai¹, S. Heike², M. Fujimori², Y. Suwa²,
T. Hashizume^{2,3} and H. Shinohara^{1,4,5}

¹Department of Chemistry, Nagoya University, Nagoya 464-8602, Japan

²Advanced Research Laboratory, Hitachi, Ltd., Hatoyama, Saitama 350-0395, Japan

³ Department of Physics, Tokyo Institute of Technology, Tokyo 152-8551, Japan

⁴Institute for Advanced Research, Nagoya University, Nagoya 464-8602, Japan

⁵CREST, Japan Science and Technology Corporation, c/o Department of Chemistry,
Nagoya University, Nagoya 464-8602, Japan

Double-wall carbon nanotubes (DWNTs) are known to exhibit unique electronic and mechanical properties of various kinds [1]. These novel properties stem from very thin graphite layer structures with an excellent graphitization compared to those of single-wall carbon nanotubes (SWNTs) and multi-wall carbon nanotubes (MWNTs).

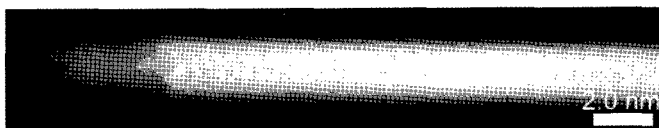
The characterization of inter-layer interaction of DWNTs has been performed by spectroscopic techniques such as Raman spectroscopy and photoluminescence which can provide information on the chirality and band structures of DWNTs [1]. However, the information obtained by such techniques show generally on the bulk sample.

To investigate the inter-layer (i.e., inner and outer tube) interaction of an isolated DWNT in detail, one of the best ways is to observe interference of the electronic states between the inner and outer tubes with scanning tunneling microscopy (STM) which was succeeded to clarify inter-layer interactions in graphite [2]. Here, we investigate inter-layer interactions exerted in DWNTs by using ultra-high vacuum STM (UHV-STM).

DWNTs were prepared by the pulsed-arc discharge method [3] and were dispersed in chloroform by ultra-sonication. Solutions of DWNTs were deposited onto clean Au(111) using the pulse-jet injection method under high-vacuum[4]. The sample was transferred to an UHV chamber and was annealed at 700K to remove the residue solvents. All STM measurements were performed in UHV conditions at room temperature.

STM images obtained show that some DWNTs exhibit a periodic super-structure along the tube axis caused by the interference between the inner and outer tubes [4] (Fig.1). The most of DWNTs, however, do not show such a super-structure on the surface of DWNTs.

The super-structure due to inter-layer interactions should have close relationships with inter-layer distance and their diameters. We will discuss the super-structures in terms of the interference of the electronic states of the inner and outer tubes based on the STM images of the DWNTs.



[1] N. Kishi et.al., J. Phys. Chem. B, 110,24816(2006)

[2] W. T. Pong et.al., Surf. Sci., 601, 498 (2007)

[3] T. Sugai et.al., Nano. Lett., 3, 769 (2003).

[4] N. Fukui et.al., Abstracts of The 30th Fullerene-Nanotubes General Symposium, Jan 7, 2006, Nagoya, Japan

Corresponding Author: Hisanori Shinohara

TEL: +81-52-789-2482, FAX: +81-52-789-1169, E-mail: noris@cc.nagoya-u.a.jp

In Situ Manipulation and Engineering of Carbon Nanotubes Inside a Transmission Electron Microscope

○Chuanhong Jin, Kazu Suenaga, and Sumio Iijima

*Research center for Advanced Carbon Materials, National Institute of Advanced Industrial
Science and Technology (AIST), Tsukuba 305-8565, Japan*

Since their discovery in 1991 [1], carbon nanotubes (CNTs) have been recognized as particularly important materials because of their extraordinary mechanical and electronic properties. Among them, realization of interconnection of CNTs as the building blocks of future nanoelectronics is of particular interest for the bottom-up process to generate all-CNTs based devices. Although previous in situ transmission electron microscope (TEM) studies have made CNTs junctions available ('wall to wall' and Y type), these junctions were produced under irradiations of ultra-high energy electrons [2, 3]. Near-atomic precision to realize the site-assigned joining (such as 'cap to cap') has not yet been achieved. In this report we will present a simple in situ Joule heating can realize the serial connection of two CNTs with the precise control when their chiral indices are identical or even 'close' to each other [4, 5]. Both single-walled carbon nanotubes (SWNTs) and multi-walled carbon nanotubes (MWNTs) have been successfully joined. Moreover, for those CNTs with a large mismatch in their diameters (chirality also), with the introduction of metal catalyst, they could also be well joined. Using simple technique, in principle, we could make any length of tubes.

[1] S. Iijima, *Nature*, 354, 56 (1991)

[2] M. Terrones et al, *Science*, 288, 1226 (2000).

[3] M. Terrones et al, *Phys. Rev. Lett.*, 89, 075505 (2002)

[4] C. H. Jin, K. Suenaga and S. Iijima, submitted

[5] C. H. Jin, K. Suenaga and S. Iijima, in preparation

Acknowledgement: This work was partially supported by a Grant-in-Aid for Scientific Research from the Japan Society for the Promotion of Science.

Corresponding Authors: Chuanhong Jin and Kazu Suenaga

TEL: +81-29-861-5694, **FAX:** +81-29-861-4806,

E-mail: chuanhong-jin@aist.go.jp & suenaga-kazu@aist.go.jp

Predominance of small bundles within vertically aligned SWNT arrays

○Erik Einarsson¹, Takahisa Yamamoto², Zhengyi Zhang¹,
Yuichi Ikuhara³, Shigeo Maruyama¹

¹*Dept. of Mechanical Engineering, The University of Tokyo, Tokyo 113-8656, Japan*

²*Dept. of Advanced Materials Science, The University of Tokyo, Kashiwa 277-8561, Japan*

³*Institute of Engineering Innovation, The University of Tokyo, Tokyo 113-8656, Japan*

Here we report recent TEM observations of the internal structure of vertically aligned single-walled carbon nanotube (VA-SWNT) arrays synthesized from alcohol. It was found that the SWNTs within the aligned array form into thin bundles, typically containing fewer than ten nanotubes. This small bundle size is significant in that it results in reduced tube-tube interactions, allowing the SWNTs to retain more of their one-dimensional nature[1].

The VA-SWNTs investigated in this study were synthesized by the alcohol catalytic chemical vapor deposition (ACCVD) method [2]. Figure 1a shows a VA-SWNT array approximately 4 μm thick. TEM observations were performed by transferring the array onto a TEM grid using a hot-water transfer method [3]. The VA-SWNTs were then observed along the alignment direction. Inside the TEM, we obtained cross-sectional images at different depths into the array, shown by dashed lines in Fig. 1a, by shifting the focal plane. An image corresponding to 600 nm into the array is shown in Fig. 1b. We also studied these VA-SWNTs by high-resolution Raman spectroscopy (Fig. 2). Using a 488 nm excitation laser, the broad peak at 180 cm^{-1} was found to consist of four separate, sharp peaks. The origin of these peaks is still unclear, but since they do not appear in random SWNTs bundles [2], they are thought to be related to the small bundles or isolated SWNTs within the vertically aligned arrays.

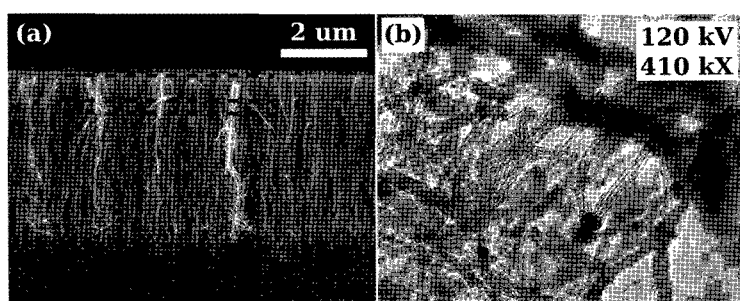


Fig. 1: (a) SEM image of a 4 μm thick VA-SWNT array. Dashed lines show depth of cross-sectional TEM images. (b) TEM image at 600 nm down into the array.

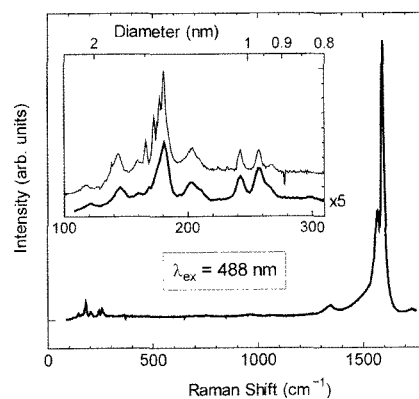


Fig. 2: Raman spectra from VA-SWNTs. Inset shows splitting of the 180 cm^{-1} peak (thin, upper line is high-resolution).

[1] E. Einarsson, H. Shiozawa, C. Kramberger, M.H. Rmmeli, A. Grneis, T. Pichler, S. Maruyama, *submitted to J. Phys. Chem. B* (2007).

[2] S. Maruyama, E. Einarsson, Y. Murakami, T. Edamura, *Chem. Phys. Lett.* **403**, 320 (2005).

[3] Y. Murakami and S. Maruyama, *Chem. Phys. Lett.* **422**, 575 (2006).

Corresponding Author: Shigeo Maruyama

TEL: +81-3-5841-6421, FAX: +81-3-5800-6983, E-mail: maruyama@photon.t.u-tokyo.ac.jp

Effect of Chemical Modification for SWNTs-FET Properties

○Ryotaro Kumashiro¹, Yuki Abe¹, Takeshi Akasaka², Yutaka Maeda³,
Nagao Kobayashi⁴, and Katsumi Tanigaki¹

¹*Department of Physics, Graduate School of Science, Tohoku University, Sendai, Japan*

²*Center for Tsukuba, Advanced Research Alliance, University of Tsukuba, Tsukuba, Japan*

³*Department of Chemistry, Tokyo Gakugei University, Tokyo, Japan*

⁴*Department of Chemistry, Graduate School of Science, Tohoku University, Sendai, Japan*

Abstract: Single wall carbon nanotubes (SWNTs) having semiconducting properties are promising as electronic materials for nano-scale devices in the future, and the electrical properties of SWNTs are of significantly fundamental and practical interests. It is well known that the field effect transistors (FETs) fabricated using semiconducting SWNTs show high performance in terms of the mobility. However, carriers in pristine SWNTs are mostly holes, therefore, SWNTs -FETs usually show p-type properties. For applying CNTs to electronic devices, it is necessary to control the both carriers of electrons as well as holes, that is, the electron carrier doping should be established. We reported the FET properties of SWNTs exohedrally modified by Si-containing organic molecules of in the previous meeting, and demonstrated that p-type nanotubes can be converted to n-type ones. However, because of ununiformity of the surface silylation of SWNTs, the confirmation of charge transfer from the exohedral functional groups to SWNTs is extremely difficult. In this meeting, we will discuss the effect of surface chemical modification on the SWNTs-FETs properties in more detail by FET and spectroscopic methods. In this study, we used the organic molecule adsorbed SWNTs to make clear the effect of modification, and it was demonstrated that an n-type property can be enhanced by $(\text{Si}(\text{ph})_2^t\text{Bu})_2$ adsorption also in a similar manner to the surface silylated ones (Fig.1). We will also discuss the possibility of charge transfer by using spectroscopic methods.

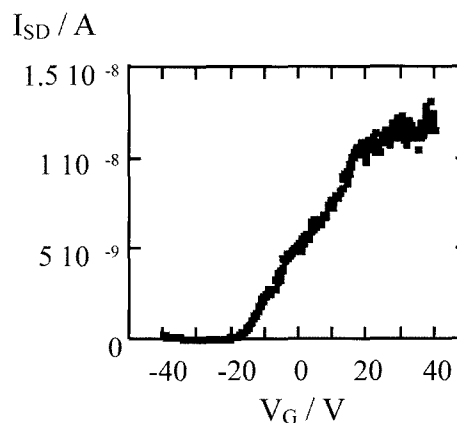


Figure 1. I_{SD} - V_G curve of $(\text{Si}(\text{ph})_2^t\text{Bu})_2$ adsorbed SWNTs -FET.

Corresponding Author: Ryoraro Kumashiro

E-mail: rkuma@sspns.phys.tohoku.ac.jp

Tel&Fax: +81-22-795-6468 (tel), +81-22-795-6470 (fax)

Threshold Energy of Low-Energy Irradiation Damage in Single-Walled Carbon Nanotubes

○Satoru Suzuki and Yoshihiro Kobayashi

*NTT Basic Research Laboratories, NTT Corporation, Atsugi, Kanagawa 243-0198, Japan
and CREST, Japan Science and Technology Corporation*

We have shown that low-energy electron and photon irradiation to single-walled carbon nanotubes (SWNTs) creates defects, which have unique characteristics [1]. The activation energy of the defect healing has been estimated to be about 1 eV [1]. On the other hand, the exact threshold energy of the damage has not been determined yet, although our previous study [2] has shown that it is less than 20 eV. Determining the threshold energy would be very important for clarifying the mechanism of the low-energy irradiation damage. Here, we study irradiation effects of photons whose energy is less than 20 eV.

SWNTs were grown by using the thermal chemical vapor deposition (CVD) method. Ethanol was the carbon source. Photon irradiation was performed at beamline BL-1B of the Ultraviolet Synchrotron Orbital Radiation Facility (UVSOR), Institute for Molecular Science, Okazaki. All the irradiations were carried out at room temperature and in an ultra-high vacuum of $\sim 5 \times 10^{-7}$ Pa. The irradiation dose was $\sim 5 \times 10^{17}$ cm $^{-2}$. After the irradiations, Raman spectra were measured in air with an excitation wavelength of 785 nm.

Figure 1 shows the Raman spectrum of SWNTs irradiated by 3- to 7-eV photons and that of unirradiated SWNTs. A G-band intensity decrease and D-band intensity increase were observed for SWNTs irradiated at 6 and 7 eV, although they were not observed at 5 eV or below. The result strongly suggests that the threshold energy of low-energy irradiation damage is within an energy range of 5 to 6 eV.

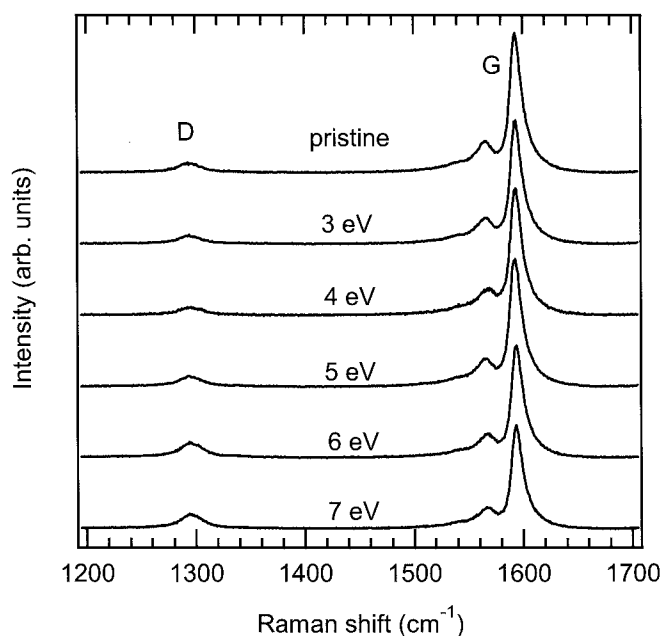


Figure 1. Raman spectra of pristine and photon-irradiated SWNTs.

The authors thank Mr. M. Hasumoto of UVSOR for his technical support in the irradiation experiments.

References:

- [1] S. Suzuki and Y. Kobayashi, *J. Phys. Chem. C* 111 (2007) 4524-4528, and references therein.
- [2] S. Suzuki and Y. Kobayashi, *Chem. Phys. Lett.* 430 (2006) 370-374.

Corresponding Author: Satoru Suzuki
ssuzuki@will.brl.ntt.co.jp
TEL: +81-46-240-3632
FAX: +81-46-240-4711

Regulated near-IR optical properties of individually dissolved semiconducting SWNTs via redox reaction

○Kohei Hirayama, Yasuro Niidome, Naotoshi Nakashima

*Department of Applied Chemistry, Graduate School of Engineering, Kyushu University,
744 Motoooka, Nishi-ku, Fukuoka 819-0395, Japan*

Carbon nanotubes (CNTs) have been in the forefront of nanoscience and nanotechnology because of their many unique properties. However, their insolubility in solvents has hindered chemical approaches using CNTs. We have reported the fundamental properties and applications of soluble carbon nanotubes in aqueous and organic systems [1-3]. Individually dissolved CNTs show the inherent properties of the CNTs that are not seen in bundled ones.

Semiconducting single walled carbon nanotubes (SWNTs) exhibit interesting optical properties via redox reactions [4-6]. Here, we report the finding that near IR absorption and photoluminescence spectra of individually dissolved SWNTs in aqueous micellar solution are regulated by the addition of a chemical reducing agent. The details will be reported at the presentation.

References:

- [1] N. Nakashima, T. Fujigaya, H. Murakami, "Soluble Carbon Nanotubes", in Chemistry of Carbon Nanotubes, eds, V. A. Basiuk, and E. V. Basiuk, American Scientific Publisher, (2007), in press.
- [2] H. Murakami, N. Nakashima, *J. Nanosci. Nanotechnol.*, **6**, 16 (2006).
- [3] N. Nakashima, *International J. Nanoscience*, **4**, 119(2005).
- [4] G. Dukovic, B. E. White, Z. Zhou, F. Wang, S. Jockusch, M. L. Steigerwald, T. F. Heinz, R. A. Friensner, N. J. Turro, L. E. Brus, *J. Am. Chem. Soc.*, **126**, 15269 (2004).
- [5] M. Zheng, B. A. Diner, *J. Am. Chem. Soc.*, **126**, 15490 (2004).
- [6] M. J. O'connell, E.E.Eibergen, S. K. Doorn, *nature materials*, **4**, 412 (2005).

Corresponding Author: Naotoshi Nakashima

E-mail: nakashima-tcm@mbox.nc.kyushu-u.ac.jp

Tel & Fax: +81-92-802-2840

Optical Properties of High-Purity Single Wall Carbon Nanotubes Sorted by Electronic Structure

○Yasumitsu Miyata^{1,2}, Kazuhiro Yanagi², Yutaka Maniwa¹ and Hiromichi Kataura²

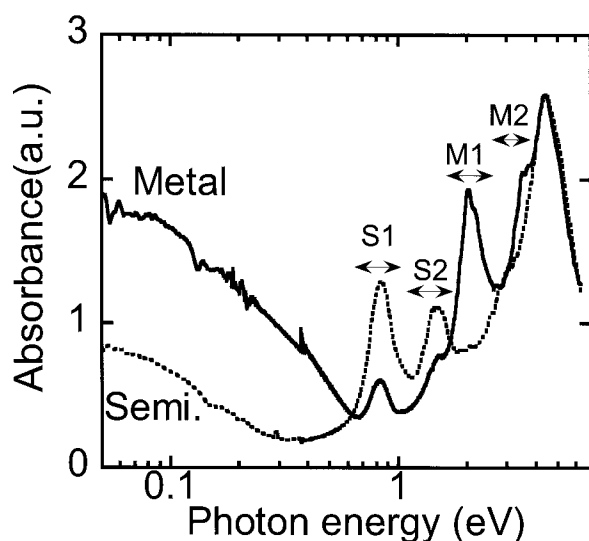
¹*Department of Physics, Tokyo Metropolitan University, 1-1 Minami-Osawa, Hachioji, Tokyo 192-0397, Japan*

²*Nanotechnology Research Institute (NRI), National Institute of Advanced Industrial Science and Technology (AIST), 1-1-1 Higashi, Tsukuba 305-8562, Japan*

Single wall carbon nanotubes (SWCNTs) exhibit remarkable electronic and optical responses originating from the one-dimensionality of the system. However, these responses have not yet been fully understood because most of previous studies have been conducted on a mixture of metallic and semiconducting SWCNTs. Thus, high-purity SWCNTs with a single electronic type is strongly required for more precise understanding of these physical properties.

In this work, we investigated the optical properties of high-purity metallic and semiconducting SWCNTs mainly by optical absorption and Raman spectroscopy. The separation of metallic and semiconducting SWCNTs was achieved through density-gradient centrifugation processes [1]. Figure 1 shows the optical absorption spectra of metal-enriched (M-) and semiconductor-enriched (S-) SWCNT thin films. The spectra were normalized at the peak of 4.4 eV caused by π plasmon resonance. Since the numbers of π electron are identical for both semiconducting and metallic SWCNTs, the optical absorption due to the π plasmon excitation should be the same. Although S1 absorption band is still observed in M-SWCNTs, the purity of each type of SWCNT is very high compared with the previous works. Unexpectedly large M1 and M2 absorption bands were observed. Importantly, it can be seen that the infrared absorption intensity of the M-SWCNTs is about two times higher than that of

the S-SWCNTs at the long wavelength limit. This indicates, as a matter of course, higher conductivity of M-SWCNTs than S-SWCNTs. Raman spectra and the other optical properties will be discussed.



References: [1] M.S. Arnold et al., *Nature Nanotechnol.*, 1, 60 (2006)

Corresponding Author: Hiromichi Kataura

E-mail: h-kataura@aist.go.jp

Tel: +81-29-861-2551, **Fax:** +81-29-861-2786

Fig. 1. Optical absorption spectra of the thin films of metal-enriched and semiconductor-enriched SWCNT bundles.

Environmental effects on photoluminescence of carbon nanotubes

○Y. Ohno, S. Iwasaki, Y. Murakami, S. Kishimoto, S. Maruyama, and T. Mizutani

Department of Quantum Engineering, Nagoya University
PRESTO/Japan Science and Technology Agency
Department of Mechanical Engineering, The University of Tokyo

In order to understand the optical properties of single-walled carbon nanotubes (SWNT), it is important to understand the environmental effects. In this study, we have studied the dielectric screening effect by the surrounding material around the nanotube. The dependence of exciton transition energy on dielectric constant of surrounding material has been investigated in the range of dielectric constant from 1.0 to 37, by means of photoluminescence spectroscopy [1].

The sample with free-standing SWNTs (Fig. 1) was immersed in various organic solvent with different dielectric constant. With increasing dielectric constant, both E_{11} and E_{22} exhibited a redshift by several tens meV and a tendency to saturate at a dielectric constant about 5 with an indication of small (n,m) dependence (Fig. 2). The redshifts can be explained by the decrease in the electron-electron repulsive interaction which exceeds that of electron-hole attractive interaction [2]. The energy shift was larger for the nanotube with a smaller diameter.

References:

- [1] Y. Ohno et al., arXiv:0704.1018v1 [cond-mat.mtrl-sci] (2007).
 [2] Y. Ohno et al., Phys. Rev. B 73, 235427 (2006).

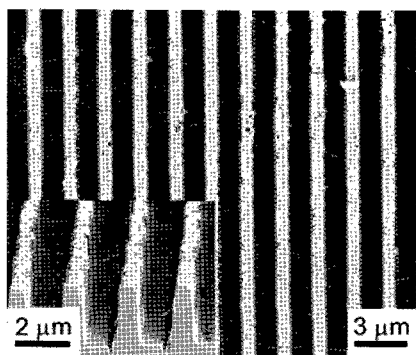


Fig. 1 Free-standing SWNTs.

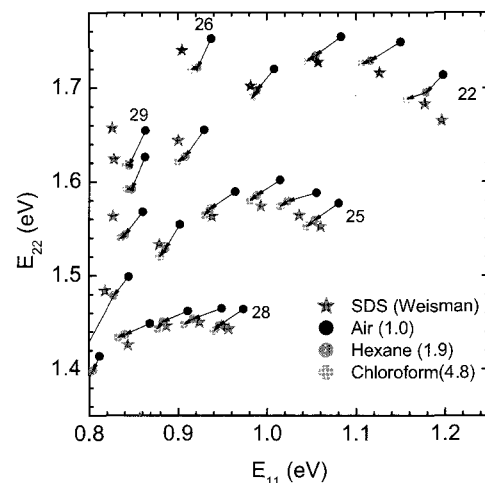


Fig. 2 E_{22} - E_{11} plots in various environmental conditions.

Corresponding Author E-mail: yohno@nuee.nagoya-u.ac.jp, Tel&Fax: 052-789-5387

Ethanol Gas Pressure Dependence of Photoluminescence from SWNTs

○ Shohei Chiashi, Satoshi Watanabe, Tateki Hanashima and Yoshikazu Homma

*Department of Physics, Tokyo University of Science
1-3 Kagurazaka, Shinjuku-ku, Tokyo 162-6801, Japan*

Understanding of the environmental effects of photoluminescence (PL) from SWNTs [1, 2] is important for elucidating their electric structures and optical properties. To investigate the environmental effects, we measured PL from the suspended SWNTs between quartz pillars in an environmental vacuum chamber, which controlled sample temperature and ambient gas conditions (gas species, its pressure and velocity). Figures 1(a, b) show the PL maps of a suspended (9,7) SWNT measured at room temperature (a) in ethanol gas (5.3×10 Torr) and (b) in vacuum (2.5×10^{-2} Torr). The E_{11} and E_{22} energies of SWNTs in the ethanol gas were almost the same as those of suspended SWNTs in air [3, 4]. However the PL peak was blue-shifted in vacuum as shown in Fig. 1(b). Figure 1(c) shows the ethanol gas pressure dependence of emission peak wavelength (E_{11} energy) of the suspended (9,7) SWNT. The E_{11} energy exhibited a slight and continuous blue-shift with decreasing ethanol gas pressure in a high pressure range, while it drastically blue-shifted [2] at transition pressure (approximately 3 Torr). Below the transition pressure, the energy was independent of the gas pressure. All suspended SWNTs had the similar ethanol gas pressure dependence in PL and the transition pressure was dependent on SWNT tube diameter and temperature. Independent of chirality indices, the thinner SWNTs had higher transition pressure and the transition pressure increased with increase of temperature.

We assumed that SWNT surface was covered with ethanol molecules above the transition pressure while it was perfectly clean below the transition pressure, and that the dielectric constant of the SWNT environment, which changed both E_{11} and E_{22} energies, depended on the absorbed amount of ethanol molecules.

[1] J. Lefebvre, *et al.*, *Phys. Rev. B*, **70** (2004) 045419.

[2] P. Finnie, *et al.*, *Phys. Rev. Lett.*, **94** (2005) 247401.

[3] Y. Ohno, *et al.*, *Phys. Rev. B*, **73** (2006) 235427.

[4] J. Lefebvre, *et al.*, *Appl. Phys. A*, **78** (2004) 1107.

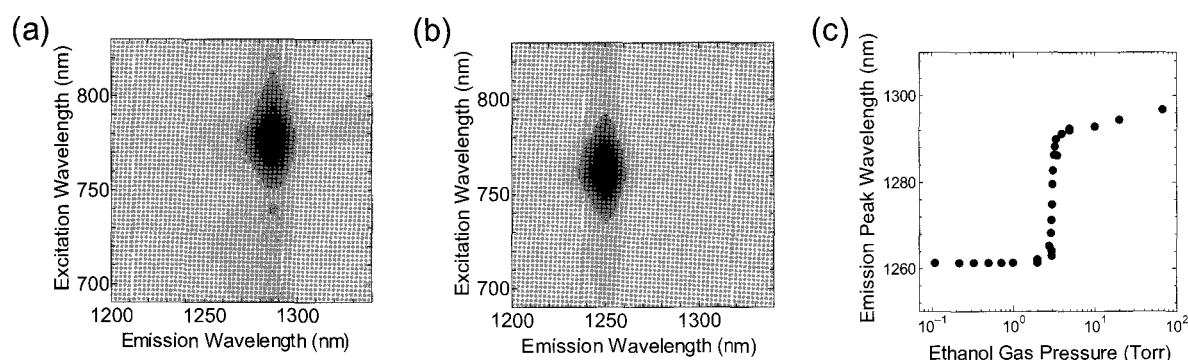


Fig. 1 PL maps from suspended (9,7) SWNT measured at RT (a) in ethanol gas and (b) in vacuum. (c) Ethanol gas pressure dependence of emission peak wavelength (E_{11} energy).

Corresponding Author: Shohei Chiashi

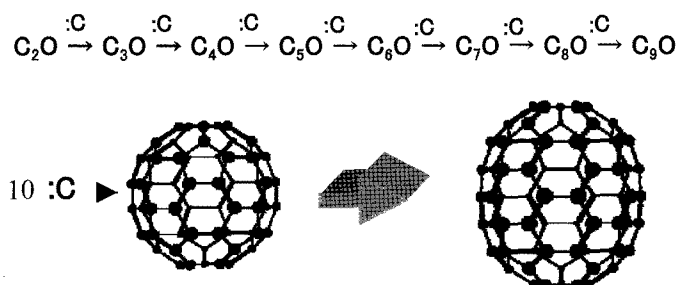
E-mail: chiashi@rs.kagu.tus.ac.jp, Tel: +81-3-5228-8244, Fax: +81-3-5261-1023

Synthesis of Fullerene C₇₀ from C₆₀ by Gaseous Carbon Insertions into CC bonds

○Teruhiko Ogata¹, Tetsu Mieno², and Yoshio Tatamitani¹

¹Department of Chemistry and ²Department of Physics, Shizuoka University, Shizuoka 422-8529, Japan

We report the synthesis of fullerene C₇₀ from C₆₀ by gaseous carbon insertion into CC bonds. Gaseous carbon atoms :C “jump” into CC bonds without cleavage of the overall molecular structure and without significant side reactions [1]. The carbon insertion reactions,



are simple, clean, efficient, and require only :C and a CC bond. As an extension of the carbon insertion reactions into CC bonds, we have formed fullerene C₇₀ from C₆₀ by insertion of carbon atoms created in the photolysis of C₃O₂. The reactions were made at 800~1000°C. A significant amount of fullerene C₇₀ was formed with negligible side products and was confirmed by HPLC and TOF-MS spectrometries. The fact that in this reaction system, carbon carbenes :C were the only chemically active species which were known to jump into CC bonds spontaneously and fullerene C₇₀ has been formed without occurrence of side reactions, implies the carbon insertion reactions should have occurred without cleavage of the C₆₀ structure. That is, insertions of ten carbon atoms :C into the CC bonds in the C₆₀ cage followed by annealing and arrangements have formed fullerene C₇₀ (Figure).

There are many experimental evidences supporting the formation mechanism of fullerene C₇₀ from C₆₀ mentioned above. In the reaction of fullerene C₆₀ with carbon, abundance mass spectra of C₆₀C_q⁺ clusters show that there is no preference for clusters containing an even number of carbon atoms in such experimental conditions that carbon atoms are softly attached to a C₆₀, however, the photofragmentation of C₆₀C_q⁺ clusters displays fragmentation sequences similar to what is observed in experiments on “ordinary” C_{60+q}⁺ fullerenes such as much more intense fragments for C₆₀⁺, C₆₂⁺, and C₇₀⁺ [3]. Reaction of C⁺ with C₆₀ shows that ¹³C⁺ projectile with no activation energy undergoes exchange with C atoms in the target of the C₆₀ cage [4]. Photolysis of diazomethane adduct of C₆₀ afforded the C₆₁H₂ cyclopropanes and annulenes indicating the :CH₂ insertion into the C=C and C—C bond, respectively [5].

[1] K.D. Bayes, *J. Am. Chem. Soc.*, **84**, 4077-4080 (1962); T. Ogata et al., *Chem. Lett.* **1985**, 1797-1798; T. Ogata et al., *J. Am. Chem. Soc.*, **109**, 7639-7641 (1987); T. Ogata et al., *J. Phys. Chem.*, **96**, 2089-2091 (1992).

[2] T. Ogata, Y. Ohshima, Y. Endo. *J. Am. Chem. Soc.*, **117**, 3593-3598 (1995); Y. Ohshima, Y. Endo, T. Ogata. *J. Chem. Phys.*, **102**, 1493-1500 (1995).

[3] M. Pellarin et al., *J. Chem. Phys.*, **117**, 3088-3097 (2002).

[4] J.F. Christian, Z Wan, and S.L. Anderson, *J. Phys. Chem.*, **96**, 3574-3576 (1992).

[5] A.B. Smith III et al., *J. Am. Chem. Soc.*, **117**, 5492-5502 (1995).

Corresponding Author: Teruhiko Ogata Tel&Fax: +81-54-238-8529 E-mail: sctogat@ipc.shizuoka.ac.jp

Structural study of Sc₂C₈₄(II)

○Koji Nakajima¹, Yuko Iiduka¹, Takatsugu Wakahara¹, Takahiro Tsuchiya¹, Yutaka Maeda²,
Takeshi Akasaka^{1*}, Naomi Mizorogi³, Shigeru Nagase³

¹Center for Tsukuba Advanced Research Alliance, University of Tsukuba, ²Department of
Chemistry, Tokyo Gakugei University, ³Department of Theoretical and Computational
Molecular Science, Institute for Molecular Science

Endohedral metallofullerenes have attracted special attention as new spherical molecules with unique properties unexpected from empty fullerenes. Among them, scandium metallofullerenes are of special interest because of their high variety in fullerene size. Sc₂C₈₄ isomers(I, II and III) have been known as one of most abundant scandium fullerenes. Their structures have been ever widely believed to have the form of Sc₂@C₈₄ on the results of ¹³C NMR spectral determination and powder X-ray diffraction analysis.[1,2] Interestingly, recent investigations by ¹³C NMR spectral determination[3], single crystal[4] and powder X-ray diffraction analyses[5] reveal that one of three isomers, Sc₂C₈₄(III), is a scandium carbide-encapsulated metallofullerene, Sc₂C₂@C₈₂.

Herein, we present that the structure of Sc₂C₈₄(II) is also not Sc₂@C₈₄ but Sc₂C₂@C₈₂, which has a C₈₂(C_{2v}) cage, by means of the ¹³C NMR spectral analysis. We successfully synthesized adamantylidene derivative of Sc₂C₂@C₈₂(II) for single crystal X-ray analysis, which was characterized by MALDI-TOF mass, UV-vis-NIR absorption, CV and ¹³C NMR spectroscopic analyses.

[1] Inakuma, M. et al., *J. Phys. Chem. B* **2000**, *104*, 5072-5077.

[2] Takata, M. et al., *Phys. Rev. Lett* **1997**, *78*, 3330-3333.

[3] Iiduka, Y. et al., *Chem. Commun.* **2006**, 2057-2059.

[4] Iiduka, Y. et al., *Angew. Chem.* in press.

[5] Nishibori, E. et al., *Chem. Phys. Lett.* **2006**, *433*, 120-124.

Corresponding Author: Takeshi Akasaka

TEL&FAX: +81-29-853-6409 E-mail: akasaka@tara.tsukuba.ac.jp

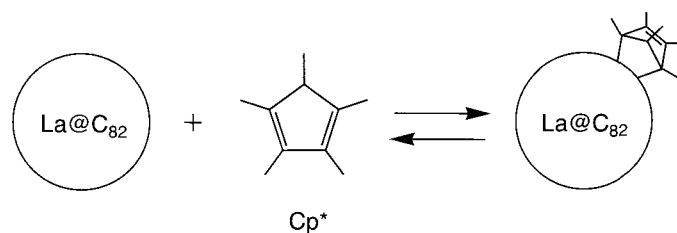
Reversible Reaction of La@C₈₂ with Cyclopentadiene Derivatives

○Satoru Sato,¹ Yutaka Maeda,² Koji Inada,² Tadashi Hasegawa,² Michio Yamada,¹ Takahiro Tsuchiya,¹ Takeshi Akasaka,¹ Tatsuhisa Kato,³ Naomi Mizorogi,⁴ Shigeru Nagase⁴

¹Center for Tsukuba Advanced Research Alliance, University of Tsukuba, Tsukuba, Ibaraki 305-8577, Japan, ²Department of Chemistry, Tokyo Gakugei University, Koganei, Tokyo 184-8501, Japan, ³Department of Chemistry, Josai University, Sakado, Saitama 350-0295, Japan

⁴Department of Theoretical Molecular Science, Institute for Molecular Science, Okazaki, Aichi 444-8585, Japan

Endohedral fullerene is a new type of carbon cluster that contains one or more atoms inside the hollow fullerene cage. Especially, endohedral metallofullerenes have attracted broad attention because of their novel properties due to the intramolecular interaction between the metal atom and the fullerene cage.¹ New electronic properties, such as the low oxidation and reduction potentials, induced by the interaction would allow new application of fullerenes. Reversible addition reaction² is one of the useful methods for separation of empty fullerenes³ and protection of their reactive sites.⁴ Recently, we have reported the reversible and regioselective addition reaction of La@C₈₂ with cyclopentadiene (Cp), in which the kinetic parameters for the retro-reaction of La@C₈₂Cp were determined.⁵ This retro-reaction proceeds much faster than that of C₆₀Cp. In this context, it is important to retard the retro-reaction of La@C₈₂Cp. It has been reported that an adduct of C₆₀ with pentamethylcyclopentadiene (Cp*) is less prone to undergo the retro-reaction than C₆₀Cp.⁶ Herein, we report the reversible addition reaction of La@C₈₂ with Cp* and the stability of its adduct.



References

- [1] *Endofullerenes: A New Family of Carbon Clusters*; Akasaka, T., Nagase, S., Eds.; Kluwer Academic Publishers: Dordrecht, The Netherlands, 2002; pp 133-151.
- [2] Tsuda, M. et al., *J. Chem. Soc., Chem. Commun.* **1993**, 1296.
- [3] Nie, B. et al., *J. Org. Chem.* **1996**, *61*, 1870.
- [4] Lamparth, I. et al., *Angew. Chem., Int. Ed. Engl.* **1995**, *34*, 1607.
- [5] Maeda, Y. et al., *J. Am. Chem. Soc.* **2005**, *127*, 12190.
- [6] Meidine, M. F. et al., *J. Chem. Soc., Perkin Trans. 2* **1994**, 1189.

Corresponding Author: Takeshi Akasaka

TEL & FAX: +81-29-853-6409, E-mail: akasaka@tara.tsukuba.ac.jp

Optical Emission of Nitrogen Plasmas Yielding the Synthesis of Nitrogen Atom Encapsulated Fullerenes

○S. Nishigaki, T. Kaneko and R. Hatakeyama

Department of Electronic Engineering, Tohoku University, Sendai 980-8579, Japan

Many works related to the properties of a nitrogen atom encapsulated fullerene C_{60} ($N@C_{60}$) are reported [1, 2], but the synthesis with high yield and high purity of $N@C_{60}$ has not yet been realized. Although $N@C_{60}$ has been produced by several plasma methods, the yield of $N@C_{60}$ is extremely low ($N@C_{60}/C_{60} = 10^{-3} - 10^{-2} \%$). The purpose of this research is to elucidate a formation mechanism of $N@C_{60}$ in order to improve the yield using a radio frequency (RF) discharge plasma. In this study, the high purity of 0.02 - 0.05 % is achieved for $N@C_{60}$, which is the highest value compared to that has ever been reported.

The nitrogen plasma is generated by applying an RF power with a frequency of 13.56 MHz to a spiral-shaped RF antenna and is controlled by the applied power, a nitrogen gas pressure, a substrate potential V_{sub} and a potential V_g of a mesh grid (20 meshes/cm) with a supporting rod, which is set up in the area between the RF antenna and the substrate [3]. C_{60} is sublimated from an oven and deposited on the water-cooled cylindrical substrate. The nitrogen plasma is continuously irradiated to C_{60} on the substrate. The C_{60} compound including $N@C_{60}$ deposited on the substrate is analyzed by electron spin resonance (ESR) and UV-vis absorption spectroscopy to calculate the purity ($N@C_{60}/C_{60}$).

Figure 1 shows a dependence of the purity of $N@C_{60}$ on the optical emission intensity of nitrogen molecule radicals N_2^* normalized by that of nitrogen molecule ions N_2^+ (N_2^*/N_2^+), which is estimated according to the strongest peaks at 337.13 nm (N_2^*) and 391.44 nm (N_2^+) observed in the nitrogen plasma. It is found that the plasma with low N_2^*/N_2^+ can synthesize the high purity $N@C_{60}$. It is expected that the decrease in N_2^*/N_2^+ means the increase in nitrogen atom radicals N^* or nitrogen atom ions N^+ , which could enhance the synthesis of $N@C_{60}$. However, the optical emission peaks of N^* and N^+ are not observed in this experiment. Another possible reason is that the reduction of an emitted ultraviolet from N_2^* suppresses the destruction of $N@C_{60}$.

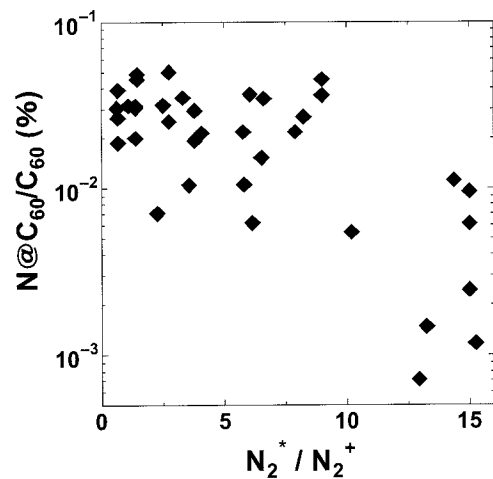


Fig. 1: Dependence of the purity of $N@C_{60}$ on the optical emission intensity of N_2^* normalized by that of N_2^+ (N_2^*/N_2^+).

[1] M. Waiblinger *et al.*, *Phys. Rev. B*, **64**, 159901 (2001).

[2] S. C. Benjamin *et al.*, *J. Phys.: Condens. Matter*, **18**, S867 (2006).

[3] S. Nishigaki *et al.*, *Abstract of the 32nd Fullerene-Nanotubes General Symposium*, 155 (2007).

Corresponding Author: Shohei Nishigaki

TEL: +81-22-795-7046, FAX: +81-22-263-9225, E-mail: nishigaki@plasma.ecei.tohoku.ac.jp

Ultrasonication Induced Structural Change of SWNTs Dispersed in the CMC Aqueous Solution.

○Shigekazu Ohmori¹, Takeshi Saito^{1,2}, Satoshi Ohshima¹, Motoo Yumura¹
and Sumio Iijima^{1,3}

¹ *Research Center for Advanced Carbon Materials, National Institute of Advanced Industrial Science and Technology (AIST), Ibaraki 305-8565 Japan*

² *PRESTO, Japan Science and Technology Agency, Kawaguchi 332-0012, Japan*

³ *Department of Materials Science and Engineering, 21st century COE (Nanofactory), Meijo University, Nagoya 468-8502, Japan*

Recently, it would come easy to get high quality SWNTs because of the research progress in the synthesis method, such as direct injection pyrolytic synthesis (DIPS)[1] and super-growth[2] methods. The high purity of these SWNTs can applied them to various uses without further purification. As the next step, SWNT should be capable to perform a liquid process on a large scale from the viewpoint of the industrial application. Many researchers try to disperse SWNT into solution and some polymers such as sodium carboxymethylcellulose (CMC) have excellent performance as the surfactant in dispersing SWNTs in water by ultrasonication. Although ultrasonication is very useful method for the preparation of the SWNT dispersion, it is reported that the ultrasonication induces damages to the molecular structure of SWNT[3]. In addition, Koshio et. al. reported that SWNT degeneration is enhanced by using polymer solution[4]. This problem will become important when the liquid process for the application of SWNTs is evolved.

Here we examined ultrasonication effect of the CMC solution dispersed SWNTs with cross flow filtration. Structural changes of the retentated and permeated SWNTs observed by the atomic force microscopy (AFM) will be discussed in detail.

References

- [1] T. Saito, et. al., *J. Phys. Chem. B*, **109**, 10647 (2005)
- [2] K. Hata, et al., *Science*, **306**, 1362 (2004)
- [3] K. B. Shelimov, et. al. *Chem. Phys. Lett.*, **282**, 429 (1998)
- [4] A. Koshio, et. al., *Chem. Phys. Lett.*, **341**, 461 (2001)

Corresponding author: Takeshi Saito

Tel: +81-29-861-4863, Fax: +81-29-861-3392, E-mail: takeshi-saito@aist.go.jp

Growth Window and Possible Mechanism of Millimeter-Thick Single-Walled Carbon Nanotube Forests

Kei Hasegawa¹, Suguru Noda¹, Hisashi Sugime¹, Kazunori Kakehi¹,
Zhengyi Zhang², Shigeo Maruyama² and Yukio Yamaguchi¹

¹ Dept. of Chemical System Engineering, The University of Tokyo, Tokyo 113-8656, Japan

² Dept. of Mechanical Engineering, The University of Tokyo, Tokyo 113-8656, Japan

The water-assisted growth method, so-called "supergrowth", has an outstanding growth rate of single-walled carbon nanotubes (SWNTs) [1]. However, few research groups have succeeded in reproducing it and underlying mechanism of the growth rate enhancement is unclear. We recently reproduced the "supergrowth" by a parametric study on both reaction and catalyst conditions [2]. In this work, we report in detail the effect of the conditions determined, and discuss the novel mechanism essential for rapid growth of SWNTs.

Our standard condition is 8.0 kPa C₂H₄, 27 kPa H₂, 0.010 kPa H₂O, 67 kPa Ar at 1093 K for 10 min. Figure 1a shows the nanotube sample grown by the combinatorial catalyst library [3] of 0.2-3-nm Fe on Al₂O₃/SiO₂. 0.5-nm-thick Fe grew SWNTs with diameter around 4 nm as shown in Fig. 1(b), and thicker Fe grew thicker nanotubes. Nanotube forests grew up to millimeter and sub-millimeter thicknesses for Fe and Co catalyst, respectively, only when supported on Al₂O₃ layer. When catalysts were supported on SiO₂, the thickness of nanotube films was as small as sub-micrometers. The window for the rapid SWNT growth was narrow. Optimum addition of H₂O (0.010 kPa equals 100 ppmv) increased the SWNT growth rate but further addition of H₂O degraded both the SWNT growth rate and quality. Addition of H₂ was also essential for rapid SWNT growth, but again, further addition decreased the SWNT growth rate. Because Al₂O₃ catalyzes hydrocarbon reforming, Al₂O₃ possibly enhances the SWNT growth rate by dissociating and supplying the carbon species to the catalyst particles. The origin of the narrow window for rapid SWNT growth will also be discussed.

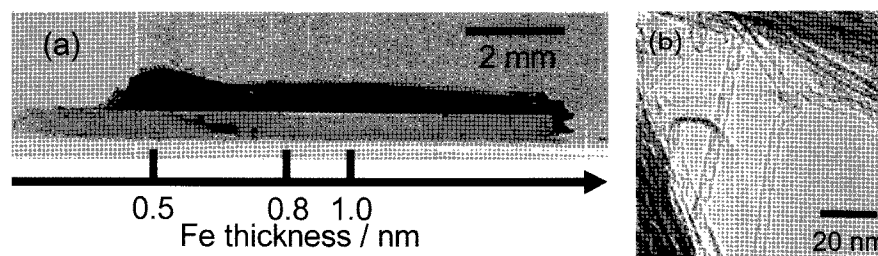


Fig. 1 (a) Photograph of Fe/Al₂O₃ combinatorial catalyst library after CVD under the standard condition. (b) TEM image of as-grown SWNTs at 0.5-nm-thick Fe under the same condition.

[1] K. Hata, et al., *Science*, **306**, 1362 (2004). [2] S. Noda, et al., *Jpn. J. Appl. Phys.*, **46**, L399 (2007). [3] S. Noda et al., *Carbon*, **44**, 1414 (2006).

Corresponding Author: Suguru Noda

TEL: +81-3-5841-7330, FAX: +81-3-5841-7332, E-mail: noda@chemsys.t.u-tokyo.ac.jp

Growth Mechanism of Horizontally-Aligned SWNTs on Sapphire Surface Studied with Patterned Catalyst

○Hiroki Ago,^{*1,2} Naoki Ishigami,² Ryota Ohdo,² Masaharu Tsuji,^{1,2}
Tatsuya Ikuta,³ and Koji Takahashi³

¹*Institute for Materials Chemistry and Engineering, Kyushu University, Fukuoka 816-8580*

²*Graduate School of Engineering Sciences, Kyushu University, Fukuoka 816-8580*

³*Graduate School of Engineering, Kyushu University, Fukuoka 819-0395*

Electronic applications of single-walled carbon nanotubes (SWNTs) require a large-scale integration of nanotubes with a controlled electronic structure on a flat substrate. We have studied this position- and direction-controlled growth of SWNTs on a sapphire substrate, because sapphire surfaces offer the horizontally-aligned growth of SWNTs in a self-assembled manner [1]. In this study, we show the patterned growth of SWNTs and their Raman mapping analyses.

The patterns of Fe-based catalyst were prepared on the surface of R-plane sapphire with an aid of electron-beam lithography. The sapphire substrate with the patterned Fe catalyst was subjected to chemical vapor deposition (CVD) in a mixed flow of CH₄/H₂ at 900 °C.

Fig. 1 shows a SEM image of aligned SWNTs grown from the patterned catalyst. The catalyst patterning was found to give better alignment than those grown on the uniformly deposited catalyst. This is because the un-patterned area of the sapphire was kept clean without contamination with the catalyst. In addition, a number of SWNTs with length over 100 μm were found on the patterned substrate. We performed the Raman mapping analysis by selectively positioning the focus to the patterned area (Fig. 2). Long SWNTs were clearly observed by the Raman mapping, which should be useful for the study of the nanotube growth mechanism as well as their characterization. At the symposium, we will also show our recent study of the growth mechanism using this Raman mapping technique.

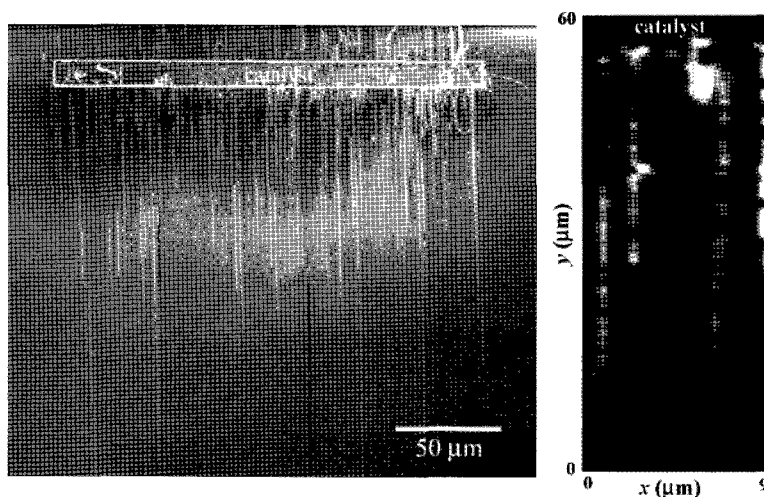


Fig. 1 (left) SEM image of highly-aligned SWNTs grown from the patterned Fe-based catalyst.

Fig. 2 (right) Mapping of the Raman G-band intensity (1592 cm⁻¹) measured for the patterned array of SWNTs (514.5 nm excitation).

Acknowledgements: This work is supported by Grant-in-aid for Scientific Research from MEXT (#18681020), Industrial Technology Research Program from NEDO, CREST-JST, and Joint Project of Chemical Synthesis Core Research Institutions.

References: [1] H. Ago *et al*, *Chem. Phys. Lett.*, **408**, 433 (2005).

Corresponding Author: Hiroki Ago (Tel&Fax: +81-92-583-7817, E-mail: ago@cm.kyushu-u.ac.jp)

First-principle Molecular dynamics study on initial stage of CNT formation from 3C-SiC (111) surface

○Hiroki Moriwake¹, Tsukasa Hirayama¹ and Michiko Kusunoki²

¹Nanostructures Research Laboratory Japan Fine Ceramics Center, Nagoya 456-8587, Japan

²Department of Chemistry, Nagoya University, Nagoya 464-8602, Japan

SiC surface decomposition method is one of the successful method for carbon nano-tube (CNT) production[1]. In this method, C-cap structure formation was thought to be critically important process. However its detail mechanism is far from fully understanding. In this study, the initial stage of CNT formation from 3C-SiC (111) surface (It is equivalent to 6H-SiC (0001) surface.) was studied by First-principle molecular dynamics(FP-MD). Theoretical calculations were performed with projector augmented wave (PAW) methods based on the density functional theory (DFT). FP-MD simulations were performed using 9 layers SiC C-surface slab model (containing 81 C atoms)with 10Å vacuum layer. To exclude the influence of complicated Si removable process from SiC surface by oxidization of Si, in the FP-MD simulation all Si atoms were deleted from our slab models. In stead of Si atoms, the position of bonded C atoms which located at surface and inside of bulk were fixed. Only the top layer (unbonded) C atoms were moved freely by FP-MD simulations. MD simulations were performed layer by layer manner (i.e. At First, only first layer atoms were moved, after that, as well as first layer atoms, second layer atoms were moved. Finally, all atoms except bottom layer were moved) for modeling layer by layer reaction at SiC surface at temperature of 2000K and 5000K. The simulation duration for one layer of 0.2psec (200MD step) were chosen by energy and structure convergence. In the MD simulation, C-C bondings are easily formed. They are sp (linear) and sp^2 (planar) bondings. No sp^3 (tetrahedron) bondings are formed. After 8 consecutive layer by layer MD simulations (1.6psec 1600MD step) at 2000K, C-cap like structure is formed. Its formation process is described as follows. Firstly, at early stage of layer by layer reaction, arch like structure (both end of the C-C chain were bonded at surface C atoms) is formed. Secondly, additional C atoms are captured by this arch structure and form additional branches. Finally, C-cap like structure are formed. Our FP-MD simulation may use a simplified model. However, our theoretical result can provide us with important insight of the microscopic mechanism of the initial stage of CNT formation from SiC surface.

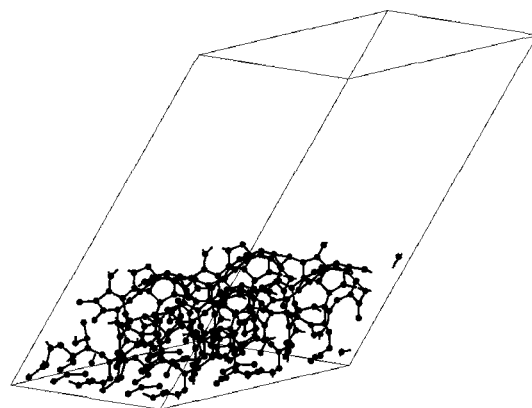


Fig. 1 Obtained C-cap like structure by 1.6ps layer by layer First-principle Molecular dynamics of SiC(111) surface at 2000 K.

[1] M. Kusunoki, T. Suzuki, T. Hirayama and N. Shibata: Appl. Phys.Lett., **77**, 531-533(2000).

Corresponding Author: Hiroki Moriwake

TEL: +81-52-871-3500, FAX: +81-52-871-3599, E-mail: moriwake@jfcc.or.jp

Optical Bandgap Modulation of Single-Walled Carbon Nanotubes by Encapsulated Fullerenes

○Toshiya Okazaki¹, Shingo Okubo¹, Takeshi Nakanishi¹, Takeshi Saito¹, Minoru Otani²,
Susumu Okada³, Shunji Bandow⁴ and Sumio Iijima^{1,4}

¹Research Center for Advanced Carbon Materials, AIST, Tsukuba 305-8565, Japan

²Institute for Solid State Physics, University of Tokyo, Kashiwa 277-8581, Japan

³Institute of Physics and Center for Computational Sciences, University of Tsukuba, Tsukuba 305-8577, Japan, and CREST, JST, Kawaguchi 332-0012, Japan

⁴Department of Materials Science and Engineering, 21st century COE (Nanofactory), Meijo University, Nagoya 468-8502, Japan

Single-walled carbon nanotubes (SWNTs) have been expected as building blocks for future molecular electronics because of their unique electronic and mechanical properties [1]. Advantageously, the local electronic band gap of SWNTs can be tuned by incorporating fullerene molecules, which results in nanometer-scale structured materials containing multiple quantum dots with length of ~ 10 nm [2, 3]. Although it provides possible design rules for proposing hybrid structures having a specific type of electronic functionality, it is yet unclear from either the experimental or theoretical point of view what is the effect of encapsulated fullerene molecules on the band gap modulations of SWNTs.

We here report systematic studies on the optical band gap modulation of C_{60} encapsulating SWNTs, so-called nanopeapods, by using two-dimensional (2D) PL excitation/emission mapping method [4]. Figure 1 shows 2D PL contour plots of the unfilled SWNTs (left) and C_{60} nanopeapods (right) as a function of emission and excitation wavelengths. It is clearly seen that overall features of PL behavior of SWNTs drastically change upon fullerene encapsulations. Detailed mechanism of band gap modulation will be discussed based on the tube diameter and the chirality dependences of the spectral shifts.

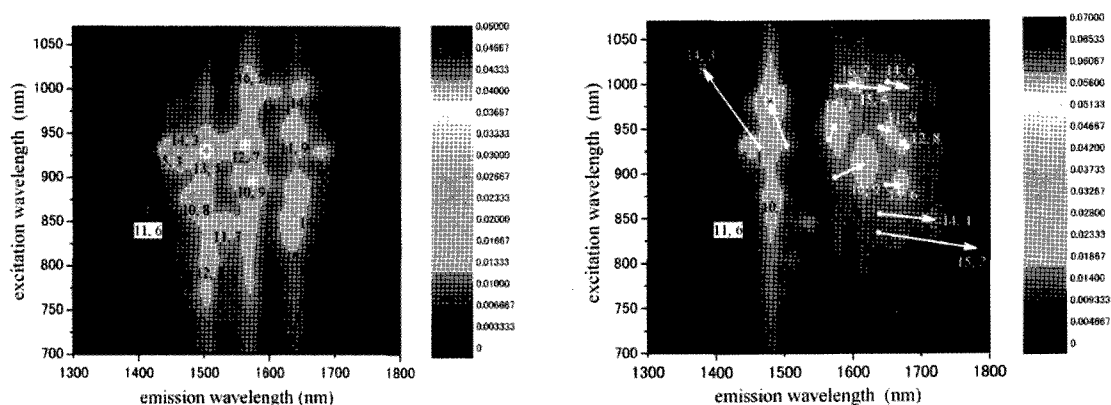


Figure 1. 2D PL contour maps of unfilled SWNTs (left) and C_{60} nanopeapods (right) of SDBS solutions.

[1] P. Avouris, J. Chen, *Materials Today*, **9**, 46 (2006). [2] J. Lee *et al.*, *Nature*, **415**, 1005 (2002). [3] D. J. Hornbaker *et al.*, *Science*, **295**, 828 (2002). [4] S. M. Bachilo *et al.*, *Science* **298**, 2361 (2002).

Corresponding Author: Toshiya Okazaki

E-mail: toshi.okazaki@aist.go.jp, **Tel:** 029-861-4173, **Fax:** 029-861-4851

Magnetically and Fluorescently Visualized Nanodiamond

○ Naoki Komatsu,¹ Masahito Morita,^{2,3} Tatsuya Takimoto,¹ Takahide Kimura,¹ and Toshiro Inubushi²

¹Department of Chemistry, Shiga University of Medical Science, Seta, Otsu 520-2192.

²Biomedical MR Science Center, Shiga University of Medical Science, Seta, Otsu 520-2192.

³PRESTO, JST

Although quantum dots and carbon nanotubes have been developed as promising fluorescent probes in modern biotechnology, they always have considerable concerns about cytotoxicity and photobleaching. Quite recently, however, proton-implanted nanodiamond (ND) powder has been reported to be successfully employed as a fluorescent probe with no photobleaching and low cytotoxicity [1]. This clearly shows the potential of ND powder as a molecular imaging agent. In continuation of our effort to develop a multi-modal imaging probe, we found that powdered ND exhibits NMR signals in a solution phase [2], a clear contrast on MR imaging [3] and fluorescence emitted from the tag on the surface [3].

The solution phase ¹³C NMR spectrum of ND is shown in Fig. 1. Such a decent spectrum was obtained after overnight accumulation, because ND has very short relaxation time ($T_1 = 0.3$ s) in the aqueous solution. A sharp contrast on MR imaging is shown in the presence or absence of ND in Fig. 2. These results are attributed to the presence of paramagnetic metals and/or defects in ND. In addition, fluorescent tag was covalently bonded on the surface of ND, making the ND to be fluorescently visualized in a cell.

This work was supported by Industrial Technology Research Grant Program in 2005 from New Energy and Industrial Technology Development Organization (NEDO) of Japan.

References:

- [1] S-J. Yu, M-W. Kang, H-C. Chang, K-M. Chen, and Y-C. Yu, *J. Am. Chem. Soc.*, **127**, 17604 (2005).
 [2] N. Komatsu, N. Kadota, T. Kimura, and E. Osawa, *Chem. Lett.*, **36** 398 (2007).
 [3] N. Komatsu, "Diamond Technology", Diamond Industry Association Ed.; NGT Co., Chapter 9, 3-7 Medicinal Application of Diamonds, pp 683-687 (2007).

Corresponding Author: Naoki Komatsu

E-mail: nkomatsu@belle.shiga-med.ac.jp, **Tel:** +81-77-548-2102, **Fax:** +81-77-548-2405

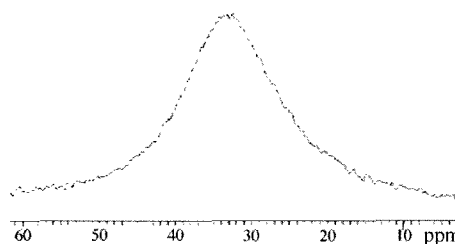


Fig. 1 ¹³C NMR of ND in water.

1% agarose
without ND

1% agarose
with ND



Fig. 2 MR image with or without ND.

Preparation and microstructural Observation of SiC nanotubes and SiC Composite Nanotubes; C-SiC, SiC-SiO₂ and C-SiC-SiO₂ Coaxial Nanotubes

○Tomitsugu Taguchi, Naoki Igawa, Hiroyuki Yamamoto and Shinichi Shamoto

Quantum Beam Science Directorate, Japan Atomic Energy Agency, Tokai, Ibaraki 319-1195, Japan

Since the discovery of carbon nanotubes (CNTs) in 1991, significant number of researches has reported about the synthesis of many nanomaterials from carbon nanotubes as the template materials. Silicon carbide (SiC) is one of the most important semiconductor materials and offers exciting opportunities in electronic devices for high temperature, high power and high frequency applications in an aggressive environment. On the other hand, SiO₂ is expected to be excellent insulator in the application of electronic devices. Furthermore, the syntheses of 1-D heterostructures with some compositions and interfaces have been of particular interest with respect to potential applications. The objective in this study is, therefore, to synthesize the SiC nanotubes and SiC composite nanotubes with heterostructures.

Carbon nanotubes as the template materials and Si powder were used. Both carbon nanotubes on the graphitic foil and Si powder were put in BN crucible. The Si powder did not contact directly with CNTs. The crucible was heated at 1100 to 1450 °C in a vacuum of around 5×10^{-4} Pa for 1 to 100 h. These reacted nanotubes were heated at 1300 °C in a vacuum of around 10 Pa for 5 to 10 h in order to sheathe with SiO₂ on the surface of SiC nanotubes.

The reacted CNTs at 1450 °C for 1h altered to the SiC nanowires, which were made of the catenated SiC grains of 50-200 nm in diameter. A few single-phase SiC nanotubes and many C-SiC coaxial nanotubes were synthesized at 1200 °C for 100 h. More than half number of nanotubes reacted at 1200 °C for 100 h were altered to single-phase SiC nanotubes by heat treatment of 600 °C for 1h in air since the remained carbon was removed [1]. The C-SiC-SiO₂ and SiC-SiO₂ coaxial nanotubes were synthesized by heating the C-SiC and SiC nanotubes at 1300 °C for 5 h in a low vacuum (Fig.1). On the other hand, almost all of the C-SiC and SiC nanotubes were altered to SiO₂ nanotubes by heating at 1300°C for 10 h in a low vacuum.

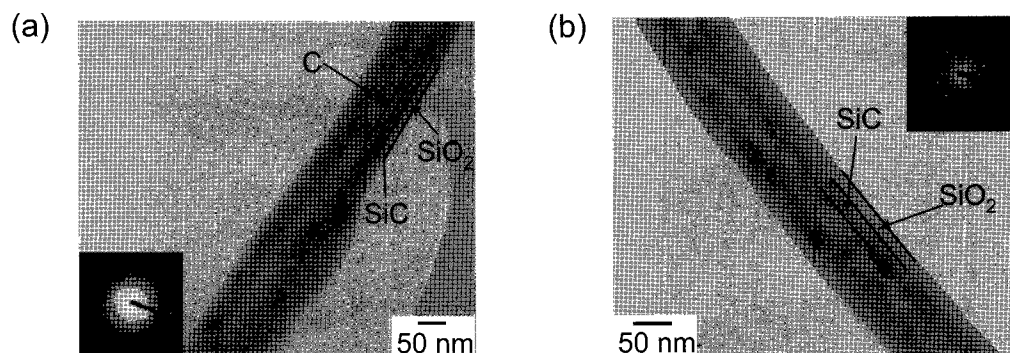


Fig.1 TEM microphotographs of (a) C-SiC-SiO₂ and (b) SiC-SiO₂ coaxial nanotubes.

[1] T. Taguchi, N. Igawa, H. Yamamoto, S. Shamoto, S. Jitsukawa, *Physica E*, 28 (2005) 431.

Corresponding Author: Tomitsugu Taguchi

TEL: +81-29-282-5479, FAX: +81-29-284-3813, E-mail: taguchi.tomitsugu@jaea.go.jp

Growth Temperature Influence on Vertically Aligned Carbon Nanofibers Containing Conical Cavity Array

○Yuta Tango, Akira Koshio, Kentaro Suzuki, Takayuki Yamasaki, and Fumio Kokai

*Division of Chemistry for Materials, Graduate School of Engineering, Mie University,
1577 Kurimamachiya-cho, Tsu, Mie 514-8507, Japan*

We previously reported that CNFs containing a conical cavity array were formed by alcohol CVD using indium tin oxide (ITO) and Fe as the metal catalysts. We named these CNFs with this unique structure “conical-cavity CNFs (CC-CNFs)”. In this study we succeeded in growing the vertically aligned CC-CNFs on a substrate by using precisely temperature-controlled CVD. We discuss what influence the growth temperature had upon the degree of vertical alignment and their inner structures.

A substrate was prepared by using the electrically controlled spray method. Ethanol solutions of InCl_3 , SnCl_2 , and FeCl_3 were used as catalysts and were sprayed on a Si plate maintained at 400°C followed by heating at 640°C for 30 min. in an Ar atmosphere. The CVD growth of the CNFs was carried out at $860\text{--}1000^\circ\text{C}$ for 30 min. at a vapor pressure of ethanol containing a small amount of CS_2 in a vacuum.

A typical CC-CNF formed after the CVD growth had a diameter of about 300 nm and an array of periodic conical cavities on the inside (Fig. 1). Figure 2 shows typical SEM images of CC-CNFs grown at $860\text{--}1000^\circ\text{C}$.

The CC-CNFs cannot grow at 860°C or less. We confirmed that vertically quasi-aligned CC-CNFs were formed at more than 870°C , and that vertically well-aligned CC-CNFs grew on the substrate at 920°C . Tangled CNFs (not vertically aligned) were formed at 1000°C . The SEM observation and precisely temperature-controlled CVD revealed the existence of two important critical temperatures and the narrow temperature range for the vertically well-aligned growth of the CC-CNFs. In addition, we investigated the relationship between the growth temperature and the inner structure by using TEM observations.

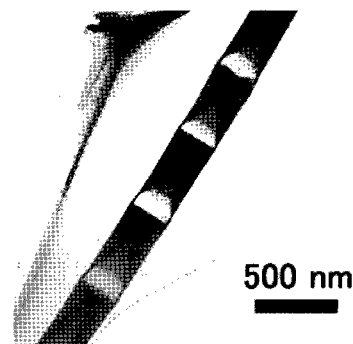


Fig.1 TEM image of CC-CNF

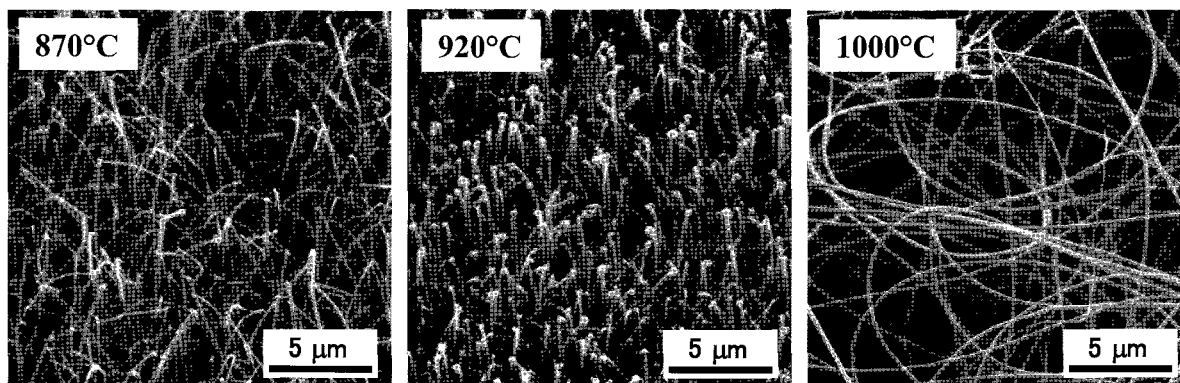


Fig. 2 Typical SEM images of CC-CNFs formed on substrate after CVD growth at $870\text{--}1000^\circ\text{C}$.

References: [1] A. Koshio *et al.*, *The 31st Fullerene-Nanotube General Symposium*, 1-18.

Corresponding Author: Akira Koshio

E-mail: koshio@chem.mie-u.ac.jp

Tel & Fax: +81-59-231-5370

Preparation and properties of rubber filled with radial single-walled carbon nanotubes

○Yoshinori Sato¹, Kenji Hasegawa², Nobuyuki Ito², Kenichi Motomiya¹, Balachandran Jeyadevan¹, Kazuyuki Tohji¹

¹*Graduate School of Environmental Studies, Tohoku University, Sendai 980-8579, Japan*

²*JSR Corporation, Mie 510-8552, Japan*

The nanotube-filler used in the rubber applications is required to be easy to disperse in polymer [1,2]. The radial single-walled carbon nanotubes (radial SWCNTs) [3] with 1.5-2.0 nm in diameter and 50-100 nm in length are grown radially around the core metal particles, which are more easily dispersed in polymer than the semi-finite long SWCNTs. Here, we report the preparation of radial SWCNTs reinforced styrene-butadiene rubber (SBR) and investigate their properties.

Ten weight percent of radial SWCNTs was blended with SBR to examine their effect on mechanical properties of the resulting composite, through the comparison with carbon black N339 (ASTM) as references. Radial SWCNTs resulted in an extraordinary hardness and low coefficient of repulsion, compared with N339. From microscopic surface analysis, the low dispersion of radial SWCNTs in the rubber matrix brought about lower fracture elongation and fracture strength as well as high hardness and low coefficient of repulsion.

[1] L. Valentini, J. Biagiotti, J. M. Kenny and M. A. López Manchado, *J. Appl. Polym. Sci.*, **89**, 2657 (2003).

[2] M. A. López Manchado, J. Biagiotti, L. Valentini and J. M. Kenny, *J. Appl. Polym. Sci.*, **92**, 3394 (2004).

[3] Y. Sato, B. Jeyadevan, R. Hatakeyama, A. Kasuya, K. Tohji, *Phys. Chem. Lett.*, **385**, 323 (2004).

Corresponding Author: Yoshinori Sato

TEL: +81-22-795-3868, FAX: +81-22-795-3868

E-mail: hige@bucky1.kankyo.tohoku.ac.jp

Stability of DNA-dissolved Carbon Nanotubes Separated by Size-Exclusion Chromatography

○Yuichi Noguchi, Tsuyohiko Fujigaya, Yasuro Niidome, Naotoshi Nakashima

*Department of Applied Chemistry, Graduate School of Engineering, Kyushu University,
744 Motoooka, Nishi-ku, Fukuoka 819-0395, Japan*

We have already reported that double-stranded DNAs (ds-DNA) and RNAs are able to dissolve SWNTs in water^{1,2)}. Water solutions of ds-DNA/SWNTs were prepared by sonication with a bath type ultrasonifier at a temperature below 10 °C, and subsequent centrifugation at 60000×g. Here, we examined high-resolution length sorting and stability of ds-DNA-wrapped carbon nanotubes by size-exclusion chromatography, which was recently developed. This system was found to separate ds-DNA/SWNTs and free ds-DNA. The result is shown in Figure 1. Furthermore, ds-DNA/SWNTs were separated into several fractions with very narrow length distribution, as confirmed directly by atomic force microscopy. The stability of ds-DNA/SWNTs was evaluated by re-injection of fractionated ds-DNA/SWNTs into size-exclusion chromatography. Details will be reported at the meeting.

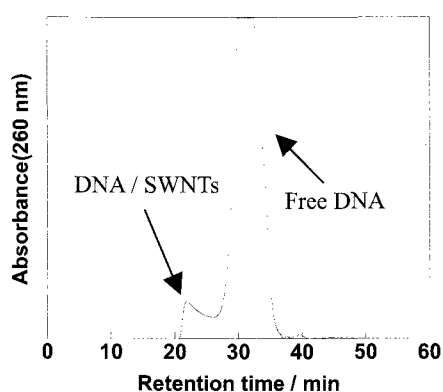


Fig. 1. Chromatogram of size-exclusion column separation of ds-DNA / SWNTs.

References:

- 1) N. Nakashima et al., *Chem. Lett.*, **32**, 456 (2003).
- 2) N. Nakashima et al., *Chem Phys. Lett.* **419**, 574 (2006).

Corresponding Author: Naotoshi Nakashima

E-mail: nakashima-tcm@mbox.nc.kyushu-u.ac.jp

Tel&Fax: +81-92-802-2840

Preparation of Carbon Nanotwist Paste for Printing-Type Field Emitter

○Y. Hosokawa^a, M. Yokota^a, H. Takikawa^a, S. Itoh^b, T. Yamaura^b,
K. Miura^c, K. Yoshikawa^c, and T. Ina^d

^a *Department of Electrical and Electronic Engineering,
Toyohashi University of Technology.*

^b *Product Development Center, Futaba Corporation.*

^c *Fuji Research Laboratory, Tokai Carbon Co., Ltd.*

^d *Fundamental Research Department, Toho Gas Co., Ltd.*

Carbon nanotwist (CNTw) is one of fibrilliform carbon nanomaterials with helical shape [1]. We have been reported the technique to synthesize CNTw in powder form with special blend catalyst [2] and this has promised to realize the mass production. However, the previous powdery CNTw included approximately 30% of catalyst. The contents of catalyst should be decreased. In the present study, first, amount of powdery CNTw production increased about 6 times compared with the case in the last report and ratio of catalyst content reduced less than 8% by improvement of catalyst application technique onto the substrate. Furthermore, by adding the third kind catalyst, amount of CNTw production increased by about 10 times, and ratio of catalyst content reduced less than 3%. As a result, larger amount of powdery CNTw production with lower cost was achieved. On the other hand, methods of pasting and printing CNTw on the substrate for field emitter have been developing. In this time, squeegee-printing method was employed. In the initial try, it was found that there were many aggregate site on the printed CNTw, due to the as-grown powdery CNTw. Thus the as-grown CNTw was milled by homogenizer. As a result of, the aggregate size became small and emission characteristics became better.

This work was partly supported by the Excellent Research Project of the Research Center for Future Technology, the Research Project of the Venture Business Laboratory, and the Research Project of Research Center for Future Vehicle, Toyohashi University of Technology; and JSPS Core University Program (JSPS-KOSEF in the field of "R&D of Advanced Semiconductor" and JSPS-CAS program in the field of "Plasma and Nuclear Fusion".



Fig. 1. SEM micrograph of CNTw synthesized in powder form.

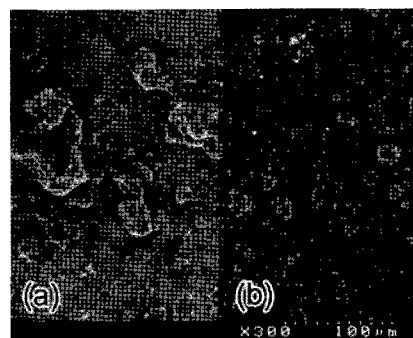


Fig. 2. Surface morphology of printed CNTw emitter; (a) as-grown CNTw and (b) after milling.

References:

- [1] T. Katsumata, Y. Fujimura, M. Nagayama, H. Tabata, H. Takikawa, Y. Hibi, T. Sakakibara, S. Itoh, *Trans. Mater. Res. Soc. Jpn.*, **29**, 501 (2004)
[2] Y. Hosokawa, H. Shiki, H. Takikawa, T. Ina, S. Itoh, T. Yamaura, *Abstracts of The 32nd Fullerene-Nanotube General Symposium*, 3P-35 (2007)

Corresponding Author: Yuji Hosokawa, Hirofumi Takikawa

E-mail: hosokawa@arc.eee.tut.ac.jp, Tel & Fax: +81-532-44-6644

E-mail: takikawa@eee.tut.ac.jp, Tel & Fax: +81-532-44-6727

Nanostructure Analysis of Carbon Nanowalls

○Ken-ichi Kobayashi ^{a)}, Makoto Tanimura ^{a)}, Hiroshi Nakai ^{b)}, Akihiko Yoshimura ^{b)},
Hirofumi Yoshimura ^{c)}, Kenichi Kojima ^{c)} and Masaru Tachibana ^{c)}

^{a)} Research Department, NISSAN ARC, LTD., 1 Natsushima-cho, Yokosuka 237-0061, Japan

^{b)} Ishikawajima-Harima Heavy Industries Co., Ltd., 1 Shin-Nakahara-cho, Isogo-ku, Yokohama 235-8501, Japan

^{c)} Graduate School of Liberal Arts and Science, Yokohama City University, 22-2 Seto, Kanazawa-ku, Yokohama 236-0027, Japan

A new type of carbon materials, so called carbon nanowalls (CNWs), has been found by Wu *et al* ^[1]. Figure 1 displays two secondary electron images of the CNWs grown on the quartz substrate, which were obtained by scanning electron microscopy. CNWs are shaped as very thin films, the average width of which is distributed in the range of 10 to 50 nm. It is reported that this two-dimensional character of CNWs originates from the stacking of several graphite sheets along the [0001] direction of the graphite structure. That is, CNWs belong to the group of graphite-based carbon materials. According to our previous report, CNWs are characterized by a high degree of graphitization in spite of the very small average size of the graphite regions ^[2]. This characteristic of CNWs greatly differs from that of ordinary graphite-based carbon materials.

In this work, in order to understand this difference, the nanostructure features of CNWs were examined by transmission electron microscopy. Our detailed analysis revealed that numerous graphite regions with an average size of about 20 nm, namely “nano-graphite domains”, were formed in the CNWs. The formation of these regions originates from the introduction of lattice defects such as dislocations and the slight rotation of the graphite sheets. On this basis, it is concluded that the nano-graphite domains are the constitutional units, the features of which would have an influence on the physical properties of the CNWs. The details of the experimental results and a nanostructure model of the CNWs will be presented.

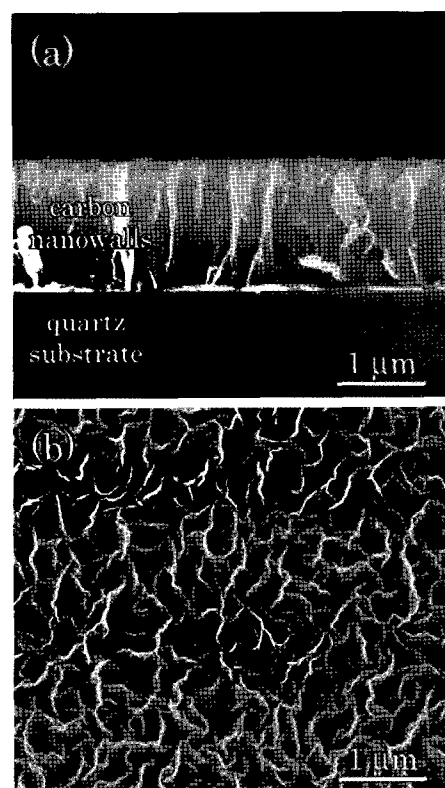


Fig.1 Secondary electron images of the CNWs grown on a quartz substrate as seen in (a) a cross-sectional view and (b) a top view.

Corresponding Author: Ken-ichi Kobayashi
E-mail: kobayashi@nissan-arc.co.jp
Tel: +81-46-867-5282
Fax: +81-46-866-5814

[1] Y. Wu *et al.*, Adv. Mater. 14, 64 (2002).

[2] S. Kurita *et al.*, J. Appl. Phys. 97, 104320 (2005).

[3] K.Kobayashi *et al.*, J. Appl. Phys. 101, 094306

Atomistic structural dynamics of carbon atomic wires by TEM-STM combined microscopy

○Koji Asaka, Kensuke Okumura, Hitoshi Nakahara and Yahachi Saito

*Department of Quantum Engineering., Nagoya University, Furo-cho,
Nagoya 464-8603, Japan*

We manipulated tips of two carbon nanotube bundles inside a transmission electron microscope and prepared carbon atomic wires supported by the two tips at the edges. The lattice imaging of structural dynamics was performed simultaneously with the electric conductance measurement. The transmission electron microscope was operated at an acceleration voltage of 120 kV. The lattice images were recorded at a time resolution of 40 ms. The variations in electric conductance were measured by the two-terminal method at room temperature.

Figures (a)-(c) show time-sequential high-resolution images of formation of a carbon atomic wire during tip manipulation. The left-hand and right-hand side regions (A) and (B) in Fig. (a) are tips of carbon nanotubes. The bright regions are the vacuum. The tip A is brought into contact with the tip B. The diameter of the nanotube of the tip B is 4.3 nm, and the nanotube is composed of walls with three atomic layers. The spacing of the atomic layers is 0.3 nm, equivalent to the interlayer spacing of graphite. When the tip A is retracted along the direction indicated by the arrow in Fig. (a) at an applied bias voltage of 0.8 V, the tip A is separated from the tip B and a carbon wire with a thickness of approximately 0.1 nm is formed between the two tips, as indicated by the arrow in Fig. (b). The thickness corresponds to a monatomic scale. The differential conductance decreased from $0.2 G_0$ (Fig. (a)) to $0.02 G_0$ (Fig. (b)), where $G_0 = 2e^2/h$ is the conductance quantum (e is the electron charge, h is Planck's constant). We assumed that the thickness of the wire is an atomic diameter of carbon, 0.15 nm, and estimated the current density of the wire to be $2 \times 10^{13} \text{ A/m}^2$. Finally, during the subsequent retraction, the monatomic carbon wire completely separates from the tip A and remains on the surface of the tip B as shown by the arrow in Fig. (c).

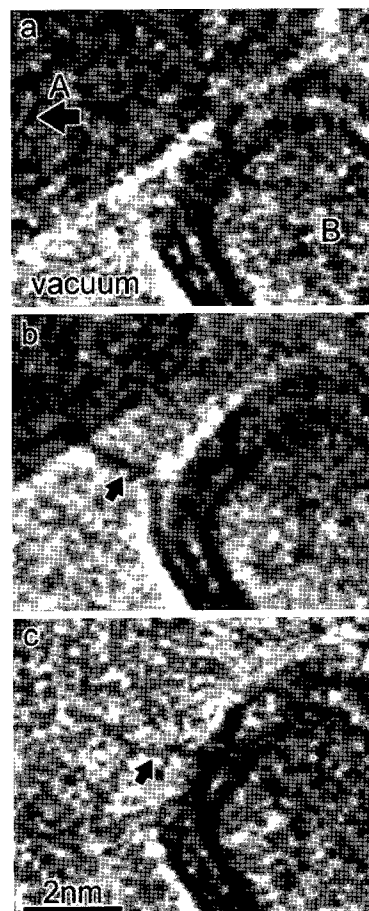


FIG. (a)-(c) Time-sequential series of high-resolution images of formation of a carbon atomic wire. The differential conductance was 0.2 and $0.02 G_0$ at the state observed in (a) and (b), respectively.

Corresponding Author: Koji Asaka

TEL: +81-52-789-4659, FAX: +81-52-789-3703, E-mail: asaka@surf.nuqe.nagoya-u.a.jp

Carbon Nanotube/Polyimide Composites

○Tsuyohiko Fujigaya, Minoru Okamoto, Ryosuke Tomokiyo, and Naotoshi Nakashima

*Department of Applied Chemistry, Graduate School of Engineering, Kyushu University,
Fukuoka, Japan*

Polymer composite materials are studied extensively and used widely in our industry due to their higher performance compared to original polymers. Carbon nanotubes (CNT) are considered as ideal filler materials because they possess extremely high mechanical strength, electric conductivity, thermal conductivity, and aspect ratio. Polyimide is one of the compounds which are most widely used in industry by taking advantage of the high thermal and chemical stability.

We have reported that total aromatic polyimide act as an excellent solubilizer for SWNT.¹ Of interest, in high concentration, solution form stable gel. Furthermore, SWNT are dispersed even in the solid state. Thus, we have successfully developed novel composite film for optical application.² Here we investigate the fabrication method and the basic properties of Kapton/CNT polymer composite. Among polyimide family, Kapton is most typically utilized especially for electronics. Single-walled carbon nanotube (SWNT) is dispersed in the *N*-methylpyrrolidinone (NMP) and polycondensation reaction of 4,4'-diaminodiphenyl ether (ODA) and 1,2,4,5-benzenetetracarboxylic acid dianhydride (PMDA) are carried out with the mixture of NMP containing dispersed SWNT. Obtained poly(amic acid) solution, precursor of the polyimide, are cast on the glass plate and dried in stepwise in vacuum with heating. It is found that SWNT are well dispersed in the resulting Kapton/SWNT composite film without any sign of aggregation even under optical microscopy observation. Mechanical properties of the composite film were examined and found that the Young modulus of the composite film (1.35 GPa) are increased compared to the film without SWNT (1.07 GPa). This is the first report describing Kapton/SWNT composite. For more effective reinforcement, anisotropic alignment of the SWNT in the film is expected to play an important role.

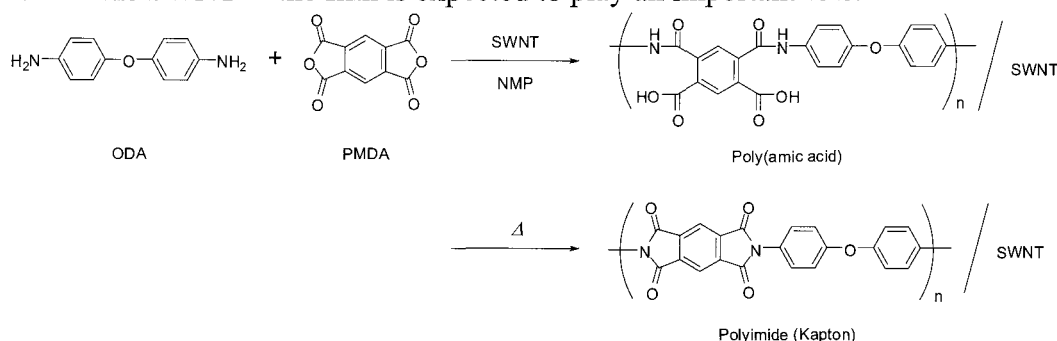


Fig.1. Synthetic scheme of Kapton/SWNT composite.

References

1. M. Shigeta, M. Komatsu, N. Nakashima, *Chem. Phys. Lett.* **418**, 115 (2006).
2. J.-H. Ryu, T. Nagamura, M. Shigeta, N. Nakashima, *Macromol. Symp.* **242**, 193 (2006).

Corresponding Author Naotoshi Nakashima

E-mail: nakashima-tcm@mbox.nc.kyushu-u.ac.jp

Tel&Fax +81-92-802-2840

Spin Injection into a Graphite Thin Film

○Megumi Ohishi, Masashi Shiraishi, Ryo Nouchi, Takayuki Nozaki, Teruya Shinjo and Yoshishige Suzuki

*Graduate School of Engineering Science, Osaka University
Machikaneyama-cho 1-3, Toyonaka 560-8531, Osaka, Japan*

Graphene¹, an atomically flat layer of carbon atoms packed into a two-dimensional (2D) honeycomb lattice, is currently one of the hottest topic in materials science and condensed-matter physics. A graphite thin film (GTF) formed from a small number of stacked layers of graphene behaves as a 2D conductor.¹ A GTF is thought to be well-suited to spin devices because of a large electron mean free path¹ and a small spin-orbit interaction. In this study, we fabricated a spin-valve device with a GTF (Fig.1) and achieved spin injection from ferromagnetic metal (FM, cobalt) into the GTF at room temperature (RT).² This is the first reliable observation of spin injection into molecular material at RT.

We employed a so-called non-local measurement scheme,³ which is able to separate a spin current path from a charge current path. Using this scheme, we can distinguish a spin-injection signal from any spurious signals such as anisotropic magnetoresistance. Figure 2 shows external magnetic field (H) versus non-local resistance (detected voltage V /applied current I) plots at RT. Depending on the magnetization directions of FM electrodes, the non-local resistance was changed and clear hysteresis can be seen, for instance from 150 to 280 Oe in upward sweeping of the magnetic field. The observed variation of detected signals clearly shows spin injection into the GTF at RT.

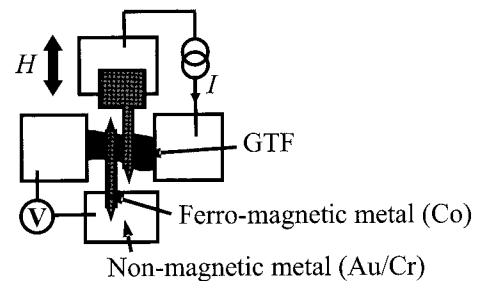


Fig. 1. A schematic diagram of a typical device structure

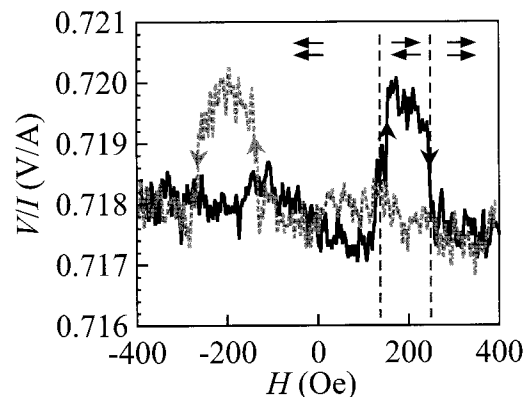


Fig. 2. Non-local signal measured at room temperature

[1] K. S. Novoselov *et al.*, *SCIENCE* **306**, 666 (2004). [2] M. Ohishi *et al.*, submitted to *Jpn. J. Appl. Phys.* [3] F. J. Jedema *et al.*, *Nature* **416**, 713 (2002).

Corresponding Author: M. Shiraishi,
E-mail: shiraishi@mp.es.osaka-u.ac.jp,
Tel&Fax: +81-6-6850-6426

発表索引
Author Index

Author Index

～ A ～

Abe, Shigeaki 1P-48
 Abe, Yuki 3P-22
 Achiba, Yohji 1-10, 1P-21, 1P-25, 2P-39,
 3-1
 Ago, Hiroki 1-2, 2P-46, 3P-34
 Aida, Takuzo 1P-5, 3-10
 Ajima, Kumiko 1P-32, 1P-33, 2-8
 Akachi, Masahiro 2-2
 Akasaka, Takeshi 3P-22
 Akasaka, Takeshi 1P-12, 2-12, 2P-10, 2P-11,
 3P-10, 3P-29, 3P-30
 Akasaka, Tsukasa 1P-48, 2P-45
 Akita, Seiji 1P-27, 2P-34
 Akiyama, Kimio 1P-13
 Akiyama, Tsuyoshi 2P-21
 Ando, Mariko 1P-13
 Ando, Yoshinori 1P-23
 Andou, Shingo 2P-15
 Aoki, Takaaki 1-11
 Aoshima, Hisae 1P-2
 Aoyagi, Shinobu 1P-14, 2-1
 Arai, Toru 3P-15
 Araki, Yasuyuki 2-4
 Asada, Yuki 2P-42
 Asaka, Koji 1P-38, 3-5, 3P-45
 Asano, Takeshi 3-9
 Atake, Toru 2P-17
 Awano, Yuji 1-17, 3-2
 Azumi, Reiko 2P-13

～ B ～

Bandow, Shunji 1-6, 1P-34, 1P-35, 1P-36,
 3P-37
 Barros, Eduardo B. 1P-41

～ C ～

Chen, Beibei 1P-23
 Chiashi, Shohei 1P-43, 3P-27
 Chikamatsu, Masayuki 2P-13
 Chitta, Rughu 2-4

～ D ～

D'souza, Francis 2-4
 Daigoku, Kota 2P-20
 Dejima, Eiji 1P-9
 Dresselhaus, Gene 1-8, 3P-18
 Dresselhaus, Mildred 1P-41
 Dresselhaus, Mildred S. 1-8, 3P-18

～ E ～

Eckert, Helmut 2P-7
 Einarsson, Erik 1P-43, 2P-29, 3P-5, 3P-21
 Endo, Morinobu 2P-40

～ F ～

Fan Jing 1P-31
 Fujigaya, Tusyohiko 2P-41, 3P-13, 3P-8, 3P-24,
 3P-42, 3P-46
 Fujimori, Masaaki 3P-19
 Fujita, Mitsuru 3-6
 Fujita, Norifumi 2-16
 Fujita, Takeshi 2-13
 Fujita, Takeshi 2P-28
 Fujiwara, Akihiko 2-15
 Fujiwara, Shinsuke 3P-7
 Fujiwara, Yoshihisa 1P-1, 2P-3
 Fukao, Tomohiro 3-9
 Fukui, Nobuyuki 3P-19
 Fukushima, Takanori 3-10
 Furukawa, Ko 1P-12
 Furukawa, Konosuke 1P-11
 Futaba, Don N. 3-8, 1-13, 3P-1

～ G ～

Ganko, Takayuki 2P-27
 Girard, Yvan 2P-1
 Goto, Tadashi 1P-2
 Goto, Yasutomo 1P-20
 Guan, Lunhui 1S-2

～ H ～

Hachiya, Makoto 2P-10
 Hanashima, Tateki 3P-27
 Hara, Takumi 2P-6
 Harada, Akira 1P-44, 1P-45
 Harada, Manabu 1P-34
 Harada, Y. 3-2
 Harima, Hiroshi 1-18, 1P-22, 1P-29
 Haruyama, J. 1P-42, 1P-43, 3-2
 Hasebe, Yuki 1-18, 1P-22, 1P-29
 Hasegawa, Kei 1-14, 1P-19, 3P-33
 Hasegawa, Kenji 3P-41
 Hasegawa, Sunao 2-3
 Hasegawa, Tadashi 3P-10, 3P-30
 Hashiguchi, Masahiko 1P-9
 Hashimoto, Kenro 2P-20
 Hashimoto, Masahiro 3P-10
 Hashimoto, Takeshi 1P-23
 Hashizume, Tomihiro 3P-19
 Hata, Kenji 1-13, 3-8, 3P-1
 Hatakeyama, Rikizo 2P-26, 3P-31
 Hatori, Hiroaki 3-8
 Hayashi, Kazuhiko 1-11
 Hayashi, Takuya 2P-40
 Hayashi, Yasuhiko 2P-28
 Heguri, Satoshi 1P-15, 1P-16
 Heike, Seiji 3P-19
 Hemme, Wilhelm 2P-7
 Hibi, Toshihide 2P-39
 Hikata, Takeshi 1-11
 Hino, Shojun 1P-11
 Hirahara, Kaori 2P-34

Hirano, Ken 2P-36
 Hiraoka, Tatsuki 1-13, 3-8, 3P-1
 Hirata, Eri 2P-45
 Hirayama, Kouhei 3P-24
 Hirayama, Tsukasa 3P-35
 Hiroki, Hibino 2-9
 Hirono, Yusaku 2P-30
 Hirotsu, Takahiro 2P-36
 Hirotsu, Tomoyuki 2P-27
 Honma, Yoshikazu 2-9, 3P-27, 2P-32
 Horie, Toshinori 2P-30
 Horikawa, Masayo 3-4
 Horn, Ernst 3P-29
 Hosokawa, Yuji 3P-43

～ I ～

Iakoubovskii, Konstantin 1-2, 3-7
 Ichiki, Takahiko 2P-4
 Ide, Mitsutaka 1P-42
 Igawa, Naoki 3P-39
 Iiduka, Yuko 2P-10, 2P-11
 Iijima, Sumio 1S-1, 1-6, 1-13, 1P-31,
 1P-32, 1P-33, 1P-34, 1P-35,
 1P-36, 2-8, 2-11, 2P-35,
 2P-37, 2P-39, 3-3, 3-8,
 3P-11, 3P-20, 3P-32, 3P-37

Iio, Yasunari 2P-15
 Ikuhara, Yuichi 3P-21
 Ikuta, Tatsuya 2P-46, 3P-34
 Imahori, Hiroshi 2P-8, 2P-38, 3-6
 Imamoto, Kenta 1-2
 Imanaka, Tadayuki 3P-7
 Ina, T. 3P-43
 Inada, Koji 3P-30
 Inagaki, Shinji 1P-20
 Inagaki, Takayuki 1P-34
 Inoue, Sakae 1P-23
 Inoue, Takashi 2-1

Inoue, Yoku	1-16, 2P-30	Jin Chuanhong	3P-20
Inubushi, Toshiro	3P-38	Jono, Jun-Ichi	3P-2
Ishibashi, Koji	1-9	Joung Soon-Kil	2P-37
Ishida, Akihiro	1-16, 2P-30		
Ishida, Masahiko	3P-12	～ K ～	
Ishigami, Itsuo	1-11	Kadota, Naoki	2P-38, 3-6
Ishigami, Naoki	1-2, 2P-46, 3P-34	Kadowaki, Hiroaki	2P-27, 2P-39
Ishihara, Masayuki	2-1	Kadowaki, Masayuki	2P-29
Ishii, Satoshi	1P-37	Takehi, Kazunori	1-14, 1P-30, 3P-33
Ishii, Tadahiro	2P-31, 2P-47, 3P-3	Kakihata, Kazuyuki	2P-30
Ishikawa, Kei	3P-5	Kakiuchi, Toru	2P-17
Ishikawa, Shinsuke	2P-9	Kamisuki, Hiroyuki	1P-49
Ishiyama, Yuichi	1P-7	Kanada, Ryo	2P-34
Isobe, Hiroyuki	2-7	Kanamori, Yusuke	2P-40
Isshiki, Toshiyuki	1-18, 1P-22, 1P-29	Kanazumi, Makoto	1P-12
Itakura, Atsushi	2P-13	Kanda, Makoto	3P-10
Ito, Nobuyuki	3P-41	Kaneko, Toshiro	2P-26, 3P-31
Ito, Osamu	2-4	Kang, Dongchul	3P-6
Ito, Yasuhiro	2-2, 2P-7	Karthigeyan, Annamalai	3-7
Ito, Yasuhiro	2-1	Kasama, Yasuhiko	1P-13, 2P-9, 2P-26, 2S-2
Itoh, S.	3P-43	Katagiri, Yoji	2P-22
Itoh, Takashi	1P-49	Kataura, Hiromichi	1P-39, 2-6, 2-11, 2P-27, 2P-39, 2P-44, 3-1, 3-4, 3P-7, 3P-17, 3P-25
Iwai, Taisuke	1-17		
Iwai, Yuki	2P-40		
Iwao, Yuriko	1P-24	Kato, Kenichi	1P-40
Iwasa, Yoshihiro	3-9	Kato, Masayuki	1P-11
Iwasaki, Shinya	3P-26	Kato, Tatsuhisa	1P-12, 3P-30
Iwasaki, Shinya	1-1	Kato, Yuko	3P-19
Iwata, Atsushi	2P-40	Kawabata, Hiroshi	2P-14
Iwata, Nobuyuki	2P-15	Kawai, Takazumi	1-3, 1P-31
Izadi-Najafabadi, Ali	3-8	Kawaji, Hitoshi	2P-17
Izumisawa, Satoru	2P-17	Kawamura, Hiroaki	1P-3
		Kawano, Gou	1P-4
～ J ～		Kawasaki, Naoko	2-15
Jeyadevan, Balachandran	1P-49, 2P-50, 3P-41	Kawasaki, Shinji	2P-40
Jie Jiang	1-1, 1-8, 3P-18	Kawashima, Junichi	2P-6
Jin, Hehua	3P-7	Kawata, Satoshi	1P-46, 3P-2
Jin, Wusong	3-10	Kazaoui, Said	2P-49, 3P-10

Kikuchi, Takashi	3P-29	Kumai, Yoko	1P-20
Kim, Yoong-Ahm	2P-40	Kumashiro, Ryotaro	2P-17, 3P-22
Kimata, Nozomu	1P-15, 1P-16	Kuroda, Norihiro	2P-3
Kimizuka, Osamu	3-8	Kusunoki, Michiko	3P-35
Kimura, Hisamichi	1P-48, 2P-50	Kuwahara, Shota	2P-42
Kimura, Takahide	2-5, 3P-38	Kuwano, Jun	1P-24
Kirimoto, Kenta	2P-12	Kuzumoto, Yasutaka	2P-8
Kishi, Naoki	1P-43, 2P-37	Kyakuno, Haruka	2P-39
Kishimoto, Shigeru	2P-43, 3P-16, 3P-26		
Kisoda, Kenji	1-18, 1P-22, 1P-29	～ L ～	
Kitada, Norihiro	1P-40	Li Yongfeng	2P-26
Kitaura, Ryo	1P-14, 1P-20, 2-2, 2P-42	Liu, Zheng	2-11
Kito, Hironobu	2P-25	Luclescu, Catalin Romeo	2P-31
Kiyooka, Yosuke	2P-20	Luculescu, Catalin Romeo	3P-3
Kobayashi, Atsushi	3P-16		
Kobayashi, Keita	1P-20	～ M ～	
Kobayashi, Ken-Ichi	3P-44	Mabuchi, Junpei	2P-22
Kobayashi, Mototada	1P-15, 1P-16	Maeda, Fumihiko	1P-28
Kobayashi, Nagao	3P-22	Maeda, Noriko	2P-47
Kobayashi, Yoshihiro	1-15, 1P-28, 2-9, 2P-32, 3P-23	Maeda, Yutaka	2-12, 2P-10, 2P-11, 3P-10, 3P-22, 3P-29, 3P-30
Kohama, Yoshimitsu	2P-17	Maekawa, Hideki	1P-13
Kohno, Hiroaki	1P-42	Maekawa, Masayuki	2P-33
Kojima, Kenichi	1-12, 1P-40, 3P-6, 3P-44	Maki, Hideyuki	1-9
Kojima, Nobuaki	1P-17, 2P-16	Makita, Yoji	2P-36
Kokai, Fumio	2P-22, 2P-25, 3-11, 3P-40	Malik, Sudip	2-16
Kokubo, Ken	1P-2	Maniwa, Yutaka	1P-39, 2P-27, 2P-39, 3P-17, 3P-25
Komatsu, Koichi	1P-8, 2P-17		
Komatsu, Mitsuo	1P-6	Maruyama, Shigeo	1-1, 1-14, 1P-18, 1P-19, 1P-26, 1P-30, 1P-43, 2P-29, 3P-5, 3P-10, 3P-21, 3P-26, 3P-33
Komatsu, Naoki	2-5, 3P-38		
Komuro, Takashi	1P-13, 2P-9		
Kondo, Daiyu	1-17		
Koretsune, Takashi	1-7	Matano, Yoshihiro	2P-38, 3-6
Koshino, Masanori	2-7	Matsuda, Kazuyuki	2P-27, 2P-39
Koshio, Akira	2P-22, 2P-25, 3-11, 3P-40	Matsudaira, Masaharu	1P-43
Koumura, Nagatoshi	2P-49	Matsukawa, Tomohiro	3-5
Krashennikov, Arkady	2P-19	Matsumoto, Hajime	2P-49
Kubozono, Yoshihiro	2-15	Matsumoto, Shuichi	2P-12

Matsuo, Jiro	1-11	Murakami, Tatsuya	1P-32, 1P-33
Matsuo, Yutaka	2-13, 2P-4	Murakami, Toshiya	1-18, 1P-22, 1P-29
Matsuoka, Ken-Ichi	2P-21	Murakami, Yoichi	3P-26
Matsuoka, Yohei	2P-28	Murakoshi, Kei	1-4
Matsushige, Kazumi	2P-14	Muramatsu, Hiroyuki	2P-40
Matsuura, Takanori	1P-3, 2P-5, 2P-6	Murata, Michihisa	1P-8
Mieno, Tetsu	2-3, 3P-28	Murata, Naoyoshi	1P-42, 1P-43
Mikami, Masafumi	1P-24	Murata, Yasujiro	1P-8, 2P-17
Mimura, Hidenori	1-16, 2P-30		
Minakata, Satoshi	1P-6	～ N ～	
Minami, Nobutsugu	1-2, 2P-49, 3-7, 3P-10	Nagano, Takayuki	2-15
Misawa, Yoshihiro	2P-49	Nagasawa, Hirosi	1P-21
Miura, K.	3P-43	Nagase, Shigeru	2-12, 2P-10, 2P-11, 3P-10, 3P-29, 3P-30
Miura, Noriko	3-9		
Miyahara, Katsuya	2P-18	Nagata, Hideya	2P-36
Miyako, Eijiro	2P-36	Nagayama, Hiroyuki	2P-20
Miyamoto, Yoshiyuki	1-3, 2P-19	Naito, Ryoji	1P-22
Miyata, Yasumitsu	1P-39, 2-6, 2P-39, 3P-17, 3P-25	Naitoh, Yasuhisa	3-4
		Naitou, Tsunahiko	2P-28
Miyauchi, Yuhei	1-1	Nakahara, Hitoshi	3-5, 3P-45
Miyawaki, Jin	1P-31, 1P-33, 2-8	Nakahodo, Tsukasa	3P-29
Miyazaki, Takafumi	1P-11	Nakai, Hiroshi	3P-44
Miyazaki, Takamichi	1P-13	Nakajima, Koji	2P-11
Mizorogi, Naomi	2-12, 2P-10, 2P-11, 3P-29, 3P-30	Nakamoto, Yoshiaki	1P-44, 1P-45
		Nakamura, Eiichi	2-7, 2-13
Mizubayashi, Jun	3-2	Nakamura, Eiichi	2P-4
Mizukoshi, Tomoyuki	1-11	Nakamura, Genki	3P-14
Mizuno, Naoki	2P-25	Nakamura, Hidetsugu	1P-4
Mizutani, Takashi	1-1, 2-2, 2P-43, 3P-16, 3P-26	Nakamura, Jin	1P-43
Moribe, Hiroe	2-1	Nakamura, Tetsuya	2-2
Moribe, Shinya	1P-1	Nakanishi, Takeshi	3P-37
Moriguchi, Isamu	3S-1	Nakashima, Naotoshi	2P-41, 3P-13, 3P-14, 3P-8, 3P-24, 3P-42, 3P-46
Morita, Masahito	3P-38		
Moriwake, Hiroki	3P-35	Nakayama, Ken-Ichi	2P-36
Moriyama, Hiroshi	2-14	Nakayama, Takashi	1P-25
Morokuma, Shingo	1P-19	Nakayama, Yoshikazu	1P-27, 2P-34
Motomiya, Kenichi	1P-49, 2P-50, 3P-41	Namura, Masaru	1P-49, 2P-50
Mrzel, Ale?	2-11	Narimatsu, Kaori	3P-14

Natori, Masato	2P-16	Ohno, Masatomi	1P-10
Neo, Yoichiro	1-16	Ohno Yutaka	1-1, 2-2, 2P-43, 3P-16, 3P-26
Nihey, Fumiyuki	3P-12, 3S-2	Ohshima, Satoshi	2P-39, 3P-11
Niidome, Yasuro	3P-24, 3P-42	Ohshima, Satoshi	3P-32
Nikawa, Hidefumi	3P-29	Ohta, Yohei	2-15
Nishibori, Eiji	1P-14, 2-1	Oizumi, Wataru	1P-49
Nishide, Daisuke	3-1	Okada, Hiroshi	1P-13, 2P-9
Nishigaki, Shohei	2P-26, 3P-31	Okada, Susumu	1-5, 3P-37, 2P-24, 2P-23
Nishimura, Toshifumi	1P-47	Okamoto, Minoru	3P-13, 3P-46
Nishino, Hidekazu	3P-1	Okawa, Jun	2P-29, 3P-5
Nishio, Koji	1-18, 1P-22, 1P-29	Okazaki, T.	3-2
Nobukuni, Shingo	3P-15	Okazaki, Toshiya	2-2, 2P-37, 3P-37
Noda, Suguru	1-14, 1P-19, 1P-26, 1P-30, 3P-33	Okigawa, Yuki	2P-43
Nodasaka, Yoshinobu	2P-45	Okimoto, Haruya	1P-11, 1P-14, 2-2, 2P-7
Noguchi, Yuichi	2P-41, 3P-42	Okubo, Akira	2P-50
Nokariya, Ryou	2P-15	Okubo, Shingo	2-2, 3P-37
Nomura, Shinya	1P-47, 2P-18	Okumura, Kensuke	3P-45
Nouchi, Ryou	2P-44, 3P-47	Okutsu, Takashi	1P-37
Nozaki, Takayuki	3P-47	Omote, Kenji	1P-13, 2S-2, 2P-9, 2P-26
Nozawa, Kyouko	1P-43	Ono, Shoichi	1P-13, 2P-9
Numao, Shigenori	1-6	Osedo, Hiroki	1P-3
Numata, Youhei	1P-3, 2P-6	Oshima, Hisayoshi	1P-18
		Oshima, Takumi	1P-2
		Osuka, Atsuhiko	2-5
~ O ~		Otani, Minoru	3P-37
Ochi, Yuta	1P-8	Otsuka, Yasuyuki	2P-32
Ogasawara, Syunsuke	2P-39		
Ogata, Teruhiko	3P-28	~ P ~	
Ogawara, Showgo	1P-37	Pan, Lujun	1P-27, 2P-34
Ogino, Shin-Ichi	1P-49	Park, Jin Sung	1P-41, 3P-18
Ogoshi, Tomoki	1P-44, 1P-45	Peng, Xiaobin	2-5
Ogura, Akio	2P-44		
Ogura, Kazuaki	2P-29, 3P-5	~ R ~	
Ohara, Kenji	1-16	Rachi, Takeshi	2P-17
Ohdo, Ryota	3P-34	Rahaman, G. M. Aminur	3P-29
Ohishi, Megumi	3P-47		
Ohmori, Shigekazu	2P-14, 3P-11, 3P-32	~ S ~	
Ohno, Yutaka	1-1, 2-2, 2P-43, 3P-16, 3P-26	Saito, Masatoshi	1P-42

Saito, Morihiro	1P-24	Shiraishi, Masashi	2P-44, 3-9, 3P-47
Saito, Riichiro	1-1, 1-8, 1P-41, 3P-18	Shizume, Rumi	3P-4
Saito, Susumu	1-7, 2P-2, 3P-36	Shoji, Satoru	1P-46, 3P-2
Saito, Takeshi	2P-39, 3P-11, 3P-32, 3P-37	Slanina, Zdenek	3P-29
Saito, Yahachi	1P-38, 3-5, 3P-45	Soga, Tetsuo	2P-28
Sakai, Yosuke	2P-33	Solin, Niclas	2-7
Sakata, Makoto	1P-14, 2-1	Someya, Chika	2-12
Sakurai, Yoshiaki	1-11	Suda, Yoshiyuki	2P-33
Samsonidze, Georgii G.	1P-41	Suenaga, Kazutomo	2-7, 2-11, 3P-20
Samukawa, Seiji	3P-12	Suga, Hiroshi	3-4
Sandanayaka, Atula	2-4	Sugai, Toshiki	1P-11, 1P-43, 2-2, 2-10, 2P-42, 3P-19
Sano, Masahito	3P-9	Sugawara, Hirotake	2P-33
Sasaki, Takeo	2P-5	Sugime, Hisashi	1-14, 1P-26, 3P-33
Sasamori, Ken-Ichiro	1P-48	Sugiura, Takahito	2-14
Sato, Kentaro	1-1, 1-8, 3P-18	Sumii, Ryohei	1P-11
Sato, Satoru	3P-30	Sun, Yong	1P-4, 2P-12
Sato, Shintaro	1-17	Suwa, Yuji	3P-19
Sato, Testuya	1-9	Suzuki, Tomoko	1P-23
Sato, Tohru	2P-8	Suzuki, Hidemasa	1P-46
Sato, Yoshinori	1P-48, 1P-49, 2P-45, 2P-50, 3P-12, 3P-41	Suzuki, Hidetoshi	1P-17
Sawa, Hiroshi	2P-17	Suzuki, Hidetoshi	2P-16
Sawada, Hirohide	1P-33	Suzuki, Kentaro	3-11, 3P-40
Seki, Toshio	1-11	Suzuki, Satoru	1P-28, 2-9, 2P-32, 3P-23
Sekido, Masaru	1P-10	Suzuki, Shinzo	1P-21, 1P-25, 2P-39
Senna, Mamoru	1P-7	Suzuki, Tomoko	2P-46
Seo, Hidetaka	2P-21	Suzuki, Yasunobu	1P-38
Shamoto, Shinichi	3P-39	Suzuki, Yoshiaki	3P-4
Shi, Zujin	2P-37	Suzuki, Yoshie	2P-31
Shimazu, Tomohiro	1P-18	Suzuki, Yoshinobu	1P-18
Shimizu, Taisei	1P-43	Suzuki, Yoshishige	3P-47
Shimizu, Tetsuo	3-4	~ T ~	
Shimote, Yoshikazu	3P-15	Tachibana, Masaru	1-12, 1P-40, 3P-6, 3P-44
Shinjo, Teruya	3P-47	Taguchi, Tomitsugu	3P-39
Shinkai, Seiji	2-16	Tajima, Isamu	2P-31
Shinohara, Hisanori	1P-11, 1P-14, 1P-20, 1P-43, 2-1, 2-2, 2-10, 2P-7, 2P-42, 3-1, 3-2, 3P-19	Tajima, Yusuke	1P-3, 2P-5, 2P-6
		Takagi, Daisuke	2-9, 2P-32

Takahashi, Katsumune	3P-4	Togaya, Kyoko	1P-2
Takahashi, Kohsuke	3P-15	Tohji, Kazuyuki	1P-48, 1P-49, 2P-45, 2P-50, 3P-12, 3P-41
Takahashi, Koji	2P-46, 3P-34	Toita, Sho	3P-6
Takahashi, Toru	2P-48	Tokunaga, Ken	2P-8, 2P-14
Takakura, Tsuyosi	1P-4	Tomanek, David	2P-19
Takano, Yoshihiko	1P-37	Tominaga, Masato	1P-47, 2P-18
Takase, Tsuyosi	1P-4	Tomioka, Fumiaki	1P-37
Takata, Masaki	2-1	Tomita, Haruo	2P-44
Takeda, Norihiko	1-4	Tomokiyo, Ryouosuke	3P-46
Takematsu, Yuji	1P-12	Tsuchida, Kunihiro	1P-33
Takenobu, Taishi	3-9	Tsuchiya, Takahiro	1P-12, 2-12, 2P-10, 2P-11, 3P-10, 3P-29, 3P-30
Takesue, I.	3-2	Tsuda, Shunsuke	1P-37
Takeuchi, Tsuneharu	1P-24	Tsuji, Masaharu	1-2, 2P-46, 3P-34
Takikawa, H.	3P-43	Tsuruoka, Ryoji	1P-6
Takimoto, Tatsuya	3P-38	Tsuruoka, Yasuhiro	1P-25
Tamaoki, Nobuyuki	2P-49	~ U ~	
Tamura, Goshu	1P-36	Uchida, Katsumi	2P-31, 2P-47, 3P-3
Tanabe, Fumiyuki	1P-8	Uchida, Katsumi	3P-4
Tanaike, Osamu	3-8	Uchida, Kazuyuki	1-5
Tanaka, Katsutomo	1P-9	Uchida, Takashi	1-12, 1-15
Tanaka, Kazuyoshi	2P-8	Ueda, Nobuteru	1P-43
Tanaka, Takatsugu	2-7	Ueda, Shinya	1P-37
Tanaka, Takeshi	3P-7	Ueno, Yusuke	2P-2
Tanamura, Masaki	2P-28	Umemoto, Hisashi	1P-11, 2-1
Tanemura, Akina	3P-3	Umesaka, Takeo	2P-43
Tango, Yuta	3-11, 3P-40	Umeyama, Tomokazu	2P-38, 3-6
Tanigaki, Katsumi	2P-17, 3P-22	Uo, Motohiro	1P-48, 2P-45
Taniguchi, Isao	1P-47, 2P-18	Urata, Keisuke	1P-21
Tanimoto, Yoshifumi	1P-1, 2P-3	~ W ~	
Tanimura, Makoto	3P-44	Wada, Akira	3P-12
Tashiro, Kentaro	1P-5, 2S-1	Wada, Keisuke	3P-9
Tatamitani, Yoshio	3P-28	Wakabayashi, Tomonari	2P-20, 3-1
Tazawa, Masaya	1-15	Wakahara, Takatsugu	1P-12, 2-12, 2P-10, 2P-11, 3P-10, 3P-29
Terada, Tomohito	2P-5		
Terauchi, Ikuya	2-1		
Terayama, Takashi	2P-16		
Tezuka, Noriyasu	2P-38, 3-6		
Tobita, Hiromi	1P-13, 2P-9		

Wakamatsu, Nobuo	2P-41	Yamasaki, Takayuki	3-11, 3P-40
Waki, Ippei	2P-50	Yamashita, Tetsuya	3-5
Wakita, Shinya	2P-12	Yamashita, Yusuke	1P-17
Wakita, Yuya	1P-1, 2P-3	Yamaura, T.	3P-43
Watanabe, Hiroto	1P-7	Yamazaki, Akira	1-15, 2P-32
Watanabe, Kazuyuki	2P-1, 2P-48	Yamazaki, Daisuke	1P-3
Watanabe, Kenchi	3P-8	Yanagi, Kazuhiro	1P-39, 2-6, 3-4, 3P-17, 3P-25
Watanabe, Makoto	3P-5	Yanagisawa, Makoto	1P-5
Watanabe, Satoshi	3P-27	Yano, Tomomi	1P-9
Watanabe, Tohru	1P-37	Yase, Kiyoshi	2P-13
Watari, Fumio	1P-48, 2P-45	Yasuda, Satoshi	3-8, 1-13
~ X ~		Yokoo, Kuniyoshi	1P-13, 2P-9
Xu Jianxun	2P-35	Yokota, M.	3P-43
~ Y ~		Yokoyama, Atsuro	2P-45
Yagi, Yuko	1P-43	Yonemura, Hiroaki	1P-1, 2P-3
Yajima, Hirofumi	2P-31, 2P-47, 3P-3	Yoshida, Hiromichi	3P-19
Yajima, Hirofumi	3P-4	Yoshida, Masaru	2P-49
Yamada, Michio	2-12, 3P-30	Yoshida, Yuji	2P-13
Yamada, Sunao	1P-1, 2P-3, 2P-21	Yoshii, Takamori	2P-12
Yamada, Takeo	3-8, 3P-1	Yoshikawa, K.	3P-43
Yamada, Tomoya	3P-29	Yoshimura, Akihiko	3P-44
Yamagishi, Tada-Aki	1P-44, 1P-45	Yoshimura, Hideyuki	2P-32
Yamagiwa, Kiyofumi	1P-24	Yoshimura, Hirofumi	3P-44
Yamaguchi, Takashi	1P-35	Yoshitake, Tsutomu	3-3
Yamaguchi, Masafumi	1P-17, 2P-16	Yoza, Kenji	2-12, 3P-29
Yamaguchi, Masao	1P-27	Yudasaka, Masako	1P-31, 1P-32, 1P-33, 1P-35, 1P-36, 2-8, 2P-35, 3-3
Yamaguchi, Takahide	1P-37	Yuge, Ryota	1P-31, 3-3
Yamaguchi, Yoshihiro	1P-24	Yumura, Motoo	1-13, 2P-39, 3-8, 3P-11, 3P-32
Yamaguchi, Yoshitaka	1-17	Yutaka Kitamura,	1P-14
Yamaguchi, Yukio	1-14, 1P-19, 1P-26, 1P-30, 3P-33	~ Z ~	
Yamamoto, Hiroshi	2P-15	Zhang, Minfang	2P-35
Yamamoto, Hiroyuki	3P-39	Zhang, Zhengyi	3P-21, 3P-33
Yamamoto, Takahiro	2P-1, 2P-48	Zhang, Guanxin	3-10
Yamamoto, Takahisa	3P-21	Zhang Minfang	1P-32, 1P-33, 2-8, 3-3
Yamamoto, Kazunori	3P-29	Zhao, Xinluo	1P-23

複写される方へ

本誌に掲載された著作物を複写したい方は、(社) 日本複写権センターと包括複写許諾契約を締結されている企業の方でない限り、著作権者から複写権等の行使の委託を受けている次の団体から許諾を受けてください。著作物の転載・翻訳のような複写以外の許諾は、直接本会へご連絡下さい。

〒107-0052 東京都港区赤坂 9-6-41 乃木坂ビル (法) 学術著作権協会

TEL : 03-3475-5618

FAX : 03-3475-5619 E-Mail : naka-atsu@muj.biglobe.ne.jp

アメリカ合衆国における複写については、次に連絡して下さい。

Copyright Clearance Center, Inc.

222 Rosewood Drive, Danvers, MA 01923 USA

Phone : (978)750-8400 FAX : (978)750-4744

Notice about photocopying

In order to photocopy any work from this publication, you or your organization must obtain permission from the following organization which has been delegated for copyright clearance by the copyright owner of this publication.

Except in the USA

Japan Academic Association for Copyright Clearance, Inc.(JAACC)

6-41 Akasaka 9-chome, Minato-ku, Tokyo 107-0052 Japan

TEL : 81-3-3475-5618

FAX : 81-3-3475-5619 E-Mail : naka-atsu@muj.biglobe.ne.jp

In the USA

Copyright Clearance Center, Inc.

222 Rosewood Drive, Danvers, MA 01923 USA

Phone : (978)750-8400 FAX : (978)750-4744

2007年7月11日発行

第33回フラーレン・ナノチューブ総合シンポジウム 講演要旨集

<フラーレン・ナノチューブ学会>

〒464-8602 愛知県名古屋市千種区不老町
名古屋大学大学院理学研究科 物質理学専攻
篠原研究室内

Tel : 052-789-5948

Fax : 052-789-1169

E-mail : fullerene@nano.chem.nagoya-u.ac.jp

URL : <http://fullerene-jp.org>

印刷 / 製本 門司印刷(株)

Hitachi Koki
HITACHI

RX II series

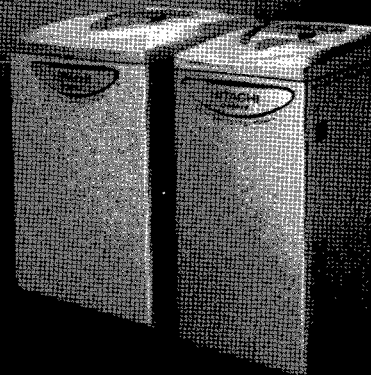
日立微量高速遠心機



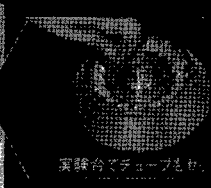
RX II series

●用途に応じて選べる豊富なロータバリエーション●のせるだけの“ロータウイックセッティング方式”を採用●低速から高速まで素早い加速、減速を実現●遠心加速度表示、設定機能を採用●ロータ自動判別機能を採用●耐インバランス駆動装置を搭載●強力な冷却能力を発揮●CE マーキング適合

毎分回転数	CF15RXII 15,000rpm	CF15RXI 15,000rpm	CF15RXIII 15,000rpm
最大容積、最大質量	21,900 x 7	21,900 x 7	21,900 x 7
回転制御範囲	400 ~ 16,000rpm	400 ~ 16,000rpm	400 ~ 16,000rpm
タイマ	5 ~ 99分、1 ~ 99分、HOLD	5 ~ 99分、1 ~ 99分、HOLD	5 ~ 99分、1 ~ 99分、HOLD
温度設定範囲	0 ~ 40℃	0 ~ 40℃	0 ~ 40℃
本体寸法 (mm)	430(W) x 415(D) x 652(H)	370(W) x 415(D) x 652(H)	370(W) x 415(D) x 652(H)
電源	AC100V、1.10V、0.6A/1.2、1.5A	AC100V、1.10V、0.6A/1.2、1.5A	AC100V、1.10V、0.6A/1.2、1.5A
質量	105kg	82kg	82kg
標準価格、税別	900,000円	790,000円	790,000円



全てのロータで使える「のせるだけ」方式



実験台でチューブもセット



結露管ロータ



多本架スイングロータ



マイクロプレート用ロータ

株式会社日立ハイテクノロジーズ

日立ハイテクノロジーズ営業部
本 社 〒105-8717 東京都港区新橋 丁目4番14号 電話 03-3504-7211 (ダイヤル)
東京都

北海道 011-221-7241 東北 022-264-2211 関東 0256-25-4811
中 部 052-219-1083 東 京 054-262-0861 西 京 055-389-7571
北 海 06-4807-2651 京 都 075-241-1341 西 京 087-325-9977
中 国 062-221-4514 九 州 0921-721-0501

日立工機株式会社

本社工場 〒312-8502 茨城県ひたちなか市武田1-060 8-40
東京：トリスセンター 〒151-0051 東京都渋谷区宇田川町5-8-2 電話 03-3226-7110
日立遠心機お客様相談センター【フリーダイヤル】 0120-02-4126 / 受付時間 9:00~17:00 (土曜S/S)
〒500-0001 長久保株式会社 052-405-7577

情報満載! **55078025** <http://www.hitachi-koki.co.jp/himac/>

住友商事のカーボンナノチューブ

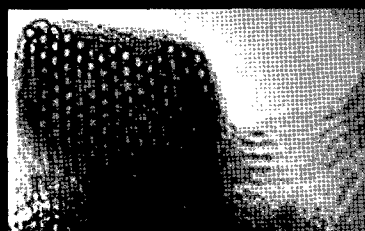
Produced by Carbon Nanotechnologies Inc. (CNI)

- ◆ 住友商事はCNI社の日本・アジア地域での総代理店として、学術研究用途から事業化・応用開発用途まで、各種用途に適した製品のご提供に加え、共同開発の推進や事業化支援プロジェクトの実施など、カーボンナノチューブの応用製品開発を総合的に支援しています。

● HiPco® 単層カーボンナノチューブ

直径約1nmの単層カーボンナノチューブです。基礎研究や高機能用途向けに、触媒残留率の異なる下記3製品をご提供しております。

製品名	触媒残留率
HiPco® As Produced (未精製品)	< 35 wt%
HiPco® Purified (精製品)	< 15 wt%
HiPco® Super Pure (超高純度品)	< 5 wt%



* Bucky Plus™(フッ化カーボンナノチューブ)など修飾品も対応可能です。

■ 単層カーボンナノチューブ ■

● CNI Xシリーズ

CNI社独自の製法で製造された、用途別産業応用向けカーボンナノチューブです。量産性に優れ、導電性付与(EMI, ESD, Anti-Static)、フィールドエミッション用途などに、安定した製品供給が可能です。詳細につきましては、下記連絡先までお問合せください。

● 二層カーボンナノチューブ

CNI社独自の製法で製造された、直径約2nmの二層カーボンナノチューブです。



■ 二層カーボンナノチューブ ■

上記製品群を中心に、研究用から量産対応品、また共同開発によるカスタマイズ対応など、用途に応じたカーボンナノチューブの開発を進めています。弊社までお気軽にお問合せ下さい。

本件に関するお問合せ先

住友商事株式会社 電子材事業部 (担当:河本/青木)

E-mail : nano@em.sumitomocorp.co.jp

TEL : 03-5166-4546 FAX : 03-5166-6234

住所 : 〒104-8610 東京都中央区晴海1-8-11

URL : www.sumitomocorp.co.jp/section/joho/nanotube.shtml

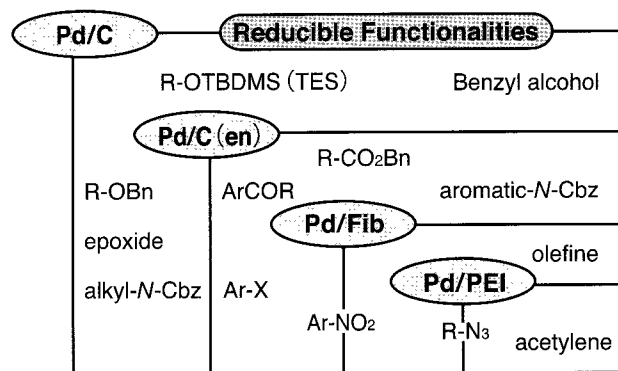


官能基選択的還元触媒 パラジウム-フィブロイン(Pd/Fib)

フィブロインにPdを担持した新規不均一系接触還元触媒

特長

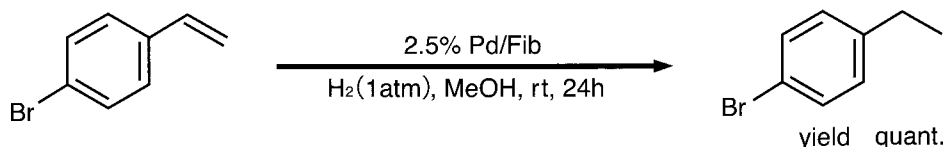
- 芳香族ハロゲン、ベンジルエステル及びN-Cbz基に対して反応性を示しません。
- 上記官能基共存下、オレフィン、アセチレン及び、アジドを選択的に還元可能。
- 従来のPd触媒に見られるような発火性を示しません。
- ろ過により再利用可能。



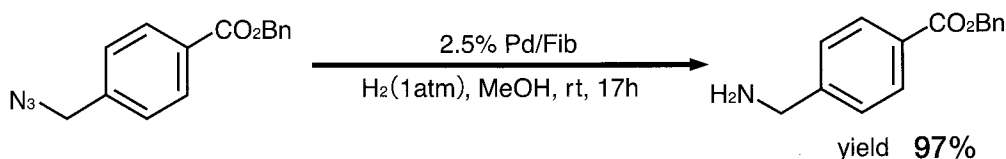
触媒活性の比較

反応例

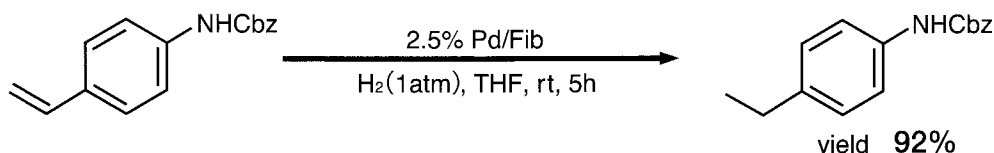
1. 芳香族ハロゲン化合物存在下での選択的還元反応



2. ベンジルエステル基存在下での選択的還元反応



3. 芳香族系アミンのCbz基保護下での選択的還元反応



コード NO.	品名	規格	容量
167-22181	Palladium-Fibroin 略名: Pd/Fib	有機合成用	1g
163-22183			5g

和光純薬工業株式会社

本社: 〒540-8605 大阪市中央区道修町三丁目1番2号
東京支店: 〒103-0023 東京都中央区日本橋本町四丁目5番13号
営業所: 北海道・東北・筑波・横浜・東海・中国・九州

問い合わせ先

フリーダイヤル: 0120-052-099 フリーファックス: 0120-052-806

URL: <http://www.wako-chem.co.jp>

E-mail: labchem-tec@wako-chem.co.jp

溶液中の粒子のナノレベル微細化・分散に

BRANSON 超音波ホモジナイザー

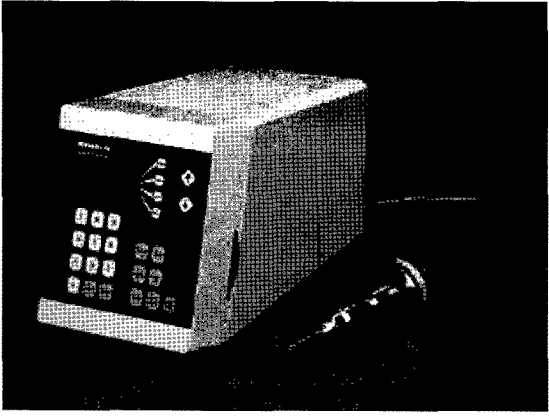
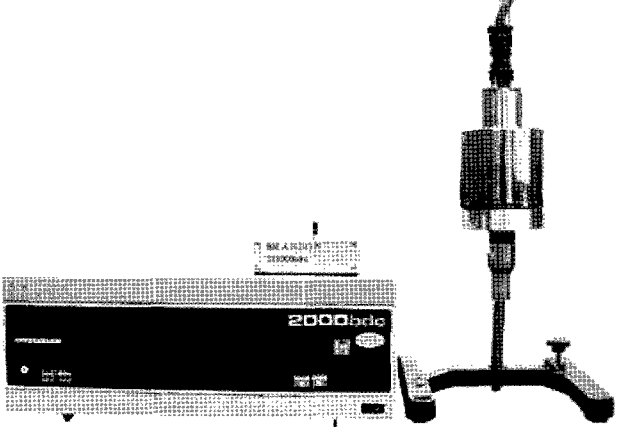
ホーン先端部の振幅の安定性を、より高めた Advance タイプ になりました。

近年のナノテクノロジーの発展及び粉体関連技術の向上により、より微細な粒子に対する乳化分散処理の要望が増えてまいりました。

超音波ホモジナイザーを使用し、均質な乳化分散処理を行い、安定させることにより製品の機能は向上します。

ブランソン社では 20kHz 機と、40kHz 機の 2 タイプを用意しております。

1 次粒子の凝集力にも抛りますが、20kHz 機では 100nm 程度までの分散力があります。40kHz 機は、さらに細かいレベルで分散ができる可能性があります。

20KHz 超音波ホモジナイザー BRANSON SONIFIER シリーズ	高周波 40KHz 超音波ホモジナイザー BRANSON SONIFIER4020 シリーズ
	

ブランソン社の製品は、ホーン先端部の振幅の安定性が高く、強力なキャビテーションが得られ、効率良くまた、再現性の高い分散処理が行えます。

主なアプリケーション

分散

カーボンナノチューブ 有機顔料 無機顔料 セラミック セメント 感光体 記録材料

磁性粉 粉末冶金 酸化鉄 金属酸化物 シリカ アルミナ カーボンブラック

ポリマー ラテックス ファンデーション

研磨剤 電池 フィラー 光触媒 触媒 ワクチン 体外診断薬 歯磨き粉 シャンプー 製紙

半導体 電子基盤 液晶 貴金属 金属 宝石 タイヤ 発酵菌類 その他

乳化

エマルジョン製剤 農業 トナー ラテックス 界面活性剤 クリーム 乳液 クリーム 等

株式会社 **セントラル** 科学貿易

本社 / 111-0052 東京都台東区柳橋 1-8-1

大阪支店 / 533-0031 大阪府大阪市東淀川区西淡路 1-1-36 新大阪ビル

福岡営業所 / 812-0016 福岡県福岡市博多区博多駅南 1-2-15 事務機ビル

札幌出張所 / 001-0911 北海道札幌市北区新琴似 11 条 13-9-3

TEL 03-5820-1500

FAX 03-5820-1515

TEL 06-6325-3171

FAX 03-6325-5180

TEL 092-482-4000

FAX 092-482-3797

TEL 011-764-3611

FAX 011-764-3612

URL <http://www.cscjp.co.jp/>

E-mail tokyo@cscjp.co.jp

E-mail osaka@cscjp.co.jp

E-mail fukuoka@cscjp.co.jp

E-mail csc-matsuda@cscjp.co.jp



atomistix

第一原理量子輸送計算プログラム

Atomistix ToolKit & Virtual NanoLab

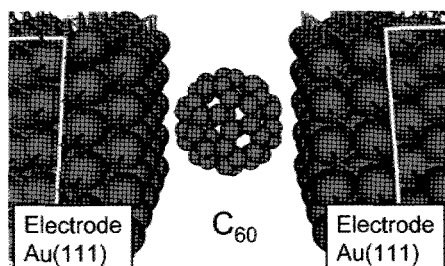
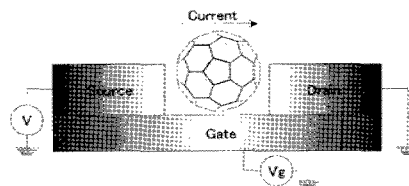
Atomistix ToolKit とは？

2つの半無限の電極に挟まれたナノスケール構造体の電気伝導特性を計算できる、世界唯一の商用第一原理電子状態計算プログラムです。

Virtual NanoLab とは？

Virtual NanoLab は、Atomistix ToolKit のためのユーザーフレンドリーな操作環境を提供します。Virtual NanoLab を用いれば、モデルのセットアップから Atomistix ToolKit を用いた計算の実行、結果の表示まで GUI を使って簡便に行うことができます。

お問い合わせは
サイバネットシステム株式会社 新事業推進室
E-Mail: atomistix-info@cybernet.co.jp



サイバネットシステムは金電極に挟まれたフラレン単分子デバイスの電気伝導特性を ATK を用いて解析し、第32回フラレン・ナノチューブ総合シンポジウムにて報告しました。



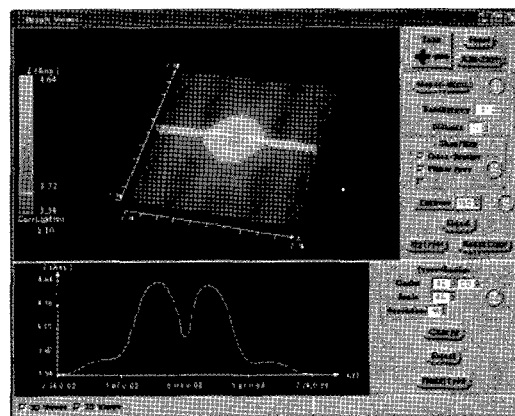
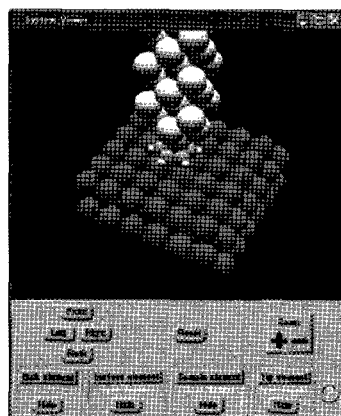
NANO times

STMシミュレータ

Nanotimes社製 Nt_STM

Nanotimes社製のSTMシミュレータNt_STMを用いると、GUIツールの操作によって容易に試料や表面、STMチップのセットアップを行うことができます。STM像のシミュレーションでは、STMチップと試料間の電流を計算してSTM像を得ることができます。

右図はそれぞれセットアップしたモデルを可視化した画面と、シミュレーションで得られたSTM像です。このモデルでは、Cu(100)面にベンゼン環を載せ、STMチップにW(110)を使用しています。



お問い合わせは
サイバネットシステム株式会社 新事業推進室
E-Mail: s-hirose@cybernet.co.jp

サイバネットシステム株式会社

本社 千101-0022 東京都千代田区神田練馬町3 富士ソフトビル
Tel: (03) 5297-3246 Fax: (03) 5297-3637

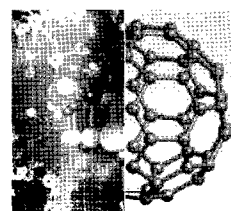
CYBERNET

つくる情熱を、支える情熱。

$$C \times \text{TOYO TANSO} = \infty$$

私たちの炭素の夢は、未来へと無限に広がります。

その優れた特性によって限りない可能性を持つC（カーボン）。
 私たち東洋炭素は、無限に広がるカーボンの応用分野を求めて、
 常に人と環境にやさしくをモットーに、未来技術の創造にチャ
 レンジしています。金属内包フラーレンやカーボンナノチューブ合
 成用原料の開発など、今、私たちに求められているものは何かを
 常に考え、21世紀に貢献する未来型企業を目指し続けます。



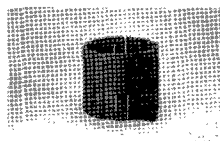
TOYO
 (K) 東洋炭素株式会社

URL <http://www.toyotanso.co.jp/>

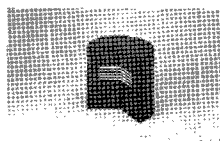
【本社】〒555-0011 大阪市西淀川区竹島5-7-12 TEL 06-6473-7912
 【工場】詫間事業所・大野原技術開発センター・萩原工場・いわき工場
 【営業所】東北・つくば・東京・北陸・静岡・名古屋・大阪・広島・四国・九州
 【国内関係会社】東炭化工株式会社・大和田カーボン工業株式会社

<主な製品>

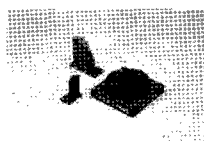
特殊黒鉛製品



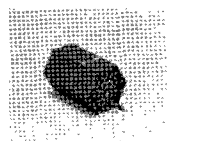
半導体用



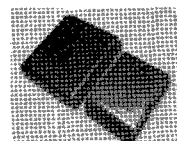
冶金工業用



放電加工用



原子力用



核融合装置用

一般カーボン製品



機械用



電気用

複合材その他製品



SiCコーティング
製品



黒鉛シート

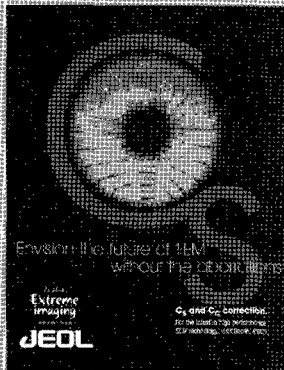


C/Cコンジット
製品



オンサイト
フッ素発生装置

収差補正(Cs)レンズで 世界最高性能の電子顕微鏡



JEM-2100F

フィールドエミッション電子顕微鏡

次世代超高性能電子顕微鏡

レンズの球面収差を補正することにより、分解能を飛躍的に向上させた次世代超高性能収差補正装置（球面収差補正電子レンズ）を、電子光学技術で高い技術を誇るドイツのCEOS社との共同開発により完成させ、最新のTEMに導入しました。

主な特長

照射系（コンデンサ）レンズの収差補正により、非常に細い電子ビームが形成され、走査透過電子顕微鏡（STEM）の分解能や元素分析などを行う際の空間分解能が飛躍的に向上

対物レンズの収差補正により、点分解能が0.12nmまで向上し、ブリッジが解消され、高精度での微小結晶界面などの特定が可能



お問い合わせは、電子光学機器営業本部（E0販促グループ） ☎042(528)3353

JEOL
Serving Advanced Technology

日本電子株式会社

<http://www.jeol.co.jp/>

本社・昭島製作所 〒196-8558 東京都昭島市武蔵野 3-1-2 ☎(042)543-1111
営業統括本部 〒190-0012 東京都立川市曙町2-8-3 新鈴巻ビル3F ☎(042)528-3381
札幌 (011) 726-9680・仙台 (022) 222-3324・筑波 (029) 856-3220・東京 (042) 528-3211・横浜 (045) 474-2181
名古屋 (052) 581-1406・大阪 (06) 6304-3941・広島 (082) 221-2500・福岡 (092) 411-2381



株式会社東京プログレスシステム

住所:107-0052 東京都港区赤坂 2-17-68-502
電話:03-5570-0457 FAX:03-5570-0462
URL: <http://www.tokyoprogress.co.jp>
Mail: eml-omori@wonder.ocn.ne.jp

営業品目

◎ 安定同位体元素

Si, S, V, Cr, Fe, Ni, Zn, Ge, Se, Kr, Mo, Cd, Sn, Te, Xe, W, Os, Pb, Mg, K, Ca, Ti, Cu, Zn, Ga, Rb, Sr, Zr, Ru, Pd, Ag, In, Sb, Ba, La, Ce, Nd, Sm, Eu, Gd, Dy, Er, Yb, Lu, Hf, Ta, Re, Ir, Pt, Tl, Hg, Yb, Ar

◎ ダイヤモンド粉末・その他の超硬材料

1. 爆発ダイヤモンド(DD)-黒鉛に爆薬の爆発による圧力をかけ合成する。粒子は多結晶体で研磨に最適と言われている。
2. 超分散ダイヤモンド(UDD)-爆薬 TNT の分子中の炭素が爆発による高温・高圧下でダイヤモンドに変わったもの。粒径は30~50ナノのクラスターになっている。エレクトロニクス産業での高精度研磨・表面処理・潤滑剤などの用途がある。
3. 静圧合成ダイヤモンド(工業用ダイヤモンド)-黒鉛に約5万気圧・1300℃以上の圧力をかけて合成したダイヤモンドを粉砕したもの。
4. その他研磨用ダイヤモンドペースト・BN・CBN など

◎ 無機レンズ・プリズム・ウインドウ(NaCl, KCl, Si, Ge, GaAs, Al₂O₃, CaF₂, LiF etc.)

◎ MTR 社のフラーレン誘導体類

- ★C60/PCBM, 純度99.5%以上
(価格:250mg, ¥93,000- 1gr: ¥180,000- 10gr: ¥1,600,000-)
- ★C70/PCBM 純度99%以上
(価格:250mg, ¥150,000- 1gr: ¥370,000- 10gr: ¥3,200,000-)
- ★その他 C60:(C13 置換) ★C60:C70 (C13 置換)★Mixture C60 & C70(C13 置換)
- ★C60F₃₆, ★C60 F₄₀ ★Higher fullerene mixture C76, C78, C80 & C84
- ★C60CHCOOH(1.2-methanbofullerenC60)-61-carboxylic acid
- ★[η⁵(C₅H₅)₂Fe]₂*C60 ★Type A: C60HNH(CH₂)₃ COONa
- ★Type B: C60HNH(CH₂)₅ COONa ★C60C(COOEt)₂ & ★C60[C(COOEt)₂]₂
- ★C60Br₂₄ ★水酸化フラーレン:C60(OH)_n: n=18~24 など

◎ 翻訳 <英語・ドイツ語・フランス語・ロシア語など>・技術調査 など

Best for Our Customers

—すべてはお客様のために— を合言葉に、ナノテク新材料における最高のソリューションを提供します。



I 分散・凝集過程評価
 ナノ粒子径分布測定装置
 SALD-7100



I 微量CNTの純度・熱特性評価
 I CNTの結晶性と耐熱性の評価
 ミクロ熱重量測定装置
 TGA-50



I 熱分解生成物・発生ガスの分析
 ガスクロマトグラフ質量分析計
 GCMS-QP2010 Plus (熱分解システム)

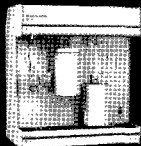


II CNTの紫外可視近赤外吸収スペクトル測定
 紫外可視近赤外分光光度計
 SolidSpec-3700



紫外可視近赤外分光光度計
 UV-3600

I 比表面積と吸着特性
 マイクロメリテックス
 高速比表面積/細孔分布測定装置
 アサップ2020シリーズ



凝集分散

微量測定

純度

I 触媒元素の測定
 ツインシーケンシャル形ICP発光分析装置
 ICPS-8100



II 直径測定
 II 結晶性と耐熱性の評価
 ラマン分光光度計
 Holo-Probe モニタリングシステム

I SWNTの近赤外PL3次元分布測定
 近赤外フォトルミネッセンス測定システム
 NIR-PL System



カイラリティ

直径

観察

※こちらの特は特製品となります

II 直径測定
 II 精製前後の観察
 II CNTとポリマーコンポジット試料の観察
 走査型プローブ顕微鏡
 SPM-9600



II あらゆるナノテク材料を観察・測定
 ナノサーチ顕微鏡
 SFT-3500



nanotech
 SHIMADZU

Total Solution focused on Carbon Nanotube

株式会社 **島津製作所**

東京支社：分析計測事業部事業戦略室マーケティングG
 東京都千代田区神田錦町1-3

TEL03-3219-5633 FAX03-3219-5557
<http://www.shimadzu.co.jp>

TORAY
Innovation by Chemistry

**そっとそばに、
東レの先端材料。**

先端材料と聞くと、なんだか遠い話だと思いかも知れません。
でも実は、意外と身近で関係しているのが東レです。

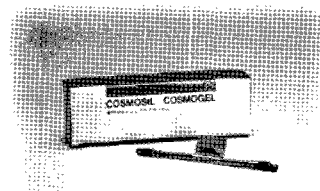
ケータイもその中の1つ。液晶画面のカラーフィルターをはじめ、
ボタン部分のシリコーンゴム、折れにくいアンテナの素材、
電子回路に使われているフィルム材料など、
他にも色々、コミュニケーションを支えているのが
東レグループの先端材料。

今日も東レは、あなたのくらしの中身をつくっています。

東レ株式会社
<http://www.toray.co.jp/>

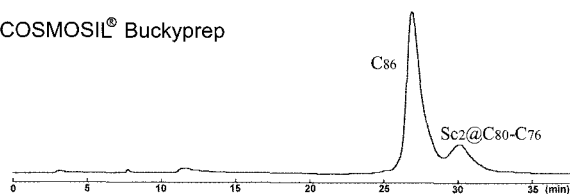
COSMOSIL® Buckyprep-M

今まで分離できなかった
金属内包フラーレンが分離可能！！

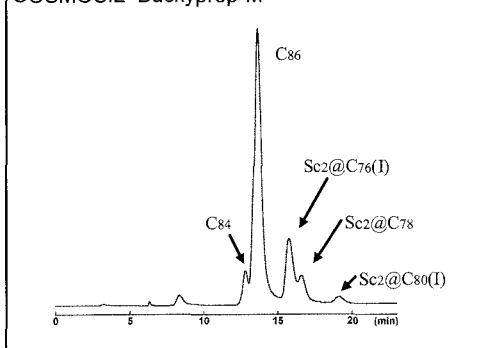


■分析例

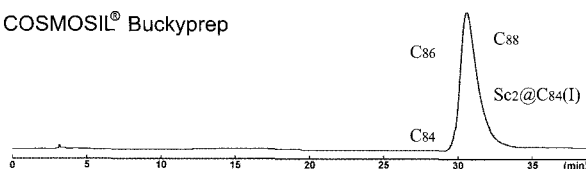
COSMOSIL® Buckyprep



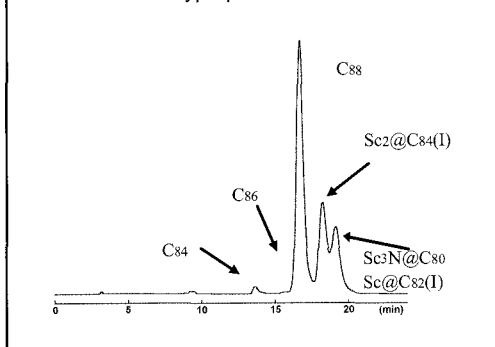
COSMOSIL® Buckyprep-M



COSMOSIL® Buckyprep



COSMOSIL® Buckyprep-M



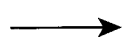
分析条件

カラムサイズ：4.6mm I.D. × 250mm 移動相：トルエン、流速：1.0 ml/min、温度：30°C、検出：UV312

資料提供：名古屋大学 大学院理学研究科物質理学専攻 篠原 久典教授

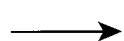
■その他COSMOSIL® フラーレン関連カラム

フラーレン分離のスタンダードカラム



COSMOSIL® Buckyprep

C₆₀, C₇₀等の大量分取に



COSMOSIL® PBB

詳しい情報はWeb siteをご覧ください。

ナカライテスク株式会社

〒604-0855 京都市中京区二条通烏丸西入東玉屋町498

価格・納期のご照会 フリーダイヤル 0120-489-552

製品に関するご照会 TEL: 075-211-2703 FAX: 075-211-2673

Web site : <http://www.nacalai.co.jp>

研究試薬・実験機器・工業薬品

株式会社三和

代表取締役社長 田村和生

本社 〒804-0082 北九州市戸畑区新池2-5-42
TEL(093)871-4821(代) FAX(093)871-4823

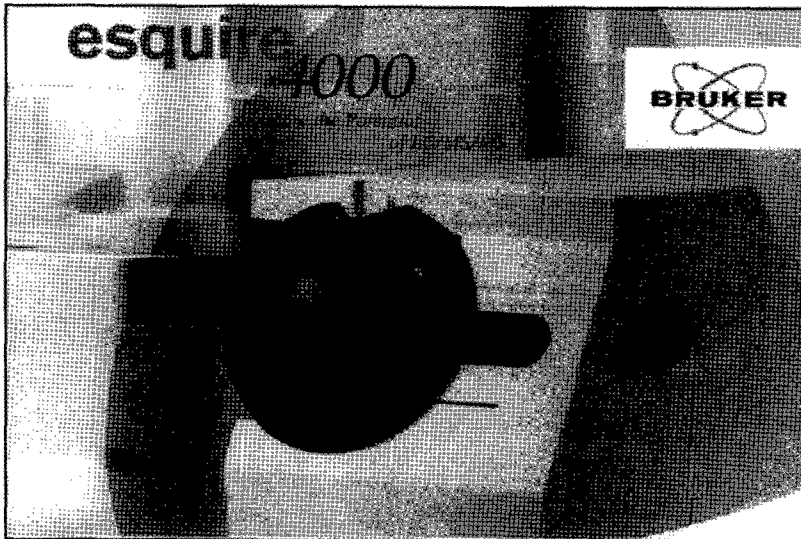
福岡営業所 〒813-0062 福岡市東区松島6-8-4
TEL(092)626-2333 FAX(092)629-2882

的確な情報で

コンサルティング

科学研究のトレンドを的確に把握した上での、サポート、アドバイス。又、将来の研究ニーズを予測し、お客様の声に耳を傾け、研究開発を飛躍的に推進させる解決策をご提案いたします。

あらゆる分野における研究機関の環境づくりに
長年にわたって携わってきた実績から、
細かなニーズにお応えする提案力が「新興精機」にはあります。



ハイレベルな **製品** のご提案

熟練のスタッフによる定期的な整備などのアフターサービス体制は万全を期しており、万一のトラブル発生の際は打てば響く迅速な対応、的確なアドバイスでサポートしています。

的確な情報で研究開発をバックアップ

九州全域をカバーする新興精機のサービスエリア

信頼の **サポート** 体制

製品のメリットデメリットを的確に判断し、厳しい基準をクリアした高品質の製品をお届けするための体制作りも積極的に推進。
国際入札への参加を通じて、厳選された機器をお客様に提供しています。

【東京営業所】

〒101-0021 東京都千代田区外神田6丁目10番12号 TEL: 03-5618-8751

【北九州営業所】

〒807-0872 北九州市八幡西区浅川1丁目18番37号 TEL: 093-603-5680

本社

〒812-0054 福岡市東区馬出1丁目18番3号

TEL: 092-641-8451

工場 〒816-0063 福岡市博多区大字会の原2丁目3番9号

TEL: 092-593-5327

【佐賀営業所】

〒849-0937 佐賀市鶴島3丁目9番6号 TEL: 0952-31-1095

【熊本営業所】

〒862-0920 熊本市月出4丁目4番130号 TEL: 096-385-6001

【宮崎営業所】

〒880-0929 宮崎市まなび野2丁目37番5 TEL: 0985-64-1533

【鹿児島営業所】

〒890-0054 鹿児島市鹿田2丁目4番14号-201号 TEL: 099-612-5461



株式会社新興精機 <http://www.shinkouseiki.co.jp>

【関連会社】～細胞保存・免疫細胞加工と先端医療技術の開発を専門とする医療支援事業専門会社～ CAセラピューティック

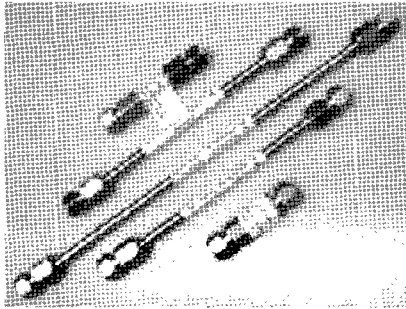


Sepax Technologies

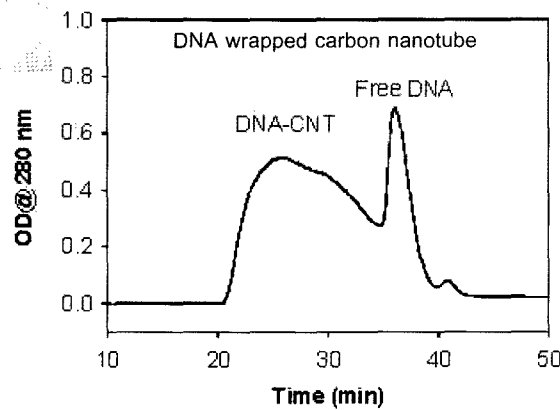
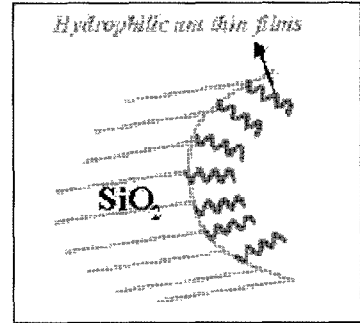
SepaxCNT SEC シリーズ

独自の表面処理技術 Nanofilm テクノロジーによりカラム樹脂表面をマスクし表面の親水性を高めることで非特異的吸着を排除し、SEC の分離原理である分子サイズに従った溶出が可能になります。

SepaxCNT SEC シリーズは、カーボンナノチューブやナノ粒子の分離に適しています。



- 長さによるカーボンナノチューブ、ナノロッドの分離
- 径によるナノパーティクルの分離
- 分析から分取まで



Columns: 4.6x250 mm, 5 μ m
 Sepax CNT SEC-300
 Sepax CNT SEC-1000
 Sepax CNT SEC-2000
 0.1 M Tris + 0.2 M NaCl
 pH 7.0
 0.25 mL/min

f21

Fraction 21
Avg. 850nm

f25

Fraction 25
Avg. 200nm

f30

Fraction 30
Avg. 100nm

Nanofilm SECにより分離されたナノチューブの各フラクション

Products	ポアサイズ	粒子径	CNT 容量範囲	pH 範囲	アプリケーション
CNT SEC-300	300 Å	5 μ m	長さ:1-100nm 径:1-5nm	2-8.5	Carbon Nanotubes, nanorods, nanoparticles
CNT SEC-500	500 Å	5 μ m	長さ: 25-250nm 径:1-10nm	2-8.5	Carbon Nanotubes, nanorods, nanoparticles
CNT SEC-1000	1000 Å	5 μ m	長さ: 100-500nm 径:1-25nm	2-8.5	Carbon Nanotubes, nanorods, nanoparticles
CNT SEC-2000	2000 Å	5 μ m	長さ: 300-1000nm 径:1-50nm	2-8.5	Carbon Nanotubes, nanorods, nanoparticles

IMS 機器株式会社



- 東京 〒162-0805 東京都新宿区矢来町113番地
TEL:(03)3235-0661 (代) / FAX:(03)3235-0669
- 大阪 〒532-0005 大阪市淀川区三国本町2丁目12番4号
TEL:(06)6396-0501 (代) / FAX:(06)6395-2588
- 福岡 〒812-0054 福岡市東区馬出1丁目2番23号
TEL:(092)631-1012 (代) / FAX:(092)641-1285

※会社名および商品名は、各会社の商標または登録商標です。
 ●規格・仕様および外観は、改良などのため予告なく変更する場合があります。

<http://www.technosaurus.co.jp>
 SEPAX_CNT SEC/nanotech2006



ハイテクの一步先に、いつも。

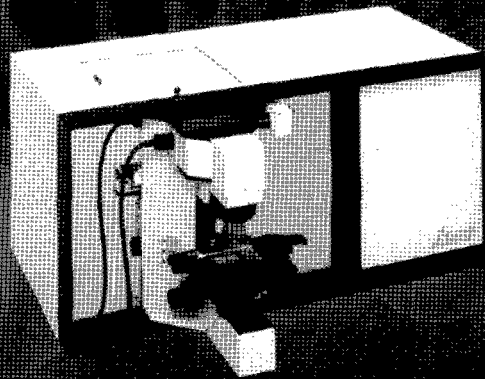
HORIBA

Explore the future

CNTの測定にはデファクトスタンダードの LabRamHR-800が最適

～RBM/フォトルミネッセンスを同一スポットで測定～

顕微レーザーラマン分光測定装置 LabRamシリーズ



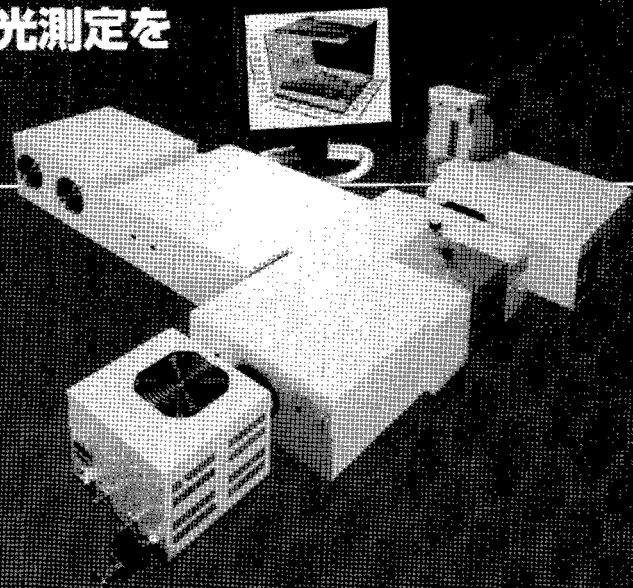
- ・244nm～1064nmのレーザによる測定が可能
- ・焦点距離800nmの分光器により高分解能測定を実現

SWCNTの近赤外領域の蛍光測定を 大幅にスピードアップ

～ ナノテクリサーチに ～

近赤外対応蛍光分光測定装置 SPEX NanoLogシリーズ

- ・InGaAsアレイ検出器による高感度測定
- ・高速・高分解能マトリックスマッピング
- ・モジュールユニットだからアプリケーションに
応じた各種NIR検出器の組み合わせも可能



HORIBA JOBIN YVON

株式会社堀場製作所

科学システム営業部 03-3861-8234

本社 〒601-8510 京都市南区吉祥院宮の兼町2 TEL(075)313-8121

- 仙台(022)308-7890
- つくば(0298)56-0521
- 東京(03)3861-8231
- 横浜(045)451-2091
- 名古屋(052)936-5781
- 大阪(06)6390-8011
- 広島(082)288-4433
- 愛媛(0897)34-8143
- 福岡(092)472-5041

製品の詳しい情報は

<http://www.jyoriba.jp>

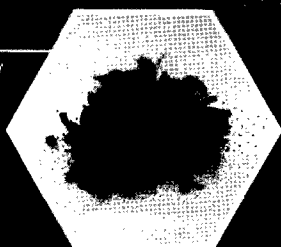
<http://www.horiba.co.jp> e-mail: info@horiba.co.jp

Lab set CNT10

1.SWNT(FH-P)

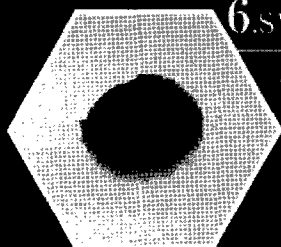
単層カーボンナノチューブ
FH精製タイプ

■ 製造法
CVD法



6.SWNT(FH-P)ペーパー

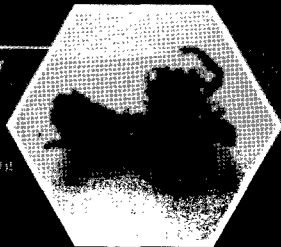
単層カーボンナノチューブ
FH精製タイプのペーパー



2.SWNT(FH-A)

単層カーボンナノチューブ
FHタイプ

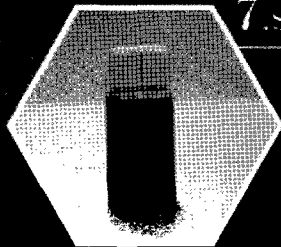
■ 製造法
CVD法



7.SWNT(FH-P)分散液

単層カーボンナノチューブ
FH精製タイプ

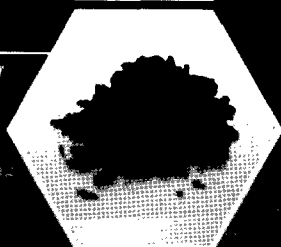
■ 分散液
分散液



3.SWNT(APJ)

単層カーボンナノチューブ
APJタイプ

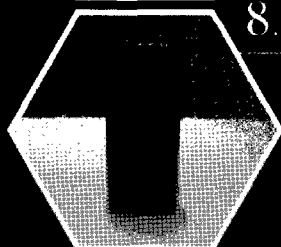
■ 製造法
CVD法



8.SWNT(FH-A)分散液

単層カーボンナノチューブ
FHタイプ

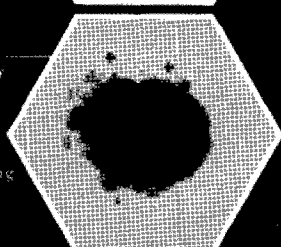
■ 分散液
分散液



4.MWNT

多層カーボンナノチューブ

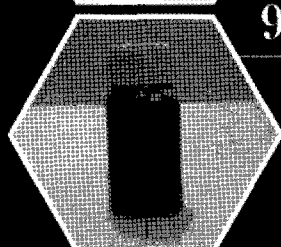
■ 製造法
CVD法



9.SWNT(APJ)分散液

単層カーボンナノチューブ
APJタイプ

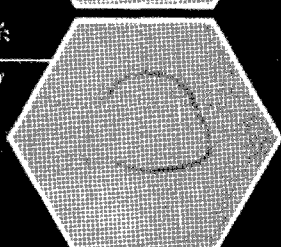
■ 分散液
分散液



5.SWNT(FH-A)糸

単層カーボンナノチューブ
FHタイプの糸

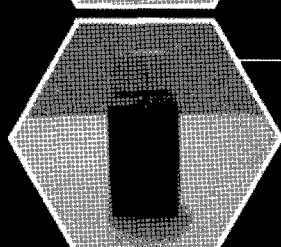
■ 製造法
CVD法



10.MWNT分散液

多層カーボンナノチューブ

■ 分散液
分散液



※ 各品類に揃って購入希望の場合、お問い合わせください。

価格 95,000円(税別)

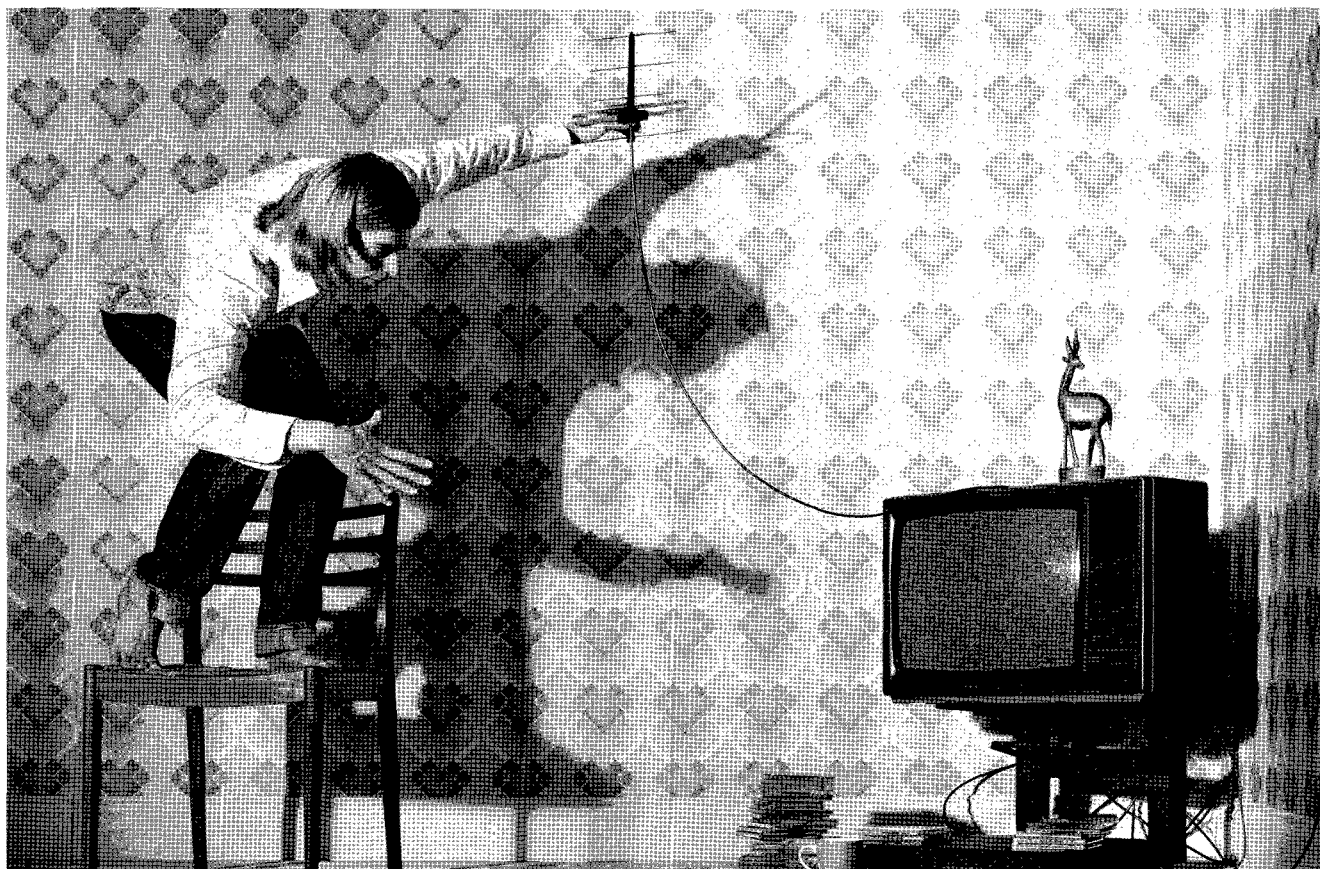
本製品は、名産ナノカーボン株式会社（〒465-0802 愛知県名古屋市中区丸の内3-4-10）にて製造されたもので、品質の向上とコスト削減に努めています。また、本製品の製造には、環境に優しい製造方法を採用しています。お問い合わせは、名産ナノカーボン株式会社（TEL:052-971-2108）までお願いいたします。



meijo nano carbon

〒160-0002
愛知県名古屋市中区丸の内 3-4-10
TEL:052-971-2108 FAX:052-955-3257

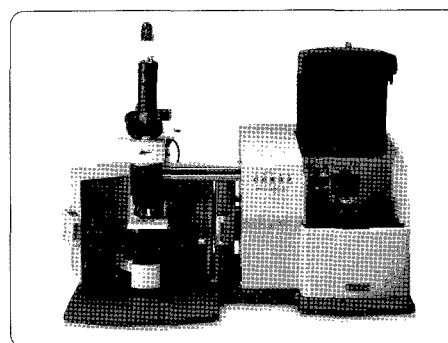
HP: <http://www.meijo-nano.com> E-mail: hashimo@cmfs.meijo-u.ac.jp



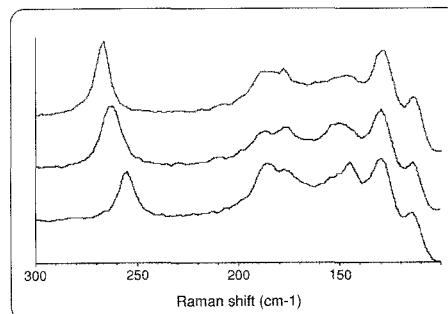
サーモフィッシャーが、ラマン分光装置の新時代を拓きます。

顕微レーザーラマンを「気難しい」装置だと思いませんか？
Nicolet Omega XRなら、自動で光路調整と較正を行うので
手間がかかりません。

- システムの自動調整、自動較正（特許）
- レーザおよびグレーティングの自動切換
- プレビュー機能とリアルタイム表示
- スマートバックグラウンド、自動露光による
高品質のスペクトル測定
- 785/780/633/532/473nmレーザ
2種類同時搭載
- クラスIレーザ安全基準適合
- ケミカルイメージングに対応



Nicolet Omega XR 顕微レーザーラマン



直径の異なるSWCNTのラマンスペクトル

サーモフィッシャーサイエンティフィック株式会社

スペクトロスコープ営業本部 IR/Raman営業部

〒221-0022 神奈川県横浜市神奈川区守屋町3-9 C棟2F

TEL. 045-453-9210 FAX. 045-453-9235

〒561-0872 大阪府豊中市寺内2-4-1(緑地駅ビル)

TEL. 06-6863-1552 FAX. 06-6863-1096

www.thermofisher.com (グローバル) www.thermofisher.co.jp (日本)

Part of Thermo Fisher Scientific



Thermo
SCIENTIFIC

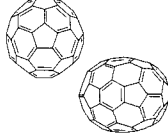
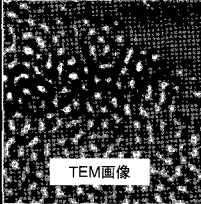
nanom

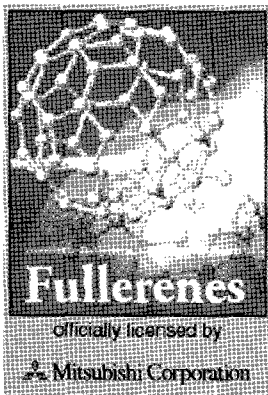
フラーレン サンプル価格一覧

フロンティアカーボン株式会社

2007年7月1日現在

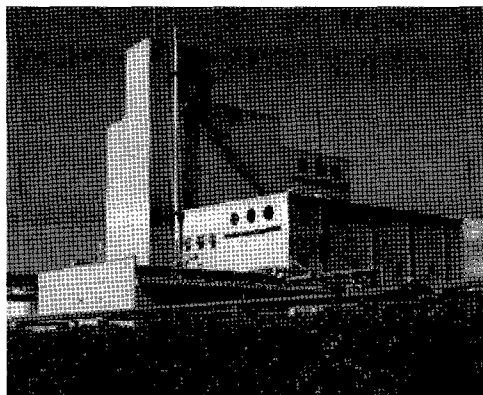
銘柄		分子構造	純度 (HPLC面積%:代表値)	販売単価	取扱数量
nanom purple フラーレンC60	ST		>99	3,000円/g	10g以上
				8,000円/g	1g以上
	TL		>99.5	10,000円/g	1g以上
	SU		>99.5/昇華精製品	15,000円/g	1g以上
	SUH	>99.9/昇華精製品	35,000円/g	1g以上	
nanom orange フラーレンC70	ST		>97	40,000円/g	1g以上
	SU		>98/昇華精製品	200,000円/g	0.5g

銘柄		分子構造	平均粒径	販売単価	取扱数量
nanom mix C60:約60% C70:約25% その他:高次フラーレン	ST		数10μm	500円/g	50g以上
				600円/g	10g以上
	ST-F		数μm	700円/g	50g以上
				800円/g	10g以上
nanom black フラーレン類似構造を有する特殊な煤 炭素含有量:96.0%以上	ST		数10μm	350円/g	100g以上
				60,000円/kg	1kg以上
	ST-F		数μm	550円/g	100g以上
				90,000円/kg	1kg以上



フロンティアカーボン株式会社は三菱商事株式会社から正規にライセンスを受け、フラーレン nanom® を製造販売しています

三菱商事株式会社は日本におけるフラーレン物質・製造特許の専用実施権を保有しております (特許第2802324号)



本格量産工場(40Ton/年)



Frontier Carbon Corporation

上記価格は予告無く変更する場合がございます。予めご了承下さい。大量のご購入の際は、別途お見積もり致します。

販売単価には消費税は含まれておりません。別途申し受けます。

御購入金額が25,000円以上(税抜)の場合、送料は弊社負担と致します。

御購入金額が25,000円未満(税抜)の場合、一律1,500円(税抜)の諸掛を申し受けます。

<お問い合わせ先>

フロンティアカーボン株式会社
営業販売センター

〒104-0031 東京都中央区京橋1-8-7
京橋日殖ビル5F TEL:03-5159-6880

<http://www.f-carbon.com>

フロンティアカーボン株式会社は、フラーレンを大量製造販売しているオンリーワンカンパニーです

銘柄	分子構造	溶解度 (wt%)				販売単価	取扱数量
		Toluene	o-Xylene	ODCB	PGMEA		
nanom spectra E100 PCBM (phenyl C61-butyl acid methyl ester)		2.2	3.1	>10	0.05	80,000円/g	1g以上
						130,000円/g	0.5g
nanom spectra E200 PCBNB (phenyl C61-butyl acid n-butyl ester)		1.9	5.3	>10	0.05	150,000円/g	1g以上
						240,000円/g	0.5g
nanom spectra E210 PCBIB (phenyl C61-butyl acid i-butyl ester)		3.5	5.9	>10	0.07	150,000円/g	1g以上
						240,000円/g	0.5g

銘柄	分子構造	販売単価	取扱数量
nanom spectra E110 C70PCBM 位置異性体の混合物です		250,000円/g	0.5g
nanom spectra E910 付加数 n=2-3 の混合物です		100,000円/g	1g以上
		160,000円/g	0.5g

銘柄	分子構造	溶解度 (wt%)				販売単価	取扱数量	
		PGMEA	乳酸エチル	CHN	MAK			
nanom spectra G100 側鎖部分の長さはカスタマイズ可能です						100,000円/g	1g以上	
		0.2	0.1	19.9	1.2	160,000円/g	0.5g	
nanom spectra Jシリーズ* 混合物です		PGMEA	価格、取扱数量、ご購入の諸条件等の詳細はお問い合わせ下さい。					
NR2 =	≥20							

銘柄	分子構造	組成	販売単価	取扱数量
nanom spectra D100 水酸化フラーレン 混合物です		C60(OH)n n=約10 (MS)	10,000円/g	1g以上
			12,000円/g	0.5g
nanom spectra B100 酸化フラーレン 混合物です		C60(O)1: 約30%	25,000円/g	1g以上
		C60(O)2: 約25%	30,000円/g	0.5g
		その他: C60, 三酸化体以上		
nanom spectra A100 水素化フラーレン 混合物です		C60(H)n n=約30 (MS)	12,000円/g	1g以上
			15,000円/g	0.5g

上記価格は予告無く変更する場合がございます。予めご了承下さい。大量のご購入の際は、別途お見積もり致します。

<お問い合わせ先>

フロンティアカーボン株式会社 営業販売センター

〒104-0031 東京都中央区京橋1-8-7 京橋日殖ビル5F TEL:03-5159-6880 <http://www.f-carbon.com>

濃厚溶液から希薄溶液まで幅広い濃度範囲に対応

ゼータ電位・粒径測定システム

ZETA-POTENTIAL & PARTICLE SIZE ANALYZER

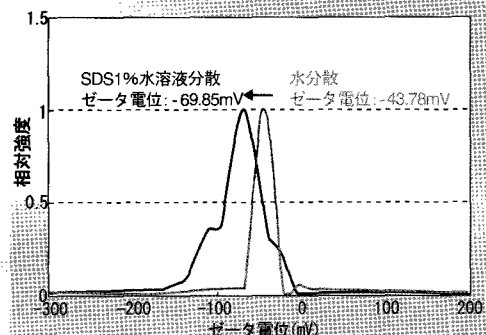
ELS-Z series



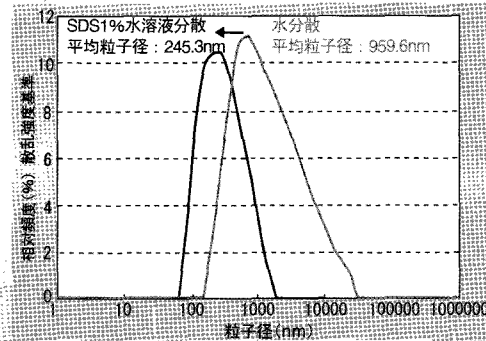
測定範囲

ゼータ電位	-100~100mV
粒子径測定	0.6nm~7 μ m
対応濃度範囲	
濃度範囲	0.001%~10%

■カーボンナノチューブのゼータ電位



■カーボンナノチューブのゼータ電位



- 希薄溶液に加え濃厚溶液でのゼータ電位測定が可能。
- 取り扱いが簡単な電気泳動セルにより操作性が向上。
- 電気浸透流を実測することで信頼性の高いゼータ電位測定が可能。
- 粒子径範囲(0.6nm~7 μ m)、濃度範囲(0.001%~10%)に対応。
- 従来のリニアスケール相関計に加えLogスケール相関計を搭載。ナノ粒子の高精度な解析や、濃厚系サンプルの解析など多様な用途に対応。

無料分析
ミニセミナー
および
分析相談会

光散乱相談室

東京会場	5/24、7/19、9/27
大阪会場	5/22、7/17、9/25

CAPI相談室

東京会場	6/28、8/23
大阪会場	6/26、8/21

お申し込みや詳しい日程は大塚電子機ホームページ
または下記の事業所までお問い合わせ下さい。

光散乱ミニセミナー

第一回	ゼータ電位測定	(東京5/24、大阪5/22)
第二回	粒子径測定	(東京7/19、大阪7/17)
第三回	分子量測定	(東京9/27、大阪9/25)

CAPIミニセミナー

第一回	原理と低分子イオンの測定	(東京6/28、大阪6/26)
第二回	ビタミン、ペプチド、糖類、 DNA、タンパク質への応用	(東京8/23、大阪8/21)

大塚電子株式会社

<http://www.photal.co.jp>

●本社 〒573-1132 大阪府枚方市招提田近3丁目26-3 TEL.(072)855-8564 FAX.(072)850-9159 e-mail: osaka.office@photal.co.jp
 ●東京支店 〒192-0082 東京都八王子市東町1-6 橋完LKビル4F TEL.(042)644-4951 FAX.(042)644-4961 e-mail: tokyo.office@photal.co.jp

週刊 **ナノテク** Nano Tech Weekly

コアテクノロジーからマーケットまで全てをカバー／ナノテクを分かりたい人、ビジネスにしたい人へのベストソリューションを提供／ナノテク国家プロジェクトからナノマテリアル、IT、バイオ、メディシン、エネルギー、MEMSに至るまで徹底取材

雑誌名：週刊ナノテク 予定頁数：16～32頁
発行日：毎週月曜日 体裁：A4変形、中綴じ
発行予定部数：15,000部 年間購読料：5万7,750円(本体5万5,000円)

産業タイムズ社

〒101-0021 東京都千代田区外神田5-5-4 第二日昌ビル
Tel.03-3834-5131 Fax.03-3834-5188
<http://www.semicon-news.co.jp/> <http://www.weeklynano.com>

〒101-0021 東京都千代田区外神田5-5-4
第二日昌ビル
Tel.03-3834-5131代/Fax.03-3834-5188

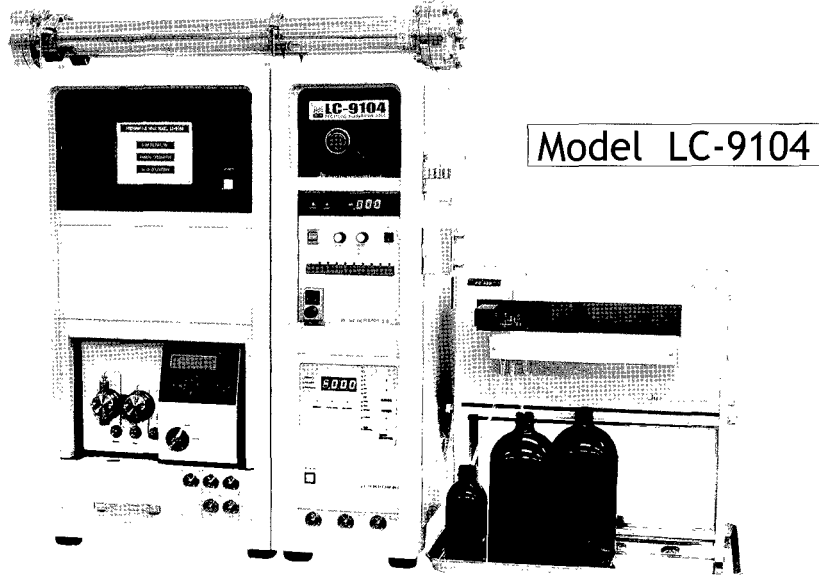
産業タイムズ社の出版案内

詳細カタログ呈
Fax.での注文も承ります。定価は税・送料込み。

- 好評発売中! **半導体産業会社録 2007年度版** 日本で唯一の半導体産業ダイレクトリ
“最新・大改訂版”
A4変形判・510頁・定価15,750円(本体15,000円)
- 好評発売中! **液晶・PDP・ELメーカー計画総覧 2007年度版** 大画面化する薄型テレビ市場へ
浸透するLCD/PDP
A4変形判・380頁・定価14,700円(本体14,000円)
- 好評発売中! **半導体工場ハンドブック 2007** 史上最高の投資に突入した
次世代ラインの全貌
A4変形判・129頁・定価3,150円(本体3,000円)
- 2007年
7月13日
発行済 **アジア半導体/液晶ハンドブック 2007** 台湾・韓国・中国・東南アジアの
メーカー別プロフィール・設備投資を一覧
A4変形判・100頁・定価4,200円(本体4,000円)
- 好評発売中! **プリント回路メーカー総覧 2007年度版** 得意分野で
さらなる飛躍に挑戦!!
B5判・292頁・定価16,800円(本体16,000円)
- 2007年
9月7日
発行済 **半導体産業計画総覧 2007-2008年度版** A4変形判・約530頁・定価19,950円(本体19,000円)
- 好評発売中! **日本半導体/FPDベンチャー年鑑 2006** 先鋭のベンチャー企業群が
日本のハイテクビジネスを変える
A4変形判・230頁・定価10,500円(本体10,000円)
- 好評発売中! **太陽電池産業総覧 2007** リニューアルエネルギーの切り札
太陽電池ビジネスに取り組む企業60社の全貌
B5判・360頁・定価18,900円(本体18,000円)
- 好評発売中! **ナノテク産業総覧** ナノテクキーカンパニー700社収録
キーパーソン300人網羅
A4変形判・540頁・定価25,200円(本体24,000円)

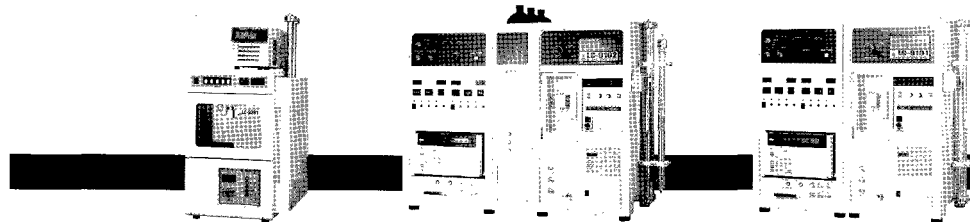
リサイクル分取HPLCはJAIのLC-9000シリーズ!

Recycling Preparative HPLC



◆LC-9104 大量分取モデル

専用のGPCカラム(40φ×600mm)を装着すれば、試料処理量は、LC-9101型の約4倍。試料注入から分取まで自動化されています。また、ODS・シリカカラムなど、大量分取用カラムの性能を最大限に引き出す装置設計がなされています。



◆LC-9201/LC-9204 コンパクトモデル

分離分取に定評のあるLC-9101型の高い性能を受継ぎながら、サイズをコンパクトにし、省スペース化と低価格化を実現しました。

◆LC-9102/9103 グラジエントモデル

グラジエントとリサイクルがワンタッチで切替えられます。

◆LC-9101 標準モデル

専用のGPCカラム(20φ×600mm)を装着すれば、分離能を落とすことなく、常時300mgを注入することができます。

—— 高分子分析の未来と取り組む! ——

分取LCに関する
新連携認定企業

Jai 日本分析工業株式会社

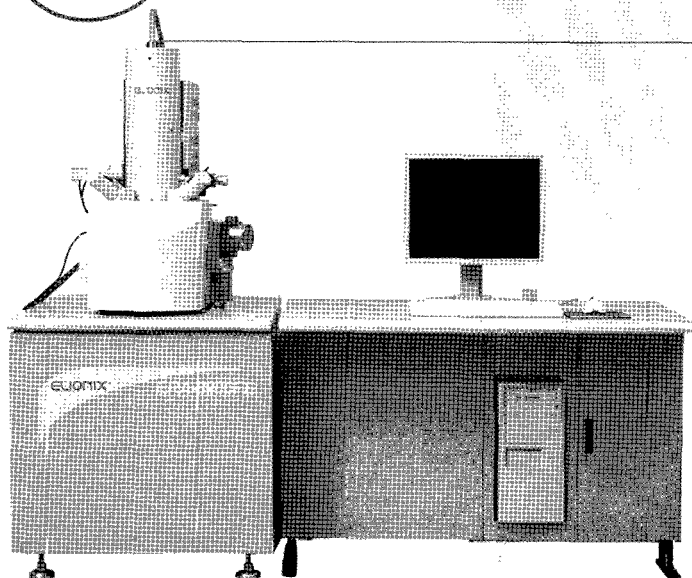
ISO9001/14001取得

URL: <http://www.jai.co.jp/> E-mail: sales-1@jai.co.jp

□本社・工場：〒190-1213 東京都西多摩郡瑞穂町武蔵208 TEL 042-557-2331 FAX 042-557-1892
□大阪営業所：〒532-0002 大阪市淀川区東三国5-13-8-303 TEL 06-6393-8511 FAX 06-6393-8525

ELIONIX

精密工学会
技術賞 受賞



Electron Probe Surface Roughness Analyzer

3D-SEMフィールドエミッション電子線三次元粗さ解析装置

ERA-8900FE

低加速でSEM観察しながら試料表面の粗さ解析が可能。

低加速領域においても簡単に高性能を発揮する新設計のTFE電子銃を搭載しました。横方向、縦方向ともに分解能が極めて高く、SEM観察視野をリアルタイムでCRTに三次元表示します。

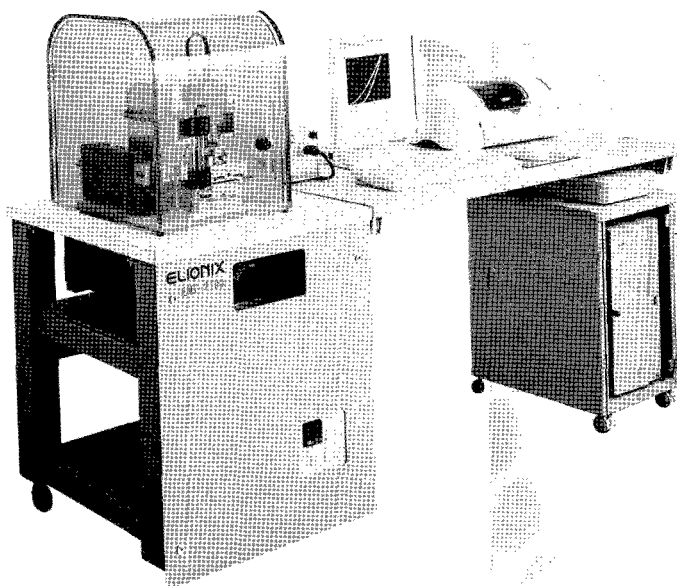
4本の二次電子検出器を搭載。

マルチ方向から凹凸(TOPO)、組成(COMPO)、通常のSEIの3タイプの画像が高分解能で得られます。従来のSEMでは困難とされた低倍率での無影照明像、微細凹凸像、緩やかなうねりなどの観察を可能としました。

Nano Indentation Tester

超微小押し込み硬さ試験機(超軽荷重型)

ENT-2100



数ナノの押し込み深さで、優れた再現性と安定性。

当社が独自に開発した定点荷重方式の採用により、サンプルに圧子を垂直に押し込むことができます。これにより正確な荷重負荷と表面検出精度を飛躍的に向上させ、最小1 μ Nという超軽荷重領域での試験を可能にしました。押し込み深さ数nmでも安定した測定ができます。

株式会社 エリオニクス

本社 〒192-0063 東京都八王子市元横山町3-7-6

大阪営業所 〒563-0025 大阪府池田市城南1-9-22 グリーンプラザ2F

<http://www.elionix.co.jp/>

TEL.042-626-0611(代表) FAX.042-626-9081

TEL.072-754-6999(代表) FAX.072-754-6990

http://atr-atr.co.jp

次世代 太陽光発電に新素材

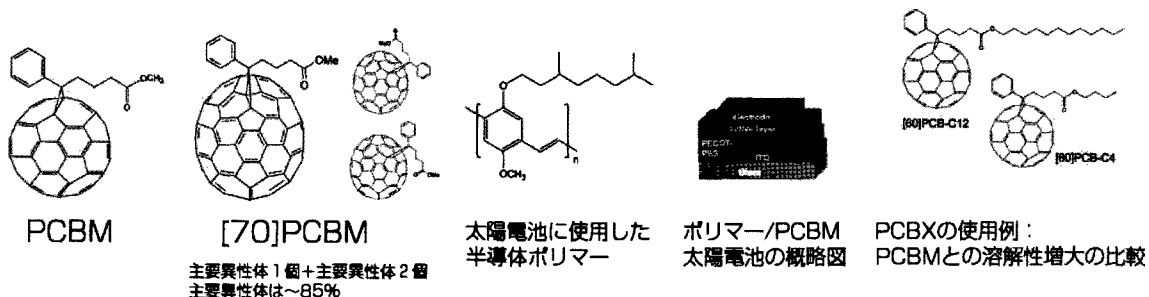
[60][70][84] PCBMフラーレン

はじめに

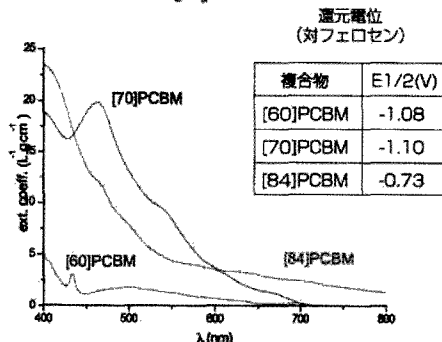
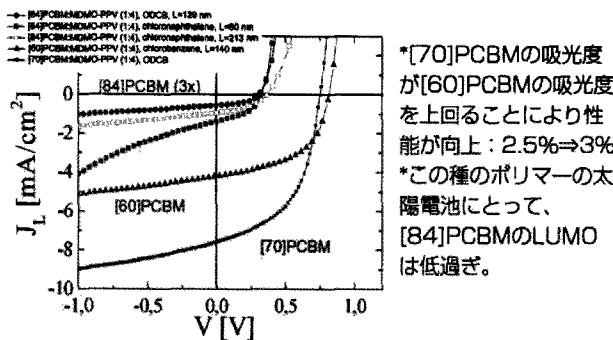
フラーレンを土台とした有機エレクトロニクスは商業的に高い可能性を秘め、業界で脚光を浴びています。例えば、半導体ポリマーに混合すれば、太陽電池、両極性の電解効果トランジスター(FET)、光検知器を低コストで製造できます。

FETには、高品質のフラーレン誘導体が使用されます。

従来、加工可能なC60-誘導体である[60]PCBMが最も多く使用されてきましたが、[60]PCBMのバリエーションや多種のフラーレン誘導体の応用によっても莫大な利益が見込めます。[60]PCBMのバリエーションは実に広く、溶解性、紫外線吸収(バンドギャップ)、安定性、還元電位などフラーレン誘導体の属性は特殊分野にも応用が可能です。以下に、[70]PCBMや[84]PCBMなどのPCBMアナログの特性と一部のPCBXの特性とを比較します。

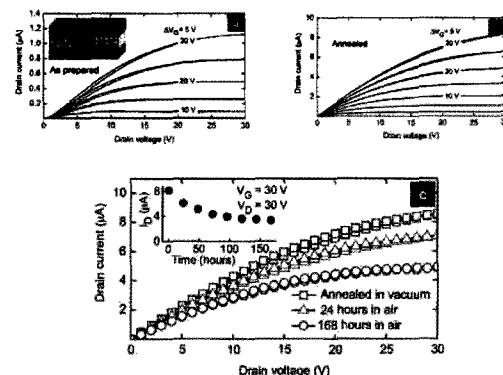


MDMO-PPV/PCBM太陽電池



UV-Vis absorbance of [60]PCBM, [70]PCBM and [84]PCBM (in toluene)

電解効果トランジスター内部の[84]PCBM



結論

- ・フラーレンの同調特性(吸光度の増加など)により、太陽電池の効率が向上。
- ・有機FET内部の[84]PCBMは、空気中で著しく安定。
- ・PCBXの使用によりフラーレンの溶解性を変化させると、加工条件は最適化される(活性層用の溶媒の加工条件など)。



Advanced Technology Research 株式会社 ATR

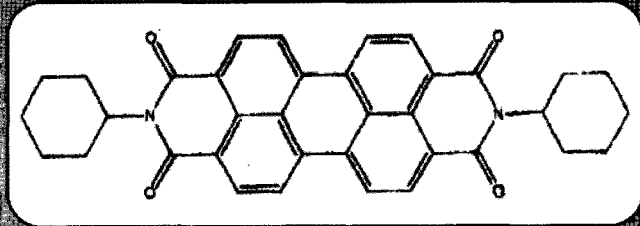
千葉県松戸市小金原7丁目10番地25 〒270-0021
TEL 047(394)2112 FAX 047(394)2100
sales@atr-atr.co.jp http://atr-atr.co.jp

<http://atr-atr.co.jp>

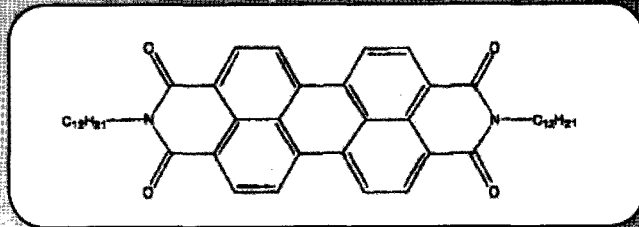
新製品 Perylene (ペリレン) — 有機半導体

- 有機電界効果トランジスタ [OFET]
両極性機能付薄膜
- 有機LEDディスプレイ [OLED]
有機EL
- 有機ソーラーセル
- 有機半導体回路
- センサラベル/蛍光ラベル

株式会社 **ATR** は株式会社
サイエンスラボラトリーズ
ナノテク部門の営業を分離
引き継いだ会社です。



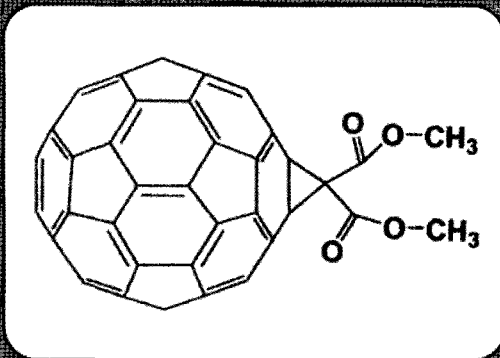
Soluble dyes



Dyes for evaporation processing

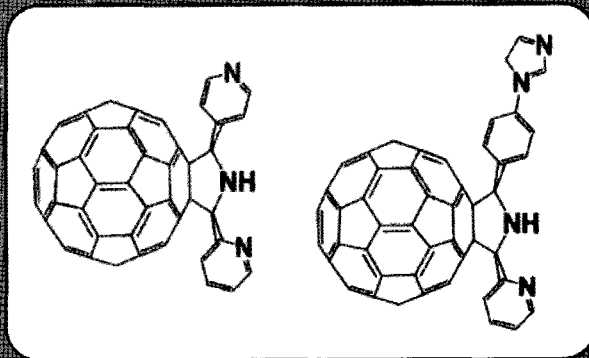
新製品 ソーラーセル・フラーレン誘導体

プラスチックソーラーセル
Malonic acid esters [FME]
有機ソーラーセル



FME-06-01

Photoresponsive
self-assembled Dyads
Mimics of natural photo
synthetic antenna [FPy]



FPy-06-01



Advanced Technology Research **株式会社 ATR**

千葉県松戸市小金原7丁目10番地25 〒270-0021
TEL 047(394)2112 FAX 047(394)2100
sales@atr-atr.co.jp <http://atr-atr.co.jp>

ナノテク材料は進化し続けている

<http://atr-atr.co.jp>

希少価値金属(レアメタル)

ニッケル:コバルト:フェロクロム:フェロマンガ:フェロバナジウム:亜鉛:チタン:スズ:アンチモン:タングステン:その他金属類

フラーレン

【60】【70】【84】PCBMフラーレン

高次フラーレン (C84)

水溶性フラーレン

C60CHCOOHカルボン酸メタフラーレン

C60(OH)6,C60(OH)22-26,C60(OH)24

アミノ酸フラーレン誘導体

アミノカプロン酸フラーレン(Anti-HIV)

ビスマロン酸エチルフラーレン

C13安定同位体置換フラーレン

Gd@C82金属内包フラーレン

La@C82金属内包フラーレン

C60-Pt,C60-Fe,C60-Ni フラーレン

ハイブリットC60フェロセン,コバルトセン

C60F36,C60F48,C60Br24フラーレン

金ナノ微粒子

金ナノ粒子,0.01%金,2~50nm

Dextranコート,0.01%金,10~50nm

PEGコート,0.01%金,5~50nm

Biotinラベル,0.01%金,5~50nm

Streptavidinラベル,0.01%金,5~50nm

各種カーボンナノチューブ

多層カーボンナノチューブ 純度95%(径~140nm 長さ~7μm)両端閉 CVD

多層カーボンナノチューブ 純度95%(径~20nm 長さ~7μm)両端閉 CVD

多層カーボンナノチューブ 純度95%(径~10nm 長さ5~15μm)両端閉 CVD

多層カーボンナノチューブ 純度90%(径5~40nm 長さ~15μm)両端閉 アーク

多層カーボンナノチューブ 純度90%(径5~40nm 長さ0.5~1μm)両端閉 アーク

単層カーボンナノチューブ 純度90%(径平均1~2nm 長さ~15μm) 両端閉 CVD

単層カーボンナノチューブ 純度50-70%

(径平均1.2~1.4nm 長さ10~50μm) 両端開 アーク

2層カーボンナノチューブ 純度15-25%(径3~5nm 長さ5~15μm) アーク

水溶性ナノチューブ各種

ナノ微粒子群

元素材料

[Au, Ag, Al, Bi, C, Cu, Fe, In, Mo, Ni, Si, Ti, W, Zn] 各種

非酸化化合物ナノ材料

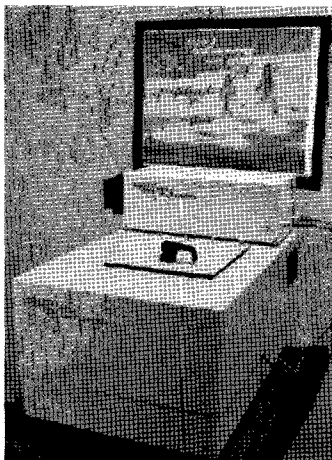
[Bn, GaP, InP, SiC, TaN, TiC, TiN, WC, WC/Co] 各種

酸化物ナノ材料

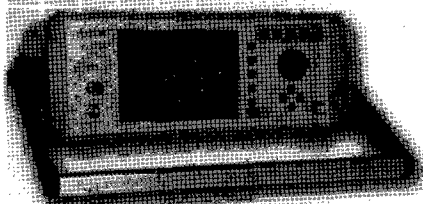
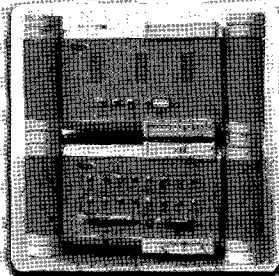
[Al2O3, BaSO4, Bi2O3, CeO2, CoFe2O4, CrO3, CuO, Er2O3, Eu2O3, Fe2O3, Gd2O3, HfO2, In2O3, MgO, Nd2O3, NiO, Sb2O3, SiO2, Sm2O3, SrCO3, SiTiO3, TiO2, V2O3, WO3, Y2O3, ZnO, ZrO2] 各種

ナノスペクトライザー

(Applied Nano Fluorescence社)
米国ライス大学ワイズマン教授
が開発した単層カーボンナノ
チューブ測定器。



SPMコントローラー



eLockIn204型デジタル2位相
ロックインアンプ

特長・仕様

- 6つ以上のフィードバックモードをデジタル制御
- 高性能ロックインアンプを搭載
- どのような装置にも簡単接続可能
- 複数の装置に同時接続可能
- 全てのチャンネルで同時計測可能
- 24ビットコンバーター
- 8チャンネルの低ノイズDAC、ADC
- スキャン領域を自由に設定可能
- コンピューター制御によるオートメーション位置決め
- SNOM、STM、AFM、SECM等のシステムに最適
- 低価格

微弱信号計測にはこれしかない

他社 (N社、S社、A社など) のロックインアンプとは格段優れた性能を持つデジタル2位相ロックインアンプがドイツから日本に初上陸。ドイツ ベンチャー企業Anfatec社がケンニッツ大学と共同開発し、技術性能を大きく向上させた画期的なデジタル2位相ロックインアンプです。



Advanced Technology Research 株式会社 ATR

千葉県松戸市小金原7丁目10番地25 〒270-0021

TEL 047(394)2112 FAX 047(394)2100

sales@atr-atr.co.jp <http://atr-atr.co.jp>